Conference Book

5th International Conference on Fog, Fog Collection and Dew

25 – 30 July 2010

Münster, Germany

www.FogConference.org

5th International Conference on Fog, Fog Collection and Dew
25 – 30 July 2010, Münster, Germany

The abstracts in this book can be also found on the conference homepage:

http://meetings.copernicus.org/fog2010/home.html

Compiled by:

University of Münster
Climatology Working Group
Robert-Koch-Str. 28
48149 Münster
Germany
http://kli.uni-muenster.de

Cover compilation: Julian Deventer
Cover Illustration: Melanie Köhler
Back side picture: Anna Westbeld

Author index

5th International Conference on Fog, Fog Collection and Dew
Münster, Germany, 25–30 July 2010
FOGDEW2010-1

Polycyclic Aromatic Hydrocarbons Transformations in an Urban Fog

K. Valsaraj, M.J. Wornat, J. Chen, and F. Ehrenhauser

Louisiana State University, Chemical engineering, Baton Rouge, United States (valsaraj@lsu.edu, 225-578-1476)

Polycyclic aromatic hydrocarbons (PAHs) are generated from incomplete combustion of fuels, coal-fired power plants and other anthropogenic activities. These are ubiquitous in all environments, especially the atmosphere. PAHs generally are found in the gaseous form and associated with the particles in the atmosphere. They are also found in the atmospheric water present in the form of fog, mist, rain, snow and ice. Particles (aerosols) in the atmosphere invariably contain a thin film of water which tends to have a high affinity for the adsorption of gaseous PAHs. Molecular dynamic simulations clearly show that the air-water interface is a preferable surface for adsorption of large molecular weight PAHs and atmospheric oxidants (e.g., O3, OH, 1O2, NO3). Thus, photochemical transformation of adsorbed PAHs in fog droplets is a possibility in the atmosphere. This could lead to the formation of water-soluble oxy-PAHs which are potential precursors for secondary organic aerosols (SOAs). Field work in Baton Rouge and Houston combined with laboratory work in thin film reactors have shown that this hypothesis is substantially correct. Field data on fog and aerosols (pre- and post-fog) will be enumerated. Laboratory work and their implications will be summarized. The thin film surface environment resulted in enhanced reaction kinetics compared to bulk phase kinetics. The influence of surface reactions on the product compositions is evaluated by performing experiments with different film thicknesses.

5th International Conference on Fog, Fog Collection and Dew
Münster, Germany, 25–30 July 2010
FOGDEW2010-2

Feasibility studies for water harvesting from fog and atmospheric moisture in Hormozgan coastal zone (south of Iran)

A. Esfandiarnejad (1), R. Ahangar (1), U.R. Kamalian (1), and T. Sangchouli (1)
(1) Water Research Institute, Tehran, Islamic Republic Of Iran (a.esfand@wri.ac.ir / Fax: +98-21- 77311959)

Abstract

The level of precipitation in the coastal towns & islands of the Hormozgan province is very low, but the relative humidity so high that wets the soil at below dew point temperatures and could therefore be utilized for relieving the water shortage, to some extents by employing water harvesting systems from fog & air moisture. The inhabitants of Qeshm Island have made efforts from the ancient times to collect air moisture along rainwater gathering. The reminders of these efforts are 366 small wells drilled in stone, which are now a tourist attraction. This method is also applied today in a less elaborate manner.
This research has been carried out to study the feasibility of water harvesting from fog and air moisture in the coastal towns and islands of the Hormozgan province of Iran on the northern shores of the Persian Gulf.
To examine the potential water in the atmosphere, the data from Bandar Abbass synoptic station with a statistical period of 1961-2005 was reviewed and the humidity values of over 70% and wind speed less than 5m/s were analyzed. The average water content of each cubic meter of air in Bandar Abbas in its most dry condition is 16.2g which amounts to 19.5g in its most humid state. The maximum water yield by applying this method could be harvested from 22 June until 22 September. The recorded data show that highest rate of moisture in each cubic meter of air occurred in 1961 while the highest extractable water potential was in 1995. Mentioning these facts, somehow indicate the importance of parameters effecting water harvesting such as wind speed and direction and the amount of moisture in the air.
Field observations and archaeological artefacts approve the results obtained by the conducted estimations showing the feasibility of water harvesting from fog & air moisture in this region and its rates in the different seasons.

1. Introduction

In the coasts and islands of southern Iran, the relative air moisture is high so that its value during summer reaches over 98 percent; but rainfall is very low in this region. Also, in this region, areas like Kish Island have over 150 foggy days in year, and Bandar Abbas, Jask, and Lenge Port have over 100 foggy days during each year. Among other important issues in this region is that in contrast to northern coastal areas in Iran where most fog occurs during winter, most fog occurs during warm months and summer in the southern coasts [1].
The residents of the coastal cities and islands of Hormozgan Province experience the contact of air moisture to solid material, e. g. metal objects like the structure of an ongoing construction, parked cars, stones and concrete blocks, etc., and their concentration into water drops making them wet during summer nights and early mornings. At times even water turns to small streams in the streets.
The use of the outlet water from air conditioning devices and coolers for watering plants in small gardens, the little streams of water and dews from putting plastic covers on plants, and the creating of small ponds for gathering the waters are common practice.
Dr. Kardovany, one of the scientists working in the field of dedesertification, proposed a project for harvesting water from air humidity for watering gardens and farms in this area in 2001. He believes that by burying metal plates in the fields, the plants can live with no need for rainfall and by only using the dew created by high air humidity[2].
Thus, if the water resources in this area do not suffice for drinking, air humidity can be used, especially during summer. This research studies the feasibility of harvesting water from air humidity and fog in the coastal regions and islands of Hormozgan using meteorological statistics and information from Bandar Abbas and Gheshm.

2. Area Under Study

relatively high during the year and its value increases from west to east. The location of Hormozgan with a sultry period of over 6 months is shown in Figure 1 [3].

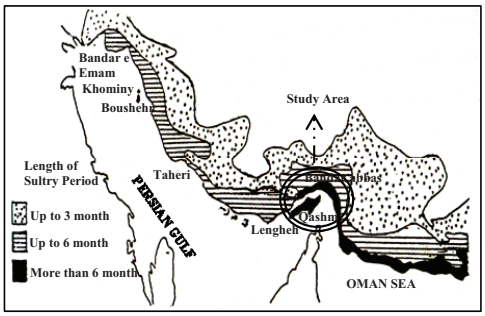

Figure 1: Sultry period in the southern coasts of the Persian Gulf

According to the results from Bandar Abbas synoptic station with a statistic period of 1961-2005 and Gheshm synoptic station with a statistic period of 1996-2005, the maximum annual relative air humidity in Bandar Abbas is 100% which includes 33 years of the 45 years of statistics. The average maximum annual relative air humidity is 99.4% and the average annual relative air humidity in the 45 years of statistics is 65.3%.

In Gheshm, the maximum annual relative air humidity has been reported as 100% which includes 7 years of the 10 years of statistics. The average maximum annual relative air humidity in Bandar Abbas is 99.4% and the average relative air humidity in the 10 years of statistics is 69.0%.

Also, according to Figure 2, which shows the occurrence diagram and probability curve of relative humidity in Bandar Abbas area, in approximately 8 to 10 percent of the year, the humidity has been reported as over 90% and the maximum occurrence rate in Bandar Abbas is recorded as 60 to 70%, which is 70 to 80% in Gheshm.

During 80% of the year in Bandar Abbas and 85% of the year in Gheshm, the relative air humidity has been reported to be over 50%. During about 55% of the year, the relative air humidity has been recorded as over 70% in Gheshm (approximately 50% of the year in Bandar Abbas).

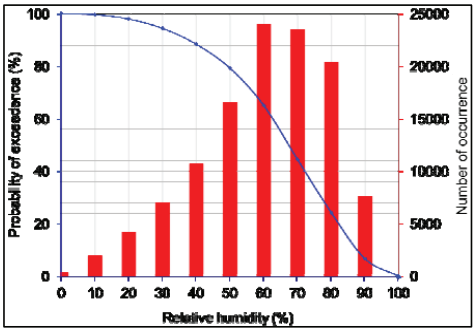

Figure 2: Frequency of occurrence and probability curve of relative humidity in Bandar Abbas s. station

3.Feasibility Study Criteria & Bases

Based on the thermodynamic parameters of the air mass, including the relative humidity and air temperature, the amount of water in the air and its conditions for saturation by the dew point can be calculated. This means that the conditions in which the ratio of humid air mixture $r(p,t)$ should get close to the ratio of saturation mixture $r_w(p,t_d)$ are that the dew point temperature should be less than air temperature $(t_d < t)$, for the $r = r_w$ condition to occur. Concentration occurs after the following processes.

- First, processes in which water vapor in the air is kept constant, and by decreasing the temperature, becomes lower. This can be shown as below:

Initial Condition	Temperature Decrease	Final Condition
$r_w > r$	→	$r_w = r$
Humid Air		Saturated Air

- Second, processes in which the maximum water vapor which a particle can absorb, i. e. r_w, is kept constant, and the water vapor in the particle is increased [4].

Initial Condition	Water Vapor Increase	Final Condition
$r_w > r$	→	$r_w = r$
Humid Air		Saturated Air

Generally, a process in which the r_w of an air mass can be decreased to r or less (first process), is the basis for water harvesting from fog and air humidity.

In the relations above, p stands for air pressure, t for air temperature, and r the ratio of humid air mixture.

Also, td is the dew point temperature and r_w is the ratio of saturated air mixture.

In the feasibility studies based on the smallest dew point temperature to reach saturation, values of 70% to approximately 92% of relative humidity have been used for conditions to harvest water from air humidity and relative humidity between 92% to 98% in additions to concentration cores for fog production with a wind speed of less than 6m/s have been used for feasibility studies. Thus, all other values for air humidity and wind have been omitted.

As to the elaborate statistics during the 45 years in Bandar Abbas, the years 1961 and 1992 were determined for maximum and minimum potential water in air humidity and the year 1995 was chosen as the 45-year average and studied. The data from Gheshm station was only used for control purposes due to similar results. The average air humidity of the area in the year 1995 is shown in Figure 3.

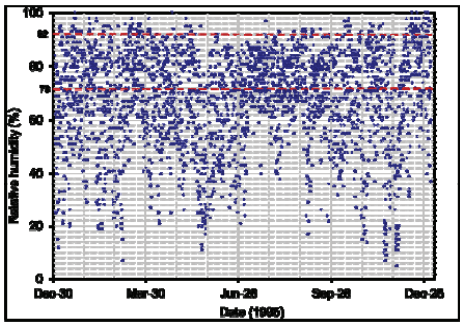

Figure 3: Relative humidity and fog average time-series diagram in Bandar Abbas synoptic station

The time-series diagram of wind in Bandar Abbas in the year 1995 is shown in Figure 4. As it is known, minimum wind speeds open the way for maximum water harvesting.

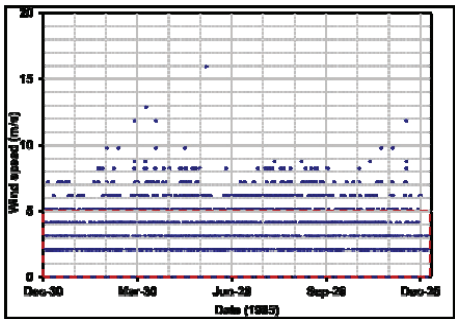

Figure 4: Wind time-series in Bandar Abbas station

3.1. Water Value in Air

To calculate the water value in the air, humidity indicators were considered for the whole year and as it can be seen in Table 1, the sum of the existing water or the annual net humidity has been divided by number of occurrences.

Table 1: Calculation of Water Value Indicator

Year	Water Value (Yearly)	Number of Occurrences per Year	Water Value Indicator (gr/m3)
1961	28450	1460	19.5
1992	47540	2928	16.2
1995	50936	2917	17.5

Thus, the average water value in 1m3 of air in Bandar Abbas in its driest conditions is 16.2gr, 19.5gr in its most humid conditions, and 17.5gr in average conditions. In Figure 5, the harvestable water is shown in contrast with the non-harvestable water.

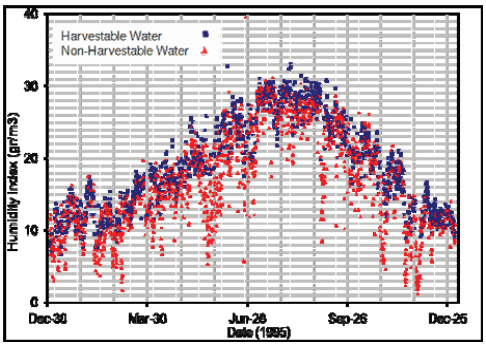

Figure 5: Harvestable water time-series diagram in Bandar Abbas synoptic station

Since the meteorology data is recorded with a time period of 3 hours, the considered harvestable water volume should be calculated with the wind speed value for 3 times. For example, in one specific 3 hours, for 2gr/m3 water and a wind speed of 1m/s, the maximum harvestable water volume would be:

2 (humidity indicator) × 1 (wind speed) × 3600 (one hour) × 3 (time indicator) × 100% (harvesting indicator) = harvestable water volume

= 21.6 (lit/m3 per 3 hours)

In Table 2, the maximum harvestable water in different years, the monthly, daily, and hourly average have been shown.

In Table 2, the maximum harvestable water in different years, the monthly, daily, and hourly average have been shown.

Table 2: Calculation of Maximum Harvestable Water (lit/m3)

Year	Yearly Sum	Monthly Average	Daily Average	Hourly Average
1961	113935	9495	312	13.01
1992	84294	7025	231	9.62
1995	221392	18449	607	25.27

Since the water cannot be completely harvested and the harvested volumes depends on both the continuity of harvesting conditions during the 3 hours and the performance of the device. Thus, for calculating the harvestable water, even if an indicator of 10% is used, according to the results obtained by different experiments by researchers around the world from the fog network device, the results can be suitable (Table 3) [5].

Table 3: Calculation of harvestable water (lit/m3) according to harvesting indicators

Harvesting Indicator	Year	Yearly Sum	Monthly Average	Daily Average	Hourly Average
10%	1961	11394	949	31	1.30
	1992	8429	702	23	0.96
	1995	22139	1845	61	2.53

The actual harvested water will be determined according to different tests in each point of the area under study.
The design which has been considered for water harvesting is shown in Figure 6 which will be tested in 3 areas for 6 months.

Figure 6: Proposed design for the water harvesting from air humidity system

3.2. Time Distribution

In Table 4, the maximum harvestable water volumes are presented by month. The maximum harvestable water is obtainable in the three months of July, August and September. In sum, in these three months in the year 1961, it has included in 55% of the year, in 1992, in 62% and in 1995, in approximately 50%. Also, the minimum harvestable water is expected in the cold months of the year.
The important point is that according to the fact that the maximum water in 1m3 of air occurred in the year 1961, thus the year 1995 has the highest potential harvestable water. This, in a way, verifies the performance of the parameters effecting the harvest, including wind and humidity.

Table 4: Calculation of Maximum Monthly Harvestable Water (lit/m3)

Month	Maximum Harvestable Water (lit/m3)		
	1961	1992	1995
January	3989	5106	7563
February	2465	3958	8353
March	10739	3751	14313
April	9475	6052	16028
May	7170	1272	11942
June	5972	4508	19622
July	26090	17797	39614
August	14754	20734	42393
September	20996	13147	26551
October	5250	3002	11878
November	3074	1252	10716
December	3962	3716	12418
Total	113935	84294	221392

4. Analysis of Resuts

In the feasibility studies based on the smallest dew point temperature to reach saturation, values of 70% to approximately 92% of relative humidity have been used for conditions to harvest water from air humidity and relative humidity between 92% to 98% in additions to concentration cores for fog production with a wind speed of less than 6m/s have been used for feasibility studies. Thus, all other values for air humidity and wind have been omitted.
The average water value in 1m3 of air in Bandar Abbas in its driest conditions is 16.2gr, 19.5gr in its most humid conditions, and 17.5gr in average conditions.

The maximum harvestable water is obtainable in the three months of July, August and September. In sum, in these three months in the year 1961, it has included in 55% of the year, in 1992, in 62% and in 1995, in approximately 50%. Also, the minimum harvestable water is expected in the cold months of the year.

The actual harvested water will be determined according to different tests in each point of the area under study. The design which has been considered for water harvesting is shown in Figure 6 which will be tested in 3 areas for 6 months.

According to the high potential of Hormozgan for water harvesting, it seems that air humidity and fog are suitable sources for supplying water shortages for houses and even farms.

It is obvious that in the mentioned area, due to shortage of superficial water and saltiness of the underground sources, the harvested water from fog and air humidity can be of important sources for water suppliance for the residents of the area due to their cost-efficiency.

References

[1] Rahimi M., Baradaran R., Fog Collection as a New Method of Water Supply, Iran Meteorological Organization, 2002.

[2] Dr. Kardavani p., the drought and contrasting styles with that in Iran, Tehran University Press 2001.

[3] Geography and Iranian Islands of Persian Gulf, Iranian Geography Publications, 1382

[4] Triple J.P., Rouch G., Translated by Shahrokhi J., General Meteorology, Center for University Publications, Tehran, 2001.

[5]www.fogquest.org,www.rexresearch.com/airwells

5th International Conference on Fog, Fog Collection and Dew
Münster, Germany, 25–30 July 2010
FOGDEW2010-3

DANGEROUS FOG ANALYSES AND FORECAST IN THE MACEIO AIRPORT, BRASIL

Natalia Fedorova, Aliton Oliveira da Silva, Vladimir Levit , Evanilson Vicente dos Santos
Institute of Atmospheric Science, Federal University of Alagoas, Brazil natalia@dimin.net

ABSTRACT
A small airplane fatal accident has occurred near Maceio Airport, on the coastal region on 26 July 2007. Low visibility in the intensive fog has provoked this accident. Weather forecast analysis, published in the local and central Brazilian newspapers during 2007, showed fog forecast absence during whole year. A study of the fog formation causes was elaborated using the high and low resolution satellite data, radar data, different products of NCEP reanalysis data and high resolution regional MM5 model simulation. The trade winds with a weak cyclonic curvature at the low levels have generated the humidity convergence at the superficial layers up to 850hPa on the coastal region. An anticyclonic circulation at the middle and higher levels and weak ascendant motion (by NCEP data) supported a weak convection development. The low levels clouds on the continental region and convection development over ocean were confirmed by the radar and satellite data. A thermal inversion near surface level (up to 150m) and descendent movement at the middle and high levels were identified by MM5 model. Fog formation was simulated by PAFOG model. The conventional airport observations have shown the minimal visibility of 200m between 4 and 7a.m. Moreover visibility less than 1000m between 4 and 7a.m. with the minimal visibility of 136m was simulated by PAFOG model.

Keywords: fog, fatal accident, PAFOG model.

1. INTRODUCTION

Fog was not observed frequently on the northern coast of Brazil; only one – two events per year were registered (Fedorova et al, 2008). At the same time rare meteorological stations don´t present complete information about the phenomenon.

A small airplane fatal accident has occurred near Maceio Airport on 26 July 2007 (figure 1). Low visibility in the intensive fog has provoked this accident.

Figure 1 Airplane fatal accident near Maceio Airport on 26 July 2007

Weather forecast analysis, published in the local and central Brazilian newspapers during 2007, showed fog forecast absence during whole year.

Fog/stratus formation on the northern coast of Brazil is associated, in general, with Wave Disturbance in the Trade Winds (WDTW) (Fedorova et al., 2008). The fog /stratus clouds were observed only together with altostratus and cumulus clouds in this tropical region. No stable layers in the vertical profiles were registered and the humid layer was very narrow in all studied cases.

The main research goal is the investigation of the fog formation causes, which provoked this fatal accident. The study results can support short-term weather forecasting in Maceio city (9ºS, 36ºW), Alagoas State on the northern coast of Brazil.

A forecast model (PAFOG) was developed by Bott and Trautmann, for radiation fog and low-level stratiform clouds in Germany (Bott and Trautmann, 2002). This model testing for intense fog formation event in the tropical region is the second goal of the study.

2. DATA SOURCE AND METHODOLOGY

The hourly conventional meteorological data (relative humidity, air temperature, dew point temperature, wind direction and velocity, pressure) at the Airport Station were used for the fog identification. The satellite and radar

information show the clouds types and synoptic scale systems near the study region.

The NCEP reanalysis date and MM5 model result (by Institute of Atmospheric Science, Federal University of Alagoas -UFAL) were used for synoptic scale systems description, vertical profiles simulation and as initial data for PAFOG model.

The WDTWs identification was elaborated by using streamline maps and vorticity at low levels (1000 and 925hP) and satellite images according to Molion and Bernardo (2002).

The PAFOG model input data are presented in 4 sections.
Section 1:
geographical data (latitude, longitude and altitude of meteorological station);
ground (ground type by Bott & Trautmann, 2002);
vegetation (height and covering);
meteorological station data (pressure; air and dew point temperatures and relative humidity at the 2m; temperature at the ground; visibility).

Section 2: cloudiness at the low, middle and high levels.

Section 3: radiosonde data (pressure; air and dew point temperatures; geostrophic wind velocity; level).

Section 4: ground temperature and humidity at different depth.

The PAFOG model was used for forecasting of the fog formation with 24h antecedence. The hourly conventional meteorological data were used as input for Sections 1and 2. Because of radiosonde data absence in the Maceio region, the MM5 model data were used in Section 3. The input data for Section 4 was constant (UV=0,25) because of the absence of any information (observational and by model).

3. RESULTS

3.1 Intensive fog formation conditions

An intensive fog was associated with the weak trough and WDTWs formation at the low levels (figure 2a). An anticyclonic circulation at the middle levels helps to humidity accumulation near the surface (figure 2b).

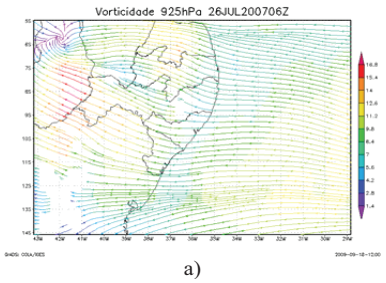

a)

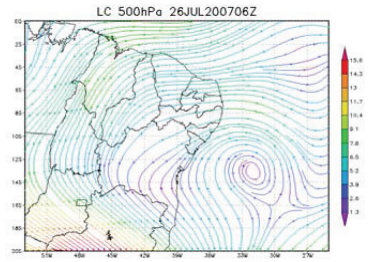

b)

Figure 2 - Streamlines at the 925 hPa (a) and 500hPa (b) near Alagoas state on 26 July 2007, 06UTC. Source: MM5, UFAL

Radar data presented the convection line development over the ocean, parallel to beach and the convection absence near the Airport (figure 3).

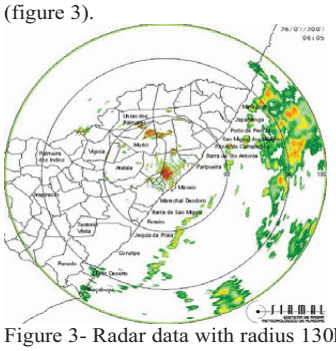

Figure 3- Radar data with radius 130km around the Airport on 26 July 2007, 06UTC.
Source: SIRMAL, UFAL

Omega vertical section show a weak ascendant movement below 900hPa near the Airport and intensive ascendant movement near beach, some kilometers over the ocean (figure 4). These data confirmed the radar information.

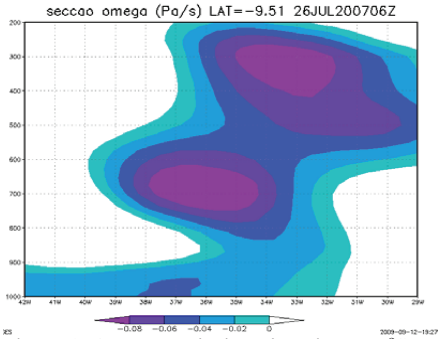

Figure 4- Omega vertical section along 9.5ºS on 26 July 2007, 06UTC. Source: NCEP

An absence of any thermal inversion or stable layer near the surface was observed by NCEP reanalysis data (figure 5a). A thermal inversion near the surface level (up to 150m) was identified by MM5 model (figure 5b).

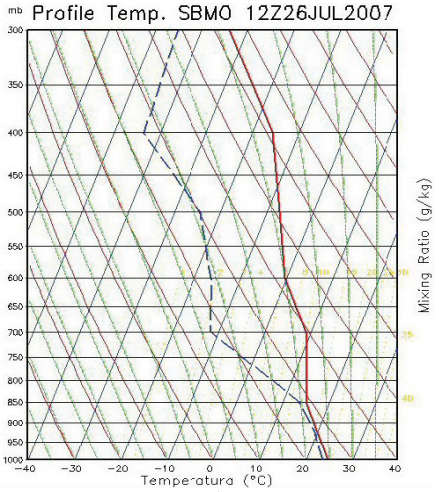

a)

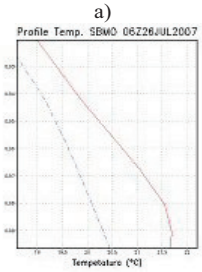

b)

Figure 5 – Vertical profiles of air temperature (line) and dew point temperature (dashed line), constructed by NCEP data (a) and in the low levels by MM5 model (b; axis y in σ) on 26 July 2007, 06UTC. Source: NCEP, MM5-UFAL

3.2 Forecast by PAFOG model with the cloudiness data

The visibility forecasts with 16-13h antecedence were lower than observed (figure 6a,b). Initial date for them used atmospheric parameters during maximal heating and maximal convective instability.

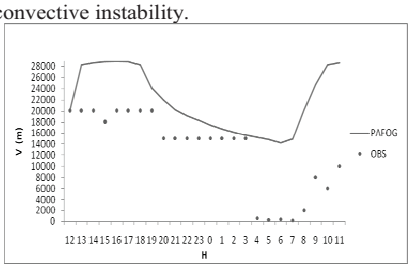

a)

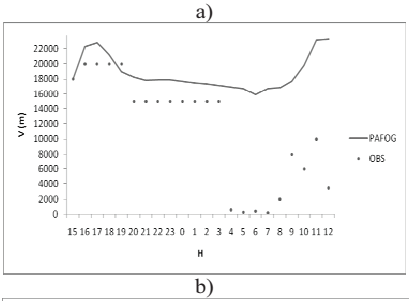

b)

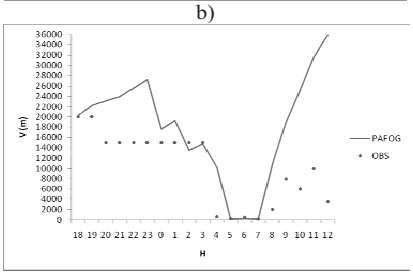

c)

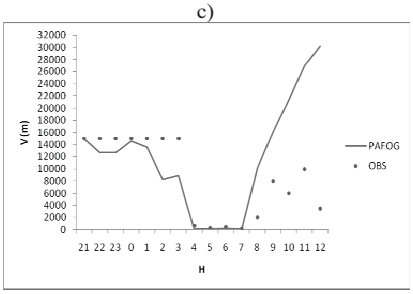

d)

Figure 6 – Visibility by observational data (points) and by PAFOG model forecast (line) on 25-26 July 2007. The forecast with 16, 13, 10 and 6h antecedence are presented at the figures a, b, c and d, respectively.

Forecast with 10h antecedence shown better result (visibility 132m between 5 and 7h local time) (figure 6c). Forecast with 6h antecedence was the best with low visibility (136m) between 4 and 7a.m. At the same time forecasted visibility after fog was higher than observed (figure 6d).

3.3 Forecast by PAFOG model for clear sky

Because of the forecast by the PAFOG model did not show satisfactory result with beginning data during maximal convective instability time, the model was tested for situation without cloudiness. The results were much better and fog formation and visibility fall were forecasted similarly to the observational data (figure 7).

After the fog event, a visibility forecast did not show satisfactory results. The model predicted a finish of the low visibility period (visibility predicted was 16-22km). But the observational data presented the haze (visibility < 2000m) up to 8h and then a visibility variation between 8 and 10km

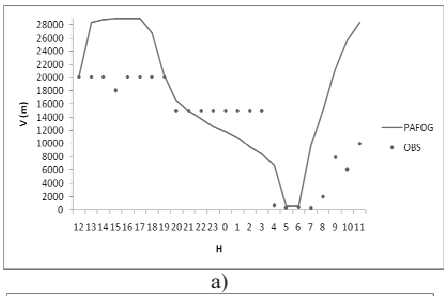

a)

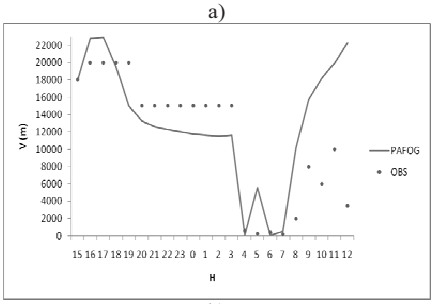

b)

Figure 7 – Visibility by observational data (points) and by PAFOG model forecast (line) on 25-26 July 2007. The forecast for clear sky with 16 and 13h antecedence are presented at the figures a and b, respectively.

4. CONCLUSION

The intensive fog, witch provoked fatal accident near Maceio Airport, was formed by next principal causes:
1) wind velocity was decreased brusque during the change of daily sea breeze (from east) to land night (from north west); the visibility in this moment decries from 15 km to 1.5km during 1 hour;
2) existence of the stable superficial layer (weak thermal inversion up to 925hPa by MM5 model);
3) weak ascendant movement at the low levels and weak descendant movement between 800 and 700hPa and at high levels by MM5 model.
All theses processes help to humidity accumulation at the low levels.

Fog forecasting by the PAFOG model presented a satisfactory result with 10h antecedence. Fog was not predicted with the beginning data during maximal convective instability time. These beginning data presented a good result for clear sky situation.

5. ACKNOWLEDGEMENTS

To Prof. Andreas Bott, Meteorological Institute, University of Bonn, Germany, by the possibility of the PAFOG model utilization.

Partial financial support was provided by FAPEAL (Research Support Foundation of the Alagoas State), CNPq (National Council of Scientific and Technological Development) and CAPES (Coordination of the Level Superior Personal Improvment).

6. REFERENCES

Bott, A. and T. Trautmann (2002) PAFOG – A new efficient forecast model of radiation fog and low-level stratiform clouds. *Atmos. Res.* **64**, 191 – 203, 2002.

Fedorova, N., Levit, V. and D. Fedorov (2008) Fog and Stratus Formation on the Coast of Brazil, *Atmos. Res.*, **87**, 268-278.

Molion and Bernardo (2002) Uma revisão da dinâmica das chuvas no Nordeste Brasileiro. *Revista Brasileira de Meteorologia*, v 17(1), 1-10.

5th International Conference on Fog, Fog Collection and Dew
Münster, Germany, 25–30 July 2010
FOGDEW2010-4

HAZE FORMATION ON THE NORTHERN COAST OF BRAZIL

Vladimir Levit, Deydila Michele Bonfim dos Santos, Natalia Fedorova

Institute of Atmospheric Science, Federal University of Alagoas, Brazil vladimirle@gmail.com

ABSTRACT

Two types of haze formation on the northern coast of Brazil were investigated. Comparisons of the thermodynamic and synoptic processes for haze associated with rain (HR) and without one (H) were elaborated. The hourly surface data at the Maceio International Airport were used for HR and H identification.

Thermodynamic processes were studied by temperature and humidity vertical profiles, elaborated by two methods: 1) NCEP reanalysis data for Maceio and 2) Air Parcels Trajectories of the HYSPLIT model at the 10 pattern levels. Vertical profile forecast, using the HYSPLIT model, was elaborated with 12, 24, 36 and 48h antecedence. High humidity of the superficial layer (up to 925hPa) and humidity convergence were confirmed by the both models and this layer was forecasted up to 48h antecedence. Weak ascendance motions at the superficial and high layers and subsidence in the middle layers have provoked a superficial humidity accumulation for H days. More intensive ascendance motions at the same levels were observed for HR days.

Synoptic situations before and during HR and H events were analyzed using different products of NCEP reanalysis, of high resolution (10km) ETA model results and infrared satellite images. All H and HR phenomena were accompanied by weak wave disturbances in the trade winds field.

HR was associated with one type of the synoptic scale systems and H events with other type at the middle levels. Different trough types were observed by both models for H days. An influence of the cyclonic circulation, which was identified only in the middle levels, was registered by NCEP data and was confirmed by satellite images for HR days.

Low visibility forecasting presented satisfactory results for H and HR days with 24h antecedence.

1. INTRODUCTION

Low visibility on the Northern Coast of Brazil (NEB) was not observed with high frequency (Fedorova et al, 2008) and therefore a few investigations were elaborated. At the same time, low visibility events caused different accidents. For example, intensive fog provoked fatal accident near Maceio Airport on 26 July 2007.

The first investigation about haze formation shown that the phenomena, with visibility of 1-2km, was observed on the northern coast of Brazil during 33 hours per year with the greatest frequency in June (Levit et al., 2007). The low visibility of 2–4km was detected during 236 hours per year with the highest frequency in a rainy season.

Processes formation analysis of haze associated with rain (HR) and without one (H) was the principal study goal. Also, the models (high resolution ETA and HYSPLIT) verification capacity for haze forecast was the second goal.

2. DATA SOURCE AND METHODOLOGY

The haze and rain occurrence was identified by hourly conventional meteorological data at the Maceio International Airport during 2004.

Synoptic analysis

Synoptic situations before and during phenomena was analyzed using different information:

1. Satellite data (www.cptec.inpe.br/satelite) in the infrared channel;
2. Products of reanalysis data by National Centers for Environmental Prediction/National Center for Atmospheric Research (NCEP/NCAR), each 6h: 1) streamlines at the low, middle and high levels, 2) omega vertical sections along 10ºS.
3. Products of high resolution (10km) ETA model each 3h: 1) streamlines at the low, middle and high levels and 2) humidity characters at the low levels (relative humidity, humidity advection, humidity confluence).

The WDTWs identification was elaborated by using streamline maps and vorticity at low levels (1000 and 925hP) and satellite images according to Molion and Bernardo (2002).

Thermodynamic analysis
Vertical profiles by NCEP reanalysis data in Maceio were used as *real profiles (Pr)* because of a radiosond data absence.

Forecast of vertical temperature and humidity profile (Pf) was elaborated with 12, 24, 36 and 48h antecedence (Figure 1). Firstly, air parcels trajectories of the HYSPLIT model at the 10 levels were constructed. Afterwards, the NCEP reanalysis of the vertical profile on the beginning trajectory points (latitude and longitude) were elaborated for each level trajectory. Then, forecast of vertical temperature and humidity profile was elaborated, using the temperature and humidity data at the beginning points (altitude) of each vertical profile.

Comparison of *Pf* and *Pr* was made by instability indexes K-Index (K), Total Totals (TT), Lifted Index (LI) and also by three parameters:
1. $|Tf - Tr| \leq 2^oC$; *Tf* and *Tr* are temperatures by *Pf* and *Pr* at the low and middle levels.
2. Humidity ($(T - Td) \leq 3^oC$) layer occurrence at the low levels.
3. Stability layer existence at the low levels.

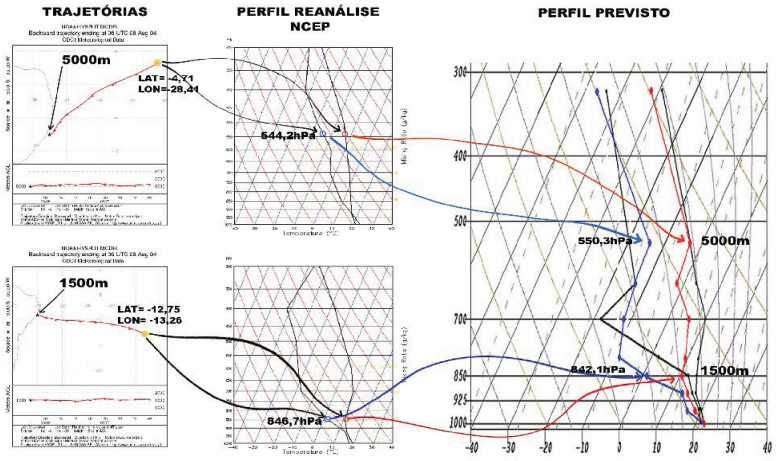

a) b) c)

Figure 1 – Forecast vertical profile elaboration (c), using Air Parcels Trajectories of the HYSPLIT model at the 10 levels (a; figure show only 2 levels) and NCEP reanalysis vertical profile for Maceió on the beginning points of each trajectories (b)

3. RESULTS

3.1 Synoptic processes of haze formation

Synoptic scale events analysis on the NEB shown the absence of principal systems, such as Intertropical Convergence Zone and Frontal zones of extrotropical baroclinic cyclones for the H and HR events (Figures 2 and 3). At the same time, any influence of Cyclonic Vortex, which is localized only at the Middle Levels (CVML), was detected for HR event (Figures 2b and 3d). The CVML cloudiness was identified by satellite images: it was up to high levels near CVML center and only at low levels on the cyclonic periphery over NEB (Figure 2b). The CVML occurrence was confirmed by cyclonic center existents at the middle levels (Figure 3d) and the center absence at the low and high levels (Figures 3b and 3f).

Weak Wave Disturbance in the Trade Winds field (WDTW) was accompanied the haze formation in all H and HR events and was identified by NCEP reanalysis data and by high resolution ETA model (Figures 3a and 3b). But WDTW was more intensive for HR event. By Rodrigues et all. (2010), 87% of the troughs near surface are associated with WDTW. At the same time, High center was localized nearest to the Southern America continent for H events, than for HR event.

Streamlines at the middle level present different trough types (Figures 3c and 3d). The trough in the HR event was associated with the CVML in the Southern Hemisphere and trough in the H event was linked with North Hemisphere Low. The east region of high level trough was identified in the HR and H events (Figures 3e and 3f). But the streamlines hade anticyclonic curvature for H events and cyclonic curvature for HR event.

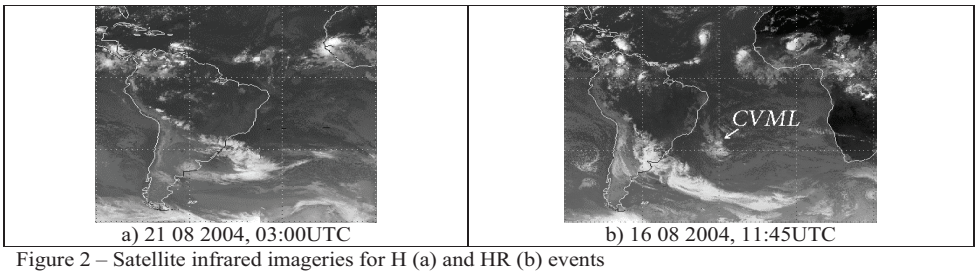

a) 21 08 2004, 03:00UTC b) 16 08 2004, 11:45UTC

Figure 2 – Satellite infrared imageries for H (a) and HR (b) events

The ETA model and NCEP reanalisys shows similarly air currents at the low and high levels. But at the middle levels ETA model shows a High above the event region for the HR event and trough axis for the H event.

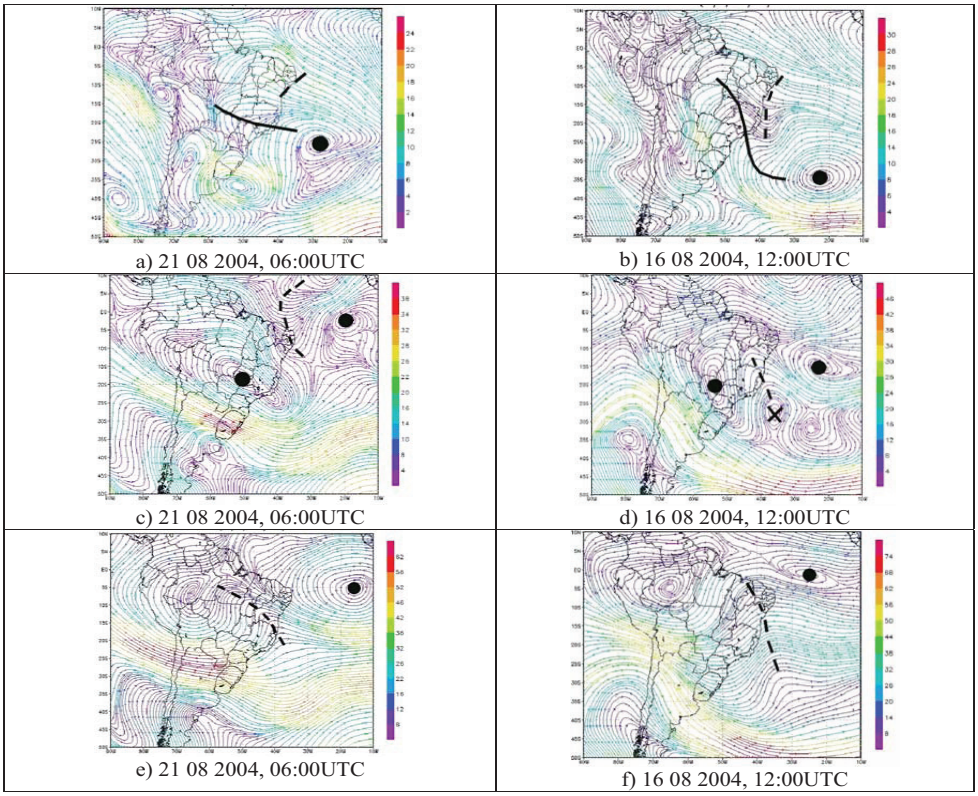

a) 21 08 2004, 06:00UTC b) 16 08 2004, 12:00UTC

c) 21 08 2004, 06:00UTC d) 16 08 2004, 12:00UTC

e) 21 08 2004, 06:00UTC f) 16 08 2004, 12:00UTC

Figure 3 Streamlines at the low (925hPa, a and b), middle (500hPa, c and d) and high (200hPa, e and f) levels for H (a, c, e) and HR (b, d, f) events. CVML- cruz, High – circle, ridge- line, trough- dotted line.

3.2 Thermodynamic processes of haze formation

The *Pf* and *Pr* comparison presented the satisfactory results for temperature at the low and middle levels and for humidity only at the low levels.

High humidity of the superficial layer (up to 925hPa) was registered for H and HR events by *Pr* and ETA model and was forecasted with success by *Pf* up to 48h antecedence (figure 4). Humidity convergence, also, was identified and forecasted by the same model up to 48h antecedence (figure 5).

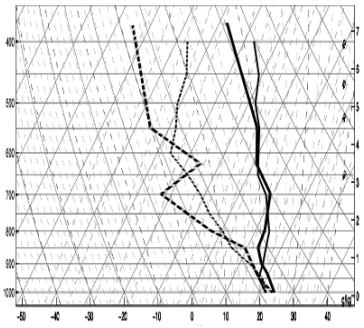

a) 21 08 2004, 06:00UTC

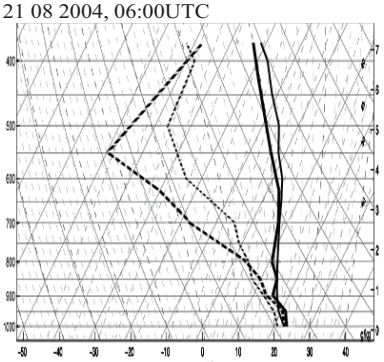

b) 16 08 2004, 12:00UTC

Figure 4- Comparison of *Pr* (thin lines) *with Pf* (thick lines) with the 24h antecedence for H (a) and HR (b) events.

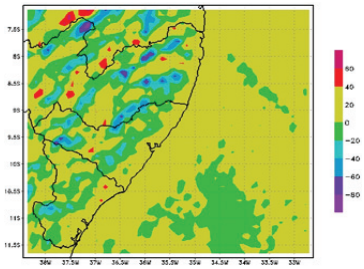

Figure 5 Humidity convergence by ETA model at the 1000hPa for H event, 21 08 2004, 06:00UTC

Weak ascendance motions at the low layers up to 850hPa and subsidence in the middle layers provoked a superficial humidity accumulation for H days (Figure 6a).

More intensive ascendance motions at the low (up to 820hPa) and high levels with thin subsidence motion layer nearly 700hPa were observed for HR day (Figure 6b).

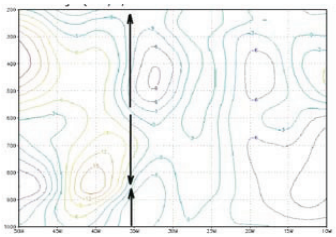

a) 21 08 2004, 06:00UTC

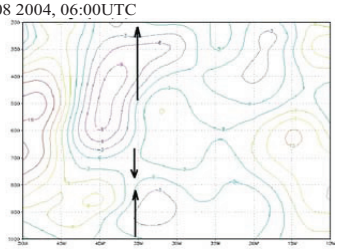

b) 16 08 2004, 12:00UTC

Figure 6 – Omega vertical sections ($*10^{-2}$ $Pa.s^{-1}$) along 10ºS for H (a) and HR (b) events

4. CONCLUSION

Weak Wave Disturbance in the Trade Winds field was associated with the haze formation in all H and HR events.

Satisfactory results of the HYSPLIT and ETA models used for the low visibility forecasting with 24h antecedence were obtained for H and HR days.

5. ACKNOWLEDGEMENTS

Partial financial support was provided by CNPq (National Council of Scientific and Technological Development).

6. REFERENCES

Fedorova, N., Levit, V. and D. Fedorov (2008) Fog and Stratus Formation on the Coast of Brazil, *Atmos. Res.*, **87**, 268-278.

Levit, V., Fedorova, N., Santos, D.M.B., Rodrigues, L. R. L., Costa, S. B., Santos, A.S. (2007) Visibility in Stratus Cloud days on the northern coast of Brazil. In: *Fourth International Conference On Fog, Fog Collection And Dew*, La Serena, Chile, 81-84.

Molion, Bernardo (2002) Uma revisão da dinâmica das chuvas no Nordeste Brasileiro. *Revista Brasileira de Meteorologia*, v **17**(1), 1-10.

Rodrigues L.R.L., Fedorova N., Levit V., (2010) Adverse meteorological phenomena associated with low level baric troughs in the Alagoas State in 2003. *Atmospheric Science Letters*, DOI: 10.1002/asl.**273.**

5th International Conference on Fog, Fog Collection and Dew
Münster, Germany, 25–30 July 2010
FOGDEW2010-5

Observational Study on Jump Features of Macro and Microphysical Structures of a Fog Event in Nanjing, China

C. Lu (1), S. Niu (1), J. Yang (1), X. Liu (1,2)

(1) School of Atmospheric Physics, Nanjing University of Information Science & Technology, Nanjing, China (luchunsong110@gmail.com), (2) Jiangsu Meteorological Science and Technology Service Center, Nanjing, China

A comprehensive fog experiment was carried out in the north suburb of Nanjing, China with many instruments, e.g., tethered balloon system, fog droplet spectrometer, visibility meter. Using the data of boundary layer profiles, fog droplet spectra, visibility and conventional meteorological elements as well as NCEP reanalysis, a fog case on December 14th, 2006 was chosen to study the jump features (sharp strengthening and weakening) of fog top and ground fog's density, and their causes are also discussed in detail. Result shows that the explosive development of fog top is due to upward turbulent transport of moisture and its accumulation under up-layer inversion as well as substantial temperature decrease; sharp strengthening of ground fog is mainly caused by lower saturation vapor pressure in the near-surface layer under the influence of cold advection, enhancement of inversion owing to up-layer systematic sinking motion, and moisture accumulation under inversion; during the fog top decline, turbulence happens near the fog top and up-layer sinking motion causes the occurrence of temperature increase, fog double layer structure and low-level jet; the sharp weakening of ground fog is the result of solar radiation and downward transport of momentum; sinking motion has dual roles in the fog event; fog double layer structure occurs during the sharp decline of fog top and accelerates fog top decline, which is extremely different from the former results that double layer causes fog top development.

5th International Conference on Fog, Fog Collection and Dew
Münster, Germany, 25–30 July 2010
FOGDEW2010-6-1

Impact of Turbulence on Radiation Fog

L. Zhao, S. Niu, C. Lu, J. Lv, and J. Yang

School of Atmospheric Physics, Nanjing University of Information Science and Technology, Nanjing 210044, China
(gsszyqxjzlj@163.com)

Fog is a common weather phenomenon occurring in the boundary layer, and its formation, development, and dissipation are closely related with the air motion and the radiation balance of the boundary layer. The transition period between autumn and winter (November-December) is the time period of the highest fog frequency in one year in Nanjing, China. Turbulence characteristics within the surface layer and its impact on radiation fog in the north suburb of Nanjing City in autumn-winter season were analyzed using the boundary layer comprehensive observations at a site in Nanjing University of Information Science and Technology (NUIST) from 13 December to 15 December 2007. A three-dimensional sonic anemometer-thermometer instrument(CSAT3, Campbell, USA) with a sampling frequency 10 Hz was used in the experiment to measure the fluctuations of u, v, w components and acoustic virtual temperature, and a Fog Monitor(FM-100) to measure the fog particle size spectrum, and a automatic weather system to measure temperature, humidity and wind near the surface.
The critical turbulent exchange coefficient (Kc) was used to analyze these two fog processes, and found that Kc was larger than the actual turbulence exchange coefficient (K) in the formation, development, and mature fog stage, but smaller than K before the fog formation. This parameter can be used to forecast the formation of radiation fog. The explosive strengthen of the radiation fog corresponds with the obvious increase in turbulence intensity. Stronger turbulence is beneficial to produce larger droplets, broaden the fog particle size spectrum, and heighten the fog layer. During the fog development stage, the fog explosively strengthens near the surface first, and then explosively heightens. Based on the synthesized analysis of turbulence, radiation, macro- and microphysics parameter, it is found that longwave radiation is the main factor for cooling and condensation during the development of radiation fog, the turbulence caused by droplets condensation is the dynamic factor to increase the vertical development of fog, but the near-surface layer warming and turbulent motion caused by increasing solar shortwave radiation directly prompts the fog dispersal.

5th International Conference on Fog, Fog Collection and Dew
Münster, Germany, 25–30 July 2010
FOGDEW2010-7

Application of Fuzzy-Logic NWP Fog Guidance to Perth Fog Forecasting Decision Support System

Y. Miao (1), R. Potts (1), X. Huang(2), G. Elliott (3), R. Rivett(3), M. Manickam(1)
1. The Centre for Australian Weather and Climate Research, Bureau of Meteorology, GPO Box 1289, Melbourne VIC 3001, Australia (y.miao@bom.gov.au / Fax: +61-3-96694468)
2. National Meteorological and Oceanographic Centre, Bureau of Meteorology, GPO Box 1289, Melbourne VIC 3001, Australia
3. Western Australia Regional Office, Bureau of Meteorology, PO Box 1370, West Perth, WA 6872, Australia

Abstract

An objective Fuzzy-logic based NWP fog guidance is developed for Perth Airport. Its performance over a five year period is assessed to be useful in cool season. A rule-based fog forecasting decision making process incorporating this guidance and other fog tools demonstrated its superiority, on average, to any of the tools used individually. This process led to the development of a more streamlined IT infrastructure called Fog Forecast Decision Support System for Perth Airport.

1. Introduction

Fog forecasting is an important issue at Perth Airport (31.58°S, 115.49°E, altitude 20m), the largest airport along the southwest coast of Australia. Although fog is an infrequent weather phenomenon there, any unforecast fog events will be detrimental to international long-haul flights due to the lack of suitable alternate airports for diversion. Even the closest ones - Learmonth Airport to the north and Adelaide Airport to the east are still three hours away.

Fog can form at Perth Airport in many different synoptic conditions: pre-frontal, post-frontal, in between fronts, slow-moving or east-drifting cut-off lows to the south etc. Often the key drivers to fog formation are precipitation followed by radiative cooling but the development of nocturnal winds over uneven terrain frequently determines the location and timing of fog formation [2].

For quite a long time, synoptic pattern recognition and physical reasoning by a forecaster are the primary fog forecasting approaches for Perth Airport. The lack of objectivity and heavy reliance on experience and local knowledge of a forecaster made it difficult for the Western Australia Regional Forecasting Centre (WARFC) to achieve a more consistent fog forecasting performance. Although various NWP models from overseas and Australia are available to the centre, their primary function is to help forecasters with their identification of synoptic conditions conducive to fog rather than to provide direct and reliable fog forecasts.

To take advantage of the constantly improving NWP model performance and to provide forecasters with an additional forecasting tool that is both objective and independent, in 2003 a fuzzy-logic based NWP fog guidance for Perth Airport was developed. Since then, it has become an essential tool to WARFC in their routine aviation fog forecasting. In the meantime, the introduction of the guidance has prompted the centre to adopt a more structured fog forecast process that makes use of the guidance and other tools in a systematic way. Recently this process has led to the development of a streamlined IT infrastructure called Fog Forecasting Decision Support System (FDSS) for Perth Airport.

This paper will first provide background information regarding fog events and forecast products for Perth Airport. The NWP fog guidance will then be described and discussed. This will be followed by the introduction of the structured forecast process and FDSS. Discussion and Summary will be provided at the end.

2. Background

2.1 Fog Definition

The meteorological definition of a fog is that the prevailing horizontal visibility is less than 1000m. However because aviation forecasting is more

concerned about the weather conditions below the Special Landing Alternate Minima (SLAM) and because of difficulty in ascertaining whether visibility reduction over a sector could lead to widespread fog event, WARFC and this paper define a fog event as when the minimum visibility for any sector is at or below SLAM condition, i.e., 2000m for Perth Airport. According, this paper defines a mist event as the minimum visibility being larger than 2000m but equal to or less than 5000m.

2.2 Fog Climatology

Figure 1 provides the fog event monthly distribution based on the 22-year observation dataset between 1988 and 2009. It is apparent that fog is more frequent in cool months between April and October with the average of 1.5 fog events per month and the total of 10.4. For the warmer months between Nov and Mar, the average is only 0.3 per month and the total is just 1.3. Therefore it is convenient to define two "fog seasons"- warm and cool with the warm season being Nov to Mar inclusive and cool season being Apr to Oct inclusive.

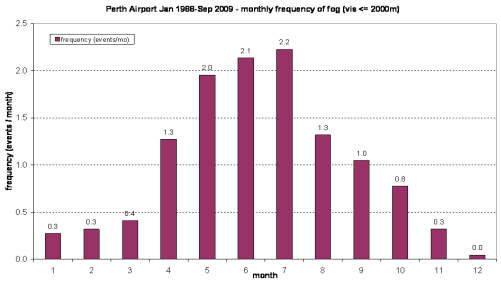

Figure 1: Perth Airport monthly distribution of the observed fog events based on the 22-year observations from 1988 to 2009.

2.3 Fog Forecast Products

For long lead-time aviation forecasting, two products are issued for major airports in Australia, the Code Grey advices and Terminal Area Forecasts (TAFs). TAFs are the standard products for the international aviation community and are issued at 6-hourly interval in UTC or zulu time (Z), namely 00Z, 06Z, 12Z and 18Z, plus any amendments. However Code Grey advice is unique to Australia. It is specially designed to help long-term planning of long-haul flights by providing advice on the small but non-negligible chance of such aviation hazardous weathers as fog, low cloud and thunderstorm. While TAFs are used for forecasting fog probability of 30% or higher, the Code Grey advices are used when fog probability is between 1 to 29%. In practice, the probability of 5, 10% or 20% are normally specified on Code Grey advices.

The critical products to long-haul flight planning are the 06Z TAF and the 06Z Code Grey advice. They are used to forecast whether fog is likely the next morning.

3. Fuzzy-Logic NWP Fog Guidance

While NWP models can provide useful fog-sensitive fields such as relative humidity, pressure gradient and wind for forecasters to assess fog risk likelihood, very few can directly simulate the detailed fog process for operational fog forecasting application [3]. In the face of this, forecasters are looking for a tool that can produce fog forecasts automatically and objectively from the best NWP model available to them.

3.1 Fuzzy-Logic Concept

A fuzzy-logic approach is considered suitable for this purpose because it caters for both model inaccuracy and the inexact relationship between a fog predictor and the likelihood of fog occurrence. For example, it is uncertain that the wind speed of 6 m/s will definitely lead to a no-fog event. However, it is appropriate to say that this wind strength is more likely associated with a no-fog event than a fog event.

Use of fuzzy-logic concept gained popularity in recent years. It has been used in the classification of atmospheric circulation Patterns [1]. Hansen [4] reported a sophisticated analog method using fuzzy-logic concept to forecast ceiling and visibility for 190 airports in Canada.

3.2 NWP Model

The **MESO_LAPS_PT125** (**MESO**scale **L**imited **A**rea **P**rediction **S**ystem **P**oin**T 125**) is chosen because it was the highest resolution and arguably the most accurate operational model available for Australian region at the time of development between 2001 and 2003. This model belongs to the LAPS model family developed by Puri et al. [6]. Some of

its specifics include a horizontal resolution of 0.125° (~12.5km), 29 levels in vertical, running twice daily at 00Z and 12Z out to 48 forecasting hours.

3.3 Fog Predictors

To be chosen as a fog predictor, it needs to meet two criteria. The first is that it is sensitive to fog occurrence thus providing better distinction between fog and no-fog events. The second is that the model is capable of simulating it well so that the modelled value behaves similarly to the observed one as far as assigning a fuzzy function value is concerned.

Extensive investigation of observations and the archived **MESO_LAPS_PT125** model dataset in the cool season identified the following four predictors for the 00Z guidance.

- Mean wind speed at 200m above mean sea level (AMSL) overnight
- Bias-corrected minimum dew point depression at 200m and 600m AMSL overnight. Bias is calculated as the dew point depression difference between the observed and modelled value at around 60m AMSL at analysis (i.e., 00Z).
- Bias-corrected minimum dew point depression difference between the +24 forecast hour and analysis at 600m AMSL.
- Minimum dew point depression difference between the +24 forecast hour and analysis at 200m and 600m AMSL.

Here overnight refers to the time that fog is most likely present, i.e., between 15 and 24Z. Apart from the wind speed, the other three predictors are not totally independent to each other. These boundary layer dew point depressions and their overnight trend are considered important to fog. Their interdependency is considered by the reduced weighting when combining fuzzy functions for final fog risk outcome.

An apparent absence from the list is the surface dew point depression. This is because that the model has large errors in predicting surface parameters and that the surface dew point depression generates high false alarms even from observations. Many rain events correspond to low dew point depression but don't necessarily lead to fog events.

For the 12Z guidance, some change to the predictor list is made with increased emphasis on observations due to the proximity to the fog onset. The list is as follows.

- Mean wind speed at 200m above mean sea level (AMSL) overnight
- Bias-corrected minimum dew point depression at 200m AMSL overnight.
- Observed dew point depression at 60m AMSL at analysis (i.e. 12Z)
- Minimum dew point depression at 200m AMSL overnight

3.4 Fog Risk Categories

Four fog risk categories are classified in the guidance aimed at matching them with the WARFC's fog forecast decision categories of NoFog, low percentage fog forecast on code grey advice (hereafter as Code Grey) and prob30 or higher fog forecast on TAF (hereafter as Prob30). They are F0, F5, F15 and F30 representing increased fog risk from very low to high.

3.5 Fuzzy Functions

Fuzzy function for each predictor is generated after the synergetic consideration of behaviour of both observational and model data in their predictability of fog events. More weight has been given to observations to ensure that future improvement in model performance will naturally lead to the improved fog guidance without having to adjust the fuzzy functions. The function ranges from 0 to 1, representing the degree of likelihood of a fog risk category from unlikely to very likely.

Figure 2 provides an example of fuzzy functions for each fog risk category of F5, F15 and F30. No function is provided for F0 category because it is always unity when a predictor does not even score any fuzzy function for F5. In the example, it is when the minimum dew point depression difference is at least 5 degrees.

Taking a value of 3 degrees, three fuzzy function scores can be worked out from the graph. This is 0.85 for F5, 0.4 for F15 and 0 for F30, representing high chance for F5, medium chance for F15 and no chance for F30.

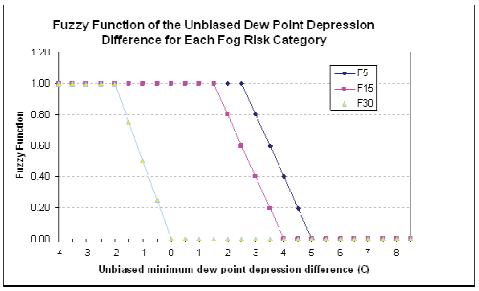

Figure 2: Fuzzy function plot for the 00Z guidance predictor of the minimum dew point depression difference between the +24 forecast hour and analysis at 200m and 600m AMSL

3.6 Fog Risk Outcome

Once a fuzzy function is assigned to each fog risk category for each predictor, a composite fuzzy function is produced for each fog risk using a fuzzy rule. Essentially this rule is to find the lowest fuzzy function out of the four predictors for each fog risk category with more weighting given to the wind speed predictor due to the interdependence of the other three.

The final fog risk outcome is then decided by finding out which fog risk category attracts the highest composite fuzzy function.

3.7 Performance and Discussion

Five year (2004-2008 inclusive) archived guidance outcomes are used to assess the performance of the guidance. Only the 00Z guidance is assessed because it is the long lead-time fog forecasting that is more important to long-haul flights.

Figure 3 displays the distribution of the percentage of times when a particular fog risk forecast is made and fog is observed. The distribution looked encouraging for cool season but not the warm season. In cool season, there is a clear increase trend from the lower risk categories of F0 and F5 to F15 and F30. For example, there is 15% chance that when F30 is forecasted, fog will be observed. This compared with the 2% times that a fog is observed when a F5 is forecasted. The 2% percentage for F0 and F5 forecast categories are however not satisfactory even though it looked like a small percentage. This is because when multiplied by the number of forecasts in these two categories, the number of times that fog is observed but unforecasted is actually not small.

For warm season, the performance is quite poor. Apart from the F0 category which is at the desired very low percentage, little distinction is made among three other categories with the highest percentage only 3% coming from FM15. As discussed earlier, fog only occurs about once per warm season and the guidance is developed based on the cool season datasets. Therefore, the guidance is not suited for warm season fog forecasting. If insisting on using it, then the categories of F15 and F30 should be treated as if they were F5.

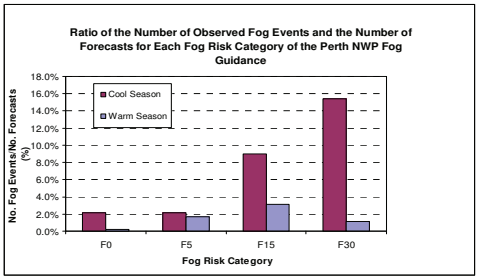

Figure 3: Ratio of the number of observed fog events and the number of forecasts for each fog risk category of the fuzzy-logic based guidance

4. Forecasting Process and FDSS

Thompson [7] demonstrated that improved accuracy may be achieved when optimally combing independent forecasts. The availability of more tools including this guidance has prompted WARFC to investigate if fog forecasting performance can be improved through a rule-based decision making process.

There are three main forecasting tools that WARFC identified as useful for Perth Airport fog forecasting. They are the synoptic pattern matching and human reasoning (generically known as subjective method), the GASM which is the analog method based on modeled data and the guidance just introduced (for simplicity, hereafter the name NWPFOG is also used). The subjective method asks a forecaster to check if and how well the current synoptic pattern matches with any of the known fog-conducive patterns. It then allows the forecaster to make subjective assessment of fog risk likelihood even if

the pattern is not favorable to fog. Once this is done, this method is treated the same as the other two methods in the rule-based decision making process with slightly more weighting given in certain situations.

This process has led to the development of the web-based system recently called FDSS that streamlines the process from data input, to methods, to rule-based final outcome and to the ultimate forecast decision. All data used are archived for view or verification.

The performance of the 06Z FDSS is compared with that of the 00Z NWPFOG which the 06Z FDSS requires, for the same 5-year period of 2004 to 2008 for cool season only. In FDSS, the NWPFOG fog risk categories are assigned to one of the three forecast categories with F0 and F5 corresponding to NoFog, F15 to Code Grey and F30 to Prob30.

Figure 4 compares the percentage of fog being observed out of all forecasts of a category from NWPFOG and FDSS. While little difference can be found in Prob30, significant improvement can be found in FDSS in the NoFog category. FDSS reduces the NWPFOG percentage of 2% down to almost zero. There is also difference in Code Grey percentage between the two but this is not considered as important.

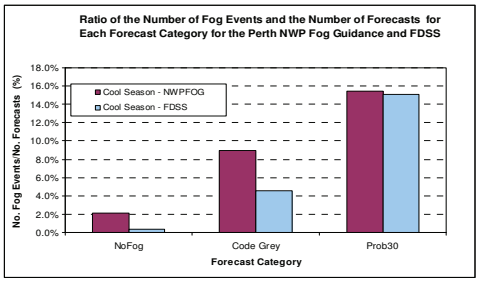

Figure 4: Comparison between NWPFOG and FDSS on the ratio of the number of fog events and the number of forecasts for each forecast category for cool seasons of 2004 -2008.

To illustrate more clearly how significantly FDSS has improved on the NWPFOG results, the frequency of the observed fog events captured by each forecast decision is plotted on Figure 5. It showed that NWPFOG missed more than 20% of the total number of fog events which is unacceptable to airlines particularly considering how important Perth Airport is to them. On the other hand, FDSS only missed 3%. While still not ideal, this is a significant improvement over NWPFOG.

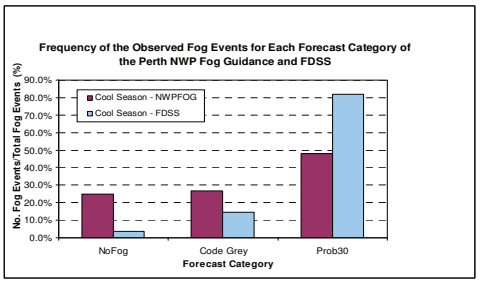

Figure 5: Comparison between NWPFOG and FDSS on the ratio of the number of fog events and the total number of fog events for each forecast category for cool seasons of 2004 -2008. The NoFog category equates missed fog events.

5. Discussion and Summary

This paper first provided some background information about the importance of fog forecasting at Perth Airport, the largest one over the southwest Australia. It then described the method and performance of a fuzzy-logic based NWP fog guidance for Perth Airport. Following that, the structured fog forecasting process which recently evolved into a web-based IT system called FDSS was introduced.

The performance of the guidance is shown to be reasonably satisfactory in cool season but not so in warm season which the guidance is not designed for. Although the guidance demonstrates a clear upward trend in its ability to capture more of the fog events when moving risk category higher, the percentage is too high for category F0 and F5. This shortcoming is alleviated by the structured process and later FDSS, further confirming that it is possible to improve forecast accuracy when optimally combining independent forecasts.

Future work will target both the guidance and the FDSS system. The guidance has now been adapted to the new modeling system called ACCESS due to the imminent cease of the LAPS model family. The new

guidance is expected to perform better than the current version but detailed verification is required before further development work is carried out. The current FDSS system relies on the rule-based decision making process which may be improved by the introduction of Bayesian Network. Such a network has been shown by Newham et al [5] powerful to improve the fog forecasting performance for Melbourne Airport.

References

[1] Bardossy, A. and Duckstein, L.: Fuzzy rule-based classification of atmospheric circulation patterns. International Journal of Climatology, 15, 1087-1097, 1995.

[2] Golding, B. W.: A study of the influence of terrain on fog development. Mon. Wea. Rev., 121, 2519-2541, 1993.

[3] Gultere, I., Tardif, R., Michaelides, S. C., Cermak, J., Bott, A., Bendix, J., Muller, M. D., Pagowski, M., Hansen, B., Ellrod, G., Jacobs, W., Toth, G., and Cober, S. G.: Fog research: a review of past achievements and future perspectives, Pure Appl. Geophys., 1121-1159, 2007.

[4] Hansen, B.: A fuzzy logic-based analog forecasting system for ceiling and visibility, Weather and Forecasting, 22, 1319–1330, 2007.

[5] Newham, P., Boneh, T., Weymouth, G., Bally, J., Nicholson, A., Korb, K.: Fog forecasting at Melbourne Airport using Bayesian Networks (http://www.bom.gov.au/events/9icshmo/manuscripts/PT_Db8_Newham.pdf), a poster presentation at the 9th International Conference on Southern Hemisphere Meteorology and Oceanography, 9 to 13 Feb 2009, Melbourne, Australia.

[6] Puri, K., Dietachmayer, G., Mills, G.A., Davidson, N.E., Bowen, R.A., and Logan, L.W.: "The new BMRC Limited Area Prediction System, LAPS." Australian Meteorological Magazine Vol 47, No 3, 203-223, 1998.

[7] Thompson, P. D.: How to improve accuracy by combining independent forecasts. Mon. Wea. Rev., 105, 228–229, 1977.

5th International Conference on Fog, Fog Collection and Dew
Münster, Germany, 25–30 July 2010
FOGDEW2010-8

Observational Research on Fog Physicochemical Properties in Nanjing, China

S. Niu, C. Lu, L. Zhao, J. Lv, and J. Yang

School of Atmospheric Physics, Nanjing University of Information Science & Technology, Nanjing 210044, China (niusj@nuist.edu.cn)

A comprehensive fog in situ observation was carried out at Pancheng in Nanjing area of China during December 2006 and December 2007, including the measurement of fog droplet spectra, surface meteorological elements, boundary layer structure and visibility as well as the collection of fog water. Some new microphysical features and the reasons why low visibility (less than 50 m) lasts for around 40 h in an unusual fog event (12/24/2006-12/27/2006) are examined. The 5-min-average maximum value of liquid water content (LWC) is found extraordinarily higher than 0.5 g m-3. But it is reasonable partly because of high fog top, long-wave radiative cooling, and partly because of the significant positive correlations of number concentration (N) vs. average radius (ra) and droplet spectra standard deviation (SD) vs. ra. The possible causes for the positive correlation of N vs. ra are studied. In general, the development of collision and coalescence can consume small droplets, causing decrease of N and increase of ra. However, due to warm and moist air and sufficient cloud condensation nuclei in this site, small droplets are reproduced through nucleation and condensation. As a result, N is proportional to ra. Furthermore, the correlation between liquid water content (LWC) and N is also positive. Prolonged low visibility is directly caused by the synchronous high LWC and N, and essentially by stable boundary layer structure under the influence of warm advection, sufficient water vapor provided by moisture advection and substantial cloud condensation nuclei (CCN) in the observation site. In addition, with the 37 fog water samples in 9 fog events, fog chemistry is analyzed. Total ionic concentration (TIC), electrical conductivity (EC) in fog samples and local emissions of pollutants are one or two orders of magnitude higher than those found in Europe or South America for instance. Scavenging of NH3 and coarse particles by fog droplets are the main causes for high mean pH value, 5.9 S/LWC (S: the surface area of fog droplets per unit volume of air) is supposed to be a better index to describe the relationship between TIC and microphysics with respect to LWC. A formula between TIC and S/LWC is derived and the related parameters are discussed. Depositions of chemical species by fog events are estimated and result shows that deposition is sufficient.

5th International Conference on Fog, Fog Collection and Dew
Münster, Germany, 25–30 July 2010
FOGDEW2010-9

Burst evolution of a deep dense fog by combining with low-level cloud

J. Yang, L. Wang, D.-Y. Liu, and Z.-H. Li

Laboratory for Atmospheric Physics & Environment, Nanjing University of Information Science and Technology, Nanjing, China (jyang@nuist.edu.cn)

Field experiments were conducted during a deep dense fog event that occurred in Nanjing 13-14 December 2007. This fog event persisted 14 hours, including 4 hours of super dense fog stage. The boundary layer structure and physical mechanisms of the fog were analyzed based on the field observations from tethersonde system, eddy covariance system, fog droplet spectrometer, and automatic weather station, etc. Formed through radiative cooling, the surface fog layer was followed by a cloud layer caused by low-level cold advection. The thickness of surface fog layer increased and cloud layer descended to lower altitudes in the development stage. With the influence of weak cold advection just above ground, the surface fog layer entered its burst evolution and some microphysical parameters of fog droplets increased significantly in 15 minutes, such as number concentration, liquid water content, mean and maximum diameter. The rising surface fog combined with descending low-level clouds to form the deep dense fog with visibility less than 15 meters, and the thickness of the combined fog layer reached 600 meters. Both the vertical momentum and downward long-wave radiation fluxes increased significantly in the beginning of the burst stage, and the net radiation fluxes approached zero at the same time. A strong surface inversion layer persisted throughout the successive stages of fog evolution because of the successive weak cold advection in the ground layer and the radiative cooling of the lower fog layer restrained by the upper fog layer.

5th International Conference on Fog, Fog Collection and Dew
Münster, Germany, 25–30 July 2010
FOGDEW2010-10

Acid fog deposition and the declining forest in Tanzawa mountains, Japan.

M. Igawa, A. Shigihara, S. Goto, and B. Nanzai

Department of Material and Life Chemistry, Kanagawa University, Kanagawa-ku, Yokohama 221-8686, Japan.
(igawam01@kanagawa-u.ac.jp)

Since 1988, we have investigated fog chemistry in Mt. Oyama, Tanzawa mountains, Japan, and acid fog has been frequently observed there. We have observed fog on Mt. Oyama by using a night view video camera placed at the base of the mountain, by using a visibility meter at the top of the mountain, and by an active fog sampler at the mountainside. We have reported the fog frequency at the top of Mt. Oyama to be 46% measured by the video camera, but it was overestimated. The visibility measured at the top of the mountain is the most reliable index, and the top of the mountain is covered with fog for about 30%. The frequency of about 15% was added for the case of the visibility of a few km when it was measured by a night view video camera placed at the base of the mountain (8.5 km far from the top). Fog-water deposition increases with the increasing altitude to be much larger than the rain-water deposition. The factors affecting on the occult precipitation intensity were investigated by the simultaneous measurement of the rainfall intensity under a canopy, the wind speed and direction, and the visibility at the top of the mountain. Air pollution has been improved recently in Japan, but acid fog is not improved and has been affecting the leaves of the trees. In Tanzawa mountains, many fir trees and beech trees are declining, while cedar trees show no decline symptoms. We have investigated the effect of acid fog on the trees of these species by exposing simulated acid fog on the seedlings of the species. Seedlings of fir and beech are much damaged by the long term exposure of pH 3 fog, while cedar seedlings are not affected by the acid fog. By the exposure of simulated acid fog, the epicuticle wax is eroded at first, then the cross linking polycation between sugar chains of cell wall is ion-exchanged with proton and the cell wall is swollen, and the membrane calcium is desorbed from the membrane, which lowers the tolerance of the trees to the climate change. Fir and beech trees in Tanzawa mountains are damaged by acid fog, although ozone also affects them additively.

5th International Conference on Fog, Fog Collection and Dew
Münster, Germany, 25–30 July 2010
FOGDEW2010-11

Synthetic roving: A numerical technique to estimate fog water dripping below the canopy

C.M. Regalado and A. Ritter
Instituto Canario de Investigaciones Agrarias (ICIA), Apdo. 60 La Laguna, 38200 Tenerife, Spain

Oppositely to the fixed arrangement of gauges, the 'roving' technique consists on the regular random relocation of gauges among different positions below the canopy. By doing so the area over which water dripping below the canopy is integrated increases. Also extreme throughfall values are average out. Thus variability of measurements and bias due to sampling of a particular canopy fraction are reduced. These issues may be particularly relevant when dealing with fog water dripping because of the low amounts of water that have to be measured. Consequently the roving technique may be considered a more accurate and precise method to measure horizontal precipitation. However such superiority claims of the roving versus the fixed technique are restricted to particular field experiments, which cannot take into account all possible spatial combinations of gauges. By synthetic roving we refer to a numerical algorithm whereby a representative number of computer-generated random iterations, reproduce possible combinations of moving gauges via Monte Carlo simulations. This permitted us to investigate suitable statistics of both the fixed and synthetic roving arrangements, such as mean dispersion or bounds of the coefficient of variability. The method is illustrated via a case study from throughfall measurements carried out with a set of 22 fixed gauges, placed below a subtropical cloud forest in the Garajonay National Park (La Gomera, Spain) during an eight-month period.

5th International Conference on Fog, Fog Collection and Dew
Münster, Germany, 25–30 July 2010
FOGDEW2010-12

Parameter estimation for a detailed atmosphere-soil-vegetation model including fog deposition onto vegetation (SOLVEG) by inverse optimization

A. Ritter (1), G. Katata (2), C.M. Regalado (1), and H. Nagai (2)

(1) ICIA, Suelos y Riegos, Valle de Guerra, Spain (aritter@icia.es, +34 922 476303), (2) Japan Atomic Energy Agency. 2-4 Shirakata-shirane, Tokai Ibaraki 319-1195 Japan

SOLVEG is a one-dimensional multilayer atmosphere-soil-vegetation model including fog deposition onto vegetation. However the complexity of the processes described by SOLVEG involves the use of many parameters not always readily available. We describe how an inverse parameter estimation algorithm, based on the Global Multilevel Coordinate Search (GMCS), coupled to SOLVEG can be used to determine model parameters. Focusing on the soil hydraulic parameters, which typically suffer from large uncertainty, we applied this inverse GMCS procedure to optimize such parameters from top soil water content time series measured in a laurel cloud forest of the Garajonay National Park (Canary Islands, Spain).

5th International Conference on Fog, Fog Collection and Dew
Münster, Germany, 25–30 July 2010
FOGDEW2010-13

Fog-Water Chemicals and PAHs in PM10 of Foggy Days in Nanjing

S.X Fan (1), X.Z. Yang (1), H.L. Huang (1), T. Fan (2), and H.S. Li (1)

(1) School of Atmospheric Physics, Nanjing university information science & technology, Nanjing,210044, China , (2) Ningxia Environmental Monitoring Center, Yinchuan,750021, China

Fog water samples during six heavy fog events were collected at Nanjing University of Information Science and Technology (NUIST) during 15 November 2007 to 31 December 2007. Five kinds of water-soluble anion and fourteen kinds of metal element concentration were detected by the ion chromatograph and the plasma emission spectrometer. The results showed that the pH values ranged from 4.64 to 6.88 among these fog water samples. The average SO42- anion concentration (2864.9μmol•L-1) was the highest in fog water, followed by Cl-(1584.4μmol•L-1) and NO3-(736.0μmol•L-1). The average concentration of heavy metal elements Cu, Ni, Pb, Cd and Cr were 2.30,1.46,0.42,0.41and 0.37μmol•L-1 respectively while the Ca, K, Na, Mg, Al and Zn concentration with big value. The concentration of metal elements in fog water was high at the initial fog stage, then decreased with the fog development, whereas increased significantly after sunrise during traffic peak period. Obvious diurnal variation of NO2- was manifested as higher value at the night while very low or disappearing after sunrise. The average pH of fog water(6.20) was higher than rain water(4.91), but the conductivity of fog water was 10.5 times higher than that of rain water. The concentration of heavy metal elements(Cd,Cr,Ni,Cu and Pb) and water-soluble anions(SO42-,NO3-,Cl-) in fog water was far higher than rain water.

Based on meteorological data and aerosol samples from Nov.15 to Dce.30,2007 in the north suburb of Nanjing, size distribution characteristics of polycyclic aromatic hydrocarbons (PAHs) in PM10 in foggy and sunny days were studied, and the concentrations of 16 PAHs were analyzed by gas chromatography with mass selective detection (GC-MS).The average concentrations of aerosols in the night (PM2.1:120.34μg•m-3; PM9.0:215.92μg•m-3) are close to those in the daytime (PM2.1:126.76μg•m-3; PM9.0:213.41μg•m-3) in fog days. The average concentrations of aerosols are higher in the night (PM2.1:71.45μg•m-3; PM9.0:114.33μg•m-3) than those in the daytime (PM2.1:41.02μg•m-3; PM9.0:74.38μg•m-3) in fine days. And we also find that the total concentrations of 16 PAHs in PM2.1 (49.97ng•m-3) and PM9.0 (59.45ng•m-3) in foggy days are 1.50 and 1.46 times of those (PM2.1:33.30ng•m-3; PM9.0:40.80ng•m-3) in sunny days separately. The average maximum concentrations of individual PAHs are fluoranthene, which are higher (PM2.1:7.98ng•m-3;PM9.0:9.99ng•m-3) in foggy days than those (PM2.1:5.23ng•m-3;PM9.0:6.77ng•m-3)in fine days, and the average concentrations of benzo-a-pyrene are higher in fog days (PM2.1:1.77ng•m-3;PM9.0:1.99ng•m-3) than those in sunny days (PM2.1:1.46μg•m-3; PM9.0:1.84ng•m-3).

5th International Conference on Fog, Fog Collection and Dew
Münster, Germany, 25–30 July 2010
FOGDEW2010-14

Bowen's signal is not present in Czech fog series

L. Hejkrlik and R. Tolasz
Czech Hydrometeorological Institute, Prague, Czech Republic (hejkrlik@chmi.cz, +420 47 2706024)

In the 1960's it was demonstrated that extreme precipitation events occur more frequently on the third to fifth day after syzygies. The effect is sometimes called Bowen's signal and similar lunar or semi-lunar modulation of meteorological parameters was later found also in ozone concentrations, sunshine, thunderstorm frequencies and in global temperatures observed by polar orbiting satellites. The original explanation suggested by Bowen was the variation of ice nuclei of meteoric origin, leading to variation of precipitation. Since that time alternative mechanisms have been proposed like rotation of the Earth around Earth-Moon barycentre or light reflected by the Moon (both effects small in magnitude), tidal influence on heat redistribution on the Earth or on the waves in the atmosphere. Possible source of variation of condensations nuclei in troposphere are also galactic cosmic rays affected by solar activity and the variability of their capture efficiency as a result of lunar distortion of the Earth's magnetosphere.
Recently we tried to study the possibility that also formation of fog, which depends on the number of effective condensations nuclei, may exhibit kind of lunar variation. We examined daily data about fog occurrence at two different meteorological stations in the Czech Republic in period 1961-2008. Mountain station Lysá hora (1322 m asl) is located in North-eastern Moravia and the lowland station Doksany (158 m asl) represents the lowest parts of Bohemia. The data were analysed by method of superposition of epochs with synodic month as epoch and the date of new moon as the null day. The resulting binary matrix consisting of 595 rows and 29 columns was then sub-divided by various criteria in order to uncover possible temporal or seasonal relations. The sums of individual columns (numbers of days with fog) were the signal we examined.
No quasi-periodical semi-lunar variation was registered at both stations neither in the whole series nor in any of sub-intervals 1961-1979, 1980-2008, winter, summer, DJF, MAM, JJA, SON. This is no surprise at Lysá hora, where fog was registered even in summer in 64% of studied days (during winter it was as high as 79%) and variation coefficient of signal was merely 2.16%. Similar picture was observed at Doksany station, even though the occurrence of fog was much less, 23% in winter, 14% in summer with =18.68%. The possible conclusion is that synoptic and microclimatic effects dominate the formation of fog in so far that they mask any other physical causes.

5th International Conference on Fog, Fog Collection and Dew
Münster, Germany, 25–30 July 2010
FOGDEW2010-15

'Dew nucleation' by hygroscopic particles on leaves

J. Burkhardt (1), M. Hunsche (2), and S. Pariyar (1)

(1) University of Bonn, Crop Science and Resource Conservation, Plant Nutrition, Bonn, Germany (j.burkhardt@uni-bonn.de), (2) University of Bonn, Crop Science and Resource Conservation, Horticulture, Bonn, Germany (mhunsche@uni-bonn.de)

Theoretical explanations of dew formation usually consider a pure, plain surface and do not include any contributions of hygroscopic material present on this surface. A significant amount of hygroscopic material, however, is present on most real leaves, due to accumulated deposited aerosols, salt exudations, leached ions, or agricultural sprays. Similarly to cloud nucleation, hygroscopic material on leaves leads to a significant reduction of saturation vapor pressure and enables ‚dew nucleation', where the condensation of minute amounts of water is still too small to be visible without a microscope. This may happen at humidities far below saturation, dependent on the composition and deliquescence point of the particles; additionally plant transpiration often raises the humidity on the leaf surface.

While the amounts of water involved are not significant in terms of the energy or water balance, the ecological consequences of such condensation mechanisms on leaves may be considerable. Highly concentrated but mobile solutions are formed by the deliquescence of hygroscopic particles, which may provide important nutrients for the plant. Their chemistry differs considerably from dilute solutions. When viewed by an environmental scanning electron microscope (ESEM), oscillating humidity led to the expansion of salts even on hydrophobic leaf surfaces. This may lead to the 'hydraulic activation of stomata (HAS)', a process leading to the extension of liquid water films into the plant and subsequent transport of liquid water and solutes on the stomatal pathway, a meanwhile well-proven contradiction to previous concepts.

Apart from the nutritional aspects, hygroscopic substances on leaves will interact with plant water relations. Depending on the degree of stomatal activation, this may trigger useful hydraulic signaling or provoke deleterious wicking and reduced drought tolerance of the plant.

5th International Conference on Fog, Fog Collection and Dew
Münster, Germany, 25–30 July 2010
FOGDEW2010-16

Studies of the Fog-water Chemical Characteristics in China

D.Y. Liu (1), Z.H. Li (1), F. Yang (2), Z. Bin (1), and J. Yang (1)

(1) School of Atmospheric Physics,Nanjing University of Information Sceince & Technology, Nanjing, China (liuduanyang2001@126.com), (2) Huai An weather bureau of Jiangsu Province, Huai An 223001, China

Research of chemical characteristics of fog-water developed rapidly in China since 1980. Observation, sampling and analysis have been done in cities , on the alps and beside the sea-sides. Studies about the acidity of cloud-fog water and the source of acid fog at each place have been done. The basic characteristics of fog water chemical composition also been detected. In many compositive fog observations , there explored the related factors of fog-water chemical characteristics as well as continuous fog-water collection, and studied the primary factors which affect the concentration of the fog water chemical composition. The paper presents the primary studies of fog-water chemical characteristics in China the last 30 years. Fog –water sampling and analysis have made marked progress. the cloud-fog water chemical composition and acidity were confirmed in many cities and mountain areas. Many efficacious works have been done about the source of chemical composition. The studies shown that the cloud-fog water in many of Chinese cities and mountain areas have been acidified. Fog-water in cities was polluted with high ion concentrations and jeopardize people's health. It's very urgent to control pollutant discharge, raise the vegetation plant cover rate, and improve ecological environment. The fog chemical research should be continue in-depth and development.

5th International Conference on Fog, Fog Collection and Dew
Münster, Germany, 25–30 July 2010
FOGDEW2010-17

Numerical Simulations of Fog Events over Mexico City's Airport

F. García-García and E. S. Caetano Neto
Centro de Ciencias de la Atmósfera - Universidad Nacional Autónoma de México, Mexico City, México

Fog events in the Mexico Basin, where Mexico City's International Airport (AICM) is located, are not very frequent. However, when present, fog affects air-transport operations and, consequently, has important economic impacts because the AICM is the major airport in the country. Climatological data indicate that fog days in the region reach annual average local maxima of up to 7 fog-days per month, but the monthly maxima in the summer and early fall amount to up to 12 fog-days per month. These frequencies of occurrence are related to seasonal atmospheric conditions in the area. In winter, when fog events are more persistent and take longer to dissipate, local terrain and land use features, as well as the presence of nearby small water bodies, modify and reinforce mesoscale circulation systems with suitable conditions for the development of fog. On the other hand, during the rainy season - summer and early fall -, the atmospheric characteristics are modified by the enhancement of air and soil humidity due to rainfall.

In this work, the results obtained from numerical simulations of fog events under different seasonal conditions carried out for the Mexico Basin are reported. The Weather Research and Forecasting (WRF) Model was used as a diagnostic tool for historical fog events in Mexico City's International Airport that occurred both in winter and summer. WRF simulations agreed well with the observed temperature and specific humidity, and reproduced the occurrence of relatively thick fog events. The temperature inversion layer near the surface that develops overnight, the stable air stratification and the weak winds in the region, are found to be the main mechanisms for the formation, developing and dissipation of fog.

5th International Conference on Fog, Fog Collection and Dew
Münster, Germany, 25–30 July 2010
FOGDEW2010-18

Ozone suppression by dew formation

N. Takenaka, W Shimazaki, Y Sadanaga, and H Bandow

Graduate School of Engineering, Osaka Prefecture University, 1-1 Gakuen-cho, Naka-ku, Sakai-shi, Osaka, 599-8531, Japan
(takenaka@chem.osakafu-u.ac.jp / (+81)72-254-9322)

Dew forms in the night and absorbs water-soluble gaseous substances near the ground surface. Some of the water-soluble gaseous substances, such as nitrous acid and formaldehyde, affect ozone buildup after the sunrise. These gaseous compounds are decomposed by sun light to produce OH radicals. OH radicals affect ozone concentrations. If these gaseous compounds are absorbed in the water droplets such as dew, fog or surface water, and if these compounds in the aqueous phase are decomposed before release into the atmosphere by drying, ozone concentration could be suppressed. We investigated the effect of dew on the ozone buildup by using real air sample. The ambient air was sucking by a pump and divided into two lines. The air in the one line was passed above water droplets and was introduced in a UV transmitting Teflon bag, and the air in the another line was introduced directly into the other Teflon bag without passing through water droplets. Two bags were placed outside and natural sun light was irradiated. After several hours of irradiation, ozone concentrations in two bags were measured. As a result, we found that the ozone production was depressed in the air passing through the water droplets compared to the air which did not pass through water droplets. This could be due to the removals of nitrous acid and formaldehyde by water droplets. The next questions are which compound of nitrous acid and formaldehyde is more effective on the ozone suppression, and is there any other water-soluble compounds to affect ozone concentrations. Now, we investigate the each effect on the ozone buildup, that is, only nitrous acid is removed from the ambient air by using a sodium carbonate denuder. The results will be reported in the conference. In the last conference, we reported that nitrous acid was decomposed when dew dries. However, the fate of formaldehyde in the dew has not been clarified. Therefore, the above results give us some information of the fate of formaldehyde. In the presentation, we will report the effect of dew formation on the ozone concentration by using experimental results, monitoring results and calculation results by a BOX model.

5th International Conference on Fog, Fog Collection and Dew
Münster, Germany, 25–30 July 2010
FOGDEW2010-19

Effects of Chinese Urban Development on the Fog

Z.H. Li (1), J. Yang (1), C.E. Shi (2), M.J. Pu (3), and D.Y. Liu (1)

(1) School of Atmospheric Physics, Nanjing University of Information Sceince & Technology, Nanjing, China (liuduanyang2001@163.com), (2) Anhui Institute of Meteorological Science, Hefei , 230061, China, (3) Meteorological Bureau of Jiangsu Province, Nanjing, 210009, China

Since China adopted the reform and opening-up policy in late 1978, the national economy as well as urbanization have developed rapidly, causing urban growth and population growth. In consequence, the urban heat islands strengthen and air pollution increase but the vegetation cover decreases, leading to the relative humidity decreases. These changes led directly to the city's foggy day reduction, fog liquid water content (LWC) and droplet-scale decreases, droplet number concentration increases, visibility degradation sharply in fog, fog-ion concentration and acidity larger, which increase the traffic hazard and endanger human health seriously. In this paper, a large number of observations and numerical simulations have been done to demonstrate these conclusions. Suggestions that air pollution controlling, virescence and improving the urban ecological environment was given at the end of the particle.

5th International Conference on Fog, Fog Collection and Dew
Münster, Germany, 25–30 July 2010
FOGDEW2010-20-2

The basic properties of non-local parametrization of a turbulent exchange

V.M. Voloshchuk (1), S.G. Boychenko (2), and I.V. Voloshchuk (3)

(1) Ukrainian Hydrometeorological Research Institute, Kyev, Ukraine (klimat@mail.univ.kiev.ua, 38 044 2656555), (2) Institute of geophysics NAS of Ukraine., Kyev, Ukraine (uaclimate@gmail.com, 38 044 4502520), (3) Presidential University of the Inter-Regional Academy of Personnel Management Kyev, Ukraine (wenqeer@gmail.com, 38 044 490-95-00)

At mathematical modeling of the dispersion of gas-aerosol impurity is used basically local parameterization of a turbulent exchange. In this case is supposed, that of a turbulent diffusion flow is proportional to a gradient of defunding substances concentration (n). This assumption is applicable only then when the characteristic size (l) of inhomogeneities of n essentially exceeds the characteristic size L of turbulent "moles". However, at solution of various applied problems rather frequently meet situations, when $l \leq L$. It is natural, that in this case parameterization of a turbulent exchange should have non-local character.

In this research one of possible scheme of non-local parameterizations of a turbulent exchange for situations, when $l \sim L$, is supposed and proved. This scheme is based on idea of representation of a turbulent flow **j** as Fredholm's convolution of function n and the function K, describing intensity of turbulent fluctuation of environment, namely

$$\mathbf{j} = -\operatorname{grad} \int K(\mathbf{r} - - \xi) \cdot n(\xi)\, dV,$$

where V is a volume of dispersion of a gas-aerosol impurity, $\mathbf{r} \in V$, $\xi \in V$, integrating carried out on a variable ξ, grad is the linear differential vector-operator (gradient) influencing on a variable **r** (other representation grad=$\partial/\partial\mathbf{r}$), the function K is a non-local analogue of coefficient of diffusion (this function at $L/l \to 0$ turn to Dirac's delta-function).

The problems for which it is possible to receive the analytical solution of the equation of diffusion with the supposed non-local parameterizations of a turbulent exchange are formulated. The solutions of these problems are based on an opportunity of application of Fourier's transformation of the equation of diffusion.

The analysis of these solutions is carried out with the purpose of an establishment what new features during a turbulent exchange appear at their mathematical modeling with the help of non-local parameterizations. It is proved, that for a situation $l \leq L$ the adequate mathematical modeling of a turbulent exchange possible only in view its non-local character.

5th International Conference on Fog, Fog Collection and Dew
Münster, Germany, 25–30 July 2010
FOGDEW2010-22

Study on the Fog Weather Process and Ionic Species Concentration Variation of The Fog Water in Beijing

Jiang Yuhua[1 3], Wang Qiang[2], Xu Xiaobin[1], Wang Zhengxing[2]

(1, CMA, Chinese Academy of Meteorological Sciences, China Beijing,100081；2, CMA, Training Centre, China Beijing,100081； 3, Chongqing Municipal Meteorological Bureau, China Chongqing, 401147

Abstract： To study the heavy fog formation mechanism as well as the urban fog pollution in Beijing, a heavy fog with horizontal visibility under 100 meters was observed in the Beijing Observatory which locates in the south suburb (39°56′N ， 116°17′E) during 11 to 12 Dec. 2006.The synoptic system and fog water ionic species concentration are analyzed. It has demonstrated that the observed fog process is an advection-radiation fog with a deep layer more than 150 meters and a low visibility less than 100 meters. The formation and development stage of the heavy fog event accompany with an air pollution index Ⅴ(API Ⅴ). Comparing with 1999 Beijing's fog water sample, the PH rises, electric conductivity rate descents, the anion's concentration has decreased generally, but the cation's risen. The chemistrical composition, ion component and concentration of the fog water has improved obviously. Studies have shown that Beijing's city government has taken measures to reduce the heavy fog's frequency and fog water's pollution in recent years.

Keywords: Beijing urban Heavy fog, Advection-radiation fog, Ionic species concentration of the fog water

5th International Conference on Fog, Fog Collection and Dew
Münster, Germany, 25–30 July 2010
FOGDEW2010-23-2

Numerical study of fog deposition onto a mountainous forest using atmosphere, aerosol chemical transport and land surface models: Chemical and physical properties of fog and aerosols

M. Kajino (1), G. Katata (2), T. Hiraki (3), M. Aikawa (3), and T. Kobayashi (3)

(1) Research Center for Advanced Science and Technology, University of Tokyo, Tokyo, Japan (kajino@atmos.rcast.u-tokyo.ac.jp), (2) Japan Atomic Energy Agency, Ibaraki, Japan, (3) Hyogo Prefectural Institute of Environmental Sciences, Hyogo, Japan

In order to predict water and matter deposition to forests, accurate estimation of chemical and physical properties of fog and aerosols are indispensable. We have developed a new aerosol chemical transport model (EMTACS) coupled with a meteorological model (WRF) and applied it to investigate uplift fog events occurred over a mountainous forest (Mt. Rokko, Japan). The EMTACS model is unique to dynamically solve temporal evolutions of mixing states of fog and aerosols, in addition to their chemical compositions and size distributions, and thus aerosol-fog interaction processes are considered in one coherent framework. The model performance was evaluated using meteorological and chemical observation data. Formation, evolution and acidification processes of fog and aerosols over the forest region were discussed.

5th International Conference on Fog, Fog Collection and Dew
Münster, Germany, 25–30 July 2010
FOGDEW2010-24

Physical and chemical properties of dew and rain water in the Dalmatian coast, Croatia

D. Beysens (1,2,3,4), I. Lekouch (2,3,4,5), M. Muselli (4,6), M. Mileta (4,7),
I. Milimouk-Melnytchouk (2,3,4,8), V. Šojat (7)

(1) Service des Basses Températures, CEA-Grenoble, France, (2) Ecole Supérieure de Physique et Chimie Industrielles, Paris Tech, France, (3) Université P. & M. Curie, Paris, France, (4) OPUR International, Paris, France, (5) Université Ibn Zohr, Agadir, Morocco, France, (6) Université de Corse, Ajaccio, France, (7) Meteorological and Hydrological Institute of Zagreb, Croatia, (8) Arcofluid, Pessac, France (daniel.beysens@espci.fr / Fax: +33-140795806)

Abstract

The possibility to use dew water as a supplementary source of water is evaluated in the Mediterranean Dalmatian coast and islands of Croatia, with emphasis on the dry summer season. Two sites were chosen, an exposed open site on the coast favourable to dew formation (Zadar) and a less favourable site in a cirque of mountains in Komiža (Vis Island). Between July 1, 2003 to October 31, 2006, dew was collected together with standard meteorological data. The mean yearly cumulative yields were 20 mm (Zadar) and 9.3 mm (Komiža). During the dry season (May to October), monthly cumulative dew water yield can represent up to 38% of water collected by rainfall.
The chemical properties of dew and rain water were analyzed during three years (2004 – 2006) in Zadar. The mean pH and electrical conductivity (EC) values were comparable for dew and rain water, pH ≈ 7 and EC ≈ 180 µS cm^{-1}, corresponding to low mineralization. The dew and rain water are in conformity with the World Health Organization directives for potability, except for Mg^{2+}.

1. Introduction

Dew water is the result of atmospheric vapour condensing on a substrate that has cooled down because of a radiation deficit. When the relative humidity (RH) of ambient air is high enough, typically RH > 70%, radiative cooling can allow the substrate to fall below the dew point temperature and counterbalance the latent heat of condensation. Dew water yield is limited by the available cooling energy, in the order of 25 – 150 Wm^{-2} [1-2] and the yield cannot exceed ~ 1 mm day^{-1}. In this paper we characterize the chemical properties of dew water versus rainwater in the Dalmatian area and assess to what extent dew water is potable. A three-year study was carried out from 2004 to 2006 in Zadar (Croatia). The measurement period had 408 dew events (36.3% in 2004, 37.4% in 2005 and 37.9% in 2006 and 312 rain events (34.7% in 2004, 30.8% in 2005 and 20.1% in 2006).
The first measurement site is located at the meteorological station of the Hydrometeorological Institute in Zadar (Croatia), at latitude 44°08' N and longitude 15°13' E, 5 m a.s.l., on the Adriatic coast, north of Zadar, on a peninsula at about 10 m from the sea. The direction of the dominant winds during the night is NE. Windspeed is measured at 10 m elevation.
The second site is in Vis Island at Komiža (43°03' N, 16°06' E, at 20 m a.s.l). It is a town and harbour at the foot of the Hum peak (587 m) on the western coast of the island. The city is situated in the centre of a mountainous cirque open to the sea to the SW. The Vis Island is about 140 km away from Zadar. The annual mean rainfall is 817 mm (mean computed between 2003-2005) and very erratic: the annual coefficient of variation is 65%. Because of the situation, this site is representative of a poor location for implementing dew collection; the dew yields will thus be considered as a minimum in the area.
Dew was collected on condensers of 1 m x 1 m inclined at a 30° angle from horizontal coated with OPUR condensing foil. Dew quantities were collected and its volume V measured daily in the morning, corresponding to water collected by gravity flow in a polyethylene bottle. The remaining dew drops were scraped from the surface. Classical meteo parameters were also recorded. Frost was excluded from the dataset.
The dew and rain samples were sent to the chemical laboratory in Zagreb every two weeks and in the interim the samples were stored in a refrigerator at 3°C. The following determinations

were performed (i) physico-chemical properties: pH, conductivity EC. (ii) chemical concentration; cations: NH_4^+, Na^+, K^+, Ca^{2+}, Mg^{2+}, anions: HCO_3^-, Cl^-, SO_4^{2-}, NO_3^-..

2. Dew yields

The dew yield data are shown in Fig. 1 (evolution) and the statistics are summarized in Table 1. Zadar had 408 dew days with a mean cumulative yearly dew yield of about 20 mm. The daily dew yields rarely exceeded 0.4 mm.

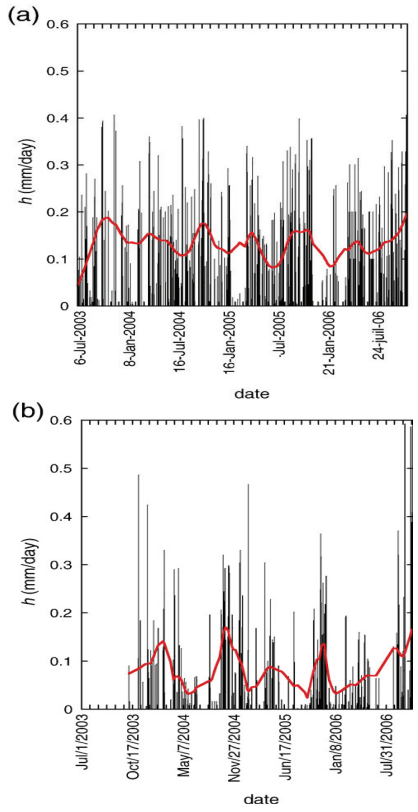

Figure 1 Dew yields *h* (mm/day) evolution for both experimental sites. The curves correspond to 10% data weighting. (a) : Zadar, (b) : Komiža.

.

3. Physico-chemical analysis

The statistical and physico-chemical analysis of the elements characteristic of dew and rain water shows that dew and rainwater are of alkaline nature. In both rain and dew water the mean average conductivity is low, EC ≈ 200 µS cm^{-1}, corresponding to low total mineralization ≈ 0.77 EC =150 mg L^{-1} (dew and rain).
The concentration of the various ions shows that the sum of the cations (Σcations) is higher than the sum of the anions (Σanions). Some anions were thus missing in the measurements, in agreement with the fact that the total measured mineralization is in the order of 85 mg L^{-1}, as compared with the above estimation of 150 mg L^{-1} from the conductivity.

Table 1: Various physico-chemical properties of rain water between 2004 and 2006

Dew: 408 events between 2004 and 2006

	2004 134 days (36.3%)			2005 136 days (37.4%)			2006 138 days (37.9%)		
Measurements	**Mean**	**Min**	**Max**	**Mean**	**Min**	**Max**	**Mean**	**Min**	**Max**
pH	6.93	5.69	7.78	6.62	5.45	7.78	6.58	5.53	7.57
EC (µS cm^{-1})	216.48	41	1117	195.66	23	1861	174.31	19	719
Ca^{2+} (mEq L^{-1})	2.11	0.08	9.7	1.79	0.17	7.49	1.25	0.12	6.7
Na^+ (mEq L^{-1})	0.42	0.00087	10.55	0.22	0.025	0.99	0.3	0.03	1.64
Mg^{++} (mEq L^{-1})	0.35	0.0016	14.52	0.14	0.014	0.56	0.2	0.002	2.66
K^+ (mEq L^{-1})	0.054	0.0019	1.25	0.073	0.004	1.16	0.05	0.004	0.26
NH_4^+ (mEq L^{-1})	0.036	0	0.18	0.017	0	0.026	0.1	0	1.4
H^+ (mEq L^{-1})	0.0002	$<10^{-4}$	0.002	0.0004	$<10^{-4}$	0.0035	0.0004	$<10^{-4}$	0.003
Cl (mEq L^{-1})	1.35	0.025	73.8	0.27	0.042	1.22	0.35	0.049	1.6
SO_4^{2-} (mEq L^{-1})	0.11	0	2.34	0.066	0.0091	0.25	0.07	0.013	0.45
NO_3^- (mEq L^{-1})	0.015	0	0.092	0.0093	0	0.062	0.01	0	0.1
HCO_3^- (mEq L^{-1})	0.0065	0.0025	0.31	0.038	0.0014	0.31	0.032	0.001	0.19

Rain: 312 events between 2004 and 2006

	2004 127 days (34.7%)			2005 112 days (30.8%)			2006 73 days (20.1%)		
Measurements	**Mean**	**Min**	**Max**	**Mean**	**Min**	**Max**	**Mean**	**Min**	**Max**
pH	6.37	4.33	7.99	6.5	4.24	8.67	6.13	4.51	7.76
EC (µS cm^{-1})	182.19	8	4850	228.53	6	4980	123.6	9	2211
Na^+ (mEq L^{-1})	0.92	0.009	35.62	1.001	0.004	21.78	0.65	0.025	19.26
Ca^{2+} (mEq L^{-1})	0.52	0.024	4.71	0.83	0	12.09	0.25	0.054	1.52
Mg^{2+} (mEq L^{-1})	0.29	0	11.66	0.4	0.007	7.32	0.27	0.029	4.3
NH_4^+ (mEq L^{-1})	0.027	0	0.58	0.019	0.0001	0.15	0.021	0	0.1
K^+ (mEq L^{-1})	0.026	0.0006	0.8	0.025	0.0007	0.4	0.02	0.002	0.4
H^+ (mEq L^{-1})	0.0028	$<10^{-5}$	0.046	0.0023	0	0.057	0.0028	$<10^{-4}$	0.031
Cl (mEq L^{-1})	0.94	0.015	34.86	1.57	0.0054	44.62	0.63	0.025	20.54
SO_4^{2-} (mEq L^{-1})	0.061	0.004	1.36	0.12	0.0013	3.74	0.038	0.0003	0.72
HCO_3^- (mEq L^{-1})	0.05	0.0001	0.5	0.113	0.0001	2.4	0.026	0.0001	0.29
NO_3^- (mEq L^{-1})	0.015	0.0016	0.095	0.013	0.0004	0.12	0.012	0.0007	0.046

3.1. pH

The evolution of pH for both dew and rain is presented in Fig. 2. The dew pH ranges between 6 and 7.5, with a mean value of 6.7 and the rain pH between 5.3 and 7.3, with a mean value of 6.4. The pH of rain is on average slightly more acidic than

the dew pH, by about 0.4 pH units. This difference between dew and rain pH can be attributed to (i) differences in the atmospheric composition of aerosols and gas at high elevation (cloud) and low elevation (dew) [3-4] and (ii) the amount of time where the rain and dew droplets are exposed to the environment [5].

3.2. Electric Conductivity (EC)

The electric conductivity (EC) of dew during the sampling period ranged from 19 µS cm^{-1} to 1861 µS cm^{-1}, with a mean of 204 µS cm^{-1} and a standard deviation of 177 µS cm^{-1}. These values are comparable to the conductivity of rain whose EC values ranged from 6 µS cm^{-1} to 4980 µS cm^{-1} with a mean EC of 132 µS cm^{-1} and a standard deviation of 214 µS cm^{-1}.

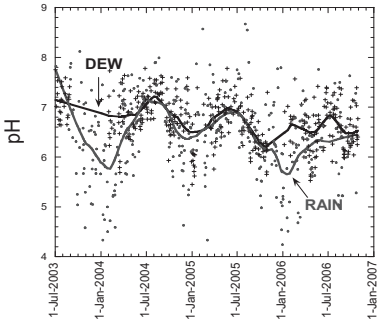

Figure 2: pH evolution for 2004 – 2006 of dew (black crosses and black curve) and rain (gray circles and gray curve). The curves are weighting functions (15% of data).

The mean values are somewhat smaller than the standard value (400 µS cm^{-1} at 20°C) for potable water as requested by the European Commission [6].

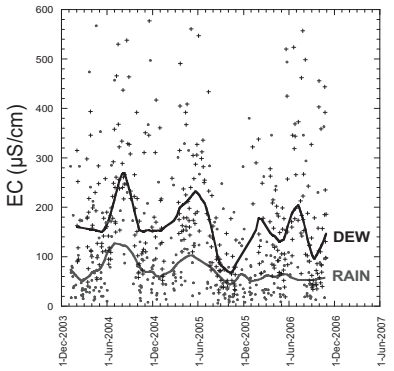

Figure 3: Evolution of dew (black crosses and black curve) and rain (gray circles and gray curve) electric conductivity. The curves are weighting functions (15% of data).

3.3. Ionic concentration

The average ionic concentrations (in mEq L^{-1}) of the major chemical species as obtained from the dew and rainwater analyses for three years are presented in Fig. 4. In dew water, the cations concentrate in different ways:
years 2004, 2005: $Ca^{2+} > Na^{+} > Mg^{2+} > K^{+} > NH_4^{+}$
year 2006: $Ca^{2+} > Na^{+} > Mg^{2+} > NH_4^{+} > K^{+}$.
The concentration of anions follows the same evolution, with $Cl^{-} > SO_4^{2-} > HCO_3^{-} > NO_3^{-}$, except in 2006 where $NO_3^{-} > HCO_3^{-}$. Concerning rainwater, the concentration of ions is different from what was observed in dew. For cations, one observes:
year 2004: $Na^{+} > Ca^{2+} > Mg^{2+} > NH_4^{+} > K^{+}$
year 2005: $Na^{+} > Ca^{2+} > Mg^{2+} > K^{+} > NH_4^{+}$
year 2006: $Na^{+} > Mg^{2+} > Ca^{2+} > K^{+} > NH_4^{+}$
In contrast, the anions evolve/move in the same way throughout the study period, $Cl^{-} > SO_4^{-} > HCO_3^{-} > NO_3^{-}$.

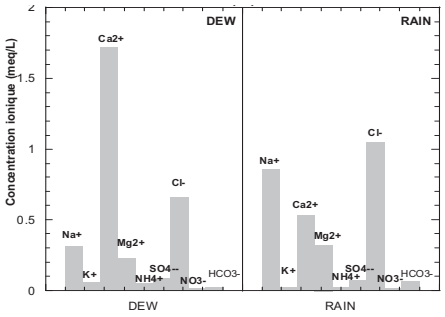

Figure 4: Mean concentration values (mEq L^{-1}) of different ions in dew and rain for 2004-2006

4. Sea contribution

In order to estimate the contribution of the different ions, the sea-salt fraction (SSF) was calculated. The other species are expressed to be as the no sea origin (no sea-salt fraction, NSSF).
The totality of Na^+ considered of sea origin is the principal reference of the calculation as well as the ionic concentration of sea water. The parameters SSF and NSSF are described by:

$$\%(SSF)_X = 100 \times \frac{(Na)(X_{sea} / Na_{sea})}{X} \quad (1)$$

Here X is the dew and rain ion concentration, X_{sea} is the concentration of ion in bulk seawater, and Na_{sea} the concentration of the Na reference ion in bulk seawater. The excess or non sea-salt fraction $NSSF_X$, is defined as (concentrations in $mEqL^{-1}$):

$$\%(NSSF)_X = 100 - \%(SSF)_X \quad (2)$$

The results presented in Table 2 show that the ratios SO_4^{2-}/ Na^+, Ca^{2+}/ Na^+, K^+/ Na^+ and NO_3^-/ Na^+ in dew were found to be higher than those in seawater. The large values in dew indicate a contribution from crustal and anthropogenic sources. The high ratios of Ca^{2+}, K^+, SO_4^{2-} and NO_3^- with Na^+ suggest a non-marine origin of these components. The values of SSF% and NSSF% support this observation. Approximately 99% of Ca^{2+}, 88% of K^+, 84% of SO_4^{2-} and 99% of NO_3^- in dew samples originate from non-marine sources. Mg^{2+} concentration in dew water is generally affected by both dust and sea-salt particles in the atmosphere, as well as the Cl^- ions (%SSF = 54%). In contrast, in rainwater the high NSSF of Ca^{2+} and NO_3^- indicates that they are not influenced by the sea, whereas the other ions show a strong sea contribution. The high contribution of Cl^- (95%) especially corresponds to sea-salt particles in the atmosphere (Table 2).

Table 2: Comparison of the ratio $\%(SSF)_X$ and $\%(NSSF)_X$ for dew, rain and sea water

Ions	Sea water ratio	Dew ratio	Rain ratio	Dew %SSF	Dew %NSSF	Rain %SSF	Rain %NSSF
Ca^{2+} (mEq L^{-1})	0.044	5.548	0.616	0.793	99.206	7.1396	92.860
Mg^{2+} (mEq L^{-1})	0.227	0.741	0.372	30.595	69.404	61.006	38.994
K^+ (mEq L^{-1})	0.022	0.190	0.0279	11.559	88.440	78.833	21.167
Cl^- (mEq L^{-1})	1.166	2.129	1.220	54.766	45.233	95.501	4.499
SO_4^{2-} (mEq L^{-1})	0.040	0.264	0.084	15.121	84.878	47.123	52.877
NO_3^- (mEq L^{-1})	0.00002	0.035	0.015	0.056	99.943	0.132	99.868

5. Conclusion

In the Mediterranean Dalmatian area, both dew and rain water generally meet the WHO requirements for potable water (except for Mg^{2+}). Passive dew harvesting could thus serve as a useful complementary source of water when other sources are lacking. The two sites investigated here provide an overview of the range of dew water production that can be obtained from an unfavorable site (Komiža, 9.3 mm/y) and a more favorable one (Zadar, 20 mm/y). In the summer dry season (May – October), the monthly contribution of dew water compared to rainfall is on order of 38% (July 2004) and has reached 120% (summers 2003 and 2006). Refurbishing abandoned traditional rain collectors (impluviums), which are numerous in the Dalmatian area, would be a viable option to collect rain and dew water.

References

1]. Garratt, J.R., Segal, M. On the contribution of atmospheric moisture to dew formation. Boundary-Layer Meteorol 45, 209–236, 1988

[2]. Nikolayev, V., Beysens, D., Gioda, A., Milimouk, I., Katiushin, E., Morel, J.P. Water recovery from dew. J. Hydrology 182, 19-35, 1996

[3]. Wagner, G., Steele, K., Peden, M. Dew and frost chemistry at a midcontinental site, United States. J. Geophys. Res. 97, 20591–20597, 1992

[4]. Jiries, A. Chemical composition of dew in Amman. Atmospheric Research 37,261-268, 2001

[5]. Beysens, D., Ohayon, C. Muselli, M., Clus, O. Chemical and biological characteristics of dew and rain water in an urban coastal area (Bordeaux, France). Atm. Environment 40, 3710-3723, 2006

[6]. Rodier, J. L'analyse de L'eau: Eaux Naturelles, Eaux Résiduaires, Eau de Mer. 8e édition. Dunod, Paris. 1365p, 1996

5th International Conference on Fog, Fog Collection and Dew
Münster, Germany, 25–30 July 2010
FOGDEW2010-26

Numerical study of fog deposition onto a mountainous forest using atmosphere, aerosol chemical transport, and land surface models: Estimation of water and matter deposition by fog deposition

G. Katata (1), M. Kajino (2), T. Hiraki (3), M. Aikawa (3), T. Kobayashi (3), and H. Nagai (1)

(1) Japan Atomic Energy Agency, Ibaraki, Japan (katata.genki@jaea.go.jp), (2) Research Center for Advanced Science and Technology, University of Tokyo, Tokyo, Japan, (3) Hyogo Prefectural Institute of Environmental Sciences, Hyogo, Japan

Water and matter input via fog deposition onto a mountainous forest (Mt. Rokko, Japan) was investigated using detailed land surface model that includes fog deposition onto vegetation (SOLVEG). Simulations using SOLVEG were carried out under meteorological and chemical fields produced by off-line coupled meso-scale meteorological/aerosol chemical transport model (WRF/EMTACS). The SOLVEG clearly underestimated the cumulative fog deposition calculated from throughfall data. This suggests that an enhancement of fog deposition by 'edge effect' which is the phenomenon that fog droplets introduced from the side are captured by leaves due to the canopy clustering and inhomogeneity. The matter deposition of atmospheric pollutants onto the forest floor due to fog deposition was estimated from the fog deposition by SOLVEG and chemical concentrations in fog water predicted by WRF/EMTACS.

5th International Conference on Fog, Fog Collection and Dew
Münster, Germany, 25–30 July 2010
FOGDEW2010-27

Influence of temporal variations and climatic conditions on the physical and chemical characteristics of dew and rain in South-West Morocco

I. Lekouch (1,2,3,4), B. Kabbachi (3), I. Milimouk-Melnytchouk (1,2,4,5), M. Muselli (4, 6), **D. Beysens** (1,2,4,7)

(1) Ecole Supérieure de Physique et Chimie Industrielles Paris Tech, France, (2) Université P. & M. Curie, Paris, France, (3) Universite Ibn Zohr, Agadir, Morocco, (4) OPUR International, Paris, France, (5) Arcofluid, Pessac, France, (6) Université de Corse, Ajaccio, France, (7) Service des Basses Températures, CEA-Grenoble, France (daniel.beysens@espci.fr / Fax: +33-140795806)

Abstract

The physical, physico-chemical and biological characteristics of rain, fog and dew water were investigated at Mirleft in the arid coastal environment of south-west Morocco for potential use as supplementary water. The study was carried out between May 1, 2007 and Avril 30, 2008 using 4 passive dew condensers and a passive fog net collector, each with 1 m² surfaces. Collecting dew increased almost 40% the water yield although fog contributes to only 3%. Dew and rain pH were neutral and the total mineralization was considerable (dew: 560 mg/L; rain: 230 mg/L). The ions concentration agrees with the World Health Organization requirements for potable water. The biological analysis shows harmless vegetal spores and little contamination by animal/human bacteria.

1. Introduction

The application of radiative cooling during the nocturnal cycle to condense water from atmospheric vapor [1] can provide relevant solutions for arid or semi-arid countries to collect water by using a natural physical phenomenon. Radiative cooling, during the day, also limits heat in buildings.
The town of Mirleft, located in a semi-arid region in south-western Morocco (43 m asl, 29° 35' N, 10° 02' W) is characterized by low average annual rainfall (215 mm) with less than 22 rainy days per year. To face the conventional water shortage and rising water prices, the use of alternative sources of water, like dew and fog, can be envisaged. The present study aims to determine the extent to which dew and fog water can supplement or augment rainfall collection in Mirleft and whether such water is potable.

2. Measurement procedure

Four plane dew condensers (1 m²), tilted 30° from horizontal to maximize dew drop gravity flow [2], were installed on a rooftop in Mirleft as illustrated in Fig. 1a.

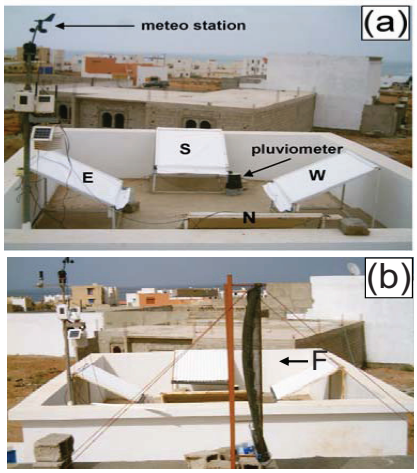

Figure 1: Measurement site located on a 3.5 m high terrace. (a) Meteorological station and 4 condensers facing north (N), east (E), south (S), west (W), with the south condenser equipped with a rain recorder. (b) Fog net collector (F) oriented east-west.

A condensing foil was used composed of material designed according to Nilsson et al. [3] (manufactured by OPUR, France, www.opur.fr). The foil is 0.35 mm thick and includes a small percentage of TiO_2 and $BaSO_4$ microspheres embedded in a matrix of low-density polyethylene (LDPE). It also contains an insoluble surfactant additive on its surface to enhance dewdrop flow. Between the foil and the condenser structure is a 2-cm thick polystyrene foam plate to provide thermal insulation. Collected water (dew and rain) by the east-, north-, west-facing condensers was measured manually every morning. Water from the south-facing condenser was recorded every 15 minutes by an automatic rain recorder. A calibration was made to properly account for the relative dew condenser/rain collecting surfaces.
In addition, a 1 m^2 fog collector oriented perpendicular to the dominant winds (east-west) was placed on a second, identical terrace within a few m from the condensers (Fig. 1b). The collector is made with two layers of polyethylene shading net (50 % transmission, ribbon width 1.7 mm).

3. Dew and rain yields

The volume corresponds to water collected through gravity flow of the drops plus the amount of the residual droplets manually scraped at the condenser surface before evaporation. During this one-year study, 178 dew events, 20 fog episodes (of which only 7 were significant) and 31 rain days were observed, corresponding to 48.8% of dew days, 2% of significant fog days and 8.5 % of rain days.

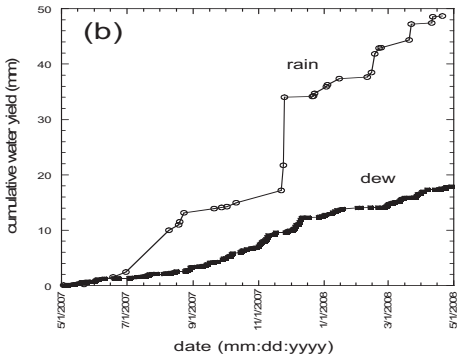

Figure 2. Cumulative dew yield (black dots, L/m^2) and rain (open circles, mm).

The cumulated amount of dew water was 18.9 mm as compared to 1.4 mm for fog water and 48.7 mm for rain water (Fig. 2). In total, the contribution of dew (and fog, although the contribution of fog is small) represents 41 % of the rain contribution and thus is significant. The dew yield was minimal in summer, in correlation with shorter night duration. The comparison of the dew yields as obtained on the 4 condensers facing north, east, south and west showed not systematic differences.

4. Physico-chemical analyses

The collection of dew and rain water was carried out from the south-facing condenser just before sunrise using sterilized polyethylene flasks. The pH and electrical conductivity (EC) measurements were performed just after water collection. Chemical and biological analyses were carried out at the National Center for Scientific and Technical Research (CNRST) in Rabat (Morocco).
The results of the analysis of the characteristic elements of dew and rain water are presented in Fig. 3. The mean dew electrical conductivity (EC) was in the order of 730 µS/cm (dew) and 316 µS/cm (rain), corresponding to a low total mineralization 0.77 EC =560 mg L^{-1} (dew) and 230 mg L^{-1} (rain). The total ions concentration averaged 534 mg L^{-1} (dew) and 287 mg L^{-1} (rain). These figures are in agreement with the EC estimation, thus showing that the chemical analysis indeed dealt with the major ions. This is also verified by the electric neutrality of cations and anions when looking at the concentrations in $mEq.L^{-1}$.

4.1 pH and EC

The dew and rain pH exhibited the same low seasonal variation, with a weak minimum during May, June, July and August (dry season). Dew pH varied between 6.75 and 7.93 and rain pH ranged between 6.49 and 7.17. Dew pH is, as usual [4], less acidic than rain because of the short time that dew is exposed to air, thus limiting the adsorption of gaseous CO_2, SO_x and NO_x. The seasonal variation of pH - lower pH when the dew yield is higher - can be explained by volume dependence.
The average values of dew and rain pH (7.4 and 6.85, respectively) are larger than the pH (5.6) of water vapour in equilibrium with atmospheric CO_2. This alkalinity is due to both the low content of sulphuric (SO_4^{2-}) and nitric (NO_3^-) acids and the large cations concentration (Ca^{2+} + Mg^{2+}) responsible for the

neutralization of these anions. The ratio (SO_4^{2-} + NO_3^-) / (Ca^{2+} + Mg^{2+}) or total acidity/total alkalinity (TA/TC), which can be regarded as an indicator of acidity, is indeed less than 1 (dew:0.4; rain:0.6).

The EC (Table 1) exhibits large fluctuations, reflecting the water mineralization variations. The dew EC ranged between 38.6 µS/cm and 2680 µS/cm, with an average value of 725 µS/cm. The rain EC varied from 14.5 µS/cm to 1081 µS/cm, with an average value of 316 µS/cm. The highest values of the dew EC were found during the dry season. Similar to the pH data, EC values decreased with increasing collected volumes, in agreement with the dissolution of particles depositing with a constant rate on the surface of the condenser. The same result was found for a study carried out in Bordeaux, France [4], Croatia [5], and in other reports concerning fog and rain in India [6,7].

Table 1: Electric conductivity (EC) (µS/cm) and total mineralization in mg/L (≈ 0.77 EC) in Mirleft as compared to other sites. (a): this study; (b): [8]; (c): [5]; (d): [9]; (e): [10]; (f) : [4].

Site	EC (µS/cm)	Total mineral (mg/L)
Mirleft (coastal, Morocco) [(a)]	725	560
Tikehau (atoll island, French Polynesia) [(b)]	580	450
Zadar (coastal, Croatia) [(c)]	204	160
Amman (near-coastal, Jordan) [(d)]	129	100
Ajaccio (island, France) [(e)]	114	88
Bordeaux (near coastal, France) [(f)]	45	35

4.2 Ionic concentrations

The mean ionic concentrations of the major chemical species obtained from the dew and rain water analyses are presented in Table 2 and Fig. 3. For both dew and rain waters, the concentration of anions are in the order $Na^+ > Ca^{2+} > Mg^{2+} > K^+$ and, for cations, $Cl^- > SO_4^{2-} > NO_3^-$. The probable source of Ca^{2+} and K^+ is from the soil, with Ca^{2+} and K^+ being suspended in the lower layer of the atmosphere and settling on the condenser surface. The presence of high concentrations of Cl^- and Na^+, and to a lesser extent Mg^{2+}, corresponds to the sea salts (the study site is within 200 m from the ocean).

Table 2. Ion concentrations for dew and rain collected from a passive dew foil condenser in Mirleft (Morocco) as compared to dew from Bordeaux (France, near the Atlantic ocean) and World Health Organization recommendations.

	Dew (Mirleft)	Rain (Mirleft)	Dew (Bordeaux)	Max WHO
pH in situ	7.4	6.85	6.26	6.5–8.5
EC (µS/cm)	725.25	316	45.1	
Ca^{2+} mg/L	48.27	32.97	1.47	
Na^+ mg/L	99.27	52.4	3.6	200
Mg^{2+} mg/L	16.19	10.81	0.36	
K^+ mg/L	9.5	5.25	0.41	
Cl^- mg/L	255.52	157.02	5.52	250
SO_4^{2-} mg/L	18.34	12.43	3.75	250
NO_3^- mg/L	14.9	11.67	2.8	50
Cu^{2+} mg/L	0.018	0.017	0.0027	2
Pb mg/L	0.005	0.006		0.01
Zn^{2+} mg/L	0.022	0.006	0.036	4
TA/TC	0.4	0.6		

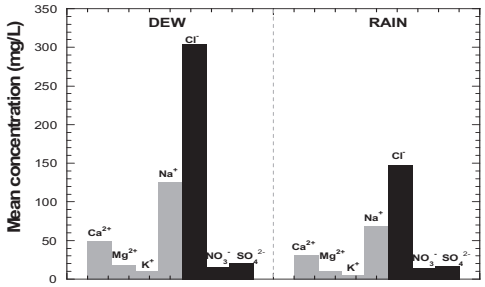

Figure 3. Mean ion concentrations for dew as compared to rain water.

The concentration of elements in dew and rain is markedly higher than in other oceanic areas such as at Bordeaux, France (see Table 2). This difference can be attributed to the strong contributions of desert particles that characterize the study area. It is noteworthy (Fig. 3) that this chemical composition is within the safety standards of the World Health Organization (WHO) for Cl^-, Mg^{2+}, and Zn.

4.4. Balance of charges

The quality of the chemical analysis can be assessed by the ion balance (sum of cations versus sum of anions). The number of charges in solution is estimated by summing the ion concentration in

mEq/L. The sum of anions and cations was well-correlated in dew and rainwater (Fig. 4) and respecting the electro-neutrality.

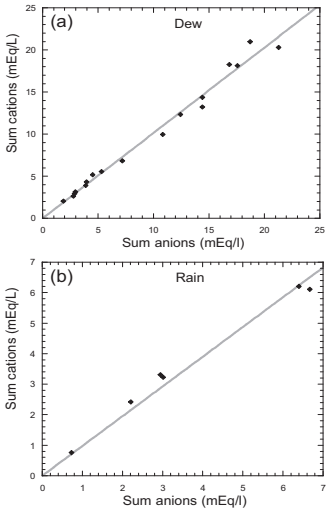

Figure 4. Correlation between total cationic and anionic charges in dew and rain water. Line: linear fit with slopes 1.01 ± 0.02 (dew) and 0.97 ± 0.03 (rain).

5. Summary and Conclusions

The annual quantity of accumulated dew corresponds to almost 40% of the yearly rain contribution. The total fog contribution remains marginal.

Dew exhibits a large mineralization, larger than rain, due to NaCl salt from marine origin and the enhanced deposition of aerosols coming from the dry, arid soil. Both dew and rain exhibit near-neutral pH. In dew are revealed the abundance of major cations Na^{+} and Mg^{2+} (marine origin), and Ca^{2+} (continental origin). The acidity from dissolved CO_2, SO_x, and NO_x is mostly neutralized by Ca^{2+}, thus giving an alkaline character to both dew and rain water.

In general, dew and rain water mean characteristics are compatible with drinking standards when compared to WHO recommendations. The small content of animal and/or vegetal bacteria makes dew water potentially drinkable after a light antibacterial treatment. Then, with little investment [11], the population of the arid and semi-arid coastal areas of south-western North Africa, characterized by high air humidity and clear skies in a wide area along the coast, could make dew water a useful supplementary potable water resource.

References

[1] Jacobs, A.F.G., Heusinkveld, B.G., Berkowicz, S.M., 2002. A simple model for potential dewfall in an arid region. Atmospheric Research Vol. 64, pp. 285–295.

[2] Beysens D, Milimouk I, Nikolayev VS, Muselli M, Marcillat J. Using radiative cooling to condense atmospheric vapour:a study to improve water yield. J of Hydrology, Vol. 276, pp. 1–11, 2003.

[3] Nilsson T. Initial experiments on dew collection in Sweden and Tanzania. Sol Energy Materials and Solar Cells;Vol.40, pp. 23-32, 1996

[4] Beysens D, Ohayon C, Muselli M, Clus O. Chemical and biological characteristics of dew and rain water in an urban coastal area (Bordeaux, France). Atmospheric Environment, vol.40, pp.3710-3723, 2006.

[5] Lekouch I, Mileta M, Muselli M, Milimouk-Melnytchouk I, Šojat V, Kabbachi B, Beysens D. Comparative chemical analysis of dew and rain water (Zadar, Croatia). , Atmospheric Research, Vol. 95, pp.224–234, 2010

[6] Ali K, Momin GA, Tiwari S, Safai PD, Chate DM, Rao PSP. Fog and precipitation chemistry at Delhi, north India. Atmospheric Environment, Vol.38, pp.4215–4222, 2004.

[7] Das R, Das SN, Misra VN. Chemical composition of rainwater and dustfall at Bhubaneswar in the east coast of India. Atmospheric Environment Vol. 39, pp.5908–5916, 2005.

[8] Clus O. Rapport d'implantation d'un condenseur de rosée sur l'atoll de Tikehau (Tuamotus, Polynesie Francaise) du 16 au 23 août 2005. Unpublished.

[9] Jiries A. Chemical composition of dew in Amman. Atmospheric Research, Vol37, pp.261-268, 2001

[10] Muselli M, Beysens D, Soyeux E. Is dew water potable? Chemical and biological analyses of dew water in Ajaccio (Corsica Island, France). J Environ Qual, Vol. 35, pp.1812-1817, 2006.

[11] Lekouch I, Kabbachi B., Milimouk-Melnytchouk I., Muselli M., Beysens D. Dew, fog, and rain as supplementary sources of water in south-western Morocco. Energy, doi:10.1016/j.energy.2010.03.017.

5th International Conference on Fog, Fog Collection and Dew
Münster, Germany, 25–30 July 2010
FOGDEW2010-28

The typical insoluble particles in fog water at Milešovka Observatory (Czech Republic)

JAROSLAV FISAK[1], VALERIA STOYANOVA[2], KRISTYNA BARTUNKOVA[1], MIROSLAV TESAR[4], ANNIE SHOUMKOVA[2]

[1] Institute of Atmospheric Physics, AS CR, v.v.i., 1404 Boční II, 141 31 Prague 4, Czech Republic, e-mail: fisak@ufa.cas.cz
[2] Institute of Physical Chemistery, Bulgarian Academy of Sciences, (IPC BAS), Sofia, Bulgaria, e-mail: valeria@ipc.bas.bg
[3] Institute of Hydrodynamics, AS CR, v.v.i., Pod Paťankou 30/5, 166 12 Prague 6, Czech Republic

Abstract:

The vicinity of Milesovka Mountain is one of the most polluted areas in the Czech Republic. In this study the input and possible sources of solid pollutants into the fog are studied. 25 sets of samples were collected in the period between August 2006 and July 2007 by different wind direction situations. Samples of fog water were filtered. Dried filters were examined by Scanning Electron Microscope. Number of particles is in the interval from 53 to 116 in every filter. Content of solid pollutants, especially elements like Al, Si, K, Fe or Ca, sizes and shapes of the particles were detected. In accordance to the content of observed elements these particles were divided into categories. After that particles in these groups were collated according to the meteorological conditions.

1. INTRODUCTION

The pollution in the atmosphere markedly influences human health and ecosystems. Formation of fog and low clouds plays a significant role in washout processes in the atmosphere. Therefore fog chemistry investigations are very important. It must be noted that some pollution in fog and low clouds is natural and the presence of condensation nuclei projects the requirement for fog and cloud genesis. It is quite necessary to examine character of the material which occurs in fog water and after that to try to determine possible sources of this pollution. It is advisable to learn how to distinguish natural and anthropogenic sources discovered in the fog samples. Identification of such sources is very complicated task.

This study is considering with the analysis of 25 samples of fog water collected at the Milešovka Mountain (837 m a.s.l.), Czech Republic. The sampling proceeded in the years 2006 and 2007 by chosen fog episodes. After that, the samples were filtered and dried filters were analyzed in the laboratory of the IPC BAS (Institute of Physical Chemistry, Bulgaria). The aim of this analysis has been to determine the typical insoluble particles in collected samples. Consequently the samples were assigned to the wind directions noticed in the day of sampling to find possible sources of detected particles. Precipitation amounts measured 24 hours before every foggy period were compared for content of particles rich in particulate element.

2. SITE OF MESUREMENT AND METHODS

The observatory Milešovka of the IAP ASCR is located on the highest mountain of České středohoří Mountains in the Czech Republic. The vicinity of this area belongs to the most polluted areas in the Republic [1] (Picture 1).

Picture 1 – Map of the biggest pollution sources (black spots) in the surroundings of Milešovka Mountain

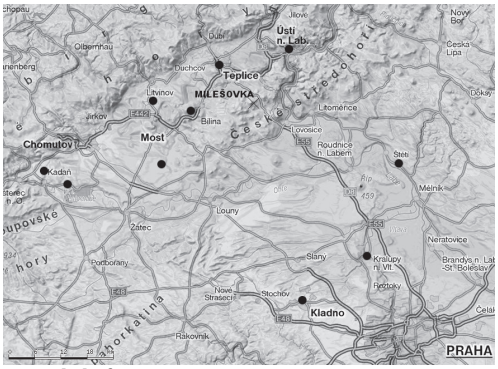

Amended after www.mapy.cz

25 fog samples were collected by the active fog water collector in the episode from August 2006 till July 2007. Nitrocellulose filters with pore sizes 0,45 µm were used to filter insoluble particles from water.

From each sample were recognized from 53 to 116 particles. Altogether that was more than 2000 particles. These filters were dried up and covered with very thin carbon coating. Each individual particle on filters was analyzed by mean of JEOL JSM 6390 scanning electron microscope. Scanning electron microscopy (SEM), coupled with Energy Dispersive X-ray Spectrometer (EDX) was used to detect parameters of the particles. In SEI mode particle's size and morphology were ascertained. BEI (backscattering) mode helped to recognize heavy metals-rich particles. EDX analysis was used to detect elemental composition of the particles [2]. Because of the necessity of covering the particles in filters by carbon layer carbon was excluded from the dataset as well as oxygen.

After getting data from analysis the statistics was made. Particles were divided into groups according to the most represented elements.

3. THE RESULTS AND DISCUSSION

3.1 Typical insoluble particles

Almost 100% of all particles in our dataset belong to PM10 (particles with size smaller than 10 µm). 62% belong to very small particles of category PM2,5 (2,5 µm diameter) (see Table 1). Approximately 23% of all particles have spherical shape. From among the spherical particles predominate those with size under 2,5 µm. Greatest shares of spherical-shaped particles have those rich in Zn (53%) and Mn (44%).
Most typical elements (Si, Al, Fe, K, Mg, Ca, P, S, Na, Ti, Mn, Zn and Cr) in fog particles were found. Representation of these elements in every fog episode is from 1,65 to 87,06 % of the whole dataset (see Table 2). The absolutely most abundant elements are Si, Al, Fe and K which are in almost 50 to 90 percent of all found particles.
Particles having more then 5% of given element were labeled as element-rich. The highest number (1752 - almost 90%) of particles includes more then 5 % of Silicium with 25% substitution of spherical particles. In between Al-rich particles there were found 26% of spherical shaped particles, in Fe-rich particles it was almost 30% and in K-rich particles it was almost 20% of particles.

There are also lots of Al-Si-rich particles, which mean particles containing 5 % and more of Al as well as Si. There are 65,47% of these particles in the dataset. In these particles quite a lot of Fe (up to 25%) and K (20%) was found. 42% of Al-Si rich particles have spherical shape.

Much less but still significantly represented are elements Ca, P, Mg, S, Na, and Ti. Each of them is represented by more then 10% in the data set.
Cl, Mn, Zn and Cr were found in more then 1% but less then 10% of all particles and were also denoted as considerable elements.

Table 1 – Sizes of particles in samples divided to 3 categories (PM2,5, PM10 and particles sizes bigger then 10 µm)

Filter	PM 2.5 [%]	PM 10 [%]	> 10 µm [%]
1	70.89	93.67	6.33
2	50.65	97.4	2.6
3	77.01	95.4	4.6
4	86.21	100	0
5	75.95	98.73	1.27
6	67.78	95.56	4.44
7	79.78	95.51	4.49
8	85.42	98.96	1.04
9	89.25	96.77	3.23
10	55.67	93.81	6.19
11	6.25	100	0
12	5.61	93.46	6.54
13	68.32	95.05	4.95
14	64.15	96.23	3.77
15	40.28	90.28	9.72
16	63.74	92.31	7.69
17	7.23	100	0
18	80.58	99.03	0.97
19	86.6	98.97	1.03
20	60	92.5	7.5
21	67.86	97.62	2.38
22	47.95	89.04	10.96
23	70.83	94.79	5.21
24	77.05	96.72	3.28
25	72.41	94.83	5.17

Table 2 – Particle quantity (PQ) and share of spherical particles (sph)

ELEMENT	PQ	PQ [%]	sph [%]
Particle total	2187	100	23.00
Si	1904	87.06	25.00
Al	1688	77.18	26.32
Fe	1321	60.4	29.72
K	1091	49.89	19.49
Mg	618	28.26	14.09
Ca	523	23.91	9.35
P	476	21.76	18.60
S	449	20.53	13.56
Na	279	12.76	10.26
Ti	265	12.12	32.77
Cl	127	5.81	7.46
Mn	56	2.56	44.44
Zn	55	2.51	52.83
Cr	36	1.65	27.27

3.2 Possible sources of fog pollution

Solid particles in the atmosphere are produced by both sources – natural and/or anthropogenic. Natural sources of air-borne dust are sea salt, terrestrial dust, volcanoes, forest fires and bioaerosol. These particles have usually size of approximately 10 µm. Anthropogenic sources are primarily combustion processes from vehicle traffic and power plant combustion, cement factories, lime-kilns, quarries and mining or particles from building sites or areas devoid of vegetation. These kinds of aerosol particles have usually smaller sizes. Another anthropogenic source of solid pollutants in atmosphere is agriculture. Solid aerosol can rise also secondarily directly in the atmosphere [3, 4].

To demark natural and anthropogenic sources of pollutants in atmosphere is very difficult. Most of elements found in our dataset are usual components of natural ambience. Also most of them can originate as products of anthropogenic activity.

The most represented elements in the dataset – Si, Al, Fe and K and also other detected particles like Ca, Na, and Mg belong to ones of the most represented elements in the crust of the earth. Silicium was found in about 90% of all particles and it is an element which is found in almost every igneous rock. Also it is second most represented particle in the earth crust. This means that significant content of these elements in fog water is natural and that most of particles with prevailing content of Si, Al, Fe, K, Ca, Na and Mg could originate from the earth. On the other hand these elements could possibly get into the fog water also from anthropogenic sources. Quite a big part of detected particles have a spherical shape. Majority of spherical particles are considered to be produced by burning processes at high temperatures (about 1200°C and more). The fact that there are lots of power plants, incineration plants and other industrial works in the surrounding of Milešovka Mountain turns out the probability of the presence of anthropogenic products in collected fog water.

Particles were divided into 3 sectors according to prevailing wind directions – NNW (north-north-west, 3 samples), WNW (west-north-west, 5 samples) and WSW (west-south-west, 5 samples). Some particles rich in particular element such as Al-rich, Si-rich or P-rich particles don't embody any significant pertinence to any sector. On the other hand certain particles show considerable dependence on wind direction. Among such particles belong primarily Cl (NNW), Cr (NNW) and Zn (WSW).

Precipitation amounts (PA) measured 24 hours before every foggy period were compared for content of particles rich in particulate element. Surprisingly there was not found significant decrease of total amount of particles in fog water. The decrease was found in Zn, Fe, Na, Cl-rich particles occurrence and on the contrary P, Ti, Mg, Si-rich particles occurrence increased by increasing PA. Investigations concerning dependence of insoluble pollutants in fog water on meteorological indicators are at the beginning and the research will continue.

5. ACNOWLAGEMENT

The results described in this paper were obtained in the frame of AS CR and BAS collaboration with support of the GACR Project No. 205/09/1918, and the IRP No. AV0Z30420517.

6. REFERENCES

[1] FISAK J., STOYANOVA V. CHALOUPECKY P., REZACOVA D., TSCHACHEVA Ts., KUPENOVA T. and MARINOV M. 2007: Soluble and insoluble pollutants in fog and rime water. In Biggs A. and Cereceda P. (eds): *Proceedings of the 4th International Conference on Fog, Fog Collection and Dew. La Serena, July 22-27, 2007, Chile,* 141-144. Pontificia Universidad Católica de Chile.

[2] STOYANOVA, V., et al. SEM-EDX identification of particles from fog in an industrially polluted region of Czech Republic. *Proceedings of 10th International Multidisciplinary Scientific Geoconference "Modern Management of Mine Producing, Geology and Environmental Protection" SGEM 2010*. 2010, 2, s. 269-276.

[3] HOVORKA, J. *Atmosféra a klima: Aktuální otázky ochrany ovzduší.* Prague : Karolinum, 2009. Atmosférický aerosol, s. 121-139.

[4] *IRZ* [online]. 2005 [cit. 2010-06-22]. Ohlašované látky - Polétavý prach (PM10) Dostupné z WWW: <http://www.irz.cz/latky/poletavy_prach>

5th International Conference on Fog, Fog Collection and Dew
Münster, Germany, 25–30 July 2010
FOGDEW2010-29

Expected Benefits from GOES-R for Fog Detection and Forecasting

J. Gurka (1), M. Pavolonis (2), and T. Schmit (3)

(1) NOAA/NESDIS, Greenbelt MD, United States (james.gurka@noaa.gov), (2) NOAA/NESDIS, Madison WI, United States (mike.pavolonis@noaa.gov), (3) NOAA/NESDIS, Madison WI, United States (tim.j.schmit@noaa.gov)

The Advanced Baseline Imager (ABI) on the GOES-R series, with a planned first launch in 2015, has been designed to meet user requirements covering a wide range of phenomena. As with the current GOES Imager, the ABI will be used for a wide range of weather, oceanographic, climate, and environmental applications. The ABI will improve upon the current GOES Imager with more spectral bands, faster imaging, higher spatial resolution, better navigation, and more accurate calibration. The ABI expands from five spectral bands on the current GOES imagers to a total of 16 spectral bands in the visible, near-infrared and infrared spectral regions. There will be an increase of the coverage rate leading to full disk scans at least every 15 minutes. ABI spatial resolution will be 2 km for the infrared (IR) bands and 0.5 km for the 0.64 micron visible band. The ABI will improve every product from the current GOES Imager and will introduce a host of new products.

The first step to improve fog forecasting is improved detection. The improved spatial resolution in the visible, near IR and IR channels will allow for detection of fog that cannot be seen on the present generation of GOES satellites. The improved temporal resolution will allow for quicker detection and improved monitoring of fog growth and decay. The increased number of channels will provide better information on cloud physics including cloud top phase and cloud top particle size distribution. Onboard visible calibration, along with improved image navigation and registration, will allow for quantitative use of visible images leading to improved short-term forecasting of fog dissipation, and improved fog climatology. Additional channels will also provide better information on aerosols and thin cirrus to allow a more accurate assessment of the actual fog brightness and thus the thickness, and expected time of dissipation. Improved information on aerosols and low level water vapor should help in the short term forecasting of fog formation both over land and water. Improved satellite derived winds and sea surface temperatures will provide additional tools for forecasting sea fog. This presentation will describe the expected new capabilities of GOES-R with respect to fog observation and forecasting and illustrate these with the use of proxy GOES-R images from MODIS (MODerate-resolution Imaging Spectroradiometer) and NOAA polar orbiting satellites.

5th International Conference on Fog, Fog Collection and Dew
Münster, Germany, 25–30 July 2010
FOGDEW2010-30

Fog water collection and reforestation at mountain locations in a western Mediterranean basin region

J.A. Valiente (1), M.J. Estrela (2), **D. Corell** (1), D. Fuentes (3) and A. Valdecantos (4)
(1) Laboratorio de Meteorología-Climatología Unidad Mixta CEAM-UVEG, Fundación CEAM (Fundación Centro de Estudios Ambientales del Mediterráneo), Paterna, Spain, (2) Laboratorio de Meteorología-Climatología Unidad Mixta CEAM-UVEG, Universitat de València, Valencia, Spain, (3) Fundación CEAM (Fundación Centro de Estudios Ambientales del Mediterráneo), Universidad de Alicante, Alicante, Spain, (4) Departamento Ecosistemas Agroforestales, Universitat Politécnica de Valencia, Gandía, Spain (josean@ceam.es / Fax: +34-96-1318190)

Abstract

An inland mountainous location in the east part of the Iberian Peninsula was selected for reforestation studies based on the fog water collection potential prevailing in the area and the high level of land degradation resulting from recurrent forest fires in the past. Prior to the beginning of reforestation and during the whole length of the campaign, a survey study of fog yields and fog-carrying wind directions was conducted by means of an instrument ensemble that consisted of a passive cylindrical fog water collector, a rain gauge, a wind direction and velocity sensor and a temperature and humidity probe. Once wind directions involved in most of the fog water collection were determined, a low-cost 18-m^2 flat-panel collector made of UV-resistant HD-polyethylene monofilament mesh was also deployed and oriented to attain maximum efficiency. Comparison between fog water collections rates in both cylindrical and large flat-panel collectors allowed the finding of a simple methodology that uses wind information to transform one variable into the other. Bulk fog-water catches were then estimated at other locations in the Valencia region for which cylindrical collector fog-water data exist. At the reforestation site, a total of 620 1-year-old seedlings of *Pinus pinaster* and *Quercus ilex* were planted in an area of about 2500 m^2. Water from the 18-m^2 flat panel collector was stored in high-capacity tanks and small timely water pulses localized deep in the planting holes were conducted during the first summer period by means of an irrigation network. Results indicate that survival rates and seedling performance of the two species planted improved with the use of small timely waterings and additional treatments with composted biosolid.

1. Introduction

The experimental site selected for the reforestation study (Mount Los Machos in Figure 1) is located in the interior of the Valencia region, western Mediterranean basin. The annual pluviometric regime ranges from 400 to 600 mm corresponding to a dry Mediterranean climate [4]. The region meets most of the geographical conditions for fog occurrence and collection potential as compiled in [5]. Previous studies using the mountain network of cylindrical collectors shown in Figure 1 have quantified fog water collection as a function of wind behavior at each of the specific stations [6], [2], [1]. The good potential shown by most of these locations brings to consider collected fog water as a new resource in restoration activities of remote areas where land degradation may be severe.

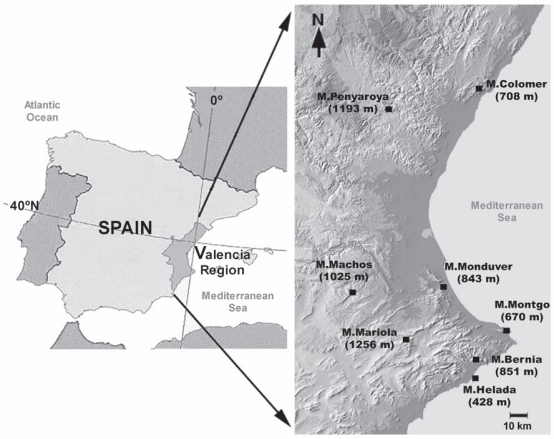

Figure 1: Map location for the restoration site at Mount Los Machos and rest of mountain stations using cylindrical collectors.

2. Methodology

The experimental site at Mount Los Machos could be divided into two parts: a fog-water collection and storing area and the reforestation plot itself, the former being 40 m above the latter. This difference in elevation alone resulted in a water pressure of about 4 atm at the end of each irrigation line. Site preparation and seedling planting took place from December 2006 to January 2007. The study uses data that extend into the whole year 2007.

At the top part of the experimental site, a cylindrical fog-water collector, an 18-m^2 flat-panel collector and three 1000-l water tanks were arranged for fog-water volume measuring, harvesting and storing. The cylindrical collector was part of an instrument ensemble holding other additional environmental sensors, being a rain gauge and a wind direction and velocity sensor the most remarkable. This cylindrical collector acts as a passive device and is handmade constructed using a pair of discs strung with nylon line to attain omnidirectional collection efficiency [2]. Additionally, an upper 60-cm diameter plastic tray carries out the function of a protective cover to avoid major rain interference [3]. The collected fog water volume per unit area (l/m^2) is calculated by dividing the collected volume by the effective collection surface of the collector (base diameter times height).

The 18-m^2 flat-panel collector was also built using low-cost materials with final dimensions of 6.4 m in width and 2.8 m in length. Fog droplets are captured on the panel mesh, and, as they become bigger, they flow downwards under gravity. Water accumulates into a tilted gutter that connects through a hose with three interconnected 1000-l tanks to store water. Water flow produced by the flat panel was measured using a level pressure sensor that was permanently maintained at the bottom of one of the tanks. According to previous data taken by the cylindrical collector, the flat panel was deployed at a fixed orientation of 55º from North in order to attain maximum efficiency during fog harvesting.

Water treatments for the two-species seedlings, *Pinus pinaster* and *Quercus ilex*, consisted of natural precipitation as the control (C), one or two water pulses of ca. 4.5 l/hole during the first summer (W1 and W2, respectively), and rainfall exclusion (-W), the latter conducted by means of a plastic sheet being deployed before a rainfall event. During an irrigation pulse, water was injected to 20-25 cm deep by means of microtubing connected to each emitter. In half of the planting holes of each treatment, composted sewage sludge from a local composting facility was applied and mixed in situ with the soil at an application rate of 22 t dry weight per hectarea.

3. Results

3.1 Fog-bearing winds

In Figure 2, the percentage of winds for which any amount of fog collection has occurred is shown in the top windrose, while the percentage of fog water in the total accumulated volume collected at a certain wind direction and velocity is represented in the bottom windrose. A noticeable component peaking between the NE and ENE (55º from North approximately) marks the most efficient direction.

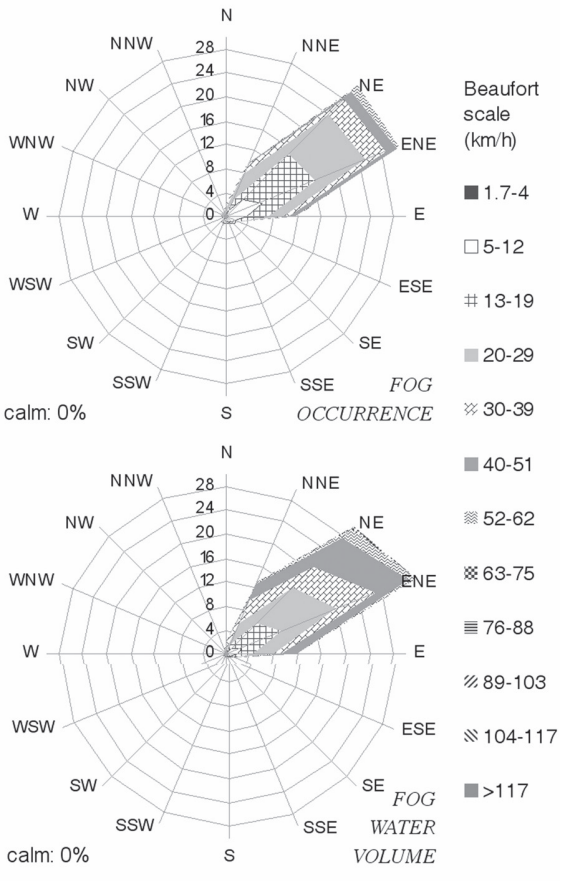

Figure 2: Wind roses that combine data from the cylindrical collector and the wind velocity and direction sensor.

3.2 Omnidirectional fog yields

Monthly fog collection and precipitation rates are obtained as the ratio of water collected volumes to the length in days of available data for each month (Figure 3). The 2007 annual rate given by the cylindrical fog collector, 3.3 l/m^2/day, contrasts with the measured rainfall rate, 1.4 l/m^2/day. Although fog collection and precipitation are distinct variables, their comparison indicates the site potential for fog water collection in relation to rainfall availability. At this experimental site, collecting fog water seems more profitable and less costly than collecting rain water since fog provides at least twice as much water.

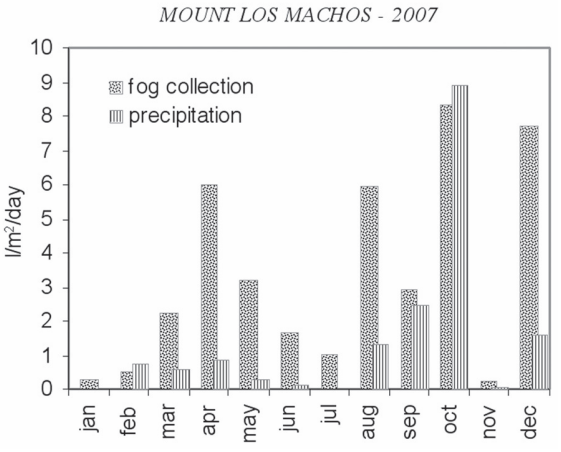

Figure 3: Monthly rates of rainfall and fog collection, given by the cylindrical collector and the rain gauge.

3.3 Seedling survival

After three years from planting, seedling survival was above 60 and 90% in maritime pine and holm oak, respectively, both for the water pulses treatments during the first summer (Figure 4). The three factors included in the analysis: two species, two types of fertilization and four water treatments, resulted in significant differences in seedling survival. Holm oak survival was significantly higher than maritime pine, and survival with compost application was slightly but significantly higher than in unfertilized seedlings. The water exclusion treatment (-W) showed the lowest survival in both species and fertilization treatments. Control seedlings showed intermediate values between the exclusion and the two water pulses treatments in most of the cases. There is a small vanishing tendency of the watering effects as time goes by.

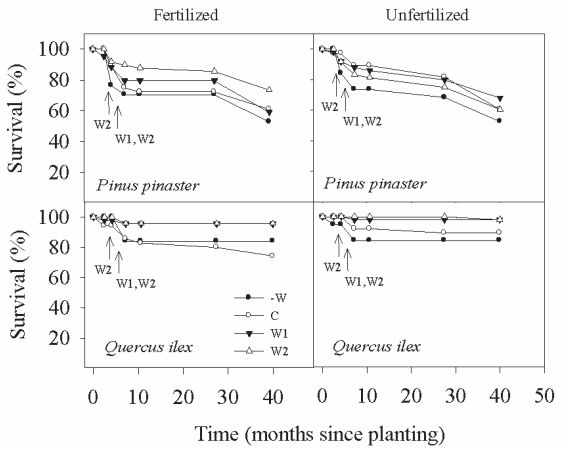

Figure 4: Dynamics of survival in *Pinus pinaster* and *Quercus ilex* seedlings according to different water and fertilization treatments.

3.4 Flat-panel and cylindrical collections

The plot in Figure 5 is obtained when comparing the hourly tank water flows with the cylindrical collector fluxes at the direction of the orientation of the flat panel, as shown by equation 1 [1]. The observed linear tendency proves a 1:1 relation within the limits of the estimation error. It is possible then to predict directional collection rates from omnidirectional data.

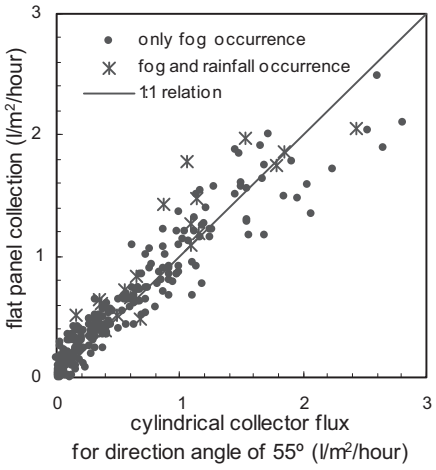

Figure 5: Scatter plot of match-up data from the flat panel and cylindrical collectors.

$$\phi_h = \sum_{1h} f_i \left|\cos(55^\circ - \theta_i)\right| \qquad (1)$$

where θ_i is the 10-min wind direction, f_i is the cylindrical fog collection in the 10-min period, and ϕ_h is the hourly fog-water flux calculated at the 55º direction, which is the orientation of the flat panel.

3.5 Estimating flat-panel yields

Equation (1) was used to estimate annual rates of fog water collection at different flat-panel hypothetical orientations that could be arranged at each mountain station of our fog collection network (Figure 6). Maximum efficiencies can be achieved at a specific orientation for each station. Some of the stations present little oscillation with respect to orientation.

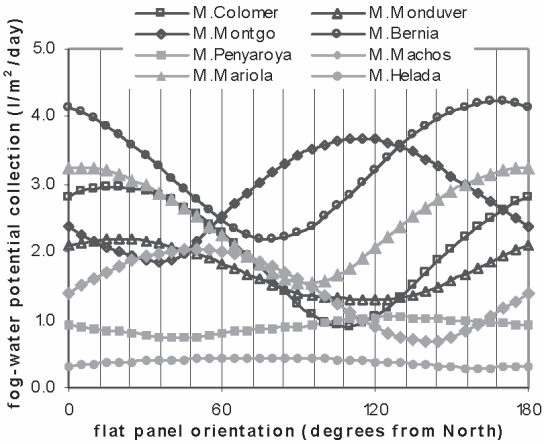

Figure 6: Annual flat-panel fog collection rates estimated by means of equation (1) versus orientation.

Finally, potential fog-water harvesting by an 18-m^2 flat-panel collector for the CEAM network is given in Table 1. The orientation for which maximum efficiency is attained varies with station as well as the ratio of flat-panel over cylindrical collection.

Table 1: Estimated fog water potential by 18-m^2 flat-panel collectors efficiently arranged at each station.

Mountain station	Orientation (º from N)	Fog water collection (l/m^2)	Ratio (flat over cylinder)	18m^2 flat panel collection (m^3)
Colomer	20	1080	0.92	19
Penyaroya	125	379	0.73	7
Monduver	20	801	0.81	14
Machos	50	746	0.91	13
Montgo	115	1343	0.83	24
Mariola	0	1188	0.83	21
Bernia	170	1539	0.82	28
Helada	85	158	0.73	3

6. Summary and Conclusions

The study has stated the use of fog water collection on mountainous locations in the restoration of degraded land in dry Mediterranean climates. In spite of the mild summer conditions during the field campaign, seedling survival was still promoted by small water pulses during the first summer. Ancillary data allowed the conversion of omnidirectional fog-water collection yields into specific directional values, as it is typical of flat-panel collectors.

Acknowledgements

The Fundación CEAM is funded by the Generalitat Valenciana and Fundación Bancaja. This research was supported by the Ministerio de Ciencia e Innovación, contract numbers CGL2005-03386 and CGL2008-04550, and the Consolider–Ingenio 2010 Programme (CSD2007-00067 GRACCIE project).

References

[1] Estrela, M.J., Valiente, J.A., Corell, D., Fuentes, D. and Valdecantos, A.: Prospective use of collected fog water in the restoration of degraded burned areas under dry Mediterranean conditions, Agricultural and Forest Meteorology, Vol. 149, pp. 1896–1906, 2009.

[2] Estrela, M.J., Valiente, J.A., Corell, D. and Millán, M.M.: Fog collection in the western Mediterranean basin (Valencia region, Spain), Atmospheric Research, Vol. 87, pp. 324–337, 2008.

[3] Juvik, J.O. and Nullet, D.: Comments on 'A proposed standard fog collector for use in high elevation regions'. Journal of Applied Meteorology, Vol. 34, pp. 2108–2110, 1995.

[4] Peñarrocha, D.: Precipitaciones: volúmenes y distribución espacial. In: Pérez Cueva , A. (Eds.), Atlas Climático de la Comunidad Valenciana (1961-1990), Consellería d´Obres Públiques, Urbanisme i Transports, Generalitat Valenciana, Valencia, pp. 86-89, 1994.

[5] Schemenauer, R.S. and Cereceda, P.: A proposed standard fog collector for use in high-elevation regions, Journal of Applied Meteorology, Vol. 33, pp. 1313-1322, 1994.

[6] Valiente, J.A., Estrela, M.J., and Corell, D.: Fog Collection Network in the Valencia Region (Western Mediterranean Basin), The Fourth International Conference on Fog, Fog Collection and Dew, 22-27 July 2007, La Serena, Chile, 2007.

5th International Conference on Fog, Fog Collection and Dew
Münster, Germany, 25–30 July 2010
FOGDEW2010-31

Meteorological Patterns and fog water in Morocco and the Canary Islands

Mª V. Marzol (1), J.L. Sánchez Megía, A. Yanes (1), A. Derhem (2) and J. Bargach (2)
(1)Department of Geography, University of La Laguna, Canary Islands, Spain (mmarzol@ull.es / Fax: +34-922317723) (2) Foundation Si Hmad Derhem (www.darsihmad.org)

Abstract

There are large monthly differences in the daily average amounts of fog water collected in Morocco (Boutmezguida) and in the Canary Islands (Anaga), from June 2006 to December 2009, which can be explained by the organization of the air pressure in the north-west Atlantic and the Sahara. Two different models of fog behavior can be identified, *the Moroccan* and *the Canary* models. The former is efficient in the winter while the latter is efficient in the summer.

1. Introduction

The stratocumulus cloud formation is very common in the Canary Islands (Spain) and on the Atlantic coast of Morocco, which are locally referred to as *mar de nubes* (sea of clouds) and *tagut* respectively. In both cases, the clouds behave like fog when they hit the mountainous relief and it is possible to collect some of their liquid content using artificial systems. This water can then be used in areas of water shortages to meet daily requirements. The source of this cloud formation is connected to the Azores anticyclone and anomalous structure of the atmosphere caused by a subsistence thermal inversion.

It is, therefore, useful to know what the organization of the surface air pressure is like (localization, frequency and intensity) in the low atmosphere of this part of the Atlantic as this would explain how this efficient natural resource providing the Canary and Moroccan ecosystems with water develops.

The University of La Laguna has been collaborating, since June 2006, with the Si Hmad Derham Foundation on a study about the viability of providing drinking water, via the construction of Large Fog Collectors (LFC)[1,2], to rural communities in areas around Mount Boutmezguida (Ifni) which are 30 km from the Atlantic coast of Morocco at the same latitude as the Canaries.

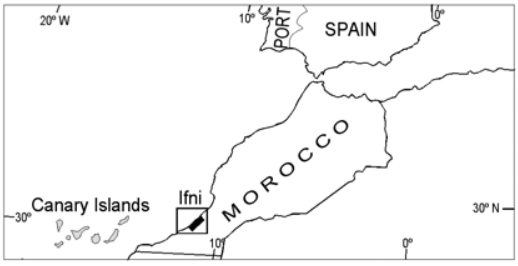

Figure 1: Location of the Ifni region where the Boutmezguida site is.

To date, the volume of the potential water that can be collected, the monthly differences and their relationship with the meteorological variables of relative humidity, wind speed and direction have been analyzed. This stage of the study has been carried out using a Standard Fog Collector (SFC) [3] and a Quarter Fog Collector (QFC) [4] connected to a Davis model automatic meteorological station, providing information on all the variables, every ten minutes, which will be used to determine the most favourable conditions for collecting the fog water with the greatest efficiency (figure 2).

The Si Hmad Derham Foundation has surveyed the local population, made up of twenty rural communities (1,547 people and 5,451 animals) about their water needs. The results of the survey show that the people in charge of looking for water are basically children (53%) and women (21%), the distance covered is more than one kilometre, this task is performed every day, only 3 out of 217 families treat the water with bleach and that the average daily consumption is very low, less than 50 litres per family per day. All these data can explain the low level of schooling of the children, the difficulty the women have in dedicating their time to more productive tasks, health problems associated with the bad quality of the water making it the main vector of diseases, etc.

Figure 2: Equipment used in the study (Morocco)

The possibility of providing these communities with drinking water via LFCs will, without doubt, improve the quality of life and contribute to sustainable development for the rural populations who have started to abandon the countryside and their roots, by emigrating to the towns and cities, as a result of the great difficulties they face in making a living in rural areas [5,6].

2. Aims and Methodology

The aim of this article is to geographically locate the areas of surface pressure on the days when there was fog in Boutmezguida (Morocco), from 6th June 2006 (starting date of the study) to 31st December 2009, and to see if there is a model of the meteorological and atmospheric conditions in the Atlantic and the Sahara which may explain seasonal differences in water fog water collection between Morocco and the Canaries.

Two SFCs with different orientations (nº3 with 300° and nº4 with 340°) were installed in Boutmezguida (1,225 m a.s.l., 29°12'30"N - 10° 01'30"W) in June 2006; the SFC nº3 was replaced by a QFC connected to a meteorological station in September 2009; the SFC nº4 was kept to fix the correlations resulting from the size of the meshes. The information collected was compared with the data, from the same period, from the station in Anaga (842 m a.s.l., 28°32'09"N - 16°14'11"W), on the island of Tenerife (the Canary Islands).

The methodology used[7] here is based on dividing the space in the Atlantic into 80 squares, 5° longitude by 5º latitude, between the longitudes 40°W and 20°E and latitudes 25° to 70°N (figure 3). This method can georeference the type of pressure centre (high and low pressure) and its values. The information is taken from daily synoptic surface maps from the Spanish National Meteorological Agency which is then introduced into a daily data base with synoptic information from the maps and data on the water from the SFC and QFC in Boutmezguida and Anaga.

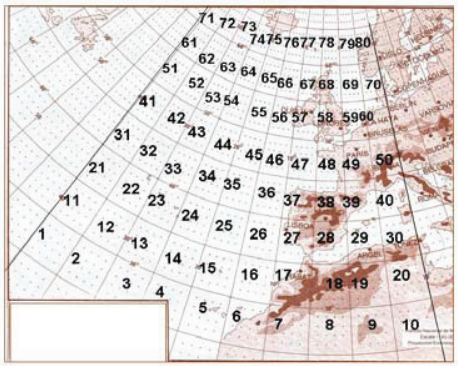

Figure 3: Grid used to take the information from the surface weather maps

3. Results

3.1 The cloud phenomenon frequency

Out of the total of 1,297 analyzed days (from 12/06/2006 to 31/12/2009, there was only fog on 33% of the days (427) in Morocco and on 381 of these 427 days there was also fog in the Canaries, i.e. 89% of the days. However, an analysis of the data for the same period in Anaga shows that there was a total of 1,250 days with fog (97%), thus the difference between Morocco and the Canaries does not mean there was a lower frequency of the cloud phenomenon but rather a lack of coincidence of the phenomenon in both places, basically in the spring and autumn.

The "interference" that rainwater can exert in determining the collection efficiency of the screens only occurs on 4% of the days of the year in Morocco and on 8% of the days of the year in the Canaries, and this only affects the months between October and March. In the case of Morocco there are very few rainy days which is why they were taken into account, whereas, in the Canaries, the fact that information is taken every 10 minutes means that rainy days can be discriminated (table 1).

3. 2 The volume of collected water

The obtained results, both in Morocco and the Canaries, support the viability of artificially

collecting part of the liquid content of the clouds because an average of 10 L/m^2/day is assured. Table 1 shows the daily amount of collected water from the screens irrespective of origin, rain and fog (1), and the fog water collected exclusively (2).
The most outstanding feature is that there are monthly models of how the efficiency of fog water collection behaves. A daily collection of 10.5 L/m^2 is assured for seven months from December to June, and only 4.8 L/m^2 per day in the other five months, whereas in the case of the Canaries, the vertical development of the clouds predominates in the winter months and reduces the efficiency of the screens as only an average of 6.5 L/m^2 /day is assured from September to May compared to 19.1 L/m^2/day in the three summer months. This volume of summer water is important from an ecological perspective because it provides the ecosystem with humidity and water at a time of greatest water stress.

Table 1: Daily mean amount of fog water at Morocco and Canary Islands (June 2006 at December 2009)

	Morocco	Canary Islands	
	(1)	(1)	(2)
	L/m^2/day	L/m^2/day	L/m^2/day
J	12.2	7.0	5.2
F	12.5	7.1	5.2
M	14.8	6.5	4.3
A	16.3	12.0	10.8
M	14.4	10.8	9.9
J	17.7	13.2	13.0
Jl	0.0	23.9	23.9
A	2.3	20.7	20.4
S	5.5	7.1	6.9
O	7.0	7.8	6.4
N	9.0	5.8	3.2
D	14.5	7.1	4.3
Mean	**10.5**	**10.7**	**9.5**

3.3 Organization of the surface pressure fields

There is a high pressure area in the eastern Atlantic on 88% of fog days in Morocco; on 60% of those days the centre of the anticyclone is between Morocco and the Canaries, with an average pressure of 1030 hPa. With less frequency (40% of days with fog) there is a relative depression over the Sahara of 1008 hPa. In addition, 5% of fog events in Morocco coincide with an area of low pressure between the Iberian Peninsula and the Canaries which corresponds to a talweg or cold advection on 500 hPa chart (figure 4).

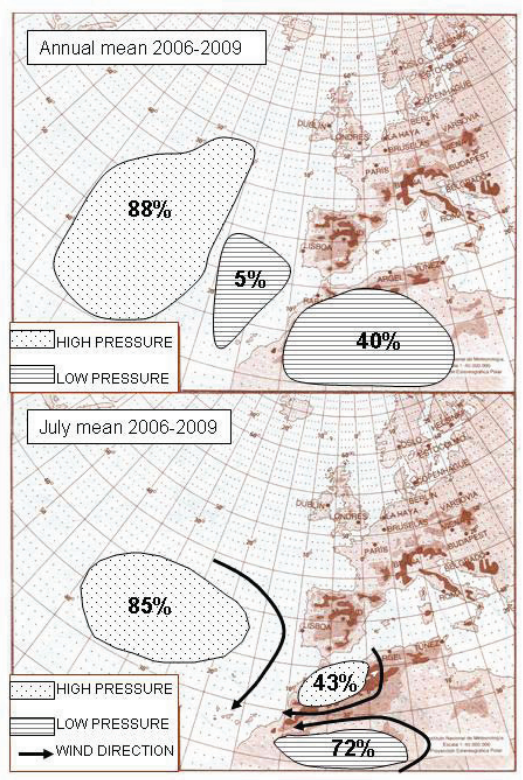

Figure 4: Location of pressure centres in the North Atlantic on fog days in Morocco (Dec-June) and on fog free days (July) in the period from 2006-2009.

3.4 July: A very dry month in Morocco and very humid in the Canaries

There is no fog water in Morocco in July in any of the four years of the study, whereas in the Canaries water is collected on 90% of days in July with a daily average of 23 L/m^2. The explanation for this large difference lies in the simplification of the regional pressure fields. The most outstanding features are:

a) The centre of the Atlantic anticyclone is nearer the Canaries on more days (85% of days in July) (figure 2). Average pressure is somewhat lower than the rest of the year (1028 hPa).

b) A greater frequency of the thermal depression over the Western Sahara (72% of days in July) with an average pressure of 1008 hPa. Its geographical location is only to be found to the south of the Atlas Mountains.

c) The appearance of a surface anticyclone over the Atlas Mountains on 43% of the days in July with an average value of 1019 hPa.

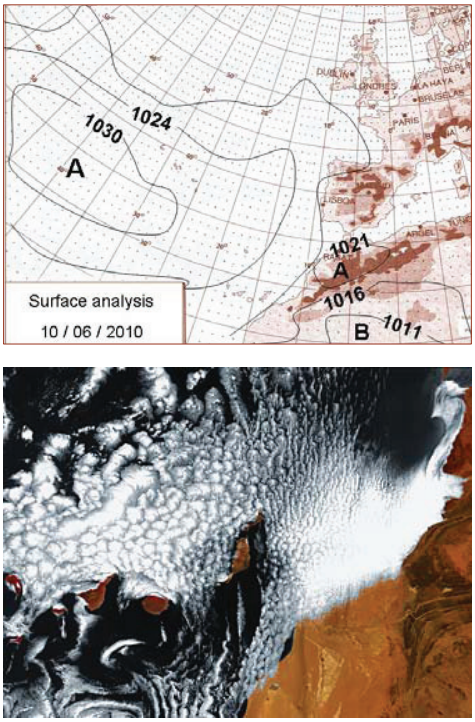

Figure 5: The surface chart and the satellite image (ENVISAT) of 6 June 2010 show the best atmospheric conditions for collecting large amounts of fog water in Boutmezguida

The three pressure centres create a steep barometric gradient giving rise to moderate NE trade winds, parallel to the Moroccan coast or from the Atlas Mountains towards the coast, which impede the Atlantic cloud from penetrating into Moroccan territory but do favour its path over the Canary Archipelago (figures 4 and 5).
However, when the winds are from the north there is a greater probability of fog on the Moroccan coast, which is what happened on 6 June 2010 (figure 5).

4. Conclusions

There is fog in Morocco on one out of every three days and in 89% of the cases this coincides with fog in the Canaries. However, the cloud phenomenon is much more common in the Islands given that it occurs on 97% of the days of the year.

There are two models of fog behavior: the *Moroccan* model which is very efficient from December to June with more than 15 L/m^2/daily and deficiency of water in July and August; and the *Canary* model which behaves inversely with a deficiency of water from September to March and an excess of water from April to August.
Finally, the organization of surface pressure systems on fog days in Morocco clearly differs to the dominating organizations on the days when there is no fog and the direction of the isobar lines is also different.

Acknowledgement

We would like to thank M. Beilla and M. Driwich for their incalculable help in collecting data and maintaining the station in Boutmezguida.

References

[5] Cereceda, P. and Schemenauer, R.: La niebla: recurso para el desarrollo sustentable de zonas con déficit hidrológico. In Marzol, Mª V., Dorta, P. and Valladares, P. (eds.) Clima y agua: la gestión de un recurso climático, Tabapress, Madrid, pp. 25-33, 1996.

[7] Dorta, P., Marzol, Mª V. and Valladares, P. Localisation et fréquence des cellules de pression dans l'Atlantique Nord, l'Europe occidentale et le nord de l'Afrique (1983-1992). Association Internationale de Climatologie, Vol. 6, pp. 452-466, 1993.

[4] Marzol, Mª V.: Fog water collection in a rural park in the Canary Islands (Spain). Atmospheric Research, Vol. 64, pp. 239-250, 2002.

[1] Marzol, Mª V., Abdelmalek, A., Sánchez Megía, J.L., and Derhem, A.: Evaluation of Fog Collection in Ifni, Morocco. Fourth International Conference on Fog, Fog Collection and Dew, 22-27 july 2007, La Serena, Chile, 2007.

[2] Marzol, Mª V. and Sánchez Megía, J.L.: Fog Water Harvesting in Ifni, Morocco. An Assesment of Potential and Demand. Die Erde, Vol. 139 (1-2), pp. 97-126, 2008.

[6] Marzol, Mª V., Sánchez Megía, JL., Yanes, A. and Bargach, J.: The viability of supplying fresh fog water to the rural population in Morocco. VII International Congress ANQUE, 13-17 June 2010, Oviedo, Spain.

[3] Schemenauer, R. and Cereceda, P.: A Proposed Standard Fog Collector for Use in High-Elevation Regions. Journal of Applied Meteorology, Vol. 33 (11), pp. 1313-1322, 1994.

5th International Conference on Fog, Fog Collection and Dew
Münster, Germany, 25–30 July 2010
FOGDEW2010-32

Polycyclic aromatic hydrocarbons in dew and frost

T. Taniguchi, N. Takenaka, K. Imamura, Y. Maeda, Y. Sadanaga, and H. Bandow
Osaka Prefecture University, Sakai, Japan (taniguti@chem.osakafu-u.ac.jp)

Dew and frost form near the ground surface and absorb water-soluble compounds. It was reported that polycyclic aromatic hydrocarbons (PAHs) absorb efficiently onto the surface of snow. It is expected that frost can also absorb PAHs efficiently. Dew and/or frost can be used as water resources, but there are few reports on measurements of the concentrations of PAHs in dew and frost so far. PAHs are well-known as strong cancerogenic substances or mutagenic compounds. Therefore, it is very important to know the concentrations in dew and frost in order to use them as the water resources. The sampling of PAHs in aqueous media is very difficult, because some PAHs are evaporated during sampling. Therefore, we examine the sampling methods of PAHs in rain and snow, and we found that PAHs can be efficiently collected when organic solvent, such as benzene and hexane, are previously put into a sampling bottle. This method was applied to dew and frost sampling. Here, we report the sampling method of dew and frost and measurement results of PAHs in dew and frost. The dew and frost were collected at about 1 m above the ground in Osaka Prefecture University, Sakai, Japan. The collected PAHs in dew and frost were extracted by liquid-liquid extraction. PAHs concentrations were analyzed by a high performance liquid chromatography with a fluorescence detection or a gas chromatography / mass spectrometer. Analyzed PAHs were fluoranthene, pyrene, benz(a)anthracene, chrysene, benzo(b)fluoranthene, benzo(k)fluoranthene, benzo(a)pyrene, dibenz(a,h)anthracene and benzo(g,h,i)perylene. The concentrations of theses compounds were several ng dm^{-3} to 20 ng dm^{-3} in rain and several tens ng dm^{-3} in snow. The PAHs concentrations in snow were higher than those in rain, and the same tendency could be observed in dew and frost. In the presentation, we will report the detail results of concentrations of PAHs in dew and frost.

5th International Conference on Fog, Fog Collection and Dew
Münster, Germany, 25–30 July 2010
FOGDEW2010-33

Observation of hydrophobic organic compounds in fog water at the summit and on the foot of Mt. Fuji during the summer

H. Okochi (1), K. Tamechika (1), S. Saga (1), K. Toshimi (1), Y. Minami (2), and H. Kobayashi (3)

(1) Waseda University, Japan (hokochi@waseda.jp), (2) Ishikawa Prefectural University, Japan, (3) University of Yamanashi, Japan

The presence of hydrophobic organic compounds (HOCs) such as PAHs, PCBs, and VOCs, which are considerably larger than expected from the surrounding gas-phase concentration and Henry's law constants, has been reported in atmospheric droplets such as fog water, rainwater, and dew water. In recent years, decrease in surface tension with respect to pure water was observed in cloud/fog sample probably because of the presence of atmospheric humic-like substances (HULIS), which have been founded to account for a substantial amount of water-soluble organic compounds (WSOC) in fog droplets and fine aerosols. Lowering of surface tension of fog droplets may influence the gas-liquid distribution of HOCs, but the influences of HULIS on the dissolution of HOCs have never been investigated in the field observation.

We performed simultaneous sampling of volatile organic compounds (VOCs) such as chlorinated hydrocarbons (CHs), monocyclic aromatic hydrocarbons (MAHs), and dicyclic aromatic hydrocarbons (DAHs) in fog water and in the ambient air at the summit and on the mountainside (1300 m a.s.l.) in Mt. Fuji during the summer from 2006 to 2009. Dew water and rainwater were also collected although there were few samples during the period. The summit of Mt. Fuji is located in the free troposphere, while the foot is located in the forest area. VOCs in fog water were determined by Head Space-Solid Phase Micro Extraction (HS SPME) / GCMS, while VOCs in the gas phase were collected in adsorbent tube, then extracted with CS2, and analyzed by a GCMS. Dissolved HULIS in fog water were concentrated on anion exchangers, then extracted by sodium chloride, and measured with a UV/VIS spectrophotometer at 400 nm, which was proposed by Hiraide et al. (1994). Among the VOCs, MAHs were much contained in fog water collected both at the summit and on the foot of Mt. Fuji than CHs and DAHs. Toluene was abundant among the determined twenty-six VOCs in atmospheric water (fog, dew, and rain) as well as in the ambient air. We will discuss the influence of HULIS on the dissolution of VOCs into fog water.

5th International Conference on Fog, Fog Collection and Dew
Münster, Germany, 25–30 July 2010
FOGDEW2010-34

Fog chemistry at the summit and on the foot of Mt. Fuji

H. Okochi (1), N. Takemura (1), S. Maruyama (1), Y. Minami (2), and H. Kobayashi (3)

(1) Waseda University, Japan (hokochi@waseda.jp), (2) Ishikawa Prefectural University, Japan, (3) University of Yamanashi, Japan

Mt. Fuji, which is the highest mountain in Japan (3776 m a.s.l.), is an isolated peak and therefore could be regarded as the tower to observe the long-range transportation from East Asia such as China and Korea to Japan, the mixing processes from the boundary layer to the free troposphere, and the nucleation/precipitation scavenging processes of various atmospheric pollutants.

We have studied fog water chemistry on the southeast foot of Mt. Fuji (Tarobo located at the starting point in the Gotemba climbing root, 1300 m a.s.l.) all over the year from 2006. Simultaneous sampling of fog water, rainwater, acidic and ammonia gases, and aerosols in the ambient air were performed at the summit and on the foot of Mt. Fuji during the summer from 2006 to 2009. Dew water was also collected on the foot of Mt. Fuji on clear nights during the summer observational campaign. The volume weighted mean pH of fog water collected on the foot of Mt. Fuji was 3.60 (range: 3.51 – 3.73, n=4) in 2006, 3.81 (range: 3.60 – 5.50, n=9) in 2007, 3.69 (range: 3.26 – 4.11, n=20) in 2008, respectively. During the 4-years summer observational campaign, the volume weighted mean pH of fog water collected at the summit was 4.68 (range: 3.72 – 5.61, n=58), while that of fog water on the foot was 3.57 (range: 3.20 – 6.03, n=20). The total concentration of major ions on the foot was 16 times lower than that at the summit of Mt. Fuji. The pH of fog water decreased as the ratio of nitrate to sulphate increased both at the summit and on the foot, indicating that the absorption of nitric acid in the ambient air into fog droplets is the dominant acidifying process in Mt. Fuji. We will discuss the scavenging mechanism of acidic substances into fog water and the long-range transportation of acidic substances from East Asia.

5th International Conference on Fog, Fog Collection and Dew
Münster, Germany, 25–30 July 2010
FOGDEW2010-35

Efficient fog harvesting by Stipagrostis sabulicola (Namib dune bushman grass)

A. Roth-Nebelsick (1), M Ebner (2), and T Miranda (2)

(1) State Museum for Natural History Stuttgart, Palaeontology, Stuttgart, Germany (rothnebelsick.smns@naturkundemuseum-bw.de, +49-(0)711-8936-100), (2) Institute for Geosciences, University of Tübingen

Stipagrostis sabulicola is an endemic species of the central Namib Desert which settles on extremely arid dune fields. Due to its ability to persistence even during exceptionally dry years it is generally assumed that water supply of this species is substantially based on fog water. In this contribution, the results of a study investigating the capability of S. sabulicola for fog harvesting are presented. For this purpose, stem flow rates of S. sabulicola during fog events, spatial gradient of soil water content (SWC) close to mounds of S. sabulicola and its leaf water potential (LWP) before and after fog events were monitored together with climate parameters.

According to the data obtained during this study, S. sabulicola is able to harvest substantial amounts of water by fog catchment from nocturnal fog events. Since culms of S. sabulicola are often stiff with an upright habitus, fog harvesting occurs via stemflow that conducts water directly towards the root zone of a plant. According to this mechanism, the stem runoff is concentrated within the area of the mound. A medium-sized mound of S. sabulicola is able to collect an amount of about 4 l per fog night. This fog harvesting leads to a considerable spatial gradient of soil water content with values decreasing with increasing distance from the mound. As a result of the water input by fog drip, SWC within the mound increases significantly, particularly close to the culm bases where SWC values increased to 2.2 % after a fog event.

Due to the uneven distribution of water by stemflow, SWC within a mound shows high spatial heterogeneity which is also illustrated by the numerous outliers and extreme values of SWC within the mound region. This heterogeneity is also due to the fact that several sagging leaves are always present causing fog drip which more or less irregularly scatters moisture. For bare soil outside of a mound, the water content is not substantially increased, amounting to 0.78 % on average during dry days and 0.89 % after fog events. Fog harvesting affects also leaf water potential: whereas leaf water potential declines during dry days, it remains more or less constant on days following fog events. Since mounds of S. sabulicola provide shelter and food for various other organisms such as ants and lizards, their ability for nocturnal fog catchment is of high significance for the ecosystem of the Namib dunes.

5th International Conference on Fog, Fog Collection and Dew
Münster, Germany, 25–30 July 2010
FOGDEW2010-36

A Fog Climatology for Cape Town International Airport

L. Van Schalkwyk (1,2) and L.L. Dyson (3)

(1) South African Weather Service, Cape Town, South Africa (lynette.vanschalkwyk@weathersa.co.za), (2) University of Pretoria, Pretoria, South Africa (lynette.vanschalkwyk@weathersa.co.za), (3) University of Pretoria, Pretoria, South Africa (liesl.dyson@up.ac.za)

Cape Town International Airport (CTIA) is situated off the cold Benguela current on the extreme southern side of the west coast of South Africa and experiences fog more frequently than any other international airport in South Africa. The aim of this research is ultimately to improve fog forecasts and to determine the characteristics of fog at CTIA by means of a comprehensive fog climatology. A fog climatology is derived making use of 06:00Z observations over a period of 31 years (1978-2008). The fog season for CTIA is observed to start in March and persists till August, while May is found to be the month with the highest frequency of fog events. Analysis of advection and radiation fog events shows that the occurrence of advection fog events dominate during the earlier part of the fog season, whilst radiation fog occurrences increase towards the latter part. Advection fog events at CTIA have been shown to occur frequently from a northwesterly and a southerly wind direction, but monthly wind roses for CTIA at 06:00Z show that a northeasterly wind (land breeze) is dominant during advection events in July and August. This suggests a third type of fog event, namely advected radiation fog, which accounts for fog that forms due to radiative processes to the east and northeast of the aerodrome, where after it is advected towards the airport when the land breeze is at its strongest prior to sunrise. The climatology is supplemented by an analysis of hourly data which are available for the limited period of 2004-2007. With the aid of hourly data, more accurate estimations of the average time of onset and dissipation of fog are determined as well as duration time: information critical to the aviation forecaster.

5th International Conference on Fog, Fog Collection and Dew
Münster, Germany, 25–30 July 2010
FOGDEW2010-38

Fog water collection under sea breeze conditions in the western Mediterranean basin (Valencia region, Spain)

C. Azorin (1,2), **D. Corell** (1), M.J. Estrela (1,3), J.A. Valiente (1)

(1) Laboratory of Meteorology-Climatology, Mixed Unity CEAM-UVEG, The CEAM Foundation, Paterna (Valencia), Spain (cazorin@ceam.es / Fax +34 96 131 81 90), (2) Group of Climatology, University of Barcelona, Barcelona, Spain, (3) Laboratory of Meteorology-Climatology, Mixed Unity CEAM-UVEG, Geography Department, University of Valencia, Valencia, Spain

Abstract

The aim of this study is to analyse the basic climatological features of fog water collection under sea breeze conditions in the eastern of the Iberian Peninsula (Valencia region, Spain). A network of five passive fog water collectors located at coastal mountain stations was used to sample water volumes during a 6-yr study period (2004-2009). The current study simultaneously applied manual and automated filters for identifying past orographic fog events associated with sea breezes. The preliminary results indicate that (a) sea breeze orographic fog episodes occur preferably in summer, but also in autumn and spring months; (b) fog water is collected during the late evening and night; and (c) collection occurs under well defined wind patterns. Orographic fog water input associated with sea breezes is particularly important for vegetation in the driest summer season.

1. Introduction

Sea breezes develop over the eastern coast of the Iberian Peninsula (IP) for almost two out of three days ([1], [9]), arriving to inland areas placed between 30 and 300 km from the nearest sea. [3] confirmed that the effect of sea breezes on cloud genera is to increase the frequency of low (*Stratus*, St) and convective (*Cumulus*, Cu) clouds. The primary impact of sea breeze flows corresponds to low stratiform clouds (St, and *Stratocumulus*, Sc) formed in the convective internal boundary layer (CIBL) due to the inflow of moist sea air at lower levels. The formation of Sc clouds is caused by the rising and cooling of turbulent moist sea air over the highest slopes of the mountains at the end of the day. In the most Sc formation, it is common to observe dense fog banks of *Stratus nebulosus* (St neb) and dew during the early next morning, covering the inland topographical depressions [7]. This multiyear study aims to verify for the first time the impact of sea breezes on fog water collection in the Mediterranean area.

2. Data source and methods

2.1 Study area and dataset

Figure 1 shows the topography features of the Valencia region, placed in the eastern fringe of the IP. The terrain is quite complex, with wide and flat coastal plains on the central coast; river valleys oriented approximately NW to SE which enhance the inland propagation of sea breezes; and the steep Iberian and Subbetic mountain ranges (Calderón is the highest mountain peak, at 1839 m.a.s.l.) located from 10-15 km inland, with coastal mountain ranges in the southern and the northern shoreline. The blocking of sea breeze flows by the mountain ranges has some impacts on the development of low stratiform clouds. This empirical study is mainly based upon a network of five passive fog water collectors maintained by the CEAM Foundation (http://www.ceam.es/ceamet/). The stations are distributed over five coastal-mountain areas (<7 km from the shore; altitudes vary between 428 and 845 m.a.s.l.) for the period 2004-2009. A cylindrical fog water instrument (i.e. omnidirectional collection efficiency) based on the ASRC (Atmospheric Science Research Centre, State University of New York) string collector is used to sample fog water volumes (FGW, in mm) on a 10-minute basis [5]. The fog water instrument is a cylinder, 26 cm in diameter and 46 cm in height (fog collection surface: 1196 cm^2), strung with five concentric rows of 0.8 mm thick nylon line. These stations also sampled 10-minute temperature (TEMP, in ºC), relative humidity

(RH, in %), wind speed (WS, in m s^{-1}), wind direction (WD, in º), and precipitation (PCPN, in mm) measurements. Furthermore, all data were subject to quality control in order to detect any unrealistic value check prior to analysis. Missing values are <0.5%, except for the Mt. Bernia (33.1%) and Mt. Helada (28.6%).

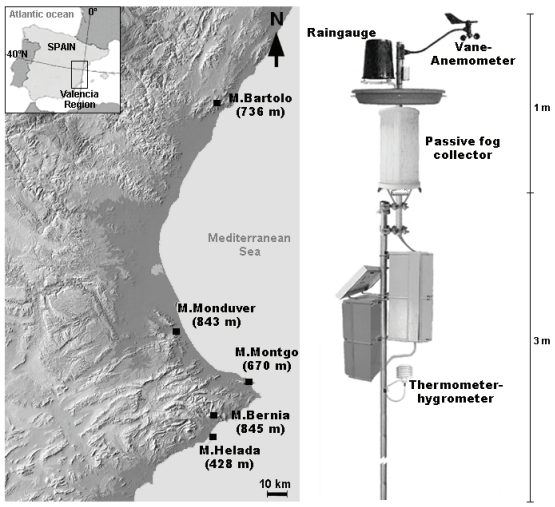

Figure 1: Map of the Valencia region showing locations of the stations (left), and the passive fog collector and meteorological equipment (right)

2.2 Selection of sea breeze fog events

Datasets of past orographic fog events associated with sea breezes were constructed applying two methodologies. Firstly, an initial manual selection consisted on the examination of the daily time series of 10-minute observations of WS, WD, TEMP, RH, PCPN and FGW for each coastal-mountain station. This manual task was considerably laborious. We selected as possible orographic fog episodes associated with sea breezes those days with FGW and PCPN below 5 mm [8]. Moreover, these fog episodes were selected if we observed distinctive features of sea breezes, i.e., a stabilization and slight downward inflection of TEMP curves, and a stabilization and upward inflection of RH curves; WS curves with a steady increase from after sunrise until noon; and a landward-moving WD shift. Those days which met the manual filters were screened using the Western Mediterranean Oscillation Index (WeMOi), as an objective filter for finding fog episodes under weak surface pressure gradients and local winds (i.e., sea breezes). The WeMOi values were computed as the daily normalized difference between the sea level pressure (NCEP/NCAR reanalysis project; [6]) at the point 35ºN, 5ºW and that at the point 45ºN, 10ºE. The [-1,1] threshold interval used here for selecting fog days associated with sea breezes was firstly proposed by [2].

3. Results

3.1 Occurrence of sea breeze Sc clouds

A subset of 192 (Mt. Montgo), 158 (Mt. Bartolo), 157 (Mt. Monduver), 72 (Mt. Bernia) and 64 (Mt. Helada) orographic fog episodes associated with sea breezes were found for the 6-yr study period (Table 1). Therefore, the probability of a day with a sea breeze orographic fog (P_1= [1]/N) is very low for the five passive fog water collectors, being greater in the Mt. Montgo (0.09), the Mt. Monduver (0.07) and the Mt. Bartolo (0.07). The lower probabilities were encountered in the Mt. Bernia (0.05) and the Mt. Helada (0.04), due in part to the missing values.

Table 1: Monthly number (ni), collected volumes (mm) and rates (r; in l/m^2/day) of sea breeze orographic fog events in the five passive fog water collectors for the 6-yr (2004-2009). Maximum values are shown in bold.

	Bartolo			Monduver			Montgo			Bernia			Helada			Σ		
Month	ni	mm	r	ni	mm	r	ni	mm	r	ni	mm	r	ni	mm	r	ni	mm	r
J	0	0.0	0.0	0	0.0	0.0	0	0.0	0.0	0	0.0	0.0	0	0.0	0.0	0	0.0	0.0
F	0	0.0	0.0	0	0.0	0.0	0	0.0	0.0	0	0.0	0.0	0	0.0	0.0	0	0.0	0.0
M	0	0.0	0.0	3	7.2	2.4	2	2.7	1.4	0	0.0	0.0	2	2.4	1.2	7	12.3	1.8
A	5	21.8	**4.4**	7	16.2	2.3	7	27.3	3.9	5	10.9	2.2	3	0.7	0.2	27	76.9	2.8
M	10	26.1	2.6	13	41.2	**3.2**	16	82.7	5.2	3	4.3	1.4	9	**11.5**	**1.3**	51	165.9	3.3
J	28	66.0	2.4	18	21.6	1.2	34	256.9	**7.6**	5	5.5	1.1	11	5.5	0.5	96	355.5	**3.7**
J	**53**	**82.2**	1.6	29	53.4	1.8	47	**325.0**	6.9	16	34.7	2.2	**14**	5.4	0.4	159	**500.6**	3.1
A	43	52.0	1.2	**47**	**110.5**	2.4	**54**	215.0	4.0	**21**	**48.3**	2.3	13	7.5	0.6	**178**	433.3	2.4
S	17	26.5	1.6	23	22.4	1.0	25	70.7	2.8	15	29.9	2.0	7	4.2	0.6	87	153.8	1.8
O	2	4.2	2.1	8	14.9	1.9	7	20.4	2.9	3	1.4	0.5	4	4.2	1.1	24	45.1	1.9
N	0	0.0	0.0	9	6.6	0.7	0	0.0	0.0	4	10.6	**2.7**	1	0.1	0.1	14	17.3	1.2
D	0	0.0	0.0	0	0.0	0.0	0	0.0	0.0	0	0.0	0.0	0	0.0	0.0	0	0.0	0.0
Σ	158	278.9	1.8	157	294.0	1.9	192	1000.8	5.2	72	145.5	2.0	64	41.5	0.6	643	1760.7	2.7

At monthly scale and for the five collectors, the absolute number of sea breeze orographic fog episodes fluctuates from a maximum of 433 episodes for the summer months (Aug. 178; Jul. 159; Jun. 96) to a minimum of 0 for the winter months (Dec., Jan. and Feb.). The remaining number of episodes is of 125 in the autumn months (Sep. 87; Oct. 24; Nov. 14) and 85 in the spring months (Mar. 7; Apr. 27; May 51), showing a marked annual cycle. Fog water volumes fluctuated from a maximum of 1000.8 mm in the Mt. Montgo and a minimum of 41.5 mm in the Mt. Helada. Maximum volumes occurred in July (500.6 mm) and August (433.3 mm) over the five collectors.

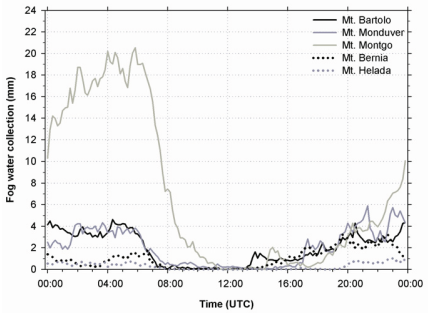

Figure 2: Daily accumulated fog water collection (in mm) under sea breeze conditions for the 6-yr study period (2004-2009)

3.2 Daily sea breeze fog water collection

Fog water collected under sea breeze episodes occurs after midday, preferably during the late evening and until the early next morning, showing a marked daily cycle. The maximum accumulated fog water volumes were found in the Mt. Montgo with 20.5 mm at 0550 h UTC. At all four sites, maximum volumes oscillated between 1 and 6 mm: Mt. Monduver 5.9 mm at 2120 h UTC; Mt. Bartolo 4.6 mm at 0420 h UTC; Mt. Bernia 3.3 mm at 2240 h UTC; and Mt. Helada 1.0 mm at 2300 h UTC (Figure 2). In contrast, the minimum amount of fog water (0 mm) was measured at about noon: Mt. Bartolo between 1140 and 1300 h UTC; Mt. Monduver at 1420 h UTC; Mt. Montgo between 1140 and 1430 h UTC; Mt. Bernia between 1020 and 1250 h UTC; and Mt. Helada between 0800 and 1850 h UTC. This fluctuation is associated with the daily cycle of sea breezes in the CIBL, which develop Sc layer clouds by the rising and cooling of turbulent moist sea air over the highest slopes during the late evening and night (nocturnal radiative cooling). Sc clouds are inhibited at noon because there may not be enough cooling in the ascending air for the water vapour to condense [4].

3.3 Prevailing wind regimes

Wind charts in the Figure 3 show a clear dominance of onshore (i.e. sea breezes) and mountain/valley winds. At Mt. Bartolo, light to moderate (>2.5-5 m s^{-1}) SSE sea breezes dominate with a frequency around 15%, whereas >16% of the fog occur under NNE and SSW winds with higher frequencies for the WS ranges from >5-7.5 m s^{-1} and >7.5 m s^{-1}. No clear dominance in WD was found at the Mt. Monduver, with light to moderate (<5 m s^{-1}) sea breezes coming from a wide range of directions: i.e., spread from NNE to SE (maximum frequency of 10%). However, at the summit of Mt. Monduver for water is collected with light to moderate winds (>2.5 m s^{-1}) coming from the NNW to NE (frequencies ~18% for the NNE direction). The wind pattern for the sea breeze events at the Mt. Montgo shows a clear SSW (~17%) and SSE (~12%) directions, with a dominant component from the NW (~20%) and moderate winds (>2.5 m s^{-1}) when fog is present. In the case of Mt. Bernia, there is a narrow SSE pattern (30-45%) for both wind roses, showing a dominance of winds greater than 5 m s^{-1} when fog is collected. Finally, the Mt. Helada is the only pilot site which displays two main sea breeze components, with light to moderate winds (<7.5 m s^{-1}) from the ESE and WSW, being most frequent (20-25%) for the fog occurrence wind rose. Despite wind roses show that WS is greater when fog is collected (i.e., wind is needed for a passive string collector, [4]), there was no statistically correlation between fog water collected and WS [8].

4. Conclusions and discussions

Sea breeze orographic fog occurrences determine water collection over the mountain ranges near the Iberian Mediterranean coast, particularly from May to September. The results have shown that sea breezes should play an important role for vegetation in the driest summer season. Future research will involve a removal of the rain component, with the aim of addressing the proportion of fog water exclusively associated with sea breezes. To conclude, other parameters should be researched in further detail, such as the influence of sea breezes and Sc development in the inland mountain ranges.

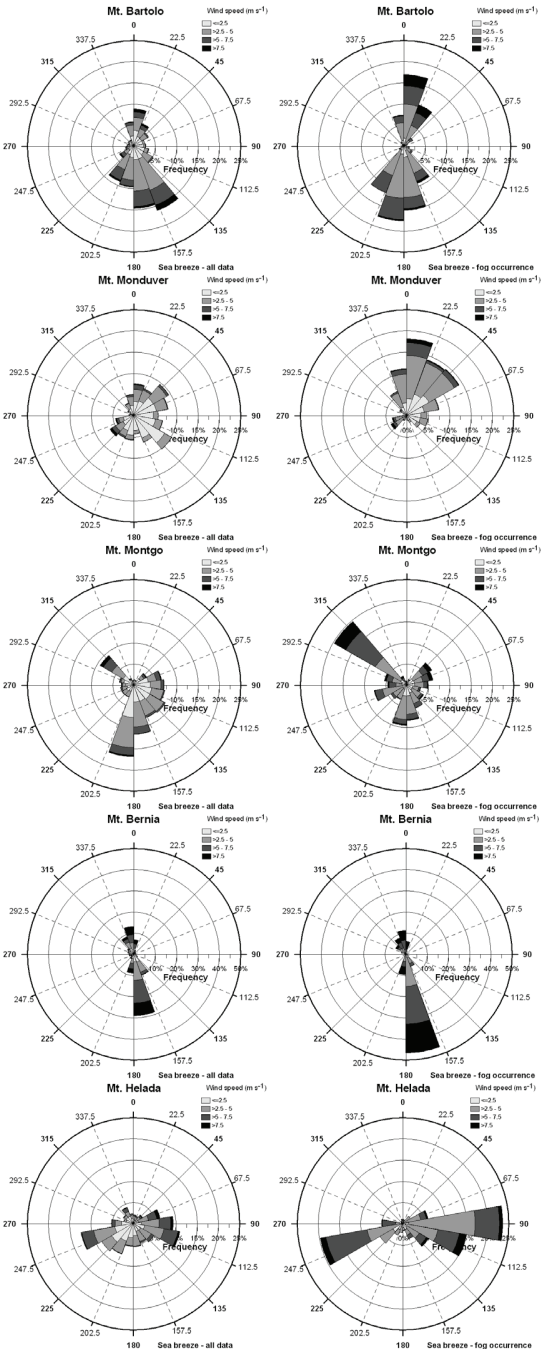

Figure 3: 6-yr wind charts from the five coastal mountain stations for (a, left) the entire dataset of sea breeze days, and (b, right) the 10-minute wind data that simultaneously collected fog water on those sea breeze episodes. Note that the frequency axis of the Mt. Bernia has been adjusted to 50%.

Acknowledgements

The CEAM Foundation is financed by the Generalitat Valenciana. This research was supported by the Spanish Ministerio de Ciencia e Innovación in the frame of the CGL2005-03386 and the CGL2008-04550 contracts, the Consolider–Ingenio 2010 Programme (CSD2007-00067 GRACCIE project) and the Torres Quevedo Program (PTQ-08-02-06762).

References

[1] Azorin-Molina, C., and Martin-Vide, J.: Methodological approach to the study of daily persistence of the sea breeze in Alicante (Spain), Atmosfera, Vol. 20, pp. 57-81, 2007.

[2] Azorin-Molina, C., and Lopez-Bustins, J.A.: An automated sea breeze selection technique based on regional sea-level pressure difference: WeMOi, International Journal of Climatology, Vol. 28 (12), pp. 1681-1692, 2007.

[3] Azorin-Molina, C., Sanchez-Lorenzo, A., and Calbó, J.: A climatological study of sea breeze clouds in the southeast of the Iberian Peninsula (Alicante, Spain), Atmosfera, Vol. 22, pp. 33-49, 2009.

[4] Estrela, MJ., Valiente, J.A., Corell, D., and Millán, M.: Fog collection in the western Mediterranean basin (Valencia region, Spain), Atmospheric Research, Vol. 87, pp. 324-337, 2008.

[5] Falconer, R.E. and Falconer, P.D.: Determination of fog cloud water acidity at a mountain observatory in the Adirondack Mountains of New York State, Journal of Geophysical Research, Vol. 85, pp. 7465-7470, 1980.

[6] Kalnay, E. and Coauthors.: The NCEP/NCAR 40-Year Reanalysis Project, Bulletin of the American Meteorological Society, Vol. 77, pp. 437-471, 1996.

[7] Kimura, K..: Origin of the fog in Namib desert in dry season, African Study Monographs, Vol. 30, pp. 57-64, 2005

[8] Marzol, M.V.: Temporal characteristics and fog water collection during summer in Tenerife (Canary Islands, Spain), Atmospheric Research, Vol. 87, pp. 352-361, 2008.

[9] Salvador, R., and Millán, M.: Análisis histórico de las brisas en Castellón, Tethys, Vol. 2, pp. 37-51, 2003.

5th International Conference on Fog, Fog Collection and Dew
Münster, Germany, 25–30 July 2010
FOGDEW2010-39

Fog and rain water chemistry in the western Mediterranean basin (Valencia region, Spain)

D. Corell (1), C. Azorin (1,2), M.J. Estrela (1,3), J.A. Valiente (1), F. Sanz (1), F. Pastor (1), S. Barceló (4)

(1) Laboratory of Meteorology-Climatology, Mixed Unity CEAM-UVEG, The CEAM Foundation, Paterna (Valencia), Spain, (dacocus@ceam.es / Fax: +34 96 131 81 90) (2) Group of Climatology, University of Barcelona, Barcelona, Spain, (3) Laboratory of Meteorology-Climatology, Mixed Unity CEAM-UVEG, Geography Department, University of Valencia, Valencia, Spain, (4) Department of Applied Statistics and Operations Research, Polytechnic University of Valencia, Valencia, Spain

Abstract

The present study attempts to characterize the chemistry composition of fog and rain water in the eastern region of the Iberian Peninsula (Valencia, Spain). This research is based upon a network of seven cylindrical fog water collectors distributed over 4 coastal- and 3 inland-mountain ranges. The fog and rain water samples were collected during the 9-month study-period April-December 2008. The fog and rain water samples were analysed for pH, Cond. and Alk., and the following ion concentrations: Ca^{2+}, Mg^{2+}, Na^{+}, K^{+}, Cl^{-}, NO_3^{-} and SO_4^{2-}. The stations also collected other atmospheric measurements such as 10-min temperature, humidity, wind speed and direction, fog and precipitation. In addition, the HYSPLIT (HYbrid Single-Particle Lagrangian Integrated Trajectory) model was used for each fog event in order to know the origin and the pathway of air masses during the previous five days. Preliminary results show two main origins of the air masses, one of them associated with recirculation processes over the Mediterranean Sea, whose fog water samples were more contaminated, and other associated with advection from the Atlantic Ocean, whose fog water samples were cleaner. The chemical composition of the fog and rain is of crucial importance for future applications of water.

1. Introduction

Since 2003, the CEAM Foundation maintains a fog collection network in the Valencia Region (Spain), in the eastern fringe of the Iberian Peninsula. Ten passive fog collectors have been installed since then, covering the region from North to South, as well as from the coast to the inland areas [8]. High fog collection rates have been measured in some of the experimental sites, which have allowed to develop a reforestation project [4]. The overall aim of this work is to describe the chemical composition of fog and rain water collected in the Valencia Region (Spain). To our knowledge, no research has yet attempted to study the chemical features of fog and its meteorological origin in Spain. Only in the Canary Islands have been carried out chemical studies about composition of fog [6], so this work is designed to gain a better understanding of fog, which is of crucial importance for future applications of collected fog water.

2. Methodology

2.1 Sites description

Seven of the ten stations of the fog passive collector network were selected for this study. Their locations covered an area bounded between 40.01º and 38.56º latitude and 0.13º and -0.89º longitude, and their altitudes ranged between 1,256 and 428 m a.s.l.. Four of the stations were located less than 7 km inland and 3 of them were placed in a distance of more than 40 km from the nearest coastline (figure 1).

2.2 Fog and rain water collection

Fog and rain water samples were collected from April to December 2008 on a fortnightly basis. The fog water was collected by using a handmade passive string fog collector (i.e., omnidirectional collection efficiency) based on the ASRC (Atmospheric Science Research Center, State University of New York) device [5]. It basically consisted of a cylinder, 26 cm in diameter and 46 cm in height (fog

collection surface: 1196 cm^2), strung with five concentric rows of 0.8 mm thick nylon line. A rain shield was attached to the top of the string collector to prevent contamination by rain as far as possible. The rain water was sampled by using a tipping bucket raingauge located at the top of the weather station (rain collection surface: 212 cm^2). Both fog and rain water, once collected by the meteorological devices, dripped into a 2 L polyethylene bottle, where remained until the next sampling date. At every sampling site, the experiment was complemented with 10-minute measurements of temperature, relative humidity, fog, rain and wind speed and direction (figure 1), which provided information about the exact time of the collected samples.

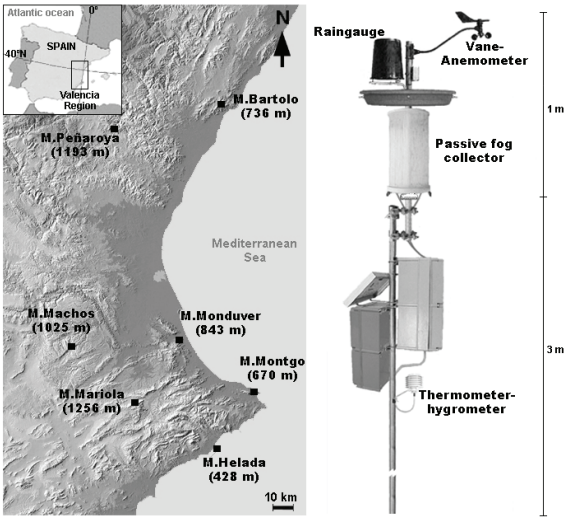

Figure 1: Terrain map of the Valencia Region showing locations of fog water collectors (left) and example of passive fog collector and meteorological measuring equipment (right)

2.3 Trajectories

Backward trajectories are a widely used method for the identification of the origin and the pathway of air masses and are often used to study the advection of air pollutants ([1], [2]). In this work, for every fog sample, we calculated the backward trajectory of every fog event which occurred during the 15-day sampling period using the HYSPLIT model ([3], [7]), (http://www.arl.noaa.gov/ready.php). Each trajectory indicated the path followed by the respective air masses during the last 5 days (120 h) at 1 m above surface level.

2.4 Chemical analysis and quality control

The rain and fog samples were stored in 250 ml polyethylene bottles at 4º C in the refrigerator prior the analysis. The electrical conductivity was measured using a conductivity meter Jenway 4520 and the pH with a pH meter Crison GLP21. Then the samples were filtered through 0.45 µm pore size Sartorius cellulose acetate filters and measured the anions (Cl^-, NO_3^-, SO_4^{2-}) by anion chromatography (Dionex DX120; AS4A column; electrical autosupression ASRS 300; and Na_2CO_3/$NaHNO_3$ eluent), the cations (Ca^{2+}, Na^+, K^+, Mg^{2+}) by optical ICP (Perkin Elmer 4300 DV) and alkalinity by Gran Titration (Crison Compact Titrator). All analyses included synthetic samples of known concentrations to check precision and accuracy of the results.

2.5 Statistical methods

As the bottles stayed in field for 15-day periods, samples could contain water from different fog and rain episodes and therefore, from different origin. To avoid this and to study the chemical composition of fog water in relation to its origin, firstly we computed, for every fog sample, the backward trajectory of every fog event, and secondly, only samples whose trajectories had similar pathways were used in the analysis. With these pure samples, two multivariate statistical analyses were performed: (a) Clustering Analysis to divide the samples into groups, and (b) Principal Component Analysis to interpret the results.

3. Results

3.1 Ion concentrations in fog and rain

119 bottle samples were collected (71 of fog and 48 of rain) during the campaign. Table 1 reports the descriptive statistics of fog and water concentration samples. Overall, conductivity, alkalinity and ion concentrations varied widely, with maximum and minimum values which showed large differences. The average pH of fog varied from 6.39 to 6.97, whereas rain presented slightly higher pH values (~7), except for two inland stations which showed a moderately acid pH (M.Machos and M.Peñaroya). In general, conductivity and ion concentrations presented the same pattern, with higher values in fog samples. At inland stations Ca^{2+} and NO_3^- were the prevailing ions, whereas at coastal stations Na^+ and NO_3^- were the dominant ions.

3.2 Origin of the collected fog water

Only 24 fog samples were used to perform this analysis. All of them could contain water collected from different fog episodes, but always with a similar backward trajectory. This ensured there was no sample with a mix of origins. The Cluster Analysis produced 2 different groups of greatest possible distinction. The cluster 1 contained 9 samples, while the cluster 2 grouped 15. The Principal Component Analysis was used to explore the data relationship. 3 components were extracted, which explained 93 % of the total variance. The component 1 explained 78 % of the total variance and was positively correlated with the ion concentration and conductivity, as well as weakly with alkalinity and pH, so it was interpreted as a size factor. The combination of both statistical analyses showed that the cluster 1 members presented higher values for the component 1, while the cluster 2 members showed lower values. To conclude, the cluster 1 contained samples with larger ion concentrations and the cluster 2 included less contaminated fog water samples (table 2).

Table 2: Chemical composition of fog water from the two clusters. Conductivity in µS cm^{-1}, Alkalinity in µeq l^{-1}, Ion Concentrations in mg l^{-1}

	Cluster 1 (n=9)			Cluster 2 (n=15)		
	avg	max	min	avg	max	min
pH	6.93	7.43	6.16	6.09	6.81	5.31
Cond	477.7	807.0	258.0	77.4	288.0	11.1
Alk	458.2	725.9	179.3	59.7	311.4	5.0
Ca^{2+}	56.8	156.9	18.6	5.1	16.3	0.6
K^{+}	2.2	4.2	0.6	0.5	1.3	0.1
Mg^{2+}	8.6	28.0	1.6	1.0	2.6	0.1
Na^{+}	48.7	179.5	5.2	5.3	16.5	0.5
Cl^{-}	48.6	102.9	10.8	10.9	40.2	0.7
NO_3^{-}	111.2	318.8	62.7	16.0	57.7	1.9
SO_4^{2-}	49.0	184.7	16.0	7.9	28.2	1.4

Backward trajectories of the cluster 1 samples were mainly associated with the Azores High, with large runs over the Mediterranean Sea (E and NE winds) and also presented recirculation processes (sea breezes). Most of them were collected in summer (figure 2, top). Backward trajectories of the cluster 2

Table 1: Chemical composition of fog and rain water from the seven mountainous sites of the Valencia Region (April-December 2008). Conductivity in µS cm^{-1}, Alkalinity in µeq l^{-1}, Ion Concentrations in mg l^{-1}

Station	M.Bartolo		M.Helada		M.Monduver		M.Montgo		M.Machos		M.Mariola		M.Peñaroya	
Type	Rain	Fog	Rain	Fog	Rain	Fog	Rain	Fog	Rain	Fog	Rain	Fog	Rain	Fog
N samples	3	8	7	6	11	18	0	2	10	12	9	12	8	13
pH avg	6.79	6.53	6.94	6.97	6.93	6.39	-	6.46	4.94	6.50	7.08	6.80	4.32	6.69
max	6.93	7.19	7.89	7.47	7.48	6.81	-	6.46	5.93	7.44	8.02	7.50	6.92	7.43
min	6.59	5.87	5.96	6.63	6.25	5.31	-	6.46	3.32	5.60	6.61	5.30	3.50	5.72
Cond avg	154.7	483.8	308.3	747.0	88.1	286.9	-	466.0	131.3	164.9	182.0	169.8	90.8	255.8
max	397.0	1024.0	535.0	1170.0	335.0	840.0	-	564.0	344.0	539.0	580.0	525.0	244.0	772.0
min	28.2	50.5	141.7	253.0	22.2	11.1	-	368.0	23.8	39.8	20.2	2.2	45.8	24.1
Alk avg	175.0	310.3	321.5	833.4	290.4	264.4	-	301.8	21.7	261.7	264.0	358.9	26.4	313.7
max	420.9	725.9	519.0	1862.2	619.1	710.3	-	349.0	71.3	1200.4	911.2	1025.4	158.3	1207.8
min	31.0	5.0	128.6	298.8	67.4	26.8	-	254.6	0.0	0.0	75.3	0.0	0.0	16.7
Ca^{2+} avg	6.6	82.6	30.3	85.6	19.8	37.6	-	55.3	13.9	15.2	32.8	68.4	8.0	41.0
max	11.5	180.8	89.5	229.9	82.4	179.2	-	57.4	74.2	57.8	183.1	491.1	41.0	190.0
min	3.5	2.4	7.5	23.3	1.9	0.6	-	53.2	1.9	2.2	2.6	1.3	1.1	2.3
K^{+} avg	0.4	4.8	1.6	8.1	1.4	1.4	-	3.4	0.9	0.8	2.2	2.0	1.3	2.0
max	0.7	10.1	4.2	16.9	7.4	4.4	-	4.0	4.8	2.2	13.7	12.3	8.0	7.3
min	0.2	0.1	0.7	3.1	0.1	0.1	-	2.7	0.1	0.2	0.1	0.2	0.1	0.2
Mg^{2+} avg	1.2	14.8	5.5	100.2	4.3	6.1	-	14.5	2.6	2.1	3.5	6.2	0.9	3.7
max	2.3	35.1	15.8	481.9	19.7	28.0	-	18.0	14.0	5.6	16.2	41.7	4.8	14.0
min	0.6	0.4	2.1	10.9	0.4	0.1	-	11.0	0.3	0.6	0.3	0.4	0.1	0.2
Na^{+} avg	6.9	92.1	31.0	151.8	21.6	30.8	-	88.9	8.6	11.0	16.2	33.4	2.4	17.7
max	13.8	240.5	83.6	446.0	129.8	179.5	-	103.8	57.4	31.8	64.3	232.0	11.1	66.2
min	3.0	1.6	7.8	66.1	0.7	0.5	-	74.1	0.6	0.8	0.8	1.3	0.2	0.5
Cl^{-} avg	18.2	56.9	39.3	98.0	16.7	28.1	-	54.9	16.2	14.4	13.8	23.9	23.5	14.7
max	45.0	102.9	67.1	231.9	102.1	84.0	-	64.3	53.6	43.5	46.4	81.7	144.3	32.6
min	4.5	6.3	14.0	11.0	1.7	1.2	-	45.4	1.8	3.8	0.6	2.0	2.6	0.7
NO_3^{-} avg	15.1	105.3	28.8	98.7	14.8	47.7	-	63.5	9.7	26.2	10.8	52.3	9.7	50.1
max	29.1	318.8	57.3	273.1	127.2	165.9	-	63.7	38.9	82.9	71.0	243.8	53.5	155.4
min	5.6	7.3	8.2	5.5	0.2	0.1	-	63.3	0.6	1.1	0.1	1.9	0.8	7.3
SO_4^{2-} avg	13.6	55.8	16.2	52.7	8.1	21.4	-	33.9	5.3	13.6	18.5	20.9	8.0	18.2
max	30.5	184.7	26.3	164.4	50.8	83.0	-	38.0	16.0	40.2	94.5	94.0	49.1	64.3
min	3.4	6.3	6.6	5.9	1.5	1.7	-	29.8	1.2	1.2	0.8	1.9	1.0	1.4

samples were associated with long-distance air masses coming from the Atlantic Ocean, which barely traveled over the Mediterranean Sea, and they were collected in spring or autumn (figure 2, bottom).

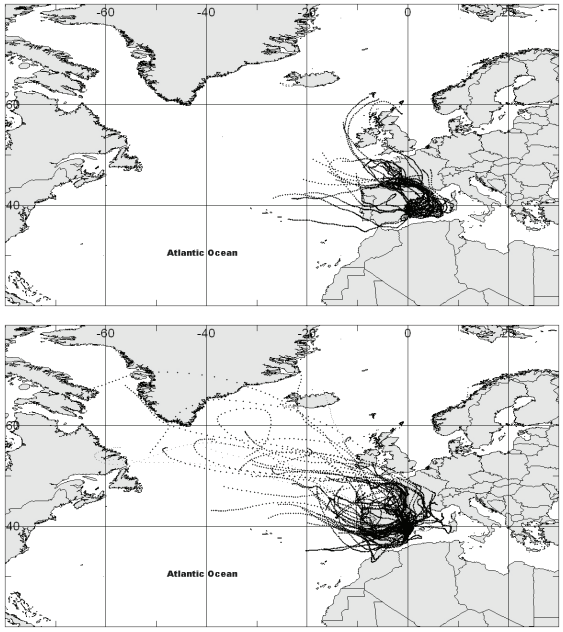

Figure 2: 120 h backward trajectories for every fog event collected for the cluster 1 (top) and the cluster 2 samples (bottom)

4. Conclusions

This study has characterized the chemical composition of the fog and rain at 7 different sites of the Valencia Region. Besides, the backward trajectories analysis has showed different ion concentrations depending on the origin of the air masses. Air masses associated with recirculation processes over the Mediterranean Sea brought water samples with larger ion concentrations than those which came directly from the Atlantic Ocean. Future studies will analyze the synoptic patterns associated with the two clusters found here, as well as the role played by dry deposition.

Acknowledgements

The CEAM Foundation is financed by the Generalitat Valenciana. This research was supported by the Spanish Ministerio de Ciencia e Innovación (CGL2005-03386 and CGL2008-04550 contracts), the Consolider–Ingenio 2010 Programme (CSD2007-00067 GRACCIE project) and the Torres Quevedo Program (PTQ-08-02-06762). The authors gratefully acknowledge the NOAA Air Resources Laboratory (ARL) for the provision of the HYSPLIT transport and dispersion model and/or READY website (http://www.arl.noaa.gov/ready.php) used in this publication. We also thank the staff of the Parque Natural de la Sierra de Mariola and the Conselleria de Territori i Habitatge for their help to collect the samples at M.Mariola and M.Monduver respectively.

References

[1] Avila, A. and Alarcón, M.: Relationships between precipitation chemistry and meteorological situations at a rural site in NE Spain, Atmospheric Environment, Vol. 33, pp. 163-1677, 1999.

[2] Beiderwieden, E., Wrzesinsky, T. and Klemm, O.: Chemical characterization of fog and rain water collected at the eastern Andes cordillera, Hydrology and Earth System Sciences, Vol. 9, pp. 185-191, 2005.

[3] Draxler, R.R. and Rolph, G.D.: HYSPLIT (HYbrid Single-Particle Lagrangian Integrated Trajectory) Model access via NOAA ARL READY Website (http://ready.arl.noaa.gov/HYSPLIT.php). NOAA Air Resources Laboratory, Silver Spring, MD, 2010.

[4] Estrela, M.J., Valiente, J.A., Corell, D., Fuentes, D. and Valdecantos, A.: Prospective use of collected fog water in the restoration of degraded burned areas under dry Mediterranean conditions, Agricultural and Forest Meteorology, Vol. 149, pp. 1896-1906, 2009.

[5] Falconer, R.E. and Falconer, P.D.: Determination of fog cloud water acidity at a mountain observatory in the Adirondack Mountains of New York State, Journal of Geophysical Research, Vol. 85, pp. 7465-7470, 1980.

[6] Marzol, M.V.: La captación del agua de niebla en la isla de Tenerife, Caja General de Ahorros de Canarias, Vol. 333, 2005.

[7] Rolph, G.D.: Real-time Environmental Applications and Display sYstem (READY) Website (http://ready.arl.noaa.gov). NOAA Air Resources Laboratory, Silver Spring, MD, 2010.

[8] Valiente, J.A., Estrela, M.J. and Corell, D.: A fog collection network in the Valencia Region (Western Mediterranean Basin), Fourth International Conference on Fog, Fog Collection and Dew, 22–27 July 2007, La Serena, Chile, 2007.

5th International Conference on Fog, Fog Collection and Dew
Münster, Germany, 25–30 July 2010
FOGDEW2010-40

Droplet distribution models for visibility calculation

F. Bernardin (1), M. Colomb (1), F. Egal (1), P. Morange (1), and J.-J. Boreux (2)
(1) Laboratoire Régional des Ponts et Chaussées, 8-10 rue B. Palissy, Clermont-Ferrand, France, (2) Université de Liège-Campus d'Arlon, Avenue de Longwy, 185B-6700 Arlon, Belgium (frederic.bernardin@developpement-durable.gouv.fr)

Abstract

In order to address the reduction of visibility due to fog, investigations are undertaken by reproducing the effect of fog by numerical simulation, namely, with a model of light scattering connected to Mie theory. This model needs to integrate droplet distributions or models of particle size in the software. The assumptions for models of particles made so far are based on the work [1] . All the data we have today thanks to experiments in natural fog, allows us to test the application of these models on new data and suggest improvements in case of divergence. This study uses simulations with Gamma and Log-normal laws. The combination of these new simulations with light scattering theory, are able to update models considered in determining road visibility.

1. Introduction

More efficient predictions of fog occurrence and visibility are required in order to improve both safety and traffic management in critical adverse weather situations. Observation and simulation of the fog characteristics contribute to a better understanding of the phenomena and to adapt technical solutions against visibility reduction. The simulation of visibility reduction by fog condition using light scattering model depends on the size and concentration of droplets (see [6]). Therefore it is necessary to include in the software some functions for the droplet distribution model rather than some data file of single measurement. The aim of the present work is to revisit some droplet distribution models of fog ([1]) in order to actualise them by using recent experimental measures. Indeed the models mentioned above were established thanks to experimental data obtained with sensors of 70's. Actual sensors are able to take into account droplets with radius 0.2 µm which was not the case with older sensors. A surface observation campaign was carried out at Palaiseau, France, between 2006 and 2007. These experiments allowed to collect microphysical data of fog and particularly droplet distributions of the fog, thanks to a "Palas" optical granulometer. Based on these data an analysis is carried out in order to provide a droplet distribution model. The first approach consists in testing the four Gamma laws proposed by [1]. The adjustment of coefficients allows changing the characteristics from advection to radiation fog. These functions did not fit the new set of data collected with the Palas sensor. New algorithms based on Gamma and Lognormal laws are proposed and discussed in comparison to the previous models. For a road application, the coefficients of the proposed models are evaluated for a visibility around 50 meters.

Determining the distribution of droplets is the first step to simulate fog and forecast visibility, as all of the fog characteristics come directly from its microphysical structure. Droplet concentration and droplet size are the two critical parameters to be determined. This distribution then allows the calculation of various parameters that will be used to determine the visibility. Once a general shape of fog distributions has been determined, it is possible to propose mathematical models that will simulate the fog distribution for various size and concentrations of droplets. Then by using the Mie theory described in the next section, the corresponding reduction of visibility can be determined.

2. Mie theory

The series of formulas used to calculate the visibility are known as Mie theory (see [5]). The amount of light that won't reach the eye of the observer is related to the extinction coefficient Ke. This coefficient is related the radius r of the droplet through the following formula :

$$K_e = \pi \int_r Q_{ext}(r) r^2 n(r) dr, \qquad (1)$$

$n(r)$ being the number of particles in a given volume. The coefficient Q_{ext} is dimensonless and depends on the droplet size and of the wavelength and varies between 1 and 4 and stabilizes around 2 for drops with a radius of a few microns (see Figure 1).

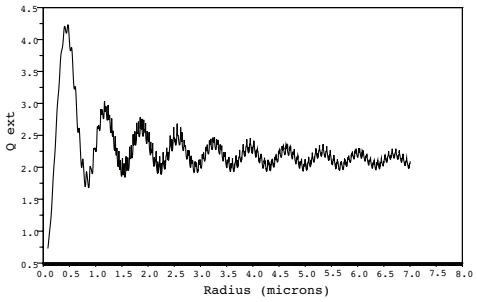

Figure 1: The function Q_{ext} versus the droplet radius for a wavelength equal to 550 nm.

If a granulometer is used to count the number of particles, the formula can be modified as follows:

$$K_e = \pi \sum_{i=1}^{N} Q_{ext}(r_i) r_i^2 N_i \tag{2}$$

where N is the number of classes of radius, N_i the number of droplets in the class of the radius r_i. It should be noted that the extinction coefficient depends on r^2, meaning that even a few large drops will have a considerable influence on fog density. Once the coefficient of extinction has been calculated, the atmospheric visibility V in meters is given by the equation:

$$V = \frac{3}{K_e}. \tag{3}$$

3. Theoretical models of fog distribution

3.1. The considered laws

We propose to revisit, using measurements by current sensors, fog distribution models still used today. This study is based on the work [2] and [1] in which two theoretical models are developped. We propose to confront experimental data collected during the 2006-2007 winter season (Paris, France). This work [2, 1] mentioned laws Log-normal and Gamma amended to model the size of the fog. Denoting $n(r)$ the number of droplets of radius r present in a sample of volume 1 cm^3, the Log-normal law is defined by:

$$n(r) = \frac{N}{r\sigma\sqrt{2\pi}} \exp\left(-\frac{(\ln r - \ln \tilde{r})^2}{2\sigma^2}\right), \tag{4}$$

where σ is the standard deviation of the experimental distribution $\ln r$ and $\tilde{r}$ is such that $\ln \tilde{r}$ is the mean of this distribution (see [2]).

The modified Gamma law (see [1]) is expressed as:

$$n(r) = a r^{\alpha} e^{-b r^{\gamma}},\ r \geq 0, \tag{5}$$

where a, b, α and γ are parameters to be determined.

We also propose in this study to consider a shifted Gamma law: aerosols whose radius is below a certain threshold r_{min} are either inaccessible by experimental measurements or are not considered as fog particles. We then assume that $n(r)$ vanish under a radius r_{min}.

3.2. Gamma laws of Shettle and Fenn

We present in Table 1 the values of the parameters a, b, α and γ of (5) given in [1]. In Figure 2, we present experimental distributions with the 4 models of [1]. We can see an inadequacy between experimental and such theoretical models.

Table 1: Values of the parameters for the four modified Gamma laws of [1].

Fog type	Model	a	α	b	γ
Advection	1	0.06592	3	0.3	1
Advection	2	0.027	3	0.375	1
Radiation	3	2.37305	6	1.5	1
Radiation	4	607.5	6	3.0	1

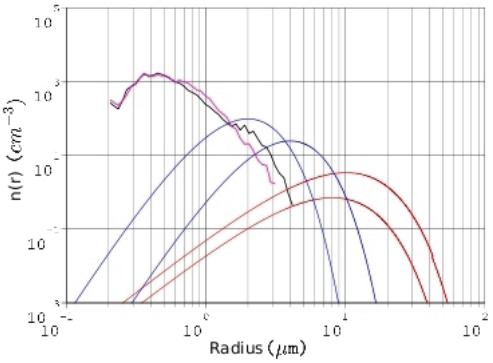

Figure 2: Shettle and Fenn models and experimental distributions.

4. Estimation of the parameters

We describe here the method allowing to estimate the parametrs of (5) from an experimental fog distribution. Let us assume that we know for a fog sampling :

- the total number N of droplets;
- the modal radius r_m;
- the number of droplets N_m for the modal radius.

The modal radius r_m corresponds to the radius for which the derivative of $n(r)$ vanishes. This leads to:

$$a = N_m r_m^{-\alpha} e^{\alpha/\gamma}, \tag{6}$$

$$b = \frac{\alpha}{\gamma} r_m^{-\gamma}. \tag{7}$$

and

$$\frac{1}{\gamma} e^{\alpha/\gamma} \left(\frac{\gamma}{\alpha}\right)^{\frac{\alpha+1}{\gamma}} \Gamma\left(\frac{\alpha+1}{\gamma}\right) = \frac{N}{r_m N_m}, \tag{8}$$

where $\Gamma(x)$, for $x > 0$ is given by:

$$\Gamma(x) = \int_0^\infty t^{x-1} e^{-t} dt. \tag{9}$$

The constraint (8) gives then *a priori* several couples (α, γ), each couple fixing, thanks to (6) and (7), the values of a and b. Assuming $\gamma = 1$ as it is made in [2, 1], only one value for α is possible and by then for a and b.

For a shifted law, that is $n(r) = 0$ if $r \leq r_{min}$ and

$$n(r) = a\,(r - r_{min})^{\alpha}\, e^{-b(r-r_{min})^{\gamma}}, r \geq r_{min}, \tag{10}$$

the previous calculations can be performed with

$$\frac{1}{\gamma} e^{\alpha/\gamma} \left(\frac{\gamma}{\alpha}\right)^{\frac{\alpha+1}{\gamma}} \Gamma\left(\frac{\alpha+1}{\gamma}\right) = \frac{N}{(r_m - r_{min})\, N_m}. \tag{11}$$

instead of (8).

5. Values of the parameters estimated from experimental data

We are interested in a fog event appeared in the night of 13 to 14 March 2007 on the site of Palaiseau (ParisFog campaign [3, 4]). In this study, we implemented the procedure described in the previous section for a visibility of 50 meters and we give in Table 2 the associated average values coefficients of the shifted Gamma and the Log-Normal laws. For this, 10 samples of experimental distributions have been used.

In Figure 3 we present the 10 experimental distributions and the theoretical ones. We can observed a good fitting of the shifted Gamma law. The calculation of the visibility for the theoretical laws is about 75 m wich is in the same order of magnitude with the target value 50 m. A better theoretical model could be carried out by adding a constraint on the visibility. Indeed, instead of taking $\gamma = 1$ for the shifted Gamma law it could be possible to research new values a, b, α and γ in order to solve (6)-(11) and a new constraint on the visibility given by (1) and (3). This approach will be the topic of futur works.

Table 2: Values of the parameters of the Log-Normal and shifted Gamma laws.

		Log-Norm.		Shifted Gamma		
Vis.	N	$-\ln\tilde{r}$	σ	α	$10^{-3}a$	b
52	1330	0.44	0.59	0.87	30,9	5.06

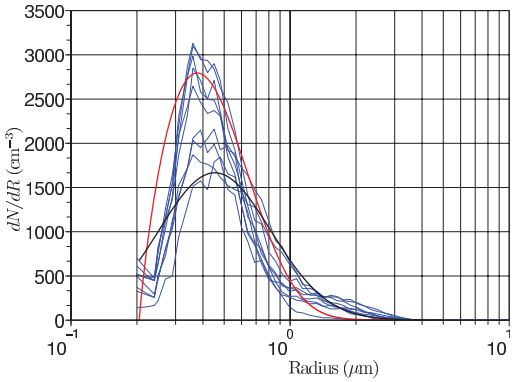

Figure 3: Experimental and theoretical distributions for a visibility around 50 meters.

6. Summary and Conclusions

This paper presents some results of simulations of droplet distribution with Gamma and Log-normal laws. This work uses a set of natural droplet distribution measured during the ParisFog experiment. These data are mostly representative of radiation fog. To extend this simulation, it will be useful to test the model on new set of data representative of advection fog and also of bi-modal distribution. Therefore some new approach with Bayesian statistical theory will be considered.

References

[1] Shettle, E.P., and Fenn, R.W.: Models for the Aerosols of the Lower Atmosphere and the Effects of Humidity Variations on Their Optical Properties, AFGL-TR-79-0214 Airforce Geophysics Laboratory, Hanscom Air Force Base, MA, USA, 1979.

[2] Tschirhart, G.: Caractéristiques physiques générales des brouillards, Monographies de la météorologie nationale, Vol. 92, 1974.

[3] Bergot, T., Haeffelin, M., Musson-Genon, L., Tardiff, R., Colomb, M., Boitel, C., Bouhours, G., Bourriane, T., Carrer, D., Challet, J., Chazette, P., Drobinski, P., Dupont, E., Dupont, J.-C., Elias, T., Fesquet, C., Garrouste, O., Gomes, L., Guérin, A., Lapouge, F., Lefranc, Y., Legain, D., Morange, P., Pietras, C., Plana-Fattori, A., Protat, A., Rangognio, J., Raut, J.c., Remy, S., Richard, D., Romand, B. and Zhang, X.: Paris-Fog, des chercheurs dans le brouillard, La Météorologie, Sér. 8, Vol. 62 , p. 48-58, 2008.

[4] Elias, T., Haeffelin, M., Drobinski, P., Gomes, L., Rangognio, J., Bergot, T., Chazette, P., Raut, J.-C., Colomb, M.: Particulate contribution to extinction of visible radiation: pollution, haze, and fog, Journal of Atmospheric Research, Vol. 92, pp. 443-454, 2009.

[5] Mie, G.: Beitrage zur Optik Truber Medien, speziell koolloidaler Metallosungen, Ann. Phys., Vol. 25, pp. 377-452, 1908.

[6] Dumont, E.: Semi-Monte Carlo light tracing applied to the study of road visibility in fog, Monte Carlo and Quasi-Monte Carlo Methods, pp.177–187, 1998.

5th International Conference on Fog, Fog Collection and Dew
Münster, Germany, 25–30 July 2010
FOGDEW2010-41-1

The role of emission background on fog chemistry at some selected mountain tops in Poland

M. Godek (1), M. Błaś (1), Z. Polkowska (2), and M. Sobik (1)

(1) Department of Climatology and Atmosphere Protection, Institute of Geography and Regional Development, University of Wroclaw, Poland, e-Mail: godek@meteo.uni.wroc.pl, (2) Gdansk University of Technology, Chemical Faculty, Department of Analytical Chemistry

Sudety Mountains and Western Carpathians form significant orographic thresholds and airflow deformation as a consequence. Fog deposition play a dominant role within the structure of the wet deposition. Intensive development of power industry in surroundings of the mountains resulted in catastrophic ecological disaster in forest ecosystems, which became clearly visible since 1978. Air pollution concentration in Western Sudetes between 1979 and 1982 achieved the highest level ever measured in Europe and pH values of fog and precipitation below 3,8 were observed frequently. Due to this situation only in Polish part of Sudety Mountains over 13500 ha of forest have been destroyed and 92,7% of remaining conifers was classified as partially damaged. Currently pollutants emission decreases, none the less still acquires high level and cumulated effect on soil and trees reacts. Since the beginning of XXI century forest disaster proceeds in the Western Carpathians and the territorial range of disaster still continous to expand.

The main goal of the project was to compare chemical structure of fog from different mountainous locations in the context of emission background and different circulation directions. There were 3 measurement points installed for collecting daily samples of fog deposition from February 2009 to January 2010. Each point has been located on the top of the mountain on the altitude range between 1200 and 1400 m a.s.l., as well as selected as a representative for wider mountainous area: Mt. Szrenica (Western Sudety Mountains), Mt. Snieznik (Eastern Sudety Mountains), Mt. Skrzyczne (Western Carpathians). They form horizontal profile from Northwest do Southeast with the lenght about 300 kilometres. Solid and liquid samples of fog were collected daily using passive fog collectors.

It was established that the efficiency of fog precipitation decreases significantly from the Western Sudety Mts to the east. Solid fog deposit amounts 4 times higher volume of water at the Mt. Szrenica when compare with the Mt. Śnieżnik (Eastern Sudety Mts). It is due to much better exposure of Mt. Szrenica for maritime air masses coming from the SW-W-NW sector. Farther to the east fog deposition efficiency slightly increases and at the Mt. Skrzyczne amounts to 30% of the Mt. Szrenica value. Mt Skrzyczne is surrounded from the west to the north by deep terrain depressions, which separates the Bohemian Massif (with the Sudety Mts) from the Western Carpathians. Efficiency of the liquid fog deposition was similar in proportion: 40% at the Mt Snieznik and 60% at the Mt. Skrzyczne, respectively.

Chemical compounds were determined for 700 fog samples. Weighted mean of pH values changed from 4,21 at the Mt. Szrenica to 4,90 at the Mt. Skrzyczne. The most important ions, within the structure of the fog water, were the following: SO42- at the Mt. Snieznik (over 0,080 meq/l) and NO3- at the Mt. Szrenica (over 0,070 meq/l).

There were also taken dendrochronological samples from the stems of upper spruce to find relations between air pollution concentration and spruce vitality, visible in the size of annual tree rings. Period of reduced vitality in the eighties of the XX century and increasing of the tree's condition in next decade is clearly visible.

5th International Conference on Fog, Fog Collection and Dew
Münster, Germany, 25–30 July 2010
FOGDEW2010-43

Climatology of dew in Poland

M. Sobik (1), M. Błaś (1), and Ż Polkowska (2)

(1) Department of Climatology and Environment Protection, University of Wroclaw, 8 Kosiby Street, PL-51670, Wrocław, Poland (sobik@meteo.uni.wroc.pl, +48-71-372-94-98), (2) University of Technology, Chemical Faculty, 11/12 G. Narutowicza St., 80-233 Gdańsk, Poland, (zaneta@chem.pg.gda.pl,+48 58 347-26-94)

It is known from earlier studies that locally in Poland dew consists a considerable component of water flux from atmosphere to the ground. The maximum reported values reach more than 50 mm annually which is around 10% of water delivered via non-wintertime precipitation. Within the present project dew collectors were installed in 12 sites representing different geographic regions of Poland and, on the other hand, different types of landuse. Samples are collected with the use of unified equipment and methodology. The deposited volume of dew/hoarfrost and accompanying weather conditions as well as ionic composition is controlled and will be controlled over one year at these sites until the end of the ongoing winter.
On the basis of daily values of water volume deposited via dew/hoarfrost, basic statistical indices will be calculated. Weather conditions that control the intensity of dew/hoarfrost deposition will be examined as well as atmospheric circulation patterns which favor dew/hoarfrost will be quantitatively characterized. Additionally local relief and landuse will be discussed as potential controls of dew/hoarfrost deposition.

5th International Conference on Fog, Fog Collection and Dew
Münster, Germany, 25–30 July 2010
FOGDEW2010-44

Some aspects of spatial distribution of dew chemistry in Poland

M. Sobik (1), Ż Polkowska (2), and M. Błaś (1)

(1) Department of Climatology and Environment Protection, University of Wroclaw, 8 Kosiby Street, PL-51670, Wrocław, Poland (sobik@meteo.uni.wroc.pl, +48-71-372-94-98), (2) University of Technology, Chemical Faculty, 11/12 G. Narutowicza St., 80-233 Gdańsk, Poland, (zaneta@chem.pg.gda.pl,+48 58 347-26-94)

We intend to present the results of one year long monitoring program of dew/hoarfrost chemical composition and pollutant deposition which takes place in this way. Within the present project dew collectors were installed at 12 sites representing different geographic regions of Poland and, on the other hand, different types of landuse. Samples are collected with the use of unified equipment and methodology. The deposited volume of dew/hoarfrost and accompanying weather conditions as well as ionic composition is controlled and will be controlled at these sites over one year until the end of the ongoing winter (February 2010).
We are planning to present a complex description of dew/hoarfrost inorganic and organic chemistry and to calculate the amount of pollutant load deposited in this way. Seasonal variations in dew/hoarfrost chemistry will be presented with the emphasis put on the controlling role of some selected atmospheric processes. Overall contribution of dew/hoarfrost to total pollutant deposition will be examined with consideration of its relation to both dry and wet deposition pathways. The final aim is the assessment of the observed dew/hoarfrost pollution structure in terms of emission sectors defined by SNAP categories.

5th International Conference on Fog, Fog Collection and Dew
Münster, Germany, 25–30 July 2010
FOGDEW2010-45

Dew chemistry near a motorway in SW Poland

G. Gałek (1), M. Sobik (1), Ż. Polkowska (2) and M. Błaś (1)
(1) Department of Climatology and Atmosphere Protection, University of Wroclaw, 8 Kosiby St., PL-51670, Wrocław, Poland, (klimagala@gmail.com, +48-71-372-94-98), (2) Gdańsk University of Technology, Chemical Faculty, 11/12 G. Narutowicza St., PL-80233, Gdańsk, Poland, (zaneta@chem.pg.gda.pl,+48 58 347-26-94)

Abstract

The main goal of this paper is to show the influence of a large linear source of air pollution on dew formation and chemistry. Dew sampling was performed during the growing season of 2009 at three sites near Wroclaw in SW Poland in the vicinity of A4 motorway. Two of the sampling sites were set in a distance of 30 meters from the motorway edge on the opposite sides (S and N) of the road to monitor dew efficiency and chemistry depending on wind direction. The third one was set 1.25 km to the NNW of the former pair to represent background rural conditions beyond the road influence. All three sites and the motorway are surrounded by vast arable grounds with intense agriculture activity. Three insulated plane radiative condensers, each 1 m^2 in area, inclined around 15º, were installed at measurement sites. Two series of measurements were performed: the first in April lasted twenty days including several days without sampling, the second in September was continuous and lasted eleven days. Altogether there were nineteen dew or hoarfrost sampling days, nine in April and ten in September. Basic meteorological data were gathered three times daily. Water yield of three condensers was compared to meteorological data and between each other. The research findings show that the most favorable weather conditions corresponding to high amounts of dew or hoarfrost were characterized by synoptic scale warm air advection, high relative humidity, moderate wind speed i.e. 2,5-3,5 m/s and radiative weather. The samples from condenser located in calm air site usually had less volume than the other in windy place. The motorway heat source imposed a strong impact on efficiency of dew. The condenser on the leeward site of the road was characterized by much smaller yield of condensed water in comparison to its windward counterpart. Both dew and hoarfrost chemistry show strong influence of the motorway. The two samplers in close vicinity of road are much more loaded by compounds commonly linked to traffic emissions. The total ionic concentration is significantly less at the site located over one kilometer from the motorway. The anions connected with car fumes i.e. NO_3^- were about two times less common than in other two. The amounts of these compounds varied as well between condensers on the opposite sides of the road. The leeward sampler was quite more loaded by these ions. In general the most abundant ions in samples were: NO_3^- (30%), SO_4^{2-} (11%), Cl^- (7%), Ca^{2+} (24%), Mg^{2+} (4%), NH_4^+ (7%), Na^+ (5%), K^+ (5%), H^+ (7%).

1. Introduction

Atmospheric pollutants are transported onto the ground in two ways: by dry deposition caused generally by gravitational sedimentation and by wet deposition where the main medium consists of precipitation particles and atmospheric deposits. One of wet deposition pathways is dew and hoarfrost. They both are mainly formed during nighttime on any surface cooled by the negative radiation balance. Dew formation [1] is the most efficient in: radiative weather conditions [3], characterized by a low level of cloudiness; large nocturnal decline of air temperature; relatively low atmospheric turbulence [4]; high absolute and relative air humidity. The process of dew formation takes place in the lowest parts of the atmospheric boundary layer, usually polluted most. This causes high pollutant concentrations in dew samples when compared with other forms of deposition [2].

The most important source of emission affecting chemical composition of dew/hoarfrost is primarily burning of fossil fuel in domestic and industrial furnaces, but also emissions associated with road transport, industrial production, agriculture, etc. An important source of some constituents is a natural, mineral dust from soil erosion.

The main goal of this study is to examine the influence of intense road traffic on dew chemistry and on pollutant deposition via dew.

2. Measurements

2.1. Study area

The field program was conducted in the vicinity of A4 motorway near Wrocław in SW Poland. This road is a part of the international route E40, which connects southern part of Poland with Germany and other EU countries. The road crosses in this section a rural landscape from ENE to WSW direction. The traffic is notoriously heavy, even at night, and lorries constitute about one third of vehicles. The density of traffic is estimated as more than 30 000 vehicles per day. Two measurement sites were located in a distance of 30 m from the motorway edge on the opposite sides (southern – AS and northern – AN condensers) (Fig.1.). The third condenser (AR) was located in a distance of 1.25 km to the NNW direction from AN and AS sites.

Figure 1: Location of three measurements sites.

The analyzed area was located in the lowland (130-150 m asl.) with a slightly wavy land relief. The area of research has an agricultural character with small isolated wood complexes. The nearest village-type loosely built-up area is situated about 1 km from the research sites. In a distance of approximately 20 km towards ENE the centre of Wrocław city is located with total population of 630 000 dwellers.

The collection sites AN and AS were set on a gentle slope within an arable ground area. Towards E and ENE, in a distance of approximately 150 m from them, there is a viaduct above the A4 accompanied by earth ridges perpendicular to the motorway axis. The AR condenser was also located in an arable ground area with a small forest to the west.

2.1. Method

Measurements were conducted in two campaigns in the year 2009 during growing season. The first one took place between 01.04.2009-20.04.2009 including some days without sampling due to logistic reasons. Nine sets of daily samples of dew/hoarfrost were obtained during this series. The second series of measurement was continuous and lasted eleven days from 18.09.2009 to 28.09.2009. During the September series 10 sets of daily samples of dew were obtained from each site.

Three insulated radiative condensers, each 1 m^2 in area, oriented towards WSW with inclination of 15° angle, were installed at measurement sites (Fig.2.). The surface was covered with polyethylene and 5 cm thick insulating layer made of styrofoam.

Figure 2: The AS dew condenser with the motorway in the background.

The condensers were cleaned up with deionized water, about sunset just before the potential start of a dew formation episode. The deposited dew/hoarfrost was collected with a use of a polyethylene scraper in polyethylene containers not later than 0.5 hours after sunrise. After that samples were stored before analysis in the dark, at about 4°C for no longer than 1 month.

During the measurements the basic meteorological data like cloud coverage, wind direction and speed, were gathered three times per a collection night. Additionally, at the sampling time, air temperature and relative humidity were measured on three near-ground levels. Another important source of continuous meteorological data was *Wrocław Strachowice* - the airport synoptic station located in a

distance of about 10 km from research sites in NE direction.

3. Results

3.1. Dew efficiency

Average daily efficiency of dew/hoarfrost formation was about 180 ml/m^2. Maximal value was reported 25.09.2009 and reached 389 ml/m^2 (Fig.3.). There has been a substantial increase in the efficiency of deposits formation between both series. In April the average volume was about 140 ml/m^2 and in September series it was approximately 210 ml/m^2. The highest average efficiency of dew/hoarfrost was found at AS (199 ml/m^2) while at AN and AR sites it was 170 ml/m^2 and 173 ml/m^2 respectively. The AR condenser was characterized by the smallest variability of samples volume. The efficiency of the deposits formation in the close vicinity of the motorway showed dependence on the direction of advection of air.

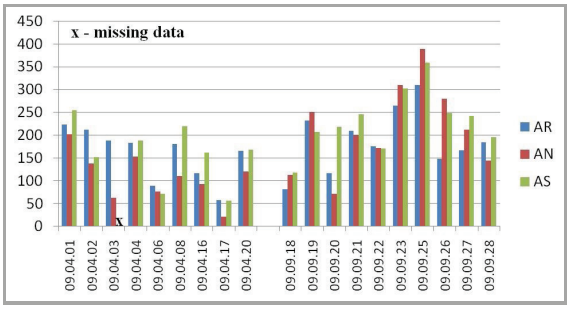

Figure 3: The volume [ml/m^2] of dew/hoarfrost daily samples at motorway (AN and AS) and background (AR) sites.

3.2. Dew chemistry

The average volume-weighted contamination of dew/hoarfrost samples defined by the TIC index (total ionic content of: SO_4^{2-}, NO_3^-, Cl^-, NH_4^+, Ca^{2+}, Mg^{2+}, Na^+, K^+, H^+) was 0.55 meq/dm^3 with strong variations depending on the series. During the April series the average value of TIC was 0.72 meq/dm^3, while in September series it was 0.45 meq/dm^3. Differences of TIC index between the measuring sites were also substantial. At the AN and AS condensers the average value reached 0.62 meq/dm^3, and for AR 0.38 meq/dm^3. The average value of conductivity was 64.4 µS/cm. The relations between series and sites were similar to these in TIC. In the structure of ions the largest share had NO_3^- and Ca^{2+} ions (Fig.4.). The other analysed constituents shared 5-11% each one. Only ions of Na^+ and H^+ showed substantial differentiation between series or sampling sites. Concentration of NO_3^- ranged between 0,003 meq/dm^3 and 0,71 meq/dm^3, while in case of Ca^{2+} between 0,02 meq/dm^3 and 0,85 meq/dm^3. Amounts of NH_4^+ changed from day to day independently of wind direction.

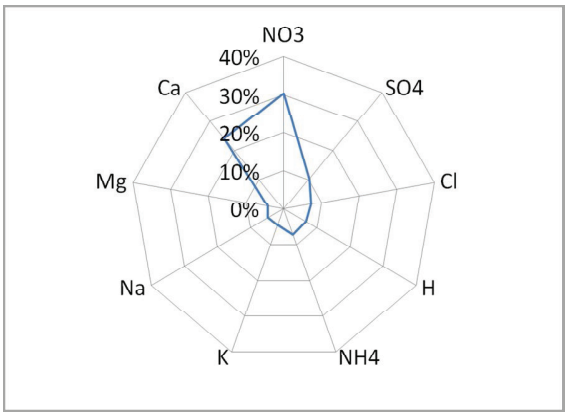

Figure 4: Relative contribution of selected ions in averaged dew samples (molar concentrations weighted by volume). Samples from all 3 sites during both April and September series were taken into account.

The overall pH (derived from H^+ concentrations weighted by volume) of the samples was strongly acidic and reached 4.4. In the April series the pH was 4.1 and in the September series it was 4.8. Parameters showing the impact of maritime aerosols on dew chemistry (Cl^-/Na^+, SO_4^{2-}/Na^+, K^+/Na^+, Ca^{2+}/Na^+, Mg^{2+}/Na^+) reached values highly exceeding those characteristic for sea water.

4. Discussion

The increased average volume of samples collected during the September series of measurement is mainly caused by higher water vapour supply due to high average temperature and relative humidity during dew formation. It was noted that the radiative weather conditions, moderate intensity of wind speed (2,5-3,5 m/s) and descending trend in minimum air temperature from day to day had a positive impact on dew formation. The least dew efficiency at AN condenser is determined by frequent impact of

motorway. In days with E-sector circulation, the AN condenser was on leeward side of the road. The air heated above the motorway was characterized by significantly increased water vapour deficit what determined lower dew yield than on the opposite side of the road. Difference between AN and AS condenser in sample volume in the same dew episode reached 3 to 1 ratio.

Contamination of the collected samples defined by TIC was relatively low if compared with earlier data gathered in Poland [5]. Higher concentrations of pollutants in April series was mainly due to larger quantities of NO_3^- and Ca^{2+} ions. AN site shows the highest difference between both series.

The results of April as well as September series confirmed the role of wind direction on dew pollution. In spring series the dominant wind direction was from the eastern sector, so inflowing air above measuring sites was earlier transformed above a long section of the motorway. Condenser AN was located in this condition on the leeward side of the road. The largest average load of pollution on AN site was in situation when wind direction was parallel to the motorway. The increased quantities of NO_3^- ions were resulted mainly from fuel combustion in vehicle engines, and Ca^{2+} ions and the other were linked with the secondary emission of pollutants from motorway surface by gusts made by fast moving vehicles. The increase was additionally strengthen by attrition of concrete surface and vehicles tires. Variable air advection in the September series caused the dew pollution on both side of motorway to be generally similar. Dependence on wind direction is clearly visible for each day of measurement. Different directions of air flow indicate no clear impact of the A4 motorway on the site AR. High Ca^{2+} share in ionic structure was additionally caused by background pollution determined by dust from industrial and urban area which could be long-transported in terms of lack of atmosphere washing-out by rain. Higher concentration of NH_4^+ ions were linked with agricultural activity.

5. Conclusions

The dew efficiency reached an average value of 180 ml/m^2 per night. The main factors determining its formation include: warm and humid air advection in synoptic scale, low cloud coverage, high relative humidity and substantial nocturnal drop of temperature. The efficiency of dew formation depends on wind direction in relation to the motorway. On the leeward side of the motorway the volume of collected samples is even 3 times smaller than on its windward counterpart.

Dew/hoarfrost chemistry in the close vicinity of the motorway remains under its strong influence. The overall level of contamination of atmospheric deposits is relatively low, however the site located on the leeward side of the road shows a significant increase in pollution. The research revealed that pollution concentrations depended on the direction of air advection, the time-lag from the last atmosphere washing-out episode and distance from the motorway. A large share in ionic structure of NO_3^- ions was caused by the combustion of fuel in car engines, while Ca^{2+} and other ions from the secondary emission of pollutants from the road surface by traffic. Ions of NH_4^+ had probably agricultural origin.

Acknowledgements

This scientific work was financially supported in 2008-2010 years by the Polish Ministry of Science and Higher Education as a research project N N305 231035.

References

[1] Beysens D., 1995*, The formation of dew,* Atmospheric Research 39 (1–3), pp. 215–237.

[2] Jiries A., 2001, *Chemical composition of dew in Amman, Jordan*, Atmospheric Research 57, pp. 261–268

[3] Muselli M., Beysens D., Marcillat J., Milimouk I., Nilsson T., Louche A., 2002, *Dew water collector for potable water in Ajaccio (Corsica Island, France)*, Atmospheric Research 64, pp. 297–312

[4] Nikolayev V.S., Beysens D., Gioda A., Milimouk I., Katiushin E., Morel J.P., 1996, *Water recovery from dew*, Journal of Hydrology 182, pp. 19-35

[5] Polkowska Ż., Błaś M., Klimaszewska K., Sobik M., Małek S., Namieśnik J., 2008, *Chemical Characterization of Dew Water Collected in Different Geographic Regions of Poland*, Sensors, 8, pp. 4006-4032

5th International Conference on Fog, Fog Collection and Dew
Münster, Germany, 25–30 July 2010
FOGDEW2010-46

Water and chemical input via hydrometeors in central European mountains with Szrenica Mt. as an example

M. Błaś (1), M. Sobik (1) Ż. Polkowska (2) and K. Cichała-Kamrowska (2)
(1) Department of Climatology and Atmosphere Protection, University of Wrocław, Poland, (2) Department of Analytical Chemistry, Chemical Faculty, Gdańsk University of Technology (blasm@meteo.uni.wroc.pl / Fax: +48-372-94-98).

Abstract

Atmospheric pollutants are transferred to the ground by the contribution of various types of hydrometeors. Due to the different techniques of measurement, comparative analyses between them are often neglected. Hence, the main goal is to compare chemistry of different types of hydrometeors and their role in both: water balance and pollutants deposition.
The results of water input and atmospheric deposits chemistry at the Szrenica Mt. during the period between XII 2008 – II 2010 are presented. The volume-weighted TIC (Total Ionic Content) of dew, hoarfrost and fogwater (both solid and liquid) was 345, 134, 425 $\mu eq \cdot l^{-1}$ respectively, while typical TIC value for precipitation was 233 $\mu eq \cdot l^{-1}$. The chemical composition of dew, hoarfrost and fog water differ significantly from each other and from precipitation, depending on background emission and atmospheric processes. Taking into account both concentration and volume of deposited water, comparison between pollutant load of hydrometeors was possible.

1. Introduction

The Szrenica Mt. [1330 m a.s.l.; φ= 50˚48', λ=15˚31'] is situated in the western part of the main ridge of the Giant Mts. located along the Polish/Czech border and falls steeply northward on the Polish side (1000 m of relative height). Giant Mts., as a part of Western Sudety Mts., are located in one of the most polluted region in Europe [3]. During typical SW-W-NW wind conditions they are exposed to highly polluted air from heavy industry densely situated at the distance of tens to hundreds kilometers on the windward side of the mountains. Atmospheric pollutants are transferred to the ground via various types of hydrometeors: atmospheric precipitation and non-precipitation atmospheric deposits i.e. dew and hoarfrost as well as rime and liquid fog.

The local climate at Szrenica Mt. is well established on the basis of 40 years of measurements made at the meteorological observatory of the University of Wrocław [9]. Precipitation is the main source of water flux at the Szrenica Mt. reaching 1430 mm annually. In general, precipitation is nonseasonal with the highest sums in June, July and August (>150 mm monthly), and the lowest in February and March (less than 90 mm). The seeder-feeder mechanism typically causes an increase in precipitation at the Szrenica Mt. of about 50% relative to the lowlands [3], [6], [13]. This effect is that orographic cloud droplets are scavenged by upper level precipitation leading to a significant increase of both precipitation and pollutant deposition.
At the Szrenica Mt. a significant part of water flux from the atmosphere is formed by direct deposition from fog. It is the most frequently observed atmospheric phenomenon, being present on average 45% of the time [2], [4]. Fog is most often of orographic origin connected with the forced ascent of humid air on a windward slope. Thus orographic fog is a kind of advective and adiabatic types of fog combined. Such kind of fog is more typical for the cold season (XI-IV) because of predominance of humid air masses and small diurnal temperature range [2], [4].
While precipitation and fog deposition is described quite well, there exist only very limited information concerning the composition of dew and hoarfrost in Poland. Dew and hoarfrost are formed especially during the anticyclonic type of weather with no wind and clear night skies, rare at summit position [1]. The annual number of days with dew in lowland part of Poland varies around 100-160 and decreases to 10-30 days per year in case of conspicuous mountain summits and ridges. Hoarfrost frequency show similar spatial distribution from less then 30 days at well exposed mountain summits to more than 80 days annually in concave landforms and central regions of Poland [5], [11].

2. Experimental

The following hydrometeors: precipitation, dew, hoarfrost, liquid fog and rime samples were collected daily during the period between December 2008 and February 2010. Cloud water samples were taken daily with the use of simple passive collector set 2 m above the ground. Liquid fog droplets (T>0˚C) were deposited on 160 strings vertically oriented and shaped by plastic hood, which reduced rain contamination. In case of rime (T<0˚C) passive collector consists of duralumin rod. It was used to measure rime efficiency expressed by the weight of ice deposit and the length of vanes of rime. A polyethylene covered cable was used to collect rime samples destined for chemical analysis. Dew and hoarfrost samples were collected using a sampler based on the design described by Muselli et al. [8]. Surface of this sampler (100 cm x 100 cm) was made of rigid polyethylene foil mounted on a wooden frame, thermally isolated from the ground with 5 cm thick polystyrene foam and mounted 50 cm above the ground with the surface at 15-degree angle. Pollutant deposition transferred via precipitation was calculated on the basis of water volume measured by standard Hellmann gauge and chemistry from the rain collector – plastic container placed on the ground or snow cover.

All samples were collected in the morning after each deposition event. To reduce the disturbing effect of ongoing dry deposition, the collecting samplers surface were cleaned before exposure, rinsed with deionized water and wiped. Selected anions and cations were quantified against synthetic rain standard using ion suppressed chromatography (ICS 3000, Dionex Corporation, USA). This synthetic standard is Reference Material No. 409 (BCR-409, Institute for Reference Materials and Measurements, Belgium) and Analytical Reference Material Rain (National Water Research Institute, Environment Canada) [10].

Information regarding chemical composition of analyzed hydrometeors was interpreted with the context of meteorological data-type of air mass, character as well as direction of atmospheric circulation. Barometric system causing synoptic airflow, 16 directions of atmospheric circulation and three pressure system types were distinguished (cyclonic, anticyclonic and transition).

3. Results

The highest values of TIC (Total Inorganic Ionic Content) were observed in case of fog (425 $\mu eq \cdot l^{-1}$), but the much lower was characteristic for hoarfrost (134 $\mu eq \cdot l^{-1}$) and precipitation (233 $\mu eq \cdot l^{-1}$, Fig. 1, Tab. 1). Because of substantial differences, dew and hoarfrost are presented separately, opposite to liquid and solid deposit of fog, similar to each other.

Differences between precipitation and fog chemistry are connected with thickness of air layer where each of them originates. Atmospheric precipitation is formed due to the processes occurring within the deep air layer, often reaching the middle or even upper part of the troposphere, where the concentration of pollutants emitted from the ground is much lower. The concentration of pollutants dissolved in fog water was 2 times higher than in precipitation, which resulted from the more polluted nature of the boundary layer than the free atmosphere. TIC for dew was significantly higher in comparison with precipitation and surprisingly twice as big as for hoarfrost. This is due to the changing depth of the atmospheric boundary layer which is frequently protruded by the Szrenica Mt. especially in wintertime anticyclonic conditions. During warmer half of the year higher vertical mixing is observed. The relative purity of hoarfrost can be explained by the suppression of vertical mixing during winter conditions and the clean air subsidence predominantly reaching the top of Szrenica summit. Air pollutant transport is limited vertically and maritime aerosol is much more important in such conditions.

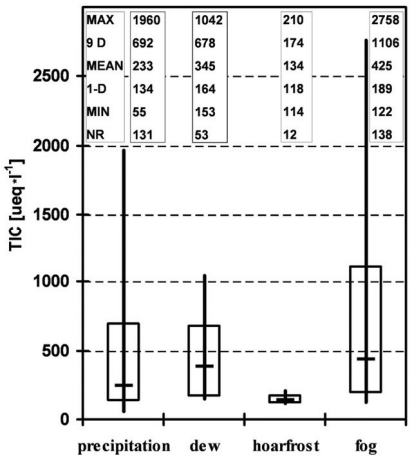

Figure 1: TIC statistical indices (max., 9th decile, mean, 1st decile, min. and the number of samples).

Table 1: Chemical composition of precipitation (P), dew, hoarfrost (H) and fog at the Szrenica Mt.

Analytes		P	Dew	H	Fog
N (samples)		131	53	12	138
Conductivity		18,0	18,2	9,9	52,8
pH		4.49	5.30	4.85	4.06
TIC	$\mu eq \cdot l^{-1}$	233	345	134	425
Na^+		19.5	25.0	17.0	31.4
NH_4^+		32.5	32.3	12.4	79.5
H^+		32.5	5.0	14.0	65.8
K^+		6.9	10.1	1.7	5.9
Mg^{2+}		4.9	30.9	12.2	12.3
Ca^{2+}		36.1	67.7	19.6	52.3
Cl^-		32.3	30.6	24.5	31.9
NO_3^-		28.8	84.3	21.7	75.2
SO_4^{2-}		39.9	30.6	11.3	70.5

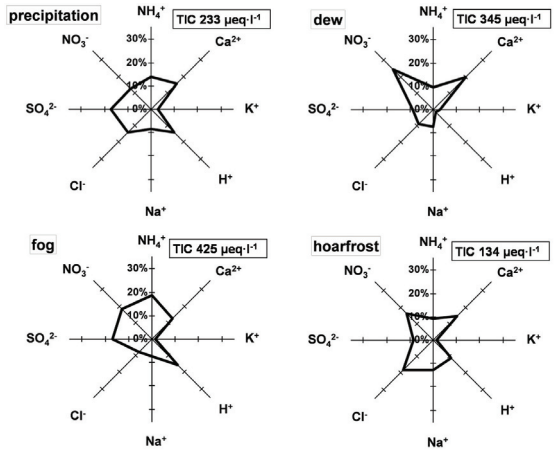

Figure 2: Ionic composition of atmospheric hydrometeors.

As the results hoarfrost chemical composition was quite different to other hydrometeors (Cl^-, NO_3^-, Ca^{2+} and Na^+ with contribution 18, 16, 15 and 13%, respectively) (Tab. 1, Fig. 2). This indicates that despite the inland location of this site, maritime components are at least significant in overall deposition.

For fog water samples equilibrium between NH_4^+, NO_3^- and SO_4^{2-} was characteristic (19, 18, 17%, respectively). Because of altitude, differences in boundary layer depth and much more vigorous circulation during cyclonic weather, fog water collected at the Szrenica Mt. may include solute contribution from emission sources located at much larger upwind distances [5], [7].

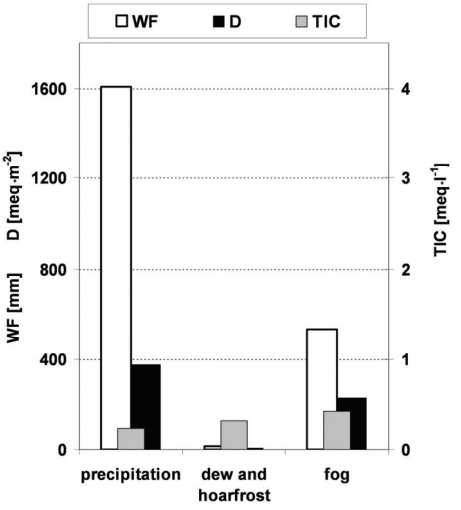

Figure 3: Water flux (WF), TIC, and pollutant deposition (D) via precipitation, fog, dew/hoarfrost sampled at the Szrenica Mt. between 1.12.2008 and 28.02.2010.

The following components: NO_3^-, SO_4^{2-}, Ca^{2+} and NH_4^+ were the principal ions in chemical structure of dew and precipitation. A relatively high contribution of Ca^{2+} especially in dew and precipitation can be attributed to the use of $CaCO_3$ in the desulphurisation process in some electric power plants and an increased construction activity in the surrounding regions.

The estimation of pollutants load accumulated by a given hydrometeor is possible when the average TIC and the volume of water reaching a unit area are known (Fig. 3). Dew and hoarfrost provide water quantities much lower than fog or rain, but is a modest supplementary source of water [12]. According to TIC value equal to 314 $\mu eq \cdot l^{-1}$ and 14,5 mm of water, pollutant load accumulated by dew/hoarfrost (between 01.12.2008 and 28.02.2010) was around 4,5 $meq \cdot m^{-2}$. This was additional 1,2% of the pollutants load delivered via atmospheric precipitation. In case of fog, due to 274 foggy days per year accompanied by high wind speed, pollutants load is much more important but substantial differences exist depending on particular location. In this case, landuse expressed by roughness is a very important factor responsible for the huge differentiation in fog droplet deposition on a microscale. At the Szrenica summit, covered by dwarf pine, water flux from fog is estimated as thirty per cent while pollutant deposition via fog constitutes a half of that via precipitation. However, on well

exposed ridges covered by coniferous forest the direct fog water flux is comparable with precipitation while fog pollutant deposition may even dominate. The highest value was recorded at the edge of a forest stand close to the tree line [3].

6. Summary and Conclusions

In all types of atmospheric deposits different ions play an important role: SO_4^{2-} and Ca^{2+} in precipitation, NO_3^- and Ca^{2+} in dew, Cl^- and NO_3^- in hoarfrost as well as NH_4^+, NO_3^- and SO_4^{2-} in fog. Chemical composition differ significantly as a result of e.g. different circulation pattern and activity, origin and the age of air masses, the range of vertical mixing. Pollutant concentrations in hoarfrost were surprisingly low, decreasing even below those observed in precipitation.

Taking into account both concentration and volume of deposited water, dew and hoarfrost form a neglectable path of pollutants flux to the ground being responsible for additional 1,2% of deposition through atmospheric precipitation. This does not apply for fog which becomes a significant component of wet deposition at mountain ridges when compared with precipitation alone, leading to the destructive environmental results.

Acknowledgements

This scientific work was financially supported by the Polish Ministry of Science and Higher Education in years 2008-2010 as a research project (N N305 231035).

References

[1] Beysens, D.: The formation of dew, Atmospheric Research, 39, 215-237, 1995.

[2] Błaś, M., Sobik, M., Quiel, F. and Netzel, P.: Temporal and spatial variations of fog in the Western Sudety Mts., Poland, Atmospheric Research, 64, 19-28, 2002.

[3] Błaś, M. and Sobik, M.: Natural and human impact on pollutant deposition in mountain ecosystems with the Sudetes as an example, Studia Geograficzne, **75**, 420-438, 2003.

[4] Błaś, M. and Sobik, M.: The distribution of fog frequency in the Carpathians, Geographia Polonica, **77**, 19-34, 2004.

[5] Błaś, M., Polkowska, Ż., Sobik, M., Klimaszewska, K., Nowiński, K. and Namieśnik, J.: Fog water chemical composition in different geographic regions of Poland, Atmospheric Research, 95, 455-469, 2010.

[6] Dore, A.J., Sobik, M. and Migała, K.: Patterns of precipitation and pollutant deposition in the Western Sudety Mountains, Poland, Atmospheric Environment, 33, 3301-3312, 1999.

[7] Möller, D., Acker, K. and Wieprecht, W.: A relationship between liquid water content and chemical composition in clouds, Atmospheric Research, 41, 321-335, 1996.

[8] Muselli, M., Beysens, D., Marcillat, J., Milimouk, I., Nilsson, T., Louche, A.: Dew water collector for portable water in Ajaccio, Atmospheric Research, 64, 297-312, 2002.

[9] Migała, K., Pereyma, J., Sobik, M., Szczepankiewicz-Szmyrka, A.: Climatic conditions at the Karkonosze during the warm half of the year 1992, Karkonoskie Badania Ekologiczne, I Konferencja, Wojnowice, 3-4 grudnia 1992, Oficyna Wydawnicza Instytutu Ekologii PAN, 47-70, 1993.

[10] Polkowska, Ż. Astel, A. Walna, B. Małek, S. Mędrzycka, K. Górecki, T. Siepak, J. Namieśnik, J.: Chemometric analysis of rainwater and throughfall at several sites in Poland, Atmospheric Environment, 39, 837-855, 2005.

[11] Polkowska, Ż., Błaś, M., Klimaszewska, K., Sobik, M., Małek, S. and Namieśnik, J.: Chemical characterization of dew water collected in different geographic regions of Poland, Sensors, 8(6), 4006-4032, 2008.

[12] Polkowska, Ż., Sobik, M., Błaś, M., Klimaszewska, K., Walna, B. and Namiernik, J.: Hoarfrost and rime chemistry in Poland – an introductory analysis from meteorological perspective, J. Atmos. Chem., Vol. 52, 5-30, 2009.

[13] Sobik, M., Netzel, P. and Quiel, F.: Zastosowanie modelu rastrowego do określenia pola rocznej sumy opadów atmosferycznych na Dolnym Śląsku, Rocznik Fizyczno-Geograficzny, Vol. VI, 27-34, 2001.

5th International Conference on Fog, Fog Collection and Dew
Münster, Germany, 25–30 July 2010
FOGDEW2010-47

Bionic development of textile materials for harvesting water from fog

Dr. Jamal Sarsour, Dr. Thomas Stegmaier, Dipl.-Ing. Michael Linke, Prof. Dr. Heinrich Planck, Institute of Textile Technology and Process Engineering (ITV) Denkendorf/Germany

The provision of drinking water turns out to be one of the great challenges of the future. Currently, about one billion people have no access to the essential wet – a problem that mainly is evident in the developing countries.
Here central water supply systems normally cannot technically and logistically be realized or the connection of remote settlements on islands, in isolated bays or higher regions is uneconomic.
For thousands of years nature has been managing on its own as regards the safeguarding of the survival of plants and animals in dry regions – by the procurement of water from the humidity of the air. In extreme desert areas especially often amazing complementary mechanisms are active in order to wrest the essential elixir. They are useful models for a corresponding technical implementation.
The development of functional products for the procurement of drinking water from fog without energy supply is the aim of a current project at the Institute of Textile Technology and Process Engineering (ITV) Denkendorf. Details about the bionic implementation are comprehensively given in the following – from the research and construction of suitable textile fabrics to lab trials regarding material analysis up to the first field trials.

- **Aims of development**

The aim of the research project at ITV Denkendorf is to analyse the biological mechanism of the separation of droplets of water from the air to design corresponding bionic implementations. Fiber-based materials for the procurement of water from morning dew and fog shall be designed and developed in that case. The textile humidity absorbers subsequently are to be used for the production of complete systems for the procurement of water and to be tested for this application.
The main focus of the investigations is on the efficiency of water separation, mechanical stability, self-cleaning behavior, and on the collection, storage and eventual treatment to drinking water.
According to the plan, larger settlement units such as multiple dwellings, schools and villages in the future will be able to independently meet their own need of water and/or to take over filtration tasks by means of the differently dimensioned fog collector systems.
For the purpose of the implementation of this plan, at first, fiber polymers and geometries have to be analyzed and – based on the findings – fibers to be produced showing a favorable behavior regarding water absorption and release.
The surface energies and spectral properties of the fiber materials, in addition, shall be optimized by a specific surface coating. The further works deal with supporting measures for the collection and leading off of the separated water – a task that can be fulfilled by functional micro and nano structures. By using the findings of filtration on coalescence, finally a spatial textile fabric has to be designed that offers with its third dimension a favorably high air permeability and an efficient aerosol separation at the same time.

- **Biological models**

Two biological systems acted as the model for the development works at ITV: the marram grass Stipagrostis subulicola and the Namib Desert beetle Onymacris unguicularis – both being natural survivalists in the Namib Desert. In the extremely dry zone at the west coast of Africa hardly any rain falls, but in certain seasons in the night there often and regularly occurs fog.
The Stipagrostis subulicola plant uses the water droplets, that are dispersed in the air, by means of a sophisticated interaction of its roots and leaves. The roots of the marram grass are in a maximum depth of 20 cm; they, however spreading over a length of 20 m forming a carpet that absorbs the water dripping from the leaves – before completely seeping away in the ground. A spatial construction of a horizontally oriented 2D-network in the ground and a vertically ramified green on the surface thus form the basis of the combing out process of the fog.
As for the grass leaf, the REM, in addition, reveals surface structures, that possibly are in conjunction with the separation efficiency. The specific interrelations are investigated at the Institute for Geoscience, University of Tübingen, under the supervision of Dr. Anita Roth-Nebelsick. Concerning the way how to handle water, the desert beetle Onymacris unguicularis developed another possibility of best practice during evolution. In the morning dew the beetle known as fog drinker exposes itself with his backside on the top of the dune and thus in the wind. The fog condenses on the shell of the beetle and flows through the grooves of the back directly into the mouth.

- **Demands to textile fabrics**

Textile-based fog separators (Fig. 1) must fulfill basic requirements regarding material properties, separation efficiency for air-transported water aerosols and profitability in the overall system.
In practice, the textiles to be developed must show favorable tear strength and air permeability so that they can reliably fulfill their function even at bad weather such as storm. The textile fabric, moreover, should have self-cleaning properties to be protected against dirt, dust and blockades of the fabric itself. In addition, maximum weathering and ultraviolet resistance is required because of extreme insolation.
As for the investments, the production and maintenance costs for the textile fabric and overall system should be as low as possible. Simple design and easy handling are the essential conditions for the use of the water separator in barren landscapes.
Last but not least, all material surfaces, that get into contact with water, must be compatible with food as the separated water is used as drinking water.

- **Trials performed in the lab**

A suitable test stand for the analysis of the efficiency of water separation of the textile materials has been designed in the lab of ITV. During the comparative investigations the test items were exposed to a shower of aerosols by a cold fog equipment with a droplet diameter from 10-100 µm. Smoke screen and inflow were realized on the basis of a reliable processing technology in order to get reproducible results.

- **Results**

In the course of a screening phase the project team of ITV conducted tests on a multitude of textile fabrics. The influence of textile-physical parameters such as polymer material, filament and fiber diameter, design, and surface energy or air permeability on separation efficiency was determined. The analyzed test items also included the Raschel meshed fabrics made of polyethylene. Based on the findings new textile constructions were developed and patented meanwhile. The favorite fog separators consist of polyester with 3D-design and – as regards conducting away water – are optimized within their spatial structure. In this way, 3D-textiles reach separation rates between 65 and 85 % at the exposure to fog – clearly improved values compared to 52 % in the case of Raschel meshed fabrics.

- **Practice tests**

The textile variants with optimum water separation rates are currently tested at the desert research station Gobabeb, Namib Desert/Namibia – under conditions of long-term field trials (Fig. 3). The first results of the field trials are promising. They confirm the results of the lab tests and certify the 3D-textiles a water yield that is 2 to 3 times higher on average compared to the materials used so far such as the Raschel meshed fabrics. The amount of water separated by the meshed fabrics was 300 ml/mm^2 fog event and that of the 3D-textiles was about 660 and 730 respectively (as of 25/09/2008).

- **Acknowledgements**

The project was funded by German Federal Ministry of Education and Research BMBF (ID: 02WT0905). Special thanks to BMBF for the financial support of the project. We also thank Mattes und Ammann KG, Meßstetten, Solar Energie Stefanakis, Stadecken-Elsheim and the Institute for Geoscience, University of Tübingen, for the support of this work.

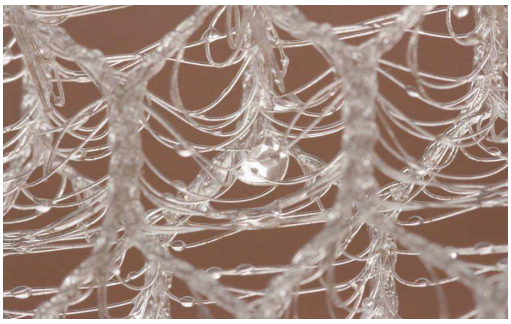

Fig. 1: Fibre-based fog collector with adhesed water droplet

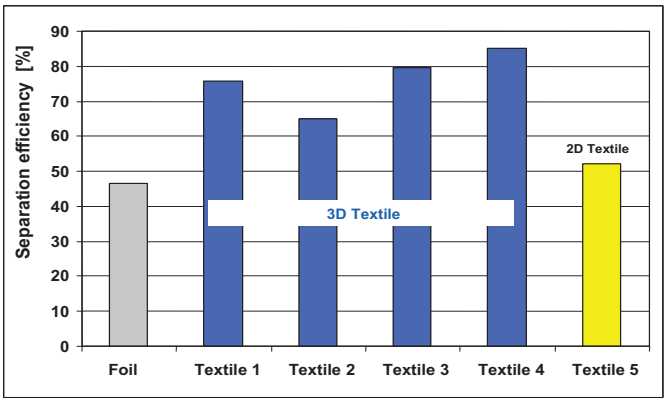

Fig. 2: Separation rates of investigated materials

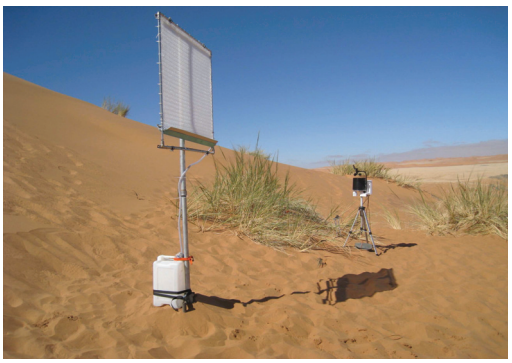

Fig. 3: Field trials at desert station Gobabeb (Namib Desert), Namibia

5th International Conference on Fog, Fog Collection and Dew
Münster, Germany, 25–30 July 2010
FOGDEW2010-48

Visibility Degradation during Foggy Period due to Anthropogenic Urban Aerosol at Delhi, India

Suresh Tiwari (1), Swagata Payra (2,3) and Deewan Singh Bisht (1)

(1)Indian Institute of Tropical Meteorology-Pune, Delhi Branch, New Delhi-110060, INDIA
(2) Remote Sensing Department, Birla Institute of Technology, Extension Centre, Jaipur, India
(3)Indian Institute of Technology Delhi, Hauz Khas, New Delhi-110016, India
(smbtiwari@tropmet.res.in / Fax: +91-11-28742020)

Abstract

Fog frequencies dominate in urban area than rural area. Increased air pollution in urban area may lead to the atmospheric reactions, resulting into the formation of secondary pollutants similar to cloud condensation processes. Northern regions of India experience severe fog conditions during the winter period (November-January) each year. In this study, simultaneous measurements of particulate mass concentration (0.23µm to 20µm), meteorological parameters and atmospheric visibility in Delhi city, India during 2007-2008 have been studied in order to understand their role in fog formation. The effects of aerosols on fog formation are discussed through an analysis of trends in fog frequency and comparison with meteorological parameters, and visibility as an indicator of aerosol load. The existing dataset of fog frequency, meteorological parameters and visibility is used to find linear regression model, that explained the variation in visibility due to depression in temperature and aerosols load.

1. Introduction

Fog is defined as visual obscurity of less than 1000 m near the surface layer due to suspended water droplets and aerosols. A very high level of ambient aerosol loadings has been recognized to intensify the fog formation in the urban areas (Mircea et al., 2002; Bergot and Guedalia, 1994; Stoelinga and Warner, 1999; Bott et al., 1990) due to the various considerable facts (Toon, 2000) and presence of ammonium, nitrate and sulphate (Frank et al., 1998).

Fog is more likely to form in an environment with large concentrations of aerosols characterized by a low activation super saturation. Organic compounds change the surface tension of pure water and can cause cloud condensation nuclei activation at lower relative humidity than that which is possible in the atmosphere of unpolluted regions (Brooks et. al., 2009). Although in a large number of fogs, the distinction between un-activated and activated droplets is not as straightforward as for other clouds types (Hudson, 1980). The properties of aerosols in the ambient air thus play an important role in fog onset due to the activation of fog droplets. Laboratory experiments have indicated that pollution/aerosol has strong effect for fog formation in favorable meteorological condition. Frank et al., (1998) studied the effect of the aerosol mass present in the fog and varied it by a factor of 4(25-100µgm^{-3}). It was found that the aerosol mass load strongly influenced the microstructure of the fog. Certain meteorological parameters alone or in combination with some air pollutants trigger fog formation in the urban area. In a metropolitan city like Delhi, with over 15 million inhabitants contributing towards the anthropogenic aerosols, coupled with the desert dust aerosols from the north-western region (Singh et al., 2006), a very high level of ambient aerosol loadings is always expected. During past one decade, Delhi has witnessed increased frequency of fog in winter season. Analysis of six years (1996-2001) of meteorological data for the winter season shows that occurrence of fog is more than 50% of the time in this mega-city (Mohan and Payra, 2008). The pollution levels in Delhi environment, especially Respiratory Suspended Particulate Matter (RSPM) concentrations are significantly high. Ali et al., (2004) reported that the anthropogenic species are higher during winter period. Despite of all the possible control measures Delhi has significant concentration of RSPM often exceeding national ambient air quality standards and therefore it is expected that increased aerosols would have an important role in the fog formation.

The main objective of the present study is thus to find the relationship with aerosol content and meteorological parameters in influencing fog formation during winter period over Delhi based on observations during winter (Nov. to Jan.) that included severe dense fog episodes.

2. Sampling Site and Techniques

Delhi ($28^0$35'N; $77^0$12'E, 218 m asl) experiences a severe weather swing between different seasons: from hot and humid weather in summer to cold and dry weather during winter. Apart from such swings of weather, the entire northern part of India, especially the Indo-Gangetic Plain, experiences a thick foggy weather during winter. During such conditions, pollutants could not be dispersed and mix with free troposphere due to trapping canopy of low boundary layer. Such conditions ultimately results in poor visibility and high levels of pollutants.

The ambient sampling of aerosols for this study was carried out at about 15m above the ground level, on the rooftop of a building situated in the thoroughly urbanized central part of Delhi. The area is primarily a residential area, and no large pollutant source exists nearby which could have influenced the sampling site directly. Sampling location is given on the road map of Delhi in Figure 1.

Figure 1. Sampling location (marked as dot) in the road map of Delhi

The GRIMM optical particle counter (GRIMM Aerosol Technich, model 1.108) - a 16 channel aerosol spectrometer was used to measure the total mass concentration of particles in the defined 16 different size ranges (Sciare et al., 2007). Counting of aerosol is measured by light scattering with the help of laser ray. Simultaneous constant flow rate (1.2 litre/min) is maintained throughout the measurements. All meteorological data for this study (2007-2008) are taken from India Meteorological Department (IMD). Aerosol concentration was taken for every minute and meteorological data was taken in every 30 min temporal resolution.

3. Results and Discussion

3.1 Total Aerosol mass concentrations and visibility

The hourly variations in Aerosol Mass Concentration (AMC) for a weeklong data in November, 2007 along with the visibility are shown in Fig. 2.

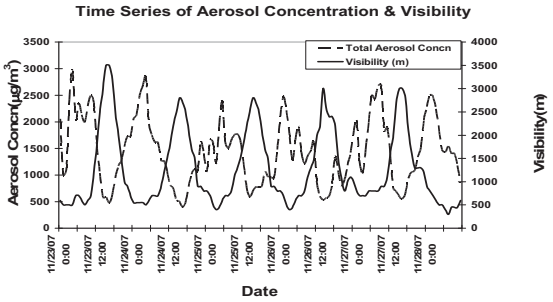

Figure 2. Time series of Visibility and Aerosol Mass Concentration (November, 2007)

The minimum and maximum values of hourly mean mass concentration of aerosols are 394.85 µg/m^3 (24th November, 4 p.m.) and 2980.34 µg/m^3 (23rd November, 4 a.m.), respectively. The corresponding visibilities are 2700m and 500m, respectively. Minimum visibility is less than 300m occurred on 28 November at 7 a.m. with mass concentration of about 1541 µg/m^3. The aerosol mass concentrations follow out of phase relationship with respect to visibility (Fig. 2). The correlation between these two shows a negative value of -0.7 which infers that more the aerosols load, less will be the visibility. This result is not surprising because the sampling site encounters almost all the times the foggy conditions with increasing aerosols concentration supporting the lesser visibility during winter.

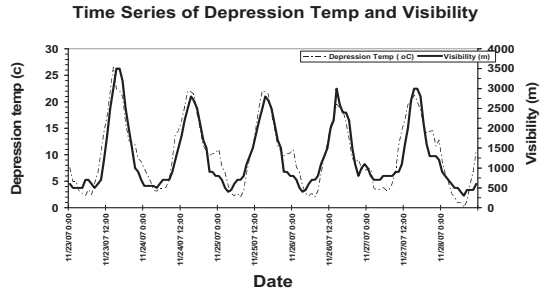

Figure 3. Time Series of Visibility and Depression Temperature (Novemeber,2007)

Figure 3 shows the time series of depression temperature and visibility during November 2007.

Most of the pure meteorological models initially considered a depression temperature less than 1^0C as fog occurrence criteria. However, it is argued that if the pollution load increases rapidly then fog may occur with a depression temperature greater than 1^0C. This study clearly shows this synergic effect of pollution and meteorological condition. The depression temperature and visibility parameter follow in-phase relationship with a high positive correlation of 0.91. The minimum depression temperature (0.1) occurs on 28 November at 7 a.m. when the visibility is the lowest (300 meter).

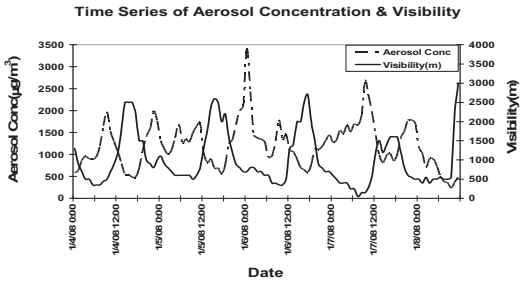

Figure 4. Time series of Visibility and Aerosol Mass Concentration (January 2008)

Hourly variations in aerosol mass concentration for a weeklong data in January 2008 along with the visibility are shown in Fig. 4. The minimum and maximum values of hourly mean mass concentration of aerosols are 233.86 µg/m^3 (8th January 2008, 9 a.m.) and 3418.65 µg/m^3 (6th January 2008 Midnight), respectively with corresponding visibilities as 550 m and 700 m, respectively. Minimum visibility is less than 50 m on 7 January at 7 a.m. with mass concentration 1670.72 µg/m^3. Like November 2007, the January 2008 data also show a negative trend between aerosols concentration and visibility with a negative correlation of -0.5. Thus the visibility trends in Fig. 2 and Fig.4 for a sampling location shows that more aerosols loading is one of the important factors for fog formation.

The time series of depression temperature for January 2008 has been shown in Fig. 5. The correlation of depression temperature with visibility is very high (0.87). The minimum depression temperature (0.9^0C) occurred on 7 January at 7 a.m. when the visibility is the lowest (50 meter). The results from winter shown in Figs. 2 to 5, for 2007 and 2008, respectively stems out that increase in pollution level (aerosol mass concentration) and less depression temperature are favorable for fog formation data.

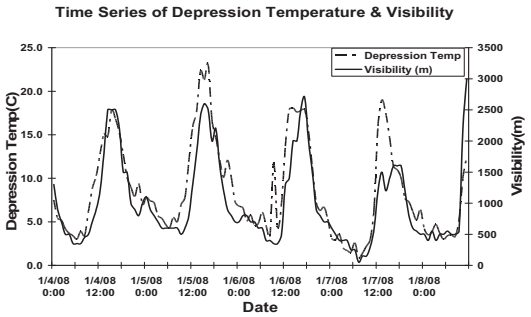

Figure 5. Time Series of Visibility and Depression Temperature (January 2008)

3.3 Linear regression model for estimating fog.

Further investigation shows that the fog formation criteria using hourly average data from 23-28 November 2007 to find linear regression amongst various parameters by due consideration of significance value. The result satisfies the precondition for using these relations even in limited data set. The model explained the variation in visibility due to depression temperature and aerosol mass concentration by the following equation:

Visibility = 545.417 - 0.214 * AMC + 103.082 * DT

Where AMC = Total Aerosol Mass Concentration

DT = Depression Temperature = Dry bulb – Dew point temp

This equation is used on 4-8 January 2008 data for validation. A visibility value of less than 1000 meter is considered as fog occurrence criteria. The predicted and observed fog occurrence is plotted in Figure 6. The estimation of fog occurrences is satisfied for 96 hours out of observed 109 hours.

6. Summary and Conclusions

Delhi is a mega-city with very high air pollution concentration levels. The increasing particulate pollution in urban areas is responsible for fog formation. The field experiments for the measurement of aerosol mass concentrations along with meteorological parameters and visibility were conducted and data analyses were performed in various ways.

Our study over a sampling location at Delhi clearly shows that high aerosols load is one of the important

factors for fog formation. The result of linear regression model depicts that increase in pollution

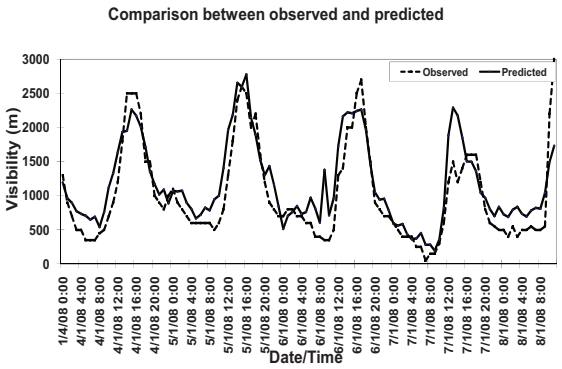

Figure 6. Comparison between of observed and predicted visibility

level (aerosol mass concentration) and less depression temperature are favorable for fog formation over sampling site in Delhi. This is a noble approach for making an idea about the dependency of pollution in favorable meteorological condition. The conclusions of the above study can be used to substantiate the future campaigns at different sites and conditions.

Acknowledgements

Authors thank India Meteorological Department, Govt. of India for providing Meteorological data during the study period. The authors are extremely thankful to Prof. B. N. Goswami, Director, IITM and Dr. P. C. S. Devara, Scientist G and Head P. M. & A. Division for their guidance and unstinted support throughout the study. Authors are also thankful to Mr. Manish Soni for his kind assistance

References

[1] Ali, K., Momin, G..A., Tiwari, S., Safai P. D. Chate, D. M., and Rao, P. S. P., 2004. Fog and precipitation chemistry at Delhi, North India. *Atmospheric Environment* 38, 4215-5422.

[2] Bergot, T., Guedalia, D., 1994. Numerical Forecasting of radiation fog. Part I : Numerical model and sensitivity tests" *Monthly Weather Review* 122, 1218-1230

[3] Brooks, S.D., Gonzales, M., and Farias, R., 2009. Using surface tension measurements to understand how pollution can influence cloud formation, fog, and precipitation. *Journal of Chemical Education 86 (7)*, 838-841.

[4] Bott, A., Sievers, u., Zdunkowski, W., 1990:A Radiation Fog Model with a Detailed Treatment of the Interaction between Radiative Transfer and Fog Microphysics, *Journal of Atmospheric Science* 47, 2153-2166.

[5] Frank, G., Martinsson, B.G., Cederfelt, S., Berg, O.H., Swietlicki, E., Wendisch, M., Yuskiewicz, B., Heintzenberg, J., Wiedensohler, A., Orsini, D., Stratmann, F., Laj, P., 1998. Droplet formation and growth in polluted fogs, *Contribution to Atmospheric Physics* Vol. 71, No. 1, 65-85.

[6] Hudson, J. G., 1980. Relationship between fog condensation nuclei and fog microstructure, *Journal of Atmospheric Sciences* 37, 1854–1867

[7]Mircea M., Facchini, M.C., Decesari, S., Fuzzi, S., Charlson, R. J., 2002. The influence of the organic aerosol component on CCN super saturation spectra for different aerosol types, *Tellus* 54B, 74-81.

[8] Mohan, M., Payra, S., 2008, Influence of aerosol spectrum and air pollutants on fog formation in urban environment of mega city Delhi, India. *Environmental Monitoring and Assessment* 151, 265 - 277

[9] Sciare, J., Cachier, H., Sarda-Estève, R., Yu, T., 2007 Semi-volatile aerosols in Beijing (R.P. China): characterization and influence on various $PM_{2.5}$ measurements, *Journal of Geophysical. Research* **112** , p. D18202 10.1029/2006JD007448.

[10] Singh, S., Nath, S., Kohli, R., Singh, R., 2006. Aerosols over Delhi during pre-monsoon months: Characteristics and effects on surface radiation forcing, *Geophysical Research Letter* 32, L13808, doi:10.1029/2005GL023062.

[11] Stoelinga, M. T., Warner., T. T., 1999. Nonhydrostatic, mesobeta-scale model simulations of cloud ceiling and visibility for an east-coast winter precipitation event. *Journal of Applied Meteorology* 38, 385-404.

[12] Toon O.B., Tabazadeh, A., Browell, E.V., Jordan., J., 2000. Analysis of lidar observations of Arctic polar stratospheric clouds during January, 1989. *Journal of Geophysical Research* 105, 20589-20616.

5th International Conference on Fog, Fog Collection and Dew
Münster, Germany, 25–30 July 2010
FOGDEW2010-49

Analysis of fog occurrence on A75 Motorway, with weather station data in relation to satellite observation

M. Colomb (1), **F. Bernardin** (1), B. Favier (1), E. Mallet (2) and O. Laurantin (2)
(1) Laboratoire Régional des Ponts et Chaussées 9-10 rue B. Palissy, Clermont-Ferrand, France
(2) Météo-France, Direction des Systèmes d'Observation, 42 av. Gaspard Coriolis, Toulouse, France
(michele.colomb@developpement-durable.gouv.fr)

Abstract

Transport is often disturbed in wintertime by fog occurrence causing delay. Fog may also be responsible for dramatic accidents causing injuries and fatalities. Fog forecast remains a difficult task. Satellite observation combined with surface measurements by a network of road weather stations could provide short-term information that could be useful to assist traffic authorities in taking decisions relating to traffic control measures or driver information. The analysis method has been tested on some case studies on the motorway E11-A75 in Auvergne region in France. Weather stations data are presented and connected to satellite images analysis in order to improve the estimation of visibility distribution.

1. Introduction

Fog occurrence may have a major impact on traffic safety on motorways. It also has an economic impact, by causing major delays in the transport of goods and passengers. Airline companies or traffic managers require more efficient forecasts of fog occurrence and visibility level. Forecasts of visibility levels would therefore assist traffic authorities in making decisions relating to driver information and traffic control measures. In order to improve forecasting methods, input data are required and satellite data have to be connected to ground observation measurements. This paper will present ground observations based upon weather station data. The analysis method is tested on some case studies on the motorway E11-A75, thanks to a network of 15 weather stations along the 300 km of motorway. In the highest area that is between 580 and 1100 m, the value of the relative humidity has been analyzed in relation to the visibility measured by a diffusometer. One particular fog event of December 2009 is selected and analyzed in this paper. The surface measurements help to discriminate between low clouds and fog. Satellite images allow to identify cloud types and are taken into account to establish a map of the risk of fog occurrence. The goal of the Météo-France fog analysis is to establish a spatialization of visibility distribution.

2. Data fusion product

A product has been developed by Météo-France/Observing Systems Direction in order to provide an hourly quantitative information about visibility, whatever the phenomenon behind the decline in visibility (fog, rain, low cloud), at each point of the domain (French emerged lands with a geographical resolution of 3 km). The first step is to spatially distribute the observed visibilities, using a multi-linear regression on meteorological and geographical predictors. One of those meteorological predictor is the Cloud Type category (developed by the French Centre de Météorologie Spatiale (CMS) of Météo-France, to provide a detailed analysis of observed clouds, [1]. In a second step, the visibility distribution is treated as a log-normal distribution whose parameters are estimated using a relationship established over 2 years of data. Thus, we will be able to provide both deciles of visibility (capped at 10000m) and the probability of observing visibilities below a given threshold (cf. Figure 1).

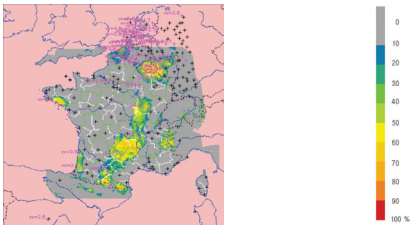

Figure 1 : Probability of observing visibilities below a specified threshold - December, 11 2009 18 UTC

3 . The Motorways 75 and the weather stations

The entire route of the motorway A75, between Clermont-Ferrand to Beziers, is about 300 km long. The mountainous part is about 200 km, it is equipped with a network of 15 weather stations. Figure 2 shows the position of these stations on a relief map, with the corresponding distances in kilometres. On the right the altimeter readings show that the stations ranged between altitudes of 580-1100 m. Figure 3 shows the longitudinal section of the A75 in the department of Cantal, indicating a motorway route with a mountain pass at an altitude of about 1100m (Col de la Fageole). This portion of the route is often affected by fog formation. One can also observe the longitudinal distribution of the 6 road weather information systems, spaced about ten miles. This area was already the test section of a preliminary study [2].

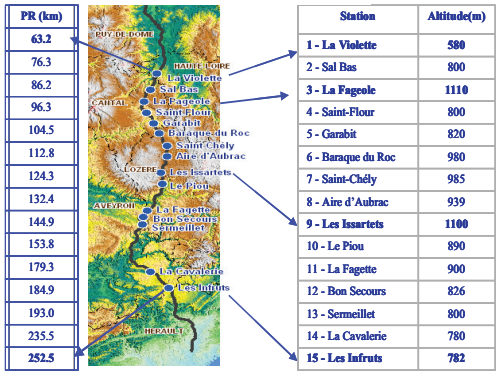

Figure 2: The 15 Weather stations on motorway E11-A75

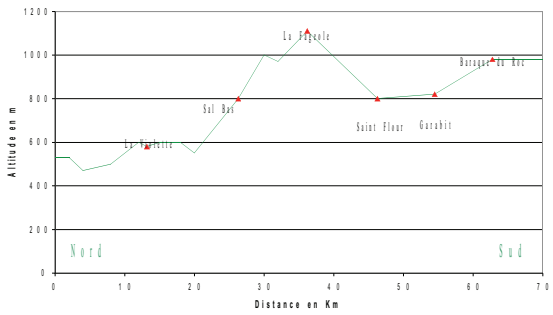

Figure 3: Altitude profiles of the highest section of the motorways E11-A75 with the 6 weather stations

4. Case study : December, 9 and 10 2009

4.1 Description of the meteorological situation

December 9, 2009 : altitude, the axis of a ridge is positioned on France and shifts slowly eastward. Surface, the warm sector of a wave covers a large part of the country. After undulating, the cold front sinks on the Northwest. It is reactivated by the dynamics of altitude during the night of December 9 to 10.

December 10, 2009 : a dynamic thalweg associated with a cold front runs quickly on the north. Then it plunges along the eastern borders. The rear of the cold front is inactive ; then, pressure increases quickly with the establishment of a ridge near the Atlantic where pressure increases in the lower layers.

Regarding the area studied, a cloud band extends Auvergne, with morning fog. Thus, on December 9 and 10, some observers report instances of fog near A75 (daily data).

4.2 Satellite data

Low clouds are detected on the A75 on December, 9 at 22 and 23 UTC (cf. Figure 4). As of December, 10, 00 UTC, clouds located at higher levels mask any low clouds. Thereby the analysis of the situation can not be based only on satellite images. Establishing a diagnosis requires merging data from different sources, including surface measurements.

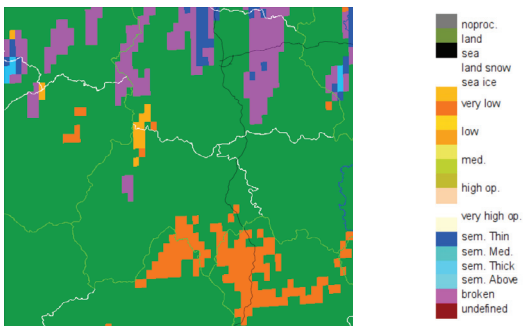

Figure 4 : Cloud Type Product - Centre de Météorologie Spatiale de Météo-France (satellite data reception and processing centre) – December, 09 2009 23 UTC

4.3 Spatialization of visibilities

Above all, it is important to note that the proposed maps do not represent an absolute reference. They are an estimate of the probability of observing visibilities below a given threshold.

We present maps of probability of observing visibility less than 1000m and compare them to the available data (weather stations on Motorway 75). The values measured by Motorway weather stations are plotted in blue. Visibility (vv) is expressed in km and is rounded to the lower hm. Relative humidity (Hu) is expressed in %.

In a first step, Figure 5 shows the map obtained by taking only the synoptic observations (threshold : 1000m). The probabilities seem to be under-estimated. This is particularly evident in the case of station 3 (probability less than 10%).

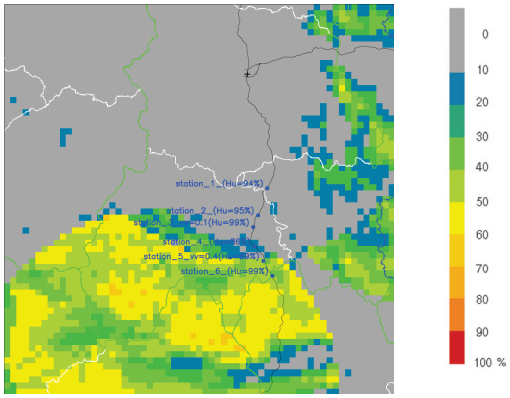

Figure 5. Probability of observing visibilities below 1000m (synoptic observations) - December, 09 2009 23 UTC

The quality of these maps depends partly on the number of point of observation where visibility is available. This is the reason why, in a second step, visibilities measured by Motorway weather stations were added to those of the synoptic network. It allows to improve the spatialization (especially in the case of station 3), as shown in Figure 6.

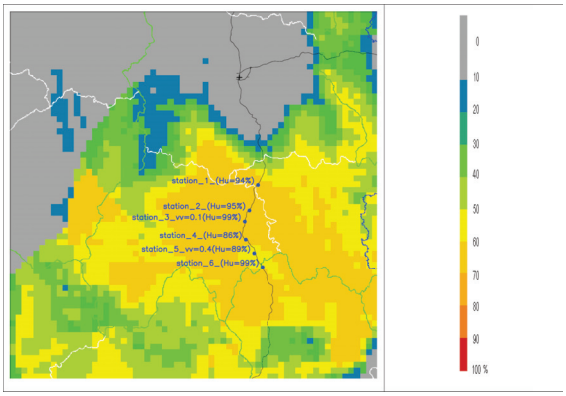

Figure 6. Probability of observing visibilities below 1000m (synoptic observations and data from road weather stations) - December, 09 2009 23 UTC

Thus, integrating data from Motorway 75 stations, and more generally, from all stations belonging to road managers, should improve the spatialization of visibilities. However it is necessary to ensure the reliability of these data (maintenance criteria, but also characteristics of the sensors).

4.4 Weather station data

For all the weather stations we have standard measurements of air temperature, relative humidity, wind speed and direction, and only for stations 3 and 5, visibility data are available from a diffusometer. Then we will focus on the data of these 2 stations. The figures 7 and 8 give the time evolution of the relative humidity (left axis) and of the visibility (right axis) during the night of the 9 to the 10 December for weather station 3 and 5.

At station 3 (figure 7), col de la Fageole, the atmosphere is saturated at 100% with very dense fog. The visibility is reduced at 50m for 3 hours and then increase to 900 m with some local fog benches during the night .

At station 5 (figure 8) Garabit, the atmosphere is a little less saturated at about 90% with moderate fog. The visibility is reduced at 450m for all the studied period.

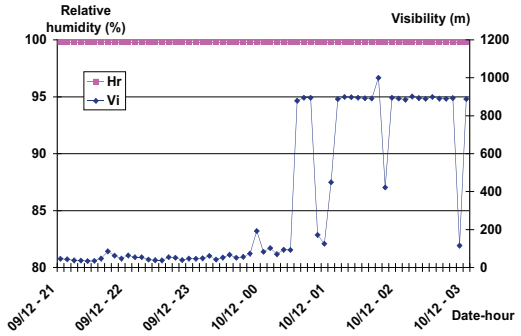

Figure 7: Time evolution of relative humidity and visibility at station 3 from 09/12 at 21h to 10/12 at 03h

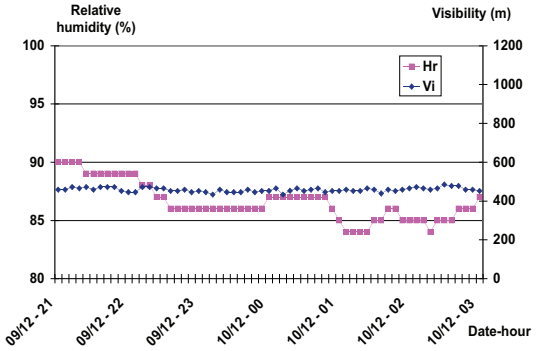

Figure 8: Time evolution of relative humidity and visibilityat station 5 from 09/12 at 21h to 10/12 at 03h

6. Summary and Conclusions

The paper presents the results of a joint study between department of transport and the national weather service Meteo-france. The purpose of the project is to improve some new data fusion product dedicated to fog occurrence and estimation of visibility distribution. This type of product could be useful for traffic authorities. A case study is analysed on the motorway E11-A75 in Auvergne region in France. Weather stations data are presented and connected to satellite images analysis. A first test of the product is made by taking only the synoptic observations. It shows an underestimation of the ground situation at the road weather station. In a second step, visibility measured by Motorway weather stations were added to those of the synoptic network. It allows to improves the spatialization of fog and by a better probability to observe fog below 1000 m visibility. This kind of analyse will be continued on other case study in order to validate these first results.

Acknowledgements

We gratefully acknowledge the motorway E11-A75 manager and winter maintenance team for their help in this study.

References

[1] Derrien, M. and Legléau, H. : MSG/SEVIRI cloud mask and type from NAFNWC, Internat. J. Remote Sensing, pp4707-4732

[2] Colomb, M., Bernardin, Fity, R., Morange, P., Laurentin, O., Tzanos, D., Spatialisation du brouillard sur un itinéraire - Étude préliminaire des paramètres des stations météorologiques de l'autoroute A75, Journée scientifique SIRTA 2009, 29 Avril, Palaiseau, France

5th International Conference on Fog, Fog Collection and Dew
Münster, Germany, 25–30 July 2010
FOGDEW2010-50

On Study of Sea Fog over the Yellow and Bohai Seas in China

G. Fu (1), S. Gao (1), Y. Yang (2), X. Xu (2), X. Wang (2), Y. Chen (3), D. Xue (3), and J. Shen (3)

(1) Dept. of Marine Meteorology, Ocean University of China, Qingdao 266100, China (fugang@ouc.edu.cn, fugang@yahoo.cn), (2) Qingdao Meteorological Bureau, Qingdao 266003, China, (3) Shandong Meteorological Bureau, Jinan 250031, China

A ubiquitous feature of the Yellow and Bohai Sea (YBS) in the eastern Asian region is the frequent occurrence of the sea fog in spring and summer season. The pioneer work on sea fog over YBS can be traced back to Prof. Binhua Wang as early as 1940's. He investigated sea fog systematically and published his book *Sea Fog* in 1985 (by *China Ocean Press* and *Springer-Verlag*). Recently, a research group in the Department of Marine Meteorology at Ocean University of China (OUC) continued sea fog research collaborated with Shandong Meteorological Bureau and Qingdao Meteorological Bureau under the financial supports of National Natural Science Foundation of China and China Meteorological Administration. Their researches involved in both observation analyses and high-resolution modeling of sea fog over YBS. In this talk, the brief history of sea fog research in China will be reviewed firstly. Then, a typical heavy sea fog event over YBS occurred in the morning of 11 April 2004 will be documented by using all available observational data and high-resolution Regional Atmospheric Modeling System (RAMS) modeling results. Finally, the applications of a quasi-operational sea fog forecasting system which was mainly based on RAMS model will be introduced.

5th International Conference on Fog, Fog Collection and Dew
Münster, Germany, 25–30 July 2010
FOGDEW2010-51

Improvement of Initial Conditions of Sea Fog Modeling with Cycling 3DVAR-WRF

S. Gao (1), G. Fu (1), W. Wu (2), and X. Xu (3)

(1) Dept. of Marine Meteorology, Ocean University of China, Qingdao 266100, China (gaosh@ouc.edu.cn), (2) Shandong Meteorological Bureau, Jinan 250031, China, (3) Qingdao Meteorological Bureau, Qingdao 266003, China

Among the seas of China, the Yellow Sea (YS) experiences sea fog most frequently, especially during the spring and summer seasons. Recent studies of sea fog modeling over YS have suggested that data assimilation is a key important issue for sea fog modeling, because simulation result is significantly sensitive to initial conditions. In this talk, a heavy sea fog over YS occurred from 6 to 7 March 2006 is carefully studied by using Weather Research and Forecasting (WRF) model. The evolution of sea fog area is demonstrated by the Multi-functional Transport Satellite (MTSAT)-1R visible imagery and infrared data using dual channel difference method. A cycling 3DVAR scheme with 12-h assimilation window is designed and employed to generate the initial conditions for this sea fog simulation. The result shows that the simulated sea fog area is greatly improved compared to the result without cycling 3DVAR. Additionally, the initial conditions with cycling 3DVAR-WRF are also used to force the Regional Atmospheric Modeling System (RAMS) model to simulate this sea fog case. We find that the simulated sea fog coverage is much better than the result with RAMS original isentropic analysis.

5th International Conference on Fog, Fog Collection and Dew
Münster, Germany, 25–30 July 2010
FOGDEW2010-53

Assessment of the unidentified organic matter fraction in fogwater using fluorescence spectroscopy

Dr. Valsaraj and Dr. Birdwell

Louisiana State University, Chemical engineering, Baton Rouge, United States (valsaraj@lsu.edu, 225-578-1476)

Dissolved organic matter (DOM) in fogwaters from southeastern Louisiana and central-eastern China has been characterized using excitation-emission matrix (EEM) fluorescence spectroscopy. The results demonstrate that fluorescence spectroscopy can be used to obtain a qualitative assessment of the large fraction of fogwater organic carbon (∼40 – 80% by weight) that cannot be identified in terms of specific chemical compounds. The method has the principle advantage that it can be applied at natural abundance concentrations, thus eliminating the need for large sample volumes required to isolate DOM for characterization by other spectroscopic (NMR, FTIR) and chemical (elemental) analyses. It was anticipated that the fogwater organic matter fluorescence spectra would resemble those of surface and rain waters, containing peaks indicative of both humic substances and fluorescent amino acids. Humic- and protein-like fluorophores were observed in the fogwater spectra and fluorescence-derived indices had values comparable to other natural waters. Biological character (intensity of tyrosine and tryptophan peaks) was found to increase with organic carbon concentration. Fogwater organic matter appears to contain a mixture of terrestrially- and microbially-derived material. The fluorescence results show that most of the unidentified fogwater organic carbon can be represented by humic-like and biologically-derived substances similar to those present in other aquatic systems.

5th International Conference on Fog, Fog Collection and Dew
Münster, Germany, 25–30 July 2010
FOGDEW2010-56

Detection of Fog/Low Stratus Using MSG SEVIRI Images

A. Erturk (1) and J. Prieto (2)
(1) Turkish State Meteorological Service, Ankara, Turkey (agerturk@dmi.gov.tr / Fax: +90-312-3606276)
(2) EUMETSAT-Darmstadt, Germany

Abstract

Under winter conditions, fog is severely affecting air, sea and land transportation. Automatic detection of fog and low stratus using satellite data is crucial in operational nowcasting. The high temporal resolution and the high spectral discrimination of MSG SEVIRI support the operational nowcasting application in the large scale. Differential droplet emissivity at 10.8 and 3.9 micron bands, and Brightness Temperature Differences (BTD) between the corresponding channels can be applied to detect fog or low stratus. Additionally, the RGB composite called "fog RGB" proves beneficial to detect fog at night time. Its derivation is simple and is described later. At high latitudes on frozen grounds, the use of 8.7μm instead of 3.9 μm is of advantage.

In this study, MSG SEVIRI applications to detect fog or low stratus are discussed. Additionally, the catastrophic fog event occurred at 20-26 November 2009 over western Turkey will be presented. Satellite-based fog detection gives new opportunities to forecasters in the very short term.

1. Introduction

Fog is meteorological phenomena with an important economic and social impact on aviation, and on marine and land transportation. Many examples have been reported of the economic benefits of early estimation of fog [6] .

Rawinsonde observations and indices such as the Fog Stability Index (FSI) [7] , the Fog Point and the Fog Threat, based on rawindsonde data, are useful tools.

Detection of fog and low stratus using polar and geostationary satellite data are providing another opportunity to the forecasters. Eyre [5] utilized NOAA AVHRR imagery to detect night time fog and low stratus, Ellrod [2] developed an algorithm using GOES imagery, Cermak and Bendix [1] applied the same approach with MSG SEVIRI imagery.

Channel differences and RGB composites present also clear information day and night for the detection of fog. Erturk [4] developed a tool called MSGView to display and analyze of MSG SEVIRI data.

In this study we present MSG SEVIRI applications to detect fog or low stratus together with a case study over north-west Turkey. In the Data and Method section we give brief information about the SEVIRI channels and the RGB composites. The next section presents a catastrophic event as a case study. The Validation section presents synoptic, rawinsonde observations and temp diagrams to show a meteorological background. In the last section we discuss existing RGB composites and provide suggestions.

2. Data and Method

The second generation of imaging radiometers on board of the European geostationary satellite Meteosat is called SEVIRI. It is a Spinning Enhanced Visible and Infrared Imager (SEVIRI), used to support nowcasting and short term forecasting.

The composition of three or more channels and their differences is used to create RGB composite images. RGB composites reflect physical properties of the scene below. The recipes for the generation of the Fog RGB composites are given at Table 1 [3].

Table 1: Range for RGB's detecting fog

Beam	Channel	Range (K)	Gamma
"night-fog RGB"			
R	IR12.0-IR10.8	-4 to 2	1.0
G	IR10.8-IR3.9	0 to 10	1.0
B	IR10.8	263 to 293	1.0
"24-hours-fog RGB"			
R	IR12.0-IR10.8	-4 to 2	1.0
G	IR10.8-IR8.7	+2 to 6	**2.0**
B	IR10.8	263 to 293	1.0

3. Fog Event over Istanbul

During the period 21-26 November 2009, a catastrophic fog event occurred over north-western Turkey, covering Istanbul airport. Hundreds of flights were cancelled or deviated to other destination airports.

The Fog RGB composite, here given on Figure 1. Fog and low clouds affected the Marmara Sea and Istanbul.

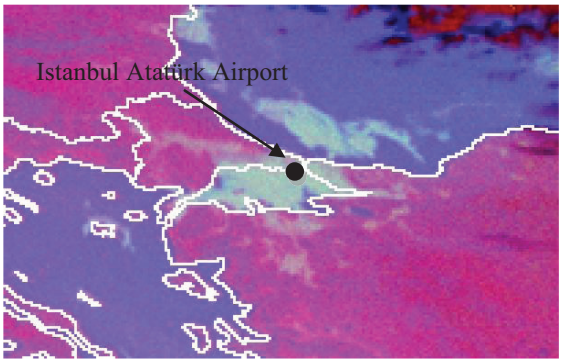

Figure 1: *Fog RGB image, 22 Nov. 2009, 04.00Z*

4. Verification

The half-hourly variation of visibility versus BTD at SEVIRI channels is given at Figure 2 for 21 November.

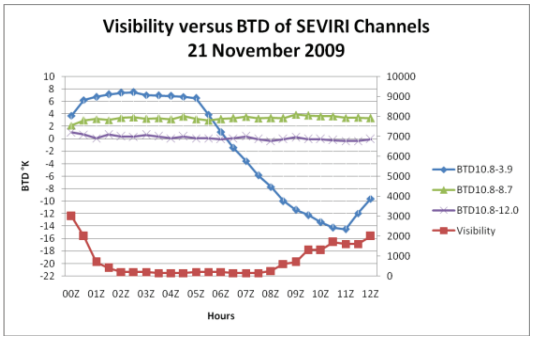

Figure 2: Half hourly variation of visibility versus BTDs of SEVIRI channels for Atatürk airport.

5. Summary and Conclusions

The detection of fog by means of MSG radiometric information is reliable. The night and 24-hour RGB products are appropriate to detect and monitor fog. Verification was performed with synoptic observations and TEMP report diagrams. The results are positive and highly correlated. They show too that the vertical and the horizontal extent of fog are not strictly related variables. The satellite is sensitive to the vertical extent, the visibility measurements are performed horizontally. MSG imagery, monitoring large areas, is crucial for fog detection and for nowcasting fog dissipation.

References

[1] Cermak, J., Bendix, J., Dynamical nighttime fog/low stratus detection based on Meteosat SEVIRI data - a feasibility study. Pure Appl. Geophys. 164, 1179–1192, 2007

[2] Ellrod, G.P., Advances in the detection and analysis of fog at night using GOES multispectral infrared imagery. Weather Forecast. 10, 606–619, 1995.

[3] Eronn, A. , Fog detection in cold winter situations at high latitudes. Final report of EUMETSAT Graduate Trainee, 2007.

[4] Ertürk A.G., MSGView : A Training Tool for Processing, Analyzing and Visualization of MSG SEVIRI Data, EGU General Assembly Vienna, 2010.

[5] Eyre, J. R. Brownscombe, and R. J. Allam, Detection of fog at night using Advanced Very High Resolution Radiometer (AVHRR) imagery. Meteor. Mag., 113, 266-271, 1984.

[6] Gultepe I., G. Pearson, J. A. Milbrandt, B. Hansen, S. Platnick, P. Taylor, M. Gordon, J. P. Oakley, and S. G. Cober. The Fog Remote Sensing and Modeling Field Project, Bulletin of the American Meteorological Society , 90: 341-359, 2009.

[7] Wantuch, F., Visibility and fog forecasting based on decision tree method, IDOJARAS, 105, 29–38, 2001.

5th International Conference on Fog, Fog Collection and Dew
Münster, Germany, 25–30 July 2010
FOGDEW2010-57

Forecast of Low Visibility and Fog From NCEP– Current Status and Efforts

Binbin Zhou[1], Geoff Dimego[1] and Ismail Gultepe[2]

[1] Environmental Modeling Center of NCEP, National Weather Service, NOAA, Camp Springs, Maryland, USA
[2] Cloud Physics and Severe Weather Research Section, MDR, Environmental Canada, Toronto, Ontario, Canada
Binbin.Zhou@noaa.gov

1. Abstract

This paper summarizes the performances of low visibility/fog predictions over North America using the operational National Centers for Environment Prediction (NCEP) forecast models. The evaluation of the results shows that the performances of the low visibility/fog forecasts from these models are still poor in comparison to those of operational precipitation forecasts from the same models. In order to improve the skills of the low visibility/fog prediction, several efforts have been made including implementations of a multi-rule fog detection scheme and a short range ensemble forecast system (SREF). How to apply these techniques in fog prediction is described and evaluated.

2. Introduction

Fog is an important hazardous weather event that affects aviation, transportation and marine traffic. A central guidance from NCEP on its thresholds is being considered and particularly emphasized in National Weather Service (NWS) of NOAA and in NextGen [1], a future Air Traffic Management System of Federal Aviation Administration (FAA), United States. However, fog is still not part of the documents of NCEP central guidance, due to its complexity and limitation of computational resources. Instead, it is only diagnosed locally by forecasters either through subjective visibility's forecast or through other variables from model outputs such as MOS (Model Output Statistics). Nevertheless, effort to add it to NCEP' central guidance is always considered to be important. As a step forward to echo the request from NWS and NextGen, presently, low visibility/fog forecast has been experimentally implemented, tested and validated using NCEP operational models. Currently, the visibility (Vis)-liquid water content relationship of Stoelinga [2] is used in horizontal visibility computation in all of the NCEP models. However, studies have shown that this visibility computation is of high error, particularly in situation of fog when droplet number concentration (N_d) is not considered [3]. Besides the error from Vis computation, bias in modeled liquid water content (LWC) near the surface is also another source of errors. The visibility computation error can be reduced by applying Gultepe's Vis versus LWC and N_d parameteri-zation [3]. Whereas reduction of modeled LWC error is extremely difficult due to low resolution of current operational models, lack of fog physics, low accuracy of LWC at the surface, and model bias itself, etc. To overcome these drawbacks in the operational models, we developed a rule based fog detection scheme recently and it is successfully applied for fog studies. It was used in NCEP's special SREF for 2008 Beijing Olympic Game Project (B08RDP) in China with a 15 km resolution [4]. Now, this scheme has also been applied and tested in the NCEP's SREF with 32km resolution over North America domain.

The objective of this paper is to evaluate (1) performance of fog prediction using the current Vis-LWC relationship based on 3 NCEP's regional models, and (2) improve the rule-based algorithm and ensemble forecast technique for fog detection.

3. Evaluation method and data

An evaluation of fog prediction over North America is generally difficult due to a lack of direct fog observations and the fact that model-based fog value represents a grid area that cannot be interpolated to the location of the observational sites. Here, Vis analysis obtained from the Aviation Digital Database System (ADDS; [5]) of Aviation Weather Center (AWC in Kansas City) of NCEP were used as truth for fog forecast evaluations. The observational data is from Nov. 1 2009 to Apr. 30 2010, covering 6 months. This time period is chosen because of high occurrence of the fog that is defined as Vis<1 km (WMO Manual, 2002). If Vis≤1 km in a grid point, the ADDS grid point is considered as fogy. By comparing model forecast Vis to observed one in a grid point, If Vis≤1 km in both observation and model points, this is assigned as a "hit", if forecast Vis≤1 km but observed Vis ≥ 1 km, this is assigned as a "false alarm", and forecast Vis ≥ 1 km but observed Vis≤1 km, the result is assigned as a" missed alarm". Using these statistical classifications,, forecast scores such as bias, probability of detection (POD), false alarm ratio (FAR), missing rate (MR), and equitable threat score (ETS) were derived. These scores are used to evaluate both single model (deterministic) forecast and ensemble probabilistic forecast performances [4].

3. Performance of current models

In this section, first, evaluation results are given for low visibility/fog forecasts from each of the three regional models. These models include a 12 km resolution North American Mesoscale Model (NAM-12 km or NMM-12 km), a 13 km Rapid Updated Cycle Model (RUC-13km) Model, and a 32 km Nonhydrostatic Mesoscale Model (NMM-13km). The NAM is used to provide regular weather guidance for NWS, the RUC is used as aviation weather guidance, and the NMM is a NCEP version of WRF model based on which other systems, such as NAM, are built.

The performance scores for all three models Vis forecasts are illustrated in Fig. 1, from which the performance scores for fog (Vis<1 km) can be examined. It can be seen that the general performances worsen as visibility threshold decreases. For the Vis threshold of fog, the POD is about 25% for RUC-13 km, 10% for NAM-12 km and only 5% for NMM-32 km. Since NAM is based on NMM-WRF regional model, it can be expected that coarse resolution model NMM-32 km has a lower hit rate (POD) than that of higher resolution (12 km) of the same model in fog prediction.

Another feature shown in Fig. 1 is that the POD for dense fog (Vis<0.5 km) is lower than that of medium fog intensity (Vis>0.5 km but <1 km). In other words, dense fog events are more difficult to detect by these operational models in fog prediction. Fig. 1b shows significant high biases for fog predictions by all 3 models (where bias ~1 means no bias). A positive bias implies an over-prediction or a false alarm of fog forecast. For shallow fog (Vis<1 km), the highest bias is 3 (or 300%) for RUC-13 km. The bias for dense fog (visibility <0.5 km) prediction is even higher. Such high positive biases for all models indicate that low visibility or fog from all NCEP regional models are highly overpredicted. The very low POD with very high bias leads to very poor performances indicated by ETS (Fig. 1c), where the ETS values for all 3 models are less than 5%. For dense fog, their ETS values become much smaller. To compare the ETS values for fog prediction to that for precipitation prediction, the average precipitation forecast ETS (~35%) from current NCEP regional models is also depicted in Fig. 1c, showing that the ETS for fog prediction is much lower than that for precipitation prediction. This means that in order to catch up the performance of precipitation forecast at NCEP we have to devote tremendous efforts to improve fog forecast. Very low POD is shown in Fig. 1a and a high bias shown in Fig. 1b and that implies the current low Vis or fog prediction from these models missed most of the fog events over North America and it overpredicted (false alarm) the fog events. To explain this point, results from an east coast regional fog event occurred on Nov.16, 2009 are shown in Fig. 2:

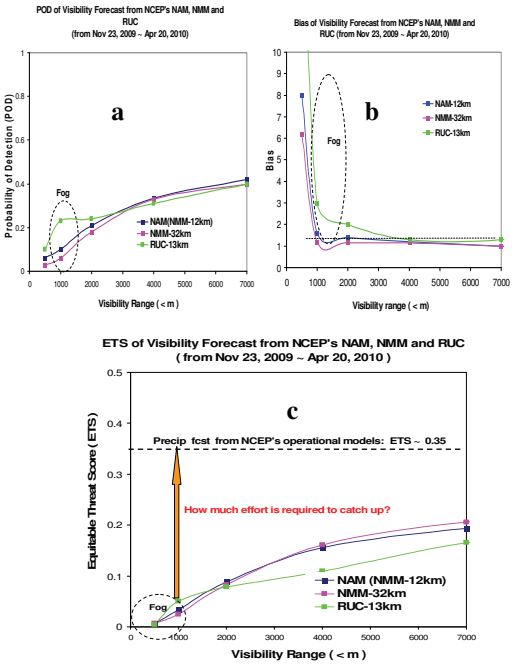

Fig. 1: The tests for Vis: POD (a), Bias (b) and ETTS (c) for each of the 3 forecast models.

Since the visibility computations in the three models are uniquely from fog LWC given at the surface, the green colors (dark, regular and light green) indicate the LWC amount (or intensity), and locations of the fog. Comparing the observed fog location and its intensity (Fig.2a) with the fog Vis obtained from NAM (Fig 2b), one can easily check that the NAM forecast missed most of the fog events in Virginia and North Carolina although it captured some of fog locations in Maryland and Delaware. But the results issued false alarms for half of Pennsylvania and New York states, and most of other northeast states as well as some regions of Canada. Fig. 2c shows that NMM-32 km forecast almost missed all of fog event locations in east coast. The differences in RUC-13 km forecasts for this case can be seen by comparing Figs. 2a and 2d. This run also missed most of locations in Maryland, Virginia, North Carolina and South Carolina, and overpredicted the fog in Pennsylvania and New York states as well as over most of the other northeast states and some regions of Canada, similar to NAM runs. This case, again, indicates much worse performance based on the lower resolution NMM-32 km model than that of the higher resolution NMM-12 km model (or NAM-12 km). Furthermore, the "large-false-alarm" feature of current forecasts of low visibility or fog from these models are also estimated. This feature reminds

us that incorrectly predicted location and amount of grid-scale fog LWC at surface may bring some difficulties to applying more precise visibility formulations in the current operational models.

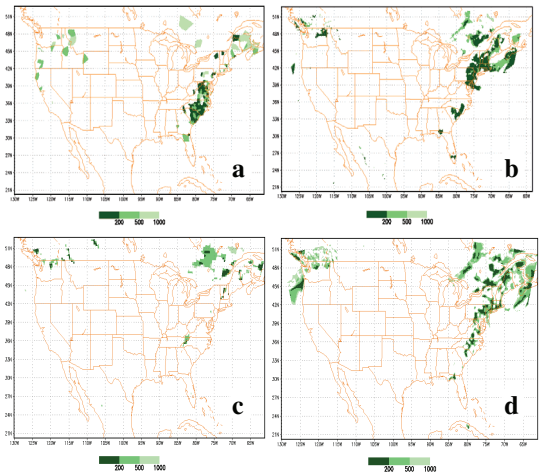

Fig. 2: Nov. 16, 2009 fog visibility observations from ADDS at 1200 UTC in east coast (a) and their forecasts from NAM (NMM-12 km) (b), NMM-32 km (c) and RUC-13 km (d) at the same time. Dark green is for visibility < 0.2 km, regular green for <0.5 km and light green for <1.0 km.

4. Model improvements

Three efforts have been dedicated to improving the performance of experimental central forecast for fog at NCEP recently. The first is testing the "multi-rule" fog diagnostic scheme in the three models, the second is conducting ensemble fog prediction in NCEP's 21-member Short Range Ensemble Forecast System (SREF), and the third is a combination of the multi-rule fog detection and the ensemble technique.

The multi-rule fog diagnostic method has been extensively evaluated in B08RDP in China, showing that the fog prediction ETS from two 15 km resolution WRF models (NCEP and NCAR WRF) was significantly raised from 0.063 with Stoelinga method to 0.192 with the multi-rule diagnosis. The multi-rule fog detection contains 3 sub-rules: (i) LWC rule, which detects fog by modeled surface LWC <0.015 g/kg, (equivalent to visibility <1 km), (ii) cloud rule, which detects fog by modeled cloud base <50 m and cloud top <0.4 km at same time, and (iii) RH-wind rule, which detects fog by RH>90% at 2 m and 10-wind speed < 2 m/s at same time. In B08RDP, the evaluation shows that the RH-wind rule has at least 50% contribution to the total ETS, while the LWC and cloud rules has 30 and 20 % contributions, respectively. This implies that radiation fog is the most frequent fog type in China since RH and calm air are two critical conditions for radiation fog. Without the RH-wind rule, the models would miss at least 50% of fog events. Recently the multi-rule fog diagnosis has also been tested in NAM, NMM-32 km and RUC-13 km over North America. The LWC and cloud rules are kept same but RH-wind rule was retuned as RH>95% and wind speed <1 m/s to better detect radiation fog over North America.

The second effort is conducting the ensemble fog forecast from the NCEP-SREF system. The ensemble forecast technique was suggested and developed recently to deal with model uncertainties and errors in numerical weather prediction (NWP) [6] and has shown many advantages over single model forecast not only for regular weather conditions but also for fog [4][7]. For example, an ensemble forecast provides not only more precise forecast but also the forecast error range and its confidence in advance. Furthermore, with an ensemble probability forecast of a specific weather, users have more freedom to determine or make decision on their own cost/loss economic benefits. Computation of a fog occurrence probability at a grid point from the NCEP SREF is relatively simple: first step is counting how many members predict fog at this grid point, and then dividing the count by total ensemble members to get the fog probability at this grid. After the fog probabilities at all of grid points are calculated, the fog probability distribution over entire domain can be obtained. Obviously, such a fog probability distribution is given in a grid-scale since the computation is grid-wide. The ensemble fog forecast was also applied and evaluated in B08RDP with a 10-member SREF and showed further improvements in forecast performance in addition to the multi-rule application [4].

To use the traditional measures in evaluation of an ensemble forecast, the SREF fog probabilistic forecast needs to be transferred to a deterministic forecast. To do this, a probability threshold, e.g. 50%, can be selected. If the fog probability at a grid point exceeds 50%, or half of ensemble members predict fog, the SREF predicts fog at this point. Different users may select different thresholds. The predictions with each threshold should be evaluated. In the analysis, 10 probability thresholds, from 10% to 100% at 10% bins, were evaluated. Then, the evaluated scores against the 10 probability thresholds are shown in Fig.3.

From Fig. 3, we can see that for different ensemble probability thresholds, the SREF ensemble forecast for fog visibility has different performance values. For a smaller probability threshold, the ensemble forecast gives a higher POD with a large bias. To decrease the bias, a larger probability threshold should be used. In this case; however, the ensemble forecast POD decreases significantly. Therefore, how to select an appropriate ensemble probability threshold in fog forecast is a trade-off. Usually, the threshold is selected as an intermediate value; not very small and large, but around 30~50%, where the ensemble forecast usually has a best performance [4].

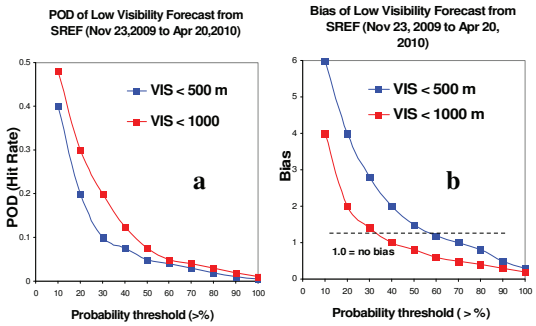

Fig. 3: SREF's fog prediction POD (a) and Bias (b) under different ensemble probability thresholds as in x-axis

The third step is to combine the first and the second efforts. This work is very straightforward and has been tested in ensemble models in the NCEP SREF. The performance of the first, second and the third efforts in comparison to the predictions without these efforts can be examined in Fig. 4. The improvements in the multi-rule effort can be expected by comparing POD or ETS between with multi-rule and without multi-rule (i.e. LWC-only) for

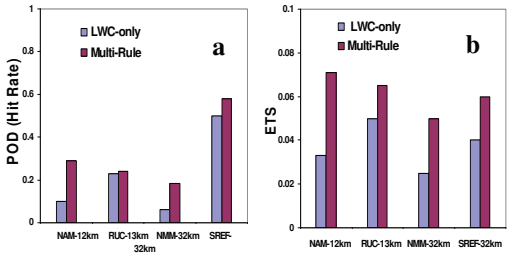

Fig. 4: POD (a) and ETS (b) of fog prediction from NAM (NMM-12 km), RUC-13 km, NMM-32 km and SREF-3 km with multi-rule fog detection and without multi-rule detection scheme (LWC-only).

detection from NAM (or NMM-12 km), NMM-32 km, and RUC-13 km. Although these improvements are not significant as those shown in B08RDP, the improvements are still obvious for NAM and NMM-32 km models, and results about 50% increases in both POD and ETS. The significant performance improvements from the ensemble technique can be observed by comparing NMM-32 km and SREF-32 km (since NMM-32 km is one of the reference models in the SREF system). The further improvements of multi-rule and ensemble combination can be seen from comparing SREF-32 km model with multi-rule and without multi-rule (i.e. LWC only). There is additional 20-30% increase in POD or ETS by using multi-rule fog detection scheme in the SREF system.

5. Conclusion

Through verifications of low visibility (<1 km) operational forecasts from NCEP's three regional models, NAM-12 km, RUC-13 km and WRF-NMM-32 km, over North America against ADDS data over 6 months time period, the performance of fog predictability were evaluated. This shows that the performances of fog predictions from the models still need improvements. The reason may be that these models are unable to predict correct locations and intensities of fog events due probably to too-coarse model resolutions, missing appropriate fog physics in the models, and model numerical bias.

Three efforts have been made to improve fog prediction at NCEP, including an application of a "multi-rule" fog detection scheme, an application of ensemble technique in SREF, and a combination of these two applications. The verifications with the same ADDS data over North America have shown obvious increases in prediction performances, suggesting that these techniques can be further applied in future North American High-Resolution Rapid Refresh Ensemble (HRRRE) Forecast System at NCEP requested by the NextGen of FAA.

Acknowledgement

This work was fully funded by FAA. Our special appreciation is given to Aviation Weather Center for providing the ADDS data to support this study.

Reference

[1]Souders, C. G., et al., 2010: NextGen weather requirements: an update. Preprint, 14th *Conf. on Aviation, Range, and Aerospace Meteorology*, Atlanta, GA, Amer. Meteor. Soc.

[2]Stoelinga, T. G. and T. T. Warner, 1999: Nonhtdrostattic, mesobeta-scale model simulations of cloud ceiling and visibility for an east coast winter precipitation event. *J. Apply. Meteor*., 38, 385-404.

[3]Gultepe, I., M. D. Müller, and Z. Boybeyi, 2006: A new visibility parameterization for warm fog applications in numerical weather prediction models. *J. Appl. Meteor*. Clim., 45, 1469-1480.

[4]Zhou, B. and J. Du, 2010: Fog prediction from a multimodel mesoscale ensemble prediction system. *Wea Forecasting*, 25, 303-322.

[5]http://aviationweather.gov/adds

[6]Toth, Z. and E. Kalnay, 1993: Ensemble forecasting in NMC: The generationof perturbations, *Bull. Amer. Meteor. Soc*., 74, 2317-2330.

[7]Roquelaure, D. S. and T. Bergot, 2008: a local ensemble prediction system (L-EPS) for fog and low clouds: Construction, Bayesian model averaging calibration, and validation. *J. Appl. Meteor. Clim.,* 47, 3072-30.

5th International Conference on Fog, Fog Collection and Dew
Münster, Germany, 25–30 July 2010
FOGDEW2010-58

Fog chemistry in central India

K. S. Patel(1), B. Ambadey(1) and B. Blazhev(2)

(1)School of Studies in Chemistry, Pt. Ravishankar Shukla University, Raipur-492010, CG, India (patelks_55@hotmail.com)

(2)Central Laboratory for Chemical Testing and control, 1330-Saofia, Bulgaria

Abstract

The investigation of fog chemistry in the urban area is of great environmental and health hazard interests. In the present work, the fog chemistry in the most polluted area of central India, Raipur and its surrounding is described. Twenty two fog samples were collected in winter season, 2007-08 and their physiochemical properties were measured. The fog is yellowish in colour with neutral pH value except in coal burning site. The volume weighted concentration of species i.e. F^-, Cl^-, NO_3^-, SO_4^{2-}, NH_4^+, Na, K, Mg, Ca, Al, Mn, Fe, Cu, Zn, Pb and Hg is ranged from 1.7 – 2.4, 14.2 – 33.1, 11.4 – 23.8, 21.7 – 116, 2.8 – 8.2, 4.6 – 33.7, 4.8 – 22.4, 2.6 – 6.7, 8.5 – 18.5, 0.570 – 1.030, 1.100 – 1.640, 0.510 – 1.290, 0.080 – 0.117, 0.058 – 0.112 and 0.004 – 0.013 mg l^{-1} with mean value of 2.0±0.2, 23.6±7.0, 16.5±4.6, 46.9±28.2, 5.0±1.4, 12.2±8.7, 11.5±4.8, 4.8±1.3, 14.2±3.4, 0.875±0.120, 1.292±0.141, 0.759±0.155, 0.100±0.010, 0.087±0.014 and 0.008±0.002 mg l^{-1}, respectively. The variations, correlations and sources of the ions and metals in the fog water are discussed.

1. Introduction

Fogs are composed of fine droplets of water suspended in the air near the Earth's surface and formed a moist air mass when cooled to its saturation point (dew point). The presence of these droplets scatters the light and thus reduce the visibility near the ground. The fog droplets are approximately 100 times smaller than rain drops, highly concentrated with respect to the chemicals [1]. The smog, a soup of smoke with fog causes low visibility, health hazard and harm agricultural production [2]. The airborne particles burden over Asia are increased significantly due to rising of population, industrialization and urbanization. A major factor contributing to fog is the chemical composition of the aerosols and radiative forcing elements associated with the aerosols. Investigations of fog chemistry and physics have become very important as nutrients and pollutants from fog water exhibit strong influence on ecosystems [3]. In mountain forest ecosystems, fog water is an important source of ion deposition [4]. The chemical characterization of fog water in several parts of the World was carried out [5-12]. In the present work, the fog chemistry (i.e. load of F^-, Cl^-, NO_3^-, SO_4^{2-}, NH_4^+, Na^+, K^+, Mg^{2+}, Ca^{2+}, Al, Mn, Fe, Cu, Zn, Pb and Hg) in the most polluted region of the central India, Raipur region is described. The variations, scavenging ratio, enrichment, correlation and sources of the fog pollution in the central India are discussed.

1.1 Study area

Five cities i.e. Raipur, Korba, Bilaspure, Akaltara, Rajnangaon and Dongargargh of central India were selected for the proposed investigation, Figure 1. These sites were selected as representative of different geography, pollution source and pollution receptor - areas. The geographical characteristics of the sampling locations are summarized in Table 1. Raipur is a capital of Chhattisgarh state with population of ≈2 million inhabitants. Several steel, sponge iron and cement industries are running in Raipur. In Korba, the most of electricity of the state is generated by thermal plants using coal as source of energy.

2. Sample collection and analysis

A passive collector prescribed by Skar˙zy´nska et al. was used for the fog collection [13]. It consists of a 2 m tall collection, of two horizontal disks 20 cm in diameter, installed vertically on frames at a distance of 40 cm from each other. Nylon strings of 0.2 mm diameter between disks were stretched into two rows. After collection, the water was filtered and physical parameters i.e. pH, conductivity and TDS values were measured. The sample was divided into two portions. The first portion was used for analysis of anions and cations. The second portion was acidified with few drops of ultrapure nitric acid (E. Merck) and used for analysis of the metals. Total 22 fog water sample from five locations: Raipur, Bilaspur, Korba, Akaltara, Rajnandgaon and Dongargargh were collected in year 2007-08. The samples were kept in airtight 250-ml polyethylene bottles and refrigerated at 4 °C for further analysis.

The fluoride content was monitored with Metrohm ion meter-781 equipped with fluoride ion selective electrode and calomel electrode. The Dionex DX120 Ion Chromatograph (Dionex Corporation, Sunnyvale, CA, USA) equipped with anion separation column (AS9-HC, 250x4 mm), cation separation column (CS12A, 250x4 mm) and conductivity detector was used for analysis of the ions. The Varian Liberty AX Sequential ICP-AES and Varian AA280FS Atomic Absorption spectrophotometer equipped VGA-77 (plasma flow: 15 l min^{-1}, auxiliary flow: 1.5 l min^{-1}, power: 1KW, PMT voltage: 650 V) were used for analysis of the metals. The GBC AAS-935 equipped with HG-3000 was used for the analysis of Hg. The E. Merck multi elements standard solutions were used for preparation of the calibration curves.

4. Results and discussion

The pH, conductivity and TDS values (n=22) are ranged from 6.08 – 7.51, 148 – 224 µS and 78 – 128 mg l^{-1} with mean value of 7.07±0.40, 180±22 µS and 96±14 mg l^{-1}, respectively. The lowest pH value is observed in fog water of Korba city due to a huge coal burning, > 35 MT Yr^{-1}. The mean volume weighted concentration of ions i.e. F^-, Cl^-, NO_3^-, SO_4^{2-}, NH_4^+, Na^+, K^+, Mg^{2+} and Ca^{2+} is ranged from 1.7 – 2.4, 14.2 – 33.1, 11.4 – 23.8, 21.7 – 116, 2.8 – 8.2, 4.6 – 33.7, 4.8 – 22.4, 2.6 – 6.7 and 8.5 – 18.5 mg l^{-1} with mean value of 2.0±0.2, 23.6±7.0, 16.5±4.6, 46.9±28.2, 5.0±1.4, 12.2±8.7, 11.5±4.8, 4.8±1.3 and 14.2±3.4 mg l^{-1}, respectively. Among them, SO_4^{2-} shows the highest concentration, may be due to huge coal burning in this region. Their distribution pattern in decreasing order is: $SO_4^{2-} > Cl^- > NO_3^- > Ca^{2+} > Na^+ > K^+ > NH_4^+ \approx Mg^{2+}$. Several folds higher concentration of almost all ions is observed in Korba city, due to higher coal burning. The equivalent ratio of sum of the total anion to cation is ranged from 0.7 – 1.0 with mean value of 0.9±0.1. The mean volume weighted concentration of metals i.e. Al, Mn, Fe, Cu, Zn, Pb and Hg is ranged from 0.570 – 1.030, 1.100 – 1.640, 0.510 – 1.290, 0.080 – 0.117, 0.058 – 0.112 and 0.004 – 0.013 mg l^{-1} with mean value of 0.875±0.120, 1.292±0.141, 0.759±0.155, 0.100±0.010, 0.087±0.014 and 0.008±0.002 mg l^{-1}, respectively. Among them, Mn exhibits the highest concentration followed with Al and Fe. Similarly, almost all metals show the highest concentration in Korba city, due to a huge coal burning.

The mean concentration of species i.e. Cl^-, NO_3^-, SO_4^{2-}, NH_4^+, Na, K, Mg, Ca, Al, Mn, Fe, Cu, Zn, Pb and Hg in the aerosols of Raipur is 4.8, 6.4, 9.5, 1.6, 2.2, 2.1, 0.7, 7.1, 6.8, 0.8, 14.5, 0.8, 1.0 and 0.015 µg m^{-3}, respectively. The mean concentration of species i.e. Cl^-, NO_3^-, SO_4^{2-}, NH_4^+, Na, K, Mg, Ca, Al, Mn, Fe, Cu, Zn, Pb and Hg in the fog water of Raipur is 30, 16, 45, 5.3, 11.3, 11.7, 5.7, 16.1, 1.0, 1.5, 0.8. 0.01, 0.07 and 0.009 mg l^{-1}, respectively.

3. Figures

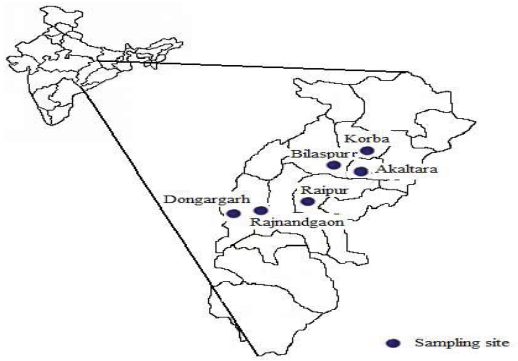

Figure 1. Representation of sampling sites

5. Tables

Table 1. Geographical characteristics of sampling locations

Site	Location	Altitude, m	Environment
Raipur	21° 13′ N, 81° 37′ E	298	Industrial and urban
Bilaspur	22° 5′ N, 82° 9′ E	346	Urban
Korba	22° 21′ N, 82° 40′ E	252	Industrial environment
Akaltara	22° 1′ N, 82° 25′ E	283	Cement plant
Rajnandgaon	21° 6′ N, 81° 1′ E	307	Urban
Dongargargh	21° 11′ N, 80° 45′ E	355	Hilly and urban

The scavenging ratio (SR) value for Cl^-, NO_3^-, SO_4^{2-}, NH_4^+, Na, K, Mg, Ca, Al, Mn, Fe, Cu, Zn, Pb and Hg is found to be 6000, 2500, 4540, 3310, 5130, 5570, 8140, 2300, 145, 1830, 56, 114, 76 and 6000, respectively. Sea salt particles i.e. Cl^-, Na^+, K^+ and Mg^{2+} exhibit the highest SR value due to most effectively scavenging out. The lower SR value of crustal metals i.e. Ca, Al, Mn and Fe is observed. The anthropogenic metals i.e. Zn, Pb and Hg show significant variation in their SR value, ranging from 76

– 6000. Calcium and aluminium are used as reference elements for evaluation of enrichment factors (EFs). Among them elements i.e. F^-, Cl^-, NO_3^-, SO_4^{2-}, NH_4^+, Na^+, K^+, $Mg^{2+}$and Ca^{2+} are highly enriched and expected to be contributed largely by anthropogenic sources i.e. coal burning, mineral roasting, industrial emissions, etc. While other elements i.e. Al, Mn, Fe, Cu, Zn, Pb and Hg are poorly to moderately enriched and more or less contributed by the dusts.

All anions and cations among themselves have fair to excellent correlation, suggesting their common origin in fog water. The Al and Fe content have fair positive correlation with Cl^- and Mn (r= 0.54-0.67). The content of three metals i.e. Zn, Pb and Hg have partial to good correlation with almost all ions and metals (except Al, Mn and Fe). The species i.e. Cl^-, NO_3^-, SO_4^{2-}, Mg^{2+} and Al with the ambient temperature have positive correlation unlikely to species F^-, NH_4^+, Na^+, Fe and Hg. All species (except F^-, NH_4^+, Al and Fe) show positive correlation with humidity. The vapour pressure and wind speed exhibit mixed correlations. Three species i.e. F^-, NH_4^+ and Fe have fair negative correlation with vapour pressure, unlikely to NO_3^-, SO_4^{2-}, Mg^{2+} and Hg. The wind speed has negative fair correlation with species i.e. Cl^-, NO_3^-, SO_4^{2-}, NH_4^+ and Mn unlikely Fe, Ca^{2+} and Al.

6. Summary and Conclusions

The chemical composition of fog water is an indicator for a lower tropospheric dust pollution of a given locations. The fog water of the central India is found to be contaminated with ions (i.e. Cl^-, NO_3^-, SO_4^{2-}, NH_4^+, Na^+, K^+, Mg^{2+} and Ca^{2+}) and metals (i.e. Al, Mn, Fe, Zn, Pb and Hg) at elevated levels due to industrial effluent emissions.

6. References

[1] Krupa S.V., Sampling and physic - chemical analysis of precipitation: a review, Environmental Pollution, 120, pp. 565 – 594, 2002.

[2] Biswas K.F., Ghauri B.M., Husain L., Gaseous and aerosol pollutants during fog and clear episodes in South Asian urban atmosphere, Atmospheric Environment, 42, pp. 7775 - 7785, 2008.

[3] Wen L., Yi Z., Hong L., Fan M., Yu L., Chang Ming W., Fog and rainwater chemistry in the tropical seasonal rain forest of Xishuangbanna Southwest China, Water Air and Soil Pollution, 167, pp. 295 - 309, 2005.

[4] Holder C.D., Rainfall interception and fog precipitation in a tropical montane cloud forest of Guatemala, Forest Ecology and Management, 190, pp. 373 - 384, 2004.

[5] Igawa M., Matsumura K., Okochi H., High frequency and large deposition of acid fog on high elevation forest, Environmental Science and Technology, 36, pp. 1 - 6, 2002.

[6] Wrzesinsky T., Klemm O., Summertime fog chemistry at a mountainous site in central Europe, Atmospheric Environment, 34, pp. 1487 - 1496, 2000.

[7] Bridges K.S., Jickells T.D., Davies T.D., Zeman Z., Hunova I., Aerosol precipitation and cloud water chemistry observations on the Czech Krusne Hory plateau adjacent 5 to a heavily industrialized valley, Atmospheric Environment, 2000, 36, 353 - 360.

[8] Fisak J., Tesar M., Rezacova D., Elias V., Weignerova V., Fottova D., Pollutant concentrations in fog and low cloud water at selected sites of the Czech Republic, Atmospheric Research, 64, pp. 75 - 87, 2002.

[9] Fišák J., Tesař M., Fotto vá D., Pollutant Concentrations in Rime and Fog Water, Soil Water Research, 3,pp. 68 - 73, 2008.

[10] Zapletal M., Kuňák D., Chroust P., Chemical Characterization of rain and fog water in the Cervenohorske Sedlo Hruby Jesenik Mountains Czech Republic, Water Air and Soil Pollution, 186, pp. 85 - 96, 2007.

[11] Lakhani A., Parmar R.S., Satsangi G.S., Prakash S., Chemistry of fogs at Agra India: influence of soil particulates and atmospheric gases, Environmental Monitoring and Assessment, 2007, 133, 435 - 445.

[12] Kulshrestha M.J., Sekar R., Krishna D., Hazarika A.K., Dey N.C., Rao P. G., Deposition fluxes of chemical components of fog water at a rural site in north-east India, Tellus B, 57, pp. 436 – 439, 2005.

[13] Skar˙zy´nska K., Polkowska Z., Namie´snik J., Sampling of atmospheric precipitation and deposits for analysis of atmospheric pollution, Journal of Automated Methods and Management in Chemistry, 26908, pp. 1 - 18, 2006.

5th International Conference on Fog, Fog Collection and Dew
Münster, Germany, 25–30 July 2010
FOGDEW2010-59

Weekly Distribution of Duration of Fogs and Haze in Dusheti (Georgia)

A. Amiranashvili (1), V. Amiranashvili (1), T. Khurodze (2) and A. Nodia (1)

(1) Mikheil Nodia Institute of Geophysics, 1 M. Aleksidze str., Tbilisi, Georgia
E-mail: avto_amiranashvili @excite.com/ avto_amiranashvili @hotmail.com, Fax: +995(32) 33-28-67

(2) Niko Muskhelishvili Institute of Computational Mathematics, 8, Akuri Str., 0193, Tbilisi, Georgia.

Abstract

In this work results of an analysis of the weekly distribution of duration of fogs (T, hour) and haze (Q, hour) in Dusheti (42.08 degrees latitude, 44.7 degrees longitude, 900 m a.s.l.) are presented. Dusheti is located in 45 km to the north of Tbilisi in the terrain with the relatively clean atmosphere. Simultaneous observations of the meteorological and atmospheric electricity parameters here are conducted during many decades. As the parameter of aerosol pollution of the atmosphere air electrical conductivity (Y, 10^{-15} ohm·m) is used. The observation period was 20 years, from 1969 to 1988. The comparison of the mean values of the indicated parameters was conducted with the aid of Student's criterion with the level of significance not worse than 0.2.

For example the following results are obtained.

In the indicated period an increase in the aerosol pollution of the atmosphere was observed. In this case, during the weekends the level of the pollution of the atmosphere was less than during the week-days (Y_{mean} = 37.5 and 33.9 for the week-days, and 38.2 and 34.5 for the weekends in 1969-1978 and 1979-1988 accordingly).
In 1969-1978 during the week-days T_{mean} = 4.08, Q_{mean} = 4.05 and during the weekends T_{mean} = 2.61, Q_{mean} = 3.68.
In 1979-1988 during the week-days T_{mean} = 3.74, Q_{mean} = 2.83 and during the weekends T_{mean} = 3.76, Q_{mean} = 3.58.

Thus, with an increase in the pollution of atmosphere the duration of fogs during the week-days and weekends becomes identical, whereas the duration of haze during the week-days becomes less than into the weekends.

1. Introduction

Fogs and haze represented an important climate forming factors. A detailed analysis of the variability of the number of fog and haze days per year, fog and haze duration and some reasons of these variability in Georgia are given in Amiranashvili et al. [1-5]. This work is a continuation of the mentioned investigations.
Several studies have reported that atmospheric pollution is associated to an changeability of the some atmospheric parameters (solar radiation, precipitation, storm activity etc.). For this purpose often carried out the analysis of the data about atmospheric parameters during the week-days and weekends [6-10].
In this work results of an analysis of the weekly distribution of duration of fogs and haze in Dusheti (Georgia) are presented.

2. Data Description

Dusheti (42.08 degrees latitude, 44.7 degrees longitude, 900 m a.s.l.) is located in 45 km to the north of Tbilisi in the terrain with the relatively clean atmosphere. Variations in following characteristics of full fog (horizontal visibility less than 1000 m, the sky is invisible to the observer) and haze are examined. Simultaneous observations of the meteorological and atmospheric electricity parameters here are conducted during many decades. As the parameter of aerosol pollution of the atmosphere summary air electrical conductivity is used.
The following designations will be used below: T- duration of fogs, hour; Q - duration of haze, hour; Y - summary air electrical conductivity, 10^{-15} ohm·m; σ - standard deviation, α - the level of significance. The estimation of difference between the investigated parameters was evaluated according to Student's criterion t with the level of significance not worse

than 0.2. The observation period was 20 years, from 1969 to 1988.

3. Results

Results of analysis in tables 1-3 are presented.

Table 1: Difference of mean values of T, Q and Y in the week-days and weekends in different years

Year	Days of week	Para meter	T	Q	Y
1969-1988	Week-days	Mean	3.84	3.68	35.7
	Weekends	Mean	3.56	3.64	36.4
	Week-days	Count	205	590	5218
	Weekends	Count	86	254	2087
	Week-days	σ	3.67	3.43	9.3
	Weekends	σ	3.47	3.29	9.2
Week-days - weekends		t	0.61	0.14	-2.8
		α	-	-	0.005
1969-1978	Week-days	Mean	4.08	4.05	37.5
	Weekends	Mean	2.61	3.68	38.2
	Week-days	Count	55	411	2608
	Weekends	Count	15	165	1044
	Week-days	σ	4.42	3.73	9.9
	Weekends	σ	1.88	2.96	9.7
Week-days - weekends		t	1.9	1.25	-1.9
		α	0.05	0.2	0.05
1979-1988	Week-days	Mean	3.74	2.83	33.9
	Weekends	Mean	3.76	3.58	34.5
	Week-days	Count	150	179	2610
	Weekends	Count	71	89	1043
	Week-days	σ	3.37	2.39	8.3
	Weekends	σ	3.70	3.85	8.2
Week-days - weekends		t	-0.03	-1.7	-2.2
		α	-	0.1	0.02
1979-88	Week-days	Mean	3.74	2.83	33.9
1969-78		Mean	4.08	4.05	37.5
1979-88		Count	150	179	2610
1969-78		Count	55	411	2608
1979-88		σ	3.37	2.39	8.3
1969-78		σ	4.42	3.73	9.9
Week-days (1979-88) - week-days (1969-78) -		t	-0.52	-4.7	-14.5
		α	-	0.001	0.001
1979-88	Weekends	Mean	3.76	3.58	34.5
1969-78		Mean	2.61	3.68	38.2
1979-88		Count	71	89	1043
1969-78		Count	15	165	1044
1979-88		σ	3.70	3.85	8.2
1969-78		σ	1.88	2.96	9.7
Weekends (1979-88) – weekends (1969-78)		t	1.75	-0.2	-9.3
		α	0.1	-	0.001

Table 2: Rations between mean values of T, Q and Y in the week-days and weekends in different years

	Week-days/weekends %		
Year	T	Q	Y
1969-1988	107.7	101.0	98.1
1979-1988	99.6	79.1	98.1
1969-1978	156.3	110.1	98.2

Table 3: Rations between T, Q and Y in the week-days and weekends in two periods of time

	(1979-1988)/(1969-1978) %		
	T	Q	Y
Week-days	91.7	69.9	90.2
Weekends	143.9	97.3	90.3

At first examine the dynamics of the aerosol pollution of atmosphere during the investigated period of time indicator of which is the air electrical conductivity.

In table 1 the mean values of Y during the week-days and weekends for three periods of time (1969-1988, 1969-1978, and 1979-1988) are presented. Y_{mean} = 35.7, 37.5 and 33.9 for the week-days, and 36.4, 38.2 and 34.5 for the weekends in 1969-1988, 1969-1978 and 1979-1988 accordingly. In the correspondence with Student's criterion the level of aerosol pollution of air during the week-days was higher than into the weekends for all three indicated periods of time (decrease of the air electrical conductivity with an increase of the aerosol pollution of atmosphere). It is interesting to note that the ratio between Y_{mean} during the week-days and weekends is practically constant for all three indicated periods of time (98.1-98.2 %, table 2).

It is also interesting to note that an increase in the aerosol pollution of atmosphere (decrease of air electrical conductivity) in 1979-1988 to comparison with 1969-1978 both for the week-days and weekends occurred practically equally. Ration between mean values of Y in two indicated periods of time is 90.2 % during the week-days and 90.3 % for the weekends (tables 1 and 3).

Let us examine changeability of mean values of fogs and haze duration during the investigated period of time.

The mean values of T and Q during the week-days and weekends for three periods of time (1969-1988, 1969-1978, and 1979-1988) in table 1 are presented. T_{mean} = 3.84, 4.08 and 3.74 for the week-days, and 3.56, 2.61 and 3.76 for the weekends; Q_{mean} = 3.68, 4.05 and 2.83 for the week-days, and 3.64, 3.68 and 3.58 for the weekends in 1969-1988, 1969-1978 and 1979-1988 accordingly.

As showed the analysis the difference between T_{mean} just as Q_{mean} during the week-days and weekends in 1969-1988 is insignificant. In 1969-1978 values of T_{mean} and Q_{mean} for the week-days accordingly are higher by 56 % and 10 %, than during weekends. In 1979-1988 the difference between T_{mean} during the week-days and weekends is insignificant, but value of Q_{mean} for the week-days is lower by 21 %, than during weekends (tables 1 and 2).

Ration between values of T_{mean} in 1979-1988 and 1969-1978 for the week-days is close to 100 %, and for weekends equally 144 %. Ration between values of Q_{mean} in 1979-1988 and 1969-1978 for the week-days equally 70 %, and for weekends is close to 100 % (tables 1 and 3).

4. Summary and Conclusions

The aerosol pollution of atmosphere has a definite effect on fogs and haze duration. With an increase in the pollution of atmosphere the duration of fogs during the week-days and weekends becomes identical, whereas the duration of haze during the week-days becomes less than into the weekends. With an increase in the air pollution for the week-days the duration of fogs does not change, but during week-days it is increases. For the haze duration another picture is observed. During the week-days the duration of haze is decreases, but during week-days it is does not change.

References

[1] Amiranashvili, A.G, Amiranashvili, V.A. and Tavartkiladze, K.A.: Spatial-Temporary Variations of the Number of Fog Days per Year in Georgia, Proc.1st Int. Conf. on Fog and Fog Collection, 19-24 July 1998, Vancouver, Canada, 1998.

[2] Amiranashvili, A.G., Amiranashvili, V.A. and Tavartkiladze, K.A.: Comparative analysis of long-term variation of number of fog days per year and various climateforming factors in Georgia, Proc. 2-nd Int. Conf. on Fog and Fog Collection, 15-20 July 2001, St. John's, Canada, 2001.

[3] Amiranashvili, A.G., Amiranashvili, V.A. and Tavartkiladze, K.A: Statistical characteristics of number of fog days per year in Georgia. Proc. 3rd International Conference on Fog, Fog Collection and Dew, 11-15 October 2004, Cape Town, South Africa, 2004.

[4] Amiranashvili, A.G., Amiranashvili, V.A. and Tavartkiladze, K.A.: Analysis of Some Reasons of Variations of Number of Fog Days per Year in Georgia, Proc. 3rd International Conference on Fog, Fog Collection and Dew, 11-15 October 2004, Cape Town, South Africa, 2004.

[5] Amiranashvili, A.G., Amiranashvili, V.A , Khurodze, T.V. and Nodia, A.G.: Long-Term Variation of Fog and Haze in Dusheti (Georgia), Proc. 4rd International Conference on Fog, Fog Collection and Dew, 22 - 27 July 2007, La Serena, Chile, 2007.

[6] Soriano, L.R. and Pablo, F. : Effect of Small Urban Areas in Central Spain on the Enhancement of Cloud-to-Ground Lightning Activity, Atmospheric Environment, v. 36, N 17, Jun. 2002.

[7] Dessens, J., Fraile, R. and Sanchez, J.L.: Weekly Distribution of Hailfalls and Hailstone Size Distributions in Southwestern France, Proc. 13th Int. Conf. on Clouds and Precipitation, vol.2, 14-18 August 2000, Reno, Nevada, USA, 2000.

[8] Amiranashvili, A.G., Amiranashvili, V.A., Bachiashvili, L.L., Bibilashvili, T.N. and Supatashvili G.D.: Influence of the Anthropogemic Pollution of the Atmosphere and Thunderstorms on the Precipitations Regime and their Chemical Composition in Alazani Valley Conditions , Proc. 14thInternational Conference on Clouds and Precipitation, 18-23 July 2004, Bologna , Italy, 2004.

[9] Amiranashvili, A.G., Amiranashvili, V.A., Kirkitadze, D.D. and Tavartkiladze, K.A.: Weekly Distribution of the Aerosol Pollution of the Atmosphere in Tbilisi, Proc. 17th Int. Conf. on Nucleation&Atmospheric Aerosols, 13-18 August 2007, Galway, Ireland, 2007.

[10] Amiranashvili, A.: Connection Between the Characteristics of Thunderstorm Activity and Air Pollution in Kakheti Region of Georgia, Proc. of IX Int. Symposium on Lightning Protection, 26-30 November 2007, Foz do Iguaçu, Brazil, 2007.

5th International Conference on Fog, Fog Collection and Dew
Münster, Germany, 25–30 July 2010
FOGDEW2010-60

The daily and annual (2007) effects of dew on a non-ventilated net radiometer

E. Malek
Utah State University, Plants, Soils, & Climate, Logan, United States (eemalek@gmail.com)

Although dew is an unimportant source of moisture in humid areas, plants and arthropods living in some arid regions depend on it for survival. On the other hand, the formation of dew mainly on the upper dome of a non-ventilated net radiometer seriously affects the measurement of available energy (net radiation). Net radiometers measure the available or net energy and are widely used for estimation of evapotranspiration throughout the world. To study the effects of dew on a non-ventilated net radiometer, a radiation station was set up which uses 2 CM21 Kipp & Zonen pyranometers (one inverted), 2 CG1 Kipp & Zonen pyrgeometers (one inverted), along with a Q*7.1 net radiometer (Radiation & Energy Balance Systems, Inc.; REBS) in a semi-arid mountainous valley in Logan, Utah, U.S.A. The pyranometers and pyrgeometers were ventilated using 4 CV2 Kipp & Zonen ventilation systems. The net radiometer was not ventilated. The ventilation of pyranometers and pyrgeometers prevents dew and frost deposition and snow accumulation which otherwise would disturb measurements. All sensors were installed at about 3.0 m above the ground, which was covered with natural vegetation during the growing season (May - September). The incoming and outgoing solar or shortwave radiation, the incoming (atmospheric) and outgoing (terrestrial) longwave radiation, and the net radiation have been continuously measured by pyranometers, pyrgeometers and a net radiometer, respectively, since 1995. These parameters have been measured every 2 seconds and averaged into 20 minutes. To evaluate the effect of dew on the non-ventilated net radiometer 6 April 2007 with early morning dew was chosen. Dew formation occurred mainly on the upper dome of the non-ventilated Q*7.1 net radiometer on this day, while the ventilated Kipp & Zonen system was free of dew. Net radiation measured by the non-ventilated net radiometer Rn,unvent. during dew periods of the above-mentioned day was greater than the ventilated ones Rn,vent. (-0.3 MJ m-2 vs. -1. 2 MJ m-2 during almost 4 hours on 6 April 2007). The reason for higher reading by the non-ventilated net radiometer during dew periods was due to emission of additional longwave radiation from water formed mainly on the upper dome of the Q*7.1 net radiometer. During 2007, net radiation measured by the non-ventilated net radiometer Rn,unvent. during dew periods was 326 MJ m-2 compared to 316 MJ m-2 for Rn,vent.

5th International Conference on Fog, Fog Collection and Dew
Münster, Germany, 25–30 July 2010
FOGDEW2010-61

Design and testing of large fog collectors for water harvesting in Asir region, Kingdom of Saudi Arabia

Habib I. Abualhamayel and P. Gandhidasan
Mechanical Engineering Department, King Fahd University of Petroleum and Minerals, Dhahran 31261, Saudi Arabia
(habib@kfupm.edu.sa/Fax:+966-3-860-2949)

Abstract

The region of Asir is located in the southwestern part of the Kingdom of Saudi Arabia between longitudes 41 – 45º E and latitudes 17 – 21º N. One of the main problems in the Asir region is the high demand for water during tourism seasons and there is urgent need to identify alternative sources of potable water.

Al-Sooda, situated at an altitude of about 3,015 m in the Asir region, was identified as the most suitable experimental site and two large fog collectors measuring 20 m by 2 m each were erected in 2009. The distance between the two sites is about 3 km. During the period from 27 December 2009 to 9 March 2010, a total of 3,128.4 L and 2,562.4 L of fog water were collected at Glider club and the Hotel sites, respectively. The results from the chemical analyses of three sets of fog water samples collected were analyzed for its quality to compare with World Health Organization drinking water standards and found to be potable. The study suggests a clear tendency that in terms of both quality and magnitude of yield, fog is a viable source of water and can be successfully used to supplement water supplies in the Asir region of the Kingdom.

1. Introduction

Water is a basic necessity of people along with food and air. Water has no substitute unlike energy sources and other essential commodities. There is no life without water. In 2007 the UN World Tourism Organization had predicted more than 7% annual growth in tourism industry in the Middle East. Flourishing tourism in the Asir region of the Kingdom of Saudi Arabia is challenged by the scarcity of water resources. It is an accepted fact that water is one of the scarcest and most limiting basic natural resources of the Kingdom. 57% of the total water use in the Kingdom relies on non-renewable water resource of deep groundwater. The use of non-conventional water resources to complement or replace the use of usual fresh water sources is important in water scarce regions such as the Kingdom. The desalinated water, water obtained by fog capturing, rainwater harvesting, groundwater harvesting, cloud seeding, etc. are included under the designation of non-conventional waters. Saudi Arabia is the world's largest producer of desalinated water with desalination meeting 70% of the country's present domestic/drinking water requirement. Capturing water from fog for household or agricultural use is a promising technology.

Fog forms in Asir Region more frequently between November and February. In the last several years, fog collection projects have been successfully implemented in arid regions of many countries in the world. In order to evaluate the effectiveness of fog water collection, three identical Standard Fog Collectors (SFCs) with two different local collection materials were designed and manufactured. Experiments were conducted in 2005 at two different locations in the area close to Al-Sooda. The study indicates that in terms of both quality and magnitude of yield, fog is a viable source of water and can be successfully used to supplement water supplies in the fog-prone Asir region in the Kingdom [1].The proposed research is devoted to investigate and identify the best site in Asir region to yield a good water production rate from the fog by constructing two Large Fog Collectors (LFCs) of 40 m² size and testing in the high yield sites. The typical experimental results are presented in the paper. Chemical analyses of the water collected are performed and also reported in this paper.

2. Site selection

The region of Asir is located in the southwestern part of the Kingdom of Saudi Arabia, as shown in Figure

1, between longitudes 41 - 45°E and latitudes 17 - 21°N.

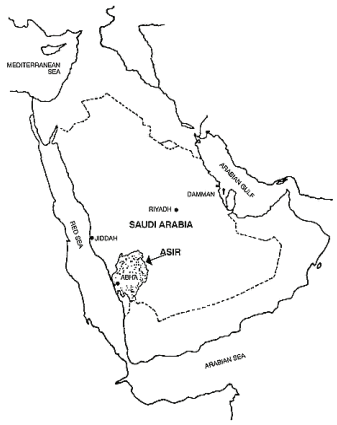

Figure 1: Study area location.

The location, roads, and available infrastructure places considerable limits on the selection of sites. The final selection of two sites to erect LFCs will be based on the fact that they must be easily accessible by road and secure from vandals. In addition, the availability of observers taking the measurements and maintenance of data quality must also be taken into consideration. It is to be noted that a large area of at least 25 m of flat vacant land is needed for the erection of LFC. It is interesting to note that Al-Sooda has the highest altitude (about 3,015 m) and is about 15 km away from Abha. It was decided to erect two LFCs at the following sites in Al-Sooda area, namely Glider club site and Inter Continental Hotel site. These two sites are about 3 km away from each other.

3. Design and manufacture of LFCs

The size of the LFC selected for this study is 20 m wide by 2 m high with a surface area of 40 m^2, as shown in Figure 2 and bases 2 m above the ground to maximize the exposure to the wind [2]. The LFCs are flat rectangular nets supported by a post at both ends and arranged perpendicular to the direction of the prevailing wind. LFC panels are designed to withstand the structural stresses imposed by wind, humidity, and friction between different parts. The area around the LFC must be relatively clear to allow a free flow of wind. The LFC surface is a black

Figure 2: The LFC at the Glider club site.

polypropylene mesh with a single layer of the mesh's fibers cover about 35% of the total area. The mesh is placed tightly on the LFC frame in a double layer. The mesh is woven in a triangular pattern and has a lifespan of about ten years. The mesh should be installed in such a way that the seams lie horizontally. As water collects on the net, droplets join to form larger drops that fall under gravity toward a trough located at the bottom of the panel. The water is then flows through a PVC pipe to a storage tank capacity of 250 L located down. A suitable water supply system must be designed to transfer the water from the trough to the reservoir or storage. The supporting structure is made of noncorrodable materials so that the collected water remains uncontaminated. The pipe must be protected from the sun's rays that can damage the PVC pipe. The distance the water travelled in the pipes must be short. The reservoir must always be covered to avoid dust and insects getting in. It must be cleaned as needed and examined on a monthly basis.

In November 2009, the final locations for the 2 LFCs were chosen. Permission to erect LFCs was obtained from the Government authorities in the Asir region. After obtaining permission, the collectors were installed during November and December 2009 at these two sites to evaluate the efficiency of fog water collection. Local inhabitants were involved to assist with the erection of the LFCs. Structural cables were employed in the construction of the LFC. These cable systems are used to provide lateral and torsional stability to the structure. Operational measurements began in the last week of December 2009 using LFCs.

4. Results and discussion

Experiments were conducted from 27 December 2009 to 23 March 2010 but data from 27 December 2009 to 9 March 2010 are used for the analysis since there were no fog events after 7 March 2010. During

the above experimental period of 72 days, there was no fog for 27 days whereas 7 days there was fog with rain and fog water were collected on 38 foggy days from LFCs. Comparison between fog water yields in liters at Glider club and the Hotel sites for experimental period spanning December 2009 to March 2010 is given in Table 1.

Table 1: Summary of experimental results

Period	Glider club site (L)	Hotel site (L)
28/12/09 - 10/01/10	692.8	645.9
11/01/10 - 26/01/10	1,329.4	1037.7
28/01/10 - 10/02/10	633.4	529.8
11/02/10 - 22/02/10	185.0	131.0
23/02/10 - 07/03/10	287.8	218.0
Total	3,128.4	2,562.4
Average (L/day)	82.33	67.43
Average (L/m^2/day)	2.06	1.69
Ratio	1.22	1.0

At Glider club site, a total of 3,128.4 L of water collected from the LFC. This gives an average yield of 2.06 L/m^2/day. Similarly at the hotel site, a total of 2,562.4 L of water were collected during the same period. The comparison between yields at Glider club site and the Hotel site reveals that the fog water yield at the former site was considerably higher. This is probably due to the increase in wind speed and the higher liquid water content of fog.

Fog collection is affected by the meteorological conditions prevailing during the experimental period. Figures 3-5 show the relationships between the amount of fog water collected by the LFC at the Glider club site and the meteorological variables. When the ambient temperature is between 5 and 10ºC, the water collection rate is high. Similarly when the relative humidity is higher than about 90%, the collection rate is high and the maximum collection is produced when the relative humidity is close to 100%. When the wind speed is about 4 m/s, the yield is high.

Water quality is of vital importance when supplying water for drinking. The actual implementation of fog collection with these collection nets should always include analysis of the quality of the collected water to ensure that the collector does not impart any chemicals that would pose a threat to the health of

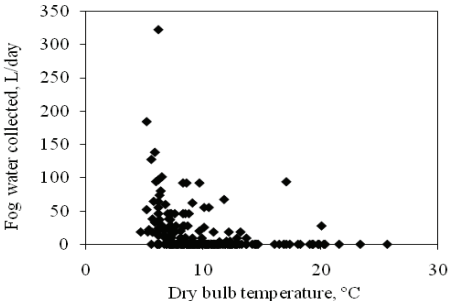

Figure 3: Fog water collected as a function of temperature.

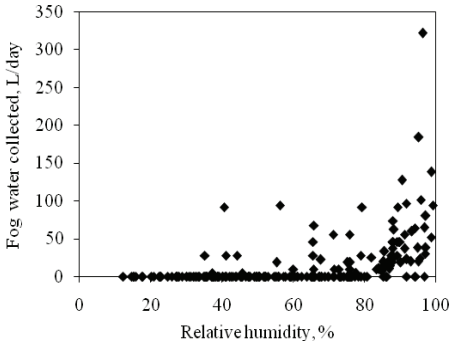

Figure 4: Fog water collected as a function of relative humidity.

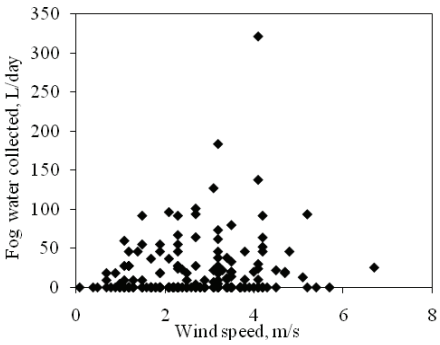

Figure 5: Fog water collected as a function of wind speed.

the users. It is, therefore, fog water quality monitoring program is carried out to identify any contaminants from the collector material and atmospheric deposition. The quality of water depends on the composition of the ambient humidity and the conditions of the fog collection surface. Chemical analysis and concentration of major cations and anions of fog-water collected were performed and the quality of water discussed in this section is based on three set of water samples collected at two different sites. The samples were analyzed for total dissolved solids (TDS), total hardness, electrical conductivity, pH, and major ions, namely, sodium, potassium, calcium, magnesium, chloride, sulphate, nitrate, fluoride, manganese, iron, etc. Samples were analyzed for anions by Ion Chromotography. Total dissolved solids and total suspended solids were determined gravimetrically. Total hardness was calculated using calcium and magnesium concentrations determined by ICP-AES. The analyses of fog water quality were assessed for its suitability [3] and are shown in Table 2.

Table 2: Chemical characteristic analysis of fog water collected (results in mg/L)

	Sample #1	Sample #2	Sample #3
pH	7.43	7.42	7.24
Cond. (ms/cm)	0.23	0.40	0.39
TDS	158	278	318
TSS	3.0	34.0	2.0
Chloride	13.6859	24.5526	27.5375
Sulphate	40.347	63.200	71.716
Flouride	0.0508	0.0981	0.0899
Nitrite	0.554	1.2607	8.0672
Nitrate	23.003	49.3663	44.0433
Carbonate	<0.020	<0.020	<0.020
Bicarbonate	40.347	63.200	71.716
As	< 0.007	< 0.007	< 0.007
Ca	25.7	49.3	50.3
Cd	< 0.0009	< 0.0009	< 0.0009
Cr	< 0.0004	< 0.0004	< 0.0004
Cu	< 0.003	< 0.003	< 0.003
Fe	< 0.0003	< 0.0003	< 0.0003
Hg	< 0.005	< 0.0005	< 0.005
K	1.62	2.97	3.47
Mg	0.966	1.69	1.64
Mn	0.003	< 0.0001	0.002
Na	7.05	12.7	12.3
Pb	< 0.008	< 0.008	< 0.008
Se	< 0.011	< 0.011	< 0.011
Si	0.128	0.145	0.245
Sr	0.102	0.185	0.199
Zn	0.051	0.041	0.019

6. Summary and Conclusions

In spite of the fact that about three months of fog events in a year is a short time to establish meteorological average values, the results obtained to date suggest a clear tendency that fog is a viable resource in the Asir region of the Kingdom of Saudi Arabia. The maximum daily fog water collections from the LFCs are 598 L and 473.8 L at Glider club and the Hotel sites, respectively. The results suggest that Glider club site has a greater potential for fog water harvesting than the Hotel site.

Acknowledgements

The authors are grateful for the financial support provided by King Abdulaziz City for Science and Technology (KACST) through Project No. AR-26-25 and the facilities provided by the King Fahd University of Petroleum and Minerals.

References

[1] Gandhidasan, P., and Abualhamayel, H. I.: Fog collection as a source of fresh water supply in the Kingdom of Saudi Arabia, Water and Environment Journal, Vol. 21, pp. 19-25, 2007.

[2] Schemenauer, R., Cereceda, P., and Osses, P.: Fog water collection manual, FogQuest, 2005.

[3] World Health Organization: Guidelines for drinking-water quality, Incorporating first addendum, Recommendations, 2006.

5th International Conference on Fog, Fog Collection and Dew
Münster, Germany, 25–30 July 2010
FOGDEW2010-62

Multiphase studies in continental and marine atmospheres

Karin Acker, Wolfgang Wieprecht, Detlev Möller
Brandenburg Technical University, Dept. of Air Chemistry (ack@btu-lc.fta-berlin.de)

Abstract

The largest uncertainty in future climate predictions is caused by aerosols and clouds and their interaction with radiation. Hydrochloric acid (HCl) in the gas phase, chloride and sodium in the particle phase were measured first time with high time-resolution and simultaneously with a number of other atmospheric components (in gas, liquid and particulate phase) as well meteorological parameters during two intensive campaigns to study the phase partitioning of chlorine. To a significant extent, sea salt already is depleted in Cl in air masses reaching the west coastal site (Mace Head) of Ireland (20±10% in marine air; 46±19% in continental influenced air) and to a much higher extent (83±13%) in air masses reaching a continental station (Melpitz) in Germany caused by acid replacement by nitric and sulphuric acid

1. Introduction

Aerosol particles have multiple impacts on atmospheric properties: response to climate by optical properties, providing cloud condensation nuclei, being a heterogeneous surface for multiphase chemical reactions, e.g. oxidation of sulphur dioxide (SO_2), and a source for reactive chlorine [4], [6]. A loss of chlorine from the marine particulate sea salt phase into the gas phase was already observed 50 years ago, years later also from continental aerosol and was found to be connected with reactions of nitric acid (HNO_3) and SO_2 on the particle surface causing degassing of hydrochloric acid (HCl) [3]. Under the assumption that sea salt aerosol (SSA) is the exclusive source of sodium in the atmosphere where it is present only in the particle and hydrometeor phase the sodium to chlorine ratio is a relevant criteria to characterise the variation in chlorine phase partitioning. Only simultaneous measurements of gaseous HCl and of chlorine and sodium in the particle phase can clarify the question if the equivalent deficit in chlorine can be found as HCl in the gas phase. Therefore two intensive field campaigns were conducted in continental (2006) and marine (2008) atmospheres.

2. Experimental

Measurements were done at two of the European Supersites for Atmospheric Aerosol Research (EUSAAR) representative of a specific climate or ecosystem and equipped with a high level of instrumentation. The Irish station Mace Head (53°19 N, 9°54 W; 5-12 m asl; Fig. 1a) is located ~88 km west of Galway city on the eastern seaboard of the North Atlantic Ocean and operated by NUI Galway [5]. The terrain is mostly low lying and undulating, the soil is predominantly peat covered in rough grasses with a significant amount of exposed granite rock. The German research station Melpitz (51°32N, 12°54 E; 87 m asl; Fig. 1b) operated by IfT Leipzig [7] is located ~40 km north east of the city Leipzig (~1 million inhabitants) and surrounded by grassland and mixed forests.

Fig. 1a and b: View to the stations Mace Head (left) and Melpitz

At both sites HCl, HNO_3 and other gaseous species were measured by a coupled wet denuder sampling / ion chromatography analysis technique. This diffusion based system separating the gaseous species from their corresponding particulate ions was extended by a steam chamber for simultaneous sampling of the soluble total suspended matter (TSP) fraction to determine components like sodium, chloride, nitrate, sulphate [1]. The whole system (beside a very short Teflon inlet) was operated in an air conditioned container at ~20°C (pre-concentration time: 30 min; sample air flow: 10 l min^{-1}; limit of quantification: 10 ng m^{-3}). Sampling of particulate matter (PM) was also done using high-volume sampler (DIGITEL) with different inlets and 5-stage Berner impactors (IfT EMEP study). Precipitation amount and composition (Eigenbrodt wet-only

sampler) have been evaluated for the data interpretation. 96h back trajectories (NOAA Hysplit model) are used to determine the air mass origins.

3. Results

In our studies the (mass) Na to Cl ratio found in sea water (R_{sea}=0.56) is used for calculation of the degree in chlorine loss in particulate matter by the relation $Cl_{loss}=1-R_{sea}/R_{sample}$.

3.1 Melpitz

Figure 2 presents detailed data from the campaign in early summer 2006. The air masses reaching this site were on average medium polluted: in continental SW air masses (19th to 22th June; Fig. 3a) NO_2 8; SO_2 4; BC 2.5; PM_{10} 22; $PM_{2.5}$ 20 µg m^{-3}; in maritime influenced westerly air masses (23th June; Fig. 3b) NO_2 6; SO_2 2; BC 1.6; PM_{10} 20; $PM_{2.5}$ 16 µg m^{-3} µg m^{-3}.

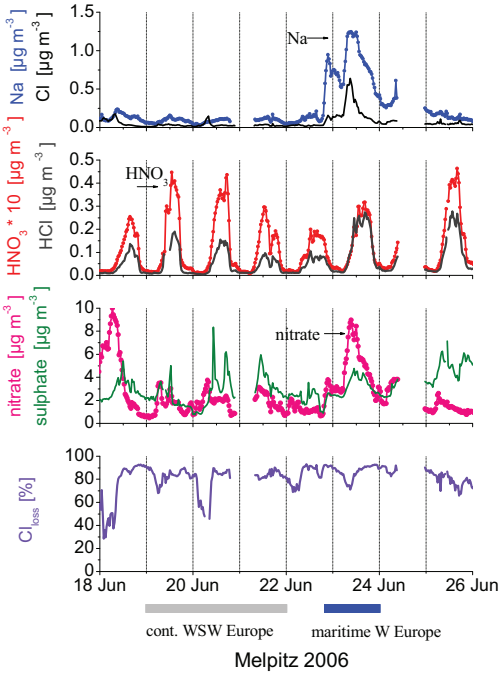

Fig. 2: Time series of particulate sodium, chloride, nitrate and sulphate, gaseous HNO_3 and HCl and the calculated loss in chlorine at Melpitz.

The mean mass Na to Cl ratio was found to be 3.6. No correlation between gaseous HCl and particulate Cl (r^2=0.03) was observed, due to faster removal of HCl during transport.

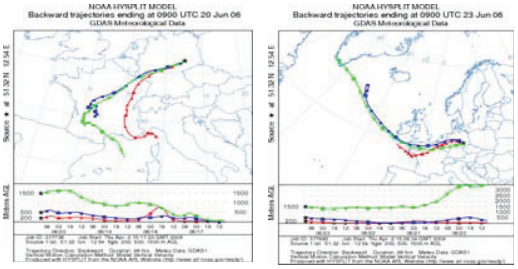

Fig. 3a and b: selected transport analysis Melpitz

A very high loss in chlorine in PM (83±13%) has been calculated, not showing a significant dependency from the air mass sector and transport percentage (25-100%) above continent. A broad HCl maximum around noon/afternoon was measured. The correlation with HNO_3 is very high (r^2=0.78). The data support that HNO_3 is responsible for Cl depletion by reaction

$HNO_3(g) + NaCl(s,aq) \rightarrow NaNO_3(s,aq) + HCl(g)$,

also because of drastically reduced SO_2 emissions in Europe compared to NO_2.

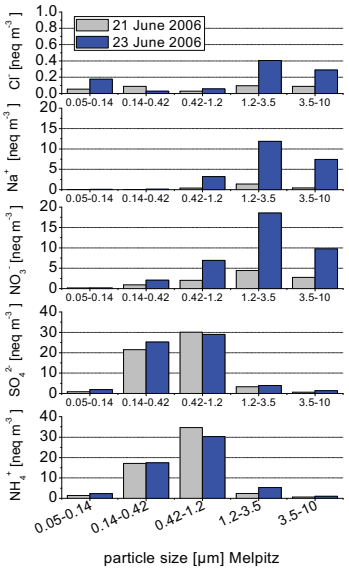

Fig. 4: Particle size aggregate sampling and chemical analysis of PM.

The data in Figure 4 confirm that HCl degassing apparently occurs on smaller particles (< 1 µm) due to sulphate formation and on larger particles due to sticking of HNO_3 (if available, what sufficient is the case only in continental air masses; in marine atmosphere exhaust plumes from ships are a source).

3.2 Mace Head

Figure 5 presents detailed data from the campaign in early summer 2008. The air masses reaching this site were very low polluted in North Atlantic Ocean clean marine air (25th to 29th June; Fig. 6a) NO_2 0.5; SO_2 0.1; BC 0.1; PM_{10} 28; $PM_{2.5}$ 8 µg m^{-3}; partly differences are found in continental influenced air masses (4th to 6th June; Fig. 6b) NO_2 5; SO_2 0.5; BC 0.4; PM_{10} 13; $PM_{2.5}$ 7 µg m^{-3}.

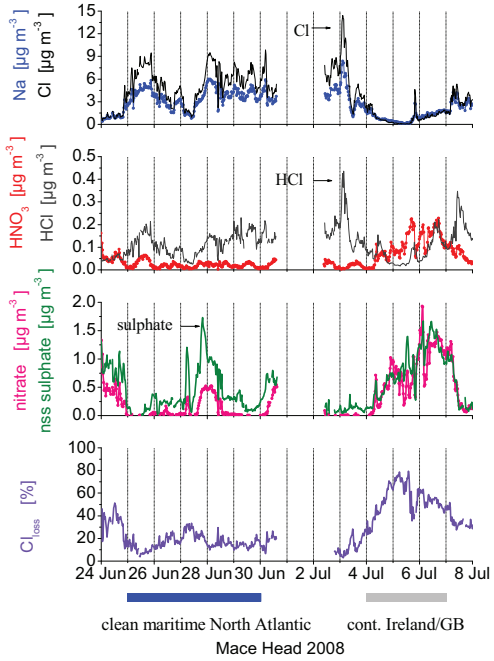

Fig. 5: Time series of particulate sodium, chloride, nitrate and sulphate, gaseous HNO_3 and HCl and the calculated loss in chlorine at Mace Head.

The mean mass Na to Cl ratio was found to be 0.74. Gaseous HCl is well correlated with particulate Cl (r^2=0.46), but to a significant extent (20±10%), sea salt already is depleted in Cl in air masses originate exclusive from the clean marine sector (180-300°; see also Figs. 6a, 8), mainly caused by HCl formation during heterogeneous sulphate formation.

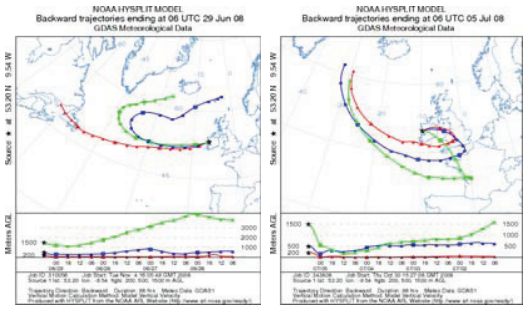

Fig. 6a and b: Selected transport analysis Mace Head

In continental influenced air masses (45-135°, mainly Ireland and Great Britain; see also Figs. 6b, 8) a higher degree in Cl_{loss} (46±19%) was found due to additional acid replacement by nitric acid; the linear correlation between HCl and HNO_3 becomes significant and positive (r^2=0.25) compared to all data (r^2=0.01). The mean mass Na to Cl ratio in Mace Head wet only rain samples (N=19) was found to be 0.69. Gas and particle scavenging processes lead to an approximation to R_{sea}.

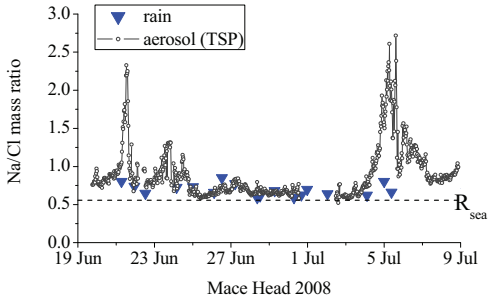

Fig. 7: Comparison of the Na to Cl ratio in Mace Head TSP and rain water

4. Conclusions

Figure 8 summarizes the wind direction dependence of the (mass) Na to Cl ratio of total suspended matter (time resolution 30 min) collected during two campaigns in a continental atmosphere as well on the border between ocean and continent.

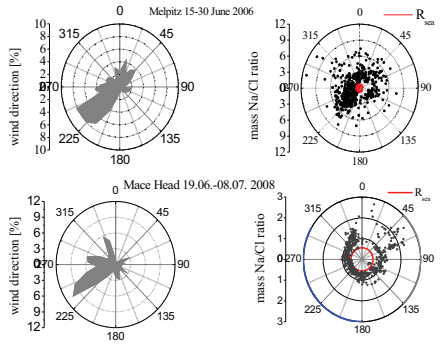

Fig. 8: Distribution of the wind direction during the field studies in Melpitz and Mace Head and comparison of the air mass history depended (mass) Na to Cl ratio.

The high loss of chlorine (as HCl) from sea salt will modify (a) the particles chemistry (mostly by nitrate enrichment) and (b) gas-phase chemistry (multiphase Cl partitioning) as well corrosive properties of the atmosphere. Possibly the global HCl formation from SSA is higher than the estimated value of 7.6 Tg a^{-1} found in the literature [2].

Acknowledgements

This work was supported by Deutsche Forschungsgemeinschaft; the study in Mace Head was also an EUSAAR TNA activity within the EU FP6 program. The authors wish to thank the colleagues from IfT Leipzig and NUI Galway for valuable assistance.

References

[1] Acker, K., Möller, D., Auel, R., Wieprecht, W., Kalaß, D.: Concentrations of nitrous acid, nitric acid, nitrite and nitrate in the gas and aerosol phase at a site in the emission zone during ESCOMPTE 2001 experiment. Atmos. Res. 74, pp. 507-524, 2005.

[2] Erickson III, D. J., Seuzaret, C., Keene, W. C., Gong, S. L.: A general circulation model based calculation of HCl and ClNO2 production from sea salt dechlorination: reactive chlorine emissions inventory. J. Geophys. Res., 104, pp. 8347-8372, 1999.

[3] Finlayson-Pitts, B.: The tropospheric chemistry of sea salt: A molecular-level view of the chemistry of NaCl and NaBr. Chem. Rev. 103, pp. 4801-4822, 2003.

[4] Möller, D.: The Na/Cl ratio in rain water and the sea salt chloride cycle. Tellus 42B, pp. 254-262, 1990.

[5] O'Connor, T.C., Jennings, S.G., O'Dowd, C.D.: Highlights of fifty years of atmospheric aerosol research at Mace Head. Atmos. Res. 90, pp. 338-355, 2008.

[6] O'Dowd, C. D., Smith, M. H., Consterdine, I. E., Lowe, J. A. Marine aerosol, sea-salt and the marine sulphur cycle: a short review. Atmos. Environ. 31, pp. 73–80, 1997.

[7] Spindler, G., Müller, K., Brüggemann, E., Gnauk, T., Herrmann, H.: Long-term size-segregated characterization of PM10, P M2.5, and PM1 at the IfT research station Melpitz downwind of Leipzig (Germany) using high and low-volume filter samplers. Atmos. Environ. 38, pp. 5333-5347, 2004.

5th International Conference on Fog, Fog Collection and Dew
Münster, Germany, 25–30 July 2010
FOGDEW2010-63

The pioneer study of fog detection and horizontal precipitation measurement at subtropical highland of Taiwan

P. H. LIN and K. L. LAI
National Taiwan University, Atmospheric Sciences, Taipei, Taiwan (polin@ntu.edu.tw)

Heavy rainfall in highland caused by the interaction of tropical storms and sharp terrain is one of the major natural disasters in Taiwan. But there is no quantitative measurement on the fog and its horizontal precipitation (HP) to estimate the storage of water by plants in the highland region of Taiwan. In this pioneer study, we studied the fog detection and its horizontal precipitation amount, existence length and monthly variation at Kuan-Wu recreation area in Shei-Pa National Park of Taiwan. The 20-year (1988∼2007) record length of meteorological data at Kuan-Wu was analyzed first to build up the background information of the local weather. The FDID (fog detection and interception device) including two fog detectors, two fog collectors and auto-shooting digital camera was delivered in this field program. The parallel experiment indoor with a fog tunnel also confirms the performance of polypropylene net used in FDID.
FDID has collected data in the field over one year, and the preliminary results show that some components of FDID present the capability of fog event detection and give quantitative data of fog interception. The digital images in 5-min interval via fog collector data detected over 90% happening of fog event in the data available days. Through the RGB diagnosis in different pixel domains (different distances to the camera) on the digital images, the fog events are distinguished into light, medium and heavy fog events. The characteristics of daily and monthly variations of fog events could be explained through the terrain and local climate effects well. We also found the horizontal precipitation from fog provides ∼11% extra water amount in the no-rain days.
The happened possibility of fog & stratus cloud with The MTSAT geostationary IR channels by Central Weather Bureau is also validated by the FDID in-situ measurement. It shows that the remote sensing product of fog detection in nighttime has good correlation with FDID ground measurement.

5th International Conference on Fog, Fog Collection and Dew
Münster, Germany, 25–30 July 2010
FOGDEW2010-64

Preliminary Fog Chemistry Analysis at two different sites: Castello Branco and Raposo Tavares Roads in São Paulo St., Brazil

Gonçalves, F.L.T. (1), Bauer, H. (2), Vasconcellos, P.C. (3), Censon , V.K. (1), Avila, S.G. (3)
(1) Dept. of Atmospheric Sciences (IAG)-University of São Paulo, Brazil, (2) Institute for Chemical Technologies and Analytics, Univ. of Technology-Austria, (3) Institute of Chemistry-University of São Paulo, Brazil

Abstract

The aim of this study is characterize the fog composition at two sites nearby the important roads, at surrounding São Paulo City, in the São Paulo State, Brazil. Both sites (CB and RT) present high number of fog events and they cause traffic problems, mainly due to radiative fogs. Castello Branco (CB) site also presents a great number of chemical industries, opposite of Raposo Tavares (RT) site. Those industries may produce CCN (sulfates, nitrates and ammonia, mainly) and due to these fog events are observed. Five events were collected from May to August 2009 at both sites. The overall results show elevated values of ammonium particularly (96 mg.L-1) at CB site as expected due to the fertilizer industries in surroundings. Additionally, it presents a high standard deviation (131 mg.L-1), perhaps due to the industry exhaustion time schedule. High values of chlorine were evaluated as well (860 mg.L-1), suggesting industrial sources, and landfill waste burning often observed in Brazilian cities1. Sodium concentrations were the highest at CB site (av. 352 mg.L-1) on June 22nd event, which may be it is from Atlantic Ocean source, despite that it is more than 100 km far. CB site also presents high values of sulfate, potassium and nitrates. Compared to RT site, all these chemical species present higher values at CB site, except nitrates, with similar concentrations. Oxalate (between 0.5 mg.L-1 at RT and 0.3 mg.L-1 at CB) and levoglucosan (0.3 mg.L-1 at RT and 0.2 mg.L-1 at CB) were found in fog water which indicates biomass burning (sugar cane) which are common during that period (May to November) of the year. It must be notified as well that the weather conditions during last winter were atypical, particularly from July to August. They were influenced by El Niño phenomena, which increased rain amount and higher temperatures at Southeastern Brazil where São Paulo site is located. The increase of rain events affected the number of radiative fogs. Advective fog events were formed, in which were difficult to collect due to its density. Additionally, at advection events, the industry impact is decreased to the air dispersion and wind. These are preliminary results which demands air mass trajectories.

1. Introduction

Fog events are characterized by visibility impacts on traffic around the whole planet. Besides, fog droplets are known to be efficient scavengers of air pollutants close to the surface as well as they are formed by them through CCN nucleation processes. Due these facts, there are many studies taking in account fog chemistry. For example, during 1980s, it was demonstrated the high acidity of fog water in southern California (Munger et al., 1983), while another study in this area showed that fogs were frequently 100 times more acidic than rain (Hileman, 1983). Since this time, a large number of studies showed very high concentrations of inorganic and organic compounds in fog water such as Munger et al, 1990; Millet et al., 1995) and organic; Richartz et al., 1990; Millet et al., 1997; and Herckes et al. (2002).

On the other hand, although night traffic represents only 10% of the total traffic, one third of accidents take place during night time. Fog events take place usually at night time, where the accidents may occur. Consequently, the traffic road managers pay a lot of attention during night time which is more propitious for fog formation. Therefore, the aim of this study is characterize the fog composition at two sites nearby the important roads, at surrounding São Paulo City, in the São Paulo State, Brazil. Both sites (Castello Branco and Raposo Tavares roads) present high number of fog

events and they cause traffic problems, mainly due to radiative fogs. Castello Branco (CB) site also presents a great number of chemical industries, opposite of Raposo Tavares (RT) site. Those industries may produce CCN (sulfates, nitrates and ammonia, mainly) and due to these fog events are observed. The impact of this study is clearly important for safety of the road passengers with impacts socio-economics.

2. Methodology

Techniques for collection of fog and cloud water have received considerable attention over the past two decades in response to a desire to better understand bow clouds and fogs process atmospheric CCN. Several instruments have been developed and utilized for collecting fog and cloud water samples for chemical analysis which have shifted somewhat to the design of instruments that can segregate collected drops by size (Collett et al., 1993, Collett et al.,1995). The primary use of most cloud water samplers is to collect cloud water samples for the analysis of chemical concentrations. Therefore the herein used sampler was developed by Dr. Collett and placed at two sites described above during the winter of 2009. Five events were collected and analyzed. The chemical methodology is divided in 2 parts: Brazilian analysis evaluated by Dr. Vasconcellos of IQ-USP, and 2- analysis made in Austria evaluated by Dr. Heidi Bauer of Institute for Chemical Technologies and Analytics, Vienna University of Technology.

3. Preliminary Results and conclusion

The overall results show elevated values of many air pollutants which may cause fog nucleation such as NH_4^+, NaCl, $SO_4^=$, NO_3^- (see Table 1). Ammonium particularly at CB site was found with high concentration (96 $mg.L^{-1}$) as expected due to the fertilizer industries in surroundings. Additionally, ammonium also presents a high standard deviation (131 $mg.L^{-1}$), perhaps due to the industry exhaustion time schedule in the area. It must be notified that the ammonium smell in the area is much punctuated. High values of chlorine were evaluated as well (860 $mg.L^{-1}$) in this site, suggesting industrial sources, and landfill waste burning often observed in Brazilian cities. Sodium concentrations were the highest at CB site (av. 352 $mg.L^{-1}$) on June 22nd event, which may be it is from Atlantic Ocean source, despite that it is more than 100 km far. Atmospheric transportation must be evaluated in order to clarify it. CB site also presents high values of sulfate, potassium and nitrates when compared to RT site. All these chemical species present higher values at CB site, except nitrates, with present similar concentrations. In Table 2, oxalate (0.5 $mg.L^{-1}$ at RT and 0.3 $mg.L^{-1}$ at CB) and levoglucosan (0.3 $mg.L^{-1}$ at RT and 0.2 $mg.L^{-1}$ at CB) were found in fog water which indicates biomass burning (sugar cane, probably) which are common during that period of the year (May to November). Other sugars (see Table 2) could also emphasize it.

It must be notified as well that the weather conditions during last winter were atypical, particularly from July to August. They were influenced by El Niño phenomena, which increased rain amount and higher temperatures at Southeastern Brazil where São Paulo site is located. The increase of rain events affected the number of radiative fogs. Some advective fog events were formed, in which were difficult to collect due to its density, usually quite soft. Additionally, at advection events, the industry impact is decreased to the air dispersion and wind. These are preliminary results which demand air mass trajectories and more events to be sampled and analyzed in which will be done in the 2010 winter time.

Table 1. Average of cations and anions in each site (mg.L-1) and their standard deviations (sd). CB means Castello Branco and RT, Raposo Tavares.

	CB	***sd***	**RT**	***sd***
Sodium	-	-	2,14	2,14
Ammonium	96.41	130.90	3.95	3.12
Potassium	87.76	77.40	1.90	2.21
Magnesium	0.11	0.10	0.35	0.35
Calcium	3.18	2.99	7.60	7.22
Fluorite	4.17	3.82	0.42	0.33
Chlorine	859.62	879.20	3.29	1.21
Nitrate	6.08	5.88	1.69	0.26
Sulfate	10.39	4.18	4.77	0.44

Table 2. Analyses made in Austria (in µg.mL^{-1} or mg.L^{-1}) for the event of June15 at RT and for the event of June 22 at CB.

		RT 15/6	CB 22/6
sugars (µg/mL)	Levoglucosan	0.597	0.328
	Arabitol	0.025	0.075
	Mannitol	0.273	0.321
	Mannosan	0.113	0.030
	Glucose	0.234	0.257
	Oxalate	0.491	0.260

4. References

Collett, Jr., J., Oberholzer, B. and Staehelin, J., 1993. Cloud chemistry at Mt. Rigi Switzerland: Dependence on drop size and relationship to precipitation chemistry. Atmos. Environ., 27A(1), 33-42.

Collett, Jr., J., Iovinelli, R. and Demoz, B., 1995. A three-stage cloud impactor for size-resolved measurements of cloud drop chemistry. Atmos. Environ., 29, 1145-1154

Herckes, P., Worthman, H., Mirabel, P., Millet, M., 2002. Evolution of the fogwater composition in Strasbourg (France) from 1990 to 1999. Atm. Res., 64, 53-62.

Hileman, B., 1983. Acid fog. Environ. Sci. Technol. 17, 117A– 120A.

Millet, M., Sanusi, A., Wortham, H., 1996. Chemical composition of fogwater in an urban area: Strasbourg.(France). Environ. Pollut. 94, 345–354.

Millet, M., Wortham, H., Sanusi, A., Mirabel, Ph., 1997. Low molecular weight organic acids in fogwater in an urban area: Strasbourg (France). Sci. Total Environ. 206, 57–65.

Munger, J.W., Jacob, D.J., Waldman, J.M., Hoffmann, M.R., 1983. Fogwater chemistry in an urban atmosphere. J. Geophys. Res. 88, 5109– 5121.

Munger, J.W., Collet Jr., J., Daube Jr., B., Hoffmann, M.R. 1990. Fogwater chemistry at Riverside, California. Atmos. Environ. 24B, 185– 205.

Richartz, H., Reischl, A., Trautner, F., Hutzinger, O., 1990. Nitrated phenols in fog. Atmos. Environ. 24A, 3067–3071.

5th International Conference on Fog, Fog Collection and Dew
Münster, Germany, 25–30 July 2010
FOGDEW2010-65

Development of a low visibility forecast tool for Munich Airport

P. Röhner (1), B.-R. Beckmann (1), M. Rohn (1), C. Mohr (2), and A. Bott (2)

(1) Deutscher Wetterdienst, Abteilung Flugmeteorologie, Offenbach, Germany (peer.roehner@dwd.de), (2) Universität Bonn, Meteorologisches Institut, Bonn, Germany

Within the frame of the German research project LuFo iPort (innovative Airport), supported by the federal ministry of economics, a low visibility forecast tool is developed in cooperation between the German Weather Service (DWD) and the Meteorological Institute of Bonn University. A model prototype is adapted to Munich Airport and initialised with both COSMO-DE runs and local meteorological observations obtained through an instrumentation installed close to the heads of the two runways. Besides the measurement of air temperature, humidity and wind speed at standard level and at different heights above ground using a 20m high tower, profiles of soil temperature and humidity as well as upward and downward radiation are recorded. In a second step, the additional value of MWRP, ceilometer and SODAR data is planned to be validated during a measurement campaign envisaged for autumn 2011.

5th International Conference on Fog, Fog Collection and Dew
Münster, Germany, 25–30 July 2010
FOGDEW2010-66

Chemical composition of fog and cloud water at the Erzgebirge summit, Germany

Stephanie Schüttauf (*), Frank Zimmermann and Jörg Matschullat

Interdisciplinary Environmental Research Center, TU Bergakademie Freiberg, D-09599 Freiberg, Germany; e-mail: stephanie.schuettauf@student.tu-freiberg.de*; frank.zimmermann@ioez.tu-freiberg.de, jörg.matschullat@ioez.tu-freiberg.de

Abstract

The Erzgebirge, part of the former "Black Triangle", was one of the most polluted forested areas in Central Europe. The local climate is characterized by above-average stable air stratification leading to an above-average amount of inversions with advection fog. "Acid fog" was thought to play an important role in the acidic deposition and in the forest decline on both sides of the Erzgebirge ridge (800 – 900 m a.s.l.). The last data on chemical composition and deposition of fog and cloud water were reported from the 1990's. This work delivers the current chemical composition of fog and cloud water from the region. Fog data are reported from two sites: (1) Zinnwald, 877 m a.s.l., eastern Erzgebirge, and (2) Fichtelberg, 1214 m a.s.l. Passive fog collectors were used. Electrical conductivity, pH-value, and the concentration of major ions and trace metals (Ba, Pb, Zn, Al, Mn, Ti, V, Ni, Cu, Sr, Cd, Sb, As, Cr) were determined.

1. Introduction

Several studies dealt with fogwater chemistry on global and local scales (Warneck 1991; Grasserbauer et al. 1994; Acker et al. 1995; Millet al. 1996; Acker et al. 1998; Collett et al. 1998; Collett and Pandis 1999; Bridges et al. 2001, Hoag et al. 2001; Bridgman et al. 2002; Marinoni et al. 2004). The key measurements related to pH, conductivity and ionic composition. Since the knowledge in this field seems to be "saturated", there where only a few studies within the last years. The environmental composition changed due to altered emission conditions in the meantime. Particularly high variations were reported for the Krusne Hory region situated in the former called "Black Triangle" by Ardo et al. (1997) and by Bridgman et al. (2002). Therefore new studies are justified to test if similar changes in fog composition can also be seen in the German part of the "Black Triangle", the Erzgebirge.

Based on newly collected data and in comparison with former studies we analysed the current chemical composition of fog water and discuss the development of the different components in the samples.

2. Sampling and Analysis

2.1 Sampling sites

Field samples were collected at two different sites: Zinnwald-Georgenfeld (ZIW) and Fichtelberg, Oberwiesental (FIB). These experimental sites are situated in the highland region of the Eastern and the Central Erzgebirge, respectively. The Fichtelberg, with 1,214.6 m a.s.l., is the highest elevation in Saxony. Due to its altitude, mountain and station are situated above the cloud base. This results in a high average fog frequency of 287 days (Zimmermann 2002, after Fojt 1970).
The experimental site Zinnwald-Georgenfeld lies at 877 m a.s.l.. The average annual air temperature is 4.3°C with a gradient of 18.1° K between July and January. The average annual precipitation reaches values up to 978 mm with a maximum in summer and a minimum in winter. This pattern reveals a continental-atlantic climate (Zimmermann 2002).

2.2 Cloud water collection and analysis

Passive string collectors were used (Zier, 1992). The samplers consist of two horizontal disks with a diameter of 20 cm, installed vertically and 40 cm apart. Nylon strings (diameter 0.2 mm) were stretched between these disks. Two samplers were used at Zinnwald-Georgenfeld (one for ion analysis and one for trace elements) and one at Fichtelberg (ion analysis). The samplers were only exposed if fog was visible for the operating staff of the weather station. The total yield of the passive collector was 40 samples for 40 different fog events between October and December 2009. The collection periods varied between 4 h 30 min and 48 h.

The samples were stored in precleaned 100 mL LDPE bottles. All samples were filtered in the laboratory prior to analysis (0.47 mm cellulose acetate for major ions and Nuclepore track-etched membrane filter for trace elements). A sample aliquot was used to determine pH and electric conductivity. Major inorganic ions (Na^+, NH_4^+, K^+, Ca^{2+}, Mg^{2+}, F^-, Cl^-, NO_2^-, Br^-, NO_3^-, PO_4^{3-} and SO_4^{2-}) were quantified by ion chromatography with DIONEX DX 120 for anions and Metrohm Ion Chromatograph 690 for cations. Trace elements were measured by ICP-MS (Perkin Elmer Sciex ELAN 9000).
Quality control of the analytical data was performed by comparing calculated vs. measured conductivity and cation vs. anion balances for each sample.

2.3 Calculation of fog water content

The liquid water content (LWC) is one of the most important parameters determining the chemical composition of fog samples. Given the lack of direct measurements, we used a parameterization developed by Queck (2003) to estimate LWC. Based on the visible range measured with meteorological conditions, the LWC is calculated as follows:

VV>100 m: $LWC=35.91*VV^{-1,15}$ (1)

VV<100 m:

$$LWC=10^{-0,49*(\log(VV))^2+1,25*\log(VV)-1,25)} \quad (2)$$

with VV: measured visible range (in m) and LWC: liquid water content (in g/m³).

3. Results

3.1 Fog frequency

Time series of fog observation from weather stations in the Erzgebirge show a significant dependence of the number of fog events on altitude: the amount of fog increases with altitude (Figure 1). There were more fog hours on Fichtelberg (1,214 m a.s.l.) than on Zinnwald (877 m a.s.l.).

The observed fog frequency is comparable to long-term observations.

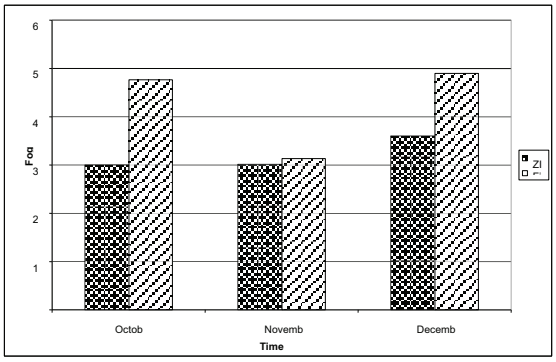

Figure 1: Distribution of fog hours at Zinnwald and Fichtelberg.

3.2 Liquid water content (LWC)

The calculated LWC for Zinnwald and Fichtelberg is presented in Table 1. Calculations are based on formula 1 and 2, respectively.

Table 1: LWC [g/m³] for Zinnwald and Fichtelberg

station	Mean value	Min	max
Fichtelberg	0,202	0,194	0,280
Zinnwald	0,204	0,035	0,323

These values are in good agreement with those mentioned by Pleßow et al. (2001) for Mt. Brocken, (475 – 625 mg/m³), a typical range for German low elevation mountains.

3.3 Composition of fog samples

The mean volume-weighted ionic concentrations of fog water samples are presented in Table 2.

The chemical composition of fog and cloud water differed considerably between the sites. Zinnwald still is polluted, influenced by the "Bohemian Fog" with high concentrations of sulphate, nitrate and ammonium, while Fichtelberg is much less influenced by air pollution. There, sodium and chloride dominated the composition. To discriminate between the marine and the non-marine origin of ions, the sea-salt and the non-sea-salt fraction was calculated for SO_4^{2-} and Ca^{2+} with Na^+ as a reference. The concentration of non-sea-salt sulphate ($nss\text{-}SO_4^{2-}$) was calculated by the formula:

$$[nss\text{-}SO_4^{2-}] = [SO_4^{2-}]_{total} - ([Na^+]*0,12). \quad (3)$$

Similarly the concentration for nss-Ca^{2+} was calculated from the ratio Ca^{2+}/Na^{+} using 0.038 as the multiplication factor (Kang et al. 2010). The large values at both sampling sites indicate a contribution from anthropogenic or crustal sources.

The minimum pH was 3.5 for Zinnwald and 3.7 for Fichtelberg (Table 2), both of phytotoxic relevance. At both sites ionic concentrations were much higher than in wet deposition: the maximum enrichment factors were observed for NO_3^- (42) at Zinnwald and for Cl^- (69) at Fichtelberg.

Table 2: Mean volume-weighted ionic concentrations in fog water at *ZIW* and *FiB* (µeq/L)

	Zinnwald	Fichtelberg
F^-	8	3
Cl	69	338
NO_2^-	1,34	1,68
NO_3^-	768	325
PO_4^{3-}	23	17
SO_4^{2-}	227	235
nss-SO_4^{2-}	218	191
ss-SO_4^{2-}	8	44
H^+	0,05	$9{,}57*10^{-5}$
Na^+	72	367
NH_4^+	347	310
K^+	13	27
Ca^{2+}	111	134
nss-Ca^{2+}	109	120
ss-Ca^{2+}	3	14
Mg^{2+}	19	91

Another aspect of our work relates to trace elements at Zinnwald. Ba, Pb, Zn, Al, Mn, Ti, V, Ni, Cu, Sr, Cd, Sb, As and Cr were detectable. The dominant species was Al (160 µg/L) followed by Zn (136 µg/L), Pb (77 µg/L) and Cu (71 µg/L). Aluminium is a marker for soil dust, while the other three elements rather indicate pollution by anthropogenic activity.

3.4 Composition development

In order to make statements about the evolution of individual components found in fog water we compared our measurements with data from Bridges et al. (2001). The results are presented in Table 3.

A clear trend could only be seen for SO_4^{2-}. The major reduction is related to decreasing sulphur emissions over the last years. The so called "Entschwefelungsanlagen" should be mentioned in this context. A related average decrease for NO_3^- was also expected, only a light decrease emerged at Fichtelberg while an increase was registered at Zinnwald (Table 3). A possible explanation is given by the hypothesis of the "new type of winter smog" (Brimblecombe 1996). Caused by low temperatures, measured during the sampling period, the normally unimportant reaction

$$2NO + O_2 \rightarrow 2NO_2 \qquad (R1)$$

can be a significant source of NO_2. Prerequisites are significant concentrations of NO which have risen considerably in line with increasing urban traffic in this region. Due to the low temperatures the rate constant for R1 increases as the temperatures falls resulting in higher production rates of NO_2. Because of the sensitivity of R1 to reactant concentration even small improvements in emission of NO (under new winter smog conditions) can yield great improvements in the NO_2 level.

Table 3: Comparison of ZIW and FIB data with those from Krusne Hory Plateau [µeq/L]

	Zinnwald	Fichtelberg	Krusne Hory Plateau
anions			
Cl^-	69	338	155
NO_3^-	768	325	726
SO_4^{2-}	227	235	625
cations			
Na^+	72	367	64
NH_4^+	347	310	203
K^+	13	27	19.4
Ca^{2+}	111	134	67.9
Mg^{2+}	19	91	20.2

Explaining the evolution of the other components is difficult because their behaviour differs significantly between the two sampling sites. One reason could be the different sample characteristic: at Zinnwald pure inversion fog was sampled while at Fichtelberg, sampling was interrupted by cloud occurrence and in this context by the composition of cloud water. To clearly explain the individual components and their

development, it is necessary to look at the sampling sites separately (not shown here).

4. Conclusion

The chemical composition of fog samples is reported from two sites: (1) Zinnwald, 877 m a.s.l., eastern Erzgebirge, and (2) Fichtelberg, 1214 m a.s.l. Fog frequency in the investigation period (10.2009 – 12.2009) was comparable to long-term observations. Modelled liquid water contents (LWC) were in the range of typical values for German low elevation mountains. Minimum pH values, 3.5 for Zinnwald and 3.7 for Fichtelberg, were still of phytotoxic relevance. The chemical composition of fog and cloud water differed considerably between the sites. Zinnwald still is a polluted site with high concentrations of sulphate, nitrate, ammonium and organic compounds, while Fichtelberg is much less influenced by air pollution. There, sodium and chloride dominated the composition. At Zinnwald, Al, Zn, Pb, and Cu showed the highest trace metal concentrations, while As, Ni, Cr, and Cd were also detected. Sulphate concentrations were lower than in 2001, while nitrate concentrations were higher than before. This is surprising in the light of decreasing NO_x emissions in Saxony and needs further investigations.

References

[1] Acker K, Möller D, Wieprecht W, Naumann S (1995) Mt. Brocken, a site for a cloud chemistry measurement programme in central Europe. Water, Air and Soil Pollution 85: 1979-1984.

[2] Acker K, Möller D, Wieprecht W, Kalaß D, Auel R (1998) Investigations of ground-based clouds at Mt. Brocken. Fresenius Journal of Analytical Chemistry 361: 59-64.

[3] Brimblecombe P (1996) Air composition and chemistry. Cambridge University Press 2nd Edition

[4] Bridges KS, Jickells TD, Davies TD, Zeman Z, Hunova I (2001) Aerosol, precipitation and cloud water chemistry observations on the Czech Krusne Hory plateau adjacent to a heavily industrialized valley. Atmospheric Environment 36: 353-360.

[5] Bridgman HA, Davies TD, Jickells T, Hunova I, Towey K, Bridges K, Surapipith V (2002) Air pollution in the Krusne Hory region, Czech Republic during the 1990s. Atmospheric Environment 36: 3375-3389.

[6] Collet Jr JL, Hoag KJ, Sherman DE, Bator A, Richards LW (1998) Spatial and temporal variations in San Joaquin Valley fog chemistry. Atmospheric Environment 33: 129-140.

[7] Grasserbauer M, Paleczek S, Rendl J, Kasper A, Puxbaum H (1994) Inorganic constituents in aerosols, cloud water and precipitation collected at the high alpine measurement station Sonnblick: Sampling, analysis and exemplary results. Fresenius Journal of Analytical Chemistry 350: 431-439.

[8] Herckes P, Wendling R, Sauret N, Mirabel P, Wortham H (2001) Cloudwater studies at a high elevation site in the Vosges Mountains (France). Environmental Pollution 117: 169-177.

[9] Hoag KJ, Collet Jr JL, Pandis SN (1999) The influence of drop size-dependent fog chemistry on aerosol processing by San Joaquin Valley fogs. Atmospheric Environment 33: 4817-4832.

[10] Kang J, Byung CC, Lee C-B (2010) Atmospheric Transport of water soluble ions (NO_3^-, NH_4^+, and nss-SO_4^{2-}) to the southern East Sea (Sea of Japan). Science of the Total Environment 408: 2369-2377

[11] Marinoni A, Laj P, Sellegri K, Mailhot G (2004) Cloud chemistry at the Puy de Dome: variability and relationships with environmental factors. Atmospheric Chemistry and Physics 4: 715-728.

[12] Millet M, Sanusi A, Wortham H (1996) Chemical composition of fogwater in an urban area: Strasbourg (France). Environmental Pollution 94: 345-354.

[13] Plessow K, Acker K, Heinrichs H, Möller D (2000) Time study of trace elements and major ions during two cloud events at the Mt. Brocken. Atmospheric Environment 35: 367-378.

[14] Queck R (2003): Fraktionierung und zeitliche Differenzierung von Depositionsraten in Waldbeständen. Unpubl. Diplomarbeit, TU Dresden, Institut für Hydrologie und Meteorologie

[15] Warneck P (1991) Chemical reactions in clouds. Fresenius Journal of Analytical Chemistry 340: 585-590.

[16] Zimmermann L, Zimmermann F (2002) Fog deposition to Norway Spruce stands at high-elevation sites in the Eastern Erzgebirge (Germany). Journal of Hydrology 256: 166-175

5th International Conference on Fog, Fog Collection and Dew
Münster, Germany, 25–30 July 2010
FOGDEW2010-67

Operational fog collection and its role in environmental education and social reintegration: A case study in Colombia

C. M. Escobar (2), A. Lopez (2), H. F. Aristizabal (3), J. M. Molina (1,4)

(2) Fundacion Occidente Colombiano, Cali, Colombia, (3) Corporacion Autonoma Regional del Valle del Cauca, Cali, Colombia, (1) Colorado State University, Civil and Environmental Engineering Department, Fort Collins, CO, United States (jmmolina@engr.colostate.edu), (4) FogQuest: Sustainable Water Solutions, Kamloops, BC, Canada

Experimental efforts with fog collection in Colombia began eight years ago, and in recent papers we have suggested the implementation of operational fog collection as an alternative to meet water requirements in rural areas of the Andes Mountain Range. Since then, an increasing number of individuals from academia and environmental organizations in the country have shown a remarkable interest on this appropriate technology, and some started its exploration in a larger scale. In this work we describe the implementation process of the first operational fog collection project in Colombia and discuss its role in rural water supply, in environmental education issues and in the process of "social reintegration" of people who have been victims of forced displacement. Both the fog collection evaluation stage and construction and administration of the operational system involved the participation of the community of a rural village. The study zone, located in the Andes Mountains of the Valle del Cauca Department and with altitudes ranging from 2600 to 2800 meters a.s.l., has serious limitations in water availability. Eight standard fog collectors (SFC) were implemented and used during the period May/2008 - Feb/2009 in order to assess the water yield from fog. The best average monthly collection rate in the period of study was around 2.0 $l.m^{-2}.day^{-1}$. The constructed large fog collector (LFC), with a vertical collection surface of 25 m^2, and the associated hydraulic system are currently managed and administered by the village inhabitants. The fog collection system benefits a rural school, and the water is mainly used in small-scale irrigation activities for horticultural crops and livestock development. The project has also brought positive impacts in the community organization, mainly comprising people who have been forced out of their rural homes by the country's nearly half-century old armed conflict. The system also allows agriculture- and environment-related issues to be incorporated in children's current education. We highly recommend exploring this technology in the search for solutions of water and food security for victims of forced displacement in Colombia. Additional efforts to increase the number of LFCs in the study zone are underway.

5th International Conference on Fog, Fog Collection and Dew
Münster, Germany, 25–30 July 2010
FOGDEW2010-68-1

Micrometeorological characteristics of sea fogs off the west coast of the Korean Peninsula

C. K. Kim and S. S. Yum
Department of Atmospheric Sciences, Yonsei University, Seoul 120-749, Korea (62beatle@yonsei.ac.kr)

Incheon International Airport (hereafter IIA) is located on a partly reclaimed island off the west coast of Korea and aircraft operation at IIA often suffers from visibility degradation due to sea fogs. The number of sea fogs that influenced the IIA area is 35 from 2002 to 2006. They are classified into cold sea fogs (27) and warm sea fogs (8), based on the temperature difference between the sea surface and the air above, i.e. the SST and the air temperature at the buoy near IIA. However, clear physical mechanisms that lead to the formation of both cold and warm sea fogs have not been identified yet. For that task, various analyses of meteorological data from micrometeorological to synoptic scales including vertical soundings must be examined. In addition, numerical modeling should be supplemented because of the temporal and spatial limitation of observation. Many scientists studying the physical processes of fog with numerical models emphasize that it is important to fully understand the effects of radiative cooling, turbulent mixing, aerosols and vegetations.
In this study, micrometeorological effects of turbulence and radiation on sea fogs are examined using both observed meteorological data at the buoy, vertical sounding measured at an island to the west of IIA, and numerical simulation results with the Weather Research and Forecast version 3 (WRFV3) model. Among the analyzed observational data, are sensible and latent heat fluxes, calculated with the meteorological data at the buoy. These are examined in association with the bulk Richardson number for each sea fog case. WRFV3 supports the Large Eddy Simulation (LES) for small grid spacing. Five nested domains of 18 km, 6 km, 2 km, 500 m and 100 m are used along with 65 vertically stretched layers. The LES is carried out only for the finest horizontal resolution. Detailed results will be shown at the conference.

5th International Conference on Fog, Fog Collection and Dew
Münster, Germany, 25–30 July 2010
FOGDEW2010-69

Fog forecasting: "old fashioned" semi-empirical methods from radio sounding observations versus "modern" numerical models

M.C. Holtslag, **G.J. Steeneveld**, A.A.M. Holtslag.
Meteorology and Air Quality Section, Wageningen University, Wageningen, Netherlands (Gert-Jan.Steeneveld@wur.nl).

Abstract

Despite the recently improved skill of numerical weather prediction (NWP) models, fog remains difficult to forecast. Hence, we examine whether empirical methods as developed in the 60s&70s are reasonable alternatives forecast tools. It appears that the so-called Fog Stability Index (FSI), solely based on routine radio sounding observations, has reasonable skill. Also, the FSI has been optimized for 12 stations in the Netherlands, after which FSI reaches a high forecast skill. It appears this skill approaches the skill of direct MM5 model output.

1. Introduction

Recent decades resulted in improved skill of high-resolution NWP models. Unfortunately, fog remains difficult to forecast due to the fog's local nature limited vertical and horizontal model resolution, relatively poor knowledge on the relevant processes, on small (radiation, turbulence, aerosols) and on larger scales (advection, subsidence; [1,2,4,8]).

Despite these difficulties, it is imperative to improve fog forecast since fog cause adverse effects in air- and sea traffic [6], leaf wetness duration, asthma when fog coincides with industrial pollution [5].

The apparent difficulties of NWP-models motivate us to evaluate the skill of empirical methods developed in the 60s&70s. The FSI is an empirical method, developed by the US Air Force [3]. Its simplicity is its main advantage: it requires only four variables that are directly available from radiosonde observations. The FSI is defined as:

$$\mathbf{FSI} = 2.(T\text{-}T_d) + 2.(T - T_{850}) + W_{850} \quad (1)$$

With T and T_d the temperature (ºC) and dew point at 2m (ºC), T_{850} and W_{850} are the temperature (ºC) and wind speed at 850 hPa respectively (i.e. outside the planetary boundary layer). The three terms in (1) represent humidity (T-T_d), stability (T-T_{850}) and wind speed (W_{850}). FSI< 31 indicates a high probability of fog formation, 31<FSI<55 implies moderate risk of fog, and FSI>55 suggests low fog risk. Unfortunately, the forecast's lead time is unclear. Fog formation is favored for high humidity (T-T_d small), the atmosphere is stable (weak mixing, T-T_{850} is small) and low wind speed (no mixing, W_{850} is small). The aims of this study are:

-To evaluate FSI against routine observations.
-To compare skill of FSI with the skill of the forecasts with the mesoscale model MM5.
-To optimize FSI for the Netherlands.

2. Methodology

2.1 Evaluation at Cabauw

First, the FSI skill for a 6h forecast is evaluated against fog observations at Cabauw (Netherlands), where a present weather sensor observes obstruction near the ground, i.e. fog. The dataset covers 01-02-2006 until 31-12-2008, of 10 min averaged visibility measurements. Input for the FSI originates from the radio sounding in De Bilt (52º11'N; 05º11'E).

In order to evaluate the FSI skill, a number of skill scores based on a contingency table have been used [10]. Fog is rare, and it is likely that by far most of the situations result in a correct no-fog forecast. These situations are less interesting since we aim to correctly forecast fog, not focus on no-fog situations. The skill score to asses FSI skill, i.e. the Critical Success Index (CSI), not dependent on the correct no-fog forecasts. CSI is the fraction of correct fog forecast of the total amount of interesting situation (both correct fog forecasts and all wrong forecasts). Ideally, the CSI=1 (all forecasts correct) and in case fog is never correctly forecasted CSI=0. Note that for rare events it is more difficult to obtain high CSI values [10]. Furthermore, note that similar conclusions were drawn based on other skill scores, as the Hansen-Kuipers score and the Extreme

dependency score (not shown). Alternatively, the Hit Rate (HR) and False Alarm Ratio (FAR) indicate which part of the *fog events* is correctly forecasted, and which part of the *fog forecasts* is incorrect respectively. A combined measure based on CSI, HR and FAR would be ideal.

2.2 Evaluation for 12 sites

The analysis from §2.1 has been extended for 12 AWS stations, for the period 01-01-2004 until 31-08-2009. For the FSI, the humidity term (T-T_d) has been determined from local observations, while the stability, and wind speed, were recorded from the radio sounding.

To optimize FSI, the data were split in two parts. The first part, from 01-01-2004 until 31-12-2005, was used to determine the exact values of new coefficients. The second part, from 01-01-2006 until 31-08-2009, was used for validation purposes. We use a Monte-Carlo approach in which the coefficients in Eq. (2) below are varied, as well as is the threshold value for the FSI. To avoid effects of fog being present at the forecast time, the forecast lead time in the optimalization is 2-6 hours. Note the current threshold for high fog risk is FSI<31, but this has never been validated for the Netherlands.

$$\mathbf{FSI} = a.(T\text{-}T_d) + b.(T\text{–}T_{850}) + c.W_{850} \qquad (2)$$

Alternatively, we enter the 10m wind speed as an additional predictor:

$$\mathbf{FSI} = a.(T\text{-}T_d) + b.(T\text{–}T_{850}) + c.W_{850} + d.W_{10} \qquad (3)$$

The relative impact of each term (3) is denoted by the coefficients *a*-*b*-*c*. Originally, *a*-*b*-*c* is 2-2-1. It is likely that a small fluctuation in the humidity term (e.g. 0.3K) might be more important for fog forecasting than a small fluctuation in the 850 hPa wind speed (0.6 ms^{-1}).

2.3 Benchmark with MM5

The FSI results on basis of the observations is compared with forecasts by MM5, The latter is a mesoscale model operationally run at Wageningen University for 48 h forecasts [7], using the MRF-PBL scheme, the NOAH land surface scheme in the evaluated set-up, using a 9 km resolution and GFS boundary conditions. Output for temperature, relative humidity, and wind speed have been used to deduced whether fog was forecasted with a lead time of 6 h [11].

3. Results

3.1 Results for Cabauw

Fig. 1 shows that the FSI with original threshold, reaches a CSI=0.38. This is surprisingly high since [9] reports a CSI = 0.35 for a complete NWP model including post-processing by model output statistics. Direct model output from MM5 provides CSI=0.22, and as such FSI seems to outperform MM5. Fig. 1 also shows that FSI skill depends on the selected threshold. Although both HR and FAR increase for larger threshold values, CSI is optimum of ~30, and as such appears to be optimizable.

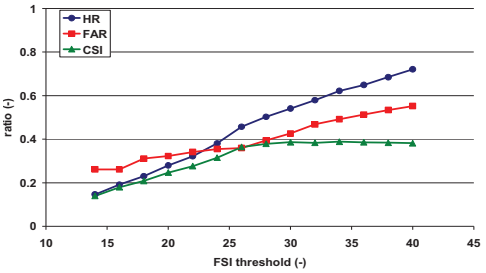

Fig. 1: Skill score for FSI, varying threshold value

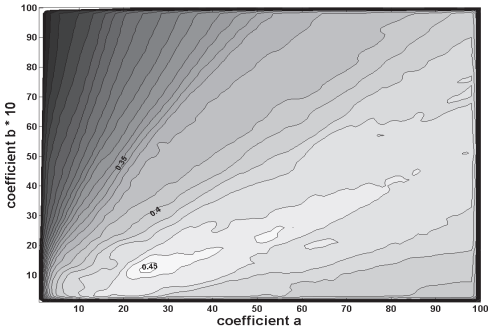

Fig 2: Contour plot of CSI a domain of for a and b, for Lelystad.

3.2 Wider verification and optimalization.

Verification on a broader dataset (see Appendix) shows FSI scores worse than for Cabauw (median CSI=0.23, Fig. 3), which might be due to the fact that Cabauw is an ideal site for fog formation (flat, humid

soil), and the sounding that feeds FSI is taken relatively close to Cabauw.

For the optimalization, detailed analysis is shown for Lelystad. §3.1 indicated modifying threshold values will likely benefit the quality of fog forecasting, the threshold values have again been modified.

For Lelystad CSI improves from 0.19 to 0.22 for adjusted threshold values. Apparently the threshold optimalization lacks the desired effect, seems to result in a worse skill since HR decrease a lot more than FAR. However, these scores are ratios and a closer look at the absolute values indicates one obtains indeed less wrong forecasts.

Subsequently, we optimize the ratio *a*-*b*-*c*. For each set of coefficients, an optimum threshold value has been determined, and the corresponding CSI values are plotted (Fig. 2). Apparently, the FSI skill would benefit a lot from modified coefficients. For Lelystad $a \cong 25$ and $b \cong 1.5$. The modified coefficients resulted in a better CSI score in the validation stage. Again HR decreased, but FAR decreased slightly more, which net resulted in a reduced amount of wrong forecasts compared to the original FSI.

Finally we analyze Eq. (3) with W_{10} included as predictor. For Lelystad the best results where found for $d = 6$, while a and b slightly changed to values 20 and 0.5. Although CSI decreases only slightly from the previous modification, HR and FAR both increased. Apparently more fog events are correctly forecasted, but there are also more false fog forecasts. It is questionable whether this is desirable or not.

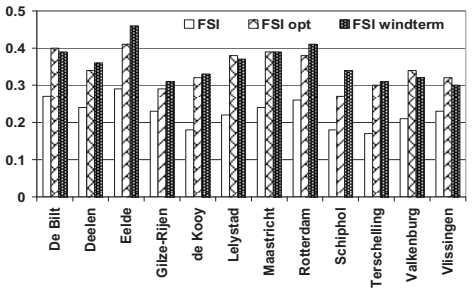

Fig 3: CSI for the validation of recalibrated FSI.

The original FSI has some potential, but the optimalization clearly made the difference, resulting in a large improvement of the skill. Whether or not the addition of W_{10} has any use is debatable, since CSI does not increase for all stations.

The original FSI formula, with optimized threshold values but with original coefficients, also has lower CSI scores compared to the Cabauw study. The CSI has a maximum of 0.29 for Eelde, and a minimum value of 0.17 for Terschelling. The modifications are beneficial for all stations, though the additional W_{10} does not provide skill improvement for all sites. Without $W_{10,}$ the CSI score vary between 0.41 (Eelde) and 0.27 (Schiphol). Including W_{10} leads on average to slight improvements. The maximum CSI value is 0.46 (Eelde) and the minimum CSI= 0.3 (Vlissingen). HR and FAR of the optimized FSI indicate the main advantage of $W_{10}$is, in general, a higher HR. Overall ~65% of all fog events are also correctly forecasted, compared to 59% if W_{10} is excluded. Unfortunately, also FAR rises slightly (53% -> 56%).
The site specific optimalizations as applied here have a side effect that a generally valid FSI formula is missing. In order to summarize our results, the mean ratio of a/b appears to be 0.09, which results in a=21 and b= 2 (Fig. 4). Hence a general FSI formula would be:

$$\mathbf{FSI = 21.(}T\mathbf{-}T_d\mathbf{) + 2.(}T\mathbf{-}T_{850}\mathbf{) + 0.5.}W_{850} \quad \mathbf{(4)}$$

The corresponding threshold value where fog is forecasted fog is found by applying this relation in the validation dataset of each station. The optimal threshold value is on average 26, varying between 22 and 30, and the corresponding CSI value is on average 0.35, varying between 0.41 and 0.28. CSI values for the threshold of 26 would be slightly lower.

For the optimized FSI, the mean CSI is 0.35. This means that for every correct fog forecast two incorrect forecasts are made. This appears to be quite inaccurate, but it has to be noted that the CSI is dependant on the observed percentage of fog events as mentioned in § 2.1. The observed fog frequency for these stations varies between 2.8% (Vlissingen) and 8.9% (Deelen). It appears that the accuracy, defined as the amount of total correct forecasts divided by the total amount of forecasts, in all situations is higher than 90%, with a maximum of 97% for observation station Vlissingen. Apparently, even though the FSI is a simplified empirical relationship, it is capable of high accuracy forecasting. Overall, ~95% of all forecasts are correct, either correct fog forecasts or correct no-fog forecasts.

Conclusions

This paper examines the skill of a modern numerical weather predication model MM5, relative to simple empirical methods based on sounding observations (FSI). It appears that FSI scores better than direct model output from MM5, and performs reasonable once optimized for site specific conditions.

Acknowledgements

We wish to acknowledge Hidde Leijnse (WUR) and KNMI for providing observational data, and Bert Heusinkveld for his advices.

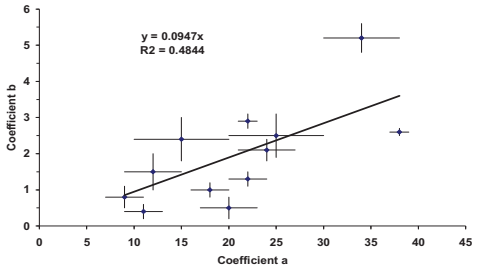

Fig. 4: Relation between coefficient a and b for Equation 2.

References

[1] Bergot, T., Terradellas, E., Cuxart, J., Mira, A., Liechti, O., Mueller, M., Nielsen, N, W., Intercomparison of single-column numerical models for the prediction of radiation fog, J Appl Meteor and Clim, 2007, 46, 504-521

[2] Fisak, J., Rezacova, D., Mattanen, J., 2006: Calculated and measured values of liquid water content in clean and polluted environments, Stud Geophys. Geod., 50, 121-130

[3] Freeman, L.E., Perkins, J.S. Meteorological Techniques, AFWA/TN-98/002, 242 p, online available at http://www.comptus.com/PDF/AFWA_TN_98-002.pdf

[4] Gultepe, I., Tardif, R., Michaelides, S.C., Cermak, J., Bott, A., Bendix, J., Müller, M.D., Pagowski, M., Hansen, B., Ellrod, G., Jacobs, W., Toth, G., Cober, S.G., 2007, Fog research: a review of past achievements and future perspectives, Pure and Applied Geophys, 164, 1121-1159

[5] Kashiwabara, K., H. Kohrogi, K. Ota, T. Moroi, 2002: High frequency of emergency room visits of asthmatic children on misty or foggy nights. J. Asthma, 39, 711-717.

[6] Pejovic, T., Noland, R.B., Williams, V., Toumi, R., 2009: A tentative analysis of the impacts of an airport closure, J. Air Trans. Manag, 15, 241-248.

[7] Skelsey, P., G.J.T. Kessel, A.A.M. Holtslag, A.F. Moene, W. van der Werf, 2009: Regional spore dispersal as a factor in disease risk warnings for potato late blight: A proof of concept. Agr. Forest. Meteor. 149, 419-430.

[8] Velde, I.R. van der, G.J. Steeneveld, B.G.J. Wichers Schreur, A.A.M. Holtslag, 2010: Modeling and forecasting the onset and duration of severe radiation fog under frost conditions, Mon. Wea. Rev., 10.1175/2010MWR3427.1

[9] Wijngaard, J., Rover de, C.J., Vogelezang, D., Bruggen van, H., Maat, N., Smit, L., Heijstek, J., Keet, M., Hove ten, R., 2008: Improved Low visibility and Ceiling forecasts at Schiphol Airport, Final report part 1, KNMI, IT 2008-07, de Bilt, The Netherlands, 43 p.

[10] Wilks, D.S., 2006: *Statistical methods in the atmospheric sciences*, Dep. Earth and Atmos. Sci., Cornell University, United States.

[11] Zhou, B., J. Du, 2010: Fog Prediction from a Multimodel Mesoscale Ensemble Prediction System. *Wea Forecasting*, 25, 303-322.

Appendix:

Fig. A1: Observation sites in The Netherlands

5th International Conference on Fog, Fog Collection and Dew
Münster, Germany, 25–30 July 2010
FOGDEW2010-70

Modeling and Forecasting the Onset and Duration of a Fog Event during Frost Conditions

Ivar R. van der Velde(1), G.J. Steeneveld(1), B.G.J. Wichers Schreur(2), A.A.M. Holtslag(1). (1) Meteorology and Air Quality Section, Wageningen University, Wageningen, Netherlands, (2) Royal Netherlands Meteorological Institute, De Bilt, Netherlands (Gert-Jan.Steeneveld@wur.nl).

1. Introduction

Low visibility due to fog and low stratus seriously affects airport and hub-and spoke operations, which has obviously direct economic consequences. In the long term, the fog frequency and predictability may even influence an airline's choice of home base. Lack of knowledge of the relevant atmospheric, hydrological and chemical fog processes inhibit successful fog forecasting. Also, an apparent feedback appears between fog occurrence and regional climate [21]. Climate projections and weather forecasts agencies use numerical weather prediction (NWP), for which fog remains a challenge. Model improvement is essential to reduce uncertainty in fog forecasting and in airport operations.

This exploratory study evaluates the performance of the WRF and HIRLAM mesoscale models for a case of thick radiation fog in the Netherlands. We aim to identify the role of model formulation, selected parameterizations and resolution in forecasting the onset and duration of fog and identify common model weaknesses. This evaluation is supported by simulations by 1D models of HIRLAM and [5, Duynkerke 1991, D91].

Studying fog onset and duration with NWP has a long history. [7] reported possibly the first feasibility study of using NWP for fog forecasting. Using 1D models, [2,3,14] showed the need for inclusion of gravitational droplet settling, radiative cooling, turbulent transport, a vegetation scheme and detailed microphysics. Sensitivity tests with the COBEL model, [1] revealed the importance of dew deposition and the initial conditions. Despite the increased understanding of fog, the NWP modeling of fog remains challenging [9, 22].

Fog studies with mesoscale models focused on advection fog in coastal regions, e.g. [8, 15]. [17] addressed the sensitivity of model results to the initial and boundary conditions for a dense fog in Ontario, Canada.

2. Synoptic situation

The synoptic situation on 24 and 25 Nov. 2004 was dominated by a high pressure system, with clear skies, light winds and subsidence, i.e. favorable conditions for radiation fog. Operations at Schiphol airport were reduced from 64 to barely 20 aircraft per hour and 107 flights were cancelled. The synoptic network, Cabauw tower observations, and AVHRR satellite products (Fig. 1) show that a 150 m deep fog layer developed in the west of the country in the early morning of 25 Nov, and which remained the full day. The fog layer was overlain by a very dry layer, and it was freezing several K close to the ground. The innovative aspects of this study are the first WRF evaluation for fog; fog occurs for T<0ºC, and the fog onset occurred relatively late at night and that the fog persisted during daytime.

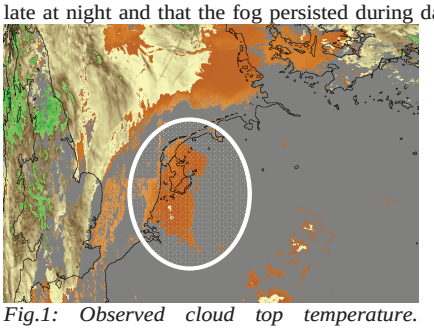

Fig.1: Observed cloud top temperature. Brown indicates low level clouds. The circle shows the fog under study. (http://wdc.dlr.de/apollo).

3. 3D model set-up and results

a) WRF

Using WRF/ARW 3.0.1 a domain was configured centered at Cabauw, on a horizontal grid of 33x33, 56x56 and 61x61 points with 30, 6, 1.2 km resolution respectively. We used 35 terrain-following σ levels, with the 1st level at σ=0.998, and 9 layers below 240 m. WRF initial and boundary conditions originate from the NCEP final analysis. Impact of lateral boundaries is expected to be limited in this case because of low winds, i.e. large scale advection is small. Land use properties were obtained from the USGS.

This study examines combinations of physics options to assess its impact on fog modeling. For microphysics we utilize Kessler, Eta-Ferrier, WSM3, and WSM6 [11]. For the PBL schemes we tested the non-local 1st order YSU model [10], and the 1.5 order TKE closure model (MYJ, [12]), in which the minimum TKE was lowered 1.10^{3} m^2s^{-2}. The NOAH [6] and the 5 soil layer land surface scheme were both permutated in the simulations. One day spin up was applied.

b) HIRLAM

HIRLAM7.2 is a short range NWP model for operational use in many European meteorological institutes. The HIRLAM project focuses on a reference version with an optimal set of parameterizations. Alternative parameterizations are present, but for research purposes only. Lateral boundary conditions are provided by the ECMWF. Fog relevant physics contain the radiation scheme by [19], the condensation scheme by [18], the [4] turbulence TKE scheme formulated in moist conserved variables and the ISBA land surface scheme [16]. Here, the model is run on a grid of 290x306 points with a spacing of 0.1º, centered at Cabauw and with 60 levels with the lowest level at 30 m. The model is run in a 6h assimilation cycle for 3 days prior to the fog experiment to allow the surface model to spin up.

c). Results

For WRF, only a few sets of parameterizations were actually able to create fog. This section presents WRF using WSM3-YSU-NOAH since it per-formed best based on incoming longwave ($L^{\downarrow}$), solar radiation ($S^{\downarrow}$), and 2m temperature (T_2). On 24 Nov., the atmosphere is fog-free, since the observed $L^{\downarrow}$ is relatively low (Fig. 2), $S^{\downarrow}$ peaks at noon, and a substantial diurnal temperature cycle is present. On 25 Nov., $L^{\downarrow}$ clearly exposes the onset and duration of the fog event since it in-creases suddenly from 250 Wm^{2} to 300 Wm^{2} at ~0300 UTC. In WRF, the fog event of 25 Nov. is not represented, but fog occurs some hours before and thus corresponds with two $L^{\downarrow}$ peaks in the early morning and two $L^{\downarrow}$ peaks in the evening of 24 Nov. On the 2nd day, HIRLAM's $L^{\downarrow}$ increase agrees well with the observed fog onset. However, fog is limited to the lowest model level and suffers from early dispersal at 0900 UTC, as seen in the plunge in $L^{\downarrow}$ at sunrise. $S^{\downarrow}$ and T_2 are reasonable well represented by both models on the 1st day. Before fog onset, T_2 decreases from 7ºC at noon to -3ºC the next day. Only in HIRLAM the T_2 decreases analogous with the observations. Clearly freezing occurs because of the late onset of fog. The fog onset may have been delayed by dewfall and hoarfrost as suggested by a small negative latent heat flux in HIRLAM in the hours prior to fog onset. The early fog onset in WRF in the evening of 24 Nov. prevents a further surface cooling to below freezing point. Apparently the coarser vertical resolution of HIRLAM does not inhibit fog formation, but may have influenced its growth to the mature stage. The extent of the fog area in HIRLAM is comparable to that in the AVHRR image, although fog over the Lake Ijssel and coastal waters is absent in HIRLAM. The absence of fog in the forecast of both models for the morning of the 25th, gives rise to an over-estimation of $S^{\downarrow}$, and correspondingly a large rise in T_2, where in reality an ice day was recorded. On 26 Nov., the passage of a cold front can be recognized in the increased friction velocity (u_*). As the fog is cleared and replaced by low stratus, the $L^{\downarrow}$ in Cabauw increases again sharply to 320 Wm^{-2} and increased the rest of the day. The $L^{\downarrow}$ in-crease in WRF agrees very well with the observations, where as the frontal passage seems to be delayed in HIRLAM. The advection of low stratus is present in both models.

4. Column model set-up and results

a) HIRLAM

The HIRLAM column model (H-SCM) consists of the full physics of the 3D HIRLAM, with 47 levels below 2 km, starting at 4 m. Initial conditions for H-SCM are derived by interpolation from the +12 3D forecast at 1200 UTC 24 Nov. Temperature, wind and specific humidity are then replaced by values from the radiosonde of 1200 UTC at De Bilt. Below 1057 m the T and q profiles from D91 (see below), are substituted, while for levels between 1057 and 2000 m a linear transition is made between the D91 and sonde observations. A time dependent geostrophic wind ($\mathbf{V_g}$) as in D91 model was coded in the 1D dynamics.

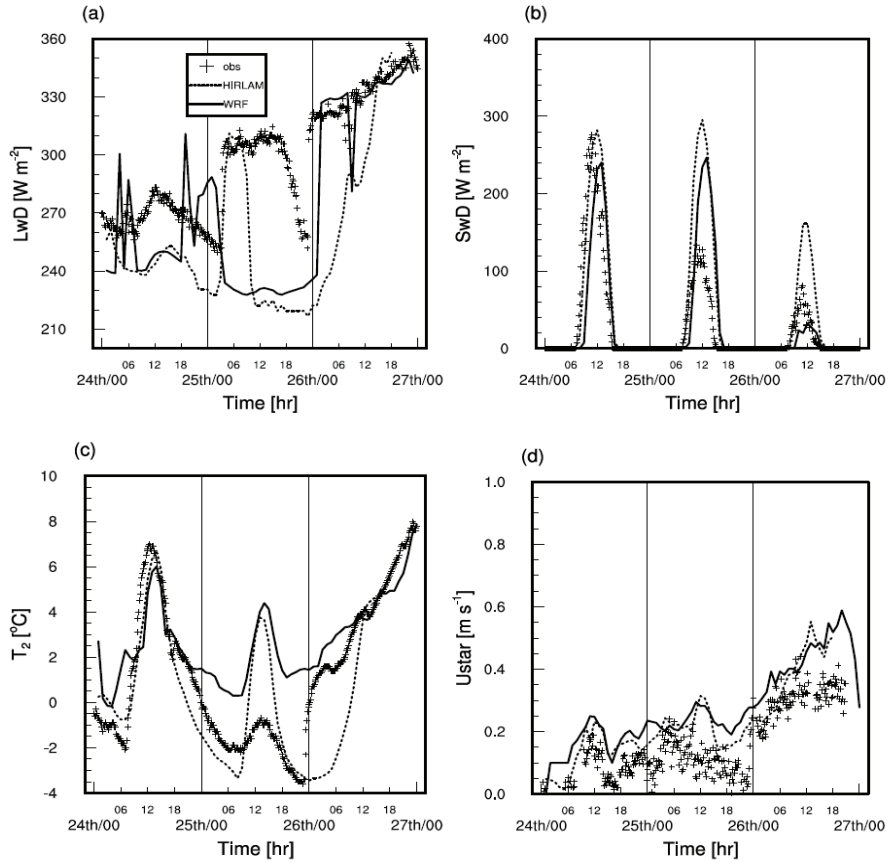

Fig 2: Modelled (3D models) and observed incoming longwave and solar radiation, 2 m temperature and friction velocity.

b. Duynkerke model (D91)

This model consists of a 1st order turbulence model based on the moist conserved variable wet equivalent potential temperature, a greybody emissivity longwave radiation model, and includes droplet settling. The heat diffusion equation is solved for a 75 cm deep soil. Soil moisture freezing and thawing was introduced, which had substantial impact on the forecast near surface temperatures. Here, the Cabauw 200 m wind is used as $\mathbf{V_g}$. The initial profiles for T and q are obtained from closest radio sonde at EHDB at 1200 UTC 24 Nov. A subsidence of $-0.5 \cdot 10^{-3}$ ms^{-1} was applied. Based on a series of EHDB radio soundings, a 5 K hr^{-1} heating was induced above 250 m, which was linearly interpolated to zero towards the surface. D91 uses 40 logdistributed levels, between 0.3 m and 1.8 km.

c. Results

Column models allow for efficient experiments with physics options. D91 acts as a reference for subsequent sensitivity studies with H-SCM. D91 is relatively successful in forecasting the fog onset and the following evolution, but is unable to forecast the fog dispersal. In practise, forecasting of fog decay and onset may be of equal importance. D91 estimates

$L^{\downarrow}$ reasonably, although fog onset is slightly too early, due to somewhat overestimated surface cooling. However, in the mature fog stag, $L^{\downarrow}$ is ~10 Wm^{-2} overestimated, which indicates a slight overestimation of the fog liquid water content (LWC). The fog decay around 0000 UTC 26 Nov. is not captured by D91 although the wind speed increase is reasonably forecasted. Thus, the correctly forecasted $L^{\downarrow}$ after midnight is spurious because clouds were observed, while the fog persists in the model. Both models estimate $S^{\downarrow}$ correctly, which is surprising for the last day considering the persistence of fog in D91. Apparently, the LWC of the modeled fog and the observed cloud do not differ substantially.

At noon H-SCM and D91 forecast the same maximum T_2 (correctly timed) about 3 K too warm, and the consequent cooling is substantially underestimated. This might be a result of the overestimated turbulence intensity (e.g. u_*) between 1800 UTC and midnight on 25 Nov. After midnight, both 1D models provide enhanced turbulence compared to the observations.

The D91 model gives the fog onset around 0200 UTC 25 Nov. and the layer gradually grows to 100 m at 0600 UTC and 180 m at 1200 UTC, and even reaches (obviously erroneously) 260 m at the end of the model simulation. At 1345 UTC 25 Nov., the near surface LWC shows a minimum, resulting in a visibility of 721 m [13]. A minimum visibility of 89 m was modeled, which is close to the reported observations. Note that the modeled visibility decreases more gradually in time than was observed. Finally, the model fails to remove the fog layer, even using substantial larger $\mathbf{V_g}$ speed as a forcing than has been observed. This occurs for different model settings and is thus a particular persistent feature. This indicates that the physical processes that control the fog dissipation are not well represented in the model physics, and further research to improve this aspect of the forecast is warranted.

As with 3D HIRLAM, H-SCM simulates the fog onset well. In the fog, the $L^{\downarrow}$ is close to the observations, which suggests the model LWC is com-parable to reality. The modeled LWC is located at the PBL top and ascends with the PBL growth. H-SCM does not completely dissolve the fog, but forms a broken stratus deck. The cooling in H-SCM is not as strong as in the 3D model. At the end of the night the fog layer is ~150 m thick and well mixed. In H-SCM at this moment LWC is concentrated around the same level. This concentration of LWC near PBL top and the model temperature profile indicate that the fog layer in the model is far from well mixed. This may point to a deficiency in the parameterization of turbulent mixing under stable conditions. H-SCM shows a small $S^{\downarrow}$ excess at noon, which is partly compensated by a negative bias in $L^{\downarrow}$. Hence, a warm bias occurs in addition to the warm bias in the preceding night. To assess the effect of resolution sensitivity tests with a 60 and a 90-layer H-SCM were carried out. Both runs accurately predict the fog onset, but the initial fog layer growth was slower and the overestimation of $S^{\downarrow}$ increased with reduced resolution, suggesting a lower LWC and a resolution dependence of the condensation scheme. In addition, with the first model level at 30 m HSCM failed to produce fog. Thus high resolution near the surface is essential for the initialization of fog. As for the 3D model, resolution is also of the essence for further growth of the layer. Finally, when the fog lifts from the surface to form a stratus layer, resolution also becomes important at higher levels. The success of the 3D model in producing fog with the same resolution must be attributed to the larger cooling rate in this model. Accurate forcing of the column model is clearly also of importance.

5. Discussion and Conclusions

A case study of a widespread 150 m thick radiative fog over the Netherlands was presented as a benchmark for mesoscale model development, in particular for very high resolution forecasts for airport operations. Both WRF and HIRLAM have difficulties with the fog evolution. WRF only fore-casts fog for a few permutations of the parame-terizations, but the fog onset is offset in time and location, and the fog is particularly scattered. This is surprising since the mean variables are well captured. HIRLAM correctly forecasts the fog on-set, but the fog layer remains at the lowest model layer. As a direct consequence, in both models fog does not persist, but is quickly dispersed. Two column models performed well for the fog onset and its mature stage, although their results were sensitive to the initial and conditions and prescribed external forcings. High vertical resolution close to the surface is essential for fog modeling. Also, resolution at higher levels becomes important when the fog lifts to a stratus layer.

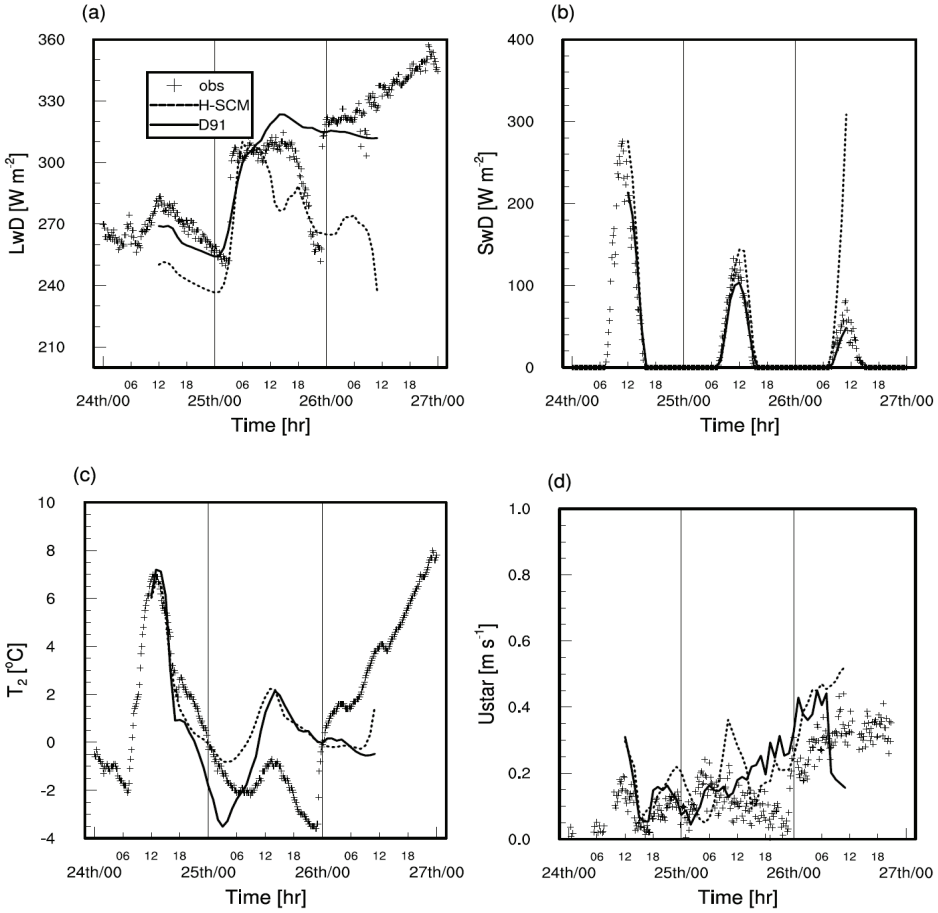

Fig. 3: Modelled (1D models) and observed incoming longwave and solar radiation, 2 m temperature and friction velocity.

In HIRLAM the fog and stratus LWC reduces with lower resolution. All models hamper during the daytime fog evolution: in D91 fog is too persistent, whereas fog in HSCM dissipates too quickly. A sensitivity experiment indicated that the turbulence scheme plays an important role in this process. Given the importance of the early morning dispersal of fog for an airport's operation this is probably the main area of research in the development of a high resolution fog model. This study has shown that despite advances in the understanding of the fog physics fog both mesoscale and column models are still not able to simulate all aspects of the fog evolution. Fog forecasting remains a challenging task.

Acknowledgements

We acknowledge KNMI for providing Cabauw observations, and S. Tijm for providing H-SCM and insightful discussion. G.J. Steeneveld acknowledges the BSIK-ME2 research programme (Climate Changes Spatial Planning).

References

[1] Bergot, T., D. Guedalia, 1994: Numerical forecasting of radia-tion fog. part I: numerical model and sensitivity tests. Mon. Wea. Rev., 122, 1218-1230.

[2] Bott, A., T. Trautmann, 2002: PAFOG -a new efficient forecast model of radiation fog and low-level stratiform clouds. Atmos. Res., 64, 191-203.

[3] Brown, R., W.T. Roach, 1976: The physics of radiation fog: II -a numerical study. Q. J. Roy. Meteor. Soc., 102, 335-354.

[4] Cuxart, J., P. Bougeault, J.L. Redelsperger, 2000: A turbulence scheme allowing for mesoscale and large-eddy simulations. Q. J. Roy. Meteor. Soc., 126, 1-30.

[5] Duynkerke, P.G., 1991: Radiation fog: a comparison of model simulation with detailed observations. Mon. Wea. Rev., 119, 324-341.

[6] Ek, M.B., K.E. Mitchell, Y. Lin, E. Rogers, P. Grunmann, V. Koren, G. Gayno, J.D. Tarpley, 2003: Implementation of Noah land surface model advances in the National Centers for Environmental Prediction operational mesoscale eta model. J. Geophys. Res., 108, doi:10.1029/2002JD003296.

[7] Fisher, E.L, P.Caplan, 1963: An experiment in numerical prediction of fog and stratus. J. Atmos. Sci., 20, 425-437.

[8] Fu, G., J. Guo, S.-P. Xie, Y. Duan, M. Zhang, 2006: Analysis and high-resolution modeling of a dense sea fog event over the Yellow Sea. Atmos. Res., 81, 293-303.

[9] Gultepe, I., et al.,2007: Fog research: A review of past achievements and future perspectives. Pure Appl. Geo-phys., 164, 1121-1159.

[10] Hong, S., Y. Noh, J. Dudhia, 2006: A new vertical diffusion package with an explicit treatment of entrainment processes. Mon. Wea. Rev., 134, 2318-2341.

[11] Hong, S.Y., J. Dudhia, S.H. Chen, 2004: A revised approach to ice microphysical processes for the bulk parameterization of clouds and precipitation. Mon. Wea. Rev., 132, 103-120.

[12] Janjic, Z. I., 2002: Non singular implementation of the Mellor-Yamada level 2.5 scheme in the NCEP meso model. NCEP Office Note 437, National Centers for Environ. Pred., 61 pp.

[13] Kunkel, B.A., 1984: Parameterization of droplet terminal velocity and extinction coefficient in fog models. J. Clim. Appl. Meteor., 23, 34-41.

[14] Musson-Genon, L.,1987: Numerical simulations of a fog event with a one-dimensional boundary layer model. Mon. Wea. Rev., 115, 592–607.

[15] Nakanishi, M., H.Niino, 2006: An improved Mellor-Yamada level-3 model: Its numerical stability and application to a regional prediction of advection fog. Bound.-Layer Meteor., 119, 397-407.

[16] Noilhan, J., J.F. Mahfouf, 1996: The ISBA land surface parameterization scheme. Global Planet. Change, 13, 145-149.

[17] Pagowski, M., I. Gultepe, P. King, 2004: Analysis and modeling of an extremely dense fog event in southern Ontario. J. Appl. Meteor., 43, 3-16.

[18] Rasch, P.J., J. E. Kristj nsson, 1998: A comparison of the CCM3 model climate using diagnosed and predicted condensate parameterizations. J. Climate, 11, 1587–1614.

[19] Savij rvi, H., 1990: Fast radiation parameterization schemes for mesoscale and short-range forecast models. J. Appl. Meteor., 29, 437-447.

[20] Skamarock, W., 2008: A description of the advanced research WRF Version 3. NCAR tech. note TN-475+STR,113 p.

[21] Vautard, R., P. Yiou, G.J. van Oldenborgh, 2009: Decline of fog, mist and haze in Europe over the past 30 years. Nature Geosci., 2, 115-119.

[22] Velde, I.R. van der, G.J. Steeneveld, B.G.J. Wichers Schreur, A.A.M. Holtslag, 2010: Modeling and forecasting the onset and duration of severe radiation fog under frost conditions, Mon. Wea. Rev., 10.1175/2010MWR3427.1

5th International Conference on Fog, Fog Collection and Dew
Münster, Germany, 25–30 July 2010
FOGDEW2010-72

Fog deposition to the Atacama desert

A. Westbeld (1), O. Klemm (2), F. Griessbaum (2), E. Sträter (3), H. Larrain (4), P. Osses (5), and P. Cereceda (5)

(1) GEO-NET, Hannover, Germany (annawestbeld@danek.com), (2) Institute of Landscape Ecology, University of Münster, Münster, Germany, (3) Landesamt für Natur, Umwelt und Verbraucherschutz, Essen, Germany, (4) Atacama Desert Center, Pontificia Universidad Católica de Chile, Santiago de Chile, Chile, (5) Institute of Geography, Pontificia Universidad Católica de Chile, Santiago de Chile, Chile

In the Atacama Desert, one of the driest places on earth, fog deposition plays an important role for the water balance and for the survival of vulnerable ecosystems. The eddy covariance method, previously applied for the quantification of fog deposition to forests in various parts of the world, was used for the first time to measure deposition of fog water to a desert. We estimated the amount of water available for the ecosystem by deposition and determined the relevant processes driving fog deposition. This is especially important for the species *Tillandsia landbecki* living in coastal Atacama at the limit of plant existence with fog and dew being the only sources of liquid water.

Between 31 July and 19 August, 2008, measurements were realized in a 31 ha large *Tillandsia* carpet at Cerro Guanaco, located 15 km south of Iquique, northern Chile. Several data quality assurance procedures were applied. For the values in compliance with the applied criteria, the mean total deposition per hour was determined (0.04 L per m^2) for foggy periods. This number was applied to estimate the amount of water deposited during the measuring period, during the entire month of August 2008, and throughout a whole year. For August 2008, a frequency of fog of 16 %, as established during the measuring period, was assumed. The frequency for a whole year was estimated from the differences of the collected amount of water obtained with standard fog collectors installed at Cerro Guanaco in an earlier study.

Calculations resulted in an amount of 2.5 L per m^2 of deposited fog water for the measuring period. During the entire August, 4.4 L per m^2 have likely been available, and for a whole year, a total of 25 L per m^2 was estimated to have reached the surface. Inaccuracies could have been caused by the low amount of data applied, and by a possible underestimation of the deposition due to additional formation of radiation fog during the fog events.

Three days were used for further analysis because of long, uninterrupted fog periods. On each of these days, turbulent upward fluxes occurred periodically. This leads to the assumption that there could have been a source of fog water near the surface. During the respective time periods, warm air was transported downward. The cold desert ground could have diminished the temperature of air layers at ground level, and therewith could have caused additional condensation. If there had been a source of droplets between the measuring height (5 m above ground) and the surface, deposition could have occurred while the instruments were measuring upward transport of fog droplets.

Westbeld, A., Klemm, O., Griessbaum, F., Sträter, E., Larrain, H., Osses, P. & Cereceda, P. (2009) Fog deposition to a Tillandsia carpet in the Atacama Desert. Annales Geophysicae 27, 3571-3576.

5th International Conference on Fog, Fog Collection and Dew
Münster, Germany, 25–30 July 2010
FOGDEW2010-73

Multimodal Size Distributions in Fog: Cloud Microphysics or Measurement Artifact?

D Baumgardner (1), G Kok (2), and P. Chen (3)

(1) UNAM, Centro de Ciencias de la Atmosfera, Mexico City, Mexico (darrel.baumgardner@gmail.com), (2) Droplet Measurement Technologies, (3) Handix Corporation

In recent years there have been a number of observations during fog events whereby the measured size distributions show more than a single mode, sometimes even three or four. These multiple modes have been explained using various physical models including entrainment and mixing, coalescence, sedimentation, and new particle activation. Whereas all of these mechanisms are physically possible, a simpler explanation may explain how these multiple modes are formed, at least in those cases where optical particle counters (OPC) are used to measure the droplet sizes.

The most frequently used OPC is the Droplet Measurement Technology (DMT) FM-100 that measures droplets from 2 – 50 μm. The technique is single particle light scattering whereby droplets pass through a focused laser beam and the light scattered in a forward, solid angle of 4-12° is collected and converted to a current in a photodetector. The relationship between scattered light and droplet size is determined from Mie theory and for the laser wavelength and collection geometry of the FM-100, this relationship is non-linear and non-monochronic, i.e. the same scattering intensity can be produced by droplets of different sizes in a number of size ranges.

This presentation will show how the ambiguities in the scatter versus size relationship in the FM-100 introduces bimodality in the measured size distributions and that the false modes tend to fall where published data has shown modes measured during fog events. These artificial peaks can be removed and size distributions can be extracted that are more representative of the ambient spectra using an inversion algorithm that accounts for the Mie scattering relationship.

5th International Conference on Fog, Fog Collection and Dew
Münster, Germany, 25–30 July 2010
FOGDEW2010-74

Temperature dependent kinetic measurements of isoprene oxidation products exposed to OH, NO3 and SO4- in aqueous solution.

L. Schöne, D. Hoffmann, and H. Herrmann
Institute for Tropospheric Research, Chemistry, Leipzig, Germany (schoene@tropos.de)

The troposphere contains a complex mixture of numerous gases, liquid water and diverse solid particles which undergo intricate processes. Volatile organic compound (VOC) emissions from anthropogenic and biogenic sources are very important for the tropospheric chemistry and other processes such as secondary organic particle mass formation. Emissions of biogenic volatile organic compounds (BVOCs) exceed those VOCs coming from human activity by a factor of 10 [1]. Isoprene (2-methyl-1,3-butadiene, C5H8) emissions represent approximately 40% of the emitted BVOCs, leading to an estimated source strength of 500-750Tgyr-1 [2]. As isoprene has a small Henry coefficient, its oxidation occurs solely in the gas phase. The formed first oxidation products methacrolein (MACR), methyl vinyl ketone (MVK), methacrylic acid (MAA) and acrylic acid (ACA) are therefore firstly located in that phase. Even if the Henry coefficients of the main isoprene oxidation products MACR and MVK are already higher than those of isoprene partitioning of theses compounds into the aqueous phase of rain, fog and cloud droplets and particles was neglected. Correspondingly, aqueous phase oxidation processes of MACR and MVK were sparsely investigated in the past. A recent study [3], however, reports much higher aqueous phase concentrations of MACR and MVK than expected from their Henry coefficients. To evaluate the importance of liquid phase reactions of early isoprene oxidation products for the organic particle mass production, kinetic studies are necessary.
Therefore, this work investigated the temperature dependence of methacrolein, methyl vinyl ketone, methacrylic acid and acrylic acid exposed to NO3, SO4- and OH radicals in the range of 278K to 318K in the aqueous phase. Furthermore, the effect of the acid–base equilibrium on the reactivity of the two acids was studied by measuring the kinetics of the dissociated and undissociated acids. The measurements were performed using a laser-photolysis laser long path absorption (LP-LLPA) technique.
The measurements' analysis confirmed in all cases the much higher reactivity of the hydroxyl radical (k∼109M-1s-1) in comparison to the sulfate (k∼108 M-1s-1) and the nitrate (k∼107M-1s-1) radical, with methacrylic acid showing steadily the highest reactivity among the investigated substances. The temperature dependence of the measured rate constants is most distinct for nitrate radical reactions and weakest for those with sulfate radicals. Referred to the two different considered pH-values of the acids, the protonated form reacts slightly faster than the unprotonated form and shows a less distinct temperature dependence.

[1] Guenther et al., 1995: Global-model of natural volatile organic-compound emissions. Journal of Geophysical Research – Atmosphere, 100(D5), 8873–8892.
[2] Guenther et al. 2006: Estimates of global terrestrial isoprene emissions using MEGAN (Model of Emissions of Gases and Aerosols from Nature). Atmospheric Chemical Physics, 6, 3181–3210.
[3] van Pinxteren et al., 2005: Schmücke hill cap cloud and valley stations aerosol chemical composition during FEBUKO (II): Organic compounds. Atmospheric Environment, 39, 4305-4320.

5th International Conference on Fog, Fog Collection and Dew
Münster, Germany, 25–30 July 2010
FOGDEW2010-75

The influence of El Niño Southern Oscillation (ENSO) on fog oases along the Peruvian and Chilean coastal deserts.

R. Manrique (1), C. Ferrari (1,2) and G. Pezzi (1,2)

(1) Plant Ecology Laboratory, University of Bologna, Via Irnerio 42, 40126 (Bologna), (2) Research Centre on Environmental Sciences (CIRSA), via S.Alberto 163-I, 48123 (Ravenna), Italy (rosa.manrique@unibo.it)

Abstract

Fog oases such as Lomas formation along the Chilean and Peruvian coasts are dependent on water inputs from oceanic fog. Vegetation is characterized by a marked seasonality which is often affected by climatic oscillations. Plant diversity and vegetation patterns are highly variable because of their fragmented spatial distribution. We hypothesize that ENSO could have influenced the spatial distribution of Lomas plant species. In particular we focus on two aspects: 1. The climate variables related to ENSO which likely affect the fog production and 2. The responses of Lomas vegetation to climate patterns during ENSO.

1. Introduction

Fog oases are found between ~6°S and 30°S in the western coasts of South America. The climate is characterized by a long dry period (austral summer) with a short and variable humid period from May to October (austral winter). This climatic pattern determines long periods of seed dormancy and short periods of growth.

Fog oases locally named “lomas” are considered “ecological islands” [6] as they are distributed in a kind of fragments or patchy way with a common climatic factor that is fog [8,21,23]. Although a floristic relationship was found between Peruvian and Chilean lomas due to some species in common [17,29,37] a floristic segmentation has been found [9,20] attributed to the hyper-arid barrier (ca. 18-20°S) between Peru and Chile that could have promoted isolation and limited plant dispersion [31].

EN (El Niño) has been observed to have positive influence in the present composition and productivity of desert flora [7,11,13]. Desert annual plants are strongly related to the rainfall availability [37], which during EN, increase primary productivity [33]. This could support the hypothesis that EN-like conditions in the past might have encouraged a continuous belt of vegetation along the Peruvian and Chilean coasts, but the enlarge of desertification fragmented such continuum [24,38]. We believed that continuous ENSO conditions may affect the lomas vegetation increasing their extension and connectivity, especially in rainy years.

To establish whether ENSO can influence the spatial distribution of lomas plant species we review two main aspects: 1. The climate variables related to ENSO event which likely affect fog production and 2. The responses of Lomas vegetation (composition, productivity, distribution) to climate patterns during ENSO.

2. Anomalies on fog seasonality

Anomalies in the fog season may be related to low-cloud anomalies associated to EN. A negative correlation between the marine Sc (Stratocumulus) amount and the warm SST (Sea Surface Temperature) has been demonstrated in the eastern Pacific [27] while convective clouds increase, especially during the austral summer. Thus, a lesser amount of Sc may reach the coast while precipitation increases.

In fact, Northern Peruvian sites receive more precipitation than southward because highly dominated by ENSO [5] while fog pattern is unknown. It is likely that fog have a negligible effect here during EN. Conversely, Southern Peruvian sites receive more precipitation in the late spring and early summer due to EN while fog and drizzle increase in winter. Northern Chile have similar pattern to south Peru but this changes south of ca. 25°S where the amount of low-clouds is negatively (positively) correlated to EN (LN) [10]. Thus, more cloud

amount in the north is related to EN and in the south with LN (La Niña).

Controversies still exist on fog-water collected during EN. Monitoring data from Chile and Peru lomas have shown more water collected during EN [14, 18]. But, whether is due to the high amount of low-clouds (fog) or more drizzle ("garúas" or "camanchacas") is not clear. The marine Sc region off the coast of Peru seems to be reinforced when unusually cool SST's are present [25]. Also colder SST and warmer air temperatures reinforce the temperature inversion and lead to a more persistent cloud deck and higher fog frequency at 30°S [10]. Thus, during EN years the fog frequency should decrease while during LN should increase. However, highest records of fog and water collection were obtained in both, northern Chile [3] and southern Peru [39] during the exceptional EN 1997-98 that depressed the thermocline in the eastern Pacific by more than 90 m in late 1997 [18] to the mid 1998 when almost instantaneously initiated LN. Apparently, the fog effect on coastal formations is higher during EN when the normal drizzle are intensified and small precipitations (during summer) may cause an impressive blooming of the desert due to the ephemeral plants establishment. Nevertheless, the coastal fog impact should be higher during the winter season when fog reaches its maximum.

3. Biological effects on fog oases

Floristic analysis have put in evidence three main groups [9,17] of lomas: North Peru (PE1, PE2, PE3), South Peru (PE4 to PE8) and Chile (CL9 to CL13). Divergence is likely due to the differences in the taxonomic relatedness between sites originated by isolation and long dry periods during the desert evolution [17] (Fig. 1).

At present, the more water availability triggered by EN (more precipitation in later spring and summer) produces extraordinary changes. During EN 1997-98, the primary productivity of southern Peru lomas reached thirteen times higher productivity (UNSA-PADOVA project report 1999) than the average value, around 1.4 g/m2/day [2,4,35] during the wet season, incrementing plant density and cover [14,21,30,33]. In some cases species that have disappeared for a long period of time reappeared [1]. Flowering and seed production increase [11,22] and so the life cycle and plant distribution following water availability [23,28,34]. More vegetation diversity has been attributed to southern Peru because more water collected from fog [21,26].

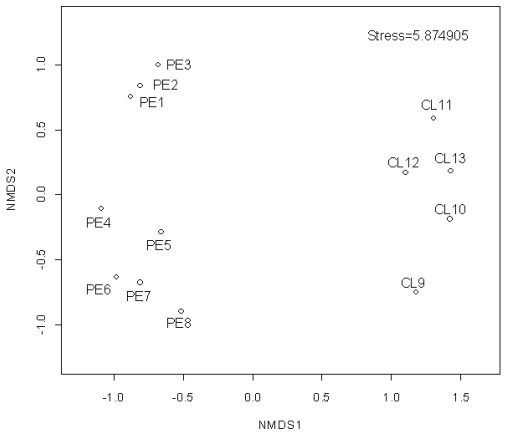

Figure 1: Divergence of lomas plant species composition (PE=Peru, CL=Chile) (from Manrique et al. 2010).

Permanent EN-like conditions in the past (3 Ma.) during the Pliocene [19] may have contributed to establish a fertile belt along the western coast of South America, which may explain the allied species found and the high quantity of endemism. Some studies showed that some species have descended in elevation due to more water availability [12,16].

According to the evidences and besides the desert barrier, it is likely that different precipitation (drizzle and fog) patterns influenced by ENSO periodic pulses may determine plant dispersion and survival of fog oases.

4. Conclusions

Contradictory results have emerged from studies on the low-cloud anomalies and the fog-collection related to EN. EN increase water availability in fog oases when fog should be less frequent due to the reduction of low-cloud amount and Sc. Because of a minor role of fog during EN is expected, especially in summer, it is likely that measurements of fog-water collection during EN are considering both, drizzle and fog at the same time. In turn the reinforced winds in winter, particularly during LN, would increase coastal low-cloud frequency and determine more fog occurrence and more fog-water collection.

Establishing which factor (drizzle or fog) is more significant to the persistence of fog oases is beyond the scope of this paper. However, we believe that the persistence of lomas is linked to both, fog (during winter) and drizzle (during summer), particularly during ENSO. Even though a short-term response in primary productivity is more related to the increase of rainfall, we assume that depending on how intense the effect is on rainfall and fog production, ENSO could modify the dynamics and plant distribution of fog oases.

Present fog-collection records are not temporally long and the latitudinal variability across the coast limits a correct interpretation of particular patterns observed in one specific site. The localized records may not have broad regional extent and may create some contradictions or unclear explanations. We believe that continuous monitoring in different points along the coast will help us to clarify some climatic patterns.

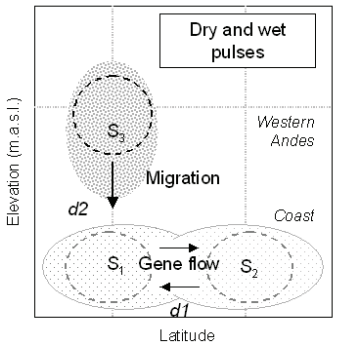

Figure 2: Divergence of lomas vegetation due to water pulses (S=species composition, d=distance). Dashed circles correspond to dry periods.

Plant composition and distribution of lomas or fog oases have changed through time. Based on the allied species found and the higher quantity of endemics, it was hypothesized that fog oases are fragments of a past continuous belt of vegetation. More paleobotanic and paleoclimatic studies are needed to clarify the real role of EN.

Two significant cases of vegetation fog-dependence show us the decline in fog frequency due to climatic anomalies such as ENSO: The Redwood forest (36°N-42°N) in California [15] and the relict forest of Fray Jorge (30°S) in Chile [10]. Thus, we infer that lomas may be influenced by ENSO events in two possible ways: 1) facilitating species migration and gene flow during wetter periods because more species abundance and 2) isolating plant communities particularly during long dry periods increasing genetic divergence (Fig. 2).

Acknowledgements

We thank the PhD program on Environmental Sciences of University of Bologna and the input of the anonymous reviewers which led to improvements in the manuscript.

References

[1] Aguero S. and Suni M. Influencia del evento El Niño 97-98 en el desarrollo de *Ismene amancaes* (Amaryllidaceae, Liliopsidae). Revista Peruana de Biologia, 118-124, 1999

[2] Arias C. and Torres J. Dinámica de la vegetación de las lomas del sur del Perú: estacionalidad y productividad primaria. Caso: Lomas de Atiquipa (Arequipa). Zonas Aridas, (6): 55-76, 1990

[3] Cereceda P. et al. The spatial and temporal variability of fog and its relation to fog oases in the Atacama Desert, Chile. Atmospheric Research, 87: 312–323, 2008

[4] Delgado A. Estimación de la productividad primaria neta en herbáceas de las lomas de Atiquipa (enero-diciembre 2003). Bachelor Thesis. Universidad Nacional de San Agustin, Arequipa, Peru, 2006

[5] Deser C. and Wallace J.M. Large-Scale atmospheric circulation features of warm and cold episodes in the Tropical Pacific. Journal of Climate, 3:1254-1281, 1990

[6] Dillon M.O. et al. The Lomas formations of Costal Peru: Composition and Biogeography History. In: Haas J. and Dillon M.O (eds.) El Niño in Peru: Biology and Culture Over 10,000 Years. Fieldiana, 43: 1-9, 2003

[7] Dillon M.O. and Rundel P.W. The Botanical Response of the Atacama and Peruvian Desert Floras to the 1982-83 El Niño Event. Elsevier Oceanography Series, (52) 487-504, 1990

[8] Dillon M.O. Lomas Formations-Peru. In: Davis S.D., Heywood V.H., Herrera-McBryde O., Villa-Lobos J., and Hamilton A.C. (eds). Centre of Plant Diversity, A Guide and Strategy for their Conservation. WWF Information Press, Oxford. pp: 519-257, 1997

[9] Duncan T. and Dillon M.O. Numerical Analysis of the floristic relationships of the lomas of Peru and Chile. Abstracts of the American Journal of Botanist, 78 (473):183, 1991

[10] Garreaud R. et al. Interannual variability of the coastal fog at Fray Jorge relict forest in semiarid Chile. Journal of Geophysical Research, 113, G04011, doi:10.29/2008JG000709, 2008

11] Gutiérrez J.R. and Meserve P.L. El Niño effects on soil seed bank dynamics in north-central Chile. Oecologia, 134:511-517, 2003

[12] Holmgren C.A. et al. Holocene vegetation history from fossil rodent middens near Arequipa, Peru. Quaternary Research, 56:242-251, 2001

[13] Holmgren M. et al. Extreme climatic events shape arid and semiarid ecosystems. Frontiers in Ecology and Environment, 4:87-95, 2006

[14] Jimenez P. et al. Condiciones Meteorológicas en las lomas de Mejia en el Niño 1997-98 y su influencia en la vegetación. Revista Peruana de Biología, 133-136, 1999

[15] Johnstone J.A. and Dawson T.E. Climatic context and ecological implications of summer fog decline in the coast redwood region. PNAS, 107(10):4533-4538, 2010

[16] Latorre C. et al. Vegetation invasions into absolute desert: A 45 000 yr rodent midden record from the Calama–Salar de Atacama basins, northern Chile (lat 22°–24°S). GSA Bulletin, 114(3):349-366, 2002

[17] Manrique R. et al. Taxonomic diversity in the western belt of Peruvian and Chilean coasts. PhD students meeting in Ecology. Università Politecnica delle Marche, February 24-26 Ancona, Italy, 2010

[18] McPhaden M.J. Genesis and Evolution of the 1997-98 El Niño. Science, 283:950-954, 1999

[19] Molnar P and Cane MA. Early Pliocene (pre-Ice age) El Niño-like global climate: Which El Niño? Geosphere, 3(5):337-365. 2007

[20] Müller G.K. Floristic Analysis of the Peruvian Loma-Vegetation. Flora, 176:153-165, 1985

[21] Muñoz-Schick M. et al. Fog oases during the El Niño Southern Oscillation 1997-1998, in the coastal hills south of Iquique, Tarapacá region, Chile. Rev. Chil. His. Nat. 74(2):389-405, 2001

[22] Ohga N. Buried seed population in the herbaceous lomas on Loma Ancon in the coastal desert of central Peru. Ecological Research, 7:341-353, 1992

[23] Oka S. and Ogawa H. The distribution of lomas vegetation and its climatic environments along the Pacific coast of Peru. Tokyo. In: Geographical Reports. Tokyo Metropolitane University, 19:113-124, 1984

[24] Ono M. Definition, classification and taxonomic significance of the lomas vegetation. In: Taxonomic and ecological studies on the Lomas vegetation in the Pacific Coast of Peru. Makino Herbarium, Tokyo Metropolitan University, 1986

[25] Oreopoulos L. and Davies R. Statistical dependence of albedo and cloud cover on sea surface for two tropical marine stratocumulus regions. Journal of Climate, 6:2432-2447, 1993

[26] Osses P. et al. Differences et similitudes du brouillard entre Iquique (Chili) et Mejia (Perou). Rev. Geografia Norte Grande, 25:7-13, 1998

[27] Park S. and Leovy C.B. Marine Low-Cloud anomalies associated with ENSO. Journal of Climate, 17(17):3448-3468, 2004

[28] Péfaur J.E. Dynamics of plant communities in the Lomas of southern Peru. Vegetatio, 49:163-171, 1982

[29] Pinto R. and Luebert F. Data on the vascular flora of the coastal desert of Arica and Tarapaca, Chile, and its phytogeographical relationships with southern Peru. Gayana Bot. 66(1):28-49, 2009

[30] Pinto R. et al. Monitoring fog-vegetation communities at fog-site in Alto Patache, South of Iquique, Northern Chile, during "El Niño" and "La Niña" events (1997-2000). Second Conference on fog and fog collection, Canada, 293-296, 2001

[31] Rundel P.W. et al. The phytogeography and ecology of the coastal Atacama and Peruvian Deserts. Aliso, 13:1-50, 1991

[32] Sotomayor D.A. and P. Jiménez. Meteorological conditions and vegetal dynamics of the Atiquipa Lomas (Caravelí-Arequipa) coastal ecosystem in the South of Peru. Ecología Aplicada, 7(1,2):1-8, 2008

[33] Squeo F.A. et al. ENSO effects on primary productivity in Southern Atacama desert. Advances in Geosciences, 6:273-277, 2006

[34] Thompson M.V. et al. Multi-annual climate in Parque Nacional Pan de Azúcar, Atacama Desert, Chile. Rev. Chil. His. Nat. 76: 235-254, 2003

[35] Torres J. and C. López. Productividad primaria neta y sus factores ecológicos en lomas de la costa central del Perú (1977-1979). Zonas Aridas, 1982

[36] Tu T. et al. Phylogeny of Nolana (Solanaceae) of the Atacama and Peruvian deserts inferred from sequences of four plastid markers and the nuclear LEAFY second intron. Molecular Phylogenetics and Evolution, 49:561-573, 2008

[37] Vidiella P. et al. Vegetation changes and sequential flowering after rain in the southern Atacama Desert. Journal of Arid Environments. 43:449-458, 1999

[38] Villagrán C. and Hinojosa L.F. Esquema biogeográfico de Chile. 33:551-577. In: Regionalización Biogeográfica en Iberoámeríca y Tópicos Afines, Jorge Llorente Bousquets and Juan J. Morrone, eds.) Universidad Nacional Autónoma De México, 577 pp., 2005

[39] Villegas L. et al. Evaluation of fog moisture absorption, in Lomas of Atiquipa (Arequipa – Peru) from 2002 to 2006. Fourth International Conference on fog, fog collection and dew. La Serena, July 22-27, Chile, 2007

5th International Conference on Fog, Fog Collection and Dew
Münster, Germany, 25–30 July 2010
FOGDEW2010-76

Experiments on fog prediction based on multi-models

Chune Shi, Lei Wang, Hao Zhang, Xueliang Deng

Chun.e.shi@gmail.com

Anhui Institute of Meteorological Sciences, Hefei, 230031, P. R. China

1. Abstract

A 1-D fog model (PAFOG) is coupled to MM5. MM5 provided the initial and boundary conditions (IC/BC) and some other necessary input parameters for PAFOG. Thus, we can run PAFOG for any interested area. Then, nine fog events observed in Nanjing during the winters of 2006 and 2007 are simulated by the two models. General performances of the two models for the nine fog cases are presented. The results of MM5 and PAFOG for two cases are verified against the field observations in detail. PAFOG outperformed MM5 in simulating radiation fog; however, MM5 performed better than PAFOG in simulating advection fog. The coupling method still needs improvements. The impacts of advection on fog should also be included in the 1-D model.

2. Introduction

The low visibility on fog days usually endangers all kinds of transportation and causes huge economic losses. Therefore, it brought more and more attentions of meteorologists in the world.

Although the numerical weather prediction (NWP) has been improved evidently with the development of computer technology, fog is still not a direct model product by any current NWP models (Zhou and Du 2010). Gultepe et al (2007) summarized the achievements on fog researches during the past several decades and pointed out that the future direction to study and forecast fog would be utilizing both 3D regional model and 1-D fog model.

Since neither 3D NWP nor 1D fog model is perfect for fog prediction currently, the objectives of this paper are: 1) to carry out experiments on fog prediction based on multi-models, a meso-scale model and a 1-D fog model; 2) To investigate whether the model profiles can be used to run the 1D fog model.

3. Study region and observational data

The region of interest covers provinces in eastern China, including Anhui, Jiangsu, Shandong, Henan, Hubei, Jiangxi, Zhejiang and Shanghai (See Fig 1 in Shi et al, 2009). Among those provinces, Anhui, Jiangsu and Zhejiang have higher fog occurrence frequencies, exceeding 20 day/year in most areas and even over 60 day/year for some areas (Liu et al, 2006). Usually, October to April are months with highest fog occurrence frequencies, especially in December and January (Zhou et al, 2007). By statistics on routine data of Anhui province during the past half century, Shi et al (2008) found that the maximum fog occurring time is 05 to 08 LST in the morning.

Around 800 routine meteorological stations, including 3-h ground level observations, in CMA (Chinese meteorology Agency) network were selected in this study. At the same time, profiles of temperature, humidity, wind and pressure from a sounding station in Nanjing (118.8°E, 32.0°N) were also used. In addition, field observations of fog were conducted by the Nanjing University of Information Science and Technology (NUIST) on NUIST campus (118.72°E,32.21°N) in northern suburb of Nanjing during the winters of 2006-2008 (Pu et al, 2008). Abundant data have been accumulated, based on which a series of scientific papers were published (Yang et al 2009).

Based on the routine visibility data, we analyzed the visibility distributions at 08 LST on fog days (Yang et al 2009). It was found that the fogs observed in Nanjing are not isolated. Almost all fog cases are parts of regional fog events. The regional characteristics of these fogs have been studied and identified (Zhou et al 2007).

4. Models and coupling method

Two models, MM5 and a one-dimensional fog model (PAFOG) are used in this study.

4.1 MM5 and configurations

MM5 and its configurations are mainly the same as those used in Shi et al (2009), except that different first-guess fields and boundary conditions are used here. In this paper, first-guess fields and boundary conditions for the coarse domain for every 6 hours were obtained from NCEP FNL (1°×1°). The simulations began at 08LST before the fog event day to 20 LST of the fog day, 36 h in total.

4.2 PAFOG

The 1-D model PAFOG (Bott et al,) was derived from the detailed spectral microphysical model MIFOG (Bott and Trautmann, 1990). The PAFOG was once used by Muller et al (2007) to set up an ensemble fog forecast system. The grid of our PAFOG model domain is divided into two subregions like Bott and Trautmann (2002). The simulations started at 20LST before the fog event day to 20 LST of the fog day, 24 h in total.

4.3 Coupling method between MM5 and PAFOG

To run PAFOG, we need to provide the initial temperature, humid, pressure in the PBL, geostrophic wind and soil data, etc. In this paper, we use MM5 output to provide the necessary input data for PAFOG, including the initial and boundary conditions (IC/BC), the high, medium and low cloud covers, and so on, so that, PAFOG can be run for any area of interest.

5. General descriptions of model performances on fog events in Nanjing

During the winters of 2006 and 2007, nine fog events were captured on the NUIST campus by the NUIST fog research group (Yang et al, 2009). Utilizing MM5, PAFOG and the above coupling method, simulations were conducted for the nine fog events in this study.

Table 1 compares simulated fog duration with measurements on NUIST campus. As for NUIST, if we use the LWC-only criterion, LWC>0.01g/kg, to decide fog production, MM5 reproduced 7 out of 9 Nanjing fog events successfully, although the simulated fog dissipated earlier than the observed fog. However, if we looked at the MM5 output for the two failed cases carefully, we found that MM5 produced relative humidity (RH) reached 100% at the lowest model layer (See Fig.1, 3, 4). If we use RH>98% as another criterion for

fog production like Yang et al(2010), MM5 succeeded in reproducing all fog cases in Nanjing.

As for the situations in the model domain, the distributions of LWC and RH at 08LST are compared to the corresponding observed visibility distributions (See Fig.1 and 3). If the LWC-only criterion is used, the MM5 simulated fog regions are generally smaller than the observed fog area. MM5 performs well for those advection-radiation fog cases, e.g. fog events during December 25-27, 2006 and December 20-21, 2007. Although there are still false alarm and missing forecast in those cases, MM5 basically reproduced the major part of the fogs. For those fog cases mainly resulted by radiation cooling, the simulated fog regions are generally smaller than the observations, and the simulated fog area do not match the observations well in some cases. However, if we also use the criterion of RH (>98%), then the simulated fog regions cover the observed ones for all cases, even larger. It is easy to deduct that if we use some restrictive conditions, e.g., wind speed, cloud bottom like Zhou et al (2010), the false alarm area will be reduced.

Due to the availability of field observations, PAFOG was only used for NUIST by now. The results of PAFOG were evaluated using the measurements from the field observations, including LWC, visibility, etc. Generally, PAFOG captured almost all fog events, even for the advection-radiation fog on December 25, 2006. For the two cases on December 25-27, 2006 and December 14, 2007, for which we have the field measurements at hand, the simulated fog depths are shallower than the measurements.

In conclusion, MM5 performs better for the advection-radiation fog than for radiation fog; while PAFOG performs better for radiation fog.

6. Evaluations of model performances for two typical fog events

Considering the availability of data, the simulations of two fog cases were compared with the field observations in detail. The two fog cases are the advection-radiation fog occurring on December 25-27, 2006 and the radiation fog occurring on December 14, 2007.

6.1 The advection-radiation fog on December 25-27

An unusually dense regional advection-radiation fog event occurred in eastern China during Dec. 25-27, 2006. It reduced visibility to 100 m or less in much of Anhui, Henan, and Jiangsu provinces, even zero meters in Nanjing, the provincial capital of Jiangsu province, lasting more than 36 hours in some places (Shi et al, 2009).

Fig. 1 shows the distributions of simulated RH and LWC at the lowest model layer and the observed visibility at 08LST on Dec 25. Comparing Fig. 1a with Fig.1b, c, it can be seen that MM5 caught the major part of the dense fog if only LWC was considered; However, if RH>98% was used, the simulated fog area covers all observed fog area with some false alarm.

Fig. 2 presents the variations of simulated and measured ground-level LWC and visibility. It can be seen that MM5 caught the trend of LWC well, especially on Dec 25 and 26, with a correlation coefficient of 0.6. Affected by low clouds by MM5, PAFOG produced lower liquid water on Dec 25; however, the PAFOG produced LWC was consistent with that of MM5 (r=0.74). Also, PAFOG over-estimated the ground-level LWC on Dec 27, like MM5. Although the MM5 simulated fog did not consecutive, it did catch the major fog episodes. PAFOG produced much lower fog water on Dec 25, while its visibilities closely related with the measured ones (r=0.73) on Dec 26-27, although large differences were noted for some times. This might be related to the model spin-up, especially under the situations that fog already existed at the simulation beginning time (Muller et al 2007).

In a word, from the comparisons of ground-level LWC and visibility with measurements, MM5 outperforms PAFOG in this case. The performance of PAFOG depends on the IC/BC provided by MM5.

6.2 The radiation fog on Dec 24, 2007

A strong dense fog event was recorded in Nanjing on Dec 14, 2007. It lasted about 14 hours, with a maximum height of 600 m. The fog was first formed through radiation cooling in the ground-level, and then followed by a cloud layer caused by low-level cold advection (Yang et al, 2010).

Fig. 3 shows the distributions of simulated RH and LWC at the lowest model layer and the observed visibility at 08LST on Dec 14. Comparing Fig. 3a and Fig.3c, it can be seen that MM5 failed to catch the major part of the dense fog, which was located in Anhui and Hubei, if only LWC was considered; However, if RH>98% was used, the simulated fog area covers all observed fog area with some false alarm.

Fig. 4 presents the variations of PAFOG simulated and measured ground-level LWC and visibility, and MM5 simulated ground-level RH. Although MM5 did not produce LWC in Nanjing, it did forecast saturated RH. The MM5 predicted RH steady with 100% from 00LST to 08LST on Dec 14. Therefore, we can say that MM5 also has some capability on this case. Due to the rapid radiation cooling by clear sky, PAFOG produced fog water soon after its startup. The PAFOG simulated LWC reached maximum at about 06 LST. In observations, although high humidity (RH>98%) and low visibility (V<km) were observed quite early (around 21LST on Dec 13) (Fig. 4b), evident liquid water was not measured until 05LST, Dec 14. It is worth noting that both the simulated and observed times with maximum LWC and fog dissipation are quite consistent. Considering the fact that the concentrations of manmade aerosol, especially the hygroscopic aerosol like sulfate, are high in most China, the hygroscopic increase in aerosol size decreases the visibility to under 1km even without liquid water. For example, the observed visibility changed from fog (V<1km) to dense fog (V<500m) from 22LST, Dec 13 to 05LST, Dec14, while the measurable liquid water (0.01g/kg) appeared until 06LST on Dec 14 (Fig 4a). In Fig.4b, due to the earlier formation of liquid water, the simulated visibilities were lower than observations in the initial stage (before 06LST), in the late stage (after 10LST) , the simulated liquid water disappeared and simulated visibilities increased to over 1km soon, while the observed visibilities increased slower than simulation. However, the variation trends were quite consistent with a correlation coefficient of 0.82. Accordingly, we think that PAFOG predicted the formation and dissipation of this radiation fog successfully.

7. Summary and Conclusions

MM5 and a 1-D model (PAFOG) were coupled and used to simulate nine fog events in Nanjing. Through verifications of simulated high RH or LWC area against observed low visibility area, the simulated hourly LWC and visibilities against the measurements in the field observations in NUIST, the performances of MM5 and PAFOG on fog predictability were evaluated. The results show that both models can reproduce most fog events; MM5 performs better for advection-radiation fog than for radiation fog, while PAFOG performs better for radiation fog than for advection-radiation fog; coupling between two models does work in most cases; Cloud cover is a key factor for fog production in the 1D fog model; The LWC-only method by NWP is not enough, both liquid water content and relative humidity should be considered to diagnose fog occurrence. The coupling method still needs improvements.

Acknowledgement

This work was supported by funds from the National Natural Science Foundation of China (40775010)，Project of New Technology Application of China Meteorology Agency (CMATG2010M16) and the Special Funds for Public Welfare of China （Grant No. GYHY200906012）.

References

Bott, A., Sievers, U., Zdunkowski, W., 1990: A radiation fog model with a detailed treatment of the interaction between radiative transfer and fog microphysics. J. Atmos. Sci. 47(18), 2153-2166.

Bott, A.,Trautmann T, 2002. PAFOG-a new efficient forecast model of radiation fog and low-level stratiform clouds. Atmospheric Research,64,191-203

Gultepe I., R. Tardif, S. C. Michaelides,et al, 2007: Fog Research: A Review of Past Achievements and Future Perspectives. Pure and Applied Geophysics 164, 1420-9136.

Liu X, H. Zhang, Q. Li, et al., 2005: Preliminary research on the climatic characteristics and change of fog in China. Journal of Applied Meteorological Sciences (in Chinese) 16(2),220-271.

Muller M D, C Schmutz and E Parlow, 2007: A one-dimensional Ensemble Forecast and Assimilation System for Fog Prediction. Pure and Applied Geophysics, 164,1241-1264

Shi, C., Roth, M., Zhang, H., Li, Z., 2008:Impacts of urbanization on long-term fog variation in Anhui Province, China. Atmos. Environ. 42, 8484-8492

Shi C., J.Yang, M. Qiu, et al, 2009: Analysis of an extremely dense regional fog event in Eastern China using a mesoscale model. Atmospheric Research, 95(4), 428-440

Yang J, Y Xie,C Shi et al, 2009: Differences in lonconpositions of winter fog water between radiation and advection-radiation fog episodes in Nanjing. Transactions of Atmospheric Sciences, 32,776-782

Yang J, L. Wang, D Liu. 2010: Boundary layer structure and evolution mechanisms of a deep dense fog. Acta Meteorologica Sinica (in Chinese), in press

Zhou B., Du, J., 2010: Fog prediction from a multi-model mesoscale ensemble prediction system. Wea. Forecasting, 25, 303-322

Zhou, Z., Zhu, Y., Ju, X., 2007 : Dense fog events in the Yangtze Delta and their climatic characteristics. Progress in Natural Science 17(1), 66-71.

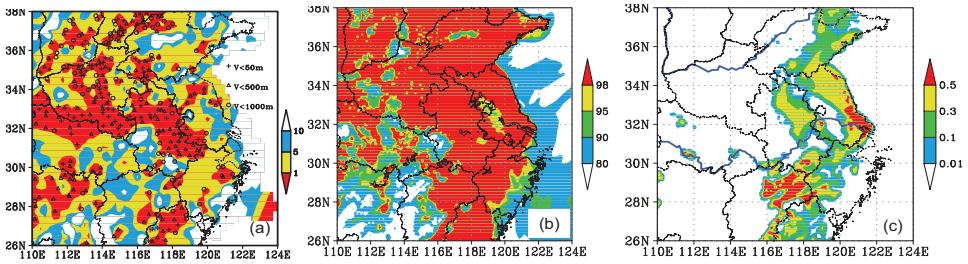

Fig. 1 Distributions of measured visibilities (a), simulated RH (b), and simulated LWC (c) by MM5 at 08LST on Dec 25, 2006

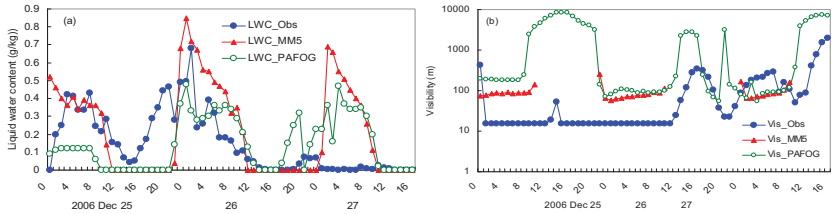

Fig. 2 Variations of simulated and observed LWC (g kg^{-1}) and visibility (m) on the NUIST campus on Dec 25-27,2006

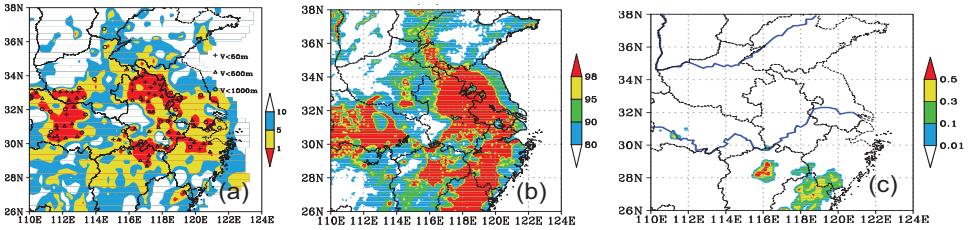

Fig.3 Distributions of measured visibilities (a), simulated RH (b), and simulated LWC (c) by MM5 at 08LST on Dec 14, 2007

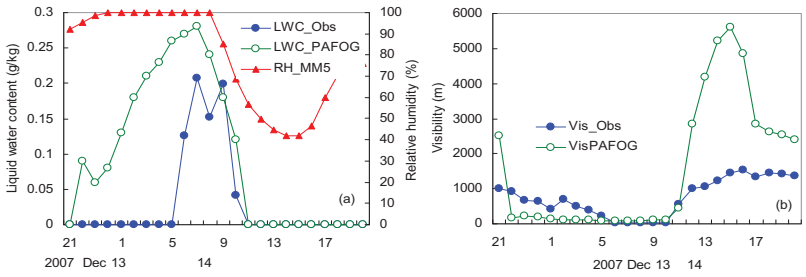

Fig.4 Variations of simulated and observed LWC (g kg^{-1}) (a)and visibility (m) (b)on the NUIST campus on Dec 14,2007

Table 1 General descriptions model performances for Nanjing fog events

Day	Observation (h)	MM5 (h)	PAFOG V<1km	PAFOG CLW>0.01g/kg
12/12,2006	11T23-12T11	***No CLW*** 11T23-12T08	11T22-12T13	11T22-12T12
12/14,2006	13T23-14T12	14T02-09	13T22-14T11	13T22-14T11
*12/25-27, 2006	24T22-27T14	24T22-25T10 25T19-26T11 26T19-27T10	24T22-25T08 25T22-26T12 26T17-27T10	24T22-25T08 25T22-26T12 26T17-27T10
12/14,2007	13T23-14T11	***No CLW*** 13T23-14T08	13T22-14T11	13T22-14T10
12/18,2007	18T03-18T11	17T21-18T09	17T22-18T20	17T23-18T20
12/19,2007	18T16-19T12	18T23-19T08	18T22-19T12	18T22-19T12
12/20,2007	19T17-20T16	20T00-20T10	19T21-20T11	***No CLW***
*12/21,2007	20T18-21T19	20T21-21T20	20T22-21T07	***21T01-21T03***
12/23,2007	23T01-23T05	22T22-23T10	22T22-23T11	22T22-23T11

*: advection-radiation fog

5th International Conference on Fog, Fog Collection and Dew
Münster, Germany, 25–30 July 2010
FOGDEW2010-77

The relation between moisture and liquid water content in fog - an experimental approach

S. Gonser (1), F. Griessbaum (1), S.-C. Chang (2), H.-S. Chu (2), Y.-J. Hsia (2), and O. Klemm (1)

(1) Institute of Landscape Ecology, University of Muenster, 48149 Muenster, Germany, (stefan.gonser@uni-muenster.de), (2) Institute of Natural Resources, National Dong Hwa University, 974 Hualien, Taiwan

In July 2009, microphysical measurements of orographic fog were performed above a montane cloud forest in north eastern Taiwan (Chilan mountain site). At this location, orographic fog appears almost every day. The goal of this work was to study the short term variations of the droplet size distribution (DSD), temperature, and relative humidity (RH), with a temporal resolution of 3 Hz. The relative humidity was calculated from precise temperature readings and absolute humidity (AH) measurements, recorded by a temperature sensor with an accuracy of 0.002°C (Model TR-1050, RBR Ltd.) and an infrared gas analyzer (Model Li-7500, LI-COR Biosciences), respectively. DSD's were measured by an optical droplet spectrometer (Model FM100, Droplet Measurement Technologies). It provides droplet spectra between 2 and 50 μm diameter. The liquid water content (LWC) of the fog was deduced from the measured DSD's.

Data showed that orographic fog is composed of various air parcels of different size, RH and DSD. Three general types of fog parcels have been identified via the recorded DSD's. DSD-type 1 is characterized by narrow spectra with maximum concentrations in the smallest size class and a continuous decrease towards greater diameters, DSD-type 2 represents slightly broader spectra with a plateau or second peak around 10 μm, and DSD-type 3 exhibits broad spectra with the droplet number concentrations peaking around 15 μm diameter. The appearance of the three different DSD-types is strongly related to RH and the general evolutional state of the fog. At the onset of a fog event, DSD's are largely dominated by small droplets (DSD-type 1). Later on the spectra tend to become broader, RH shows relative low values, and DSD-type 3 is dominating the DSD's. A statistical analysis of the characteristics of these parcels was performed and yielded large variability in persistence, RH, and LWC. DSD-type 2 showed the shortest durations and can, therefore, be regarded as a transitional state between the other two DSD-types.
Further, the 3 Hz data revealed an inverse relation between RH and LWC. In principle, this finding can be explained by the diffusional growth theory for droplets containing soluble or insoluble materials. Droplets with greater diameters are able to exist at lower ambient RH's than smaller droplets. If, on the other hand, the large observed variabilities of both LWC and RH can be explained through these considerations, remains unclear so far. Likely, local disequilibrium between the fog droplets and the bulk gas phase during turbulent transport is a cause for the observed effects. More analyses including fog droplet chemistry and dynamic microphysical modeling are required to further analyze these findings. To our knowledge, this is the first experimental field observation of the anti-correlation between RH and LWC in fog.

5th International Conference on Fog, Fog Collection and Dew
Münster, Germany, 25–30 July 2010
FOGDEW2010-78

iPort-VIS: Site Specific Fog Forecasting for Munich Airport

M. Rohn (1), G. Vogel (1), B.R. Beckmann (1), P.R hner (1) Ch. Thoma (2), W. Schneider (2), A. Bott (2)
(1) Deutscher Wetterdienst, Germany, (2) University of Bonn, Germany

Abstract

The German Weather Service (DWD) together with University at Bonn attempts to implement a site specific fog forecasting system at Munich International Airport. The presentation provides an overview of the project and links to other presentations during this conference which focus on the instrumental setup at the airport as well as the scientific aspects of the PAFOG model development. The integration of all components within DWD is outlined including technical aspects necessary to ensure a stable prototype for evaluation at the end of the project.

1. Introduction

The German ministry for economy and technology is instigating improved effectiveness and competitiveness of the German aviation industry by funding an aviation research program. This supports among other activities forecasting techniques for various weather related phenomena affecting airport management and traffic including poor visibility. DWD in cooperation with University Bonn and the German Aviation Control (DFS) is implementing a site specific fog forecasting system for Munich International Airport. The planned system aims at coupling the one-dimensional version of the fog forecasting model PAFOG with the high-resolution model COSMO-DE of DWD. Following experiences of other institutes on fog forecasting [1] local observations will be integrated using a nudging approach in order to integrate local observations during the model run. Therefore, additional instruments will be installed close to the runways to provide an observational data base for both model initialization and model diagnostics.

2. The fog forecast model PAFOG

The fog forecast model PAFOG has been developed during recent years. Beside many scientific details, one technical requirement was the implementation of a fast model which, ideally, could be integrated within a meteorological workstation enabling aviation forecasters to perform sensitivity studies as part of the routine forecast work by manually varying the initial conditions. This resulted in a parameterization of the cloud microphysics as described in detail by Bott and Trautman in [2]. As part of the present project, the previously pure scientific model has been migrated to DWD software standards as being used with the COSMO consortium. The radiation module has been substantially upgraded. Since the model has to rely on assumptions of aerosol particle concentrations one modification tries to estimate aerosol concentration using observed visibility. These modifications for initialization with visibility measurements under fog and non-fog conditions are expected to be of particular use on airports where visibility measurements are taken on a regular basis. Finally, the most important extension to the previous PAFOG version is the introduction of nudging terms within the prognostic equations in order to perform a nudging with measured temperature and humidity profiles above the ground and close to the surface.

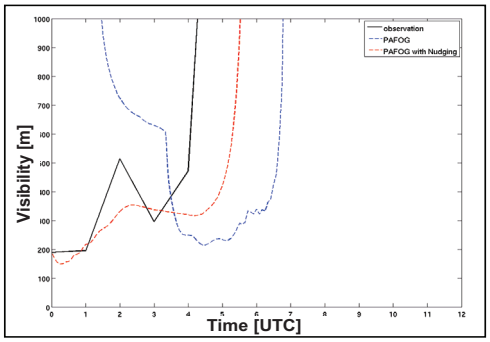

Figure 1: PAFOG case study for September 14, 2005 initialized at 00 UTC.

First trials using both visibility measurements under fog conditions and temperature and humidity measurements from the 98 m tower at the DWD Lindenberg Meteorological Observatory show the systems potential. Figure 1 shows a case study for September 14, 2005 – 00 UTC. The blue curve depicts the surface visibility forecasted by PAFOG without nudging. PAFOG together with nudging of the measured temperature and humidity profile from the 98m tower at the Lindenberg site results in an improved representation of the surface visibility (red line). The observed visibility (automatic measurement) is indicated by the black line. The details of the scientific model development are described in more detail by Thoma during this conference [4].

3. Instrumentation at the airport

A further challenge of this project is to provide the measurements on the airport site. Various discussions with both meteorological and technical experts took already place during the initialization of the project.

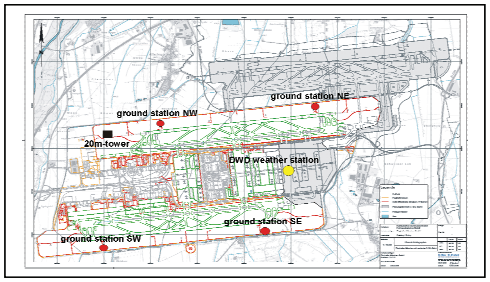

Figure 2: Overview of the instrumentation locations at Munich Airport.

The required instrumentation needed to be specified in great detail prior to the actual procurement of all components of the measuring system. The instruments are currently being installed at their designated locations on the airport. Soil profile measurements are taken at the official wind measurement poles close to the heads of the two runways. Radiation measurements are done on the routine observation field of the DWD observation network. Instruments for temperature, humidity, and wind observations above ground are mounted at an existing 20m tower being installed during the project RegioExakt as part of the "KlimaZwei initiative of the Federal Ministry of Education and Research [5].

The details on all aspects of the instrumentation are outlined by R hner during this conference [3].

4. Application aspects

The final goal of the project is to provide a prototype which can be evaluated in respect of its potential benefit within the forecasting routine at the airport. Therefore, the application aspects have to be addressed at an early stage. The planned evaluation strategy is based on a field campaign towards the end of the project in autumn/winter 2011/2012. In order to enable the potential stakeholders to assess the value of the system within a routine environment, regular information exchange with both, aviation forecasters and air traffic controllers, with focus on the visualization of the final forecast product is a key issue.

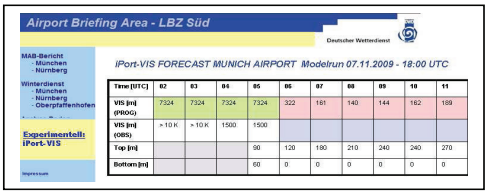

Figure 3: Presentation of visibility forecast with the meteorology briefing system at DWD.

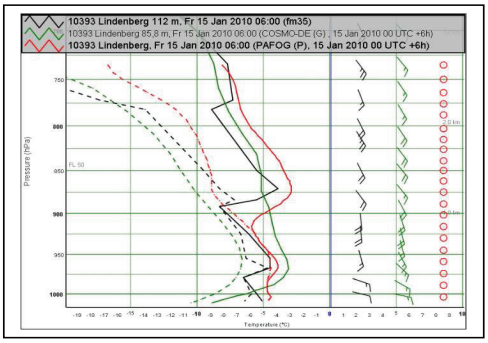

Figure 4: Visualization of prognostic temperature and dew point profile from PAFOG for a t+6h time step together with the observed radiosonde profile. The COSMO-DE profile is marked by Green, PAFOG in Red, and the observed sounding in Black.

One option is to provide very condensed information in a tabular form with a browser based information system of the DWD aviation meteorology office at

the airport as shown in Figure 3. In order to provide a more detailed insight, the forecasted vertical profile could, for example, being visualized by the DWD meteorological workstation NinJo (Figure 4).

5. Technical integration at DWD

Finally, all aspects of the development need to be integrated within the DWD infrastructure in order to meet the necessary quality management standards.

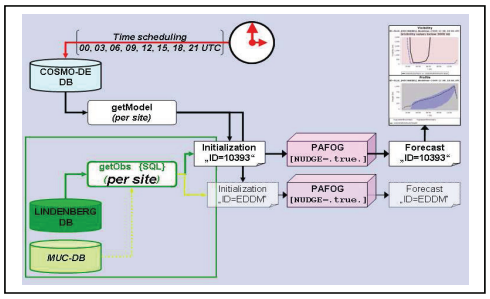

Figure 5: iPort-VIS workbench as framework to integrate all technical aspects of the visibility forecasting system.

This covers aspects such as software configuration management, the operationally used interface to the model data as well as the observational data base. Therefore, it is attempted to provide all measurements from the airport site via a relational data base as it is being used for measurements of the Lindenberg Meteorological Observatory of DWD. Since the system is developed on the base of measurements from the observatory the project follows a similar data flow in order to reduce the technical adaptation necessary to transfer the system from the Lindenberg site to the airport location and its instrumentation. Currently, a stable test system is running based on a regular initialization with each newly available COSMO-DE model run (update every 3h). From Lindenberg observed soil profiles for initialization and atmospheric temperature and humidity profiles from the 98m tower for four consecutive hours of nudging are integrated. An overview of the test system is illustrated in Figure 5.

6. Summary and Conclusions

The project “LuFo iPort-VIS focuses on the implementation of a site specific visibility forecast module based on the 1D fog forecasting model PAFOG and additional measurements. The 1D fog model PAFOG has been extended in order to integrate temperature and humidity observations by a nudging technique. In parallel to the scientific extension of PAFOG, the required instrumentation is currently being installed on the airport. In order to test the model and perform diagnostics before the installations are completed, the model is currently applied to the location of the Lindenberg Meteorological Observatory of DWD which provides an optimum data base for model initialization and verification. The project will be concluded by a field campaign which aims at deciding on the usefulness of the entire system for operational aviation forecast and air traffic management in the vicinity of the terminal area.

Acknowledgements

The project is funded by the Federal Ministry of Economics and Technology (BMWi/LUFO-20V0801C). The work is performed in cooperation with Deutsche Flugsicherungs GmbH (DFS) and Flughafen München GmbH (FMG). The cooperation of the RegioExakt partners and particularly the support by Dr. Nikolai Dotzek (DLR) for the use of the existing measuring tower is highly acknowledged.

References

[1] Bergot, T., Carrer, D., Noilhan, J., and Bougeault, P.: Improved Site-Specific Numerical Prediction of Fog and Low Clouds: A Feasibility Study, Weather and Forecasting, Vol. 20, pp. 627 – 646, 2005.

[2] Bott, A., Trautmann, T.: PAFOG – A new efficient forecast model of radiation fog and low-level stratiform clouds, Atmospheric Research, Vol. 64, pp. 191-203, 2002.

[3] R hner, P., Beckmann, B.-R., Rohn, M., Thoma, Ch., and Bott, A.: Development of a low visibility forecast tool for Munich Airport, 5th International Conference on Fog, Fog Collection and Dew, FOGDEW2010-65, 2010.

[4] Thoma, Ch., Schneider, W., Rohn, M., R hner, P., Beckmann, B.-R., Masbou, M., Bott, A.: Development of the one dimensional Fog Model PAFOG for operational Use at Munich Airport, 5th International Conference on Fog, Fog Collection and Dew, FOGDEW2010-94, 2010.

[5] Mahammadzadeh , M., Biebeler, H., Bardt, H.: Klimaschutz und Anpassung an die Klimafolgen, Strategien, Maßnahmen und Anwendungsbeispiele, ISBN 978-3-602-14847-9 , 310 p., 2009.

5th International Conference on Fog, Fog Collection and Dew
Münster, Germany, 25–30 July 2010
FOGDEW2010-79

Fog Water Systems in South Africa: An Update.

J Van Heerden (1), J. Olivier (2), L. Van Schalkwyk (3,4)

(1) Dept. of Geography, Geoinformatics and Meteorology, University of Pretoria, South Africa (jvhplett@mweb.co.za), (2) Dept. of Environmental Science, UNISA, (3) Dept. of Geography, Geoinformatics and Meteorology, University of Pretoria, South Africa, (4) South African Weather Service

This paper reports on fog water harvesting in South Africa. Ten semi-operational fog water catchment systems were erected at rural schools in South Africa between 1999 and 2007. These systems copied the basic design features of the systems at El Tofo, Chili, modified for South African conditions. Major problems were experienced due to poor maintenance and vandalism. Another serious problem was the abrasion of the 40% shade cloth netting against the supporting cables. Gale force winds also led to the complete failure and collapse of the systems. It thus became obvious that the simple flat screen structure is not suitable for South African conditions.

Co-operation with Mesh Concepts cc and Cloud Water Concepts cc resulted in the development of a new design for fog/cloud water collection. This design comprises three 40 m2 panels joined together to form the sides of an equilateral triangle. Four such triangles are linked together to form a 9 panel system. The six 6 m poles supporting the 9 panels are 11 m apart and all structure and net support cables are anchored, in line, with the sides of the panels. The system is 5.5 m high and the 9 panel system exposes 360m2 to the cloud/fog. The system is stable and wind forces are transferred to the anchors via nylon pulleys housed in brackets bolted to the poles. The mesh material is a poly yarn co-knitted with stainless steel that provides strength and stability to the mesh. An added advantage is that several 9 panel systems can be linked and expanded to cover the available space.

There are currently three such systems in place - at Brook's Nek (1650 m MSL) in the mountains of the Eastern Cape (684 m2) and at Lamberts Bay and Doring Bay (both 360 m2) on the West Coast. An experimental 3-panel system has been established on the Zondachsberg (1142m MSL), 35 km north of Plettenberg Bay. Preliminary data from this site indicate that orographic cloud forms against the mountain side soon after the wind turns to the south. Average yields of 3 lm-2day-1 were obtained during the worst drought in the last 135 years.

5th International Conference on Fog, Fog Collection and Dew
Münster, Germany, 25–30 July 2010
FOGDEW2010-80

THE COMBINED FOG MONITORING SYSTEM OF ARPAV OVER THE VENETO REGION, PO VALLEY – ITALY

F. Domenichini, A. Rossa, F. Zardini, M. Monai, M. Calza, A. Della Valle, V. Gaspari.
ARPAV – Meteorological Centre of Teolo, Veneto Region Italy (fdomenichini@arpa.veneto.it)

1. INTRODUCTION

The presence of fog is a frequent problem in the Po Valley. The consequent reduction in visibility has a strong impact on the road, air, ship and railway traffic. Both, fog monitoring and forecasting, constitute significant challenges, not least due to the high spatial and temporal variability of the phenomenon. In the last 10 years new opportunities were given by the *Meteosat Second Generation* satellite (*www.eumetsat.int*) and by the availability of different methods for the monitoring of visibility (visibility sensors, webcam).
The monitoring systems, from the ground as from the sky, present different values and problems; a system that can take advantage from the values of different methods, merging the information, would provide a more complete estimation on visibility reduction.
The many issues of the COST 722 'Short-range forecasting methods of fog, visibility and low clouds', has given some important starting ideas for the realization of the work presented in this paper (*COST 722 Reports: 2005 and Final Reports*).
The impact of fog conditions is important in general, and for Italy represents about a 0.5-1.5% of the total road accidents. In the Veneto Region only, the economic loss (total social cost) due to road accidents in low visibility conditions is close to 35 millions of euro per year (*Italian Central Institute of Statistics, Automobile Club Italia*). ARPAV, the Regional Agency for Environmental Prevention and Protection of Veneto, is the regional meteorological service of the north-eastern Italian region Veneto and, as such, is responsible for meteorological support to institutional and private users. Since real-time visibility information over an extended area would represent an interesting product for road and transport safety, ARPAV, in the framework of the FP7 project ROADIDEA*, on road safety and traffic control, proposed and developed the system described in the present paper, as a pilot system for the fog monitoring. (*ROADIDEA Project involves 14 partners from 8 countries, it started on December 2007, and will finish on August 2010).
The main idea of this fog monitoring methodology is to merge information derived from different observation platforms, i.e. satellite low stratus cloud classification, direct visibility monitoring, statistical estimation of low visibility from meteorological parameters at the ground. Each information is translated into probability maps of fog occurrence, with a weight attributed to the estimation itself, on a common grid (4x4 km) covering the flat portion of the region Veneto. These three different information are combined, taking into account the weight of single information, into the final fog probability map.
A probabilistic verification applied to the resulting product yields encouraging results, and is systematically more skillfull than the fog probabilities derived from the individual data sources. First real-time products are now available on the ARPAV Fog Pilot website for a group of specific users (motorway head office, road police, national railways and others) and are under testing.
Address of the test site:
http://85.42.129.76/ROADIDEA

2. DATA

2.1. Screen–level visibility network

The in situ fog monitoring requests instruments for direct observation of the visibility at screen level (height of 2 or 10 meters). For this aim ARPAV has purchased 10 visibilimeters, and installed them in their surface station network, in the plain part of Veneto, in an average resolution of 30 km. The instruments are included in the real time calling procedure (every hour).

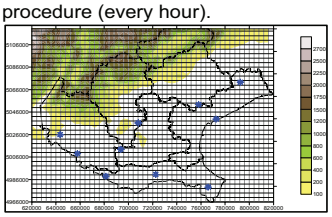

Figure 1: Map of the actual visibilimetry network, working since Jan 2009.

2.2. SAFNWC Cloud Classification

For the area of northern Italy the second generation geostationary satellite of EUMETSAT, Meteosat 8-9, is an essential source of information. The SAFNWC system is a software developed over the last years by a consortium involving many different organizations (*http://www.nwcsaf.org – SAFNWC documentation*). Of the set of 12 products available by the SAFNWC, we use the "Cloud Classification Type" (CT) product; this product provide an estimation on the type of

cloudiness covering a point on the satellite optical range, including low and very low clouds.
At the Meteorological Centre of Teolo the SAFNWC software was installed in order to obtain from Satellite a good estimation on cloud coverage, derived from combination of satellite imagery and meteorological models. The CT product takes part of the operational chain, contributing with the satellite-derived information.

2.3. CALMET and PBL parameters

CALMET (*Scire et al., 2000*) is a meteorological diagnostic model, normally used as a pre-processor for CALPUFF, pollution dispersion model. The starting data are coming from ground stations, Synop data, description of the cloud coverage.
In the framework of the ROADIDEA FOG PILOT the CALMET model output is used to estimate the meteorological conditions at the lower levels of atmosphere, including relative humidity, temperature and mixing height.
The relation between our surface station meteorological data and the visibility is established by a statistical non parametric analysis method, more precisely the "Classification And Regression Tree" ('*Classification and Regression Trees', Breiman et al. 1984*).

2.4. Grid of the Probabilistic Fog diagnostic system

Each information about visibility have to be related to the same geographical grid. We have opted for the geographical grid UTM32, used by the CALMET model in our operational settings. The UTM32 is a metric reference system, that allows to calculate directly the real distance between two points (important for the weight calculation). The grid spacing is 4x4 km; this size well matches with the dimension of the basic cell of the SAFNWC output at the lat-lon of northern Italy.

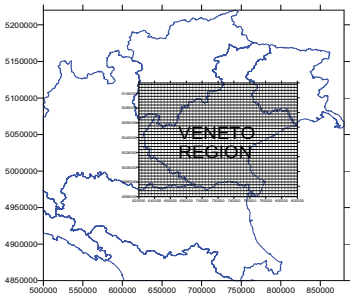

Figure 2: the metric grid UTM32 with cell size of 4x4 km, used in the probabilistic fog diagnostic system.

3. METHOD

3.1. Model elements, measures and its representativity

Using data sources presented in the previous chapters, we have three different sources of information/estimation available:

- Visibility sensors network information (10 points);
- Satellite derived cloud classification;
- Meteorological surface observations preprocessed by CALMET.

These pieces of information are different in essence; the visibilimeters network reports a set of local deterministic measurements; the Satellite CT reports an estimation of a condition that presents a relationship with the visibility reduction; the estimation derived by statistical method from meteorological ground stations returns a probability based on the analysis of a large set of observations.
In order to combine the available information, which are inherently uncertain, we opted for a probabilistic approach.
The merging method of the Fog Pilot will take into account the following conditions as essential:

- Each observation/estimation takes the form of a probability of an event occurrence (e.g. visibility less than 500 meters);
- Each observation/estimation has the form of a 2D field of probability, on the same geographical grid;
- Each observation/estimation must be linked to its level of uncertainty, expressed by a weight;
- The resulting product, obtained by merging the single information fields, will be more or less reliable depending on the specific reliability of the different information sources.

3.2. Probability derivation and weight of information

The information deriving from each monitoring system is translated into the "probability of visibility under 500 meters, within the cell".
The information given by CALMET or ground stations will be translated into probability with a decision three obtained by a CART analysis on meteorological data and visibility reports. The result of the three is an histogram counting the number of historical fog cases. This allows to derive a probability, and the dispersion of the histogram gives a measure of the weight of the probability estimation.
From the visibility sensors network a value of probability is derived from each instrument (probability=1 with visibility less than 500 meters, decreasing to probability=0 if visibility is upper 1 km). Then this values are interpolated on the entire grid of the system.
The Cloud Classification obtained by SAFNWC provide and information that can be divided into 3

classes: clear sky, overcast (medium-high coverage), low or very low clouds. To each class a value of probability of reduced visibility (under 500 m) was empirically assigned. The empirical values are checked only by a posteriori verification; in particular we assigned a probability of 70%, even if with the last analysis this value were found to be overestimated. Once recorded a year of complete data (August 2010) the values of probability will be reassigned more opportunely, with a specific statistical analysis.

3.3. Weighted average

The combination of available data is then performed with a simple weighted average. Once found the correct weight for every point in each field, a further weighting constant will be applied to each field, in the final merging procedure ('sigma').
To summarize, the single point probability of event is:

$$P(x,y)=\frac{\sigma_{sat}\cdot w_{sat}(x,y)\cdot P_{sat}(x,y)+\sigma_{vis}\cdot w_{vis}(x,y)\cdot P_{vis}(x,y)+\sigma_{carr}\cdot w_{carr}(x,y)\cdot P_{carr}(x,y)}{\sigma_{sat}\cdot w_{sat}(x,y)+\sigma_{vis}\cdot w_{vis}(x,y)+\sigma_{carr}\cdot w_{carr}(x,y)}$$

the 'sigma' parameters have been introduced to have an overall relative weight for the three data sources. These can be chosen plausibly or determined as the result of an optimization of the model.
It's well known how all the mentioned information sources about fog presence shows pros and cons.

Data source	Preprocessing	Pros	Cons
VISIBILIMETERS	Spatialization on the model grid	Good reliability	Very local information
Ouput by CALMET (or from STATIONS)	Statistical treatment	Instruments already available	Reliability very variable, local information
SATELLITE	Cloud Typing with SAFNWC	Coverage of the territory	Reliability very variable

Table 1: characteristics of data sources.

This merging process aims at reducing the individual limitation of the single data sources for fog estimation. In particular it is expected that:

- the surface information helps the distinction between low clouds and fog in the satellite information;
- satellite maps help the interpolation of the information even in areas not covered by instruments at the ground.

3.4. Performance measures

Verification is of principal importance for establishing the "goodness" of the fog probability maps and warnings that are output from the Fog Pilot. The verification process was chosen to act on the products derived from the individual data sources, as well as on the final merged product. The verification was performed for different periods during the winter 2009-2010, for a total of around 30 days (per 10 instruments, make available more than 7000 hourly samples). The following statistical indices and methods were applied:

- Reliability diagram, which compares the probability estimates with the effectively observed fog frequency given the probability estimate from the fog model;
- Probability of Detection (POD), Probability of False Detection (POFD, i.e. false alarms) and ROC curve diagram (ROC area);
- "TOTAL COST" (lower is better), or the directly derived "Economic Value" (higher is better), here calculated for a c/L ratio of 0.2.

Ref. *'Statistical Methods in the Atmospheric Sciences' (Wilks 2006)*.

3.5. Model parameters to be tuned

The system contains a certain number of parameters that can be varied to find the best performance with the present processing; in particular:

- The range of influence of visibilimeters; an exponential decreasing factor that determines the loss of weight of the information from a visibilimeter;
- Parameters for the correction of SAFNWC-derived probability field; 2 parameters that depending on visibility sensors records increase or decrease the weight of the satellite derived field;
- Relative weights for the calculation of final product; the 3 sigma parameters, ranging from 0 to 1, that determine the overall weight of the three fields we are merging with the weighted mean.

The optimization of these parameters allows a consistent increase of the model performances.
The mentioned parameters were tuned by a verification of outputs, performed varying the parameters value; the behaviour of the indeces we used for the tuning were reported on a 1-dimensional graph (for single parameters, such as distance factor) or 2-dimensional graph (for coupled parameters, such as relative weights of fields or correction factors).

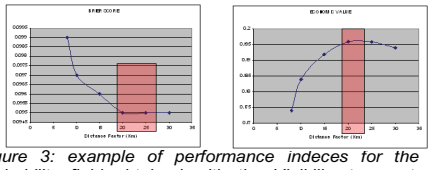

Figure 3: example of performance indeces for the fog probability field obtained with the Visibilimeters network, varying the Distance Factor; the optimal results are obtained for a factor close to 20 km.

4. Tuning And Performance Evaluation, added value of the merging procedure

Table 2 summarizes the performances, including the economic value, of various warning system setups, i.e. never warn, always warn, individual components as well as the merged version of the Fog Pilot. It can be observed that all the individual components of the Fog Pilot have a value, and that the merged product yields the best performance, also in terms of cost minimization and relative economic value.

	never	always	CART	SAF	VIS	MERGED
BEST POD	0	1	0.52	0.43	0.76	0.73
BEST POFD	0	1	0.23	0.008	0.22	0.18
COST (L)	1	1.2	0.8254	0.74	0.6229	0.6049
Economic value	0	-20%	17%	26%	38%	40%

Table 2: comparison of the performance indices between the individual components and the merged Fog Pilot products for a cost/Loss ratio of 0.2; the reference values are the absence of action (never protect) and the maximum of the security (always protect).

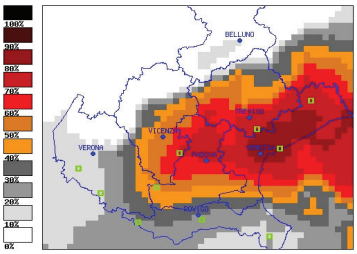

Figure 4: an example of the merged product; map of fog probability on 25 february 2010.

5. CONCLUSIONS

5.1. Overview of present Fog Pilot monitoring system

The Fog Pilot system in its current version, processes in real-time the data retrieved from a dedicated visibilimeter network of 10 stations, from the cloud classification scheme of the Meteosat Nowcasting Satellite Application Facility (SAFNWC), and from meteorological observations preprocessed by CALMET software.

The data of each source are transformed into a probability of fog occurrence based on a visibility threshold (500 m in our case, but in principle it's possible to implement other thresholds), and a weight representing the data quality is assigned. Then the three fields are merged taking the relative quality into account. The issues are hourly real-time maps of probability of reduced visibility under 500 meters at the ground level. The final product shows a POD up to 76% and a POFD lower than 10% (best performance verified by webcam records in Venice).

The results are encouraging for an operational employment of the Fog Pilot as a base for a warning system.

5.2. Operational applications, warnings and forecast

The present and potential applications of such a system are:

- To support the operational activities of the forecasters;
- To provide a base for warning about low visibility along road stretches;
- To provide an information, with known quality, to support the implementation and the improving of automatic forecasts of visibility reduction.

The information provided by the system can be directed to a large set of "private" users (drivers) and "great" users (police and public emergency services, heavy goods transport companies, motorway managements). A good exploitation of such information can have an impact on the huge amount of social costs caused by fog related accidents.

5.3. Futures perspectives

The potential, or already planned, developments are:

- Use of PBL parameters: parameters describing the boundary layer (Mixing height, vertical gradient of temperature), require a further statistical treatment to be related with the ground visibility; [PLANNED]
- Statistics on Cloud Type: a statistical analysis shall be performed on the Cloud Classification Type, in order to assess numerically the probability attributed to the visibility reduction from the Cloud Type field (this step requires at least 1 year of data, august 2010). [PLANNED]
- Extension of the system: more visibility sensors can be installed on the Veneto plain; [PLANNED]
- Involvement of neighbouring regions (Po plain area), in order to complete the monitoring over a climatologically coherent basin; [POTENTIAL]
- Integration of extra observations into the system: automatic or human reports, information from webcams, others. [POTENTIAL]

References:

1. COST 722 - Short range forecasting methods of fog, visibility and low clouds. Final Report, COST Office, Brussels, Belgium, 2007, online available at http://lcrs.geographie.uni-marburg.de
2. SAFNWC software documentation, available at www.nwcsaf.org
3. Scire et al (2000). J.S. Scire, F.R. Robe, M.E. Fernau and R.J. Yamartino. A User's Guide for the CALMET Meteorological Model, Earth Tech Inc., available at www.src.com
4. Breiman, L., Friedman, J. H., Olshen, R. A., & Stone, C. J. (1984). Classification and regression trees. Monterey, CA: Wadsworth & Brooks/Cole Advanced Books & Software
5. Wilks, D.S., 2006. Statistical Methods in the Atmospheric Sciences, 2nd Ed. International Geophysics Series, Vol. 59, Academic Press, 627 pp.

5th International Conference on Fog, Fog Collection and Dew
Münster, Germany, 25–30 July 2010
FOGDEW2010-81

Fog Forecasting using Synergy between Models of different Complexity: Large-Eddy Simulation, Column modelling and Limited Area Modelling

G.J. Steeneveld (1,2), M. Masbou (2), C.C. van Heerwaarden (1), C. Mohr (2), W. Schneider (2), M. Müller (3), A. Bott (2), and A.A.M. Holtslag (1)

(1) Wageningen University, Meteorology and Air Quality Section, Wageningen, Netherlands (gert-jan.steeneveld@wur.nl), (2) University of Bonn, Meteorological Institute, Bonn, Germany, (3) University of Basel, Basel, Switzerland

Fog is a hazardous weather phenomenon with a large impact on the environment and human life. In particular the transportation sector is vulnerable to fog; but fog is also important for agriculture, for leaf-wetness duration in particular, and for humans with asthma or related diseases. In addition, fog and low level clouds govern to a large extent the radiation balance of the polar regions in summer, and as such fog also influences the regional climate. Hence a thorough understanding of the fog governing processes is essential. However, due to the complexity and small scale nature of the relevant physical processes, the current understanding is relatively poor, as is our ability to forecast fog.

In order to improve our knowledge, and to identify key deficiencies in the current state of the art fog forecasting models, we present an experiment in which the synergy between models of different complexity and observations is used to evaluate model skill. Therefore, an observed case study (Cabauw; The Netherlands) of a well developed radiation fog will be innovatively run with a large eddy simulation model which allows us to evaluate the key issue of turbulent mixing. In addition, operational and research column models (PAFOG; Duynkerke, 1991) will be employed to evaluate their skill on the local scale, while at the limited area models WRF-NMMFOG (Mueller et al 2010) and COSMO-FOG will be evaluated on their skill for the regional scale. Special focus will be given to the representation of the boundary-layer vertical structure and turbulence in the latter two model types versus the LES results with its solid physical ground.

5th International Conference on Fog, Fog Collection and Dew
Münster, Germany, 25–30 July 2010
FOGDEW2010-82-1

On the potential of numerical short range fog forecast and low clouds with three-dimensional fog forecast models

M. Masbou (1), M. D. Müller (2), G. J. Steeneveld (3), J. Cermak (4), and A. Bott (1)

(1) University of Bonn, Meteorological Institute, Bonn, Germany (mmasbou@uni-bonn.de), (2) Institute of meteorology, Climatology and Remote Sensing, University of Basel, Switzerland, (3) Meteorology and Air Quality section, University of Wageningen, Netherlands, (4) Institute for Atmospheric and Climate Science, ETH Zurich, Switzerland

The presence of fog and low clouds in the lower atmosphere can have a critical impact on both airborne and ground transports and is often connected with serious accidents. An improvement of localisation, duration and variations in visibility therefore holds an immense operational value for the field of transportation in conditions of low visibility. However, fog is generally a small scale phenomenon which is mostly affected by local advective transport, radiation, turbulent mixing at the surface as well as its microphysical structure. Therefore, a detailed description of the microphysical processes within the three-dimensional dynamical core of the forecast model is necessary.

For this purpose, three-dimensional fog forecast models with a high vertical resolution with different microphysical complexity have been developed. COSMO-FOG and NMMFOG include a new microphysical parameterisation based on the one-dimensional fog forecast model. The implementation of the cloud water droplets as a new prognostic variable allows a detailed definition of the sedimentation processes and the variations in visibility. Also, we compare WRF mesoscale model results using different boundary-layer schemes that ignore or account for specific fog microphysics.

In some realistic fog situations (radiative fog) the potential of these three-dimensional fog models will be presented. The fog spatial extension will be compared with MSG satellite products for fog and low cloud. It will be shown that the initialisation and the interaction between the earth's surface and the atmosphere is one of the most important issues for reliable fog forecasts.

5th International Conference on Fog, Fog Collection and Dew
Münster, Germany, 25–30 July 2010
FOGDEW2010-83-3

Cloud chemistry in eastern China: Observations from Mt. Tai

J. L. Collett (1), X. Shen (1), T. Lee (1), X. Wang (2), Y. Li (1), W. Wang (2), T. Wang (2,3)

(1) Colorado State University, Atmospheric Science, Fort Collins, CO, United States (collett@atmos.colostate.edu), (2) Environment Research Institute, Shandong University, Jinan, China, (3) Department of Civil and Structural Engineering, The Hong Kong Polytechnic University, Hong Kong, China

Until recently, studies of fog and cloud chemistry in China have been rare - even though the fate of China's large sulfur dioxide emissions depends, in part, on the ability of regional clouds to support rapid aqueous oxidation to sulfate. Sulfur dioxide oxidized in regional clouds is more likely to be removed by wet deposition while sulfur dioxide that undergoes slower gas phase oxidation is expected to survive longer in the atmosphere and be transported over a much broader spatial scale. Two 2008 field campaigns conducted at Mt. Tai, an isolated peak on the NE China plain, provide insight into the chemical composition of regional clouds and the importance of various aqueous phase sulfur oxidation pathways. Single and two-stage Caltech Active Strand Cloudwater Collectors were used to collect bulk and drop size-resolved samples of cloudwater. Collected cloudwater was analyzed for key species that influence in-cloud sulfate production, including pH, S(IV), H2O2, Fe and Mn. Other major cloud solutes, including inorganic ions, total organic carbon (TOC), formaldehyde, and organic acids were also analyzed, as were gas phase concentrations of SO2, O3, and H2O2.

A wide range of cloud pH was observed, from below 3 to above 6. High concentrations of cloudwater sulfate were consistent with abundant sulfur dioxide emissions in the region. Sampled clouds were also found to contain high concentrations of ammonium, nitrate, and organic carbon. Peak TOC concentrations reached approximately 200 ppmC, among the highest concentrations ever measured in cloudwater. Hydrogen peroxide was found to be the dominant aqueous phase S(IV) oxidant when cloud pH was less than approximately 5.4. Despite its fast reaction with sulfur dioxide in cloud droplets, high concentrations of residual hydrogen peroxide were measured in some clouds implying a substantial additional capacity for sulfate production. Ozone was found to be an important S(IV) oxidant when cloud pH was high. Oxidation of S(IV) by oxygen, catalyzed by Fe (III) and Mn(II) was generally the second or third fastest pathway for sulfate production. Differences between the pH and trace metal concentrations of small and large cloud droplets were observed, giving rise to aqueous phase sulfate production rates that were drop size-dependent for the ozone and metal-catalyzed pathways.

5th International Conference on Fog, Fog Collection and Dew
Münster, Germany, 25–30 July 2010
FOGDEW2010-84

Chemical composition of fog water at Mt. Tateyama near the coast of the Japan Sea in Central Japan

K. Watanabe (1), H. Honoki (2), H. Yamada (1), M. Aoki (1), Y. Saito (1), K. Iwatake (1), S. Mori (1) and Y. Uehara (3)
(1) Toyama Prefectural University, Toyama, Japan (nabe@pu-toyama.ac.jp / Fax: +81-766-56-0396), (2) Toyama Science Museum, Toyama, Japan, (3) Kyushu University Forest, Fukuoka, Japan

Abstract

Measurements of the chemical composition of fog water at Murododaira (altitude, 2,450 m), on the western slope of Mt. Tateyama near the coast of the Japan Sea, were performed during the summers of 2004 and 2008. Strong acidic fogs (pH < 4) containing high concentrations of $nssSO_4^{2-}$ were observed in 2008, when the air mass at Mt. Tateyama originated mainly from the polluted regions of Asia. The mean ionic concentrations in the summer of 2008 were higher than those in the autumn from 2004 to 2007. The ratio of $NO_3^-/nssSO_4^{2-}$ in fog water was relatively high in 2004, when the air mass originated from central and western Japan. Transport processes of air pollution may significantly influence the chemical characteristics of fog water at Mt. Tateyama.

1. Introduction

Acid fogs are thought to contribute to the decline of forests at high elevation locations, where mountain slopes are frequently immersed in fog or cloud water (e.g., Blank 1985). Chemical measurements of fog water have been performed at high elevation sites, especially in the United States and Europe (e.g., Mohnen and Kadlecek 1989; Collett et al. 1990). The chemical composition of cloud or fog water has also been measured in East Asian countries, such as China (Lu and Niu 2009), South Kores (Kim et al. 2006) and Japan (Igawa et al. 1998; Watanabe et al. 1999, 2001, 2006; Tago et al. 2006). However, there is a shortage of fog water chemistry data from high elevation sites in Japan, where the decline of forests has become a serious environmental problem.

Recently, large amounts of acidic species have been deposited in the Hokuriku District, along the Japan Sea coast in central Japan (Honoki et al. 2007). Mt. Tateyama, a part of the mountain range in the Hokuriku District, is near the Japan Sea coast, where a large amount of air pollution may be transported from Asia as well as from industrial regions in Japan. In previous studies of Mt. Tateyama, high concentrations of pollutants derived from the continent, such as O_3, SO_2, and aerosols, were observed (Kido et al., 2001; Osada et al. 2009). Preliminary measurements of the chemical constituents of several fog water samples were also made at Mt. Tateyama in 2003 (Watanabe et al. 2005). A strong acidic fog, probably affected by trans-boundary air pollution, was detected. Furthermore, a serious decline of the forest in the vicinity of Mt. Tateyama has been observed (Kume et al. 2009). Air pollution may contribute to the damage to vegetation.

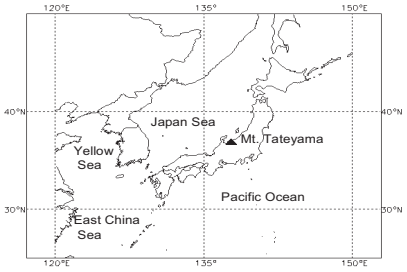

Fig. 1. Map of Japan showing the location of Mt. Tateyama.

From 2004, we systematically performed fog chemistry observations at Mt. Tateyama, and the chemical composition of fog water in the autumn (September and October) was described (Watanabe et al. 2010). The chemical characteristics of cloud or fog showed year-to-year variation. According to Osada et al. (2009), the volume concentration of submicrometer aerosols near the summit of Mt. Tateyama was significantly higher in the summer than in the autumn. To evaluate vegetation damage by acid fogs, it is important to understand the fog water chemistry during the summer. In this paper, the chemical characteristics of the fog water sampled at Murododaira near the summit of Mt. Tateyama in the summer are discussed.

Table 1. Summary of the chemistry of fog water at Murododaira (altitude, 2,450 m) during the summer. The units of the ionic concentrations are micro-equivalents per liter. N denotes the number of samples.

Year	N	pH	Cl^-	NO_3^-	SO_4^{2-}	$nssSO_4^{2-}$	Na^+	NH_4^+	K^+	Mg^{2+}	Ca^{2+}	$nssCa^{2+}$
2004	7	4.4-5.1	8-16	15-83	38-69	35-65	12-30	15-82	1-5	3-14	11-59	10-57
2008	4	3.7-4.2	23-35	63-146	146-296	138-293	27-31	77-181	0-4	8-14	26-58	25-56

2. Methods

Fog water collection was performed at Murododaira (altitude, 2,450 m), which is located on the western slope of Mt. Tateyama near the Japan Sea coast and far from the heavy industrial areas of Japan, from late July (21 July 2004 and 24 July 2008) to the end of August of 2004 and 2008. A map of Japan with the location of Mt. Tateyama is shown in Fig. 1. Due to severe conditions, such as heavy snow cover from winter to early summer, observation can be usually carried out only in the summer and autumn. Unfortunately, fog water sampling was not made during the summer from 2005 through 2007. Fog events are usually observed by extended clouds (not local upslope fogs) at Murododaira because local upslope fogs are mainly observed at altitudes below 2,000 m (lower than the altitude of Murododaira) at Mt. Tateyama.

Floud water was collected using a passive thin-string sampler (Model FWP-500) from Usui Kogyo Kenkyusho, Inc., as described in detail by Watanabe et al. (2005). The passive sampler, which does not require electricity, is advantageous for use at high elevations and has been used at Mt. Fuji (Dokiya et al. 2001; Watanabe et al. 2006). A hood with a diameter of 1 m for keeping out rain droplets was also mounted. However, perfect sampling of fog water without contamination of rain or drizzle may be impossible. Dry deposition of particles onto thin-strings during clear days may also affect the chemical composition of samples. In this study, water collected using the passive sampler is regarded as a fog water sample. The fog water collected with the sampler was stored in a tank with a volume of 5 liters and recovered every 3-14 days. The weight (volume) of the cloud water samples was measured *in situ*. The samples were carried back to Toyama Prefectural University and stored in a refrigerator. The fog water sampler as well as the tank was washed using pure water every 3-14 days after recovery of the fog water samples. The collection efficiency of the passive sampler is affected by the wind speed. In particular, the volume of fog water samples is small when wind velocity is low. Wind speed is usually relatively high during fog occurrence at the sampling site, therefore, cloud water could be collected effectively even with the passive sampler. In this study, the mean chemical concentrations in fog water were calculated by the concentrations and the weight (volume) of the samples.

The pH of the fog water was measured with an electrode using a pH meter. The analysis of the dissolved ionic species was performed using an ion chromatograph.

3. Results and Discussion

Table 1 shows the range of the concentrations of major ions and pH in fog water at Murododaira during the summers of 2004 and 2008. The pH of fog water ranged from 3.7 to 5.1. The acidity of fog water in the summer was comparable with that in the autumn. The pH of fog water at Murododaira ranged from about 3.5 to 6.3 in September and October from 2004 through 2007 (Watanabe et al. 2010).The chemical characteristics of fog water at Murododaira was dramatically different during those two years. Highly acidic fogs were frequently observed in 2008, on the other hand, the pH of fog water was relatively high in 2004. The concentrations of $nssSO_4^{2-}$ were high during the summer of 2008.

The volume-weighted mean concentrations of major ions in fog water during the summers of 2004 and 2008 are shown in Fig. 2. The mean pH of cloud water in 2004 and 2008 was 4.5 and 4.0 (3.95), respectively. The concentrations of chemical constituents in 2008 were much higher than those in 2004. The mean ionic concentrations in the summer of 2008 were also higher than those in the autumn from 2004 to 2007 (Watanabe et al., 2010). First of all, the chemical concentrations in fog water are highly dependent on the liquid water content (LWC) or fog duration. Unfortunately, the LWC was not directly measured with a LWC analyzer in this study. The total weight of all samples which correlates with the LWC and fog duration was about 1.5 times higher in 2004 than in 2008 (about 6,000 g/month in 2004 and about 4,000 g/month in 2008). The concentrations of total ions in 2008 were 3 times

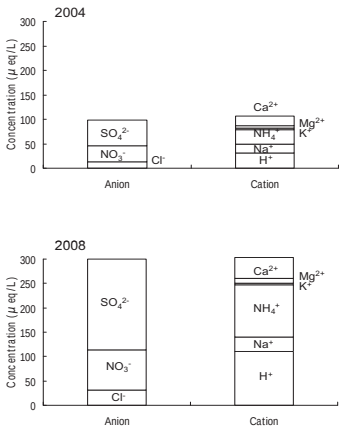

Fig. 2. Weighted mean concentrations of major ions in fog water at Murododaira in the summers of 2004 (upper panel) and 2008 (lower panel).

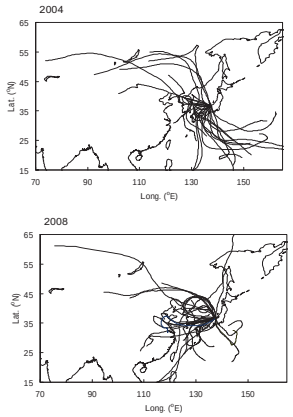

Fig. 3. Results of the 5-day backward trajectory analysis at altitudes of 2,500 m in the summer of 2004 (upper panel) and 2008 (lower panel). The trajectories are plotted once daily, and the starting time is 9:00 JST (0:00 UTC).

higher than those in 2004 (Fig. 2). The chemical characteristics in the two years cannot be explained by the amount of samples alone. Osada et al. (2009) showed submicrometer aerosols in the summer (August) at Murododaira were much higher in 2008 than in 2004. Air pollution might have been easily transported in the summer of 2008.

The $nssSO_4^{2-}$ concentration was usually higher than the NO_3^- concentration at Murododaira, and the equivalent ratio of $NO_3^-/nssSO_4^{2-}$ in fog water was quite different from the ratio in fog water at the mountainous sites near the industrial regions of Japan. The NO_3^- concentration is usually higher than the $nssSO_4^{2-}$ concentration (the $NO_3^-/nssSO_4^{2-}$ ratio is higher than 1) in fog or cloud water highly affected by polluted air from urban areas in Japan (Igawa et al. 1998; Tago et al. 2006). The $NO_3^-/nssSO_4^{2-}$ ratio at Murododaira seems to show year-to-year variation. While the concentration of NO_3^- was lower than that of $nssSO_4^{2-}$, the ratio of $NO_3^-/nssSO_4^{2-}$ was relatively high in 2004. Some samples showed that the concentrations of NO_3^- were higher than those of $nssSO_4^{2-}$ in 2004 (Table 1). The $NO_3^-/nssSO_4^{2-}$ ratio in the summer of 2004 was also higher than that in the autumn (Watanabe et al. 2010). The most predominant cation other than H^+ was NH_4^+ (Fig. 2).

The chemical characteristics in the two years might have been due to the difference in the transport processes of air pollution. The results of a 5-day backward trajectory analysis arriving at altitudes of 2,500 m during the sampling periods of 2004 and 2008 are shown in Fig. 3. The trajectories are plotted once daily. Fig. 3 presents predominant transport processes of air mass during both years. The analysis was based on the HYSPLIT4 (Hybrid Single-Particle Lagrangian Integrated Trajectory) Model, 1997 (Web address: National Centers for Atmospheric Research (NCEP-NCAR)

The air mass usually came from central and western Japan in the summer of 2004, whereas that at Murododaira in 2008 was mainly derived from Asia, especially from the coasts of the Yellow Sea and East China Sea, where SO_2 (and NH_3) emission is large (Ohara et al. 2007). In the summer, central Japan is usually under the influence of a maritime air mass, however, the continental air mass seemed to be predominant in 2008. Predominant air mass must significantly influence the chemical compositions of fog water at Murododaira, Mt. Tateyama. Watanabe et al. (2010) examined the relationship between the chemistry of fog water collected intensively (every 2-4 hours of sampling) at Murododaira in the autumn and transport processes of the air mass. High concentrations of $nssSO_4^{2-}$ and low pH were observed under the influence of the air mass transported from the polluted regions in Asia (Watanabe et al. 2010). Large amounts of air pollutants, such as sulfate aerosols (e.g., $(NH_4)_2SO_4$), might have been easily transported from the Asian continent to Mt. Tateyama in the summer of 2008.

The acidification of fog water must be accelerated by the trans-boundary pollution. According to the results of the backward trajectory analysis in 2008, the cloud water chemistry might also have been affected by the air pollution from western Japan. Therefore, the ionic concentrations might have been high in the summer of 2008. On the other hand, chemical constituents in cloud water in 2004 might have been mainly affected by the air pollution from the industrial regions of Japan, where SO_2 emission is restricted. As a result, a relatively high $NO_3^-/nssSO_4^{2-}$ ratio was observed in 2004.

4. Summary and Conclusions

Strong acidic fogs that contained high concentrations of $nssSO_4^{2-}$ were observed at Murododaira, Mt. Tateyama in the summer of 2008. The mean ionic concentrations in the summer of 2008 were also higher than those in the autumn from 2004 to 2007. According to the results of the backward trajectory analysis, the air mass at Mt. Tateyama was derived primarily from the polluted regions of Asia in 2008, and the trans-boundary air pollution might have contributed to cloud water acidification at Murododaira. In the summer, central Japan is usually under the influence of a maritime air mass, however, the continental air mass seemed to be predominant in 2008. On the other hand, acidic clouds might have been produced by pollutants from central and western Japan in 2004, and the ratio of $NO_3^-/nssSO_4^{2-}$ in fog water was relatively high.

Acknowledgements

This work was supported in part by a Grant-in-Aid for Scientific Research from the Ministry of Education, Culture, Sports, Science and Technology (No. 16710011, No. 18310022, and No. 20310113).

References

[1] Blank, L.W., 1985: A new type of forest decline in Germany, Nature 314, 311-314

[2] Collet, J.L. Jr., B.C. Jr. Daube, D. Gunz and M.R. Hoffmann, 1990: Intensive studies of Sierra Nevada cloudwater chemistry and its relationship to precursor aerosol and gas concentrations, Atmos. Environ., 24A, 1741-1757.

[3] Dokiya, Y., T. Yoshikawa, T. Komada, I. Suzuki, A. Naemura, K. Hayashi, H. Naoe, Y. Sawa, T. Sekiyama and Y. Igarashi, 2001: Atmospheric chemistry at the summit of Mt. Fuji: a challenging field for analytical chemists, Analy. Sci., 17, i809-i812.

[4] Honoki, H., K. Watanabe, H. Iida, K. Kawada and K. Hayakawa, 2007: Deposition analysis of non sea-salt sulfate and nitrate along to the northwest winter monsoon in Hokuriku district by a snow boring core and bulk samples, Bull. Glaciol. Res., 24, 23-28.

[5] Kido, M., K. Osada, K. Matsunaga and Y. Iwasaka, 2001: Diurnal variation of ionic aerosol species and water-soluble gas concentrations at a high elevation site in Japan, J. Geophys. Res., 106, 17335-17345.

[6] Kim, M.-G., B.-K. Lee and H.-J. Kim, 2006: Cloud/fog water chemistry at a high elevation site in South Korea. J. Atmos. Chem., 55, 13-29.

[7] Kume, A., S. Numata, K. Watanabe, H. Honoki, H. Nakajima and M. Ishida, 2009: Influence of air pollution on the mountain forests along the Tateyama-Kurobe Alpine Route, Ecol. Res., 24, 821-830.

[8] Lu, C. and S. Niu, 2009: Fog and precipitation chemistry in Nanjing, China. 3rd International Conference on Bioinformatics and Biomedical Engineering, ICBBE 2009, art. no. 5162865.

[9] Mohnen, V.A. and J.A. Kadlecek, 1989: Cloud chemistry research at Whiteface Mountain, Tellus 41B, 79-91.

[10] Ohara, T., H. Akimoto, J. Kurokawa, N. Horii, K. Yamaji, X. Yan and T. Hayasaka, 2007: An Asian emission inventory of anthropogenic emission sources for the period 1980-2020, Atmos. Chem. Phys., 7, 4419-4444.

[11] Osada, K., T. Ohara, I. Uno, M. Kido and H. Iida, 2009: Impact of Chinese anthropogenic emissions on submicrometer aerosol concentration at Mt. Tateyama, Japan, Atmos. Chem. Phys., 9, 9111-9120.

[12] Tago, H., H. Kimura, K. Kozawa and K. Fujie, 2006: Long-term observation of fogwater composition at two mountainous sites in Gunma Prefecture, Japan, Water Air Soil Pollut., 175, 375-391.

[13] Watanabe, K., Y. Ishizaka and C. Takenaka, 1999: Chemical composition of fog water near the summit of Mt. Norikura in Japan, J. Meteor. Soc. Japan, 77, 997-1006.

[14] Watanabe, K., Y. Ishizaka and C. Takenaka, 2001: Chemical characteristics of cloud water over the Japan Sea and the Northwestern Pacific Ocean near the central part of Japan: airborne measurements, Atmos. Environ., 35, 645-655.

[15] Watanabe, K., C. Natori and H. Honoki, 2005: Chemical composition of fog water on Mt. Tateyama, J. Japan Soc. Atmos. Environ. 40, 122-128 (in Japanese with English abstract).

[16] Watanabe, K., Y. Takebe, N. Sode, Y. Igarashi, H. Takahashi and Y. Dokiya, 2006: Fog and rain water chemistry at Mt. Fuji: a case study during the September 2002 campaign, Atmos. Res., 82, 652-662.

[17] Watanabe, K., H. Honoki, A. Iwai, A. Tomatsu, K. Noritake, N. Miyashita, K. Yamada, H. Yamada, H. Kawamura and K. Aoki, 2010: Chemical characteristics of fog water at Mt. Tateyama, near the coast of the Japan Sea in central Japan, Water Air Soil Pollut., doi: 10.1007/s11270-009-0307-2

5th International Conference on Fog, Fog Collection and Dew
Münster, Germany, 25–30 July 2010
FOGDEW2010-85

Is dewfall an important source of water in semiarid coastal steppe ecosystems in SE Spain?

O.M. Uclés (1), M.J. Moro (2), L. Villagarcía (3), L. Morillas (1), Y. Cantón (4), F. Domingo (1,5)

(1) Estación Experimental de Zonas Áridas. Carretera de Sacramento s/n. 04120 - La Cañada de San Urbano Almería, (Spain). oucles@eeza.csic.es; lmorillas@eeza.csic.es; poveda@eeza.csic.es., (2) Departamento de Ecología. Universidad de Alicante. Apdo 99. Alicante (Spain). mj.moro@ua.es , (3) Departamento de Sistemas Físicos y Químicos, Universidad Pablo de Olavide, Carretera de Utrera Km1, 41013 – Sevilla, (Spain). lvilsai@upo.es., (4) Departamento de Edafología y Química Agrícola. Universidad de Almería. La Cañada de San Urbano s/n. Almería, (Spain). ycanton@ual.es., (5) Departamento de Biología Vegetal y Ecología, Escuela Politécnica Superior, Universidad de Almería. Carretera de Sacramento s/n. 04120 - La Cañada de San Urbano Almería, (Spain)

Dewfall phenomena is widely recognised as an important source of water, leading in recent years to an increasing interest in its study. Dewfall deposition can be a significant source of moisture in arid and semiarid ecosystems, thus contributing to improve daily and annual water balances. Occurrence, frequency and amount of dewfall were measured in a Mediterranean semiarid ecosystem (Balsa Blanca, Almería, SE Spain) from January 2007 to December 2009. This area has a sparse vegetation cover dominated by Stipa tenaccisima combined with bare soil and biological soil crusts.

Wetness sensors were used to detect occurrence and frequency of dew events. The single-source Penman—Monteith equation simplified for potential water condensation was used to calculate potential dew amount. Micro-meteorological conditions during dew formation were also measured.

Dew condensation was recorded over 79% of nights during the study period. Dewfall length varied from 1.5 to 16 hours per night with an average of 10.1 $\pm$ 2.9 hours per night. The average dew amount was 0.21 $\pm$ 0.14 mm per night and it was mostly dependent on dew duration. Dew episodes were longer in late autumn and winter and decreased along spring.

Annual dewfall was 41.5 mm in 2007, 57.2 mm in 2008 and 71.1 mm in 2009, which represents, respectively, 13.7%, 18.8% and 18.0% of total rainfall. 2007 and 2008 were average years with 264 mm and 246 mm of rainfall, respectively whereas 2009 was a wetter year with 324 mm of rainfall. The comparison of the contribution of dewfall to the local water balance during a wet (September – November 2008, 146.3 mm rainfall) and a dry period (June - Augustus 2009, 0.8 mm rainfall), represented a dew contribution (dew / rainfall) of 8.4% for the wet but of 2602.0% for the dry period.

These results highlight the relevance of dewfall as a relatively small but constant source of water in arid ecosystems, as well as its significant contribution to the local water balance mainly during dry periods.

5th International Conference on Fog, Fog Collection and Dew
Münster, Germany, 25–30 July 2010
FOGDEW2010-86-2

What is the contribution of fog to sulphur deposition? Estimation based on high-resolution model for the territory of the CR.

I. Hunova, M. Conkova, P. Kurfurst, and J Maznova

Czech Hydrometeorological Institute, Ambient Air Quality Department, Prague, Czech Republic (hunova@chmi.cz, ++420244032468)

The precipitation chemistry is monitored over the Czech territory in the long run and maps of atmospheric deposition are regularly published. The contribution of the fog deposition has so far been neglected, however. The chemistry of fog is measured only on a very limited number of sites and so the data which are at the disposal cannot be used for estimation of the fog contribution to deposition of ambient air pollutants. Nevertheless it is widely accepted that the fog contribution is likely to account for substantial portion of the total atmospheric deposition both regarding its quantity and quality, particularly in elevated sites.
We present the estimation of contribution of fog to total atmospheric sulphur deposition over the territory of the CR, based on differences in two deposition models for forested area: 1. the throughfall sulphur deposition and 2. the sulphur deposition calculated from dry S deposition plus wet-only S deposition. The S deposition maps in 1x1km resolution and trends of S deposited in fog over the last 10 years are presented and the dependence of the fog contribution to sulphur deposition on altitude is calculated.
The preliminary results indicate that the contribution of fog to sulphur deposition varies in a wide range. For 2008 the fog contribution to sulphur deposition over the Czech forested area was up to 70 % depending on the altitude.

5th International Conference on Fog, Fog Collection and Dew
Münster, Germany, 25–30 July 2010
FOGDEW2010-87

The roles of circulation and aerosols in the decline of mist and dense fog in Europe over the last 30 years

G. J. van Oldenborgh (1), P. Yiou (2) and R. Vautard (2)
(1) KNMI, De Bilt, The Netherlands (2) LSCE/IPSL, laboratoire CEA/CNRS/UVSQ, Gif-sur-Yvette Cedex, France
(oldenborgh@knmi.nl)

Abstract

Fog and mist are meteorological phenomena that have significant contributions to temperature variations. Understanding and predicting them is also crucial for transportation risk management. In previous work has been shown that low visibility phenomena over Europe have been declining over the past three decades (Vautard et al., 2009). The trends in mist and haze have been correlated to atmospheric aerosol trends. More recently the same analysis was extended to dense fog, together with an examination of the roles of synoptic atmospheric circulation and aerosol content on the trends of dense fog (van Oldenborgh et al., 2010). It was shown that sulphur emission trends are spatially correlated with visibility trends, with a maximum correlation when visibility is between 1 km and 10 km. Atmospheric dynamics overall contributes up to 40% of the variability of the frequency of fog occurrences. This contribution is spatially variable and highly depends on the topography and the season, with higher values in the winter. The observed long-term circulation changes do not contribute much to the trends in low visibility found in the data. This process is illustrated on three stations (De Bilt, Zürich Airport and Potsdam) for which a long-term visibility data and a thorough meteorological description are available. We concluded that to properly represent fog in future climate simulations, it is necessary to include realistic representations of aerosol emissions and chemistry, land surface properties and atmospheric dynamics.

1 Data

Horizontal-visibility data have been taken from the 6-hourly NCEP ADP land surface observations available at the National Centre for Atmospheric Research (NCAR) server `http://dss.ucar.edu/datasets/ds464.0`. We selected 329 European stations (out of 4479) within [10°W–30°E; 35°N–60°N]. Stations were selected that had data over at least 1980–2000, at least 10 years with at least two observations per day, and at least 30 observations in all half-year seasons between 1980 and 2000 (excluding 1997). The details of the selection procedure are given in Vautard et al. (2009). We also excluded 9 high-altitude stations (above 1000 m). Six stations showed very obvious breaks in a visual inspection of the time series. Due to a change in the observing system the years 2002–2006 were disregarded for all Dutch data. The other four stations were removed entirely.

About two-thirds of the stations correspond to airports or airfields, at which low visibility observations are very important and often performed with more care. When plotting the results separately for airports/airfields and other stations it is apparent that the latter subset indeed contains more noise (not shown). However, there do not appear to be other systematic differences between the two subsets. In the following we present results for the complete dataset.

We also use longer time series of daily minimum visibility observed at De Bilt 1955–2001 (available from the KNMI web site), Zürich Airport (courtesy of MeteoSwiss) and Potsdam (Deutsche Wetterdienst).

2. Observed trends

Mist and Fog occur most frequently over eastern Europe and is more rare in summer, around the Mediterranean, and along the Atlantic coasts (Fig. 1a–d). The occurrence of fog and mist have decreased sharply over the last 30 years, as was shown for 1 km visibility in Vautard et al. (2009). The number of days with minimum visibility less 2 km has declined by a factor two over his period in most areas in Europe where fog is common (Fig. 1e–f). The same holds for dense fog with visibility less than 200 meter. This decrease has a high field significance.

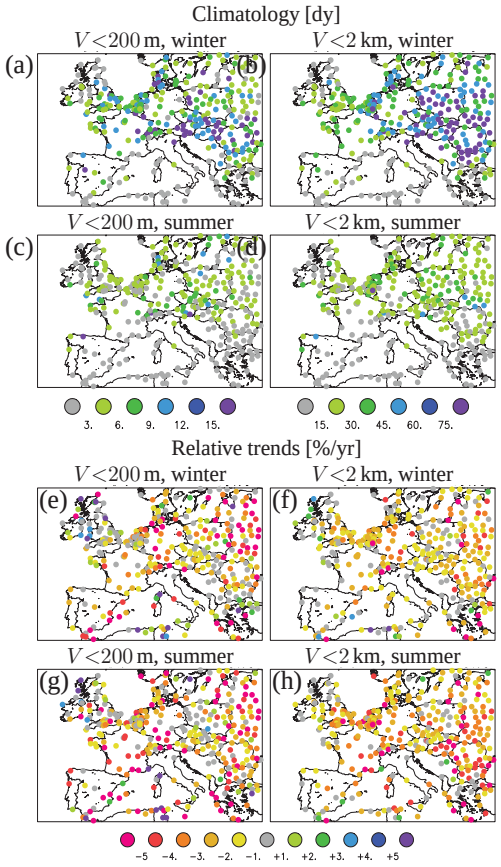

Figure 1: Mean number of days per half year with low visibility over 1976–2006 in winter (a) and (b) October–March, and summer (c) and (d) April–September. In (a) and (c) the number of days with dense fog (visibility less than 200 m) is shown, in (b) and (d) the number of days with visibility less than 2 km. (e)–(f) Relative trend in low visibility [%/yr] over 1976–2006.

3 Aerosol emissions and urbanisation

The spatial pattern of the absolute declines in numbers of fog and mist days matches the pattern of SO_2 emission trends over 1990–2007 (Streets et al., 2006) in Europe, suggesting that the improvements in air quality over Europe over this time contributed to the decrease. This relation is strongest for 5 km visibility, but is statistically significant for all ranges down to 100 m (Fig. 2). This is in agreement with micrometeorological modelling studies of fog Bott (1991) and von Glasow and Bott (1999), who found that urban aerosols cause higher water content and longer-lasting fog than rural aerosols.

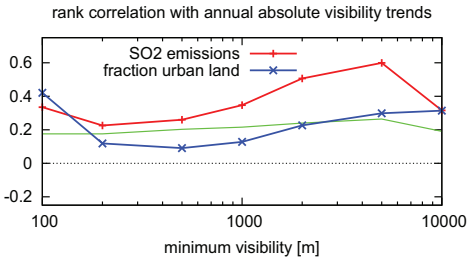

Figure 2: Spatial rank correlation of the trend in the annual number of days with minimum visibility less than a range of cut-offs with the trend in EMEP SO_2 emissions 1990–2007 (Streets et al., 2006) and with the trend in the fraction of urban land (Hurtt et al., 2006) (with sign changed) on a $2.5° \times 2.5°$ grid covering 10° W–35° E, 37°–60° N. The green line indicates the correlations that have p=0.05, using a number of degrees of freedom deduced from the spatial autocorrelation.

A few stations with longer observations show an increase in fog days up to 1970 (Zŕich Airport) or 1985 (De Bilt, Potsdam), and a decrease afterwards at almost all visibilities (Fig. 3). As the visibility at 5 km is directly correlated to aerosol concentrations, this reinforces the notion that aerosols also play a large role at lower visibilities.

The agreement of fog trends with urbanisation trends 1976–2005 (Hurtt et al., 2006) is much weaker: the largest absolute fog reductions have been observed in eastern Europe, whereas the largest increases in urban area have been in western Europe. Urbanisation also cannot explain the peak in fog and mist occurrences in the 1970s at Zürich Airport and the 1980s at De Bilt in Fig. 3.

4 Atmospheric circulation

Weather types obviously influence fog formation, both directly by creating circumstances favourable for fog

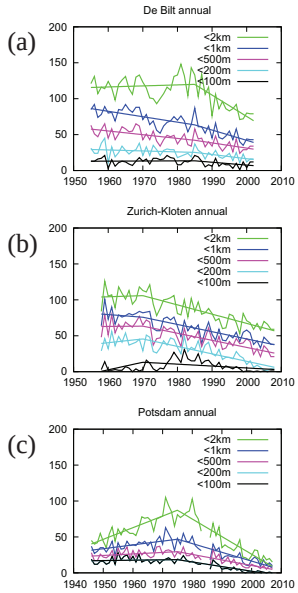

Figure 3: The annual number of days with visibility less than 100 m, 200 m, 500 m, 1 km and 2 km at (a) De Bilt, (b) Zürich Airport and (c) Potsdam. The straight-line fits include a break-point estimated from the 5 km visibility.

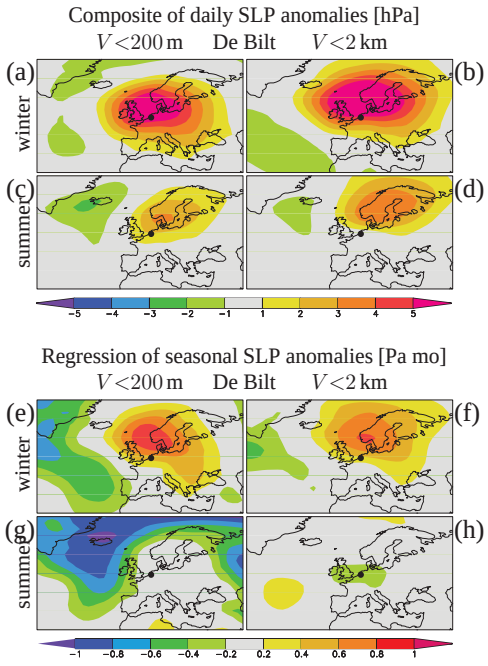

Figure 4: Composite of daily mean sea-level pressure anomalies [hPa] at days with low visibility in De Bilt, the Netherlands (dot) in winter (a) and (b) October–March, and summer (c) and (d) April–September. In (a) and (c) SLP anomalies at days with dense fog (visibility less than 200 m) is shown, in (b) and (d) at days with visibility less than 2 km. (e)–(f) Regression of the seasonal mean sea-level pressure on the number of days with low visibility in De Bilt [Pa month], the Netherlands (dot).

formation and indirectly by increasing aerosol concentrations near the ground. In winter the daily patterns associated with individual fog events (Fig. 4a,b) are similar to the seasonal mean weather patterns associated with seasons with many occurrences of fog or mist (Fig. 4e,f). However, in summer there is no such correspondence: the average circulation patterns of seasons with many fog days (Fig. 4g,h) are not the same as the circulation patterns on the fog days themselves (Fig. 4c,d). A study of De Bilt data shows that fog in July and August is associated with dry weather and clear skies in these months, but with rainy weather the months before. We hypothesise that the rain in late spring and early summer supplies the moisture needed for fog formation in high summer.

At three test locations the dependence of fog and mist occurrence on the atmospheric circulation can be parametrised well by local sea-level pressure gradients: the geostrophic wind components and vorticity (see also Clark and Hopwood, 2001; van Ulden and van Oldenborgh, 2006). There is no way to distinguish the direct effect of the circulation (low wind speeds for low geostrophic wind, clear nights associated with negative vorticity) with the air quality effects (advection of polluted air, stably stratified atmosphere, no precipitation).

In Central Europe, north of the Alps, westerly flows in winter with clean air, strong winds and cloudy skies are associated with fewer fog and mist days. Just north of the Alps and in eastern Europe, southerly flows also increase the number of fog days. High pressure (negative vorticity) increases fog and mist everywhere except the eastern edge of the study area (see

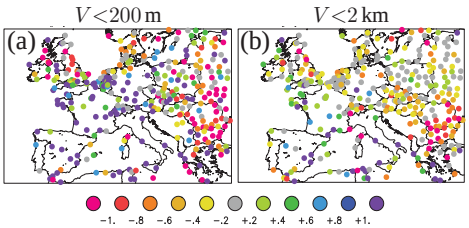

Figure 5: Relative trend in visibility [%/yr] due to circulation changes in January–March. (a) dense fog (200 m), (b) mist (2 km).

van Oldenborgh et al., 2010, for the figures).

The study period 1976–2006 has seen an increase in westerly flow over much of Europe in January–March (see e.g. van Oldenborgh and van Ulden, 2003; Osborn, 2004; van Oldenborgh et al., 2009). However, the effect of this increase on the decrease of fog days is much smaller than the other factors influencing fog trends (compare Fig. 5 with Fig. 1e–f, note the factor 5 difference in the colour scale) and only occurs in second half of winter.

5. Summary and Conclusions

This study only addressed the associations of fog and mist with aerosols, urbanisation and atmospheric circulation. Other factors, such as the availability of moisture due to water table management, the stability of the atmosphere and possible decreased nighttime cooling due to greenhouse warming have not yet been addressed. However, as these trends are unlikely to change sign over the next decades, projected further increases in air quality, increases in westerly circulation in winter and maybe drought in summer will likely further decrease the occurrence of fog and mist.

References

Bott, A.: On the influence of the physico-chemical properties of aerosols on the life cycle of radiation fogs, Bound. Layer Meteor., 56, 1–31, doi:10.1007/BF00119960, 1991.

Clark, P. A. and Hopwood, W. P.: One-dimensional site-specific forecasting of radiation fog. Part I: Model formulation and idealised sensitivity studies, Meteorol. Appl., 8, 279–286, doi:10.1017/S1350482701003036, 2001.

Hurtt, G. C., Frolking, S., Fearon, M. G., Moore, III, B., Shevliakova, E., Malyshev, S., Pacala, S. W., and Houghton, R. A.: The Underpinnings of Land-use History: Three Centuries of Global Gridded Land-Use Transitions, Wood Harvest Activity, and Resulting Secondary Lands, Global Change Biol., 12, 1208–1229, doi:10.1111/j.1365-2486.2006.01150.x, 2006.

Osborn, T. J.: Simulating the winter North Atlantic Oscillation: the roles of internal variability and greenhouse gas forcing, Clim. Dynam., 22, 605–623, doi:10.1007/s00382-004-0405-1, 2004.

Streets, D. G., Wu, Y., and Chin, M.: Two-decadal aerosol trends as a likely explanation of the global dimming/brightening transition, Geophys. Res. Lett., 33, L15 806, doi:10.1029/2006GL026471, 2006.

van Oldenborgh, G. J. and van Ulden, A. P.: On the relationship between global warming, local warming in the Netherlands and changes in circulation in the 20th century, Int. J. Climatol., 23, 1711–1724, doi:10.1002/joc.966, 2003.

van Oldenborgh, G. J., Drijfhout, S. S., van Ulden, A. P., Haarsma, R., Sterl, A. Severijns, C., Hazeleger, W., and Dijkstra, H. A.: Western Europe is warming much faster than expected, Clim. Past., 5, 1–12, doi:10.5194/cp-5-1-2009, 2009.

van Oldenborgh, G. J., Yiou, P., and Vautard, R.: On the roles of circulation and aerosols in the decline of mist and dense fog in Europe over the last 30 years, Atmos. Chem. Phys., 10, 4597–4609, doi:10.5194/acp-10-4597-2010, 2010.

van Ulden, A. P. and van Oldenborgh, G. J.: Large-scale atmospheric circulation biases and changes in global climate model simulations and their importance for climate change in Central Europe, Atmos. Chem. Phys., 6, 863–881, doi:10.5194/acp-6-863-2006, 2006.

Vautard, R., Yiou, P., and van Oldenborgh, G. J.: Decline of fog, mist and haze in Europe over the past 30 years, Nature Geoscience, 2, 115–119, doi:10.1038/NGEO414, 2009.

von Glasow, R. and Bott, A.: Interaction of Radiation Fog with Tall Vegetation, Atmos. Environ., 33, 1333–1346, 1999.

This page is purposely left blank.

5th International Conference on Fog, Fog Collection and Dew
Münster, Germany, 25–30 July 2010
FOGDEW2010-89

Fog Collection and Sustainable Architecture in Atacama Coast

Dr. Cristian Suau
Cardiff University, Welsh School of Architecture, suauc@cardiff.ac.uk

Abstract

It seems imperative to integrate renewable energy and climatic design in zero-carbon buildings in arid lands by employing natural and social science-based innovation applied in natural or built environs. The aim of this initial study is twofold: On one hand, to establish general climatic design codes for potential fog collection in different scales and, on another hand, augment rate and yield of fog collection used for drinking and irrigation in natural and urban areas.

The purpose is to integrate zero-carbon design in sustainable landscape and architecture and thus envision potential inhabitation through autonomous space-frame configurations along the coast of Tarapacá Region in Chile. In a sequential way, this study distinguishes three scales of interventions: territorial, local and domestic.

This research integrates climatic, structural and constructional factors by employing agile space-frame fogtraps; implementing appropriate low-passive energy technologies and combining hydrophobic and shading fabrics. Design is upgrading the following aspects:
1. Increasing rate and yield of advection fog by taking into account harvesting rate and climatic parameters
2. Structural reinforcement of fog collectors through lightweight, modular and deployable polygonal space-frames
3. Reducing installation and maintenance of fog collection (material research)
4. Purification of drinking water due to concentrations of pollutants
5. Lowering frame impacts on ground and surrounding mainly in *lomas*
The survey methods consist of literature review; fieldwork; comparative analysis of existing fog collection's techniques and climatic design simulations.

1. The cost of Atacama desert: a hyro-eolic lab

It is well-know that the phenomenon of desertification is caused by both climate change and the manned actions (United Nations Environment Programme). In the case of Chile, the land degradation of arid, semi-arid and dry sub-humid areas is the result of two main variables: El Niño's climatic performance and massive mining activities along the Andes Range, which require large amount of surface and subterranean water resources by extracting, processing and transporting minerals.

Parts of Atacama Desert have not reported a drop of rain since recordkeeping began. Somehow, more than a million people squeeze life from this parched land.

Stretching 1000 kilometres from Peru's southern border into northern Chile, the Atacama Desert rises from a thin coastal shelf to the *'pampas'*[1]. There are sterile, intimidating stretches where rain has never been measured. Without moisture, nothing rots. Everything turns into perpetual. Settlements are established into coastal cities, mining complexes, fishing villages, and oasis towns. Along much of the coast of northern Chile, rainfall is so scarce that remote communities long had to import water by trucks, a quite expensive and inefficient supply process, in order to survive. In the Atacama's coastline, a dense fog known as *'Camanchaca'* is abundant. Despite its aridity, the Atacama Desert hosts an impressive variety of plant life. The fog feeds flora called *'lomas'*, isolated islands of vegetation that can contain a wide variety of species, from cactuses to ferns.

[1] Lifeless plains that dip down to river gorges layered with mineral sediments from the Andes.

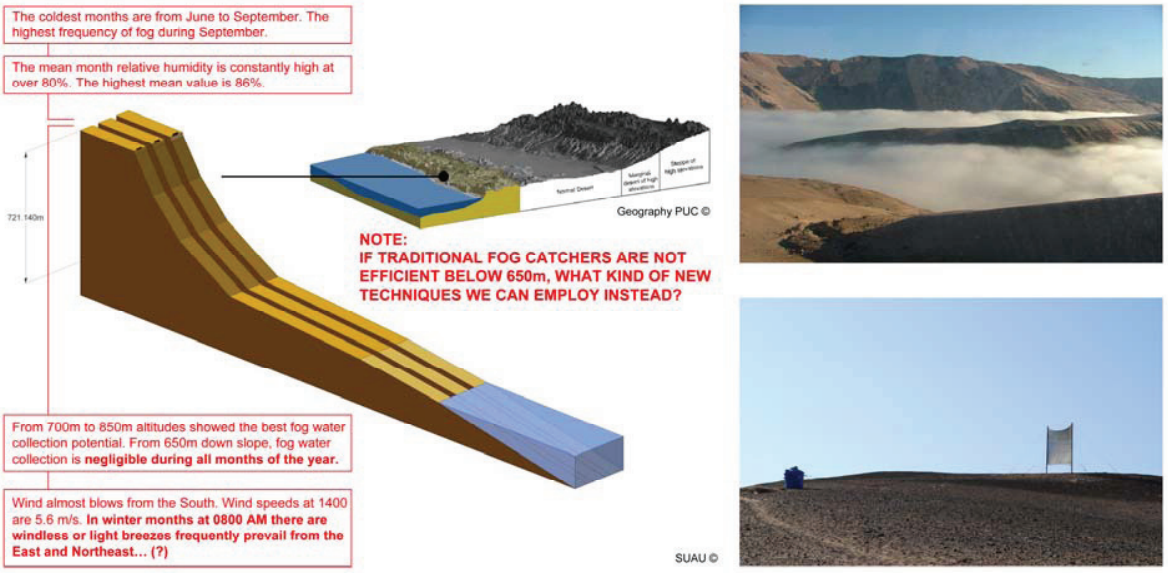

Figure 1. Atacama Desert and its 'Camanchaca' phenomenon: Section and views of the cliff facing S-SW winds in the fog oasis of Alto Patache. Source: Suau.

According to environmentalist and activist groups about 34% of the Atacama's total land surface is affected by this dehydration process. With no rainfall, the depletion and pollution of freshwater sources, and the existing pressures of urban population densities in the port cities, the current administration seems bland in the attempt to mitigate and trim down the precious water exploitation caused by the mining sector.

Demographic data shows how rural settlements are shrinking or simply depopulating and emigrating to port cities such as Antofagasta or Iquique. So it is urgent to map an atlas that shows how this territory is at risk by exposing current water resources; the shrinkage of rural settlements and degradation of fertile hectares used for agriculture.

Water scarcity intrudes just as harmfully on communities less accustomed to managing with freshwater shortages: from the high valleys of the mountains to coastal hillside of slums. As result this fragile ecological linkage is experiencing the loss of regional biodiversity. Demographic data shows how rural settlements are shrinking or simply depopulating and emigrating to port cities such as Antofagasta or Iquique.

So it is urgent to map an atlas that shows how this territory is at risk by exposing current water resources; the shrinkage of rural settlements and degradation of fertile hectares used for agriculture. Water scarcity intrudes just as harmfully on communities less accustomed to managing with freshwater shortages: from the high valleys of the mountains to coastal hillside of slums. As result this fragile ecological linkage is experiencing the loss of regional biodiversity.

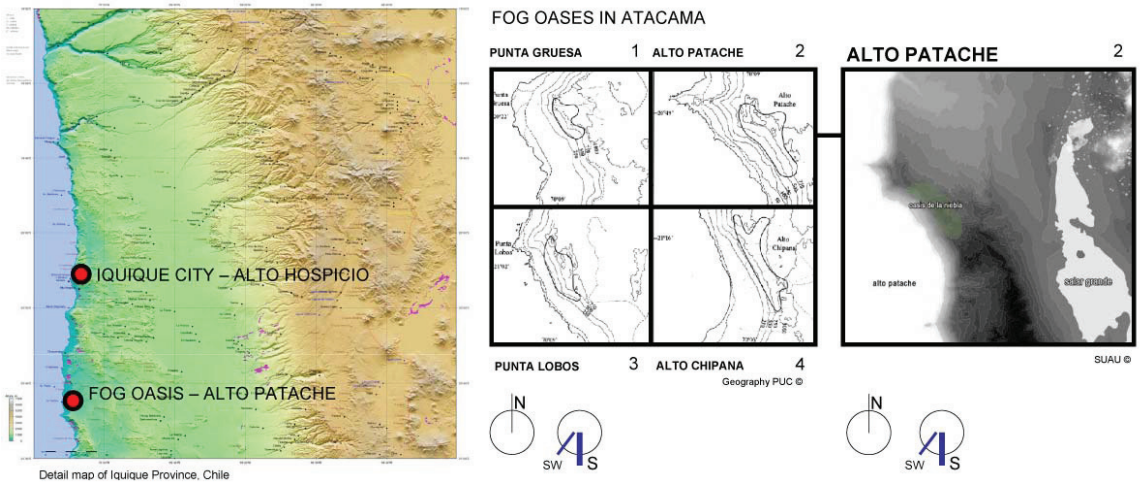

Figure 2. Map of coastal fog oases in the Region of Tarapaca, Chile: Alto Patache and Cerro Guanaco (nearby Alto Hospicio, Iquique). Source: Suau, 2010.

2. Research by design

It is imperative to integrate energy and climate into architecture by providing a more effective and holistic management of renewable energy like solar, wind and water supplies, particularly when it is reinforced by science-based innovation in the landscape, urban and domestic scale. This study is determined as much by climatic, geographic and biological factors as by any alternative for appropriate technologies. The main aim is stopping desertification by repairing endangered fog oases ecosystems; harvesting water for drinking and irrigation and fostering potential inhabitation in self-sufficient polyhedral configurations along the coast of the Tarapacá Region, Chile. Due to existing winds we also can obtain regular wind-based electricity.

Decades of pioneer applied research developed by *University del Norte* (1957) and recently continued by the *Centro del Desierto de Atacama* (CDA) have demonstrated that some of the most influential responses to these scarcities have been mounted at the level of fog oasis, farming fields, local villages and impoverished neighbourhoods.

The initial research stage (2010) has critically revised the studies made by the hydrologist Christiaan Gischler[2] and three-dimensional fogtrap prototypes (so called macro-diamonds) developed by Carlos Espinosa and Ricardo Zuleta in Camanchaca laboratory. Based on these precedents, this survey updated and collected climatic and geographic data provided by CDA combining meeting with experts and fieldwork in two fog oases: Alto Patache and Cerro Guanaco. Both are unique natural environments, nevertheless the latter is close by an urban settlement and it is more vulnerable.

The final stage was to elaborate standard design codes for 3D fog catchers and integrate the principles of polyvalence in each design. To achieve fog collectors' shape, frame and components I took into account three main climatic factors: Wind (direction and speed), humidity and temperature. Parametric design was used to test various solutions of water collection in different scales, from landscape to domestic ones.

[2] Gischler, C. *The Missing Link in a Production Chain*. 1991, UNESCO/ROSTLAC, Montevideo

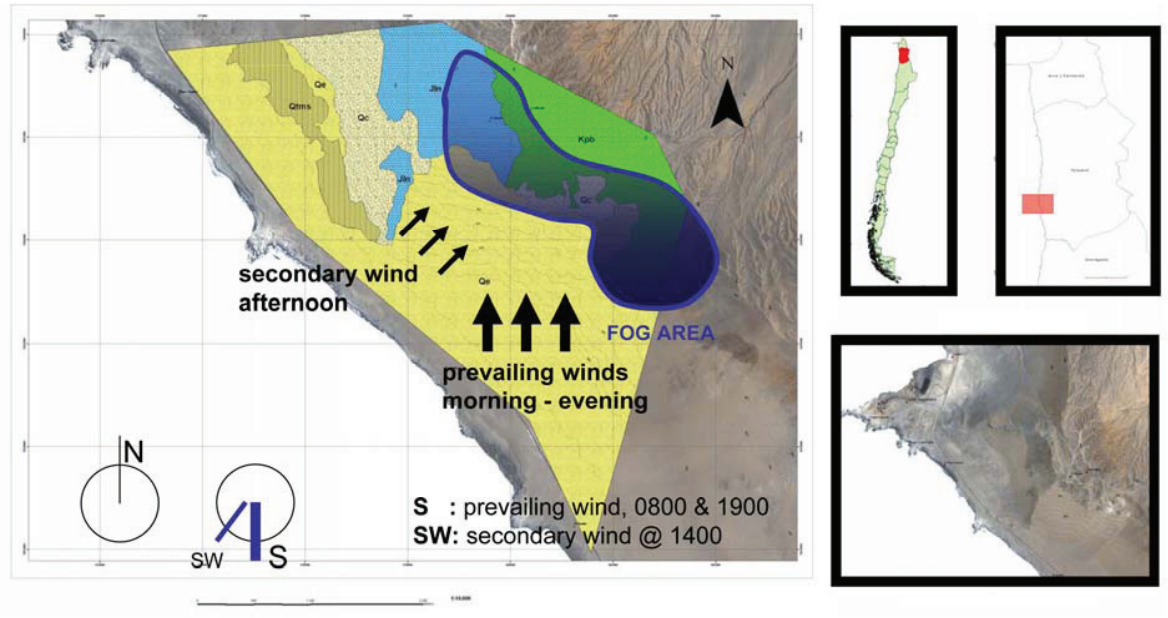

Figure 3. Geological map of Alto Patache overlapped by the fog area along the ridge. Source: Suau.

3. A glance about two-dimensional fogtraps

The more fog, the more wind. Fog catchers are structurally fragile devices. Nets tear, pipes leak, and wind can blow the whole structure over. Metal frames and tensors normally corrode and birds attack nets in joining areas ruining the process of fog trapping.

The conventional fog collectors[3] utilised in Chile are two-dimensional tensile devices waving delicately on the tops of coastal arid cliffs. These structures are long and light nets mostly made with polypropylene, glistening with moisture, transforming fog into precious water for reforestation, cultivation fields or small communities on the slopes below. Fog collection deals with horizontal precipitation. It actually imitates the missing link of trees. Once trees grow, they serve as natural fog catchers. A forest in a waterless area can trap and drip as much water into the dry soil as any idyllic rainfall.

These nets stand perpendicular to the prevailing wind, which blows fog into the woven plastic mesh. From there, droplets group and then fall into gutters that carry the water to collection tanks. The collector itself is completely passive, and the water is conveyed to the storage system by gravity. If topographic conditions are favourable, the stored water can also be conveyed by gravity to the point of use. The storage and distribution system usually consists of a plastic channel or PVC pipe approximately 110 mm in diameter which can be connected water hose for conveyance to the storage site/point of use. Storage is usually in a closed cistern. Chlorination of storage tanks may be necessary if the water is used for drinking purposes.

Nevertheless there are some technical aspects that need to be upgraded:

- The current technology represents a significant risk investment unless a pilot project is first carried out to quantify the potential rate and yield that can be anticipated from the fog harvesting rate and the periodicity of the fog within the area.

[3] The fog catchers are plastic (nylon or polypropylene) nets, measuring 30 M2 average. They catch the water, which condenses and is collected in tanks (with a capacity of about 18000 litres each) or earthen basin with a capacity of about 65000 litres. You require fine mesh netting facing the prevailing damp wind, so water is condensed on its filaments (1 mm wide and 0.1 mm thick, in a triangular weave); then collect in troughs and drain to where it is needed.

- Community participation in the process of developing and operating these technologies to reduce installation, operating and maintenance costs.
- If the harvesting area is not close to the points of use, the installation of the pipeline needed can be very pricey, especially in abrupt areas.
- The technology is very sensitive to changes in climatic conditions, which could affect the water content and frequency of occurrence of fogs. A backup water supply to be employed during low-harvest periods is recommended.

In Chile fog water has failed to meet drinking water quality standards because of concentrations of chlorine, nitrate, and some minerals derived from mining sector. It is mostly used for horticulture and forestry.

4. Design factors for fogtraps in Atacama desert

It is well-know that the occurrence of fogs can be assessed from reports compiled by climatic stations (i.e.: airports, research units, etc). To be successful, this technology should be located in areas where favourable climatic conditions exist such as fog oases along Atacama coast. Since fogs are carried to the harvesting site by winds, the topographic shape and orientation towards prevailing winds; solar position and wind speeds/directions will be prominent in determining the success of fog collectors. Nevertheless, in order to increase the yield and harvesting of water collection, we have to augment the size and material properties of nets (colours, patterns, filaments types and hydrophobic features). The study highlights several factors we should be considered in selecting an appropriate site for fog harvesting in Atacama coast:

Wind speed and velocity
The high-pressure area in the eastern part of the South Pacific Ocean produces onshore, southwest winds in northern Chile for most of the year. Prevailing/secondary winds (S-SW) are ideal for advent fog collection. Wind almost blows from the South. Wind speeds at 14.00pm rose 5.6 m/s. In winter months at 08.00am is windless or with light breezes below 2m/s in April.

Air temperature and fog water content
The higher is the formation the lower is the air temperature. In the coast of Tarapacá Region, the cooler months are from May to October. Hot seasons are from November to March [4] . For instance, in Alto Patache the high average temperature reaches 18C and the low temperature reaches roses 9.9C; daily temperature lap is 7.7 C. The highest frequency of fog condensation occurs during September. There is a relationship between temperature and fog collecting: The cooler is the mesh surface, the more water is collected.

Relative humidity
The higher is the formation the high is the relative humidity. The mean month relative humidity is constantly high at over 80%. The highest mean value is 86% in hot season (July).

Topography
It is necessary to have sufficient topographic relief to intercept the fogs/clouds; in terms of continental scale, it includes the coastal cliffs of Atacama Desert, and, in a local scale, isolated high obstacles or coastal lomas.

Relief in the surrounding areas
It is imperative that there be no major blockage to the wind within a few kilometres upwind of the site (i.e.: Alto Patache and Cerro Guanaco). In arid coastal regions, the presence of an inland depression or basin that heats up during the day can be advantageous, as the localized low pressure area thus created can enhance the sea breeze and increase the wind speed at which marine cloud decks flow over the collection devices.

Altitude
The breadth of the stratocumulus clouds and the height of their bases vary with location. As a rule of thumb, a desirable altitude is at two-thirds of the cloud thickness above the base. This portion of the cloud will normally have the highest liquid water content. In Atacama coast, the best fog water collection potential favourable altitudes range from 700m to 850m above sea level. From 700m to 850m altitudes showed the best fog water collection potential. From 650m down slope, fog water collection is negligible during all months of the year.

[4] Data extracted from Project FONDECYT 1971248, published by Pablo Osses et al., PUC, Chile (1998)

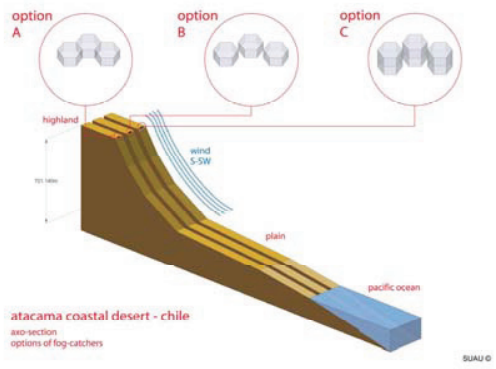

Figure 4. FogHive©, options of three-dimensional fog collector's arrays in the fog oasis of Alto Patache. Option1: Attached; option 2: detached; and option 3: stacked. Source: Suau.

Orientation of the topographic features:
It is vital that the longitudinal axis of the formations be perpendicular to the direction of the dominant winds that convey the clouds from the ocean. The advent clouds flow over the ridge lines and pass through, often dissipating onto the downwind side.

Distance from the coastline
There are many high-elevated coastal formations with frequent fog covered by transport of upwind advent or orographic clouds. In both cases, the distance to the coastline is irrelevant. However, highlands nearby the coastline are generally preferred sites for fog harvesting.

Length/height ratio and spacing between collectors
The best length/height ratio of any fog collectors is 1:1 or 1:2 (as proportional dimensions)[5]. If we do increases the length, it diminished its relative yield. Ridge lines and the upwind edges of flat-topped formations are high-quality fog harvesting zones. When long fog water collectors are installed, these should be placed at intervals of at least 5.00m to allow airflows in-between.

Crestline and upwind locations
Slightly lower-altitude upwind locations are as acceptable as constant-altitude locations on a flat terrain. But locations behind a front ridge or hill, especially where the wind is flowing down slope, should be avoided.

[5] Gischler, C. *The Missing Link in a Production Chain*. 1991, UNESCO/ROSTLAC, Montevideo. Fig 24, p28

5. Design factors for polyhedral fogtraps: FogHive©

The earth sciences taught that due to the occurrence of water in three phases: gas, liquid and solid, solar energy keeps the hydrological cycle going, shaping the earth surface while regulating the climate and thus allowing smart technologies to interfere in the natural process by rerouting water and employing its yield for natural and human environments' subsistence. This is the case of traditional fog collectors implemented along the Atacama coast through vertical tensile mesh or macro-diamonds structures.

Nevertheless, these basic prototypes require urgently to be upgraded, mainly through new shapes, fabrics and frameworks' types by following the principles of lightness, transformability, portability and polyvalence.

So it is necessary to establish new design alternatives. Not just alternative forms but also alternative sites, fabrics, and arrays. So this study questions how this varies as we vary the alternative forms and so on. These alternatives are variables under our control; there are other variables affecting deposition rate over which we have no control. These include wind speed, air temperature, and humidity. There are several routes to understanding the relationship between the variables. One is based on experience from tradition, which might be able to affirm which materials work well in which specific locations. Another one is through experiments that researchers have done and yielded empirical relationships, such as between wind speed, fog density, and deposition rates.

For instance, canvas in a conventional fog collector contains too much stressed at each joints and as result it becomes vulnerable. So this initial research has explored the relative yield in parallel flat planes with polyhedral systems with hexagonal footprint, and then few large cases with lots of smaller ones by optimizing fabric area and selecting alternative types.

In order to increase yield of collected fog water, this study has searched for suitable natural and semi-urban placements that contain high rates of fog's accumulation: Alto Patache and Cerro

Guanaco. As important as the chosen sites is also the building and structural reliability of these collectors that will be installed. Both frames and skins have to provide an optimal shape that can deal with dynamic wind directions and be resistant against high speed and rust. Its fabric necessitates increasing its hydrophobic condition, being elastic and containing lighter colours (high emittance) to ease dripping/drainage and thus avoid ultra-violet deterioration. In addition, structural supports should be well-embraced and lightweight too.

FogHive© (Suau) explores climatic design parameters combined with the agile structural principles of Tensegrity and Geodesic widely developed by Bucky Fuller and Frei Otto. The design methods mainly consisted of literature review; fieldwork; comparative analysis of existing fog collection's techniques and climatic design simulations. FogHive© is a lightweight, polyvalent and modular space-frame, fully wrapped with a light hydrophobic mesh, which can collect water fog. It also performs like a shading/cooling device and a soil humidifier for greenery and potential inhabitation. Being a transformable construction, it can easily be installed on flatten or uneven grounds. Its footprint is hexagonal.

Regarding the scale of intervention, FogHive© unit varies its dimensions. Landscape model has 12m side; local model 9m side and domestic model has 6m side.

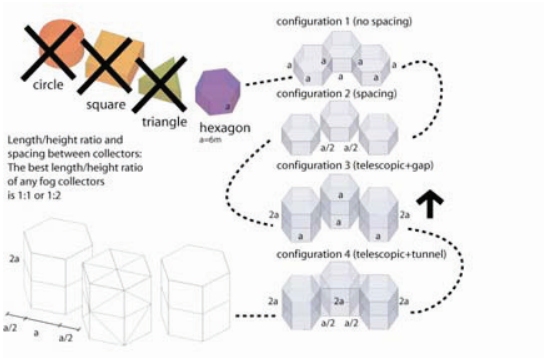

Figure 5. The hexagonal footprint seems the most efficient way to response climatically to shading and fog water capture aspects. It secures the best length/height ratio for 3D fog collectors, which is 1:1 or 1:2 (proportional dimensions). Source: Suau.

A. Territorial scale model:
It is a large polyhedral telescopic fog catchers (hexagonal footprint, side equal 12m) aligned in strategic sides of natural creeks or valleys, which will impede desertification in rural settlement or natural landscapes. Those devices bring micro-agriculture back and repair fragile ecosystems (native flora and fauna) by harvesting and distributing mainly crop water. Study area: Fog oasis in Tarapacá Region. The strategic allocation of fog collectors can not only bring local agriculture back and decrease rural emigration but also repair existing fragile ecosystems in several fog oases by harvesting and distributing mainly crop water.

B. Local scale model:
It is a mid-size polyhedral standing alone fog catcher (hexagonal footprint, side equal 9m) to supply both water and electricity to small communities (sustainable micro-agriculture and rural electrification) in natural and urban environments. Study area: Cerro Guanaco – Alto Hospicio. This space-frame fog collector can be allocated in Cerro Guanaco, a fog oasis nearby Alto Patache, a low-income sprawl. It can provide water and electricity to small communities through forestation, sustainable micro-agriculture and electrification.

C. Domestic scale model:
It is an autonomous small polyhedral space-frame (hexagonal footprint, side equal 6m) manufactured with timber, galvanised steel or carbon fibre. This inhabitable unit is modular, deployable and lightweight; with an adjustable textile system that perform as water-repellent skins when it faces South and SW winds and shading fabrics (mainly roof and North–NE-NW sides); plus blades plugged in the base frame. Water collector, filtering (purification) and irrigation network consider available materials and techniques.

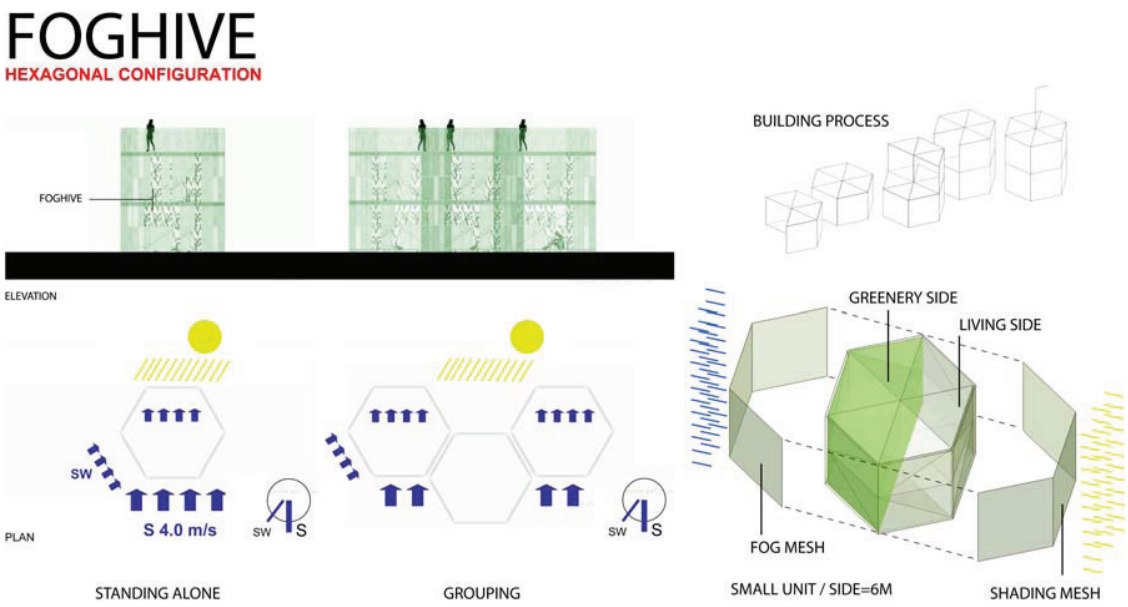

Figure 6. Plan, elevation and axonometric model of FogHive©, domestic version. Source: Suau.

Perhaps the most revealing aspect of FogHive© is that it can be also understood as a polyvalent measurement device. Prior to implementing any prototype, a pilot-scale assessment of the water fog collection; humidity and shading systems should be undertaken. It cannot replace the role of CDA neblinometers [6]. However it should be equipped with an anemometer to measure wind speed and a vane to measure wind direction. FogHive© can be connected to a data logger.

6. New questions

Despite the fact that technology meets the requirement for small volumes of water, future development work should be directed toward increasing the yield from the harvesters for small, intermediate and large applications. In particular, if this goal is to be achieved, studies need to be aimed at design levels that might increase the flows of fog towards the collection area. In addition, it is important to bear in mind that, while the technology has proved satisfactory, its successful implementation depends on the existence of the correct intersection of geographical and meteorological conditions.

Thus, a rigorous study of meteorological parameters must precede any further proposed application of polyhedral systems, not only to determine if the correct combination of geographic and climatic conditions exists but also to contribute to the understanding the complexity of these factors so that their occurrence may be predicted properly. When needed a socio-cultural development project should also be conducted at the same time to ensure that an appropriate organization exists to manage the system in an appropriate and efficient manner.

We need to be able to make some quite simple judgements of the kind that you are interested in, such as the form of the catchers. The more than we know, the more challenging are the possibilities than we can explore. What climatic factors we need to ask for, or what properties of cloth we need to study, cannot be answered confidently until we understand in-depth geographic and climatic parameters.

[6] This tool has been developed at the Catholic University of Chile (Carvajal, 1982). There are four different types of neblinometers: (a) a pluviograph with a perforated cylinder; (b) a cylinder with a nylon mesh screen; (c) multiple mesh screens made of nylon or polypropylene mesh; and (d) a single mesh screen made of nylon or polypropylene mesh. The devices capture water droplets present in the fog on nylon filaments that are mounted in a metal frame. It is a fixed device only facing prevailing winds and cannot response dynamically to daily wind changes.

Figure 7. Outer view of FogHive© array situated along the ridge. Source: Suau.

In terms of climatic issues, we would know more about the timing and nature of the fog events. There are not climatic stations in our chosen sites. The existing data is primarily averages, either aggregates of several events or averaged over a long period. If it is known that the current fog water efficiency of two dimensional fogtrap is low, then there is scope for improvement. According to the literature review we require more dynamic climatic data to understand the *Camanchaca* phenomena to exploit it. Hence the suggestion of a time lapse film ideally attached with accurate atmospheric measurement might help well. This study still have to establish the efficiency of the capture; e.g. of the total latent water in the air, how much can be extracted. That would give us an idea of how far the FogHive© concept could be pushed. One way to establish this is to measure the total water content of the air during any fog episode so-called total water content (TWC), expressed in g/m3. One simple method to do this is from a measure of visibility: The denser the fog, the greater the water. Based on the initial research of hydrophobic fabrics, we still have to explore about the size (or range of sizes) of the droplets. It could be useful in deciding on the mechanisms for fog capture, and so inform on the size of net filaments, level of porosity, etc.

The polyhedral structures' meshes not just respond to fog catching collection but also allow the potential inhabitation for endangered local flora and fauna or mini-agriculture due to they are performs like shading spaces or *umbraculos*. The modules also allow the possibility for temporary or transient accommodation at the collection sites; for instance, maintenance workers, water "harvesters", farmers or even eco-tourists.
There is a regional concern over the issue of collecting and concentrating atmospheric pollutants into the soil when untreated water is used for irrigation. There might also be concern over the impact of different net types and its durability due to birds' intrusion searching for water.

What we can play instead? There is a scientific collaborative agreement between CDA and WSA (June 2010) and we are searching for international funding to develop the advanced stage of FogHive©.

Acknowledgements

I thank the support and collaboration of Imke Höhler from Muthesius Academy of Fine Arts and Design Kiel, Industrial Design, Technical Design, Germany. Her research on Sustainable Design and new technologies applied in nomadic fogtraps has been very fruitful to orientate my design.

Apart from this, I cannot forget the brainstorming sessions, discussion and presentations carried out at the Welsh School of Architecture where Dr. Mike Fedeski and Dr. Don Alexander gave me their expertise guidance in the fields of Physics and Sustainable Environments.

Special gratitude towards the team of *Centro del Desierto de Atacama* (CDA) led by Pilar Cereceda in Chile. They provide the updated climatic and geographic data of my research; and co-ordinating my fieldwork in the fog oases of Alto Patache and Cerro Guanaco, Iquique. Finally, this research was possible due to the support of two exceptional researchers: Dr. Pablo Osses and Dr. Horacio Larrain, who make possible my on-site design tests and climatic verifications.

References

Atlas del Agua by Pietro Laureano, UNESCO, LAIA editors, Barcelona, 2001
Water: Our Thirsty World, National Geographic Magazine (special issue), Voume 210, No. 4, 2010
The Missing Link in a Production Chain by C. Gischler, UNESCO/ROSTLAC, Montevideo, 1991
The Climate of the Coast and Fog Zone in the Atacama Desert of Tarapacá Region, Chile, Atmospheric Research, Volume 67, Nº 3-4, pp 301-311, 2008
The Spatial and Temporal Variability of Fog and Its Relation to Fog Oases in The Atacama Desert, Chile by P. Cereceda, Larraín H., Osses P., Farías M. and Egaña I. Atmospheric Research, 2007

Advective, Orographic and Radiation Fog in the Tarapacá Region, Chile by Cereceda, P.; Osses, P.; Larraín, H.; Lázaro, P.; Pinto, R. and Schemenauer, R.S. Atmospheric Research, Elsevier Science Volume 64, pp 261-271, 2002

Los Atrapanieblas, Tecnología Alternativa para el Desarrollo Rural by P. Cereceda. Revista Medio Ambiente y Desarrollo, CIPMA, Vol. XVI – Nº 4: 51-56. Chile. 2000

Human Occupation and Resources in a Fog-covered Site in Alto Patache (South of Iquique, Northern Chile) by Larraín, H.; Cereceda, P.; Schemenauer, R.S.; Osses, P.; Lázaro, P. and Ugarte, A. Proceedings of the First International Conference on Fog and Fog Collection, Vancouver, Canada, pp 217-220, July 1998

Camanchaca as a Potential Renewable Water Resource for Vegetation and Coastal Springs along the Pacific in South America by Gischler, C., Cairo, Egypt, UNESCO/ROSTAS, 1977.

LINKS (accessed in 05/07/2010)

http://ngm.nationalgeographic.com/ngm/0308/feature3/#know

http://www.fogquest.org/

http://www.uc.cl/geografia/cda/

http://www.oas.org/dsd/policy_series/5_eng.pdf

http://www.idrc.ca/index_en.html

http://www.fogharvesting.com/

http://www.inhabitat.com/2007/04/16/watair-turning-air-into-water/

http://www.wateraid.org/

5th International Conference on Fog, Fog Collection and Dew
Münster, Germany, 25–30 July 2010
FOGDEW2010-90

Long-lasting Fog in the Ebro valley: a high-resolution mesoscale simulation

J Cuxart and M.A. Jimenez
University of the Balearic Islands, Physics Dpt., Palma de Mallorca, Spain (joan.cuxart@uib.cat)

A 48-hour simulation of a radiative fog event in the Ebro Valley (in the NE part of the Iberian Peninsula) is made. The fog extends over the complete lowlands of the valley, which are about 350 km along the river axis and near 100 km transversally. It is established during the first night and does not lift and dissipate until midday of the second day, therefore lasting more than 30 hours.

The simulation is able to reproduce the overall behaviour of the fog event, which is monitored making use of METEOSAT imagery and the network of meteorological stations. The simulation allows a short lifting of the fog during a pair of hours of the first midday in some areas that did not take place in reality. The evolution is compared to a pure single-column run to evaluate the importance of the lateral detraining of fog by basin motions according to the model.

The simulated fog has its top at approximately the same height above the sea level everywhere, therefore being deeper in the low terrain areas. The depth of the fog evolves up to 500 m over the terrain, generating a well mixed fog layer driven by top-bottom convection due to radiative and evaporative cooling at the top. Above the fog a sharp inversion is generated. The air above the fog behaves disconnected from the fog layer, interacting with the fog at its limits over the slopes.

5th International Conference on Fog, Fog Collection and Dew
Münster, Germany, 25–30 July 2010
FOGDEW2010-91

An analysis of the fog distribution in Beijing for the 2001-2005 period using NOAA and FY data

J.L. Wang (1), S.M. Li (2), and X.L. Liu (3)

(1) Institute of Urban Meteorology, China Meteorological Administration, Beijing 100089, China (jlwang@ium.cn) , (2) National Satellite Meteorological Center, Beijing,100081, China, (3) Beijing Meteorological Information Center, Beijing, 100089, China

Based on the various fog remote sensing information products abstracted from the polar orbit meteorological satellite data (NOAA and FY), this paper analyses the characteristics of the frequency and distribution that dense fogs have taken place in the Beijing district from 2001 to 2005. Among those information products, the statistical graph of the foggy days in Beijing from 2001 to 2005 by means of satellite-remote-sensing reflects the frequency that dense fog has occurred in the different regions in Beijing; and the statistical graph of the foggy days of each season by satellite-remote-sensing shows the characteristics of the temporal and spatial change of the fog distribution in the Beijing in different seasons; the fog degree index(like pixel-level spatial measurement) by satellite-remote-sensing reflects the fog frequency difference on unit area in different counties of Beijing. Meanwhile, based on the satellite-remote-sensing pictures, data on the main meteorological elements that contribute to the formation of fog, geographic information, and DEM data, this paper makes an analysis in 3 areas, the traits of the fog distribution in the different regions of Beijing in different seasons; meteorological causes for temporal and spatial changes the main fog types(advection fog, radiation fog). This paper also gave a brief introduction to the general principles of meteorological satellite remote sensing fog, fog information extraction method, as well as the process of satellite orbit selecting according to the ground visibility, data processing and product generation.

5th International Conference on Fog, Fog Collection and Dew
Münster, Germany, 25–30 July 2010
FOGDEW2010-92

Highly effective fog-water collection with Pinus canariensis

A. Groh
(arnold.groh@tu-berlin.de)

Fog-collecting nets require constant manpower in terms of maintainance. Also, those nets are made of artificial material, and they do not really fit into the natural environment. They are, by far, not as effective as plants that are specialised for catching humidity from the air.

The probably most effective plant to serve this purpose is Pinus canariensis, a tree native to the Canary Islands. It is well-known for its capability of collecting air moisture, and has already been used for many centuries for this purpose. This tree would allow a much more effective and environmentally friendly way of supplying arid regions with drinking water than this could be done with fog-catching nets. Moreover, it would also help to establish or re-establish vegetation in a natural way. Agriculture would profit from it, too, because vegetables could be produced, watered with the help of P. canariensis.

In those places, where the net-projects are currently running, it is the right time now to plant P. canariensis seedlings underneath the nets, which they will soon replace. The surface of the trees is much larger than the surface of the nets, thus enabling much more water to condensate. Within a few years, a population of P. canariensis will be established that collects many times more water than the nets. With regard to ecological aspects, the introduction of P. canariensis into the environments concerned do not cause a problem, since in those desert areas, there are no native trees that could be superseded, and the P. canariensis trees are easy to control. They are a natural alternative to the unnatural plastic nets, and can even help to enhance any local flora.

5th International Conference on Fog, Fog Collection and Dew
Münster, Germany, 25–30 July 2010
FOGDEW2010-93

Fog harvesting on the verge of economic competitiveness

K. J. Tiedemann and A. Lummerich
Alimón e.V., Akazienweg 3, 41372 Niederkrüchten, Germany (alimon@alimon.org)

Water scarcity is the bottleneck for agriculture and development of Peru's coast and subject to aggravation due to climate change. Until present day, Peru's coast in general and the Lima Metropolitan Area (LMA) in particular have enjoyed to a great extend the effect of the country's high altitude glaciers that serve as a buffer for the capital's water demand during the highland dry season. However, climate models predict the disappearance of this buffer system below 5.500 masl by 2015, leaving one of the driest places on earth with yet another decrease in freshwater supply (Zapata 2008). The deviation of water resources from the highlands has led already to allocation conflicts. Peru is in urgent need of new concepts for water management.

Fog harvesting was introduced to South America in the 1980s and has since been implemented at various locations in North and Central America, Europe, Africa, Asia and Australia. The Standard Fog Collector (SFC) as described by Schemenauer and Cereceda (1994) has proven to be a successful instrument for this purpose. Apart from a number of small scale investigations, the design of the collector has barely been changed over the past three decades (e.g. Gioda et al. 1993). Within the framework of the presented project, financed primarily by the Global Exploration Fund of the National Geographic Society and Bayer AG, new fog collectors were designed at pilot and full scale.

Best results in terms of simplicity of construction and water yield were obtained by a metal frame structure called Eiffel. While covering the same amount of space as an SFC and using the same Raschel 65% shadow net, the Eiffel collector harvested up to 2.650 liters of water within a frame of 8x4m compared to up to 600 liters of water harvested by a SFC at the same location. In combination with a simplified maintenance concept, our collectors present an economically competitive alternative to water supply by truck delivery in a region that is not likely to be connected to a centralized water supply system within the next two decades. At the given water price and a given location, we calculate a break-even point after 8-9 years following the investment.

5th International Conference on Fog, Fog Collection and Dew
Münster, Germany, 25–30 July 2010
FOGDEW2010-94

Development of the one dimensional Fog Model PAFOG for operational Use at Munich Airport

C. Mohr (1), W. Schneider (1), M. Rohn (2), P. Röhner (2), B.-R. Beckmann (2), M. Masbou (1), and A. Bott (1)
(1) Meteorological Institute, University of Bonn, Germany, (2) German Meteorological Service (DWD), Offenbach, Germany

Reduced visibility due to heavy fog is a hazard for land, sea, and air traffic. Especially for air transportation systems, reduced visibility leads to significant cost increments. Therefore, it is of particular importance to predict poor visibility fog events at airports accurately. In iPort-VIS, part of an aviation research program funded by the German Ministry for economy and technology, a site specific fog forecast system for Munich airport will be developed in cooperation between DWD, the German Aviation Control (DFS) and University of Bonn. The principal component of this forecast system is the one dimensional fog forecast model PAFOG (PArameterised FOG) that will be upgraded to operational use.

The model consists of a parameterised microphysics scheme. The particle size distribution of cloud droplets is taken into account by a lognormal distribution and the visibility is calculated dependent on liquid water content and droplet concentration based on the Koschmieder formula. The turbulence in the atmospheric boundary layer is treated by the Mellor and Yamada closure scheme of order 2.5 in which a prognostic equation for the Turbulent Kinetic Energy (TKE) is solved. Radiative transports are considered by a Delta-Two-Stream Method with 18 spectral bands.

Due to the fact that fog is a small scale complex phenomenon with high spatial and temporal variability, detailed knowledge of the atmospheric boundary layer structure is fundamental to get a realistic fog forecast. A time nudging scheme has been developed for integrating local observations (vertical profiles of temperature and specific humidity) periodically during the forecast. The system has been tested in several case studies with data from Lindenberg observatory and will be adapted to Munich airport with a new measurement system that will be installed by DWD.
A second version of the nudging scheme, driven by the forecast of the high-resolution COSMO-DE model by DWD, is currently under development.

5th International Conference on Fog, Fog Collection and Dew
Münster, Germany, 25–30 July 2010
FOGDEW2010-95

European fog/low stratus climatology from satellite and ground data

J. Cermak (1), R.M. Eastman (2), J. Bendix (3), and S.G. Warren (2)

(1) ETH Zurich, Institute for Atmospheric and Climate Science, Zurich, Switzerland (jan.cermak@env.ethz.ch), (2) Department of Atmospheric Sciences, University of Washington, Seattle, USA, (3) Laboratory for Climatology and Remote Sensing (LCRS), Faculty of Geography, Philipps-Universität Marburg, Germany

Knowing the climatological distribution of fog and low stratus would allow for regional risk assessments and to estimate the radiative effect of these clouds. The study presented here uses geostationary satellite data (Meteosat Second Generation SEVIRI) to detect low stratus and fog, and to produce climatological maps on this basis. The maps are compared to ground-based observations. The focus of this study is on Europe.

The satellite technique used is based on a sequence of spectral and spatial analyses and validated against METAR observations. The methodology allows for the retrieval of low stratus clouds as well as ground fog situatiuons; it is found to be reliable and without a regional bias. Averaged maps covering several winter seasons of satellite data are analysed and compared to a cloud climatology based on a 26-year record of ground-based visual cloud observations. Maps are presented for the relative frequency of low stratus situations as well as for the number of hours with ground fog, making use of the very high temporal resolution available from a geostationary platform. The spatial patterns found in both products are found to be in good agreement and plausible.

5th International Conference on Fog, Fog Collection and Dew
Münster, Germany, 25–30 July 2010
FOGDEW2010-96

Study of fog characteristics by using the 1-D model COBEL at the airport of Thessaloniki, Greece

S. Stolaki, I. Pytharoulis and Th. Karacostas
Department of Meteorology and Climatology, School of Geology, Aristotle University of Thessaloniki, Greece
(sstolaki@geo.auth.gr / Fax: +30-2310-995392)

Abstract

An attempt is made to couple the one dimensional COBEL - ISBA (COuche Brouillard Eau Liquide - Interactions Soil Biosphere Atmosphere) model with the WRF numerical weather prediction model. This accomplishment will improve the accuracy of the short-term forecasting of fog events, which is of paramount importance -mainly to the airway companies, the airports functioning and the community as well- and will provide the means for the implementation of extensive studies of fog events forming at the "Macedonia" airport of Thessaloniki. Numerical experiments have been performed to study in depth the thermodynamic structure and the microphysical characteristics of the fog event that was formed on 6th of January 2010. Moreover, the meteorological conditions that prevailed during the formation of the fog event are also investigated. Sensitivity tests with respect to the initial conditions of temperature and relative humidity profiles have been performed to illustrate the model's performance. The numerical results have been thoroughly studied and the findings have been evaluated and discussed.

1. Introduction

Accurate and reliable information on expected visibility conditions at the airport of Thessaloniki-Greece, is of high importance, concerning safety and operational expenses for the airport and the airway companies. On the other hand, the life cycle of fog involves complex interactions among dynamical, turbulent, microphysical and radiative processes that are still not fully understood. Therefore, the implementation of an integrated weather-fog numerical model could be a very helpful tool, for understanding in depth the physical processes involved in the different stages of fog formation and consequently to accurately predict fog conditions. Several efforts have been made towards the forecast of low-visibility and fog conditions, either through the use of three-dimensional (3D) models ([5], [7], [8], [6], [11]), or the use of one-dimensional (1D) models ([1], [3], [2]).

The main objective on this work is to couple the 1D boundary layer model COBEL-ISBA (COuche Brouillard Eau Liquide - Interactions Soil Biosphere Atmosphere) with the version 3.1.1 of the WRF-ARW (Weather Research and Forecasting) regional non-hydrostatic atmospheric model, at the "Macedonia" airport of Thessaloniki (LGTS). High-resolution numerical experiments were performed in order to study the thermodynamic structure and the microphysical characteristics of the fog event that was formed on the 6th of January 2010 at the airport. This is an overview of a first attempt, with the means of a single column model, for a better understanding of the formation and dissipation of the fog event in Thessaloniki.

2. The COBEL-ISBA model

The COBEL model [developed in collaboration between the Laboratoire d'Aérologie-Université Paul Sabatier/Centre National de la Recherche Scientifique (CNRS) and Météo-France/Centre National de Recherches Météorologiques (CNRM)] is coupled with the land-surface scheme ISBA, as documented in [2] and it possesses a high vertical resolution, which consists of 30 levels between 0.5 and 1360 m, with 20 levels being below 200 m. ISBA is run with 7 levels in the ground, from 1 mm to 1.7 m below the surface level. The model input are the initial conditions and mesoscale forcings. The first are given by a two-step assimilation scheme, using local observations [2] consisting of: 2 m temperature and humidity, visibility and ceiling, temperature and humidity observations at 1, 5, 10 and 30 m from a measurement mast, radiative fluxes (short-wave and long-wave) at 2 and 45 m and soil temperature and water content at the surface, -10, -20, -30 and -40 cm. The available observations for the airport of Thessaloniki (40.52^{o}N, 22.96^{o}E) are very limited and consist of the operational half hour information provided by the station's METARs. Neither radiative fluxes data, nor mast measurements are available; therefore parts of the model code that make use of them have been deactivated. Mesoscale forcings are given by the WRF-ARW Numerical Weather Prediction (NWP) model. Since soil

temperature and moisture observations were unavailable, the forecast values of the NWP model were used.

3. The WRF model

The non-hydrostatic Weather Research and Forecasting model with the Advanced Research dynamic solver (WRF-ARW Version 3.1.1) was utilized in the numerical experiments. It is a flexible, state-of-the-art numerical weather prediction system, designed to operate in both, research and operational mode ([9], [12]).

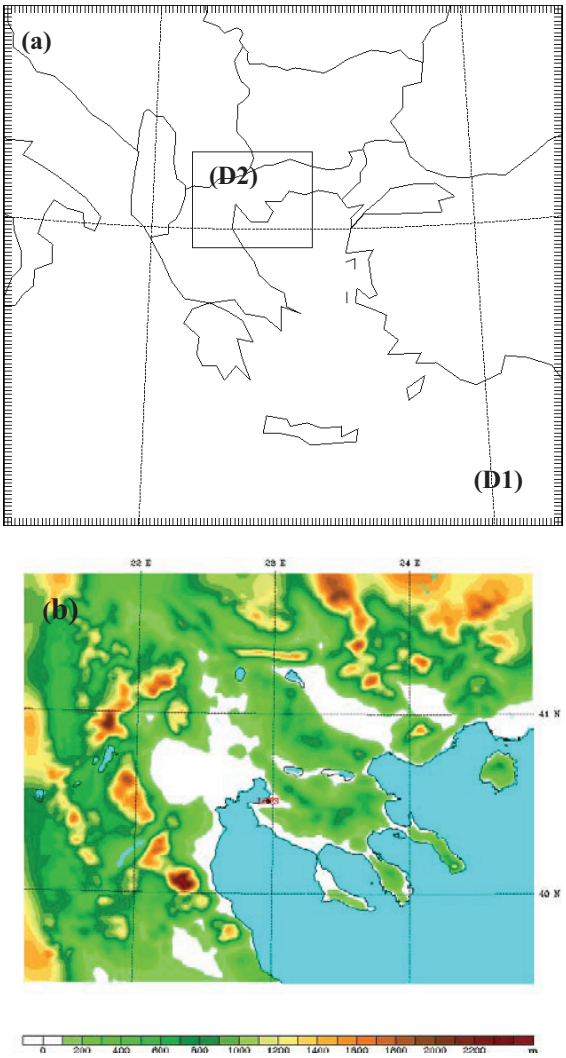

Figure 1. (a) The two nests used by WRF-ARW in the numerical experiments. (b) The topography of the inner domain (D02) and the location of the airport.

Two interactive model domains (Figure 1a) covering Balkans and the wider area of Macedonia (Figure 1b) at horizontal grid-spacings of 10km x 10km (D1) and 2km x 2km (D2), respectively, utilizing the staggered Arakawa C grid. Fine-resolution data (30''x30'') were used in the definition of topography, land use and soil type. Six-hourly ECMWF analyses at a horizontal resolution of 0.25^{o}x0.25^{o} were used as initial and lateral boundary conditions for the coarse domain, while the fine inner domain was two-way nested to the larger one. The sea-surface temperatures were also derived from the ECMWF analysis and were kept fixed to their initial values throughout the simulations. In the vertical, 38 sigma levels (up to 50 hPa) were used by both nests. The GFDL scheme, the Monin-Obukhov (Eta), Mellor-Yamada-Janjic, the NOAH Unified model and the Ferrier Eta scheme were used in both nests to represent longwave/shortwave radiation, surface layer, boundary layer processes, soil physics and microphysics, respectively. Cumulus convection was parameterized only in the coarse nest by the Betts-Miller-Janjic scheme.

Among the NWP mesoscale forcings that COBEL requires are the downward shortwave and longwave radiation under clear skies at the ground. In order to get the former, the GFDL shortwave radiation scheme was used. However, the latter is not provided by the NWP, therefore, it was estimated though the equation provided by [4] formula. This formula was chosen among others.

4. The fog event of 6th January 2010

Thessaloniki's International Airport is located 15 km south-southeast of city-center in a fog-prone coastal region with several geomorphological complexities (valley, mountain, coastline, urban and rural areas). The existence of the nearby Anthemountas valley and of the Chortiatis mountain (~1200 m) are of high importance, since a breeze, originated within the valley, descends from the slopes of the surrounding hills to the airport area, transferring already formed fog or providing the area with cold air from the valley [10].

On the 6th of January 2010, fog that extended to an area covering the whole airport and the surroundings -that is up to a radius of 5 km- formed and was quite thick, with estimated minimum visibility reaching 100 m (Figure 2). The fog event started at 05:20 UTC and ended at 10:50 UTC. According to the surface

synoptic conditions (Figure 3), northern Greece was influenced by an upper air low pressure system that resulted in a warm front affecting the region, while the airport area was mainly influenced by the warm sector of the front. A variable direction light breeze was prevailing a few hours before the fog onset.

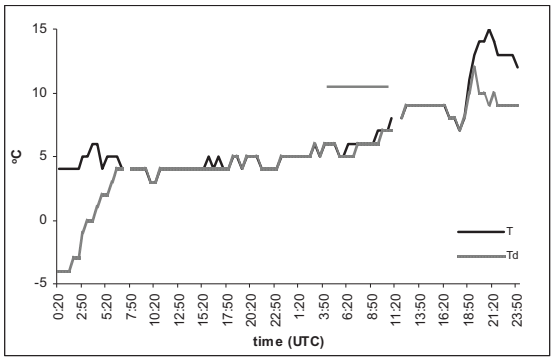

Figure 2. Temporal evolution of the 2 m temperature, dew point temperature for 5-6 January 2010. The fog period is highlighted with a grey line.

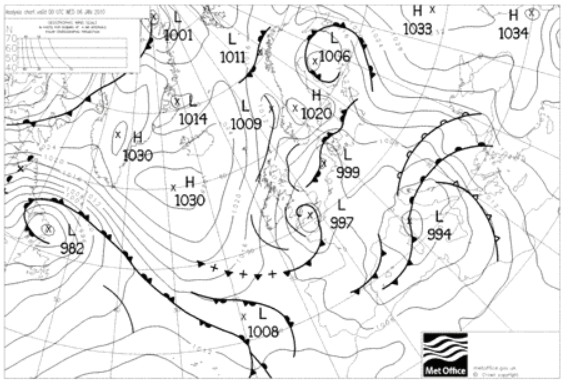

Figure 3. Surface synoptic conditions on the 6th January 2010, 00UTC.

4. Results

One of the first tasks, in order to successfully forecast the occurrence of fog at the airport of Thessaloniki, was the coupling of the COBEL-ISBA model with the WRF-ARW. To achieve this, an interface between the two models was developed, that vertically interpolates 16 meteorological fields, needed as mesoscale forcings for the initialization of COBEL, from the WRF vertical sigma level format into the COBEL format (the 15 required height levels above ground are at: 20, 50, 100, 250, 500, 750, 1000, 1250, 1500, 2000, 2500, 3000, 4000, 5000, 6000 m). The WRF data used in the interpolation correspond to 1h frequency forecasts, with initialization time on the 05/01/2010 at 1200 UTC. The simulation of COBEL was initialized at 1800 UTC on 05/01/2010 (before the fog onset) and a 24h forecast was produced. Moreover, the initial fog thickness was set a fixed value, since no radiative fluxes measurements were available.

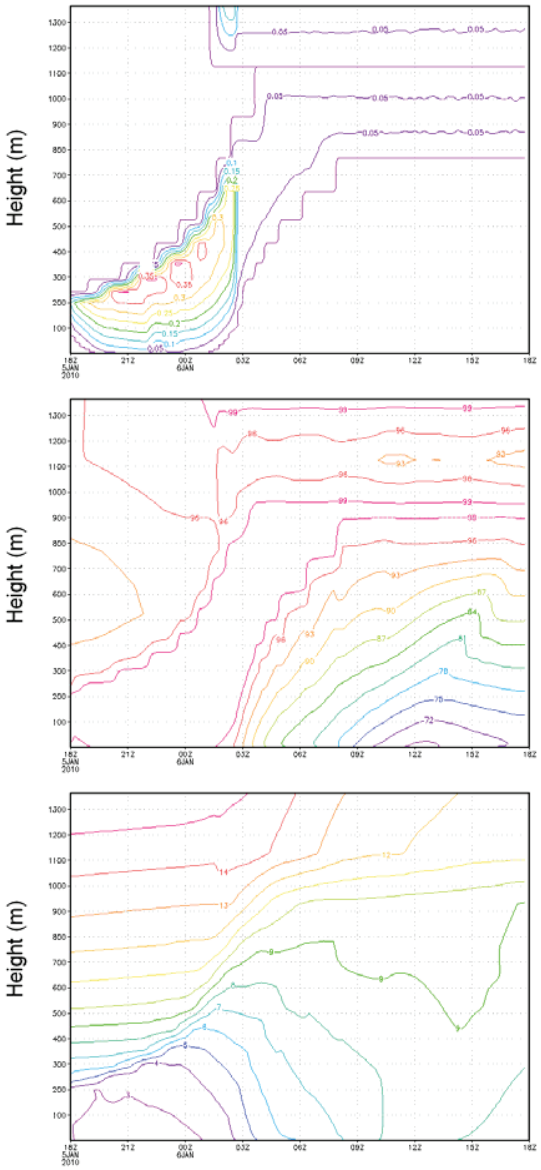

Figure 4. Time-height cross sections of the liquid water mixing ratio (gkg^{-1}), relative humidity (%) and potential temperature (^oC) by COBEL-ISBA, initialized at 1800 UTC, 06/01/2010.

The time-height cross sections of the liquid water mixing ratio, the relative humidity and the potential temperature simulated by COBEL-ISBA are presented in Figure 4. The integrated WRF and COBEL-ISBA modeling system did not manage to predict accurately the onset time of the fog event. Nevertheless, the high values of existing relative humidity and of the liquid water mixing ratio, are strong evidences of fog forming potentially on that day. Moreover, the values of the liquid water mixing ratio (0.05-0.35 gkg^{-1}), are found to be of the same magnitude as the ones in the literature for COBEL-ISBA outputs. Finally, the potential temperature cross section depictes a typical stable nocturnal boundary layer around 0000 UTC.

5. Summary and Conclusions

This study demonstrates the first attempt that has been made in order to simulate a fog event that occurred at the airport of Thessaloniki. For first time COBEL-ISBA model is used in a fog prone area of Greece, as a forecasting tool, coupled with WRF NWP model. The high values of liquid water mixing ratio and relative humidity indicate the ability of the model to simulate the potential of fog formation. However, the integrated WRF and COBEL-ISBA modeling system did not manage to simulate accurately the onset time of the fog event. Other model experiments regarding the study of the thermodynamic and microphysical structure of fog, as well as sensitivity tests in respect of the initial model conditions, are under way and will be presented during the 5th International Conference on Fog, Fog Collection and Dew, in Germany.

Acknowledgements

The authors would like to thank Météo-France/Centre National de Recherches Météorologiques (CNRM) for providing the 1D COBEL-ISBA local forecast system. Many thanks are also given to Dr. T. Bergot and Dr. S. Remy for their valuable help and support in accomplishing the adaptation and run of COBEL-ISBA at the area of Thessaloniki's airport.

References

[1] Bergot, T., and Guédalia, D.: Numerical forecasting of radiation fog. Part I: Numerical model and sensitivity tests. Mon. Wea. Rev., Vol. 122, pp. 1218–1230, 1994.

[2] Bergot, T., Carrer, D., Noilhan, J., and Bougeault, P.: Improved site specific numerical prediction of fog and low clouds: a feasibility study. Weather and Forecasting, Vol. 20, pp. 627–646, 2005.

[3] Bott, A., and Trautmann, T.: PAFOG-a new efficient forecast model of radiation fog and low-level stratiform clouds, Atmos. Res., Vol. 64, pp. 191-203, 2002.

[4] Brutsaert, W.: On a derivable formula for long-wave radiation from clear skies, Water Resour. Res., Vol.11, pp. 742-744, 1975.

[5] Clark, D.A.: The 2001 demonstration of automated cloud forecast guidance products for San-Francisco international airport. Proc.10th Conf. on Aviation, Range,and Aerospace Meteorology, AMS, 2002.

[6] Hikari, S., Kundan, L.S., Akira, K., Akikazu, K., and Yoshio, I.: Fog simulation using a mesoscale model in and around the Yodo River Basin, Japan. J. Environ. Sci., Vol. 20, pp. 838-845, 2008.

[7] Koračin, D.I., Businger, J.A., Dorman, C.E., and Lewis, J.M.: Formation, evolution, and dissipation of coastal sea fog, Bound.-Layer Meteor., Vol. 117, pp. 447–478, 2005.

[8] Müller, M.D., Masbou, M., Bott, A., Janjic, Z.: Fog prediction in a 3D model with parametrized microphysics. Proc. WWRP Int. Symp. on Nowcasting and Very Short-Range Forecasting. 6.26, 2005. http://www.meteo.fr/cic/wsn05/resumes longs/6.26-96.pdf

[9] Skamarock, W.C., Klemp, J.B., Dudhia, J., Gill, D.O., Barker, D.M., Duda, M.G., Huang, X-Y, Wang, W., and Powers, J.G.: A description of the Advanced Research WRF Version 3.NCAR/TN-475+STR, pp. 113, 2008.

[10] Stolaki, S.N., Kazadzis, A.S., Foris, D.V., Karacostas, T.S. Fog characteristics at the airport of Thessaloniki, Greece, Nat. Hazards Earth Syst. Sci., Vol. 9, pp.1541-1549, 2009.

[11] Tang, Y.M., Capon, R., Forbes, R., and Clark, P.:fog prediction using a very high resolution numerical weather prediction model forced with a single profile, Meteorol. Appl., Vol. 16, pp. 129-141, 2009.

[12] Wang, W., Bruyère, C., Duda, M., Dudhia, J., Gill, D., Lin, H-C, Michalakes, J., Rizvi, S., and Zhang, X: ARW Version 3 Modelling System's User Guide, NCAR-MMM, pp. 312, 2010.

5th International Conference on Fog, Fog Collection and Dew
Münster, Germany, 25–30 July 2010
FOGDEW2010-97

Contribution of cloud water to the groundwater recharge in Madeira Island: preliminary isotopic data

Susana Prada (1,2), José V. Cruz (2), Manuel O. Silva (1) and Celso Figueira (2)
(1) Centro de Ciência Exactas e da Engenharia da Universidade da Madeira, Campus Universitário da Penteada 9000-390 Funchal, Madeira, Portugal
(2) Centro de Estudos da Macaronésia, Campus Universitário da Penteada, 9000-390 Funchal, Madeira, Portugal
(3) Centro de Vulcanologia e Avaliação de Riscos Geológicos, Universidade dos Açores, 9501-801 Ponta Delgada, Portugal
(4) Departamento de Geologia da Faculdade de Ciências da Universidade de Lisboa , Edifício C6 – 2º Piso Campo Grande 1749-016 Lisboa, Portugal

Abstract

Situated about 600km southwest of mainland Portugal, in the North Atlantic, Madeira is the bigger and more populated island of the archipelago with the same name. It has a total area of 747km^2 and its northern slope forms a barrier that opposes the prevailing north-easterly trade winds, thus resulting in a very frequent windward fog belt, between 800-1600m a.s.l. Madeira has a 125km^2 area of indigenous altitude forests inside the windward fog belt, between 800-1600m a.s.l. This area is characterized by very steep slopes, mainly exposed to the prevailing winds. When combined, factors like steep slopes, great exposure to the humid trade winds and presence of forest vegetation facilitate fog precipitation. This is why we assume that fog precipitation is a generalized phenomenon throughout Madeira's northern slope area.

To ascertain whether or not fog water contributes to groundwater recharge, a study on the stable isotopic composition was made. For that purpose, assuming a difference between isotopic composition in rain and fog (fog being enriched in heavier isotopes ^{2}H and ^{18}O relative to rain at the same altitude and region), several samples of fog water, rain water and groundwater were collected for stable isotopic analysis. Groundwater was collected, according to from springs and tunnels representing perched and basal aquifers, respectively; fog water was collected on trees by hand by placing a funnel in a collection bottle and dabbing droplets which collected on the foliage, in rainless days of intense fog, under 98-100% relative humidity conditions, thus preventing sample evaporation enrichment; rain water was collected in containers with a 1cm thick layer of mineral oil to prevent evaporation, representing a sample of several rain events.

The preliminary stable isotopic compositions of fog, rain and groundwater samples collected are plotted in figure 1 along with the Global Meteoric Water Line (GMWL). The rain samples are the most isotopically depleted and fog samples the most enriched ones. Groundwater data is plotted in an intermediate position between the stable isotopic ratios for rain and fog waters.

The composition of groundwater may be explained by evaporation of the rain prior to infiltration. However, the isotopic composition of groundwater does not appear to depict any evaporative effects. So, the best explanation is that some of the fog water infiltrates and recharges the groundwater system of the Madeira Island, as observed in other regions.

1. Introduction

Situated at about 600km southwest of mainland Portugal, in the North Atlantic, Madeira is the biggest and more populated island of the archipelago with the same name. This volcanic island was originated more than 5.6 Ma ago by an oceanic hot-spot in the African Plate (Ech-Chakrouni, 2004). With a total of 737km^2, its rugged relief reaches a maximum altitude of 1861m a.s.l., at Pico Ruivo. The island forms an E-W oriented mountain range, resulting in a barrier to the prevailing north-easterly trade winds. The adiabatic cooling of the air masses that are pushed up the slopes of the island originates a very frequent windward cloud belt, between 800-

1600m a.s.l. This leads to events of thick, very moist and turbulent ground fog that can last for several days. Cloud water interception occurs when cloud droplets (essentially fog droplets of various sizes and sometimes drizzle) coalesce on foliar and woody surfaces as the cloud base passes through the canopy (Bruijnzeel *et al.*, 2005; Holder, 2003, 2004; Prada *et al.* 2009; Brauman *et al.*, 2010). In the absence of the vegetation, this water would not precipitate into the soil in significant quantities (Cunha, 1964; Davis and DeWiest, 1991). Different factors influence the amount of cloud water intercepted. Among these, cloud droplet size, cloud liquid water content, vegetation size and morphology, site exposure to wind and wind velocity are the most important. The cloud belt occurs in an area that is characterized by steep slopes, mostly covered by indigenous altitude forest (Prada *et al.,* 2008) and it is assumed that cloud interception is a common phenomenon along the area (Prada *et al.*, 2010).

Groundwater is the most important water supply source in Madeira. As such, knowledge about the island's water cycle is important for a correct management and evaluation of water resources. The objective of this work was to determine if cloud water contributes to groundwater recharge. Cloud water is normally enriched in the heavier isotopes ^{2}H and ^{18}O relative to rain at the same altitude and region (Ingraham and Mathews 1988, 1995; Clark and Fritz, 1997). By comparing the isotopic composition of both of them with groundwater, it is possible to determine if recharge occurs essentially through rain infiltration, or if it is a mixture of rain and cloud water.

2. Materials and Methods

Groundwater samples were collected, according to Clark and Fritz, (1997), from springs and tunnels throughout the island, representing perched and basal aquifers, respectively. Cloud water was collected on trees by hand by placing a funnel in a collection bottle and dabbing droplets which collected on the foliage, in rainless days of intense fog, under 98-100% relative humidity conditions, thus preventing sample evaporation enrichment. Rain water was collected in containers with a 1 cm thick layer of mineral oil to prevent evaporation according to Clark and Fritz (1997) and School *et al.*, (2002), representing a sample of several rain events. Both rain and cloud water were only sampled at altitudes above 1000m a.s.l., due to the fact that groundwater recharge mainly occurs above this level (Prada *et al.*, 2005).

3. Results and discussion

The preliminary stable isotopic compositions of fog, rain and groundwater samples collected are plotted in Figure 1 along with the Global Meteoric Water Line (GMWL), first described by Craig (1961). The rain samples are the most isotopically depleted and fog samples the most enriched ones. Groundwater data is plotted in an intermediate position between the stable isotopic ratios for rain and fog waters.

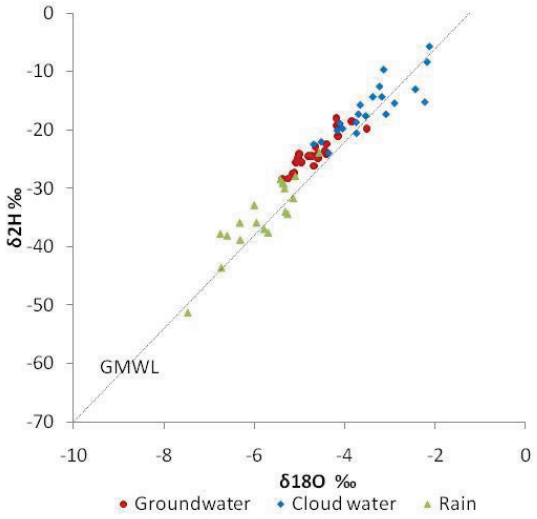

Figure 1: Graphic with plotted rain, cloud water, groundwater and the GMWL. Groundwater (red circles) is isotopically enriched when compared to rain water (green triangles). This shows evidence that cloud water is an alternative source of groundwater recharge.

The composition of groundwater may be explained by evaporation of the rain prior to infiltration. However, the isotopic composition of groundwater does not appear to depict any evaporative effects. So, the best explanation is that some of the fog water infiltrates and recharges the groundwater system of the Madeira Island, as observed in other regions by Ingraham and Matthews (1988; 1995).

4. Summary and Conclusions

The preliminary isotopic results show that groundwater in Madeira has a different isotopic composition from that of the meteoric water in the recharge area. There is evidence that at least some cloud water infiltrates and recharges the aquifers. Further analysis of the data is currently being performed. With this, we expect to refine Madeira's hydrological model through a better understanding of recharge altitudes, water origins and groundwater dynamics.

Acknowledgements

We would like to thank Ana Nunes, Ricardo Ramalho, Bárbara Lucas, Isabel Sengo, Ana Pontes and Ana Luísa Fernandes for their work during the sample collection campaigns. We also thank the INTERREG III B "AQUAMAC" project.

References

[1] Brauman, K.A., Freyberg, D.L., Daily, G.C.: Forest structure influences on rainfall partitioning and cloud interception: A comparison of native forest sites in Kona, Hawai'i. Agr. Forest Meteorol. 150, pp.265-275, 2010

[2] Bruijnzeel, L. A., Eugster, W., Burkard, R.: Fog as a hydrologic input, in: Anderson, M. G., McDonnell, J. (eds.), Encyclopedia of Hydrological Sciences. John Wiley & Sons, Ltd., Chichester, pp. 559-582, 2005

[3] Clark, I. and Fritz, P.: Environmental isotopes in Hydrogeology. Lewis Publishers, 1998

[4] Craig, H.: Isotopic variations in meteoric waters. Science, 133, pp. 1702-1703, 1961

[5] Cunha, F.: O problema da captação da água do nevoeiro em Cabo Verde. Garcia de Orta 12, pp.719-756, 1964

[6] Davis, S.N. and De Wiest, R.J.M. Hydrogeology. Krieger Publishing Company, Florida, 1991

[7] Ech-Chakrouni, S.: Géochronologie et paléomagnétism de l'île de Madère et dês îles Desertas. Une contribution à la volcanostratigraphie et à l'évolution de l'archipel de Madère, et à l'échelle de polarité du champ magnétique. PhD thesis Vrije Universiteit, Brussell., 2004

[8] Holder, C.D.: Fog precipitation in the Sierra de las Minas Biosphere Reserve, Guatemala. Hydrol. Process. 17, pp.2001-2010, 2003

[9] Holder, C.D.,: Rainfall interception and fog precipitation in a tropical montane cloud forest of Guatemala. Forest Ecol. Manag., 190, pp.373-384, 2004

[10] Ingraham, N. L. and Matthews, R. A.: Fog drip as a source of ground water recharge in Northern Kenya. Wat. Resour. Res. 24, pp.1406-1410, 1988

[11] Ingraham, N. L. and Matthews, R. A.: The importance of fog-drip water to vegetation: Point Reys Peninsula, California. Journal of Hydrology, 164, pp.269-285, 1995

[12] Prada, S., Menezes de Sequeira, M., Figueira, C., Prior, V., Silva, M.O., 2010. Response to "Comment on fog precipitation and rainfall interception in the natural forests of Madeira Island (Portugal)". Agr. Forest Meteorol., 150, 1154-1157

[13] Prada, S., Menezes de Sequeira, M., Figueira, C., Silva, M. O.: Fog precipitation and rainfall interception in the natural forests of Madeira Island (Portugal). Agr. Forest Meteorol. 149, pp.1179-1187, 2009

[14] Prada, S., Menezes de Sequeira, M., Mesquita, S., Gaspar, A., Figueira, C., Pontes, A., Silva, M.O.: Avaliação preliminar do contributo global da precipitação oculta para os recursos hídricos da ilha da Madeira. CD-ROM das comunicações do 9ºCongresso da Água, pdf 21, Cascais, Portugal, 2008

[15] Prada, S., Silva, M.O. and Cruz, J.V.: Groundwater behaviour in Madeira, volcanic island (Portugal). Hidrogeol. J., 13, pp.800-812, 2005

[16] Scholl, M. Gingerich, S., Trible, G.W.: The influence of microclimates and fog on stable isotope signatures used in interpretation of regional hydrology: East Maui, Hawaii. J. Hydrol. 264, pp.170-184, 2002

5th International Conference on Fog, Fog Collection and Dew
Münster, Germany, 25–30 July 2010
FOGDEW2010-98

Alto Patache fog oasis in the Atacama Desert: Geographical basis for a sustainable development program

M . Calderón, P. Cereceda, H. Larrain, P. Osses, L. Pérez and M . Ibáñez
Atacama Desert Center, Pontificia Universidad Católica de Chile (mccalderon@uc.cl, dcereced@uc.cl / Fax: +56-2-5526028)

Abstract

Alto Patache coastal fog oasis is a State protected area due to its rich biodiversity. It is located south of Iquique, Northern Chile, being presently in charge of the Atacama Desert Center (ADC) of the Pontificia Universidad Católica de Chile. On 2007, the Chilean Government bestowed a land stretch covering 1,114.5 hectares to ADC for scientific research, ecosystem protection and environmental education. This oasis has been studied since 1997 from different aspects like climate, fog collection, geomorphology, soil survey, biogeography, flora and fauna distribution, conservation, history and archaeology.

During 2009, a study of the geographical basis to elaborate a general management plan was undertaken to collect information to accomplish the planned out objectives. Through this study, geo-referenced strategic information was compiled to evaluate future actions conducting to a sustainable development within the protected area. This information was translated into geographical thematic maps showing the spatial distribution of the specific variables. The methodology used was the analysis of remote sensing imagery, intensive and systematic field work and GIS as an integration tool.

The paper's core shows that three climate types influence the geography and ecosystems of the area. The biogeographical contrast between the foggy section, and the areas located below the stratocumulus cloud influence and the hills out of its influence in the "sunshine", show important features for the understanding of the area complexity. Two soil types could be found: Entisols (Torriorthent) and Aridisols. Vegetation consists not only of a very rich lichen and soil crust cover along the foggy area, but also of endangered vascular species associations constituting a very fragile sub-tropical coastal desert community. Fog oasis runs from 600 - 850 m a.s.l.

Future human activities at place should be restricted to scientific studies, ecosystems conservation, experimental site, environmental education and eco-tourism of special interest. The uniqueness and the fragility of the place are here the most important issues. Questions are: how, where and when these activities can be practiced inside the oasis without risking its vulnerability.

1. Introduction

The fog oasis of Alto Patache in the Tarapacá Region has been given in concession by the Chilean Ministry of Bienes Nacionales to the Pontificia Universidad Católica de Chile for 25 years with the objectives of protection and conservation of the ecosystems, research activities and environmental education. It covers 1,114.5 ha lodged in a desert environment possessing significant geographical features. These are: a littoral plain, an abrupt cliff more than 600 m of elevation, a huge climbing sand dune and the first mountains of the Cordillera de la Costa, a major geoform in the Atacama Desert. Its most important trait is the plant ecosystem, where several species of plants and animals survive mainly on the water provided by fog and dew (fog has been studied; dew is an aspect which has to be tackle with in the future).

The main goal of this study was to undertake a detailed survey of all the geographical and cultural features being necessary for the design of a master plan of occupation and protection. It is necessary to do a sustainable use of the area, especially in connection with the future scientific research. The place is seen as a laboratory to test different results of applied research, such as energy resources (eolian and solar), water (fog and dew), architecture (houses and materials designed for arid conditions), land art, environmental education, tourism of

special interest, amongst others. Certainly it is a challenge for arid land sustainability and an example for other similar places in Chile and in deserts of the world.

To exactly define zones for the future different uses of the fog oasis based on its environmental fragility and the needs of creating a natural laboratory for scientific research, is the main purpose of this study.

2. The study area

Alto Patache is located in the Tarapacá Region in the north of Chile. It lies in the Coastal Atacama Desert where the precipitation is the minimal in the country, averaging 0.2 mm per year in the last 30 years. Tarapacá has a surface of 42,226 km2, with a population of 240,000 inhabitants, mainly located in the neighbor cities of Iquique and Alto Hospicio (95%). Because of its aridity and lack of conditions for agriculture, the rural population is scarce and is located mainly in valleys and inland. At the coast, people live in small villages and are dedicated to fishing activities. Less than 1.000 persons live in that littoral area, mainly because of lack of water which is only available by truck. Mining is the main regional economical activity; the most important copper mines are located in the high Andes; people live in the two coastal cities and work in turns in modern settlements near the mines. In the Cordillera de la Costa population is practically absent (Fig.1).

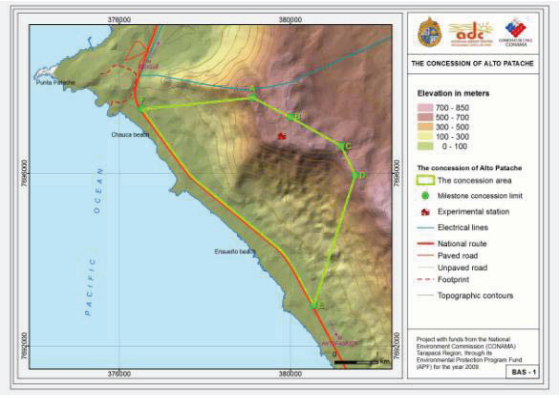

Figure 1: The study area in the Tarapacá Region.

3. Methodology

The general objective of the study was to evaluate the geographical conditions of the fog oasis of Alto Patache with all its natural and cultural features, which may allow tracing a master plan of site occupation. The specific objectives were: a) to make a detailed survey of the climate types and fog present in the area; b) to study its geology, geomorphology, ecosystems, soils, flora and fauna; and c) the cultural aspects such as archaeology and historical evidence.

Almost all the information needed was extracted from our own studies done during the last 12 years [1-9]. The Geomorphology and Soils required a specific study only [10].

Several geographical studies of fog oases have been presented by our team in the four Conferences on Fog and Dew, since 1998 being Tarapacá the area showing the great majority of investigations related to fog and its spatial and temporal distribution. The climatic zones presented here were defined based on 3 official Meteorological Stations and 2 years of temperature and humidity sensors in Patache [2, 5]. Fog water potential collection comes from Standard Fog Collectors (SFCs) located at different elevations and exposures in the Alto Patache oasis [1, 3].

The geological and geomorphological surveys were practiced using satellite-photo-interpretation of the area geo-forms and substrate identification [10] The soil survey was done through soil morphology evaluation, to answer explanations about some important properties of arid soils, digging trenches in specified sites to get samples for soil texture and structure, bulk density, electrical conductivity and others, distributed in a soil map, showing soils types and properties at a 1:10.000 scale.

Site ecosystems were studied during the last 12 years; vegetation has been surveyed following different soil features influenced by the stratocumulus cloud, fog and wind direction [4]. Botanical studies identified the species present [8] and the botanical ADC team has been working in spatial distribution and seed bank studies. The entomological chart was constructed on the basis of 5 year trapping records already published in several papers, including a Fog Conference [9]. The cultural aspects reflected in the archaeological and historical record, were based on several field surveys and two student theses now in process [6, 7].

4. Results

According to the objectives and the methodology described, the following results were obtained. Alto Patache fog oasis was mapped in ARC GIS 9.3 with the official boundary and official marks; important sites such as the field station, experimental nursery and the educational site, the location of SFCs, trails, were marked in map together with the local denominations assigned by the team.

Two different climates types according to the Chilean classification can be found in the study area: at the coast, BWn, that is "Desert with Abundant Cloudiness" and BW "Normal Desert". After the researches done in Patache, a BW fog type of climate for Chile has been proposed. [3]. These maps also include areas of light and dense fog (Fig. 2).

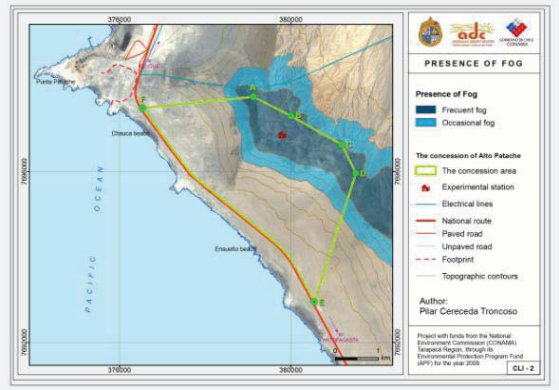

Figure 2: Presence of fog.

Fog oases are located usually near the coast, in mountain slopes, cliffs or plains at altitude between 600 and 1200 m a.s.l. The marine cliff represents a major geomorphic feature near Iquique dated from Upper Miocene age with Pliocene transgression reaching 800-900 m of altitude in Alto Patache area. At the base of coastal cliffs area, sea sandy terraces are found from 0-300 m (Fig. 3).

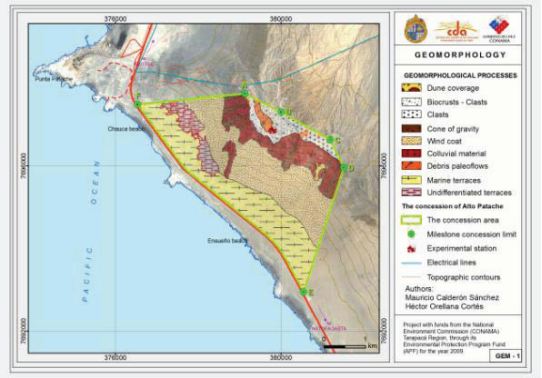

Figure 3: Geomorphology map

The Patache soils from the coastal area were classified as Torriorthent, with sandy texture, low organic matter content and salt abundance in profile

while the soils located at cliff barriers are classified like gypsic and sodic Solonchack, with a 100% base saturation percentage and a 15-52 dS/m of Electrical Conductivity. The traditional land use pattern of these soils is basically used for wildlife, with a land use capacity type VIII and extensive problems of eolic erosion.

A special map shows the different vegetal associations in their exact location in relation to altitude and topography, indicating the species present in the area. The local flora appears only in the foggy area, and their distribution is strongly related to topographical factors such as the relief, exposure to the winds, type of substrate and soils (Fig. 4).

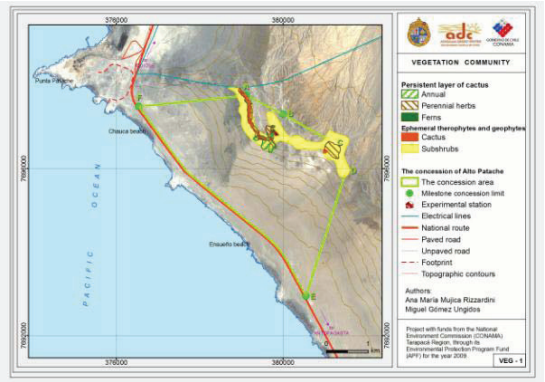

Figure 4: Vegetation map

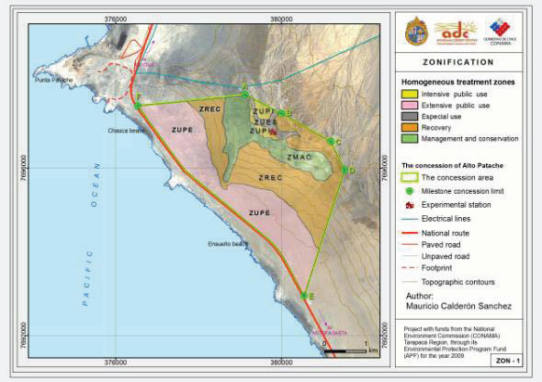

Figure 5: Zonification map

Alto Patache ecosystem shows a variety of shrub and herb species, depending on altitude, type and orientation of relief, plateau or cliff. Furthermore, this geomorphic aspect are relevant in soil types formation with high level of salts, dry profile and scarce evolution, where despite its aridity some cacti, perennials and annual plants occur, generating the "lomas" formations, restricted to fog-zone locations. The results of the surveys were summarized in a map offering a first proposal of management, where 5 homogenous zones were identified: i) intensive public area, ii) extensive public use, iii) special use, iv) recovery and v) conservation (Fig. 5).

5. Conclusions

Alto Patache fog oasis has been studied from several viewpoints, since 1997. A set of 12 maps scale 1: 10.000 show the variety of themes so far studied. More than 30 publications (including doctoral thesis) have been edited.

Totally isolated, its fauna and flora reveals a high percentage of endemism. Several species of small arthropods, lichens and soil crusts wait still for a scientific identification. Various insect and flora local species have been identified as new species since 2000. Oasis ecosystem, being very fragile, urgently needs special protection. At present, it shows many plant specimens dying or decaying.

Alto Patache fog oasis suffers nowadays a severe desiccation process due to global heating, decrease of precipitations and probably also to nearby industrial processes contaminating the whole area.

Until present, this northern coastal fog oasis is the only one in Chile to be subjected to diversified studies dealing with geography, archaeology, history, climatology, biology, pedology and specially about the possibilities of community involvement in its use.

The spot, showing a defined new type of climate in Northern Chile, seems particularly apt for environmental education. Hundreds of local school children have been instructed in situ on the peculiarities of this fog ecosystem and is open to students of the region, Chile and of the world.

Acknowledgements

We are grateful to PUC, CONAMA and CONICYT for the support of our researches. Special thanks to the many professors and students that have worked with the authors of this article (no space for names...).

References

[1] Cereceda, P., Larrain, H., Osses, P., Schemenauer, RS., and Farías M. Radiation, advective and orographic fog in the Tarapacá Region, Chile. Atmospheric Research, Volume 64, Issues 1-4, Pages 261-271, 2002.

[2] Cereceda, P., Larrain, H., Osses, P. Farías M. and Egaña, I.: The climate of the coast and fog zone in the Atacama Desert of Tarapacá Region, Chile. Atmospheric Research Volume 87, Issues 3-4, 301-311, 2008.

[3] Cereceda, P., Larrain, H., Osses, P., Farías, M. and Egaña. Spatial and temporal behavior of fog and its relation to fog oases in the Atacama Desert, Chile. Atmospheric Research volume 87 Nº Issues 3-4, Pages 312-323. 2008.

[4]Egaña, R. Pinto, P. Cereceda, H. Larrain, P. Osses y M. Farías (2004). Estudio biogeográfico de la comunidad arbustiva del farellón costero de Punta Patache, Chile. Revista de Geografía Norte Grande 31: 99-113, 2004.

[5]Larrain, H., Velásquez, F., Espejo, R., Pinto, R., Cereceda P., Osses P. and Schemenauer R.S. Fog measurements at the site "Falda Verde, (Chile) compared with other North Chilean fog stations. Atmospheric Research, Volume 64, Issues 1-4, Pages 271-284, 2002.

[6]Larrain, H., González, B., Velásquez, F., Cereceda, P., Osses, P. Archaeological and geographical evidence of guanaco (lama guanicoe müller 1776) hunting at the fog-site of Alto Patache (20º40´s & 70º 09´w), south of Iquique. 2nd Southern Deserts Conference: Human - Environment Interactions in Southern Hemisphere Deserts: Past, Present, and Future" Chile, 2005.

[7]Navarro M., Larrain H., Pérez and Cereceda P. Collection of atmospheric water at Alto Patache Fog Oasis by coastal prehistoric inhabitants new archaeological perspective. Proceedings Fourth Internacional Conference on Fog, Fog Collection and Dew, Chile 247-250, 2007

[8]Pinto, R., Larrain, H., Cereceda, P., Lázaro, P. Osses P., and R.S.Schemenauer. Monitoring fog-vegetation communities at a fog site in Alto Patache Chile, during El Niño and La Niña events. Proceedings Second conference on fog and fog collection 293-296 Canada, 2001.

[9]Sagredo, E., Larrain, H., Cereceda, P., Ugarte, A., Osses, P., y M. Farías Variación espacio-temporal de la entomofauna de Coleópteros en el oasis de niebla de Alto Patache (20°49´S; 70°09´W) y su relación con factores geográficos. Revista de Geografía Norte Grande, 29: 121-133, 2002.

[10]Orellana H. 2010Aspectos geodinámicos del desierto costero de Atacama, sector Alto Patache (Oasis de Niebla) y Bajo Patache. Memoria para optar al título profesional de Geógrafo. Universidad de Chile, Santiago. 2009.

5th International Conference on Fog, Fog Collection and Dew
Münster, Germany, 25–30 July 2010
FOGDEW2010-99

Studies of the multiphase cloud system at Mt. Brocken

G.P. Frank (1), K. Acker (2), S. Sjögren (1), M. Berghof (1), D. Kalass (2), W. Wieprecht (2), B.G. Martinsson (1), and D. Möller (2)

(1) Lund University, Dept. of Physics, Lund, Sweden (goran.frank@pixe.lth.se), (2) Brandenburg Technical University, Department of Air Chemistry, Cottbus, Germany

Aerosol particles, particularly via their interaction with clouds, have been identified to exert most of the uncertainties in current quantifications of climate change forcing. The intricate interaction of aerosol properties and meteorology in cloud development is a challenging task to investigate. In addition, every single cloud is unique, since the aerosol properties and meteorological conditions are highly variable with space and time.

Here we will present results from detailed studies of cloud microstructure and aerosol-cloud interactions in the cloud formation process. Focus will be on warm clouds occurring at Mt. Brocken (1142 m a.s.l., Harz Mountains, Germany).

Central to the measurements is the Droplet Aerosol Analyser (DAA) (Martinsson, 1996; Frank, 2001). The DAA is an instrument especially developed for studies of fog and clouds, and measures the ambient diameter of individual droplets and interstitial particles in a fog or a cloud. It then measures the diameter of the individual residual particle after evaporation of the water in a diffusion drier. It also counts the number of dry particles of each size. This gives a unique three-parameter data set that connects ambient size to dry size and to the number of particles and droplets, thus connecting ambient number size distribution to dry residual number size distribution.

An improved version of the instrument was tested during September-October 2009 at Mt Brocken. Continuous studies will start in spring 2010. Concurrently a number of other atmospheric components (reactive gases, meteorological parameters) and relevant cloud physical features (e.g., liquid water content, cloud base height) are measured. The results of these studies will be discussed in detail within this contribution. Comparisons will be made with results from fog studies in Lund.

References:
Martinsson, 1996: Physical Basis for a Droplet Aerosol Analysing Method, J. Aerosol Sci., 27, 997-1013
Frank, 2001: Experimental Studies of the Interaction of Atmospheric Aerosol Particles with Clouds and Fog, PhD thesis, http://nuclearphysics.pixe.lth.se/theses/gf.asp

5th International Conference on Fog, Fog Collection and Dew
Münster, Germany, 25–30 July 2010
FOGDEW2010-100

Recent Fog trends and its impact on wheat productivity in NW plains in India

S. Singh and D. Singh

Department of Agricultural Meteorology, CCS Haryana Agricultural University, Hisar-125004, India
(surendersd@yahoo.com / Fax: +91-1662-234952)

Abstract

Observations on fog events recorded at Agrometeorological Observatory at Hisar, India (Lat: 29°10'N, Long: 75°41'E and Alt: 209.1 m amsl) representing North-west plains in India during winter season for the recent period 1993 to 2008 have been analyzed. The study period was so chosen because of significant climatic aberrations reported by IPCC[1]. In the region, the fog season is generally considered from November to February, with the months of December and January witnessing the longest durations of dense fog. The cumulative foggy days in the region ranged between 18 to 52 during the winter/rabi seasons (1992-93 to 2007-08). The maximum (52) and minimum (18) numbers of foggy day were observed during winter/rabi season 2007-08 and 1997-98, respectively. On an average, the dense fog was witnessed for just 3-5 hours during the months of November and February while December and January experiences about 95 per cent of dense fog durations under reference. The conditions became conducive for formation of dense fog as there was little difference between day and night temperatures with no winds. Interestingly, an increasing trend (@ ~ 2 day/season) in occurrence of fog events was seen during the period under report. Maximum foggy events (25) in a month were recorded in December, 1998. Average maximum foggy events (12) recorded in a month were observed in January. All the Niño years (SST>0.5°C) received above normal rainfall (50.0 mm) in fog season, but the deficient rainfall was recorded during Niña years (SST<-0.5°C); though, there seems no direct correlation between seasonal rainfall and teleconnections but the foggy events prevailed during/after the passage of WDs. The seasonal rainfall's associated weather system i.e. Western Disturbances (WDs) coming over NW plains in India from far west countries Afganistan & Pakistan. The WDs and fog events showed strong relation over the region. The growth and development of winter wheat was adversely affected due to reduced or no PAR available for photosynthesis, cold stress and congenial conditions for diseases and insect-pest development in the region.

1. Introduction

Fog season is generally considered from November to February, with the months of December and January witnessing the longest durations of dense fog in North-west plains of India[2, 3]. Fog is nothing but cloud at ground level condensation of invisible water vapor in air into visible droplets of water. Fog occur most of the time during cold and nearly calm conditions when the air is saturated (a RH around 100 %). Fog plays an important role in the earth's ecosystem being a medium for the exchange of water and pollutants between the atmosphere and the biosphere[4]. The feasibility of a fog water collection system depends on the availability of a site where relatively large amounts of water can be collected and fog may be measured on top of canopy to estimate its impact on the crop beneath[5]. Fog which often occurs in the winter time during stable weather situations plays an important role in tropics affairs and air quality all over the world. Fog climatology based on satellite remote sensing using time series data is important because long term knowledge of regional changes in fog frequency and fog properties are of over all importance for Global Circulation Model simulations dealing with global climate change[6]. The frequency of occurrence of fog is so high that the foggy conditions persist for number of days together over a larger area in winter season (November through February). The study of fog intensity and its continuity over NW plains is of paramount importance as being sensitive indicator of regional climate change. Therefore, an attempt has been made here to characterize the fog events and their impact on winter wheat productivity in semi-arid NW plain region in India.

1.1 Study domain and data base

Systematic meteorological records during the winter seasons (November to February) for period 1992 to 2008 for Hisar (Latitude 29°10'N. Longitude 75°41'E and Altitude 209.1 meters) representing semi-arid NW plain region of India have been considered for aforementioned study. The fog data were taken from CWS 27 (b) format of India Meteorological Department recorded at Agrometeorological Observatory at Research Area of Department of Agricultural Meteorology, Chaudhary Charan Singh Haryana Agricultural University, Hisar, India. Daily records on maximum and minimum temperature, relative humidity, bright sun-shine hours and number of foggy days and their duration have been taken for calculating monthly and seasonal values. The relevant data on teleconnections, WDs and wheat productivity were taken from e-resources of BOM, Darwin, IMD and Statistical Abstract of Haryana, respectively.

2. Foggy events and associated weather variables

During the entire winter season (wheat growing season), the more number of foggy events were observed in coolest months (December and January) and minimum events in comparatively warmer (November and February) months. However, the range of foggy events was highest (4 to 25) in January month (Table 1). The foggy days in entire winter season ranged between 18 to 52 during the whole growing period under study. Maximum foggy events (25) in a month were recorded in January, 2003. Average maximum foggy events (12) too were recorded in the month of January. In a particular winter season, the highest foggy events (52) were recorded during 2007-08 and the minimum (18) during 1993-94 (Figure 1). Interestingly, an increasing trend (@ ~ 2.0 day/season) in occurrence of fog events was noticed.

Table 1. Foggy events and associated weather variables

Events /Variable (s)	November	December	January	February
Foggy Days	3 (1-16)	9 (3-20)	12 (4-25)	4 (2-9)
T_{max} (°C)	28.4 (26.2-30.6)	21.3 (17.1-24.3)	18.6 (14.4-23.2)	21.5 (16.2-23.8)
T_{min} (°C)	9.3 (2.9-11.5)	5.0 (2.2-6.7)	3.8 (0.9-5.8)	4.8 (2.7-7.8)
RH_{mor} (%)	88	92	90	86
BSS (hrs)	6.3	5.9	5.7	7.2

About 41 per cent of variability in foggy events can be explained over the time due to regional climatic variability. {y = 1.69 x + 16.72 (R^2=0.41)}. Such occurrence in foggy events may be attributed to sharp fall in temperatures and above 95 per cent relative humidity along with calm conditions in the atmosphere. Satellite based remote sensing monitoring of the region showed continued prevalence of foggy conditions (3-4 weeks) for days together (Figure 2) which helped considerably in weather forecasting and impact assessment of such events on crop productivity. The minimum temperature during winter season ranged between 2.9 to 11.5°C as against normal range of 4.6 to 9.6°C. Similarly, maximum temperature ranged between 14.4 to 30.6°C and bright sun-shine hours ranged between 5.7 to 7.2 hours as against normal range of 20.5 to 28.7°C and 7.3 to 8.5 hours, respectively during the winter seasons of study period (Table 1). These wide ranged fluctuations in weather variables too indicted regional climatic variability in global climate change perspectives.

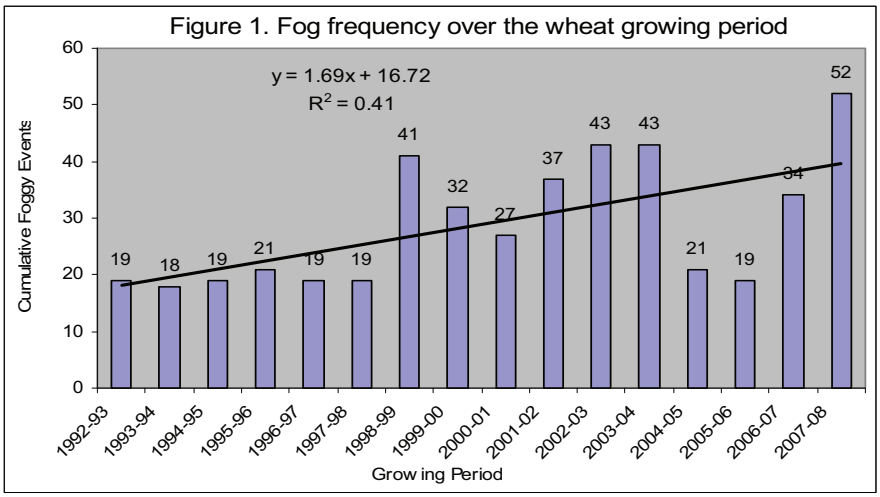

2.1 Teleconnections and their impact

All the Niño years (SST>0.5°C) received above normal rainfall (50.0 mm) in fog season, but the deficient rainfall was recorded during Niña years (SST<-0.5°C); though, there seems no direct correlation between seasonal rainfall and teleconnections but the foggy events prevailed during/after the passage of WDs. The seasonal rainfall's associated weather system i.e. Western Disturbances (WDs) coming over NW Indian region from far west countries Afganistan & Pakistan. The WDs and fog events showed strong relation over the region.

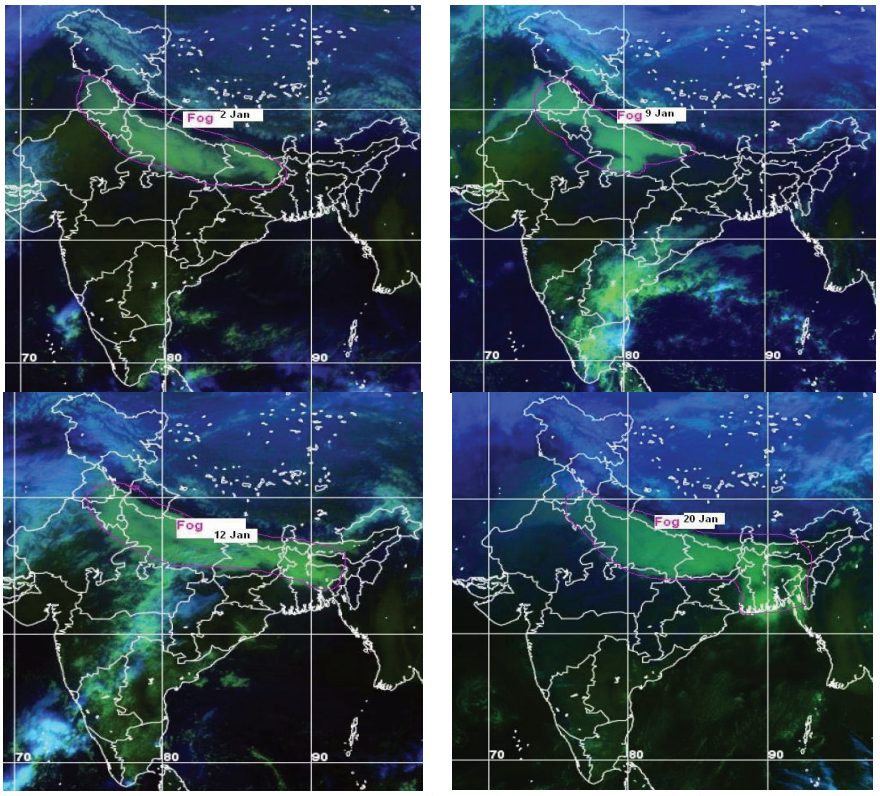

Figure 2. Recent Persistence Foggy conditions (January, 2010) in the NW plains

3. Summary and Conclusions

Frequency and duration of foggy events have increased in winter season of 1993 through 2008 as compared to long term normals at Hisar, India. Such type of continued and varied climatic situations in the region affecting the agricultural productivity adversely and symbolized the shift in local climates due to global climatic changes. Continued foggy conditions for days together especially more than a week caused considerable damage to field crops like wheat The growth and development of winter wheat was adversely affected due to reduced or no PAR available for photosynthesis, cold stress and congenial conditions for diseases and insect-pest development in the region. Simple and multiple regression equations using fog events explained 45 to 60 per cent variations in wheat productivity. It may be concluded that the regional climatic variability may be the reason of increased duration and frequency of foggy events in the region and thus, the meteorological variables need to be monitored carefully for better predicting of ensuing foggy conditions and to negotiate these conditions up to some extent particularly for crop production operations for sustainable agricultural development. Thus, strategies are needed to predict the sustenance of foggy conditions over the region using remotes sensing technology viz., satellite monitoring of the region[7] which may provide a better approach in getting useful information essential for fog forecasting and dew research for water trapping/collection in continued foggy weather for sustainable wheat production in otherwise moisture deficit semi-arid region of NW plains in India.

References

[1] Intergovernmental Panel on Climate Change.: Climate Change: Impacts, Adaptation and Vulnerability, Contribution of Working Group II to the Fourth Assessment Report of the Intergovernmental Panel on Climate Change, Cambridge Univ Press, Cambridge, UK, 2007.

[2] Verma, R.K.: Fog over Lucknow airport. Vayu Mandal, Vol. 19 (1-2), pp. 39-42, 1989.

[3] Samui, R.P. and Gupta, D.C.: Fog in relation to elevation and topographical features at two stations in Sikkim. Mausam,Vol. 45 (4), pp. 369-371, 1994.

[4] Schemenauer, R.S., Banic, C.M. and Urquizo, N.: High elevation fog and precipitation chemistry in Southern Quebec, Canada, Atmospheric Environment, 29, pp. 2235-2252, 1995.

[5] Klemm, O., Wrzesinsky, T. and Clemens Scheer, C.: Fogwater flux at a canopy top: Direct measurement versus one-dimensional model. Atmospheric Environment, Vol. 39 (29), pp. 5375-5385, 2005.

[6] Singh, S., Singh, D. and Rao, V.U.M.: Fog and Dew Analysis at Hisar, India Journal of Agrometeorology. Vol. 9 (1), pp. 118-121, 2007.

[7] Uematsu, M., Hattori, H., Nakamuraa, T., Naritaa, Y., Junga, J., Matsumotoa, K., Nakaguchib, Y and Kumar, M.D.: Atmospheric transport and deposition of anthropogenic substances from the Asia to the East China Sea. Marine Chemistry, Vol. 120 (1-4), pp. 108-115, 2010.

5th International Conference on Fog, Fog Collection and Dew
Münster, Germany, 25–30 July 2010
FOGDEW2010-101-4

Fog collection and deposition modelling – EcoCatch Lunz

M.W. Koller (1), C. Ramírez-Santa Cruz (1), K. Leder (1), H. Bauer (1), M. Dorninger (2), F. Hofhansl (3), W. Wanek (3), and A. Kasper-Giebl (1)

(1) Institute of Chemical Technologies and Analytics, Vienna University of Technology, Austria, (2) Department of Meteorology and Geophysics, University of Vienna, Austria, (3) Department of Ecology and Ecosystem Research, University of Vienna, Austria

The area of Lunz am See (N 047.855°, E 015.068°, 650 m a.s.l.) in Lower Austria has been subject to long term monitoring of meteorological parameters as well as wet deposition. Even though Lunz is known for its good air quality, with about 200 days of precipitation per year reaching an annual average of 1500 mm deposition, immission fluxes reach levels of critical loads. For instance, nitrogen input from wet deposition of nitrate and ammonium is > 14 kg ha^{-1} a^{-1}, and sulphur input from sulphate is 5 kg ha^{-1} a^{-1}.

In the framework of the EcoCatch project[1)] wet, dry and occult deposition have been investigated in detail in an alluvial forest near the Biological Station (Lunz/See) since September 2008. The overall contribution of dry and occult deposition was expected to be comparably low and only of importance in times of decreased wet deposition.

Collection of fog samples was performed with an active fog sampler, regulated by a Vaisala PWD-12 sensor monitoring visibility. Temperature, relative humidity, wind speed and direction were logged by a HOBO weather station. Filter stacks were used for sampling of aerosol particles and gaseous components and a Wet And Dry Only Sampler (WADOS) was used to sample precipitation. Solute analysis was carried out via ion chromatography. Alkali and earth alkali metals, chloride as well as ammonium, sulphate and nitrate were quantified in rain, aerosol and fog samples on an event basis. In addition dry deposition included nitrogen oxide and dioxide, sulphur dioxide and ammonia measurements. A site specific relation of liquid water content (LWC) to visibility was established using the collection rate and the known collection efficiency of the fog sampler. A modified version of the fog deposition resistance model devised by G.M. Lovett was used to quantify occult deposition onto the alluvial forest. The surface area index of local vegetation was measured with a SunScan System and tree height was determined using a Vertex IV/GS.

Between September 2008 and October 2009 roughly 560 hours of fog were observed and about 380 hours thereof were sampled. Duration, frequency as well as density of fog events showed strong seasonal variations. As expected, spring and autumn seasons exhibited the highest frequencies and durations of fog events. Concentrations of nitrate in fog samples during the cold season (Nov-Mar) were 10-fold higher than in rain, reaching monthly averages of 50 mg L-1 in January and February. With 15-25 mg L^{-1}, sulphate was 11-fold higher in fog compared to rain. Ammonium reached on average 14 mg L^{-1} in fog samples and was thus 15-fold higher than in rain.

[1)]EcoCatch – Understanding the effects of global change on ecosystem processes and services at catchment scale (funded by Amt der Niederösterreichischen Landesregierung, and Clean Air Commission, Austrian Academy of Sciences).

5th International Conference on Fog, Fog Collection and Dew
Münster, Germany, 25–30 July 2010
FOGDEW2010-102-3

Cloud water composition over the southeastern Pacific

K.B. Beem, T. Lee, X. Shen, Y. Li, and J.L. Collett Jr.
Department of Atmospheric Science, Colorado State University, Fort Collins, CO

Cloud water was collected over the remote southeastern Pacific off the coast of northern Chile in October and November 2008. Samples were collected with an axial-flow cloud water collector aboard the NSF/NCAR C-130 aircraft. Multiple samples were collected during each flight in a wing pod canister. Sample pH was measured on-site after each flight while samples for peroxide, formaldehyde, a suite of organic acids, total organic carbon, sulfur (IV), trace metals and major ions (Cl^-, NO_3^-, SO_4^{2-}, Na^+, NH_4^+, K^+, Ca^{2+}, and Mg^{2+}) were preserved on-site and analyzed after the field campaign. Over the 5 week study period there were 14 flights and 73 samples collected. Our work provides a set of key cloud chemistry measurements for this remote region of the world. The results presented here will address the chemical composition of marine clouds present in the study region, examine spatial variability in cloud composition, and address the relative importance and rates of aqueous S(IV) oxidation by hydrogen peroxide, by ozone, and by oxygen (catalyzed by iron and manganese).

Sample pH varied somewhat significantly over the course of the campaign, the highest pH measured was 7.2 while the lowest was 2.9. Concentrations of major anions and cations also varied significantly from flight to flight and on some flights from sample to sample. Unsurprisingly, an average of all samples indicates that Na^+ and Cl comprised the largest fraction of measured anions and cations followed by SO_4^{2-}, Mg^{2+}, NH_4^+, Ca^{2+}, NO_3^-, and K^+. In addition, total mass was dominated by inorganic species with organic matter contributing only 4% of the mass. The majority of organic species have not been identified. Of the identified organic species formaldehyde, oxalate, formate, and acetate contributed the most to the mass and combined account for 10% mass of organics. Cloud processing is an important pathway for oxidation of SO_2 to sulfate. Aqueous S(IV) oxidation by hydrogen peroxide, by ozone, and by trace metal-catalyzed auto-oxidation are all potentially important pathways. Oxidation by hydrogen peroxide was typically found to be fastest, except under high pH conditions. Observed cloud water S(IV) concentrations ranged from 0.09-3.3μM while concentrations of peroxide were much higher, ranging from 1.8-611 μM. These observations suggest that in-cloud sulfate production is typically unlikely to be oxidant-limited in the region during the spring study season.

5th International Conference on Fog, Fog Collection and Dew
Münster, Germany, 25–30 July 2010
FOGDEW2010-103

Fog monitoring using a new 94 GHz FMCW cloud radar

B. Thies, K. Müller, F. Maier, and J. Bendix

Philipps-University Marburg, Faculty of Geography, Laboratory for Climatology and Remote Sensing (LCRS), Marburg, Germany (thies@lcrs.de, +49 06421 2828950)

A new solid state frequency modulated continuous wave (FMCW) cloud radar and its potential for monitoring the life cycle of fog and low stratus is presented. The radar operates at a frequency of 94 GHz, which is ideal for observing clouds as it lies within a part of the spectrum which experiences relatively low absorption in the atmosphere. With a wavelength of approximately 3 mm, scattering from cloud droplets is by Rayleigh scattering. So the new 94 GHz FMCW radar provides best resolution of cloud and fog in the lower troposphere. Due to the FMCW technique, the radar can detect clouds with a minimum range of ∼30 m making it ideal for monitoring fog and low stratus. A vertical resolution of 4 m from the surface to 2 km permits fine vertical cloud structures to be resolved. The high temporal resolution of 10 seconds makes it highly suitable to capture and analyze the dynamics of fog development and its evolutionary stages. Since the radar reflectivity is strongly related to the cloud liquid water content within the respective scan level, it is possible to retrieve and analyze this essential microphysical cloud parameter with a high vertical and temporal resolution.

Only some studies investigated the profile of the liquid water content during fog events so far. Very few of them combined the vertical and the temporal component by investigating the variation of the liquid water content profile during different fog evolutionary stages. This is mainly due to the laborious measurement techniques using balloon-borne sensor platforms.

In this context the radar offers new insights into fog development and the associated liquid water content based on continuous profile measurements. Such a continuous monitoring of fog and its vertical structure has applications for aviation as well as for climatological and meteorological research.

The poster presents the vertical fog structure and its temporal dynamic for selected fog events and investigate the existence of distinct evolutionary stages as concluded from former studies.

5th International Conference on Fog, Fog Collection and Dew
Münster, Germany, 25–30 July 2010
FOGDEW2010-104

Fog Studies for University Students and High School Teachers

M.Witiw (1), S.Ladochy (2)
(1) Embry-Riddle Aeronautical University Worldwide, Everett, Washington, USA (witiw170@erau.edu / Fax: 01-425-898-1456)
(2)California State University, Los Angeles, California 90032 USA (sladoch@calstatela.edu/ Fax: 01-323-343-6494

Abstract

Over the past few years, fog studies have been introduced as part of courses in Earth system science for both university students and high school teachers. In the undergraduate course, about three hours are devoted to the study of fog starting with a discussion of sustainable water systems. This is followed by presentations on types of fog, the role of fog in the biosphere, biogeochemical cycles and fog, human influences on fog, fog intensity, and remote sensing of fog. We end with a description of fog collection. Fog education efforts increased for students when we were able to obtain fog collecting equipment from Richard Jagels at the University of Maine. The equipment included active and passive fog collectors as well as infrared-beam fog detectors. Two graduating students took on fog collection as their senior project. After setting up the donated equipment, the students designed a fog collection project for the University's Whidbey Island location on Puget Sound. They built a passive fog collector and determined where to place it on the Island. Future projects planned include implementing a water system based upon fog collection on Whidbey Island. We have also implemented a new module on fog for the Earth System Science Education Alliance – The Camanchaca: Fog in the Earth System. Aspects of fog in the Earth system are discussed and teachers are led to see the important role fog has throughout the Earth system. This module was successfully piloted as part of an Earth system science course for teachers in June-July, 2009.

1. INTRODUCTION

Fog as an academic topic can be incorporated on different levels and as part of courses in different disciplines. At Seattle Pacific University, fog studies have been incorporated into senior engineering projects, undergraduate general education courses and specialized graduate problem-based learning courses for teachers. Earth system science studies the Earth by examining interactions between the various components of the Earth system - the atmosphere, hydrosphere, biosphere and lithosphere. The effect of human activities is also included. In the undergraduate course, the role of fog in the Earth system is studied along with its importance in all of Earth's spheres – biosphere, atmosphere, hydrosphere and lithosphere. As an aide to studying Earth's spheres, Earth system science also incorporates remotely sensed data, mainly from satellites. The module on fog ends with a description of fog collection activities. For the teachers' course, problem –based learning is used and the module on fog can be incorporated into a course that typically will use three content-based modules.

2. BACKGROUND

During the 2007 Fog Conference, Professor Richard Jagels offered his fog collection equipment to other universities. We were fortunate to obtain the equipment and two students used it for two parts of their senior project. Initially, the equipment was used to put together an active fog collection system. Subsequently, as a follow-on project, the students built two passive fog collectors. Fog modules are now routinely incorporated into undergraduate general education courses and teacher courses in Earth system science at both Seattle Pacific and at the California State University at Los Angeles.

3. FOG COLLECTOR CONSTRUCTION

Two students with a desire to apply their engineering skills to a sustainable water project, chose the design and construction of two passive fog collectors a their engineering senior design project (Viducich, 2009). The goal was to ultimately deploy these collectors at the University's Physics Research Station on Whidbey Island. This is an island in Puget Sound and the University's property borders the Sound. The area is prone to frequent advection fog off the water with a climatological maximum of 18 days of dense fog in August.

In designing their passive fog collectors, the students made use of works on fog collector design by Schemenauer and Cereceda (1994) and the Fog water collection manual (Schemenauer, Cereceda and Osses , 2005). Some minor changes were made to the materials due to availability and cost. One of the students, although not currently working on fog collection is working on sustainable water projects in Madagascar.

Future plans for engineering projects at Seattle Pacific University include designing a water system on Whidbey Island that will make use of the new passive fog collectors.

4. UNDERGRADUATE MODULE

As part of an Earth system science course, about three hours are devoted to fog. The module begins with fog being defined as a cloud that is attached to the surface where visibility is less than 1,000 meters. Different types of fog are then discussed including steam fog, radiation fog, advection fog and upslope fog.

Fog's role in all of Earth's systems is described**.** This begins with the roles of the atmosphere and hydrosphere in the formation of fog. The role of fog in the biosphere is then discussed and references are made to locations where this is important such as the California Redwoods, wheat growing in India (Singh, Sing and Rao, 2004) and the complex roles of both fog and dew in supporting the biosphere in the the Namib desert (Henschel and Seely, 2004).

We next explore the role of fog in some of the biogeochemical cycles**.** Fog is an important part of the hydrologic cycle. It provides moisture to areas that may otherwise be dry. It can dissolve pollutants and transport them to other regions – thereby influencing the carbon, nitrogen and sulfur cycles. Numerous conference papers have addressed this function of fog; Blas, Sobik and Twarowski (2004) and Husain (2004) for example.

We look at the role humans have played in the formation and intensity of fog. In areas with heavy particulate concentrations, dense fog is common. In recent years, with a decrease in the number of particulates, we have seen the occurrence of dense fog in the Los Angeles basin greatly diminish. We then look at how fog influences human activities and discussed transportation issues, free space optics and fog collection. Emphasis was made on current fog collection efforts, the type of fog that is most readily collected, and the need for testing in certain areas before setting up large scale fog collection operations.

For the undergraduate module, students were shown an example of how fog can be detected on infrared as well as visible satellite imagery (LaDochy, 2007).

5. TEACHER MODULE

The teacher module is designed to fit a three week schedule and is usually one part of a course that contains from two to four content modules plus a module on inquiry based learning. The development of this module was described by Witiw and LaDochy (2007). Other modules in the course will cover other aspects of the Earth system. (For a complete list of modules see: http://esseacourses.strategies.org/modules.php?action=list&sort=bytitle)
The initial module which was designed for undergraduate university students was modified and expanded to fit a three week module that is part of an inquiry-based course for teachers that will include modules on other aspects of the Earth system as well. This module is now available for use by all. The three week module for the teacher course involves an initial week where some background and a scenario are provided to the teachers. In the second week, teachers develop their own Earth system models and in the last week, they develop lesson plans to be used in the classroom. As in the undergraduate course, material was drawn from resources that included papers presented at the fog conferences. Increased emphasis is placed on the remote sensing of fog by satellite. Educational resources for this module include the Digital Library for Earth System Education (2010) and the Cooperative Program for Meteorology, Education and Training (2007).

6. COMET FOG MODULES

The University Corporation for Atmospheric Research runs the Cooperative Program for Operational Meteorology, Education and Training (COMET, 2007). COMET now has over 50 modules in Spanish and 15 in French with plans for translation into Russian and Portuguese (UCAR Staff Notes, 2010). COMET currently has 14 modules on fog and low stratus; ten of which have been translated into Spanish. Although COMET modules

are designed for the professional meteorologist, they can be easily be used use in the classroom or individually (METED, 2010).

7. REFERENCES

Blas, M., Sobik, M., and Twarowski, R.: Changes in cloud water chemical composition in the Western Sudety Mts., Poland. Programme Abstracts The 3rd International Conference on Fog, Fog Collection and Dew, Capetown, Republic of South Africa, 2004.

COMET: Cooperative Program for Operational Meteorology, Education and Training Online at: http://www.comet.ucar.edu/, 2007.

Digital Library for Earth System Education, Online at: http://www.dlese.org/library/index.jsp, 2010.

Earth System Science Education Alliance (ESSEA): The Camanchaca: Fog in the Earth system. Online at: http://esseacourses.strategies.org/module.php?module_id=54, 2008.

Earth System Science Education Alliance (ESSEA): List of modules. Online at: http://esseacourses.strategies.org/modules.php?action=list&sort=bytitle, 2010.

Henschel, J. R., and Seely, M. K.: First approximation of the ecophysiology of fog and dew-A tribute to Gideon Lowe. Programme Abstracts The 3rd International Conference on Fog, Fog Collection and Dew, Capetown, Republic of South Africa, 2004.

Husain, L.: In situ heterogeneous oxidation of SO_2 in fog and cloud drops. Programme Abstracts The 3rd International Conference on Fog, Fog Collection and Dew, Capetown, Republic of South Africa, 2004.

LaDochy, S.: Learning about fog from satellites. Satellite Educators Association Newsletter, February, Online at: http://sated.org/newsletter_2_07.htm#Paula, 2007.

METED: Fog and low stratus. Available online at: http://www.meted.ucar.edu/topics_fog.php, 2010

Schemenauer, R. and Cereceda, P.: A proposed standard fog collector for use in high elevation regions. Journal of Applied Meteorology, 33, 1313-1322, 1994.

Schemenauer, R., Cereceda, P. and Osses, P. Rogwater Collection Manual. FogQuest, Thornhill, 2005

Singh, S., Singh, R. and Rao, V.U.M. (2004) Temporal dynamics of dew and fog events and their impact on wheat productivity in semi-arid regions of India. Programme Abstracts The 3rd International Conference on Fog, Fog Collection and Dew, Capetown, Republic of South Africa.

UCAR Staff Notes (2010). COMET's international reach. Online at: http://www2.ucar.edu/staffnotes/news/comets-international-reach

Viducich, J. (2009). Passive fog collector design for Whidbey Island physics research station. Unpublished manuscript, Seattle Pacific university, Department of Engineering

Witiw, M. R.,and LaDochy, S., (2007) Fog studies as a module in an Earth system science course for teachers. Programme Abstracts The 4th International Conference on Fog, Fog Collection and Dew, La Serena, Chile.

5th International Conference on Fog, Fog Collection and Dew
Münster, Germany, 25–30 July 2010
FOGDEW2010-105

Pollution Levels in Fog at the Chilean Coast

E. Str ter[1, 2], O. Klemm[1], and A. Westbeld[1,3]

[1]University of Münster, Climatology Working Group, Robert-Koch-Str. 26, 48149 Münster, Germany 2
[2]*Present address:* North-Rhine Westfalia State Agency for Nature, Environment, and Consumer Protection, Leibnizstr. 10, 45659 Recklinghausen, Germany
[3]*Present address:* GEO-NET Umweltconsulting GmbH, Große Pfahlstraße 5a, Hannover, 30161, Germany

Abstract

During July and August 2008 fog water was collected for chemical analysis in Patache, at the coast of northern Chile, 60 km south of Iquique (20 49'S, 70 09'W). Advective fog events occur regularly at the cliff in the coastal range at about 800 m above MSL. People collect these types of fog water at some places along the coast with Large Fog Collectors (LFC) for domestic use and for watering field crops. So far, no chemical analysis of fog water was performed in Patache. Pure fogwater samples (38 samples from 8 fog events) were taken by using a passive Scientific Cylindrical Fog Collector. Major ions and trace metals were quantified.

The analyses indicate very high ionic concentrations (mean 3500 eq/l) and very low pH values (mean 3.3). The mean H^+-concentration represents 16 % of the total ionic equivalent concentration. Sulfate is the anion exhibiting the highest concentrations. A mean value of 880 eq/l was found, which accounts for 24 % of the total mean concentration. In contrast to sulfate, nitrate shows only a low percentage of 8.1 %. Further major ions are sodium (20 %) and chloride (19 %), which are typical seasalt ions in coastal fog.

High correlations between the measured ions suggest a causal link between concentration in the fog samples and the liquid water content (LWC) of the cloud. The higher the liquid water content the lower are the ionic concentrations.
Enrichment factors with sodium as reference ion were calculated to identify potential emission sources contributing to the observed pollutant levels. We found that K^+, Na^+, Mg^{2+} and Cl^- mainly result from seaspray. Sulfate, however, is enriched by a factor of 13. The measured trace elements are highly enriched by factors up to hundreds of thousands (Zn: 50, Ni: 1800, As: 2400, Cd: 3900, Fe: 100000, Cu: 96000, Pb: 250000). A cluster analysis supports the conclusion that sulfate and the trace elements originate from anthropogenic activities. The sulfate cannot primarily originate from oceanic dimethylsulfide (DMS).
With regard to the back trajectories, the air masses generally reach the study site from southerly directions after travelling along the Chilean coast. Presumably the air masses pick up pollutants in the densely populated cities, industrial plants and power plants along the Chilean coast and transport them over hundreds of kilometers to Patache. Here, they were detected as ingredients in fog water and lead to high pollution levels therein.

References

Str ter, E., Westbeld, A. and Klemm, O. (2010): Pollution in coastal fog at Alto Patache, Northern Chile. Accepted for publication in Environmental Science and Pollution Research.

5th International Conference on Fog, Fog Collection and Dew
Münster, Germany, 25–30 July 2010
FOGDEW2010-106

Retrieving fog liquid water content using a new 94 GHz FMCW cloud radar

F. Maier, B. Thies, and J. Bendix

Philipps-University Marburg, Faculty of Geography, Laboratory for Climatology and Remote Sensing (LCRS), Marburg, Germany (frank.maier@staff.uni-marburg.de)

The vertical distribution of the liquid water content (LWC) in fog and low stratus is a critical microphysical parameter since it essentially influences the interaction between these low level clouds and the solar and terrestrial radiation.
Despite of this importance there are only few investigations concerning LWC-profiles during fog events, which are mainly restricted to balloon borne measurements and suffer from a low temporal resolution. Therefore, no continuous records covering the whole life cycle of fog events can be provided for climatology studies.
A new ground based frequency modulated continuous wave (FMCW) cloud radar has the po-tential to fill this lack of knowledge. Working at a frequency of 94 GHz (wavelength 3 mm) it is ideal for monitoring low level water clouds. The radar can detect clouds at a minimum height range of ∼30 m and provides a vertical resolution of 4m: This offers the potential to retrieve detailed vertical structures of fog and low stratus.
The reconstruction of the LWC-profile can be accomplished due to the close relationship be-tween the cloud LWC and the detected radar reflectivity. However, this relationship depends strongly on the drop size distribution within the cloud. The strength of the radar reflectivity is related to the sixth power of the drop size distribution and the LWC is related to the latter by the third power.
Former studies yielded the existence of different fog evolutionary stages with characteristical drop size distributions. In order to explore the effect of the different drop size distribution on the relationship between the radar reflectivity and the LWC we conducted radiative transfer calculations with characteristical drop size distributions and LWC-profiles taken from the literature.
For this purpose we adapted the radiative transfer model (RTM) QuickBeam developed for the Cloudsat satellite to our ground based microwave radar. Beside the adaptation to the verti-cal resolution of the ground based cloud radar, the so-called modified gamma distribution, suitable to describe the drop size distribution in fog and low stratus, was implemented into the RTM. By applying representative coefficients for different fog evolutionary stages to the modified gamma distribution together with typical fog LWC-profiles the resulting radar re-flectivity was calculated.
The poster presents the findings of the sensitivity study together with the conception of a new technique to retrieve fog LWC-profiles by means of a novel ground based 94 GHz FMCW cloud radar.

5th International Conference on Fog, Fog Collection and Dew
Münster, Germany, 25–30 July 2010
FOGDEW2010-107-4

The structures of the atmospheric boundary layer in the Yellow Sea summer fog-a comparison study with the spring fog

S.-P. Zhang (1), Z.-P. Ren (1,2), Y.-Q Yang (3), X.-G. Wang (3), and X.-L. Xu (3)

(1) Ocean University of China, College of Physical and Environmental Oceanography, Dept. of Marine Meteorology, Qingdao, China (zsping@ouc.edu.cn), (2) Pingdu Weather Observatory, Qingdao Meteorological Bureau, China, (3) Qingdao Meteorological Bureau, China

The Yellow Sea is a highly foggy area in spring-summer (April to July) seasons. A Yellow Sea fog case occurred on July 7-11, 2008 is investigated by the data from the sea buoy stations, high-resolution digital sounding instruments and other observations and from a three-dimensional mesoscale model (WRF). Espcially, the boundary layer structure are analyzed and simulated, and the comparison is made between the summer fog case and a spring fog case in May 2-3, 2008. The results are as follows [U+FF1A](1) In summer fog, the marine atmospheric boundary layer (MABL) is less stable (almost no temperature inversion)than that in spring fog and the summer fog is thicker in elevation due to the development of turbulence and plenty of moisture supply advected by the East Asian summer monsoon in the low level of the MABL; whereas in spring fog the MABL is very stable with pronounced temperature inversion and the moisture is mainly transported by a shallow local anticyclone in the Yellow Sea surface and traped close to a very low level, thus leading to thin fog. (2) In summer, the southerly air column in the MABL is of similar physical features since it comes from the southern ocean, producing the less vertical gradient both in temperature and in humidity (no obvious dry layer). In contrast, in spring the southerly sea surface air is cooling gradualy as it passes the cold Yellow Sea, but the air at about 950 hPa is westerly from inland that is dry and warm by the increased solar radiation, thus forming temerature inversion and evident dry layer over the sea. (3) The surface air temperature (SAT) is obviously higher than the sea surface temperature (SST) in the process of the summer fog, and the SAT does not derease or even increase in the fog, which is related to the weaker long wave radiation at the fog top and the huge amount of latent heat; while in spring sea fog the SAT decreases rapidly and is even lower than the SST in the peak phase of the fog due to strong long wave radiation at the fog top and the turbulence cooling, which is similar to the haar in the North Sea. The cooling effect can reach to the sea surface readily possibly due to the thin fog, the small amount of moisture, and the robust cooling at the top. (4) The turbulent layer in the summer fog is at 100 -300m high in the upper level of fog and the long wave radiation is weaker due to the inexistence of dry layer, thus the cooling effect at the fog top can hardly influence the bottom air; while in spring fog the long wave radiation cooling effect can quickly reach the bottom of the fog. These results are helpful for understanding the formation of the mechanism of the sea fogs.

5th International Conference on Fog, Fog Collection and Dew
Münster, Germany, 25–30 July 2010
FOGDEW2010-108

SPACCIM simulations of chemical aerosol-cloud interactions with the multiphase chemical mechanism MCM-CAPRAM3.0i

A. Tilgner, R. Schrödner, P. Bräuer, R. Wolke, and H. Herrmann
Leibniz-Institut für Troposphärenforschung, Leipzig, Germany (tilgner@tropos.de)

Heterogeneous and multiphase processes in fog droplets, cloud droplets and deliquescent particles can potentially alter the physico-chemical composition of the tropospheric aerosol on global scale. In order to model such complex tropospheric multiphase chemical interactions of clouds, fogs and deliquescent aerosol particles, chemical mechanisms with a detailed description of chemical processes in both the gas and aqueous phase are required. Currently, both near-explicit gas and aqueous phase mechanisms are available. However, a near-explicit chemical multiphase mechanism was still missing. Therefore, the near-explicit chemical gas phase mechanism MCM v3 (Master Chemical Mechanism, Saunder et al., 2003) with about 13502 reactions and the explicit aqueous phase mechanism CAPRAM3.0i (Chemical Aqueous Phase Radical Mechanism, Herrmann et al., 2005) with about 777 reactions were coupled and integrated into the model framework SPACCIM (SPectral Aerosol Cloud Chemistry Interaction Model; Wolke et al., 2005). The parcel model SPACCIM combines a complex microphysical and multiphase chemistry model.
First SPACCIM simulations have been carried out for different environmental conditions using a non-permanent cloud scenario. The model studies were aimed to investigate multiphase chemistry in tropospheric deliquescent aerosol particles, fogs and clouds in more detail. The model investigations were focused on the multiphase chemistry of tropospheric radical oxidants such as OH and NO3, organic compounds and closely linked chemical subsystems. The model results have been analysed including time-resolved reaction flux analyses. The obtained model results of the near-explicit multiphase mechanism MCM-CAPRAM3.0i have been compared with results of former model studies using the non-explicit gas phase mechanism RACM-MIM2ext and CAPRAM3.0i (Tilgner and Herrmann, 2010).

Herrmann, H., Tilgner, A., Barzaghi, P., Majdik, Z., Gligorovski, S., Poulain, L., and Monod, A.: Towards a more detailed description of tropospheric aqueous phase organic chemistry: CAPRAM 3.0, Atmos Environ, 39, 4351-4363, 2005.
Saunders, S. M., Jenkin, M. E., Derwent, R. G., and Pilling, M. J.: Protocol for the development of the Master Chemical Mechanism, MCM v3 (Part A): tropospheric degradation of non-aromatic volatile organic compounds, Atmos Chem Phys, 3, 161-180, 2003.
Tilgner, A., and Herrmann, H.: Radical-driven carbonyl-to-acid conversion and acid degradation in tropospheric aqueous systems studied by CAPRAM, submitted to Atmospheric Environment, 2010.
Wolke, R., Sehili, A. M., Simmel, M., Knoth, O., Tilgner, A., and Herrmann, H.: SPACCIM: A parcel model with detailed microphysics and complex multiphase chemistry, Atmos Environ, 39, 4375-4388, 2005.

5th International Conference on Fog, Fog Collection and Dew
Münster, Germany, 25–30 July 2010
FOGDEW2010-110

Will the southern African west coast fog be affected by climate change?

A. Haensler, S. Hagemann, and D. Jacob
Max Planck Institute for Meteorology, Land in the Earth System, Hamburg, Germany (andreas.haensler@zmaw.de)

Fog and dew constitute an important water source along the hyperarid and arid parts of the southern African west coast. In this region the annual amount of precipitation due to fog substantially exceeds water input of surface rainfall. As a consequence of these unique climate characteristics, many fog dependent species established along the southern African west coast. Furthermore, as the region's ground water levels are receding and rainfall is rather unreliable, fog harvesting can be a valuable additional water source for drinking water supply.

A major portion of fog precipitation along the southern African west coast region constitutes of advected fog, which generation is related to the transport of moist air masses over the cold sea surface of the Benguela Current. Because of its advective nature, fog patterns are directly linked to the region's circulation activities. Therefore, potential changes in future land sea circulation characteristics might significantly influence the occurrence of fog along the southern African west coast. To assess potential changes in future fog precipitation we implemented a basic fog diagnostics scheme based on Kunkel (1984) into the regional climate model REMO. The REMO model has already been applied over the southern African region in previous studies, e.g. for the generation of long-term high-resolution climate change projections (without a fog diagnostic). Here it has been shown, that REMO ably reproduces the regions climate characteristics. In the present study, we apply the REMO model including the fog diagnostics in two 10-years time slice experiments for current and future climate conditions. Potential changes in the future fog characteristics will be highlighted and the driving processes will be discussed.

5th International Conference on Fog, Fog Collection and Dew
Münster, Germany, 25–30 July 2010
FOGDEW2010-111

FTS (Fog To Snow) conversion process During the SNOW-V10 project

I.Gultepe and G. A. Isaac
Cloud Physics and Severe Weather Research Section, Environment Canada, Toronto, Ontario M3H5T4, Canada
Ismail.gultepe@ec.gc.ca

Abstract

The objective of this work is to understand how winter fog which occurred on Whistler Mountain on 3-4 March 2010 developed into a snow event by the means of the FTS (Fog_To_Snow) process. This event was documented using data collected during the Science of Nowcasting Winter Weather for Vancouver 2010 (SNOW-V10) project that was supported by the Fog Remote Sensing and Modeling (FRAM) project. The FTS resulted in a snow event at about 1850 m height where the RND (Roundhouse) meteorological station was located. For both days, there was no large scale system that affected local fog formation and its development into snow. The patchy fog occurred in the early hours of both days and was based below 1500 m. Clear skies at night likely resulted in cooling, the valley temperature (T) was about -1°C in the early morning, and snow was on the ground. Winds were relatively calm (<1 m s^{-1}). At the RND site, T was about -3°C. Weather at RND was clear and sunny till noon. When fog moved over the mountain peak/near RND, light snow started and lasted for about 4-5 hrs and was not detected by precipitation sensors except the Ground Cloud Imaging Probe (GCIP) and Laser Precipitation Sensor (LPM).

In this work, the FTS process is conceptually summarized. Because clear weather conditions over the high mountain tops can become hazardous with low visibilities and significant snow amounts (<1.0 mm hr^{-1}), such events are important and need to be predicted.

1. Introduction

Mountain weather systems change quickly because of various boundary layer processes such as radiative heating, turbulence, lifting over the sloped surfaces. Time and space scales for changes in microphysical, dynamical, and radiative processes over mountain surfaces can be much shorter than those associated with flater terrain. Fog usually forms when relative humidity with respect to water (RHw) reaches to ~100%, and reaching this point can be effected by various conditions e.g. radiative cooling, lifting, turbulence, and evaporative mixing [1].

The objective of this work is to understand how winter fog at low levels (below 1500 m) which occurred on Whistler Mountain on 3-4 March 2010 developed into a snow event by the means of the **FTS** (**F**og_**T**o_**S**now) process that was documented for the first time (Fig. 1). This event occurred during the Science of Nowcasting Winter Weather for Vancouver 2010 (SNOW-V10, [2]) project that was supported by the Fog Remote Sensing and Modelling (FRAM [1]) project. The FTS resulted in a snow event at about 1850 m height where the RND (Roundhouse) meteorological station, with several precipitation and visibility sensors, was located. For both days, there was no large scale system that affected local fog formation and its development into snow.

2. Observations

At the RND site during SNOW-V10, there were several instruments [3;4] measuring visibility, surface precipitation, wind, radiation, and particle type. The deployed sensors are shown in Fig. 1-f that includes Vaisala FD12p, Sentry, Geonor, YES TPS, VRG101, RID, SVI, FMD, GCIP, MRR, 2D and 3D-Yonge, WXT520, HMP45C, OTT-ParSiVel, Biral MRR and LPM, SR50, CRN1, and SPN1. In case of failure of one of the sensors, measurements of important parameters were usually made by more than one instrument.

Figure 1: Pictures taken during the FTS process: a) low level fog at VOL station (early morning), b) elevated fog taken from the RND station, c) increasing cloudiness at RND (early afternoon), d) clear sky conditions at the RND, e) developed stratus/altostratus clouds and fog seen at RND, and f) snowing and cold fog at RND station (late after noon).

The ground imaging probe (GCIP) measurements of particle shapes and sizes from 7.5 micron up to 960 micron over 62 bins (64 diodes) with 15 micron resolution are used for snow/fog particle detection together with a fog device (DMT-FMD). A 7.5 micron particle travelling directly over the diodes' centre in the receiver could meet the 50% shadowing criteria and can be detected. The GCIP instrument is adapted for ground-based applications and is based on a DMT CIP probe which is usually mounted on an aircraft. The heated inlet is used to keep the surfaces clean and primary suction is provided by the two-six inches ports giving a flow rate of 25 m s^{-1} at the measurement area. Three distinct zones of heat control are provided and the entire horn exterior is insulated to reduce thermal losses. The flow cross-sectional diameter varies from 12" at the inlet to 4" between the CIP arms. A VAISALA ceilometer measurement of cloud base height, and T and RHw profiles obtained along Whistler mountain slope are shown in Fig. 2a and 2b, respectively.

3. Analysis and Results

The patchy fog occurred in the early hours of both days and its top height was below 1500 m (Fig. 1a). Figures 1a-f show time development of the FTS process. Clear skies at night likely resulted in radiative cooling, and the valley temperature (T) at VOL station on March 4 (March 3) was about -1°C (+3°C) in the early morning (Fig. 3a), with snow on the ground on both days (Fig. 1). Here, the results from only the March 4 will be summarized. Winds on this day were relatively calm (<1 m/s) and T was about -6°C at 15 UTC at RND. (Fig. 3b). The RHw was 100% before 15 UTC (Fig. 3c). Fig. 3e shows Vis ~100 m at VOL during the fog event. The foggy air at VOL lifted to higher elevations (Fig. 1b) before local noon. Weather at RND was clear and sunny until noon (Fig. 1c). When shortwave (SW) radiation provided additional heat at the low levels and sloping surfaces, the fog started to lift over a 3-4 hr time period gaining additional moisture from melting snow (Fig. 1d). Then, the fog layers were eventually converted to cumulus/altocumulus. In the afternoon, at about 01:30 PM, the entire valley was filled with a

fog/cloud mixture (Fig. 1e). Figs. 3d-f show that at RND T was less than 0°C and RHw was ~80%. When the fog moved over the mountain peak/near RND (Fig. 1f), light snow started (0.2 mm h^{-1}; Fig. 3f) with Vis~2-3 km (Fig. 4) and lasted for about 4-5 hrs. Snow was not detected by weighing precipitation sensors (Fig. 3f) except with the Ground Cloud Imaging Probe (GCIP; Fig. 4a) and disdrometers (e.g. Laser Precipitation Sensor (LPM) and OTT (Figs. 3f and 4b, correspondingly).

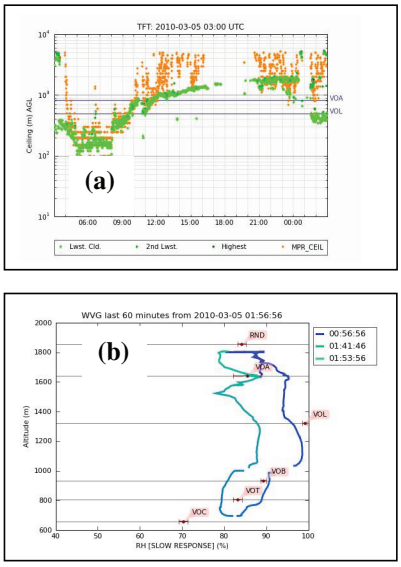

Fig. 2: Times series of fog base height measured at the Whistler Mountain base for March 4: a) green dots represent VAISALA ceilometer and brown dots represent the MPR (Microwave Profiling Radiometer, Radiometrics Inc.), b) profiles of RH measured by the sensors mounted on a Gondola along the Whistler Mountain slope.

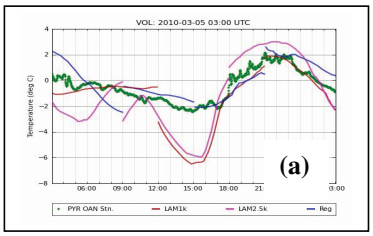

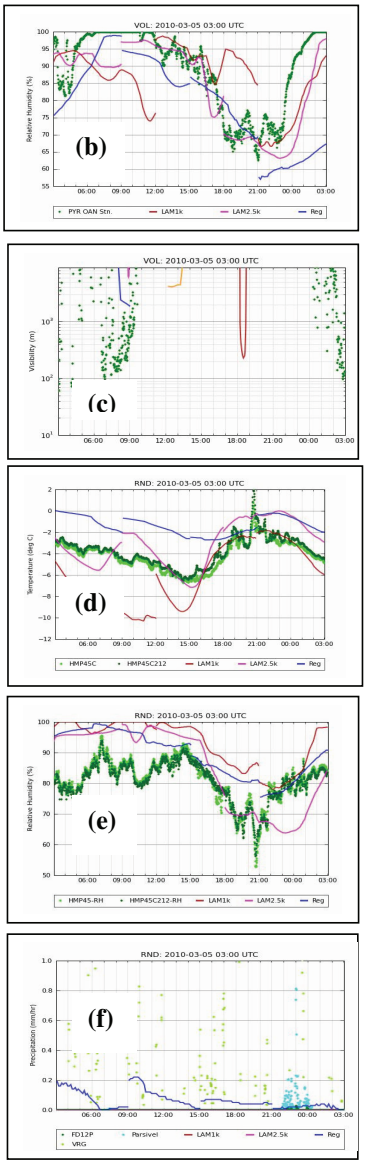

Fig. 3: Time series of T, RHw, and Visibility for VOL station and T, RH, and precipitation rate from FD12P, VRG101, and OTT ParSiVel for RND station. The VRG measurements are an artefact due to wind speed. The colour solid lines are predicted parameters obtained from the Canadian GEM model.

3

4. Summary and Conclusions

During the FTS process, snow occurred at high elevations but this was not predicted with any model simulation. It was detected by some sensors but most of the sensors missed this precipitation type which occurred as a result of the FTS process.

The following conclusions are obtained from this work:

- Visibility was low at the low levels early in the morning but it became worse during the FTS at high elevations after 3 pm local time.
- Forecast of the FTS process is important to meteorologists because it lowers mountain Vis down to 2-3 km from a clear sky condition and increases snow precipitation rates up to 0.2-0.5 mm h^{-1}; meanwhile its is not predicted by the models.
- Cloud base decreased gradually at the high elevations and it was not detected by the model predictions.
- Solar radiation played an important role over the sloped surfaces by increasing radiative heating at low levels, resulting in a moisture source for high level fog and snow formation.
- GCIP sensor measurements were effective at measuring the light snow amounts e.g. snow particles and its spectra.

Acknowledgements

The author would like to thank to science team of Environment Canada and other SNOW-V10 participants who helped make this project a success. This project was funded by the office of the DND SAR and EC.

References

[1] Gultepe, I., R. Tardif, S.C. Michaelides, J. Cermak, A. Bott, J. Bendix, M. Müller, M. Pagowski, B. Hansen, G. Ellrod, W. Jacobs, G. Toth, S.G. Cober, 2007: Fog research: a review of past achievements and future perspectives. *J. of Pure and Applied Geophy*., Special issue on fog, edited by I. Gultepe. Vol. 164, 1121-1159.

[2] Isaac, G., P. Joe, J. Mailhot, M. E. Bailey, S. Belair, F. S. Boudala, M. Brugman, E. Campos, R. L. Carpenter, S. G. Cober, B. Denis, C. Doyle, D. E. Forsyth, I. Gultepe, T. Haiden, L. Huang, J. A. Milbrandt, R. Mo, R. M. Rasmussen, T. Smith, R. E. Stewart, and D. Wang, 2010: Nowcasting winter weather in complex terrain—Experiences from SNOW-V10 AMS Mountain Meteorology, San Diego, CA, USA, accepted.

[3] Gultepe, I., G. Pearson J. A. Milbrandt, B. Hansen, S. Platnick, P. Taylor, M. Gordon, J. P. Oakley, and S.G. Cober, 2009: The fog remote sensing and modeling (FRAM) field project. *Bull. Of Amer. Meteor. Soc*., v.90, 341-359.

[4] Gultepe, I., G. A. Isaac and R. Rasmussen, 2010: GCIP measurements of precipitation and fog during SNOW-V10 and FRAM projects. The 13th Conference on Cloud Physics, 28 June-2 July 2010, Portland, Oregon, USA. Accepted.

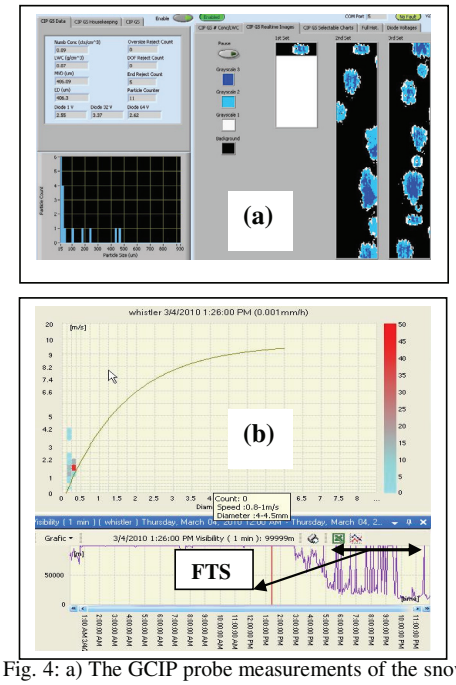

Fig. 4: a) The GCIP probe measurements of the snow particle shape and spectra, and b) LPM measured snow particle counts as a function of particle fall speed and size, and LPM snow visibility (bottom panel).

5th International Conference on Fog, Fog Collection and Dew
Münster, Germany, 25–30 July 2010
FOGDEW2010-112

Visibility Parameterization For Forecasting Model Applications

I. Gultepe[1], J. Milbrandt[2], and Z. Binbin[3]
[1]Cloud Physics and Severe Weather Research Section, MRD, Environment Canada, Toronto, Ontario, Canada
[2]Numerical Weather Prediction Research Section, MRD, Environment Canada, Toronto, Ontario, Canada
[3]NOAA/NCEP/Environmental Modeling Center, and Science Appl. Inter. Corporation, Camp Springs. Maryland, USA.
Ismail.Gultepe@ec.gc.ca

Abstract
In this study, the visibility (Vis) parameterizations developed during Fog Remote sensing And Modelling (FRAM) projects, conducted in central and eastern Canada, and Barrow, Alaska, US will be summarized and their use for forecasting/nowcasting applications will be discussed. Parameterizations developed for reductions in visibility due to 1) fog, 2) rain, 3) snow, and 4) relative humidity (RH) during FRAM will be given and uncertainties in the parameterizations will be discussed. Observations used in this study were obtained using a fog measuring device (FMD) for fog parameterization and a Vaisala all-weather precipitation instrument called FD12P for rain and snow visibility parameterizations.

1. Introduction
Because fog can form over time and space scales of minutes and meters, high-resolution models have been developed to better nowcast fog [1]. Unfortunately, high-resolution models are not always available; therefore, visibility parameterizations have been used in forecasting models. Gultepe et al [2] performed three field projects to study warm fog conditions and developed microphysical parameterizations suitable for application to fog and precipitation measurements. Presently, visibility parameterizations related to the precipitation type in forecast models are not adequate because they represent mid-latitude cloud systems [3]. Some previous work concerning snow visibility (Vis) has shown that particle phase is an important factor in the visibility calculation but usually it is ignored [4]. The objective of this work is to summarize the relationships of Vis versus RH with respect to water (RH_w), fog liquid water content (LWC) or ice water content (IWC), and precipitation rate (for rain; PR_R or snow; PR_S); these parameters were obtained using surface observations. Also, Vis versus both droplet (ice) number concentration (N_d(N_i)) and LWC (IWC) were derived for non-precipitating boundary layer conditions.

2. Observations
Surface observations during the FRAM field project were collected 1) at the Center for Atmospheric Research Experiments (CARE) site near Toronto, Ontario and Pearson Airport in Toronto, Ontario during the winter of 2005-2006 (FRAM-C), 2) in Lunenburg, Nova Scotia during the summers of 2006 and 2007 (FRAM-L), 3) at the DOE ARM NSA site, Barrow, Alaska in the April of 2008 during the Indirect and Semi-Direct Aerosol Campaign (ISDAC) field program (called ISDAC-FRAM-B), and 4) at the Mirabel Airport from 3 November 2003 to 12 February 2004 during the Alliance Icing Research Study (AIRS 2; [5]). The main observations used in the analysis were fog droplet spectra from a FMD (DMT Inc.), Vis and PR from the VAISALA FD12P all-weather precipitation instrument, and RH_w together with temperature (T) from the Campbell Scientific HMP45 sensor. Figures 1 and 2 show ice fog and time series of the FD12P measurements [6].

3. Analysis and Results
In this work, the Vis (from FD12P) values were compared to RH_w, and PR for snow and rain (from FD12P). The FMD-based Vis was compared to fog LWC and N_d (also for IWC and N_i).

The extinction parameters (β_{ext}), using Koschmieder's Law and assuming a brightness contrast threshold (ε) of 0.05, is converted to Vis as follows:

$$Vis = -\ln(0.05)\beta_{ext}^{-1} . \quad (1)$$

The FD12P measurements are then used to obtain 1-min averaged values of Vis. In this work, the simulations from the Canadian GEM and US Rapid Upper Cycle (RUC) models are used for Vis comparisons. The RUC uses the parameterizations [7] given for snow, rain and fog visibility calculations. The Canadian Global Multiscale (GEM) Numerical Weather Prediction (NWP) model uses the results from the current work.

3.1 Visibility versus RH_w
The relationship between Vis and RH_w determined from a few field campaigns are shown in Fig. 3 and Table 1 where RH_w is between 30 and 100%. In general, the Vis obtained from the RUC model near RH_w=100% is about 2 times smaller than the Vis values obtained from the other data sets. Note that the total Vis in a numerical model is obtained using both Vis-RH_w and the Vis-PR relationships.

3.2 Visibility parameterization for fog
Visibility versus particle number concentration for a fog type has always been ignored in forecast models [2;6;8]. Using state of the art observations of N_d and N_i from new optical probes, such as DMT FMD, Vis versus N_d, and Vis

versus N_i as well as the best fits are shown in Figs. 4a and 4b, respectively. These relationships are obtained as

$$vis_{Nd} = 238 N_d^{-1.31} \quad (2)$$

and

$$vis_{Ni} = 18 N_i^{-0.56}, \quad (3)$$

where Vis is in [km], N_d and N_i are in [cm^{-3}]. These equations are given here to emphasize the importance of the number concentration for Vis calculations.

The aircraft in-situ observations are used to develop a parameterization for fog Vis [2] that is based on both LWC and N_d. Figure 4c shows Vis versus f(LWC;N_d). Using information that Vis decreases with increasing N_d and LWC, an empirical relationship between Vis_{obs} and $(LWC.N_d)^{-1}$ (Fig. 4c) called the "fog index" using FRAM-L observations collected at the surface is determined as

$$Vis_{obs} = \frac{0.8771}{(LWC \cdot N_d)^{0.49034}}. \quad (4)$$

This empirical fit suggests that Vis is inversely related to both LWC and N_d.

The Vis parameterization for ice fog conditions can be challenging because of unknown ice crystal number concentrations and its shape when ice crystal sizes are smaller than 100 micron. The FMD measurements from the 3 day ice fog event (April 9-11 2008) occurred during ISDAC in Barrow, Alaska are used for Vis [km] versus N_i [cm^{-3}] relationship; then Vis versus ice fog index is obtained as

$$Vis_{obs} = \frac{0.242}{(IWC \cdot N_i)^{0.5147}} \quad (5)$$

where IWC has unit of [g m^{-3}]. Note that these equations are obtained using FMD measurements at T~-18°C and RH_i>100%. The uncertainty in N_i and IWC can be very large.

3.3 Vis versus PR for rain

The Vis-PR_R observations from FRAM-L are shown in Figure 5 and the corresponding percentile fits to this data are given in Table 2. These equations given in Table 2 as a function of PR_R can be used in model simulations, depending on the rain type as follows: Using the rain rate classification (heavy rain fall: PR_R >7.6 mm h^{-1}, moderate rain fall: 2.6 mm h^{-1}<PR_R<7.5 mm h^{-1}, and light rain fall: PR_R<2.6 mm h^{-1}; [9]), the 5% fit equation curve may be used to estimate Vis when heavy rain precipitation occurs and the 95% curve can be used for Vis calculations under the light precipitation conditions.

3.4 Vis versus PR for snow

The results from the FRAM projects are presented in Figure 6 with T<-1°C, representing snow conditions. Overall, a trend for snow conditions exists with decreasing Vis for higher precipitation rates but the variability is large. Some of the data points (red dots) just above the snow condition points (black dots) are for wet snow conditions and this needs to be further researched. It should also be stated that PR_S less than 0.1 mm h^{-1} are not reliable due to sampling issues.

Using the FD12P measurements without considering specific particle density and type, Vis-PR_S relationships depending on snow type (heavy snow fall: PR > 2.5 mm h^{-1}, moderate snow fall: 1 mm h^{-1} < PR < 2.5 mm h^{-1}, and light snow fall: PR < 1 mm h^{-1}; [10]) are given in Table 3. For example, when heavy snow precipitation occurs, the 5% fit equation (Table 3) can be used to estimate Vis. It can be seen that 50% of the observed points are found above or below the 50% fit.

3.5 Integrated Vis

Next, equations given for Vis-PR_R in Table 2 combined with Vis-RH_w parameterizations given in Table 1 can be used to obtain integrated Vis values. In the case of both fog and precipitation occurring together: first, the calculated Vis values (with respect to RH_w, fog LWC, and PR_R) are converted to extinction coefficients using Eq. (1) and, then, an integrated extinction coefficient is obtained [4] as

$$\beta_{\text{int}} = \beta_{RHw} + \beta_{LWC} + \beta_R. \quad (6)$$

The final value of Vis is then calculated using (1) which utilizes β_{int} from (6). Note that the conditions set for the probability curves need to be tested for various geographical regions because of varying characteristics of CCN related to their composition and hygroscopicity.

3.6 Application

For a fog event that occurred on 11 Feb 2009 (Figs. 7a and 7b), the derived equations are applied to model runs. Figure 7c shows Vis obtained from the probabilistic parameterizations (e.g. 5%, 50%, and 95% curves), a RUC model forecast run, and an integrated fog parameterization. The results compare well with observed FD12P Vis. Integrated Vis values (black circles filled with yellow color) are found comparable to the observed Vis (green line) between 1400 UTC and 1830 UTC, and to RUC Vis (blue line with triangles) after 1500 UTC. In this plot, the GEM model, using the time dependent RH_w, PR_R, and LWC values, is used to predict Vis [11]. In the GEM simulations, LWC within the lowest model layer (<50 m) is assumed to be same as the total water content at warm temperatures.

4. Summary and Conclusions

In the present work, surface observations from the various instruments, measuring N_d, N_i, PR (for rain and snow), Vis, RH_w, and T, were used in the analysis and parameterizations are suggested. Based on the results, the following conclusions can be drawn:

- The relationships previously used in forecast models, especially for RH_w, should not be utilized because of an underestimation of Vis at values close to saturation (Fig. 3). Eq. 4 should replace the previous relationship used in the forecasting models.
- Overall, a large variability in the Vis-PR relationships suggests that these relationships need to be improved, especially for snow.
- The relationships between Vis versus N_d and N_i clearly indicate that number concentration of the particles needs to be considered for parameterizations..
- Applying observation-based parameterizations (e.g. Eq. 4) as an alternative to those based on specific hydrometeor size distribution functions can be used to compute extinction coefficients directly.

These conclusions suggest that the new visibility parameterizations can significantly improve visibility estimates but additional tests utilizing the forecasting models are needed. An ice fog project planned for 2010-2011 winter will further help to develop the new parameterizations based on measurements of a GCIP instrument.

Acknowledgements

Funding for this work was provided by the Canadian National Search and Rescue Secretariat (DND SAR) and Environment Canada. ISDAC was supported by the Office of Biological and Environmental Research of the U.S. Department of Energy (DOE) through the Atmospheric Radiation Measurement (ARM) program.

.

Fig. 1: An ice fog event occurred over Barrow, Alaska on April 10 2008 during the ISDAC-FRAM-B project.

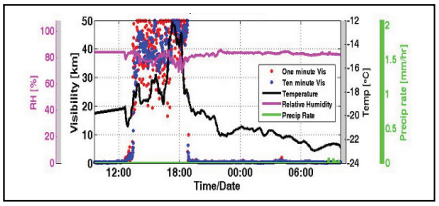

Fig. 2: A time series of RH_w, *Vis*, temperature (*T*), and precipitation rate (*PR*) on April 10 2008 for an ice fog event that occurred during ISDAC.

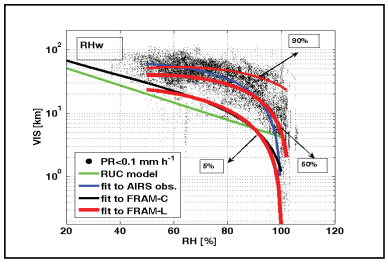

Fig. 3: Summary of FRAM observations for Vis versus RH_w. The black solid line is from the Pearson Airport site during FRAM-C. The green line represents the RUC model parameterization (Smirnova et al., 2000).

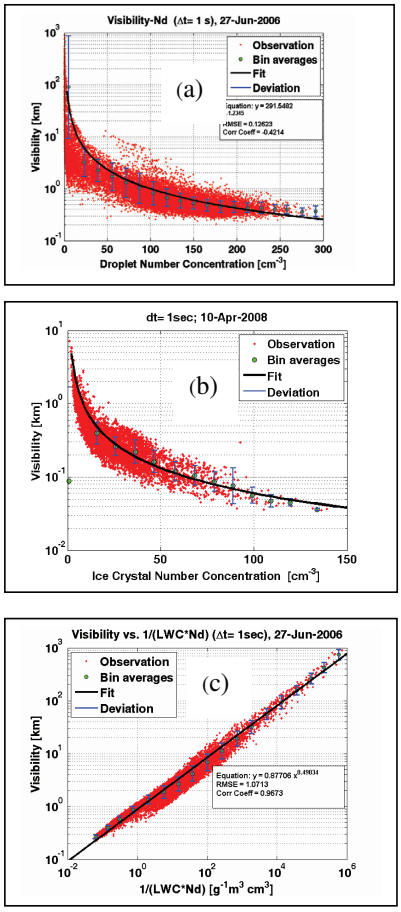

Fig.4: Visibility function of N_d (a) and f(LWC,N_d) (b) for droplets, and Vis- f(*IWC, N_i*) (c) for ice crystals on June 27 2006 and April 10 2008, respectively.

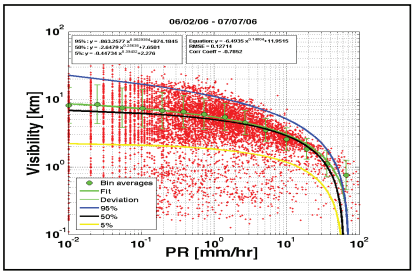

Fig. 5: The Vis versus PR for rain$_R$ from all observations (red dots) obtained during FRAM-L.

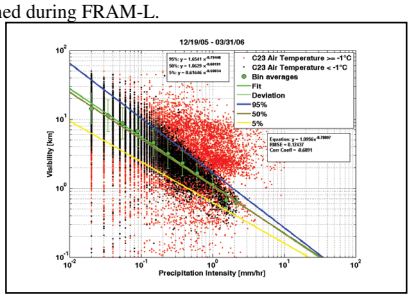

Fig. 6: The *Vis* versus *PR* for snow (black dots) from observations obtained during FRAM (November 2005-April 2006). The red dots are for T>-1°C.

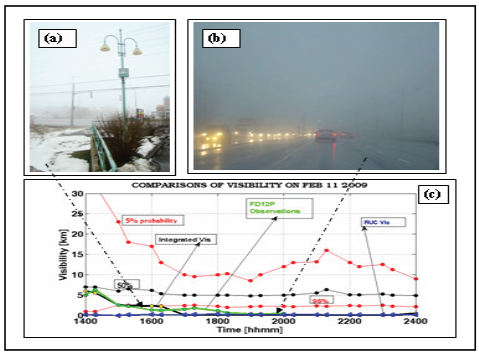

Fig. 7: A heavy fog event at 9:57 AM LST (a) and at 4:48 PM LST (b) on Feb 11 2009 after a heavy rain occurrence (T=9°C). Vis versus time is shown in (c).

Table 1: Visibility (*Vis* [km]*)* versus relative humidity (RH_w).

Percentile %	Vis-RH$_w$ relationships
Mean	$Vis_{FRAM-C} = -41.5\ln(RH_w) + 192.30$
95%	$Vis_{FRAM-L(95\%)} = -0.000114\mathrm{RH}_w^{2.70} + 27.45$
50%	$Vis_{FRAM-L(50\%)} = -5.19*10^{-10}\ \mathrm{RH}_w^{5.44} + 40.10$
5%	$Vis_{FRAM-L(5\%)} = -9.68*10^{-14}\mathrm{RH}_w^{7.19} + 52.20$

Table 2: Visibility (*Vis* [mm h^{-1}]) versus *PR* [mm h^{-1}] for rain.

Percentile %	Vis-PR$_R$ relationships
Mean	$Vis_R = -4.12PR_R^{0.176} + 9.01$
50%	$Vis_R = -2.65PR_R^{0.256} + 7.65$
95%	$Vis_R = -0.45PR_R^{0.394} + 2.28$
5%	$Vis_R = -863.26PR_R^{0.003} + 874.19$
Mean(drz)	$Vis_D = -2.66PR_R^{-0526} + 6.54$

Table 3: Visibility (*Vis* [mm h^{-1}]) versus *PR* [mm h^{-1}] for snow.

Percentile	Vis-*PRs* relationships
Mean	$Vis_S = 1.10PR^{-0.701}$
50%	$Vis_S = 1.06PR^{-0.682}$
95%	$Vis_S = 0.62PR^{-0.590}$
5%	$Vis_S = 1.65PR^{-0.795}$

References

[1] Bott, A., U. Sievers, and W. Zdunkowski, 1990: A radiation fog model with a detailed treatment of the interaction between radiative transfer and fog microphysics, ***J. Atmos. Sci., 47***, 2153–2166.

[2] Gultepe, I., M. D. Müller, and Z. Boybeyi, 2006: A New Visibility Parameterization for Warm Fog Applications in Numerical Weather Prediction Models. ***J. Appl. Meteor., 45,*** 1469-1480.

[3] Stoelinga, M. T., and T. T. Warner, 1999: Nonhydrostatic, Mesobeta-scale model simulations of cloud ceiling and visibility for an east coast winter precipitation event. ***J. Appl. Meteor., 38***, 385-404.

[4] Rasmussen, R. M., J. Vivekanandan, J. Cole, B. Myers, and C. Masters, 1999: The estimation of snowfall rate using visibility. ***J. Applied. Meteor., 38***, 1542-1563.

[5] Isaac, G.A., et al., 2005: First results from the Alliance Icing Research Study II. *AIAA 43rd Aerospace Sci. Meeting and Exhibit*, Reno Nevada, 11-13 January 2005, AIAA 2005-0252.

[6] Gultepe, I., and J. Milbrandt, 2010: Visibility parameterizations for precipitation types for modeling applications. ***J. Appl. Meteor. And Clim., 49,*** No. 1, 36–46.

[7] Smirnova, T. G., S. G. Benjamin, and J. M. Brown, 2000: Case study verification of RUC/MAPS fog and visibility forecasts. Preprints, *9th Conference on Aviation, Range, and Aerospace Meteorology,* AMS, Orlando, FL, Sep. 2000. Paper#2.3, 6 pp.

[8] Gultepe, I., G. Pearson, J. A. Milbrandt, B. Hansen, S. Platnick, P. Taylor, M. Gordon, J. P. Oakley, S.G. Cober, 2009: The fog remote sensing and modelling field project. ***Bull. Amer. Meteor. Soc., 90,*** 341-359.

[9] Gickman, T. S., 2000: *AMS Glossary of Meteorology*, Second Edition. Published by AMS, Boston, US, 855 pp.

[10] Bendickson, S., 2003: *Relationship between visibility and snowfall intensity*. Available from APS Aviation Inc. Transport Canada Pub. # TP 14151E, Montreal, Quebec. 34 pp.

[11] Milbrandt, J. A. and M. K. Yau, 2005: A multimoment bulk microphysics parameterization. Part I: Analysis of the role of the spectral shape parameter. ***J. Atmos. Sci., 62***, 3051-3064.

5th International Conference on Fog, Fog Collection and Dew
Münster, Germany, 25–30 July 2010
FOGDEW2010-113

Leaf wetness distribution within a potato crop

B.G. Heusinkveld
Wageningen University, Meteorology and Air Quality (bert.heusinkveld@gmail.com)

The Netherlands has a mild maritime climate and therefore the major interest in leaf wetness is associated with foliar plant diseases. During moist micrometeorological conditions (i.e. dew, fog, rain), foliar fungal diseases may develop quickly and thereby destroy a crop quickly. Potato crop monocultures covering several hectares are especially vulnerable to such diseases. Therefore understanding and predicting leaf wetness in potato crops is crucial in crop disease control strategies. A field experiment was carried out in a large homogeneous potato crop in the Netherlands during the growing season of 2008. Two innovative sensor networks were installed as a 3 by 3 grid at 3 heights covering an area of about 2 hectares within two larger potato crops. One crop was located on a sandy soil and one crop on a sandy peat soil. In most cases leaf wetting starts in the top layer and then progresses downward. Leaf drying takes place in the same order after sunrise. A canopy dew simulation model was applied to simulate spatial leaf wetness distribution. The dew model is based on an energy balance model. The model can be run using information on the above-canopy wind speed, air temperature, humidity, net radiation and within canopy air temperature, humidity and soil moisture content and temperature conditions. Rainfall was accounted for by applying an interception model. The results of the dew model agreed well with the leaf wetness sensors if all local conditions were considered. The measurements show that the spatial correlation of leaf wetness decreases downward.

5th International Conference on Fog, Fog Collection and Dew
Münster, Germany, 25–30 July 2010
FOGDEW2010-114

Fog Chemistry at Different Altitudes in the Swiss Alps

P. Michna (1), W. Eugster (2), and H. Wanner (1)

(1) University of Bern, Department of Geography, Bern, Switzerland, (2) ETH Zurich, Institute of Plant Sciences, Zurich, Switzerland

During two extended summer seasons in 2006 and 2007, we installed two battery driven versions of the Caltech active strand cloud water collector (MiniCASCC) at the Niesen mountain in the northern Swiss Alps. Along, we measured air temperature, relative humidity, wind, and visibility. During these two field operation phases we gained weekly samples of fogwater, where we analysed the major anions and cations, and the stable water isotopes δD and δ^{18}O. The fog collectors were installed at an altitude of 2300 and 1600 m asl to resolve altitudinal differences in fog chemistry. We found a large variability between the events, but no clear altitudinal gradient. At both sites, the most important ions were nitrate, ammonium, and sulphate. Higher concentrations occured preferably in late spring (start of sampling period) and in autumn (end of sampling). Compared to previous studies at lower elevations in the Swiss Plateau during wintertime, our measurements showed considerable lower ion loads in the fogwater. The combination of these results suggest that lowest ion loads are found in convective clouds with a short lifetime and that the highest ion loads occur during radiation fog events at lower elevations.

5th International Conference on Fog, Fog Collection and Dew
Münster, Germany, 25–30 July 2010
FOGDEW2010-115

The Continued Reduction in Dense Fog in the Southern California Region: Possible Climate Change Influences

S.Ladochy (1), M.Witiw (2)
(1) California State University, Los Angeles, California 90032 USA (sladoch@calstatela.edu/ Fax: +01-323-343-6494
(2) Embry-Riddle aeronautical University Worldwide, Everett, Washington, USA (witiw170@erau.edu / Fax: +01-425-898-1456)

Abstract

Dense fog appears to be decreasing in many parts of the world, especially in cities. An earlier study showed that dense fog (visibility < 400 m) was disappearing in the urban southern California area as well. It showed that the decrease in dense fog events could be explained mainly by declining particulate levels, Pacific SSTs, and increased urban warming. Dense fog is most prevalent along the coast and decreases rapidly inland. Using hourly data from 1948 to the present, we looked at the relationship between fog events and contributing factors in the region and trends over time. The relationship between the occurence of dense fog to the phase of two atmosphere–ocean cycles: the Pacific Decadal Oscillation (PDO) and the Southern Oscillation In addition, the influence of the urban heat island and the amount of suspended particulate matter were assessed. Results show a decrease in the occurrence of very low visibilities (<400 m) at the stations in close proximity to the Pacific Ocean. Occurrence of the frequency of low visibilities at these two locations was highly correlated with the phase of the PDO. A downward trend in particulate concentrations coupled with an upward trend in urban temperatures were associated with a decrease in dense fog occurrence at both LAX and LGB. While examining data from LAX, we saw a frequency of dense fog that reached over 300 hours in 1950, but occurrence was down to zero in 1997. Since 1997, there has been a bit of a recovery with both 2008 and 2009 recording over 30 hours of dense fog each. In the present study, we examine the relationships that control the frequency of dense fog (visibility < 400 m) in coastal southern California. To remove urban influence, we also included Vandenberg Air Force Base, located in a relatively sparsely populated area. While particulates, urban heat island and Pacific SSTs are all contributing factors, we now speculate on the direct and indirect influences of climate change on continued decreases in dense fog. Case studies of local and regional dense fog in southern California point to the importance of strong, low inversions and to a lesser contributor, Santa Ana winds. Both are associated with large-scale atmospheric circulation patterns, which have changed markedly over the period of study.

1. INTRODUCTION

The coast of California is well known as a foggy place. During the warm season, the semi-permanent Pacific high pressure remains off the California coast. The clockwise circulation around this high results in the California Current and upwelling of cold water close to the coast. Although the upwelling is strongest farther north, where summer water temperatures usually remain around 11 °C to 12 °C, temperatures remain relatively cold at latitudes well to the south including the Los Angeles area. Moist, relatively warm air moving over the cold water is chilled to its dew point, resulting in the formation of sea fog. This sea fog typically rises as it moves inland forming a low stratus deck. The density and horizontal coverage of fog and low clouds is negatively correlated with the sea surface temperature (Norris and Leovy, 1994). Usually, only the immediate coastal regions experience dense fog conditions. Even there, because of the generally large fog droplet size (resulting from the large condensation nuclei available over the ocean) very low visual ranges are rare. The main type of fog in the cool season is advection-radiation fog (Byers, 1959). Typically fog-free marine air moves inland, and frequently after the wind changes direction to an offshore component, advection-radiation fog forms. Because of the smaller fog nuclei available, this type of fog tends to produce lower visibility than advection fog (sea fog) (Leipper, 1994). October through February are characterized by a relatively

high frequency of low visibility (<400 m) at both coastal Los Angeles (LAX) and Long Beach (LGB) International Airports (Baars et al., 2002). This is also the season of lower inversion heights which are necessary for dense fog formation (LaDochy and Behrens, 1991).

In the present study, we examine the relationships that control the frequency of dense fog in coastal southern California. While particulates, urban heat island and local SSTs are all contributing factors, we now speculate on the direct and indirect influences of global warming on continued decreases in dense fog. Case studies of local and regional dense fog in southern California point to the importance of strong, low inversions and to a lesser contributor, Santa Ana winds. Both features are controlled by large-scale atmospheric circulation patterns.

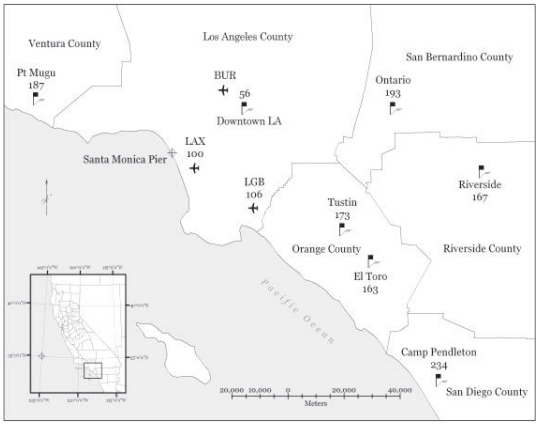

Fig. 1. Study area-Los Angeles Basin with average annual days with fog (visibility < 1km).

2. DATA AND METHODOLOGY

Visibility and significant weather is recorded hourly at the three airport stations in the coastal plains of the Los Angeles Basin, LAX, LGB and BUR (Burbank International Airport). Dense fog is recorded when visibility is less than ¼ mile (<400 m). Hourly visibility were recorded for both LAX and LGB from 1948-2009 from the National Climate Data Center, NCDC. From the mid-1960s through June 1999, downtown Los Angeles had automatic weather observations without visibility observations, resulting in visibility data being available only for the complete years 1961-1964 and 2000-2004. Burbank Airport had hourly data from 1982 through 2004, with missing data for the first half of 1998. Monthly mean, max and min temperatures for LAX and downtown Los Angeles were also obtained from NCDC for the period of the study. Monthly and annual particulate air pollution data was recorded as total suspended particulates (TSP) from 1966 to 2008 from the South Coast Air Quality Management District (SCAQMD). Monthly Pacific climatic indices, Pacific Decadal Oscillation (PDO) and Southern Oscillation Index (SOI) were downloaded from Mantua (2010) website and NOAA (2010) website, respectively, for the 1948-2009 period.

Simple linear regressions and Pearson correlations were calculated between annual totals of hourly and daily dense fog occurrences at LAX and LGB and contributing variables- annual PDO and SOI values, downtown Los Angeles annual TSP amounts, mean monthly and annual temperatures at LAX and downtown Los Angeles, and annual sea surface temperatures (SST) at Santa Monica Pier. Fog frequencies at LAX and LGB were also examined for trends. For comparisons, fog frequencies were also examined for BUR and downtown Los Angeles. As expected, dense fog frequencies were higher at locations near the ocean (Fig. 1).

3. RESULTS

Table 1 shows the average annual number of hours visibility was less than 400 m at various Los Angeles Basin locations over the study period, 1948-2008. Data for downtown Los Angeles (CBD) were only available for the two periods noted, although the station has been moved since 1999. Data for Burbank were not available for the first part of 1998 and therefore 1998 were omitted.

Table 1. Average annual hours visibility < 400m (excludes 1998 for BUR)

LAX 1948-2008	74
LGB 1948-2008	109
LAX 1982-2008	27
LGB 1982-2008	39
BUR 1982-2008	7
CBD 1961-1964	10
CBD 2000-2004	3

There has been a significant decrease in dense fog hours at all locations studied in the Los Angeles Basin. Most notable are the two coastal airports, LAX and LGB (Figs. 2 and 3). Dense fog disappeared completely in 1997 at both stations, but rebounded somewhat in more recent years.

3.1 Air-sea interactions and their influence on fog Frequencies

Previous studies found that coastal sea surface temperatures and Pacific climatic indices, such as The El Niño Southern Oscillation (ENSO) and the Pacific Decadal Oscillation (PDO) influence southern California weather and climate, including dense fog frequencies. While ENSO, as quantified by the Southern Oscillation Index (SOI), was only weakly correlated to dense fog, annual PDO values explained over 34% of the variance seen in the amount of dense fog ($p<.001$) at LAX and 18% of the variance at LGB ($p<.05$) (Witiw and LaDochy, 2008). The fact that the study period overlaps with mostly 1 cycle of the PDO from 1948 to 1997 is not trivial, although more cycles would make the analyses more rigorous. As noted by Mantua (2010), the PDO shifted from a cool phase to a warm phase at about 1977. During cool phases of PDO there are more numerous La Niña episodes and less El Niños, while the opposite occurs during the warm phase. Dense fog frequencies decrease during El Niño events (LaDochy 2005) and disappeared during the 1997-98 major El Niño event. In the same study, annual sea surface temperatures recorded along the coastline at Santa Monica Pier were found to be highly significant at explaining LAX dense fog frequencies ($p<.001$) and at LGB ($p<.001$) for the years 1950-2001.

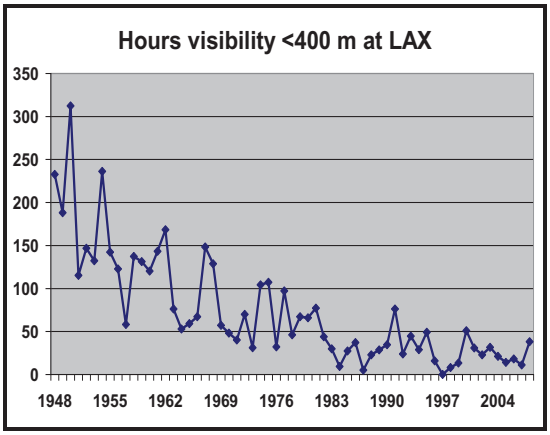

Fig. 2. Dense fog trend at Los Angeles Int. Airport, 1948-2008.

3.2 Particulate air pollution influence

Annual TSP data for downtown Los Angeles was available from 1966 to 2008 (SCAQMD 2009). The trend indicates a significant decrease throughout the period ($p<.001$), dropping to less than half the values of the 1960s by the end of the century. The last decade, 1999-2008, was the cleanest of the record. Witiw and LaDochy (2008) found TSP to be highly significant in explaining hours of dense fog variability with $R2 = .343$ for LAX and .319 for LGB. As TSP levels continue to fall, there are less condensation nuclei available for fog droplet formation. Using multiple regression analyses, the authors showed that the combined effect of TSP and PDO index increased the variance in fog hours explained to 36% at LAX and 33% at LGB for the years 1966-2004.

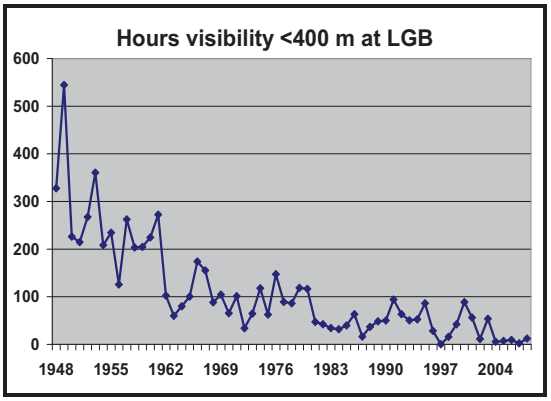

Fig. 3. Dense fog trends at Long Beach International Airport, 1948-2008.

3.3 Urban heat island influence

The temperature trend for downtown Los Angeles shows marked warming over the study period, moreso for Tmin than Tmax. Comparing downtown temperatures with annual days of dense fog, LaDochy (2005) found correlations between annual average temperatures and dense fog highly significant. As temperatures increased, dense fog frequencies decreased. PDO values and coastal SSTs also correlated highly with Los Angeles temperatures, while all three variables correlated inversely with TSP.

In order to test whether factors besides urban heating and particulates are influencing decreasing fog, we are also looking at dense fog frequencies at Vandenberg Air Force Base, approximately 130 miles (210 km) northwest of downtown Los Angeles near the central California coast. While Vandenberg is far from urban influences, it has a different fog regime, with most fog coming in the summer months, while the Los Angeles area shows a winter maximum. Preliminary data show some slight decreasing

tendencies. This may, however, be an artifact of how visibilities are calculated using automated sensors versus humans and should be examined more thoroughly. Data were incomplete from the mid-1970s to the mid 1990s when automated observing began.

4. DISCUSSION

In this study we continue to explore the relationships between atmospheric and oceanic variables and the trend in decreasing Los Angeles area's dense fog frequencies. While urban warming and decreasing pollution are definite contributors, there are also influences coming from the Pacific. PDO values, which may be shifting back into the cool (negative) phase, may nudge fog frequencies higher in the coming years. However, other large-scale influences, particularly global warming, may lead to the opposite, a continuation of decreases.

Dense fog is associated with strong, low inversions over coastal California (Leipper, 1994). Recent trends show that inversion strength has decreased over the last few decades (1960-2007) and that inversion frequencies vary partly in association with SSTs along the California coast (Iacobellis et al., 2009). This would explain one of the mechanisms linking rising SSTs with decreasing dense fog.

Hughes et al., (2009) found that Santa Ana events declined over 30% over the period 1959-2001. They believe that differential warming, that is more rapid warming inland than over the ocean, would make conditions less favorable for these offshore wind events. Santa Ana events are often followed by dense fog, such as on Feb. 7, 2007, when several stations in southern California recorded visibility at 0.0 miles. This followed a strong Santa Ana event.

Several trends in climatic variables, many driven by climate change, point to decreasing dense fog frequencies in the Los Angeles region. If the same trend is occurring along the entire west coast, this may become another important positive feedback in enhancing global warming.

5. REFERENCES

[1] Baars, J.A., Witiw, M.R., Al-Habash, A., Ramaprasad, J.: Determining fog type in the Los Angeles basin using historic surface observation data. Proceedings of the 16th Conf. on Probability and Statistics in the Atmospheric Sciences, Orlando, FL, American Meteorological Society, Boston, pp. J104-107, 2002.

[2]Byers, H.R., General Meteorology, 3rd ed. McGraw-Hill, New York, 1959.

[3]Hughes, M., Hall, A., Kim, J.: Anthropogenic Reduction of Santa Ana Winds. CEC Publication # CEC-500-2009-015f. Available at: http://www.energy.ca.gov/2009publications/CEC-500-2009-015-F.PDF, 2009.

[4]Iacobellis, S.F., Norris, J.R., Kanamitsu, M., Tyree, M., Cayan, D.C.: Climate Variability and California Low Level Temperature Inversions. CEC Publication # CEC-500-2009-020-F. Available at: http://www.energy.ca.gov/2009publications/CEC-500-2009-020-f.pdf, 2009.

[5]LaDochy, S.: The disappearance of dense fog in Los Angeles: Another urban impact? *Physical Geography* 26, 177-191, 2005.

[6]LaDochy, S., Behrens, D.: Particulate air pollution patterns over metropolitan Los Angles. In Majumdar, S.K., Miller, E.W., Cahir, J.C. (Eds.), Air Pollution: Environmental issues and health effects. Pennsylvania Academy of Sciences, pp. 444-459, 1991.

[7]Leipper, D.F.: Fog on the U.S. west coast: a review. Bull. Amer. Meteorol. Soc. 75, 1794-1796, 1994.

[8]Mantua, N.J.: PDO homepage. Available at: http://www.atmos.washington.edu/mantua/pdo.html, 2010

[9]NOAA:. ENSO homepage. Available at: http://www.enso.noaa.gov, 2010.

[10]Norris, J.R., Leovey, C.B., 1994. Interannual variability in stratiform cloudiness and sea surface temperatures. *J. Climate* 7, 1915-1925, 1994.

[11]SCAQMD: Air Quality Annual Summary, 1979-2008. Southern California Air Quality Management District, Diamond Bar, California, 1980-2007.

[12]Witiw, M.R., LaDochy, S., 2008. Trends in fog frequencies in the Los Angeles Basin. Atmospheric Research 87, 293-300, 2008.

5th International Conference on Fog, Fog Collection and Dew
Münster, Germany, 25–30 July 2010
FOGDEW2010-116

The study on estimate historic foggy days using meteorological data at Tatachia region in central Taiwan

T.H. Wey, Y.J. Lai, C.S. Chang, C.W. Shen, B.T. Guan, and P.H. Lin
Experimental Forest of National Taiwan University

The purpose of this study was to understand dew point temperature and solar radiation value during foggy time based on an additional visible sensor at Lintsushan Observatory, Tatachia region, central Taiwan. The analysis showed that the deficit of air temperature and dew point temperature (DADP) were lower than 1 [U+2103] during foggy time. The correlative regression between measured value and estimated value was y = 0.8547x + 0.8872. The correlative coefficient was 0.8341. The historical annual foggy days from 1997 to 2008 of Guanshan Observatory (latitude: 23°30'52.74", longitude: 120°54'42.72", altitude: 1,700 m) and Lintsushan Observatory (latitude: 23°28'38.68", longitude: 120°53'18.47", altitude: 2,780 m) were estimated using Magnus Model Method. The result showed that annual foggy days decreased gradually at Guanshan Observatory located on middle altitude. The annual foggy days increased gradually at Lintsushan Observatory located on higher altitude.

5th International Conference on Fog, Fog Collection and Dew
Münster, Germany, 25–30 July 2010
FOGDEW2010-117

Laboratory studies on the OH-initiated oxidation of acetone in the aqueous phase

T. Schaefer and H. Herrmann
Leibniz-Institut für Troposphärenforschung, Chemistry, Leipzig, Germany (schaefer@tropos.de)

Small organic compounds, such as acetone and its oxidation products, are emitted by a variety of natural and anthropogenic sources in the atmosphere. The degradation or transformation of these compounds can occur in the gas phase and in the liquid phase (cloud droplets, fog, rain or hygroscopic particles) of the troposphere. A special role plays the OH radical, which is one of the most reactive radicals in the atmosphere.

To study the OH radical reaction towards small organic compounds in the aqueous phase, a thermostated laser photolysis long path absorption set-up was used. The OH radicals were generated directly in the reaction cell by the photolysis of hydrogen peroxide (H_2O_2) at λ = 248 nm and monitored using the thiocyanate reference system. Furthermore, the objective of this work is to identify and characterize the various transient species formed in the OH radical reaction. In order to characterize the optical properties of the formed transient compounds (e.g. organic peroxy radicals) a laser photolysis long path absorption apparatus coupled with a CCD-camera / grating combination is used. With this technique time resolved spectra (at different delay times after the excimer laser pulse) of the reactants and products can be recorded. Within this contribution organic peroxy radical spectra of the following parent carbonyl compounds (a) acetone, (b) hydroxyacetone and (c) methylglyoxal will be presented, discussed and compared with literature data.

The optical characterization of the formed transient compound is necessary to measure rate constants of elementary reaction steps in the degradation process of the small organic compounds.

.

5th International Conference on Fog, Fog Collection and Dew
Münster, Germany, 25–30 July 2010
FOGDEW2010-118

Stable isotope techniques to investigate cloud water in forested mountain watersheds in the trade wind latitudes – Hawaii and Puerto Rico

M. A. Scholl (1) and T. W. Giambelluca (2)

(1) U.S. Geological Survey, Water Resources Division, Reston, VA, United States (mascholl@usgs.gov), (2) University of Hawaii at Manoa, Department of Geography, Honolulu, HI, United States

Fog and cloud water can contribute to stream flow, soil moisture, groundwater recharge and plant uptake in mountain watersheds in the trade wind latitudes. Results from three island sites, two in Hawaii and one in Puerto Rico, are discussed to evaluate the utility of isotopic methods in studies of fog and cloud water in watersheds. In forests that are immersed in orographic clouds, the precipitation consists of a range of droplet sizes from fog to rain. Stable isotopes distinguish precipitation source to a greater extent than precipitation size, and isotopic composition of fog-sized droplets may be similar to the smallest raindrops in a cloud. Therefore, results from isotopic methods can differ from estimates using fog collectors, canopy water balances, eddy covariance, and other methods. Examples from study sites in Hawaii and Puerto Rico illustrate these differences. East Maui in Hawaii rises 3054 m above the ocean, and clouds intercept the mountain slopes between 600 and 2200 m on both windward and leeward sides of the island. The eastern mountains of the island of Puerto Rico receive cloud water input at their highest altitudes, between 900-1100 m. In both study areas, stable isotopes of fog/cloud water and rain were measured monthly using passive fog and rain collectors. The sites on Maui were instrumented with weather stations and throughfall gages to estimate cloud water input with canopy water balance methods. Estimates of cloud water as a fraction of total precipitation input from isotopic mixing models and the canopy water balance calculations were 29% and 15%, respectively, on leeward Maui and 27% and 32% on windward Maui, using the most conservative mixing model end member for fog. Cloud water input at Pico del Este in Puerto Rico was estimated to be 45-56% of total precipitation from isotope mixing model results, compared with 10-16% from previous studies using various methods. Sources of uncertainty in using isotope mixing model analyses to distinguish fog from rain inputs include sampling precipitation on a monthly time scale, the fact that isotopes may measure a different droplet size fraction than other methods, and the use of single end-member values when isotopic composition of cloud water may be variable. The uncertainty in mixing model results may be reduced if sampling is done on a shorter (weekly to event) time scale, however, monthly isotope measurements very effectively quantified input from the orographic precipitation pattern that included fog. Isotopic composition of stream water in Maui and Puerto Rico indicated that cloud water was an important component of high-elevation streamflow year-round (62% in PR, 37% in Maui). In Puerto Rico, determining the isotopic composition and amount of rain from different weather patterns showed that streams contained a higher proportion of orographic precipitation than the bulk rainfall, suggesting that the low-intensity cloud water precipitation events were important in maintaining stream baseflow. On Maui, ohia lehua (Metrosideros polymorpha) xylem water isotopic composition indicated different water use strategies by the trees at the windward and leeward sites, which had very different precipitation regimes. Isotope analyses work very well for tracing the pathways of cloud water within watersheds, and results can lead to a better understanding of the role of cloud water in forested mountain watersheds.

5th International Conference on Fog, Fog Collection and Dew
Münster, Germany, 25–30 July 2010
FOGDEW2010-119

Fog water collection with SFC on the mountain Velebit (Croatia) during the period 2000-2009

M. Mileta, T. Likso
Meteorological and Hydrological Service, Zagreb, Croatia, (mileta.cirus@dhz.hr / Fax: ++385 1 48 51 901)

Abstract

Zavižan (1594 m above mean sea level) is the highest mountain station in Croatia and it is chosen for collecting of fog water with a standard fog collector (SFC). It is situated on Velebit Mountain which is the boundary between maritime and continental climate. The methodology of collecting fog water was described in Schemenauer and Cereceda (1994). Fog water collection with SFC started in summer 2000. With a mean air temperature of 5. 1°C the year 2000 was the warmest year in the available measurements (1953-2009). A significant increase in the annual temperature was observed during the whole period 2000-2009. Among 10 the warmest years at Zavižan, 5 were observed in this century (2000, 2007, 2008, 2002 and 2009). The paper discusses the daily fog water amounts collected during the different long periods in the warm parts of the period 2000-2009. The fog water collected in days without precipitation is analysed separately. Also a number of days with fog in the monitoring period have been compared with respect to the average values from the period 1961-1990. Maximum one day–value was 27.8 l/m² observed in October 2003, while the highest daily rate in days without rain was 19.0 l/m² observed in October 2002.

1. Introduction

The meteorological station Zavižan is equipped with the standard fog collector (SFC). It is located at the foot of Vučjak Hill on Northern Velebit, 1694 m above mean sea level (45°49' N, 14°59' E). The methodology used was described in Schemenauer and Cereceda (1994), and it is based on the use of a standard fog collector (SFC) of 1 m² of polypropylene mesh. The results presented here are the daily fog water amounts collected during different long periods in the warm part of 10 years (2000-2009). The measurements lasted until the air temperature became negative. The measurement of fog water in Croatia using the Grunow type of the fog collector (for the 30 years period) and using the standard fog collector (SFC) was presented by Mileta (1998, 2003, 2004).

1.1 The air temperature and a number of foggy days during 2000-2009

A significant increase in the annual temperatures was observed in the first decade of this century. This was the warmest decade ever recorder as shown in Figure 1. Distribution of mean monthly number of foggy days during the observing period 2000-2009 is presented in Figure 2. The number of foggy days is dependent on a season. Maximum was in December (22.4 foggy days) and minimum in July (7.2 foggy days). The number of foggy days during the period 2000-2009 in comparison with the average 1961-1990 is presented in Figure 3. During summer months (June, July and August) and also in April, May and February in the period 2000-2009 the number of foggy days was below the average 1961-1990. In other months number of foggy days exceeded the average as shown in Figure 3.

2.Results of fog water measurement

The fog water amounts in the period 2000-2009 in the warm part of the years have been analised. The data were obtained between July 27 and November 10 in 2000, May 16 and September 27 in 2001, June 26 and October 25 in 2002, July 3 and October 10 in 2003, during June and September (13-24) in 2004, between May 1 and August 31 in 2005, and June 2 and October 17 in 2006, between May 29 and October 12 in 2007 and between May 14 and September 16 in 2008 and from May 9 to October 13. The maximum one-day value was 27.8 l/m² recorded on October 8, 2003. The highest daily collection rate in days without rain was 19.0 l/m² on October 16, 2002. Synoptic situation on October 8, 2003 was characterised by west upper air current with advection of moist air from Atlantic and on October 16, 2002 was southwest upper current with advection of moist air from Mediterranean Mileta (2004).

3. Figures

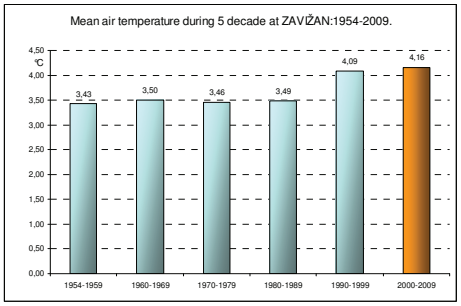

Figure 1: The mean air temperature during periods 1954-1959, 1960-1969, 1970-1979, 1980-1989, 1990-1999, and 2000-2009.

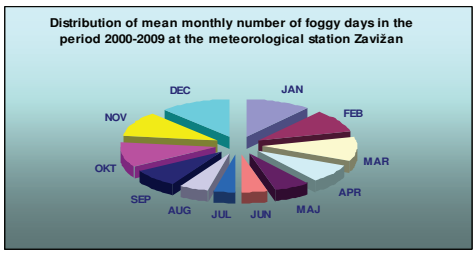

Figure 2: Distribution of mean monthly number of foggy days in the period 2000-2009 at Zavižan.

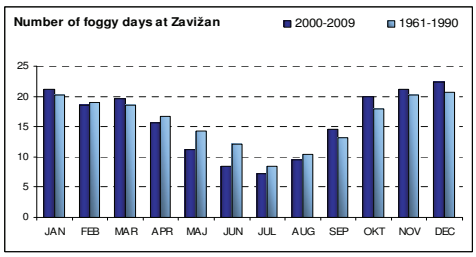

Figure 3: Distribution of mean monthly number of foggy days in comparison with the average 1961-1990.

4. Tables

Table 1: The monthly amount of fog water collected with SFC and fog water contribution with respect to rain (%)

	MAY		JUN		JUL	
	SFC	**%**	**SFC**	**%**	**SFC**	**%**
2000					0.3	15.8
2001	24.5	67.7	37.4	24.3	34.5	51.3
2002			14.3	32.9	21.0	37.5
2003					9.0	54.9
2004			61.5	59.0	-	
2005	77.1	45.9	17.4	39.5	46.9	54.5
2006			36.9	37.8	22.3	27.6
2007	27.6	58.6	46.3	35.4	16.6	61.9
2008	46.9	43.4	41.6	29.8	10.6	22.3
2009	5.1	64.1	46.0	36.5	17.4	29.9

	AUG		SEP		OCT	
	SFC	**%**	**SFC**	**%**	**SFC**	**%**
2000	1.4	20.0	80.0	32.3	177.7	63.9
2001	8.2	78.8	87.8	36.3		
2002	99.8	26.9	128.5	31.4	165.9	162.5
2003	16.6	96.0	78.2	68.3	88.2	92.2
2004	-		44.9	26.6		
2005	92.1	34.4				
2006	75.3	30.4	-		27.1	250.9
2007	50.8	26.2	94.9	36.7	38.4	297.3
2008	18.1	54.5	32.5	142.5		
2009	29.4	25.9	27.7	42.5	16.9	20.6

	NOV	
	SFC	**%**
2000	102.5	48.5
2001		
2002		
2003		
2004		
2005		
2006		
2007		
2008		
2009		

Table 2: The amount of fog water in days without rain

	MAY	JUN	JUL	AUG	SEP	OCT
	SFC	**SFC**	**SFC**	**SFC**	**SFC**	**SFC**
2000			0.1	.	5.7	32.0
2001	7.5	1.2	4.4	2.2	1.2	
2002		4.0	4.4	2.3	5.4	35.5
2003			0.8	0.3	7.3	7.2
2004		0.9	-	-	1.0	
2005	0.9	1.6	3.4	10.8		
2006		1.6	0.4	0.5	-	24.9
2007	.	3.1	2.7	2.6	2.2	2.6
2008	2.3	1.4	2.5	2.1	0.6	
2009	0.4	0.3	0.5	1.4	4.2	3.7

5. Summary and Conclusions

The studies have shown that the fog water constitutes an important water resource in the considered area. The maximum amount of fog water occurs in autumn (October, November) together with the maximum of precipitation. This is caused by the cyclonic activity over the Adriatic Sea and Mediterranean. The greatest need for water occurs during the summer season when many visitors come in National Park where is located the meteorological station. That is the reason why is necessary to start with fog water collection earlier in spring but this is dependent on snow cover and air temperature in spring. It is interesting to note that even in drought condition fog provides a consistent amount of water.

References

[1] Mileta, M.: Fog precipitation on the mountain in Croatia, 1. International Conference on Fog and Fog Collection, 20-24 July 1998, Vancouver, Canada, 1998.

[2] Mileta M.: Special measurements of precipitation and fog water, Zavižan among snow, wind and sun. Meteorological Monography (in Croatian), Zagreb, 2003.

[3] Mileta M., 2004: Results from fog water collection on Mt Velebit in Croatia, 3. International Conference on Fog, Collection and Dew, 11-15 October 2004, Cape Town, South Africa.

[4] Schemenauer, R.S., Cereceda, P.: A proposed standard fog collector for use in high elevation region, Journal of Appl. Meteo., Vol. 33, pp. 1313-1322, 1994.

5th International Conference on Fog, Fog Collection and Dew
Münster, Germany, 25–30 July 2010
FOGDEW2010-120

Large Dew water collectors in a village of S-Morocco (Idouasskssou)

O. Clus (1, 2), I. Lekouch (2,3,4,5), M. Durand (2), M. Lanfourmi (6), M. Museli (2,7), I. Milimouk-Melnytchouk (2,4,5,8), **D. Beysens** (2,4,5,9)

(1) Dhomino RD, Clapiers, France, (2) OPUR International, Paris, France, (3) Université Ibn Zohr, Agadir, Morocco, (4) Ecole Supérieure de Physique et Chimie Industrielles Paris Tech, France, (5) Université P. & M. Curie, Paris, France, (6) IMIRJANE Organization, Mirleft, Morocco, (7) Université de Corse, Ajaccio, France, (8) Arcofluid, Pessac, France, (9) Service des Basses Températures, CEA-Grenoble, France (daniel.beysens@espci.fr / Fax: +33-140795806).

Abstract

The coastal region of south Morocco presents a chronically shortage of drinkable and fresh water. Measurements in the village of Mirleft have shown that collecting dew water could provide 40 % of the rain fall. In order to show to the local population the interest of recovering dew water in addition to rain water, three pilot condensers of terrace, roof and ground type with 136 m^2 total surface area was erected in a small nearby village (Idouasskssou, 8 km SE of Mirleft). A good integration of the project by the village inhabitants was ensured by the cooperation of the local organization IMRJANE. The water production from 15-12-2008 to 31-07-2009 (6 months, 137 dew events for 47 % of days) was more than 3800 L (0.2 mm/dew day). While the devices are specifically designed to condense dew water, they also harvest rain and fog as well.

1. Introduction

Nowadays, the development of the water resources of the arid areas is centered on projects of great irrigation. These projects, however, offer few direct advantages for the small farmers or the nomads who must survive in the constraints of their environment without benefiting from new technologies that are not adapted to their needs. Fortunately, the collection of water is one of the methods of improvement of the conditions of existence of these populations. After the measurements of rain, dew and fog yield in Mirleft, south Morocco (43 m asl, 29° 35' N, 10° 02' W), it was found that the dew contribution, amounting to about 40% of rain precipitation, could not be ignored any more [1].

In a small nearby village (Idouasskssou, 8 km SE of Mirleft, about 300 m asl) some data of dew, fog and rain was collected by OPUR-type 2 m^2 dew collectors and a fog net collector on the roof of a small school by the teacher with the help of a local Organization for local development IMIRJANE. They showed indeed that a significant amount of dew water could be collected. When one of us (O.C.) obtained a 10,000 € award from the Corsica Ferries company for a project of high environmental value and promotion of sustainable development, he gave the amount to the OPUR organization that decided to implement, with the help of the above organization IMIRJANE and the local population a demonstration site at Idouasskssou. the goal was to show to the local population the interest of recovering dew (and fog) water in addition to rain water. The implication of the local population and organization was essential. Three dew condensers (135,7 m^2 total surface area), easily accessible from the ground have been constructed in a month: a roof terrace (40,6 m^2), a slope roof (21,2 m^2), a ground condenser (73,8 m^2), together with a fog collector (30 m^2)

3. Collection devices

3.1 Site

A site favorable to the installation with two water storage tanks on a slope of approximately 17° with the horizontal (Fig.1). The cistern (1) exhibits a planar surface area of 10.6 x 5.3 m^2 on its top and is used as emergency tank when the water distribution is down. The second, 4.7 x 3.0 x 1.60 m^3, not covered, was abandoned. The site is downwards the village on a slope that is not used by the inhabitants. The

installation of condensers will thus not disturb the practices of the inhabitants.
A terrace condenser (40.64 m²) was installed on the covered cistern in (1). The second cistern (2) was rehabilitated to collect water from all the condensers. It was also used to set up a two slopes roof condenser (21.2 m²). In (3), above (2), on the slope, a ground condenser was installed (see Figs. 1, 2).

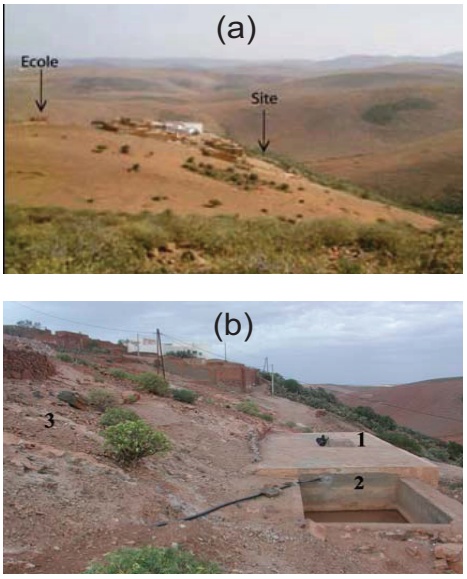

Figure 1: Site in its initial state. (a) General view. (b): (1) condenser on terrace; (2) double-slope roof condenser; (3) full condenser on ground.

3.2 Terrace condenser

The top of the cistern was firstly surmounted by a parapet in order to find a configuration of traditional terrace. The characteristic of this standard " roof " being it is easily accessible. The condensing materials is made with of 0.75 mm galvanized iron sheets painted with a special painting (OPUR) that enhances infrared cooling in the atmospheric window and keeps hydrophilic thanks to continuous photocatalytic reaction with the sun UV. Thermal insulation below the sheets are insured by 2 cm thickness Styrofoam plates.

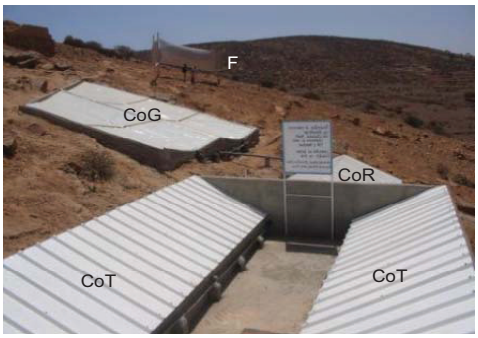

Figure 2: General view. CoT: condenser on terrace, 40.64 m²; CoR: condenser on roof, 21.2 m²; CoG: condenser on ground, 73.8 m²; F: 40 m² fog collector.

3.3 Double-roof condenser

The open cistern (2) was firstly raised by three lines of cement blocks then of a gable intended to receive the ridgepole. The condenser is then installed with the same elements as the terrace condenser.

Figure 3: Two slopes roof condenser (CoR) and condenser on terrace (CoT).

3.3 Condenser on ground

The condenser on ground required a preparation (chaining and stabilization of the ground). The design was selected to profit from the slope of the ground (17°) to collect dew water. The principal surfaces of condensation are tilted by 30° in order to increase the dew yield [2]. The surface is made with a UV treated white polyethylene foil that is commercially

available in Morocco and presents a high resistance to mechanical stress.

Figure 4: Condenser on ground CoG.

3.4 Fog collector

A 40 m^2 fog collector (F) made with two layers of polyethylene shading net (50 % transmission, ribbon width 1.7 mm), similar to that by Schemenauer et al. [3] has been installed nearby the condensers, near a crest (Figs.2, 5). No data have been collected so far.

Figure 5: Fog collector.

3. Measurements

The data were collected during 229 days, between 15/12/2008 and 31/07/2009. 137 events of dew were counted, that is, 46.9% of the period of collection with a cumulated volume of 3791.5 L. It corresponds to an output of 16.6 L / day over the complete period and 27.7 L / dew event. Unfortunately, the method to measure volume (graduated bucket) saturates at 22 L.

On Fig. 6, it is clear that many dew events should have given more water.

According to the figures above, the CoT plus double slope CoR (total: 61. 8 m^2) collect almost the same quantity of water than the CoG (73,8 m²). This can be explained by the difference of materials of collection used (foil and paint) and the method of construction for each system. Indeed, it has been shown [4] that a suspended condenser of 30 m² condenses approximately 14% more than the identical condenser built on the ground.

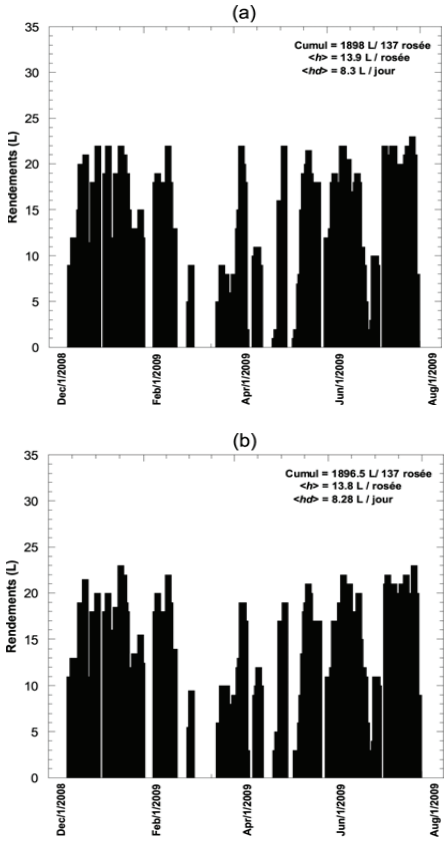

Figure 6 : Dew yield (L) for 229 measurement days. (a) CoT (40.6 m²) plus CoR (21.2 m²). (b) CoG (73.8 m²).

3. Conclusion

The construction of these demonstration condensers, of three main types; CoG on ground, CoR, on roofs and CoT on terraces led to a great satisfaction in the village community. In particular, people were amazed to see the level of water rising although there was no rain.

A year after the construction, the President of the IMRJANE organization left the village. The CoR and CoT were still working a year and a half after their construction. However, due to a severe storm, the CoG was damaged. It is still partially functioning but the foil has not (yet?) been fixed by the inhabitants. They also did not connect the fog net to the tank.

In order to be sustainable and useful on the long term to the population, this kind of project would need a clear involvement of the local authorities to go beyond the good will of small private organizations.

References

[1] Lekouch I., Kabbachi B., Milimouk-Melnytchouk I., Muselli M., Beysens D. Dew, fog, and rain as supplementary sources of water in south-western Morocco. Energy, doi:10.1016/j.energy.2010.03.017.

[2] Beysens D, Milimouk I, Nikolayev VS, Muselli M, Marcillat J. Using radiative cooling to condense atmospheric vapour:a study to improve water yield. J of Hydrology, Vol. 276, pp. 1–11, 2003.

[3] Schemenauer RS, Fuenzalida H, Cereceda P. A neglected water resource: the Camachanca of South America. Bull. Amer. Meteor. Soc., Vol. 69, pp. 138-147, 1988.

[4] Muselli M., Beysens D., Milimouk I. A comparative study of two large radiative dew water condensers. Journal of Arid Environments, Vol. 64, pp. 54–76, 2006.

5th International Conference on Fog, Fog Collection and Dew
Münster, Germany, 25–30 July 2010
FOGDEW2010-121

Three dimensional fog forecasting in complex terrain

M. Mueller (1), M. Masbou (2), and A. Bott (2)

(1) University of Basel, Institute of Meteorology, Climatology and Remote Sensing, Basel, Switzerland (mathias.mueller@unibas.ch), (2) University of Bonn, Institute of Meteorology, Bonn, Germany

Fog in complex terrain shows large temporal and spatial variations that can only be simulated with a three-dimensional model, but more modifications than increasing the resolution are needed. For a better representation of fog we present a second moment cloud water scheme with a parametrization of the Köhler theory which is combined with the mixed phase Ferrier microphysics scheme. The more detailed microphysics produce many differences to the first moment Ferrier scheme and are responsible for reproducing the typically low liquid water content of fog. With explicitly predicted droplet number concentrations, sedimentation of cloud water can be modeled without a prescribed fall speed, which mainly affects the vertical distribution of cloud water and the end of the fogs life cycle. The complex topography of the Swiss Alps and its surroundings are used for model testing. As the focus is on the models ability to forecast the spatial distribution of fog, cloud patterns derived from high resolution MSG satellite data, rather than few point observations from ground stations are used. In a continous five day period of anticyclonic conditions, the satellite observed fog patterns showed large day to day variations with almost no fog to large areas of fog. This variability was very well simulated in the three-dimensional fog forecast. The simulations also demonstrate the need for high horizontal resolutions between 1 and 3 km. For model initialization the complex topography is actually a simplifying factor, as cold air flow and pooling are dominating the more uncertain processes of evapotranspiration or errors in the soil moisture field.

5th International Conference on Fog, Fog Collection and Dew
Münster, Germany, 25–30 July 2010
FOGDEW2010-122

Not just beneficiaries: fostering participation and local management capacity in the Tojquia fog-collection project, Guatemala

M. Rosato, F. Rojas, and R.S. Schemenauer
FogQuest: sustainable water solutions, Kamloops, BC, Canada (melissa.rosato@fogquest.org/Fax:+1-250-374-1746)

Abstract

The largest fog collection project in the world at this time is the FogQuest project in the village of Tojquia, in the Western Highlands of Guatemala. While much attention in the past has been devoted to developing the fog collection technology and finding and evaluating appropriate sites, there is also an opportunity in Guatemala to focus on implementation factors for long-term success in community fog-collection projects. Drawing from the themes of appropriate technology and integrated water-resource management, this paper details the participatory and management strategies undertaken by FogQuest in the ongoing fog collection project in Tojquia. Through a collaborative effort with the community association Mam Ma Qosquix, 30 large fog collectors are in place providing a daily average of 6000 liters of water to over 130 individuals. The current critical developments, it is argued, are to have a discussion on the successes and ongoing challenges in gender mainstreaming, to ensure women's participation and capacity building, and to ensure operation and maintenance capacity are built for the long term. Lessons learned include the importance of fostering trust as a precursor to collaborative effort and recognizing that an engagement will be for the long-term. True sustainability will be reached when the beneficiaries are themselves managers of a fog water collection system. By sharing our experiences we hope to encourage reflection on these important issues, which are relevant throughout the entire planning process, especially when establishing new initiatives.

1. Introduction

An ongoing project in the village of Tojquia in the highlands of Guatemala presents an opportunity to evaluate the human dimension of fog collection technology in the department where as many as 93% of the residents live in poverty and suffer from seasonal water shortages [10]. Best estimates indicate Guatemala-wide only 15 liters per capita per day (lpcd) are available for personal consumption, which falls below the 20 lpcd minimum required for basic existence and well below the 200 lpcd for productive uses [1]. The Tojquia fog collection project aims to increase the lpcd for both personal and eventually productive uses, and contribute directly to poverty alleviation. The unique fog collection technology fits well with the small scale, context-specific solutions promoted by Integrated Water Resources Management and defined as appropriate technology. It is these kinds of solutions that will make a difference in achieving the UN's Millennium Development Goals (MDGs). The focus of this paper is to examine the participatory issues for planning and managing community fog collection projects, using the village project in Tojquia, Guatemala to draw out prominent themes in the literature. The importance of gender mainstreaming, training for Operation and Maintenance (O&M) and fostering local management are evaluated.

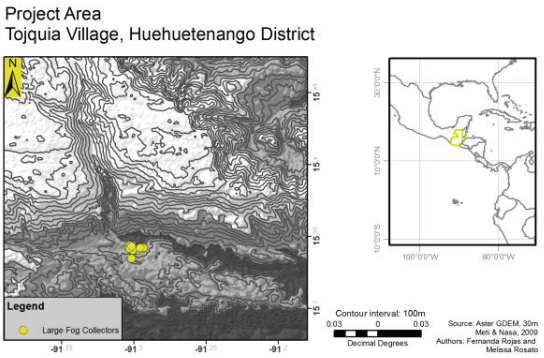

Figure 1: Map of project location, Guatemala

Initiated in 2006 [7], the current fog collection project is now providing water to over 130 people through 30 Large Fog Collectors (LFCs) [6]. Based on an evaluation indicating water resources were not communally managed in Tojquia, this project sought to uniquely implement LFCs at the household level, that is to say one or two are installed adjacent to one or several houses versus arrays of LFCs serving the community at large. This way ownership and responsibilities as well as benefits are clearly defined, and it is hoped fare better for project sustainability. Evaluation for effectiveness is ongoing. From the onset, this project placed locals at the forefront,

respecting their initial apprehension towards development projects. Instead a strong focus was placed on building trust as the key imperative. Upon completion of the first four LFCs with two willing families, the community association was ready to engage in a truly collaborative effort. All LFCs built since 2006 are functioning well giving the community confidence in the technology.

2. An Analysis of Stakeholder Participation in Tojquia – Gender Mainstreaming

An understanding of the role of community participation and community management is crucial to the management of a natural resource such as water. Attention to Arnstein's "ladder of participation" model indicates the more decision-making and management power rests with the participants, the more genuine the participation truly is [5]. With genuine participation, mechanisms are established for enduring engagement and thus success [2]. This is specified by identifying the need to move past manual labour in water projects as the primary mode of participation [8]. In the rural highlands of Guatemala, a well developed and preserved sense of organization and strength in the family unit can be found. These organizational and social structures are usually comprised of the elders, councils and committees [3]. At the same time, issues of seasonal migration are historically entrenched and can have important ramifications for planning and management [4].

In Tojquia, it appears the community is well organized and has higher social capital than in other regions [7]. The villagers have organized themselves as a community association called Mam Ma Qosquix (New Awakening). This group has fulfilled legal requirements for incorporation under Guatemalan law, is comprised of at least 88 families, and has been active for close to 10 years. As such, the community is empowered and in a legal position to seek out financial and project assistance from different government sources. Membership rests on the belief in their founding principles, commitment to the group and collaborative participation. Meetings are scheduled during hours that are sensitive to women's daily tasks, (as well-defined gender roles means women are the primary caregivers). This is especially relevant as there are at least 8 widows in the community of Tojquia. Meetings serve to establish objectives, delineate roles, (there are biannual elections), and are documented formally. This allows opportunities for concerns to be raised and decisions are consensus-based and respected.

For the purposes of the fog collection project, a water subcommittee was formed and has been coordinating the activities on the ground in Tojquia from the beginning. This has worked well and our involvement has remained minimal, both for practical and strategic reasons. Despite initial hesitation, this has not seemed to impair the abilities of the group to make decisions regarding the identification of beneficiary families, keeping track of participating members, organizing work teams, and other tasks in collaboration with FogQuest members when needed. While this is positive, challenges do exist.

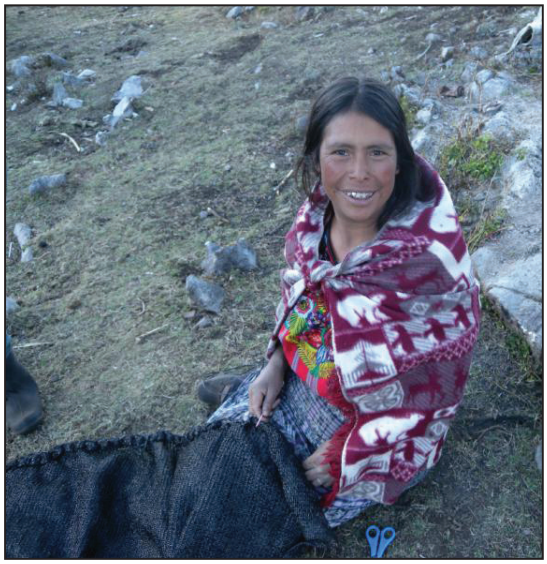

Figure 2: A village lady, Mercedes, sewing LFC mesh.

In Tojquia, there has been an emphasis to seek out women's participation from the onset, though this has been difficult as men are the family representatives and more likely to attend and participate in community meetings where a woman's attendance often indicates her widowed status. For fog collection, efforts to involve all women appropriately during the construction phase (e.g. by sewing the edges of the mesh for the collector) have provided for some engagement, yet also raises the possibility their involvement is "tokenism" [5]. How does an implementing agency both seek gender

sensitivity and respect local values when they include very traditionally-defined gender roles? This one issue demonstrates the challenges of applying theories in practice [9].

Respecting the local community's culture is not only appropriate, it is required to maintain trust and for this reason we have proceeded carefully. As one way to increase women's engagement in the project, the past several years have seen the community host several groups of 20+ individuals as FogQuest involves international students and others in the project. The women's traditional caregiver role is therefore brought into the project to carry out the cooking and other domestic duties, placing an important emphasis on their contribution to the needs of the large groups. Their increased contribution is recognized by the visiting members and also by the men of the community.

A narrow project aim necessarily limits the extent to which we can pursue issues of gender equality, though we seek to do this where feasible and possible. Many FogQuest and student volunteers who have been involved are females themselves who engage in gender-bending activities such as laboring, coordinating and leading, all with the respect of the village men. This serves as just one demonstrable example for women's participation. We hope this example of women's leadership can slowly open the discussion and possibilities to get women more involved in the technical aspects of building and maintenance and for overall empowerment. We recognize traditional and cultural barriers exist, but challenge these for the sake of improving local lives. Given the pattern of seasonal migration for labour and often extended absences by the men, the full inclusion of women is deemed essential for the ongoing operation of the water system.

3. Operation and Maintenance (O&M) Issues

For agencies and small charities such as FogQuest, local organizational capacity is a precursor to initiating a project and this should be evaluated via a comprehensive village assessment prior to any construction. In Tojquia, the community association recognizes the need to manage resources directly, and so our strategy has been to involve different local work teams directly in the builds, by choice for training purposes, but also by necessity due to the limited number of experienced fog collector builders. It is our recommendation that construction should be primarily undertaken by the locals as practice and training for the O&M that is required. In effect, the most recent builds in Tojquia have seen the locals take on more leadership and guide the process without the oversight once necessary. Their suggestion to mostly lead the next build session with only minimal involvement demonstrates the capacity that has been fostered and empowerment also.

However, it can be unreasonable to expect smooth operations to happen automatically. This is due to greatly varying capacity between community members, (case in point some owners are female widows with no experience in the build sessions). As FogQuest's mandate is to implement sustainable water projects, a continued responsibility for maintenance includes the development of local capacity to do so. Fog collector maintenance faces particular challenges inherent in teaching how to operate tools that may be unfamiliar to agriculturalists and developing a specific skill set such as tightening of the structure's cables. Safety training on minimizing risks is also essential as some men continue to be apprehensive about climbing ladders and preparing the cabling for the tightening procedure. It is recognized that not all participants will necessarily be able to maintain their own collectors, regardless of the amount of time spent on training. For this reason the development of clusters of specialists dispersed throughout the village is essential and should be organized around the water committee. In support of this, stocked toolkits have been prepared to ensure the essential tools are there. Increasing knowledge across a larger group is more challenging but necessary and an ongoing process. Future plans include increasing training sessions and, given the high illiteracy, visual manuals.

One encouraging prospect is the fact that several of the more adept villagers are undertaking basic maintenance without FogQuest involvement whatsoever. There is also local to local training happening which is very encouraging. Continuing to support and facilitate this local capacity development has been identified as a crucial objective in the next stages of the project. However, an additional barrier in Tojquia is the strong possibility the more capable young men, the ideal candidates for expedient capacity training, leave the village, as there are historical patterns of seasonal labour migration, and more recently economically attractive "outmigration" to the USA [4, 11]. The local reality dictates the

consideration of training a large pool of people, to the point where local to local training is more common and where O&M operations are viable in the long run despite migration patterns. There is evidence that payment for services, such as wage labour, exists in the area, and this creates potential jobs for those with a developed LFC building skill-set. We like to think that in the future neighbouring communities might seek out their own fog collection projects and hire the Tojquian labour force. Encouraging women to get more involved and emphasizing mutual support via the water committee are also important activities. These are but some mitigation tactics. The community should pursue what is most feasible and desirable with the support of the implementing agency. Further still, there are abundant possibilities to increase the productive uses for the fog water, through greenhouse agriculture for example, as economic development in this impoverished region is made possible by fog water.

4. Summary and Conclusions

The various applied issues outlined above indicate the complexity of ensuring community management and thus a sustainable water project in the long term. While solutions to problems require adaptive capacity at their core, some projected lessons presented here may be applied in the context of other water projects. An examination of a participatory approach was presented, indicating challenges lie with gender mainstreaming particularly in traditional cultural situations such as Tojquia. Community management and specifically the need to address O&M was indicated as a precursor to ongoing success. Clearly the management of a natural resource such as water by locals and efforts to achieve not only project success but sustainable development are a rich and expansive subject matter. The themes discussed here, and the Tojquia successes, should provide encouragement for those seeking to achieve the MDGs and to end poverty in the world, one small water project at a time.

Acknowledgements

The project in Tojquia would not have been possible without a lot of help. We at FogQuest are especially grateful to our longstanding partners: Rotary Clubs in Canada and Guatemala, the International Development Research Centre, Round Square Schools International and Mr. Marco Antonio Ortiz and his warm staff at Tocosa S.A. in Guatemala City. Our deepest gratitude goes to the people of Tojquia who have opened their hearts and homes to us, and who dare to pursue a better future.

References

[1] Gleick, P. H.: The Human Right to Water, Water Policy, 1(5), pp. 487-503, 1998.

[2] Harvey, P. A., & Reed, R. A.: Community-managed water supplies in Africa: Sustainable or dispensable? Community Development Journal, 42(3), pp. 365-378, 2007.

[3] IRC International Water and Sanitation Centre.: Water supplies managed by rural communities: Country reports and case studies from Cameroon, Colombia, Guatemala, Kenya, Nepal and Pakistan. No. 5-E. Delft, the Netherlands: IRC International Water and Sanitation Centre, 1997.

[4] Lovell, W. G.: Conquest and survival in colonial Guatemala: A historical geography of the Cuchumatan highlands, 1500-1821. Montreal: McGill-Queen's University Press, 2005.

[5] Mitchell, B.: Resource and environmental management (2nd ed.). Harlow, England; New York; Prentice Hall, 2002.

[6] Schemenauer, R.S. and Joe, P.: The collection efficiency of a massive fog collector. Atmospheric Research, 24, 53-69, 1989.

[7] Schemenauer, R. S., Rosato, M., & Carter, V.: Fog collection projects in Tojquia and La Ventosa, Guatemala. 4th Intl Conf. on Fog, Fog Collection and Dew, 22-27 July 2007, La Serena, Chile , 2007, pp. 383-386, 2007.

[8] Schouten, T. In Moriarty P.: IRC International Water and, Sanitation Centre (Eds.), Community water, community management: From system to service in rural areas. London: ITDG, 2003.

[9] Singh, N.: Equitable gender participation in local water governance: An insight into institutional paradoxes. Water Resources Management, 22(7), pp. 925-942, 2008.

[10] Steinberg, M. & Taylor, M.: Guatemala's altos de Chiantla: Changes on the high frontier. Mountain Research and Development, 28(3-4), pp. 255-262, 2008.

[11] Taylor, M. J., Moran-Taylor, M. J., & Rodman Ruiz, D.: Land, ethnic, and gender change: Transnational migration and its effects on Guatemalan lives and landscapes. Geoforum, 37(1), pp. 41-61, 2006.

5th International Conference on Fog, Fog Collection and Dew
Münster, Germany, 25–30 July 2010
FOGDEW2010-123

Fog Collection Pilot Project (FCPP) in the Eastern Escarpments of Eritrea

T. Gherezghiher
Vision Eritrea, Asmara, Eritrea, (drtseggai@gmail.com)

Eritrea is water scarce country that relies heavily on underground water reserve and more than 80% of the rural population does not have access to safe and clean drinking water. In the rural areas, shallow hand dug wells are the primary sources of water and in most cases their discharge rate is deteriorating due to the recurrent drought. Particularly, in the targeted project areas underground water reserve is hard to find due to the steep topography. However, in these parts of Eritrea one will find a sector of mountains, about 700 km long, where the wind transports moist air from the Red Sea forming fog on the highlands. The area of the FCPP is the region of Maakel, near the villages Nefasit and Arborobu. The overall objective of his FCPP was to provide supplementary water supply system from large fog collectors (LFCs) in order to increase access to safe and clean drinking water in the targeted Schools and surrounding villages. Communities and students were organized to participate in the implementation of the project. Forty LFCs were established in all the targeted areas in previously evaluated potential locations.
The project was implemented by Vision Eritrea, a National NGO in partnership with the country's' Water Resource Department; Fog Quest a Canadian NGO and Water Foundation, a German NGO, who also funded the project. The FCPP focused on introducing a new innovative water harvesting technology which is a crucial element for the survival of the people in the mountainous escarpment of the country; and with prospect of locally owned solutions for a sustainable management of and access to natural resource. Preliminary evaluation of the project showed that there was a good production of fog water, with an average of 6-8 litters/m2/day on the low intensity of fog and from 12 -18 litters on the high fog intensity. A functional water committee was established and trained on water management and maintenance of the LFC. They also developed water bylaw by which the water committee manages the water supply system. Similarly, the fog collectors have also been proved indeed to collect rain water during the wet seasons. This will extend the water harvesting period of the LFC within a year. The new fog harvest technology will further be developed in the target areas and in the long term is expected to help decrease poverty, improve food security and have a positive impact of the livelihood of target communities and neighboring villages. As a result, its dissemination and the mainstreaming of the action will be greatly facilitated to other similar part of the country where water can be harvested from fog.

5th International Conference on Fog, Fog Collection and Dew
Münster, Germany, 25–30 July 2010
FOGDEW2010-124

Characteristics of water-soluble ions before, during and after fog events

P. Li (1), H. Du (1), C. Yang (1), J. Yao (1), J. Du (2), and J. Chen (1)

(1) Fudan University, Environmental Science and Engneering, Shanghai, China (jmchen@fudan.edu.cn), (2) Baoshan Weather Administration, Shanghai, China

Two atmospheric processes of rain-fog-haze and haze-fog-rain were observed on Feb.8th and Mar. 14th, 2010 in urban Shanghai. On-line characterization of water-soluble ions of aerosol was performed before, during and after two fog episodes by an instrument of Monitoring AeRosoles and GAses (MARGA). Fog water samples were also collected to study the chemical ion characteristics for identifying the property of fogs. After rain, total water-soluble ion concentration in PM2.5 increased by 71.9%. Afterwards, a fog formation was observed as a frontal fog. Six fog water samples were collected to measure concentration of water-soluble ions, whose total concentrations decreased from beginning to end of fog. At the end of fog, the total water-soluble ion concentration of aerosol was continually increased. Meanwhile with a sharp decline of RH down to 70% in two hours, and a haze episode was observed. The reverse process, haze-fog-rain process, was also investigated. After the haze episode, total water-soluble ions concentration of aerosol rarely increased, but fog appeared with sharp increase of RH. Concentration of water-soluble ions in the fog water sample was higher than mean concentration of samples in 2009. When the fog started to disperse, the ion concentration hardly changed. As water vapor continued to increase, rain was observed. The inorganic compositions of aerosol in both fog events were dominated by sulfate and ammonium. The in situ investigation clearly illustrated that fog water mainly influenced by continental sources was dirtier and contained more sediment comparing with fog water influenced by marine sources.

5th International Conference on Fog, Fog Collection and Dew
Münster, Germany, 25–30 July 2010
FOGDEW2010-125

Spatial Variation of Dew over India

T. Madhavan (1) and G. Sharan (2)

(1) Indian Institute of Management, Ahmedabad,India (email: madhavan@iimahd.ernet.in), (2) DA Institute of Information and Communication Technology, Gandhinagar, India (gsharan@iimahd.ernet.in)

Dew harvest systems - devices to condense and collect dew water - have been developed for use in arid coastal region of the north-west India. These are installed over building roofs, over open ground and along boundary walls of large properties. Several installations, some as large as 850 m2 condensing surface, have been functioning in the region for several years. There is potential to deploy these in other areas where dew occurs and water is in short supply. However, lack of reliable data on dew occurrence hinders their adoption and diffusion. Indian Meteorological Department (IMD) monitors dew deposition using Duvdevani gauges at 79 locations in the country. Data includes dew fall amount over a six month span (October to March), number of dew nights. The north-east region has the highest dew resource. Other parts that have high accumulation are along the coast. Using data from 79 locations, spatial variation of dew amount has been characterized using variogram. Spatial clustering has been done to indicate areas with similar accumulation. Kriging is used to determine expected dew accumulation by extrapolation in areas for which measured data is not available but which lie near one or other monitoring station. The results of this analysis would be of use to those who need to assess the potential of dew harvesting in various parts of India especially in coastal zones.

5th International Conference on Fog, Fog Collection and Dew
Münster, Germany, 25–30 July 2010
FOGDEW2010-126-1

Occult precipitation as an input to the small catchment: observation, evaluation and new technics of fog water collection in the Czech Republic

M. Tesar (1), J. Fisak (2), M. Sir (1), and K. Bartunkova (2)

(1) Institute of Hydrodynamics ASCR, Pod Patankou 30/5, 166 12 Prague 6, Czech Republic (miroslav.tesar@iol.cz / +420-233324361), (2) Institute of Atmospheric Physics ASCR, 1401 Boční II , 141 31 Praha 4, Czech Republic (fisak@ufa.cas.cz / +420-272763745)

The main objectives of the present contribution are to: (i) describe the monitoring network created in the mountainous regions in the Czech Republic; (ii) assess the input of water and pollutants from the wind driven low clouds and fogs onto the forest canopy; and (iii) introduce new ground-level cloud water sampler designs.
Montane ecosystems can receive considerable inputs of water and dissolved substances from ground-level cloud and fog events. In order to study the input of water and matter from wind driven low clouds and fogs on the water balance and chemistry of mountainous forested catchments, three experimental watersheds were established: (1) the Liz basin (Sumava Mts. – southern Bohemia; 0,99 km2, 828 – 1073 m a.s.l., prevailing type of tree: spruce aged up to 120 years); (2) the Uhlirska basin (the Jizerske hory Mts. – northern Bohemia; 1,87 km2, 774 – 870 m a.s.l., prevailing type of tree: spruce aged up to 80 years); (3) the Modry potok basin (the Giant Mts. – north-eastern Bohemia; 2,62 km2, 1010 – 1554 m a.s.l., prevailing type of tree: spruce and dwarf pine 62 % and meadow 38 % of the area). These experimental catchments are placed in the main massifs of the Bohemian border mountains. They differ especially in the level of anthropogenic impacts on vegetation cover.
The hydrological and ecological significance of occult precipitation will be demonstrated. The chemistry of falling bulk precipitation sampled at the open area will be compared with the throughfall and with surface water sampled at the closing profile of each watershed. For the whole observed time period analytical results of the chemical analyses will be summarized. Based on the model predictions and on the water balance of the forest canopy the annual occult precipitation totals were estimated by the 10 % of the annual falling precipitation total in the Sumava Mts., by 10 – 15 % in the Jizerske hory Mts., and even more than 20 – 25 % in the Giant Mts. A fog water study carried out over the 16-years period proved high acidity of fog water and high values of enrichment factors. The compounds NH4+, SO42- and NO3- are the dominant species both in fog water and in precipitation.
In order to collect cloud water samples, the active and passive sample-taking devices were constructed. Besides the collectors, as described in literature, both passive and active fog water collectors of the new design were developed and installed at the selected localities.

5th International Conference on Fog, Fog Collection and Dew
Münster, Germany, 25–30 July 2010
FOGDEW2010-127

Guanaco traces and hunting strategies at Alto Patache North Chilean fog oasis

H. Larrain (1), P. Cereceda (1), and L. Pérez (2)

(1) Instituto de Geografía, Centro del Desierto de Atacama, Pontificia Universidad Católica de Chile, Santiago, Chile (dcereced@uc.cl/56-2-5526028), (2) Universidad Bolivariana, Iquique, Chile (luchonomas@hotmail.com)

1. In foregoing Fog Conferences, some of us have made explicit the rich botanic and faunistic inventory to be found at this Chilean Fog site. This was specially apparent under strong ENSO conditions, as it happened in 1997/98 in the area.
Among the mammal biggest species represented, the guanaco (Lama guanicoe Müller) merits special mention. Clear traces of their presence and eventual hunting and slaughtering by primitive populations have survived until present times. Among them, the myriads of guanaco trails still covering practically all the slopes along the foggy area, close to the sea, and their wollowing and defecating places are found. Also, although less studied, plant eating traces left behind by roaming camelids can be seen.
2. Guanaco hunting traces still visible at Alto Patache can be portrayed differently through : A) Analysis of lithic artifacts used as arms in hunting operations; B) Botanic response to animal attack; C) Examination of topographic traits used by primitive man in guanaco hunting strategies.
A. Hundreds of lithic instruments made of stone, were abandoned by hunters in situ, some of them were intact, some fragmented, which would demonstrate a direct relationship with hunting and slaughtering, and also their elaboration in workshops at place. Lithic points, scrapers and knives were found at places specially apt for hunting or slaughtering activities. Total isolation of the mountain fog site previous to our arrival in 1996, favoured their conservation at place.
B. Careful observation of some local plants showed clear traces of guanaco feeding habits. As a proof thereof, old cactus of the species Eulychnia iquiquensis show in their basal portions clear signals in the forms of scars, caused by the eating by guanacos. Guanaco faeces were found at the foot of Ephedra plants. Many dead Stipa ichu plants (Gramineae), in different areas of the oasis provide evidence of cutting close to their basis, caused by sharp guanaco tooth under severe food scarcity.
C. Special lookouts located at high places offering clear visibility were used by hunters. Some were built up, some others consisted of natural stone arrangements. The same can be said for the wollowing places, located in plains with loose or sandy soils.
Pictures showing different artifacts, plants or topographic traits used, will be presented here as evidence of guanaco hunting activity at place.

5th International Conference on Fog, Fog Collection and Dew
Münster, Germany, 25–30 July 2010
FOGDEW2010-128-2

Analyzing the spatio-temporal distribution of fog in French Guiana using ground-based and satellite data

A. Obregon, M. Hansmeier, and J. Bendix

Laboratory of Climatology and Remote Sensing, Department of Geography, University of Marburg, Germany
(obregon@staff.uni-marburg.de)

Fog occurrence is extensively studied in the outer Tropics and in tropical montane cloud forests, but investigations in tropical lowland forests are virtually lacking. The knowledge of temporal and spatial fog dynamics in tropical lowland forests is generally poor. We investigated the spatio-temporal distribution of fog in a tropical lowland forest in central French Guiana. Data of important meteorological parameters were gathered by installation of a climate station directly above the forest canopy (45 m above ground). Horizontal visibility (and thus fog occurrence) was observed by using a visibility and present weather sensor (HSS VPF-730, Biral). The spatial extent of fog was analyzed by means of night-time AVHRR and MODIS satellite data using an algorithm relying on brightness temperature differences between the long-wave and medium infrared bands. The output of the fog detection scheme was validated against horizontal visibility data from the ground station.
It is shown that fog occurs frequently in river valleys of French Guiana. During the measurement period, fog occurred on nearly all days in the dry season and on every day in the rainy season. Comparable high fog frequencies are hitherto only reported from tropical montane cloud forests. Fog frequency shows a clear diurnal course, with a maximum during early morning hours. Solar heating after sunrise leads to rapid fog clearance. First results of the satellite data analysis indicate a widespread distribution of night and morning fog in river valleys throughout the country.

5th International Conference on Fog, Fog Collection and Dew
Münster, Germany, 25–30 July 2010
FOGDEW2010-129

Secondary organic aerosol formation through fog processing of VOCs

P. Herckes and J.W. Hutchings

Arizona State University, Dept. of Chemistry and Biochemistry, Tempe, AZ 85287-1604, United States
(Pierre.Herckes@asu.edu)

Volatile Organic Compounds (VOCs) including benzene, toluene, ethylbenzene and xylenes (BTEX) have been determined in highly concentrated amounts (>1 ug/L) in intercepted clouds in northern Arizona (USA). These VOCs are found in concentrations much higher than predicted by partitioning alone.

The reactivity of BTEX in the fog/cloud aqueous phase was investigated through laboratory studies. BTEX species showed fast degradation in the aqueous phase in the presence of peroxides and light. Observed half-lives ranged from three and six hours, substantially shorter than the respective gas phase half-lives (several days). The observed reaction rates were on the order of 1 ppb/min but decreased substantially with increasing concentrations of organic matter (TOC).

The products of BTEX oxidation reactions were analyzed using HPLC-UV and LCMS. The first generation of products identified included phenol and cresols which correspond to the hydroxyl-addition reaction to benzene and toluene. Upon investigating of multi-generational products, smaller, less volatile species are predominant although a large variety of products is found. Most reaction products have substantially lower vapor pressure and will remain in the particle phase upon droplet evaporation.

The SOA generation potential of cloud and fog processing of BTEX was evaluated using simple calculations and showed that in ideal situations these reactions could add up to 9% of the ambient aerosol mass. In more conservative scenarios, the contribution of the processing of BTEX was around 1% of ambient aerosol concentrations.

Overall, cloud processing of VOC has the potential to contribute to the atmospheric aerosol mass. However, the contribution will depend upon many factors such as the irradiation, organic matter content in the droplets and droplet lifetime.

5th International Conference on Fog, Fog Collection and Dew
Münster, Germany, 25–30 July 2010
FOGDEW2010-130-1

Fog processing of polycyclic aromatic hydrocarbons (PAH)

Y. Wang (1), K. Khadapkar (2), F.S. Ehrenhauser (2), J.W. Hutchings (1), M.J. Wornat (2), K.T. Valsaraj (2), and P. Herckes (1)

(1) Arizona State University, Dept. of Chemistry and Biochemistry,Tempe AZ 85287-1604, United States , (2) Louisiana State University, Cain Department of Chemical Engineering, Baton Rouge LA 70803, United States

Polyaromatic hydrocarbons (PAHs) are a class of organic species of concern for environmental and human health. The present work will present initial finding of a comprehensive study on the fate of PAHs in multiphase fog/cloud systems and across consecutive fog/smog cycles.

Field observations were conducted in Fresno, CA in Winter 2010. Simultaneous measurements of gas phase, aerosol and fog PAH allowed to gain insights on the partitioning of PAH in a multiphase fog system. Partitioning results as well as temporal evolution of PAH concentrations across different phases will be discussed. Select known degradation products (oxy-PAH) from the processing of PAHs were also analyzed in the fog systems, although frequently their concentrations were close to or below detection limits, even in the polluted urban study setting.

The field observations are complemented by laboratory investigations on the reactivity of PAH in fog systems, both heterogeneously and in the aqueous phase. Heterogeneously a novel reactor design is being tested to simulate fog systems and allow for repeat fog/smog cycles. A separate series of measurements investigated the processing of PAH in the aqueous phase in a solar simulator set-up.

5th International Conference on Fog, Fog Collection and Dew
Münster, Germany, 25–30 July 2010
FOGDEW2010-131

The performance of sonic anemometers under foggy conditions – An intercomparision above a Taiwanese mountainous cloud forest

T. El-Madany (1), F. Griessbaum (1), F. Maneke (1), H.-S. Chu (2), C.-C. Wu (3), S.C. Chang (2), Y.-J. Hsia (2), J.-Y. Juang (3), and O. Klemm (1)

(1) Institute of Landscape Ecology, Climatology, University of Münster, Germany (tarek.elmadany@uni-muenster.de), (2) Institute of Natural Resources, National Dong Hwa University, Hualien,Taiwan, (3) Department of Geography, National Taiwan University, Taipei, Taiwan

Foggy conditions are a toughness test for anemometers because the transceivers are continuously influenced by the deposition of fog-droplets. During a period of nearly four weeks three sonic anemometers where tested for their performance under foggy conditions. The anemometers were set up on a 24 meter high flux tower in a 14 meter high Chamaecyparis obtusa var. Formosana forest. The test anemometers were a Gill R3-50, a Young 81000V, and a Campbell CSAT3 (equipped with 'dripping noses'). All anemometers were set up at one level on the highest platform of the tower. The performance was evaluated on the basis of 10 Hz data. The test site is located in the northwest of Taiwan at about 1650 m above sea level. This location is influenced by a steady diurnal wind system of valley winds during daytime and mountain winds during nighttime. The valley winds transport air masses from the coast up to the mountain where they cool down and fog development occurs. Due to this effect the site is highly frequented with fog. Results of this intercomparison will be presented.

5th International Conference on Fog, Fog Collection and Dew
Münster, Germany, 25–30 July 2010
FOGDEW2010-132

Simulation of regional fog event with WRF in North China and evaluation of visibility equations

C. Pang (1,3), J. Liu (1,3), Y. Li (1,3), and N. Niu (2)

(1) Institute of Atmopheric Physics, Chinese Academy of Sciences, Beijing, China (chengmingpang@126.com), (2) China Meteorological Administration Training Centre, Beijing, China, (3) Beijing Institute of Aviation Meteorology, Beijing, China

The fog events are adversely affecting transportation due to worsening visibility, affecting the air quality and health through accumulation of pollutants near the ground. Forecasting the fog events successfully is helpful to reduce their disadvantageous impact on visibility, air quality and health etc. The forecasting ability of numerical model for fog is currently limited. Successful simulation of fog events and evaluation of visibility equations leading to an improvement of the forecasting ability of numerical model is the focus of the paper. The fog models can almost only simulate a local fog event, but the regional fog event is more and more. So in the paper the weather research and forecast (WRF) model is used to simulate and forecast the regional fog event in North China. The fog events form in atmospheric boundary layer (ABL), even in a hundreds-meters layer near surface. So 9 σ levels are added in ABL mainly below 500 meters and appropriate parameterization schemes are adopted to localize WRF in North China. During the period of Nov. 29th to Dec. 2nd of 2009 a regional fog event is burst in North China. Using GFS 0.5ºx0.5º forecasting dataset as the initial and boundary conditions a two-way and three domains nested simulation of the fog event is run with localized WRF model. The simulated weather type is very similar to the observing one. The simulated distribution of liquid water content (LWC) on the bottom levels of model matches basically the fog area according to the stations which report fog weather. The comparisons between the model results and observing meteorological data show a good potential forecasting ability of localized WRF model for fog events in North China. Visibility is the main judging parameter for the fog event. A few visibility equations functioned by LWC or combining of LWC and number concentration of droplets (N_d) which are derived from the former studies are added into the simulation of the fog event. The derived visibility results are evaluated according to the observing visibility. The forecasting ability of the visibility method combining of LWC and N_d is better than that of the LWC one.

5th International Conference on Fog, Fog Collection and Dew
Münster, Germany, 25–30 July 2010
FOGDEW2010-133

Open path measurements of carbon dioxide and water vapor under foggy conditions – technical problems, approaches and effects on flux measurements and budget calculations

T. El-Madany (1), F. Griessbaum (1), F. Maneke (1), H.-S. Chu (2), C.-C. Wu (3), S.C. Chang (2), Y.-J. Hsia (2), J.-Y. Juang (3), and O. Klemm (1)

(1) Institute of Landscape Ecology, Climatology, University of Münster, Germany (tarek.elmadany@uni-muenster.de), (2) Institute of Natural Resources, National Dong Hwa University, Hualien,Taiwan, (3) Department of Geography, National Taiwan University, Taipei, Taiwan

To estimate carbon dioxide or water vapor fluxes with the Eddy Covariance method high quality data sets are necessary. Under foggy conditions this is challenging, because open path measurements are influenced by the water droplets that cross the measurement path as well as deposit on the windows of the optical path. For the LI-7500 the deposition of droplets on the window results in an intensity reduction of the infrared beam. To keep the strength of the infrared beam under these conditions, the energy is increased. A measure for the increased energy is given by the AGC value (Automatic Gain Control). Up to a AGC threshold value of 70 % the data from the LI-7500 is assumed to be of good quality (personal communication with LICOR). Due to fog deposition on the windows, the AGC value rises above 70 % and stays there until the fog disappears and the water on the windows evaporates.

To gain better data quality during foggy conditions, a blower system was developed that blows the deposited water droplets off the window. The system is triggered if the AGC value rises above 70 %. Then a pneumatic jack will lift the blower system towards the LI-7500 and the water-droplets get blown off with compressed air. After the AGC value drops below 70 %, the pneumatic jack will move back to the idle position.

Using this technique showed that not only the fog droplets on the window causing significant problems to the measurement, but also the fog droplets inside the measurement path. Under conditions of very dense fog the measured values of carbon dioxide can get unrealistically high, and for water vapor, negative values can be observed even if the AGC value is below 70 %. The negative values can be explained by the scatter of the infrared beam on the fog droplets. It is assumed, that different types of fog droplet spectra are causing the various error patterns observed.

For high quality flux measurements, not only the AGC threshold value of 70 % is important, but also the fluctuation of the AGC value in a flux averaging interval. Such AGC value fluctuations can cause severe jumps in the concentration measurements that can hardly be corrected for. Results of fog effects on the LI-7500 performance and its consequences for flux measurements and budget calculations will be presented.

5th International Conference on Fog, Fog Collection and Dew
Münster, Germany, 25–30 July 2010
FOGDEW2010-134-1

Coalescence of fog droplets: Differential fog water deposition on wet and dry forest canopies

C. Tobón and J. Barrero
Universidad Nacional de Colombia, Sede Medellín (ctobonm@unal.edu.co)

The Páramo ecosystem is a high-altitude (2800 - 4500 masl), natural ecosystems which comprises approximately 42000 km^2, extending across the Andes from north of Peru, Ecuador, Colombia and western part of Venezuela. Andean páramos are widely considered to be prime suppliers of large volumes of high-quality water for large cities and for hydropower production. As páramos tend to be subjected to persistent fog incidence, fog interception by the vegetation is a common process in these ecosystems, representing not only an extra input of water to the ecosystem but also to suppress evaporation. In this process, small drops of water, transported by the wind, are captured by the surfaces of the vegetation, acting as physical obstacles to the flow of fog. These drops condense in the exposed surfaces and drip towards the ground or evaporate from the surfaces. The quantification of the magnitude of these processes is important for the quantification of the water balance of river basins where these types of ecosystems exist. Although the great hydrological importance of fog in montane tropical ecosystems little is known about its physical principles related to the interception of fog by physical barriers as vegetation, notably the differential behaviour of a wet and dry vegetation in the efficiency of capturing water from the fog. To characterize and quantify this efficiency of páramo vegetation in capturing water from the fog, during wet and dry canopy conditions, an experimental design was set up at the Páramo de Chingaza (Colombia) where paired samples of espeletia branches (dry and wet) were exposed to different fog events, and at the same time Juvik cylinders were exposed by the side of the experimental site, to measured fog inputs. Cylinders were also paired (wet and dry) at the beginning of the experiments. Results indicated that exposed wet and dry samples have a significant difference on the magnitude of water intercepted from the fog, being, in average, the wet samples more efficient on capturing fog water. Same behaviour was observed from exposed cylinders, although magnitude was not similar between samples and cylinders, being the cylinders more efficient. Besides tendencies on fog interception were positively associated to the intensity and duration of the fog events, results also indicated that this differential efficiency on capturing the small drops by the wet and dry canopy seems to be related to the coalescence principle, or the interactions of drops, where the coalescence depends on the size of the drops and the humidity state of the interacting surface where the drops merge. The differences on fog interception efficiency is discussed from the physical principles of coalescence of drops impacting wet (drop – drop) and dry surfaces (drop – air).

5th International Conference on Fog, Fog Collection and Dew
Münster, Germany, 25–30 July 2010
FOGDEW2010-135

Fog collectors and collection techniques

I. Höhler (1) and Dr.C. Suau (2)

(1) Muthesius Academy of Fine Arts and Design Kiel, Industrial Design, Technical Design, Germany (gold_i@gmx.de), (2) Welsh School of Architecture, Cardiff University, United Kingdom (suaucristian@googlemail.com)

The earth sciences taught that due to the occurrence of water in three phases: gas, liquid and solid, solar energy keeps the hydrological cycle going, shaping the earth surface while regulating the climate and thus allowing smart technologies to interfere in the natural process by rerouting water and employing its yield for natural and human environments' subsistence.

This is the case of traditional fog collectors implemented by several researchers along the Atacama Desert since late '50s such as vertical tensile mesh or macro-diamonds structures. Nevertheless, these basic prototypes require to be upgraded, mainly through new shapes, fabrics and frameworks' types by following the principles of lightness, transformability, portability and polyvalence. The vertical canvas of conventional fog collectors contain too much stressed at each joints and as result it became vulnerable.

Our study constitutes a research by design of two fog-trap devices along the Atacama Desert. Different climatic factors influence the efficiency of fog harvesting. In order to increase yield of collected fog water, we need to establish suitable placements that contain high rates of fog's accumulation. As important as the location is also the building reliability of these collectors that will be installed. Their frames and skins have to be adjustable to the wind direction and resistant against strong winds and rust. Its fabric need to be more hydrophobic, elastic and with light colours to ease dripping/drainage and avoid ultra-violet deterioration. In addition, meshes should be well-tensed and frames well-embraced too.

In doing so we have conceived two fog collectors: DropNet© (Höhler) and FogHive© (Suau). These designs explore climatic design parameters combined with the agile structural principles of Tensegrity and Geodesic widely developed by Bucky Fuller and Frei Otto. The research methods mainly consisted of literature review; fieldwork; comparative analysis of existing fog collection's techniques and climatic design simulations.

DropNet© is a lightweight fog collector kit -a standing-alone web- resistant against very strong winds. It is constructed with an elastic mesh according to the required tension. Apart from this, it is ease to be transported, assemble and relocated due to its tent-like construction. As a flexible construction it can be installed on flatten or uneven grounds.

FogHive© is a modular space-frame, fully wrapped with a light waxy mesh, that can collect water fog and also performs like a shading/cooling device and a soil humidifier for greenery and potential inhabitation. Its body consists of a deployable polygonal structure with an adjustable polyvalent membrane which performs as water repellent skin (facing prevailing winds) and shading device facing Equator. In addition, a domestic wind turbine is installed within the structural frame to provide autonomous electrification.

Both models have great applicability to provide drinking water in remote place and also irrigating water to repair or re-establish flora. Water collector, filtering (purification) and irrigation network are designed with appropriate materials and techniques.

5th International Conference on Fog, Fog Collection and Dew
Münster, Germany, 25–30 July 2010
FOGDEW2010-136

Fog deposition at a windward Costa Rican cloud forest site

K.F.A. Frumau (1), L.A. Bruijnzeel (2), and C. Tobon-Marin (3)

(1) ECN, Energy research Centre of the Netherlands, Petten, The Netherlands, frumau@ecn.nl, (2) VU University, Amsterdam, The Netherlands, (3) Universidad Nacional de Colombia, Medellin, Colombia

The hydrological importance of tropical montane cloud forests is recognized increasingly, mostly with respect to the additional water inputs provided by the capture of fog by the forest canopy compared to a non-forested situation (e.g. pasture) in the same environmental setting. The deposition of fog (interception) consists of two components, viz. advectional impaction against roughness elements in the landscape, and vertical settlement both by turbulent diffusion and by gravitational settling. Turbulent diffusion being a function of the aerodynamic roughness of the surface it is typically enhanced over forest compared to pasture.

In windward montane areas fog often consists of stratus clouds being forced uphill with the cloud being "stripped" by roughness elements in the landscape. However, due to rain-generating processes these clouds rarely have fog-sized droplets only and larger drops are present as well. Under sufficiently strong wind speeds (e.g. in the trade-wind belt), drizzle-sized droplets tend to follow the terrain and behave like fog. Consequently, there is no unbiased manner in which to separate between fog and drizzle using conventional fog and rain gauges only. Similarly, hydrologically
effective precipitation (inclined rainfall) is difficult to determine in mountainous areas, which complicates the determination of fog deposition using wet-canopy water budget approaches.

The deposition of fog to a windward Costa Rican montane cloud forest was studied during a full hydrological year (between 1 July 2003 and 1 July 2004). Fog deposition was estimated from the wet canopy water budget as the difference between hydrologically effective precipitation and the sum of throughfall, stemflow, and interception loss. The results show that fog interception constituted a much smaller contribution at this site compared to wind-driven drizzle.

5th International Conference on Fog, Fog Collection and Dew
Münster, Germany, 25–30 July 2010
FOGDEW2010-137

Dynamics and evolution of tree populations and soil-vegetation relationships in Fogscapes: Observations over a period of 14 years at the experimental sites of Meija (Peru).

F. Salbitano (1), G. Calamini (1), G. Certini (2), A. Ortega (3), A. Pierguidi (1), L. Villasante (3), R. Caceres (3), D. Coaguila (3), and M. Delgado (3)

(1) DEISTAF, University of Florence, Italy (fabio.salbitano@unifi.it), (2) DI.P.S.A., University of Florence, Italy, (3) IRECA, Universidad Nacional de San Augustin de Arequipa, Peru

The Fogscapes, i.e. fog-dependent landscapes, and the sub mountain drylands of the Pacific Coast from Ecuador to Northern Chile are amongst the most fragile regions of the planet. The so-called “Lomas” (i.e. Hills) ecosystems are characterised by pre-desertic flora and vegetation where the plant phenological pattern coincides with the fog season from June to December every year. The occurance of ENSO (El Niño Southern Oscillation) affects these ecosystems inducing, occasionally, a sudden change in the characteristics of the vegetation. Relics of low-density woodlands dominated by Caesalpinea spinosa and scattered trees of the same species (which during the fog season appear as savannah-like ecosystems) are still present but becoming increasingly rare due to past and present over-grazing

In the experimental site of Las Cuchillas, located on the coastal hills close to Meija (Dept. Arequipa, South Peru) trees of native species (Caesalpinaea spinosa and Prosopis pallida) and exotic species (Acacia saligna, Casuarina equisetifolia, Parkinsonia aculeata) were planted in 1996, in order to look at the rehabilitation potential of the degraded “lomas” ecosystems. This paper deals with the results observed over a period of 14 years’ of tree growth patterns and the related results concerning the soil and habitat dynamics. Among indigenous species Caesalpinea spinosa shows the heighest rate of survival even if the height increment is low and the tree crowns tend to dry out at a height of approximately two metres, followed by the appearance of new shoots produced during the course of the seasons. The exotic Acacia saligna shows the maximum height, diameter and crown volume increments. The habitat conditions, both in term of diversity / frequency of plant and animal populations, and plant cover (LAI estimated by processing fish-eye lens images) have changed substantially over the years. A number of samples from the top mineral soil and random samples from the forest floor were collected both from the reforested test site and from the adjacent control areas were no trees had been planted. The samples were analysed for organic carbon and total nitrogen. Overall, the tree-covered soil retained much more of both elements than the non-forested areas, thus demonstrating the efficiency of the intervention carried out in terms of combatting the greenhouse effect. The various tree species planted, however, showed greatly variable capacity to promote carbon sequestration at soil level.

The results referred to above are critical in understanding the plant population dynamics of pre-desertic ecosystems in response to climate change and in assessing the potential of reforestation programmes and landscape conservation strategies for the purposes of carbon sequestration.

5th International Conference on Fog, Fog Collection and Dew
Münster, Germany, 25–30 July 2010
FOGDEW2010-138

Analysis of Paris- Fog using ground based aerosol and meteorological measurement

N. Boyouk (1), M. Haeffelin (2) J- C. Dupont (2) T. Elias(3)
(1) LMD - Ecole Polytechnique, France, (2)IPSL /SIRTA, Ecole Polytechnique, (3)IPSL/ CEA,France
(neda.boyouk@lmd. polytechnique.fr)

Abstract

Fog is important atmospheric phenomena interns of air quality. Low visibility as imperative fog factor may result due to high level of aerosol number concentration in affirmative meteorological condition and high relative humidity. This work analysis micro-physical and optical aerosol properties and meteorological condition of fog and quasi fog event to improve understanding of micro-physical process during fog occurrence and the influence of aerosol on fog formation.
Based on high decrease on visibility on foggy days(less than 1km) and quasi fog (between 1km and 2 km), we have compared the temporal evolution of aerosol parameters (mass and number concentration, extinction and absorption coefficient) for fog and near fog event. In addition, the analysis of temporal series of meteorological parameter (temperature, humidity, wind speed, wind direction) help us to better understand the micro-physical process which are the important reason for formation ,removal or modification of particle and increase of fine aerosol number concentration during fog event.
An increase in aerosol micro-physical or optical properties (mass, accumulation number, extinction coefficient) shows large variation in visibility. This variability is much higher in case of fog event compare to near fog. The chemical analysis used to find the influence of fog on aerosol type characteristic specially the aerosol acidity. The cation-to-anion ratio for explain how accumulation mode are acidity. There is a good correlation between the Pm2.5 and visibility during fog event with a correlation coefficient of R=0.84.

1. Introduction

Fog formation and low surface visibility are important to be predicted due to their influences on aviation, transport, navigation and traffic. Low visibility prediction is not easy due to complexity of formation processes which depends on physical and chemical properties of aerosol and meteorological elements. However using the ground based or remote sensing measurement and models, many studies (Baumer et al. 2008; Gultepe et al. 2009; Kokkola 2003; Nowak et al. 2008; Stolaki et al. 2009) have been acquired to understnd the microphysical and meteorological process and effect of pollution result in fog formation, but Operational forecasting of fog in Environmental centers and for numerical weather prediction is difficult due to complexity of fog and limited computing resources available for forecasting. It is necessary to present aerosol emission, related pollutant and land surface properties in fog situation for climate simulation models (Oldenborgh et al. 2010). Zhou et al (2010) have used multivariable diagnostic(lowest level liquid water content, cloud top, cloud base, wind speed, relative humidity) fog prediction method which works better than unique variable method. The application of this multivariable approach to a multi model mesoscale prediction system and performance of ensemble base forecast was statistically superior to single- value. They can found occurrence of fog but not intensity of fog.
Using satellite measurement can help us for fog prediction, The map of fog and low stratus distribution over Europe based on Satellite data have been presented by (Cermak et al. 2009). They have found general pattern of Meteosat second generation and 26 year ground base measurement of visual cloud observation are in good agreement.
Large scale atmospheric circulation influences micrometeorological conditions of formation of advection and radiation fog at ground level. Large scale circulation also indirectly could be a reason for

enhancement of aerosols concentration, advection of pollutant, height of mixed layer and probabilities of precipitation in favorable meteorological conditions and high relative humidity(Oldenborgh et al. 2010). The radiation fogs are influenced by not only local pollution but also by long range transport. Radiation fog is formed when pollutant stagnates in the surface under the anticyclonic condition with calm wind and the pollutant can settle around fog droplet (Ogawa et al. 2004).

Gultepe et al (2009) have been shown that interaction of microphysical, dynamical, radiative process and surface conditions influence on life cycle of fog. The large variability on RH and visibility parameterization has been observed. Oldenborgh et al. (2010) have shown contribution of dynamic of atmosphere depends on topography and season is about 40%. The fog duration and intensity depends on meteorological, regional, geographical parameters. Wang et al (Wang et al. 2010) based on satellite data and meteorological parameters have found that distribution of radiation fog depends on types of surface underneath. Dunkerke (1998) have compared a deep and shallow fog observations (surface net radiation, soil heat flux, Liquid water content, temperature) by a one dimensional average model for parameterization of vegetation.

Fog frequency influenced by the airborne pollutant properties (particulate matter PMx, aerosols, sulfure-dioxide,….) in megacities. An analysis of trends in fog frequency by Shi et al (2008) shows that the impact of urbanization on fog is different at various stages of urban development. The number of annual fog days in most cities studied has increased since the 1960s but decreased after the mid 1980s in large, old cities. New cities, on the other hand, are characterized by still increasing fog frequency. During the last thirty years, average fog duration increased and visibility decreased at most urban stations. Based on observations over Europe 1976-2006 it has been found a decrease in number of fog and mist days which is spatially and temporally related in SO_2 emissions. The correlation is more at 5km visibility, for dense fog the correlation are significant (Oldenborgh et al. 2010). In foggy days Diurnal variation of SO_2 and NO_2 have inverse relation with visibility due to formation of secondary pollutant sulfate and lesser extent nitrate (Mohan; Paraya 2009). Kokkola et al (2003) reveal the oxidation of SO_2 to sulfate has significant effect on fog droplet gross when hygroscopic trace gases, for example HNO3 and NH3 are present. Wen et al (2010) have analyzed the influence of airborn pollutant and meteorological parameters on visibility in Taiwan. They have found high visibility is along with low level of PM10 less than 150 μgm^{-3} with clear atmosphere. They have found a method of prediction of airborne pollutant based on visibility.

The decrease of visibility is associated to increase in the aerosol number concentration of particle less than 300nm (Baumer et al. 2008). Increase in number concentration of nucleation and accumulation mode with decrease in nucleation mode radius and increase in accumulation radius shows hygroscopic and coagulation growth of particles (Das et al. 2008). Elias et al (2009) shows that the accumulation mode have been contributed to extinction in haze condition 100%, clear sky 50% and fog condition 20% ±10. During fog condition nucleation mode is decreasing by collision to droplet. The accumulation and droplet mode are significant on extinction.

Das et al. (2008) show the relationship between aerosol optical thickness and visibility during fog days. They have found that the aerosol optical thickness increase in fog days compare to the previous day.

In this study we have chose the period of Paris fog (Jan, Feb, March 2007) in that the aerosol properties have been measured during fog and quasi fog events. Based on definition from AMS (American-meteorological-society 2000)fog is Water droplets suspended in the atmosphere in the vicinity the earth's surface that reduce visibility below 1 km (10-min averaged visibility remains below 1 km during at least 30 minutes over a 50-min time window). Mist is suspension in the air consisting of an aggregate of microscopic water droplets orwet hygroscopic particles (of diameter not less than 0.5 mm or 0.02 in.), reducing the visibility at the earth's surface to not less than 1 km. (not used in this study because it lacks precise upper boundary in visibility) Near fog are the events in that 10-min averaged visibility ranges between 1 and 5 km during at least 30 minutes over a 50-min time window. In Quasi fog events, the 10-min averaged visibility ranges between 1 and 2 km during at least 30 minutes over a 50-min time window (Haeffelin et al. 2010).

Our objective is to better understand the microphysical and dynamical processes which have the most influence on life cycle of fog. We want to find a key parameter between microphysical and meteorological elements for fog prediction. In section 2, we present the instruments which have been used to measure the visibility and microphysical, optical and meteorological parameters (number and mass concentration of aerosol and droplet, aerosol optical

thickness, backscattering coefficient, pollutant concentration; PM2.5 and PM10). In section 3, we will discuss the method which have been used to understand the process before formation of fog ; in haze regimes which occur as transition between the clear-sky and fog regimes, visibility is highly variable in this regime. Haze regime is defined as visibility smaller than 5000 m, down until fog occurrence(Elias et al. 2009). We retrieve visibility using aerosols optical thickness: AOT and backscattering coefficient for fog and quasi fog events when the atmosphere is convective and considering uncertainties in the retrieval and assumptions on the mixing of the boundary layer. In section 4, we present the meteorological condition during fog and quasi fog events. The section 5, first, present the analysis which have been acquired to find the key parameters between meteorological, microphysical properties of aerosol and pollutants (accumulation aerosols number and mass concentration, wind component and PM2.5) for formation of fog. Second the result of the retrieved visibility using aerosol optical thickness and ceilometer backscattering coefficient at lowest level is presented. In section6, the results are resumed.

2. Instrument

We have used the measurement acquired for the Paris - Fog experiment (Haeffelin et al. 2010) on the Sirta observatory (48.7°N, 2.2°E) during winter 2006 and 2007. Simultaneous measurements of dynamic, thermodynamic, radiative, microphysics of aerosols and fog properties have been monitored. During several intensive observational period (IOP) (Haeffelin et al. 2010) measurements have been acquired as manual-system . We have focused on period of Jan to march 2007. The instruments used in our study are presented in table1. A complete description of Paris -Fog and instrument can be found in Haeffelin et al (2010) and Elias et al (2009).
The degreanne visibilimeter working at height of 4m provide the ground- level visibility. For the measurement of scattering coefficient the nephelometer TSI 3563 have been used working at 450, 550, 700nm. The counting of aerosol particles has been measured by TSI smps in range of 0.01 to 0.50 µm diameter. Palas Welas 2000 particle spectrometer is sampling the particle number and size in range between 0.39-42 µm (aerosol and droplet).
A modified vaisala ceilometer ct 25k 905 nm was used to profile aerosol backscatter. The backscattered radiation caused by particles allows aerosol layers, haze, and cloud base to be identified. In rain and fog, the ceilometers is only used to measure cloud base.

Table 1 List of instruments deployed during ParisFog, parameters that can be retrieved from their measurements, instrument range (vertical range, spectral range, as relevant) and resolution, and type of operations (RT: routine operations).
T: temperature, RH: relative humidity, WS: wind speed, WD:Wind direction, AOT: aerosol optical thickness, Vis : visibility, βc: aerosol scattering coefficient , β, Back scatter by č eilometers ND: droplet number, NA: aerosol number,D: Particle diameter, PM Particle mass concentration, AO: ambient outdoor

Instrument	Model	Temporal resolution	Parameter	Uncertainity measurement	Sampling,
Thermometer, humidity sensor		1 min	T, RH		AO, RT
Sonic anemometre		1s	WS, WD		AO
sunphotometer	Cimel 318 λ= 440, 670, 870, 1020 nm	15min	AOT, ω_0	AOT 5%	AO, RT
Visibilimetre	Degreanne (DF320&DF 320+) λ= 490- 750 nm	10s	Vis	10-25%	AO
Nephleometerer	TSI3563 λ= 450, 550, 700 nm	1 min	βc	10%	PM10 inlet
Particle counter	Welas-2000 D=0.39-42 µm	5 min	ND and NA	20%	AO
Particle counter	TSI- smps D=0.01-0.5 µm	10 min	NA	20%	PM10inlet
Particle counter	Grimm-5400	1min	NA	10%	PM10 inlet
Ceilometer	Vaisala CT25K λ= 905 nm	1 min	β		PM10 inlet, RT
TOEM			PM2.5		

There are two types of measurement stations in Ile-de France region air quality monitoring network (http://www.airparif.asso.fr), 41station of air quality monitoring which are situated far from the urban circulation and near to traffic. They are classified as traffic, urban, suburban and industrial. The mean inter station distance are 2km in the urban zone and 6 km in the suburban one. The concentrations of SO2, NO, NO2, PMX, CO, O3 have continuously been monitored and data are available on an hourly basis.
In the present study we are using PM2.5 and PM10 data collected by a Tapering Element Oscillation Microbalance TEOM (Patashnick; Rupprecht 1991) operated by the regional air quality network. Comparisons of TEOM to gravimetric measurements show that routine TEOMs can underestimate PM10 by up to 35% (Allen; Ress 1997; Van Dingenen et al. 2004). TOEM at SIRTA is not working continuously. We have used the measurement of VITRY-SUR-SEINE. The two stations are in different geographical But there is a good correlation between the PM2.5 measurement. The simple regression between data shows that PM2.5(Vitry) =0.98 PM2.5(SIRTA)+3.6 with correlation coefficient R^2=0.87 (Figure.1).

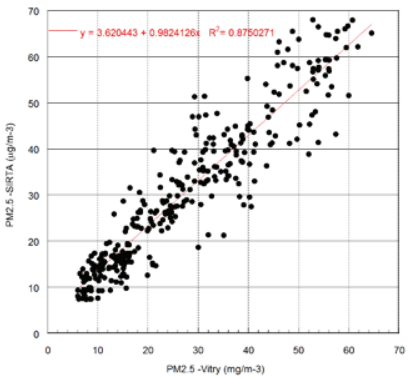

Figure 1 Relationship of PM2.5 at vitry- sur- sein and Sirta PM2.5 measurement

3. Methodology

You We have analyzed the processes taking place during fog formation versus non-formation in similar conditions (quasi-fog), in clean and polluted air masses. We know the droplet are formed in haze, causing fog outbreak then based on our main question in terms of aerosol properties difference between the pre-fog haze and near fog conditions, which are close to fog conditions we have used different method which will be described as following. The radiation fog are chosen as fog days.
First, We have analyzed the temporal variation of meteorological parameters and visibility to find out the difference which makes fog (visibility less than 1km) and quasi fog events when they have the similar situation. We have analyzed compared the hourly average of data during these events.

Second, We had analyzed the temporal variation of AOT and number concentration for the days when fog and quasi fog occur: implication of accumulation mode aerosols in visibility, AOT, relation mass-visibility. This is to check consistency of the data base as we showed in the paper for visibility and microphysics. With combination of remote sensing and ground based measurement we want to study the relationship of visibility and aerosol properties during fog and quasi fog events. We have retrieved the visibility using columnar aerosol optical thickness to find out how AOT and visibility are in good correlation. Using available hourly data of AOT of Aeronet, we have retrieved the visibility by a simple relationship between AOT($_{\lambda=440}$) and visibility. The measured visibility is averaged every 10min and AOT depends on local situation and is available just in clear sky. In the Koschmeider equation formula then visual range can be expressed in term of extinction coefficient (b_{ext}) with unity of km^{-1} (Seinfeld; Pandis 2006).

$$Vis = 3.912/b_{ext} \quad (1)$$

And aerosol optical thickness is defined by following equation in range of 0 to Z_l

$$\tau = \int b_{ext}\, dz \quad (2)$$

Combining Equation 1 and 2 we obtain the simple relationship between visibility and aerosol optical thickness as following

$$Vis = 3.912\, Z_l/\tau \quad [3]$$

We have assumed that the Z_l; is mixing layer height which can is calculated from the ceilometers measurement when the atmosphere is convective and considering uncertainties in the retrieval and assumptions on the mixing of the boundary layer.
We have then determined the altitude of the boundary layer by using a simple gradient method applied to the ceilometer profiles acquired during the day and night at a time resolution of 1 min. Under the basic assumption that the aerosol mass is well mixed in the boundary layer and that the relative humidity has a negligible impact on the extinction coefficient.
Using the first available level of the ceilometer signal, S(z) at the lowest available altitude can be used to infer the mass concentration close to the ground. We have estimated that the first level that can be used is at z = 15 m. Secondly using the first available level of the ceilometer signal, the error in estimating ground-level visibility is proportional to the error in the ceilometer backscattered signal in the first hundred meters. An additional source of error comes from the impact of the relative humidity on the aerosol optical properties. This impact can be modeled (Hänel 1976) when the aerosol type (hygroscopic factor) and the vertical profile of relative humidity are known (Raut; Chazette 2008). Since we have the relative humidity measured at the ground, we have only applied a correction factor for the ceilometer signal close to the ground following Raut and Chazette (2007) with an exponent factor of 0.55. S*(z_l) is the corrected signal:

$$S^*(z) = S(z) * \left(1 - RH\right)^{0.55} \quad (3)$$

Where RH is the relative humidity. The overall uncertainty is between 20 and 40% (Boyouk et al. 2009).

$$Vis = 3.912 / (S^*(z_l) * L) \quad (4)$$

Where it is assumed in the first level the attenuation is negligible. L is a constant value of extinction to backscatter coefficient at 905 nm.

Fog and quasi fog event are classified based on observation of visibility and to make comparison between fog event and quasi fog event we have averaged data on different time scale of 10 minute, 30 minute, 1 hours. The microphysical properties of aerosol data as mass and number concentration of accumulation, ultrafine and fog droplet have been averaged every 30 minutes. meterological data, visibility and lowest level of backscatter of ceilometer and boundary layer height is averaged over 10 minutes. PM2.5, PM10 and other pollutant which have been used in our analysis were available on hourly average (http://www.airparif.asso.fr).

Table 2 Radiation fog and quasi fog event during Jan, Feb, March 2007 –Paris fog the time is corresponded to the time of the observation of lowest visibility

FOG	Date / Time	Fogtype	Lowest visibility m	synoptic
	27/01/2007 23:30	RAD	0.07	H
	18/2/2007 22:40	RAD	0.07	H
	4/3/2007 6:30	RAD	0.15	T
	13/03/2007 23:10	RAD	0.1	H
Quasi fog	Date/ Time	Weather – condition		
	1/6/07 2:10	PCP+LowC	1.92	L
	1/29/07 19:20	SKC	1.82	H
	2/1/07 2:10	LowC	1.31	H
	2/5/07 21:00	LowC	1.99	T
	2/7/07 3:30	LowC	0.85	T
	2/19/07 20:10	SKC	0.4	H
	3/2/07 18:00	PCP+LowC	1.86	H
	3/9/07 10:20	PCP+LowC	1.78	L
	3/11/07 3:50	SKC	1.41	H
	3/27/07 0:20	SKC	1.58	L
	3/27/07 23:00	SKC	1.6	T
	3/29/07 3:10	SKC	1.12	L

4. Synoptic condition and visibility

The formation, dissipation and evolution of fog are highly depended on meteorological condition. The near fog situation has also been influenced by synoptic condition. Table 2 shows the list of the fog and quasi fog event which have been analyzed in this study. Based on the time of observation of the lowest visibility we have averaged the data on fog and quasi fog event. We have compared fog and quasi fog events in different average scale to find the key elements. The 4 days of radiation fog and 12 days of quasi fog events have been analyzed. We have studied the meteorological situation as a permanent parameter in fog formation during Jan, Feb and March 2007 for fog and quasi-fog events. The monthly average of meteorological data and visibility has been shown on Table. 3.

The visibility (Vis) is ranged between 22 and 28 km during winter. There is 6 days with daily average of Vis less than 5k during the period. Two foggy days 27 Jan and 2 Feb and 3 days of quasi fog events are included. 28 days of whole period has the daily average of visibility more than 29 km. The average of lowest visibility at fog days is 270 m and for quasi fog event is 1450m. We have considerd the time of the day, the local meteorological influence like temperature, humidity and wind speed to better describe the daily evolution of the visibility and the important keys of fog formations.

The evolution of Relative Humidity (RH)during the 3 months Jan, Feb, March have been studied (are not shown here). Before 6 Jan there is no high variation of RH. But the morning of 6 and 7 Jan RH increase to 95% the morning and decreases in afternoon. The days before fog and foggy days (1, 5, 7 and 8 Feb) in the morning the values of RH are larger than 95 %. We have observed an important variation before 18 and 19 Feb (value between 50% and 90%) during fog and quasi fog events. Radiation fog, which generally occurs as ground fog, is caused by the radiation cooling of Earth's surface. The average of temperature for whole period is about 7°C. It is primarily a night time occurrence but it often begins to form in late afternoon and may not dissipate until well after sunrise. Radiation fog is common in high-pressure system where the wind speed is usually low (less than 2.5m/s) and clear skies are frequent. Table.3 shows that we have higher pressure on January compare to March and February. The dominant wind in the whole of period is blowing

from south-west with the speed of 3m/s in Jan and Feb and 2.6 ms^{-1} on March.

Table 3 The monthly average of visibility and meteorology data during Jan, Feb and March 2007, and average of meteorological parameter and visibility at thetime of lowest visibility of fog and quasi fog event Average[min-max]

Date	VIS(km)	T(°C)	RH(%)	P(hPa)	WD(deg)	WS(m/s)
Jan	28 [0-99]	6.9 [-6-14]	86[25-99]	1002 [987-1017]	220	3.8[0.1-11.7]
Feb	22 [0.07-99]	7.4 [-1.2-17]	84[45-99]	992 [970-1017]	200	3.1[0.1-11.4]
March	23 [0.07-99]	7.1 [-1-19]	80[36-99]	998 [976-1022]	227	2.6[0.1-10.7]
Fog	0.27 [0.1-0.9]	4 [2-7]	96[92-99]	1006 [998-1017]	206[96-343]	1.4[0.4-2.4]
Quasi-fog	1.47 [0.4-1.99]	6 [1-11]	91[81-97]	999 [981-1017]	166[48-337]	1.8[0-4.8]

Mean while the table. 3 shows the10 minute average of visibility and meteorological parameters at the time of observation of lowest visibility for fog and quasi fog days. Stolaki et al (2009) have studied fog events which is mainly formed in winter in Greece. They observed that Formation of fog is around sunrise or 1 or 2 h before it in Thessaloniki. The mean duration is about 4h with density of 75%. In our study, Fog days happened normaly after sunset between 22 and 24 UTC except 4 March in that fog happened before sunrise. Lowest visibility in quasi fog event (12 days) have been observed between 0 to 3UTC, one case at 10 UTC and between18 and 23 UTC after sunset. We have higher temperature in quasi-fog days compare to fog events whereas the relative humidity is about 96 and 91 for fog and quasi fog days respectively.

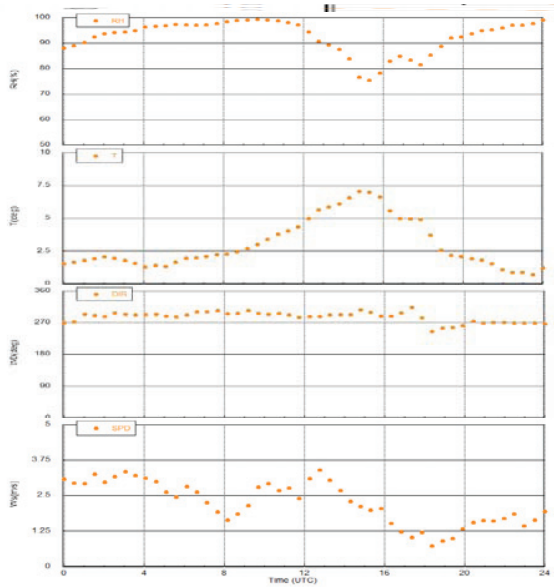

Figure 2 10 minute average of meteorological parameters of a fog condition on 27 January 2007; fog formation at 23:50 visibility, relative humidity, temperature, Wind direction speed and wind speed

In foggy days dominant wind is from south-west and for quasi fog event is south-east with the calm wind of about 1.5 m/s. Figure 2. shows the synoptic – meteorology and visibility of a fog study on winter of 2007 on 27 January. The fog has been formed at 23:50 UTC. All of the meteorological parameters have been compared by the variation of the visibility. The temporal variation of these parameters before formation of fog can help us to better understand the impact of meteorology on visibility. The visibility changes between 100 m and 15km. It can be observed that the highest value of relative humidity 99% is related to 100 m of visibility. The wind direction approximately is in NW section whole days and it changes to SW at 17UTC . The largest value of visibility is observed at 17 UTC and it changes to less than 5km (haze before fog) 2hours before formation of fog.

5. Result and discussion

Aerosol optical and microphysical (mass, number, aerosol optical thickness, extinction coefficient) properties have been analyzed during Paris –fog experiment 2007. Table.4 shows the microphysical and optical properties of aerosol which have been averaged based on the time of observation of lowest visibility. It can be observed that the AOT has the same average value for fog and quasi fog event at the time of lowest visibility. Fog event has higher AOT between 0.1 and 0.2. The available AOT data on quasi fog event is 50% and for radiation fog event 100%. The average mass concentration of ultrafine aerosol particle is higher for fog event. The PM2.5 and PM10 mass are higher in radiation fog compare to quasi fog event 65 and 83% respectively. Accumulation mode number during radiation fog days is ranged between 459 to 2973 cm-3 and their mass is ranges between 305 and 2271 µgcm-3. As the droplet are forming before the time of observation of lowest visibility then microphysical and meteorological parameters some hours before the fog formation are important to be analyzed. Table 5. shows the average of microphysical parameters 3h, 2h and 1h before observation of minimum visibility. The hourly average of the parameters has been presented after the observation of reduction of visibility 3h before formation of fog or observation of minimum visibility. 3h before observation of lowest visibility; first, the level of hourly average of visibility is decrease about 72% compare to one hour before fog formation. For quasi fog the visibility of

12 km decreases 3h before observation of lowest visibility to 10.9 km and to 9.9 km 1 h later which is about 20%.

Table 4 Average of aerosol microphysics characteristic at the time of lowest observed visibility, *UF : Ultra-Fine mode (r<0.5µm) , AC : Accumulation mode 0.4<r<2µm) , FD : Fog Dropplet (r>2µm)*

		Number of part. /m³						Mass of part. /m³	
Moyenne [Min-Max]	AOT	PM2.5 Fixy	PM10	UF	AC	FD	PM2.5 SIRTA	UF	AC
FOG	0.13 [0.1-0.2]	44 [20-66]	53 [15-81]	10553 [7280-16000]	1482 [459-2973]	76 [85-194]	34 [7-63]	4 [2-6]	1347 [305-2271]
QUASI-FOG	0.13 [0.01-0.2]	24 [9-55]	32 [12-63]	12798 [1580-28200]	103 [44-446]	2.9 [0.2-8.1]	32 [16-48]	2.7 [0.6-5.1]	144 [45-289]

Wind direction during fog days is in WS and it is approximately blowing from the same direction during 3h before formation of fog whereas in quasi fog days the wind changes from S to SW. we have higher wind speed 3h before observation of lowest visibility quasi fog days but the wind speed does not vary a lot.

Table 5 .Average of microphysical parameters before observation of minimum visibility. The hourly average of the parameters has been presented after the observation of reduction of visibility from 3h before formation of fog or observation of minimum visibility.Q-Fog are the quasi fog event.

	Vis (km)	DIR (deg)	SPD (m/s)	N1	N2	N3	M1	M2	M3
3h before Min Vis									
Q_FOG	12.0	177.4	1.9	8535.5	9515.6	142.4	30.1	2.2	91.9
FOG	8.1	208.1	1.2	5706.2	15446.3	119.5	27.7	3.3	94.1
2h before Min Vis									
Q_FOG	10.9	219.9	1.8	7333.4	11436.9	427.5		2.7	197.0
FOG	5.4	202.4	1.3	2464.8	14333.8	556.7	39.6	3.4	247.1
1h before Min Vis									
Q_FOG	9.9	221.0	1.8	7685.5	12558.8	692.1		2.9	690.2
FOG	2.2	222.1	1.4	1307.0	13562.5	1147.6	43.3	3.7	713.2

N1 (cm-3) aerosol number concentration measured by CPC, for diameter D < 3 um, N2 (cm-3) ultra fine aerosol number concentration measured by SMPS (D<0.5 um), N3 (cm-3) accumulation mode aerosolnumber concentration measured by WELAS-2000 (0.4<D<2 um), M1 (ug/m3) aerosol mass measured by TEOM, M2 (ug/m3) ultra fine aerosol mass measured by SMPS (D<0.5 um), M3 (ug/m3) accumulation mode aerosol mass measured by WELAS-2000 (0.4<D<2 um)

Number of aerosol measured by CPC is less than quasi fog days. Ultra fine particle number is decreasing about 25% in foggy days however their mass is approximately constant. The accumulation mass and number has approximately higher value of 89% and 86% 1h before formation of fog compare to 2h former. The variation in mass and number of accumulation mode in fog and quasi fog events has upward trends which is one of the most important keys in fog formation beside meteorological parameters.

5.1 Microphysiccal and optical properties of aerosol(Mass, number)

5.1.1 Particle mass concentration PM2.5, PM10 and other pollutants

The role of aerosol in fog formation not only depends on their optical properties and their size distribution of diurnal cycle of particle mass concentration on reduction of visibility and fog formation.

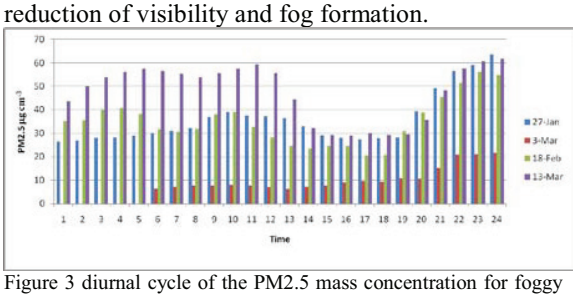

Figure 3 diurnal cycle of the PM2.5 mass concentration for foggy days, 27 Jan, 18Feb, 3 and 13 March

Figure3. shows the diurnal cycle of PM2.5 for foggy days. It can be observed that after sunset the level of PM2.5 have a high increase and is not just due to urban circulation. It can be also related to increase of humidity after sunset but the increase of humidity is not the single reason because the level of AOT in the foggy days has been high. As we are interested in the key parameters for formation of fog compare to quasi fog event that have approximately the same level of relative humidity, it seems the level of pollution can be one of the main parameter after the aerosol number concentration.

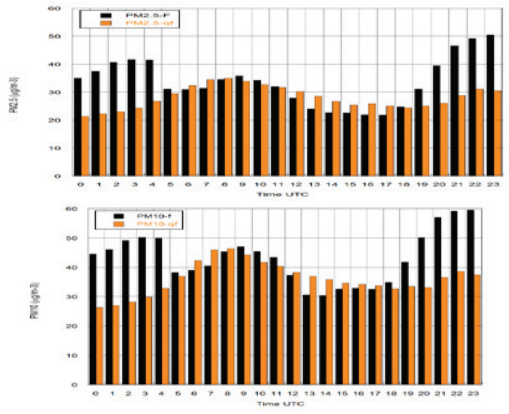

Figure 4 Diurnal cycle of PM2.5 and PM10 for fog and quasi fog

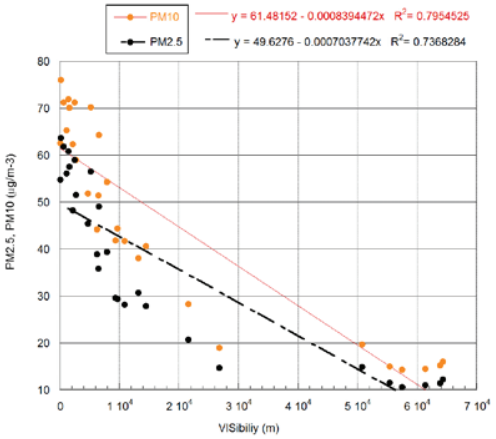

Figure 5 Relationship between the PM2.5 and PM10 and visibility between 17 UTC and 23 UTC on fog events

In figure 4 we have compared the diurnal cycle of PM2.5and PM10. The level of PM2.5 in fog days is 42% and higher compared to quasi fog event. The percentage changes from 20 to 98% after 17 UTC in the evening. No2 concentration varies between 40 to 20 % during 19 and 23 UTC. We have observed the same trend of diurnal cycle of PM2.5 and PM10 which start to have upward trend from 20 to 55 µg/m-3 and 33 to 60 respectively between 17 UTC and 23 UTC. Increase of PM2.5 and PM10 is related to decrease of boundary layer height during foggy days. The calculated boundary layer height shows the quasi fog days have higher boundary layer height compare to fog days about 25% between 17 UTC and 22 UTC is obvious reason of increasing of PM2.5 and PM10. Figure 5 shows the relationship between the hourly average of visibility and PM2.5 and PM10 between 17 UTC (time of highest observed visibility) and 23UTC. The good correlation coefficients of R2 of 0.79 and 0.73 have been observed respectively during fog events. Wen et al (2010) have found the visibility versus PM10 as exponential curves which enable the range of the range of visibility to be predicted from measured PM10 concentration. The removal and production of aerosols have been evaluated in fog. The fog top has important role in entrainment due to the mixing as a process which provides reactant to fog layer.

Fogwater concentration of nitrate and sulfate and ammonium can increase up to 30%. The fraction of scavenged aerosol by fog droplet is important for the fog effect on PM (Lillis et al. 1999). Dall'osto et al (2009) have shown the formation of the secondary aerosols during a fog event in London. They have found change in chemical properties in droplet mode. Particle which are rich on nitrate and organic carbon (200-300 nm) have been formed during fog events.
Nitrate and sulfate can be removed from the air by fog formation depends on the presence of gas phase and oxidants. The level of sulfate and nitrate differs on fog and quasi fog events.

5.1.2 Aerosol accumulation mode

To understand the influence of aerosol microphysical parameters on visibility we have compared the aerosols accumulation number and visibility for the time before a fog formation and near fog. It is clear that before fog formation we have abrupt reduction of visibility which is normally between 3 to 1 hours before fog formation. We have found the good correlation between augmentation of accumulation number and reduction of visibility for the interval of visibility on near fog (1km <Vis< 5km)(Table 4). Figure 6 shows the relationship between the visibility and accumulation number concentration during haze condition before fog formation in fog event and quasi fog event. We have chosen the visibility between 1km and 5km.

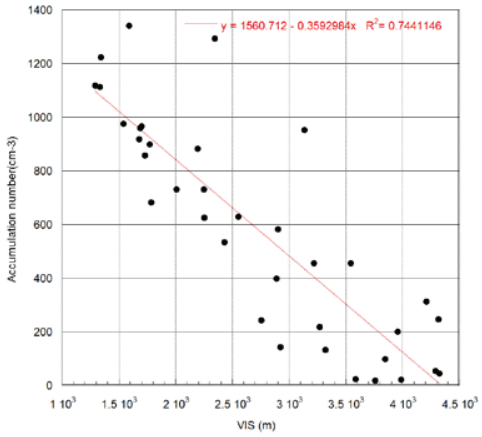

Figure 6 Correlation between accumulation number and visibility for the near fog definition range of visibility between 1 and 5 km

The simple regression coefficient of 0.86 shows the important roles of activated mode. Figure 6 shows the relationship between accumulation mass concentration and visibility. It can be observed that the correlation coefficient between visibility and mass R is decreased to 0.76. It can be conclude that aerosol activated number mode concentration are more related to visibility reduction.

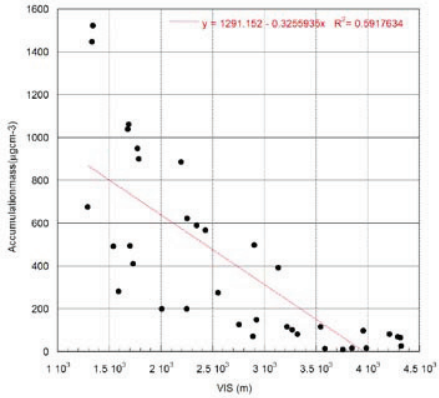

Figure 7 Correlation between accumulation mass and visibility for the near fog definition range of visibility between 1 and 5 km

5.1.1 Aerosol backscattering vertical profile and boundary layer

Figure 8 shows the structure of low level boundary layer on 27 Jan 2007 which was similar to profile of aerosol backscatter on 18 February (not shown) after 18 UTC until the formation of fog at 23:50 and 22:40 respectively. These cases have different vertical structure from 4 and 13 of mars. In all case before formation of fog the backscatter signal of ceilometers increased which is corresponded to aerosol concentration. On 27 Jan and 18 Feb we had the dense fog in that 30 minutes before the fog formation the layers gradually lowers at 22:40 and 23:50 the fog makes ground contact. As the surface visibility suddenly lower to a minimum which continues for the duration of the fog.

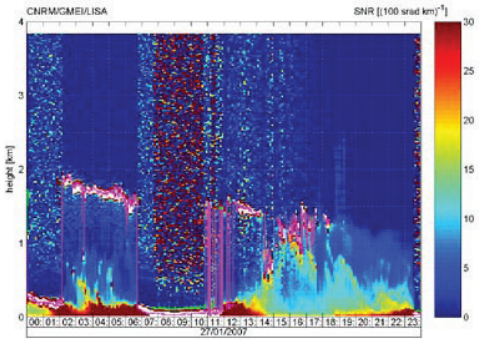

Figure 8 Ceilometer image of the radiation fog days 27 Jan

The Ceilometer plots shows the formation of fog and after some hours depends on dissipation process the fog lifts to an elevated layer for example on 19 Feb after 9 UTC (which have not been shown here) and it can be seen from the level of visibility. Surface level of relative humidity also showed a decrease in relative humidity. The ceilometers shows the presence of fog in all cases except 13 of March which have been observed a very thin layer of fog.
Hourly average of diurnal cycle of boundary layer height calculated using gradient method for fog and quasi fog events using backscatter signal of ceilometer. After sunrise the boundary layer height is increasing to have its maximum at 16 UTC late. We have observed the mixing in the boundary layer as a function of the day. We can define the period when the turbulence occurs by looking at the wind reinforcement and the temperature decrease and

relative humidity increase. The impact of the relative humidity on PM2.5 is observed for fog days and quasi fog days. We show that using additional information on the structure of the boundary layer detected by ceilometer, first we can understand better the variation of PM2.5 and PM10 in end of the day, secondly we can improve the correlation between aerosol optical thickness and ground-level visibility**.**

5.2 Retrieved visibility from Aeronet aerosol opticl thickness and backscatter signal of ceilometer

First, we compared the temporal evolution of AOT of foggy days and the day after and before. The AOT measured by aeronet are not available for all of the fog and quasi fog events. The AOT in foggy and the day after of fog between 17 and 20 February has been compared in that period 18 is the day with a dense fog and 19 is a quasi fog event. The day before the fog days has lower value of AOT_{440} of 0.098 and it change to 0.17 on 18 February. On 19 and 20 the value of AOT continuously is increasing because of long range transport. There is no available prove for the relative influence of regional transport on fog radiation. The value of AOT is about 73% higher in 18 Feb compared to 17 Feb. Secondly we have retrieved the Visibility using

the Koschemier method which is explained on the Section 3. It can be observed considering the constant value of Z=1km is not enough good for best estimation of visibility(Figure 10) because during the winter, the boundary layer height is most of the time less than 1km.We have used the boundary layer height which is obtained by backscatter signal of Ceilometer to find the best estimation of visibility.

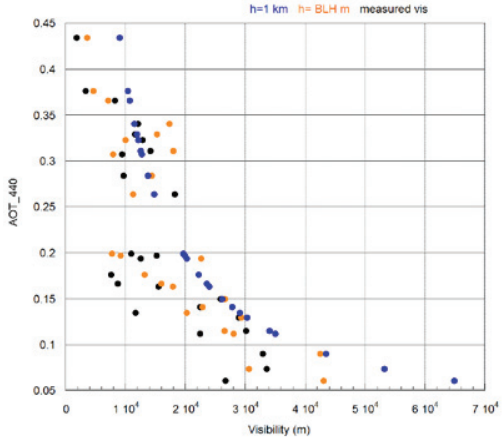

Figure 9. Retrieval of the visibility using AOT –Aeronet

The retrieved visibilities are in good agreement of calculated visibility. Figure shows the regression coefficient of R= 0.8(Figure 10).
The ceilometers –TSI is able to detect cloud layers and fog may be the base altitude could be obscure due to ground based fog. We have applied a relative humidity correction factor on the low level ceilometer signal. The regression coefficient is about R^2 =0.62(Figure 10).

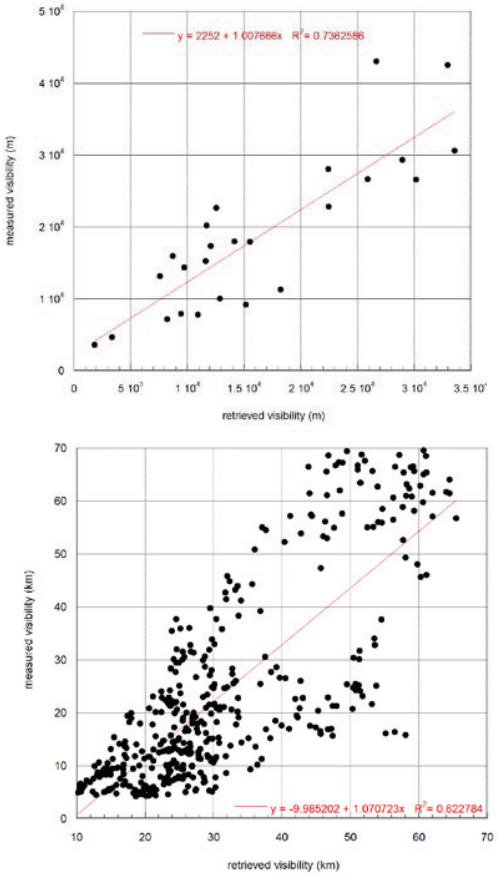

Figure 9 The regression equation between retrieved visibility a) using available aerosol optical thickness and measured visibility b)using backscatter ceilometers signal at first level and visibilty

Refrences

[1]. Alföldy, B., and Coauthors, 2007: Aerosol optical depth, aerosol compoistion and air pollution during summer and winter conditions in Budapest. *Science of the total environment*, 383, 141-163.

[2]. Allen, G., and R. Ress, 1997: Evaluation o the TEOM method for measurement of ambiant particulate mass in urban areas. *J. Air Waste Manage. Assoc.*, 47, 682-689.

[3]. American-meteorological-society, 2000: Online Glossary of Meteorology, 2nd Ed ition. *Accessed in 2009 at* http://amsglossary.allenpress.com.

[4]. Baumer, D., B. Vogel, S. Versick, R. Rinke, O. Mohler, and M. Schinaiter, 2008: Relationship of visibility, aerosol optical thickness and aerosol size distribution in an ageing air mass over South-West Germany. *Atmospheric Environment* 42, 989–998.

[5]. Boyouk, N., J.-F. Léon, H. Delbarre, T. Podvin, and C. Deroo, 2009: Impact of the mixing boundary layer on the relationship between PM2.5 and aerosol optical thickness. *Atmos. Environ.*, in press.

[6]. Cermak, J., R. M. Eastman, J. Bendixc, and S. Warren, 2009: European climatology of fogand low stratus based on geostationary satellite observations. *Q. J. R. Meteorol. Soc*, 135, 2125–2130.

[7]. Dall'Osto, M., R. M. Harrison, H. Coe, and P. Williams, 2009: Real-time secondary aerosolformation during a fog event in London. *Atmos. Chem. Phys.*, 9, 2459-2469.

[8]. Das, S. K., A. Jayaraman, and A. Misra, 2008: Fog-induced variations in aerosol optical and physical propertiesover the Indo-Gangetic Basin and impact to aerosol radiative forcing. *Ann. Geophys.*, 26, 1345–1354.

[9]. Duynkerke, 1998: Turbulence, Radiation and fog in Dutch Stable boundary layer *Boundary-Layer Meteorology*, 90, 447-477.

[10]. Elias, T., and Coauthors, 2009: Particulate contribution to extinction of visible radiation: Pollution, haze, and fog. *Atmos. Res.*, 92, 443-454.

[11]. Gultepe, I., and Coauthors, 2009: The fog remote sensing and modeling field project. *AMS*.

[12]. Haeffelin, M., and Coauthors, 2009: ParisFog, shedding new light on fog physical processes. *American Meteorological Society*.

[13]. ——, 2010: ParisFog, shedding new light on fog physical processes. *American Meteorological Society*.

[14]. Hänel, G., 1976: The properties of atmospheric aerosol particles as functions of the relativehumidity at thermodynamic equilibrium with surrounding moist air. *Adv. in Geophys.*, 19, 73-188.

[15]. Kokkola, H., et al., 2003: On the formation of radiation fogs under heavily polluted conditions. *Atmos. Chem. Phys.*, 3, 581- 589.

[16]. Lillis, D., N. C. Celia, CollettJr. b, and L. W. R. a. S. N. Pandis, 1999: Production and removal of aerosolnext term in a polluted previous termfognext term layer: model evaluation and previous termfognext term effect on PM *Atmospheric Environment*, 33, 4797-4816.

[17]. Mohan, M., and S. Paraya, 2009: Influence of aerosol spectrum and air pollutants on fog formation in urban environment of megacity Delhi, India. *Environ Monit Assess*, 151, 265-277.

[18]. Nowak, D., D. Ruffieux, J. Agnew, and L. Vuilleumier, 2008: Detection of fog and low cloud boundaries with ground-based remote sensing system. *J.of.Atmos. and Ocean. Tech*, 25, 1357-1368.

[19]. Ogawa, N., K. Youshimura, R. Kikuchi, T. Adzuhata, T. Ozeki, and M. Kajikawa, 2004: Effect of long- range

transport of Air Mass on the Ionic Component in radiation fog in northen Japan. *Analy. Sci*, 20.

[20]. Oldenborgh, G. J., P. Yiou, and R. Vautard, 2010: On the roles of circulation and aerosols in the decline of mist and dense fog in Europe over the last 30 years. *Atmos. Chem. Phys.*, 10, 4597- 4609.

[21]. Patashnick, H., and E. G. Rupprecht, 1991: Continuous PM10 measurements using the tapered element oscillating microbalance. *J. Air Waste Manage. Assoc.*, 41, 1079-1083.

[22]. Raut, J. C., and P. Chazette, 2008: Vertical profiles of urban aerosol complex refractive index in the frame of ESQUIF airborne measurements. *Atmos. Chem. Phys.*, 8, 901-919.

[23]. Seinfeld, J. H., and S. N. Pandis, 2006: *Atmospheric chemistry and physics: from air pollution to climate change, second edition.* J. Wiley & Sons, 1203 pp.

[24]. Shi, C., M. Roth, H. Zhang, and Z. Li, 2008: Impacts of urbanization on long-term fog variation in Anhui Province, China. *Atmospheric Environment 42 (2008) 8484–8492*, 42, 8484 -8492.

[25]. Stolaki, S. N., S. A. Kazadzi, D. V. Foris, and T. Karacostas, S., 2009: Fog characteristic at the air port of Thessaloniki, Greece. *Natural hazards and earth system sciences*, 9, 1541-1549.

[26]. Van Dingenen, R., F. Raes, and et al., 2004: A European aerosol phenomology - 1: physical characteristics of particulate matter at kerbside, urban, rural and background sites in Europe. *Atmos. Environ.*, 38, 2561-2577.

[27]. Wang, J., S. M. Li, and x. L. Liu, 2010: An analysis of the fog distribution in Beijing for the 2001–2005 period using NOAA and FY data. *Atmos. Res.*, 96, 575-589.

[28]. Wen, C. C., and H.-H. Yeh, 2010: Comparative influences of airborne pollutants and meteorological parameters on atmospheric visibility and turbidity. *Atmo. Res*, 96, 496-509.

[29]. Zhou, B., and J. Du, 2010: Fog prediction from a multi model mesoscale ensemble prediction system. *weather and forecasting*, 25, 303-322.

5th International Conference on Fog, Fog Collection and Dew
Münster, Germany, 25–30 July 2010
FOGDEW2010-140

The PreViBOSS project: study the short term predictability of the visibility change during the Fog life cycle, from surface and satellite observation

T. ELIAS (1), M. Haeffelin (2), D. Ramon (3), L. Gomes (4), F. Brunet (4), M. Vrac (1), P. Yiou (1), G. Hello (5), and H. Petithomme (5)

(1) Laboratoire des Sciences du Climat et de l'Environnement, Gif Sur Yvette, France (thierry.elias@lsce.ipsl.fr), (2) IPSL, Ecole Polytechnique, 91128 Palaiseau, France, (3) HYGEOS, Euratechnologies, 165 Avenue de Bretagne, 59000 Lille, France, (4) Metéo-France/CNRM/GMEI/MNPCA, 42, avenue G. Coriolis, 31057 Toulouse Cedex 01, France, (5) Metéo-France/DP, 42, avenue G. Coriolis, 31057 Toulouse Cedex 01, France

Fog prejudices major activities as transport and Earth observation, by critically reducing atmospheric visibility with no continuity in time and space. Fog is also an essential factor of air quality and climate as it modifies particle properties of the surface atmospheric layer. Complexity, diversity and the fine scale of processes make uncertain by current numerical weather prediction models, not only visibility diagnosis but also fog event prediction.
Extensive measurements of atmospheric parameters are made on the SIRTA since 1997 to document physical processes over the atmospheric column, in the Paris suburb area, typical of an environment intermittently under oceanic influence and affected by urban and industrial pollution. The ParisFog field campaign hosted in SIRTA during 6-month in winter 2006-2007 resulted in the deployment of instrumentation specifically dedicated to study physical processes in the fog life cycle: thermodynamical, radiative, dynamical, microphysical processes. Analysis of the measurements provided a preliminary climatology of the episodes of reduced visibility, chronology of processes was delivered by examining time series of measured parameters and a closure study was performed on optical and microphysical properties of particles (aerosols to droplets) during the life cycle of a radiative fog, providing the relative contribution of several particle groups to extinction in clear-sky conditions, in haze and in fog.
PreViBOSS is a 3-year project scheduled to start this year. The aim is to improve the short term prediction of changes in atmospheric visibility, at a local scale. It proposes an innovative approach: applying the Generalised Additive Model statistical method to the detailed and extended dataset acquired at SIRTA. This method offers the opportunity to explore non linear relationships between parameters, which are not yet integrated in current numerical models. Emphasis will be put on aerosols and their impact on the fog life cycle. Furthermore, the data set of ground-based measurements will be completed by spaceborne observation of visible and infra red radiance performed by the METEOSAT mission.

5th International Conference on Fog, Fog Collection and Dew
Münster, Germany, 25–30 July 2010
FOGDEW2010-141-1

Tailored fog climatology for Amsterdam Airport Schiphol

R. Leander
Royal Netherlands Meteorological Institute (KNMI), De Bilt, The Netherlands

Like many airports, Amsterdam Airport Schiphol is vulnerable to climate change. The airport is situated in a complex and fragile urban area where fundamental changes take place in design and use of the region. To maintain its competitive position, the airport is beginning to respond to changes in weather and climate by formulating adaptation strategies, based on tailored climate information.

The Royal Netherlands Meteorological Institute (KNMI), Amsterdam Airport Schiphol (AAS) and Air Trafic Control the Netherlands (LVNL) are working together to provide just that type of information. Due to safety regulations, reduced horizontal visibility on airports can have an immediate impact on the availability of runways and hence the airport capacity. Fog is therefore one of the most relevant meteorological phenomena to airport operations.

A study has started in which the statistics of fog occurrence and visibility at Amsterdam Airport are assessed. The aim is describing the current climate (from 1970 onward) as well as making projections into the future (up to 2040). For the latter, the identification and attribution of trends is relevant. Another point of interrest is the spatial pattern of fog potential over the airport, in particular the related questions whether some runways are more prone to fog occurrence than others and whether these runways require a separate forecast. To answer these questions it is crucial to distinguish between large-scale and local influences. The preliminary results of this study are presented here.

5th International Conference on Fog, Fog Collection and Dew
Münster, Germany, 25–30 July 2010
FOGDEW2010-142

Fog in a marginal agricultural area surrounded by montane Andean cloud forest during El Niño climate

G. García-Santos
University of Zurich, Geography, Zurich, Switzerland (glenda.santos@geo.uzh.ch)

The aim of the present study was to evaluate temporal variations of water inputs, rainfall and fog (cloud water), and its contribution to the water balance in a marginal agricultural area of potato surrounded by tropical montane cloud forest in Colombia. Fog in the air boundary layer was estimated using a cylindrical fog collector. Liquid water content of fog events were evaluated before and during natural climate event of El Niño. Our study shows the temporal variation of these two water inputs in both daily and monthly cycles on Boyacá at 2900 m a.s.l. Rainfall was the most frequently observed atmospheric phenomenon, being present on average 62% of the days per year, whereas fog was 45% of the time. Reflected on the lower frequency, annual amount of fog was 11% of precipitation. However during the anomalous dry climate of El Niño, total amount of rainfall was negligible and the few fog events were the only water source for plant growth. Estimated water crop requirements were higher than the water inputs. The survival of the crops was explained by meteorological conditions during dew and fog events. High relative humidity might have eased the plant's water stress by decreasing transpiration and temperature in leaves and soil, affecting the water balance and the heat exchange between the atmosphere–land interfaces in the marginal agricultural areas during exceptional dry climate.

5th International Conference on Fog, Fog Collection and Dew
Münster, Germany, 25–30 July 2010
FOGDEW2010-143

Fog, plant leaves and deposition of droplets

W. Konrad (1), M. Ebner (1), C. Traiser (1), and A. Roth-Nebelsick (2)

(1) University of Tübingen, Institute for Geosciences, Sigwartstrasse 10, D-72076 Tübingen, Germany (wilfried.konrad@uni-tuebingen.de), (2) State Museum of Natural History Stuttgart, Rosenstein 1, D-70191 Stuttgart, Germany

For various plants and animals, the accumulation of fog or dew droplets constitutes an essential part of their water supply. Understanding how water droplets deposited by fog or dew events interact with plant or animal surfaces is essential for gaining insight into the functionality of these surfaces. Besides being interesting within the realm of biology, this knowledge is indispensable for technical applications.

Frequently, it is advantageous to know (i) the growth rate of a droplet attached by surface tension to a surface which grows due to a given influx of fog particles, (ii) the maximum volume and (iii) the "lifespan" of a droplet before it detaches from the surface or starts to slide down along the plant surface, driven by gravity. Starting from principles of physics, we calculate quantitative expressions addressing questions (i) to (iii) for droplets which are attached to surfaces characterised by a high degree of symmetry, such as horizontally oriented or inclined planes, sections of spheres, cones and rotationally symmetric crevices. Furthermore, we treat the behaviour of droplets attached to a surface of non-constant contact angle. Although real surfaces never meet their geometric idealisations, results based on these often represent suitable and useful approximations to reality.

Finally, we apply our results to *Stipagrostis sabulicola*, a dune grass of the Namib desert which satisfies its water demand solely by capturing fog and dew droplets. Pictures taken with a scanning electron microscope show that the stem of *S. sabulicola* is longitudinally built up by alternating elevated and countersunk strips. Filling gaps in the experimental observation with theoretical speculation, the following picture emerges: Assuming that the elevated strips exhibit a higher contact angle than the countersunk strips, water droplets being deposited on the elevated strips are drawn towards the latter. The lower contact angle which prevails there increases the droplets' contact area with the plant surface at the expense of their thickness, thus expediting coalescence with neighbouring droplets. Once the droplets have grown to the critical size at which surface tension is overcome by gravitational attraction, the countersunk strips act as drainlike channels guiding the sliding droplets towards the basis of the stem and the roots.

5th International Conference on Fog, Fog Collection and Dew
Münster, Germany, 25–30 July 2010
FOGDEW2010-144

Wet season water distribution in a tropical Andean cloud forest of Boyacá (Colombia) during the dry climate of El Niño

G. Garcia-Santos (1) and M.B. Berdugo (2)

(1) University of Zurich, Department of Geography, Zurich, Switzerland (glenda.santos@geo.uzh.ch), (2) University of Boyacá, Department of Biology and Microbiology, Colombia

Fog has been demonstrated as the only source of moisture during the dry climate of El Niño in the tropical Andean cloud forest of Boyacá region in Colombia, yet its importance for the forest is virtually unknown. We assessed fog water distribution during the wet season inside the forest and outside in a practically deforested area. Water intercepted by plant was measured at different vertical stratus. Soil moisture in the first centimetres was also measured. During the anomalous drier wet season there was lack of rainfall and the total recorded cloud water was lower compared with the same period during the previous year. Our results indicated that the upper part of the forest mass intercepts most of the fog water compared with lower stratus when the fog event starts. However upper most stratus became rapidly drier after the event, which is explained because water is released to the atmosphere due to high heat atmosphere-leaves interface fluctuations caused by wind and solar radiation, flows towards a different water potential and drips from the leaves. Low amount of fog dripped from tree foliage into the soil, indicating a large water storage capacity of the epiphyte and bryophyte vegetation. Despite the small amount of throughfall, understory vegetation and litter remained wet, which might be explained by the water flowing through the epiphyte vegetation or the high capacity of the understory to absorb moisture from the air. Soil water did not infiltrate in depth, which underlines the importance of fog as water and cool source for seedling growth and shallow rooted understory species, especially during drier conditions.

5th International Conference on Fog, Fog Collection and Dew
Münster, Germany, 25–30 July 2010
FOGDEW2010-145

Total nitrogen and phosphorus in aerosols, sea fog and rain over the western North Pacific

Jinyoung Jung, Hiroshi Furutani and Mitsuo Uematsu
Atmosphere and Ocean Research Institute, Kashiwanoha 5-1-5, Kashiwa, Chiba 277-8564, Japan (jyjung@aori.u-tokyo.ac.jp)

Nitrogen (N) and phosphorus (P) are essential nutrients for the growth of phytoplankton in the ocean. They can be transported as aerosols or as gas phase and delivered to the surface of the ocean through atmospheric wet and dry depositions. The supply of N and P from atmosphere to ocean could be an important source of nutrients. Few studies, however, have been carried out to investigate distribution of atmospheric total (inorganic + organic) N and total P, simultaneously, over the North Pacific Ocean. In this study, atmospheric total N, total P and major ion species were determined in aerosol, sea fog and rain over the western North Pacific Ocean between 29 July 2008 and 19 August 2008 through the KH-08-2 cruise of R/V *Hakuhomaru*. Particle number concentrations (0.1 μm < D < 5 μm) of aerosols and size spectra of fog droplets (2 μm < D < 50 μm) were also measured.

During over a dozen fog events, ammonium (NH_4^+), nitrate (NO_3^-) and organic nitrogen (Org N) in aerosols were found to represent ~56% (6.5 ± 1.9 nmol N m^{-3}), ~21% (2.5 ± 1.7 nmol N m^{-3}) and ~23% (2.7 ± 1.6 nmol N m^{-3}) of total N, respectively. Similar distributions of N species in aerosols were observed during non-fog events. In comparison, contributions of NH_4^+, NO_3^- and Org N to total N in fog water (in rainwater) were ~26% (~48%), ~60% (~15%) and ~14% (~37%), respectively. These results indicate that NO_3^- was more effectively scavenged by fog water than by rainwater. It is suggested that scavenging mechanisms between fog and rain are different (e.g. in-cloud scavenging, below-cloud scavenging and hygroscopic property). In addition, the continuous particle number measurements illustrated that sea fog scavenged coarse particles (D > 0.5 μm) more effectively than fine particles (D < 0.5 μm).

Concentration of P species in aerosols during non-fog events were 0.06 ± 0.03 nmol P m^{-3} for water-soluble phosphate (PO_4^{3-}), 0.34 ± 0.19 nmol P m^{-3} for acid-leachable inorganic phosphorus ($IP_{acid\text{-}leachable}$), 0.59 ± 0.17 nmol P m^{-3} for organic phosphorus (Org P), accounting for ~6%, ~35% and ~59% of total P, respectively. On the other hand, in fog waters, contributions of PO_4^{3-}, $IP_{acid\text{-}leachable}$ and Org P to total P were ~1%, ~77% and ~22%, respectively. These results suggest that Org P is oxidized and transformed to $IP_{acid\text{-}leachable}$ under the condition of acidic fog water.

5th International Conference on Fog, Fog Collection and Dew
Münster, Germany, 25–30 July 2010
FOGDEW2010-146

Processing of carbonaceous material by fogs

P. Herckes (1), J.W. Hutchings (1), Y. Wang (1), H. Hill (1), J. Wang (2), and P.W. Westerhoff (2)

(1) Arizona State University, Dept. of Chemistry and Biochemistry, Tempe AZ 85287-1604, United States (Pierre.Herckes@asu.edu), (2) Arizona State University, School of Sustainable Engineering and The Built Environment, Tempe AZ 85287-5306, United States

Over the last years our understanding of carbonaceous material in aerosols, fogs and clouds has substantially improved. Comprehensive analytical approaches coupling chromatographic separations to bulk carbon measurements (total/dissolved organic carbon, TOC/DOC) and functional group characterization techniques (FT-IR, NMR), developed in water and soil chemistry, have been applied to atmospheric samples.

We will present novel insights on the composition of carbonaceous materials in fogs using size exclusion chromatography coupled to inline TOC detection (SEC-DOC) and spectroscopic approaches like fluorescence excitation emission matrices or H-NMR spectroscopy. SEC-DOC revealed similarities of fog water organic matter to the water soluble fraction of ambient aerosols (WSOC). However some notable differences have also been observed that will be discussed. Time resolved fog sampling allowed the observation of intra-event variability of organic matter concentrations and composition including changes in molecular size. The latter being particularly interesting as it might provide observational evidence of SOA generation or oligomerization type reactions.

Observations of carbonaceous particulate matter during foggy periods including pre-, interstitial and post-fog aerosol, allowed to gain insights on the impact of fog processing on carbonaceous matter and on the scavenging of carbonaceous matter by fogs. Observations made during a recent field campaign in Fresno (CA) will be discussed in detail.

5th International Conference on Fog, Fog Collection and Dew
Münster, Germany, 25–30 July 2010
FOGDEW2010-147-3

Use of fog water to the initial establishment of tree species under conditions of barren Lomas in the Quebrada Topará, Chincha-Perú

A. Vargas (1), R. Cabrera (1), K. Bederski (2), and A. Orellana (3)

(1) Universidad Nacional San Luis Gonzaga de Ica, Ica,Perú (aaronvargasg@gmail.com), (2) Fundo Vivero Organico Huaquina,Ica, Perú(klaus@toparaorganico.com), (3) Servicio Nacional de Áreas Naturales Protegidas por el estado-MINAM,Ica,Perú(bio_aog@hotmail.com

The Quebrada Topara is located in the Peruvian coastal desert ($13^0 12' $L.S, $76^0 09' $L.W.) and is influenced by the fog during the winter months, these conditions of high humidity allows its use to achieve the establishment of a permanent vegetation cover Huaquina hill, which is representative at the place of study.

Uncounted fog water can be captured and used for irrigation of plants. Also due to the absence of any tree species coverage in this region is not known which or which could have a better performance under these environmental conditions, We used to native species ***Caesalpinia spinosa*** "tara" and ***Schinus molle*** "molle" also introduced species ***Casuarina equisetifolia*** "Casuarina", as these could have a better adaptation. Soil analysis determined a high salinity and nitrogen poverty, preventing water infiltration into the soil and is not used by the plant so that the saline soil difficult to establish plants.

This research can be considered an exploratory phase, the objectives were: to determine the potential for fog water harvesting to capture in the study area, to assess for 20 months the initial performance of the species tara, molle and casuarina, and profit incorporation in the final sowing of organic matter and soil amendments to facilitate a better development of plants.

3 standard fog collector (SFC) proposed by Schemenauer and Cereceda (1993) were installed and we evaluated the capture water during 31 months, from June 2007 to December 2009, finding much water collected in the winter months, the average annual in the 3 SFC was similar (1.1, 1.2 and 1.1 L m $^{-2}$ day^{-1}) which allows us to plan according to necessary the best way to harness and store water to supply the plants.

It was found that native species, tara and molle were more adaptable to extreme conditions of the place that introduced casuarina species. The tara does grow faster in height and stem diameter, also achieves a good coverage to intercept fog water itself making it more viable and capable of being established. It provides statistics that indicate the beneficial effect of improving soil with organic matter and amendments in the survival rate and vegetative growth of tree species.

5th International Conference on Fog, Fog Collection and Dew
Münster, Germany, 25–30 July 2010
FOGDEW2010-148

Observations of radiation fog chemistry in the Eastern United States

D. Straub (1), J. Hutchings (2), and P. Herckes (2)

(1) Department of Earth and Environmental Sciences, Susquehanna University, Selinsgrove, PA, USA (straubd@susqu.edu),
(2) Department of Chemistry and Biochemistry, Arizona State University, Tempe, AZ, USA

The chemical composition of radiation fog in the Mid-Atlantic region of the United States has been the focus of an ongoing field campaign based in Selinsgrove, PA. This field study was established to provide a long term record that can be used to identify the effects of meteorology and air mass source regions on fog composition and to shed light on the role that fog can play in the production of secondary inorganic and organic aerosol mass. In the United States, studies that focus on radiation fog have been relatively rare. For the most part, they have been limited geographically to the Central Valley of California, though individual studies have also been conducted in the Central United States and along the Texas-Louisiana Gulf Coast.

Sample collection for the current study began during the fall of 2007. Through 2009, samples from 25 radiation fog events have been obtained. A Caltech Heated Rod Cloudwater Collector (CHRCC) having a Dp50 of approximately 8 microns was used to collect one fog sample per event. Samples were typically collected between 2:00 AM and 7:00 AM under conditions of light winds, clear skies, and recent rainfall. Sample volumes ranged from 2.9 ml to 150 ml. Following collection, samples were analyzed for pH and then one of the following: major inorganic ions, dissolved total organic carbon, N-nitrosodimethylamine (NDMA), metals, or organic speciation.

Through 2009, sample pH varied between 4.28 and 6.86 and averaged 5.03 based on H+ concentration. Ammonium and sulfate were found to be the most abundant ionic species in the fog samples. Sufficient ammonium was detected in nearly every sample to fully neutralize nitrate and sulfate. The concentrations of sulfate, nitrate, and ammonium observed in this study were lower than values reported in the literature for most other cloud and fog studies conducted in the US. Due to significant ammonium input, pH in the current study was higher than most other studies. Concentrations of total organic carbon averaged 7.22 mgC/L, which is lower than other radiation fogs studies but similar to that for many cloud studies. NDMA concentrations in two analyzed samples were considered high, but not outside the range that could be expected through equilibrium with potential gas phase concentrations.

5th International Conference on Fog, Fog Collection and Dew
Münster, Germany, 25–30 July 2010
FOGDEW2010-149

The surface learned from nature

H. Lim and W.D. Kim

Department of Printed Electromechanical Systems and Nature Inspired Mechanical Systems, Nano-Mechanical Systems Research Division, Korea Institute of Machinery and Materials, 171 Jang-dong, Yuseong-gu, Daejeon, 305-343, Korea (helim@kimm.re.kr)

In this work, I would like to introduce the emerging surface of nature. The surface in nature, has the multi and optimized function with well organized structure. There are so many examples that we learn and apply to technology.

First example is self-cleaning surface. Some plants (such as lotus leaf, taro leaf) and the wings of many large-winged insects (such as moth, butterfly, dragonfly) remain their surface clean in the very dirty environment. This self cleaning effect is accomplished by the superhydrophobic surfaces which exhibit the water contact angle of more than 150° with low sliding angle. Generally, the superhydrophobic surface is made up the two factors. One is the surface composition having the low surface tension energy. The other is the surface morphology of hierarchical structure of micro and nano size. Because almost nature surface have the hierarchical structures range from macro to nano size, their topography strength their function to adjust the life in nature environment.

The other example is the surface to use for drag reduction. The skin friction drag causes eruptions of air or water resulting in greater drag as the speed is increased. This drag requires more energy to overcome. The shark skin having the fine sharp-edged grooves about 0.1 mm wide known riblet reduces in skin friction drag by being far away the vortex.

Among a lot of fuctional surface, the most exciting surface the back of stenocara a kind of desert beetles. Stenocara use the micrometre-sized patterns of hydrophobic, wax-coated and hydrophilic, non-waxy regions on their backs to capture water from fog. This fog-collecting structure improves the water collection of fog-capture film, condenser, engine, and future building.

Here, the efforts to realize these emerging functional surfaces in nature on technology are reported with the fabrication method and their properties, especially for the control of surface wettability.

5th International Conference on Fog, Fog Collection and Dew
Münster, Germany, 25–30 July 2010
FOGDEW2010-150

Diagnosing Antarctic Fog

M. Lazzara
Antarctic Meteorological Research Center, Space Science and Engineering Center, University of Wisconsin-Madison, Madison, WI 53706 (mattl@ssec.wisc.edu / FAX: +1 (608) 263-6738)

Abstract

Fog affects aviation and other logistical operations in the Antarctic; however, limited studies have been conducted to understand fog behavior in this part of the world. A study has been conducted in the Ross Island region of Antarctica, the location of McMurdo Station and Scott Base – the main stations of the United States and New Zealand Antarctic programs, respectively. Using tools such as multi-channel satellite observations and supported by in situ radiosonde and ground-based automatic weather station observations, combined with back trajectory and mesoscale numerical models, this study discovered that austral summer fog events are advective. The diagnosis finds a primary source region from the southeast over the Ross Ice Shelf (over 72% of the cases studied) while a minority of cases point toward a secondary fog source region to the north along the Scott Coast of the Ross Sea with influences from the East Antarctic Plateau. Part of this examination confirms existing anecdotes from forecasters and weather observers, while refuting others about fog and its behavior in this environment. This effort marks the beginning of our understanding of Antarctic fog behavior.

1. Introduction

Fog is a weather phenomenon found all over the Earth, including the polar regions. A study of Antarctic fog has been conducted over the Ross Island region of Antarctic, where flight operations at Williams Field, Pegasus Field and Ice Runway are impacted by fog occurrences. Observations of fog from satellites, radiosondes, automatic weather stations and other surface observations along with analysis via back trajectory model and mesoscale model are discussed here. The study area (See Figure 1) is a 400 by 600 kilometer area. The time period analyzed covers the austral field seasons 2001 to 2007 during which there were approximately 23 fog event cases.

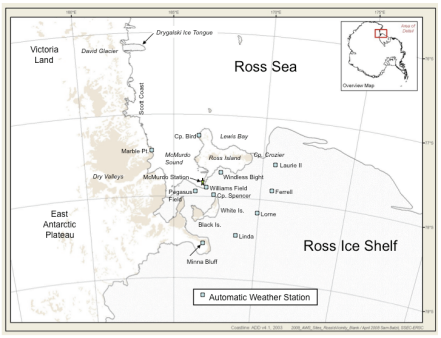

Figure 1: This is the fog study area, located over the Ross Island region of Antarctica.

2. Satellite Analysis

Principal Component (PC) Analysis (PCA) provides a means for depicting features in the satellite imagery (Hillger 1996). This offers one of the first attempts to apply this method for depicting Antarctic fog/low clouds. PCA is often performed on a dataset to reduce the redundancy in it – as is the case with the MODIS multi-spectral observations. It is also used to bring out features in the dataset, which is the objective here.

The Hillger approach (Hillger 1996) takes multiple spectral channels of a sample satellite observation, and determines the principal component "images" (PCI) for a given number of input channels. The first PCI depicts the features from the original observation that explain the most variance of the data and the features that are most common in the input channels. Similarly, the second PCI depicts the features from the observation that explain the second most variance of the data, and typically the differences between the input channels (Hillger 1996). Higher order PCs usually depict noise and other differences between the input channels. In its application here, the PCA provides information on variance spatially and spectrally, and does not offer the additional temporal

variance that most Empirical Orthogonal Function (EOF) analyses accomplish.

The PCA is conducted on a selection of MODIS bands - specifically 1, 6, 7, 20, and 31 (See Table 1; Figure 2). This combination of spectral channels offers the best visual depiction of fog in the second PCI. A combination of the first, second, and third PCI through red, green and blue color combinations provides a means of depicting characteristics of more than one PCI. The first PCI contains so much of the infrared window channel signal and some of the low clouds and fog signal, and when combined with the second PCI, which is one of the best depictions of low cloud and fog, provides a display that gives the fog and cloud features an appealing white color while having the ice features, so strongly seen in infrared imagery, blended into the blue or sepia shaded background.

Table 1: These are the MODIS channels utilized in the generation of the RGB PCI imagery.

MODIS Band	Wavelength	Description
1	0.64 μm	Visible channel
6	1.62μm	Near infrared
7	2.11μm	Near infrared
20	3.78μm	Shortwave infrared
31	11.0μm	Infrared window

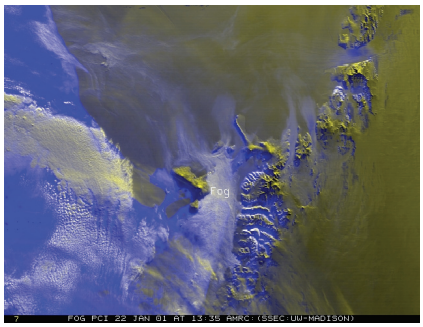

Figure 2:An RGB PCI fog depiction from 22 January 2001 at 13:35 UTC.

3. Boundary Layer Analysis

Moderate to high-resolution radiosonde observations can reveal the structure of the boundary layer. Radiosonde observations launched from McMurdo Station, with data reports every 10 seconds of flight or more recently upgraded to every 3 seconds of flight, are used to illustrate the structure of temperature, moisture and wind in the lowest 1.0 to 1.5 kilometers (km) of the atmosphere. The wind information is analyzed with a 1-2-1 smoothing. Figure 3 is a sample profile launched close to a fog occurrence at McMurdo Station and is an example of the boundary layer structure found in a majority of the fog events analyzed. The typical profiles may reveal a surface or friction layer close to the ground (not in all cases), a fog layer in the core of the boundary layer, an inversion at the top of the fog layer (which also marks the top of the boundary layer), and the lowest portion of the free atmosphere. Fog is difficult to capture via radiosonde observations that are widely spaced every 12 hours (or more in the case of missing observations). This results in radiosonde observations only providing snap shots of fog structure in the vertical during a particular stage of evolution.

The surface or friction layer is often thin in most cases and not well resolved by the radiosonde observations. Additionally, the McMurdo Weather Office practice is to assign the lowest level of the radiosonde report from the surface measurement made at the McMurdo Weather building and not by the radiosonde itself. Since that measurement is not always matched in time and is usually at a slightly different location, in most of the analysis here, this lowest observation level has been often been removed. This example, seen in Figure 3, does not have this removed, hence a surface layer between the lowest two observation points can be envisioned, although for this case, the radiosonde was launched between surface reports of fog and the surface layer may be mixed out given the wind speeds on the order of 10 meters per second (ms^{-1}).

In the example, the fog layer (~100 to 250 meters) is marked with a moist layer of air as compared to air aloft that is drier. This layer is also somewhat cooler than the air aloft. Both dewpoint and temperature have a slight decrease from the bottom to the top of the layer. Winds within this layer, in this sample, reveal an increase of the wind with height through the fog layer to the bottom of the inversion layer,

where the wind becomes geostrophic at the level of the free atmosphere (Stull 1988). Wind directions are primarily from the east, which is commonly the case for fog occurrences. In the inversion layer (between ~250 to ~350 meters), temperatures increase from the bottom to the top of the layer, while the layer becomes increasingly drier from the bottom to the top of the layer. This gives the profile a classic "goal post" shape between the temperature and dewpoint (Croft et al. 1997). In this particular example, wind speeds decrease some with increasing height as winds switch toward the southeast. Above the inversion layer is the free atmosphere (above ~350 meters) with different air mass characteristics.

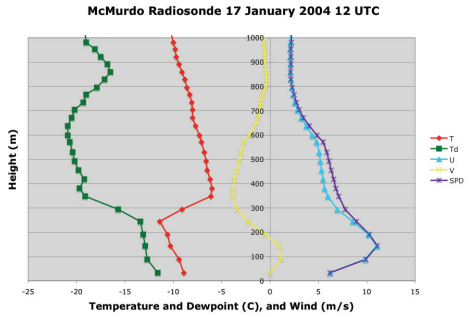

Figure 3: A sample radiosonde from 12 UTC on 17 January 2004 captures the boundary structure temporally close to a fog event at McMurdo Station.

4. Back Trajectories and Mesoscale Model Streamlines

The HYbrid Single-Particle Lagrangian Integrated Trajectory (HYSPLIT) model, available from the NOAA Air Resources Laboratory (ARL) offers a means of generating back trajectories. HYSPLIT is designed for air pollution and dispersion applications. Used in its basic form, it offers single particle forward or backward trajectories treated, in essence, as a parcel of air (Rolph 2003, Draxler and Rolph 2003). HYSPLIT version 4.8 used in back trajectory computations was initialized with conditions from the Global Data Assimilation System (GDAS) one-degree by one-degree resolution data. In only a couple of cases where input data was not available from the GDAS, 2.5 by 2.5 degree resolution NCEP/National Center for Atmospheric Research (NCAR) reanalysis data was used as an alternate initialization. All back trajectories were computed to end at the Williams Field AWS location (77.866° South, 166.983° East). Families of back trajectories are computed with final altitudes of 50, 100, 250, 500 and 1500 meters above ground level. A 48-hour back trajectory family set included six back trajectories - one inserted every 2 hours prior to the final end time. In all cases, the model's vertical velocity was used. The ending back trajectory date and time was selected from 20 fog cases, to match the occurrence of the fog. With fog often reported over several hours, the lowest visibility (or densest) portion of the fog, as reported from surface observations at McMurdo Station, was used as the final time of the back trajectory.

The results of the back trajectories are summarized in Table 2. The largest source region for air is from the Southern Ross Ice Shelf, with approximately half of the events having this characteristic (Figure 4). For 23 percent of the events, air originating purely from the East Antarctic Plateau may often come through the dry valleys over McMurdo Sound (not shown). Air from both the East Antarctic Plateau and the Ross Ice Shelf were found as well as a mix of the two source regions is seen in these cases. Finally, there is a unique case of air that originally was from the south of McMurdo Sound on the Ross Ice Shelf, but then circled over the Sound (not shown). Overall, if the two Ross Ice Shelf source are a combined, 72% of the air that leads to fog comes from the south and east of Ross Island.

Table 2: The source regions of fog as revealed with the HYSPLIT model back trajectories.

Source region	Occurrence (%)
Southern Ross Ice Shelf/Southern Ross Ice Shelf & East Antarctic Plateau mix	72%
East Antarctic Plateau	23%
South with circling over McMurdo Sound	5%

A combination of the satellite (especially reviewing time sequences), back trajectories, and Antarctic Mesoscale Prediction System (AMPS) model (Powers et al. 2003) streamlines agree that the fog impacting the region is "advective" in nature – forming over the Ross Ice Shelf and moving into the area (See Figure 5).

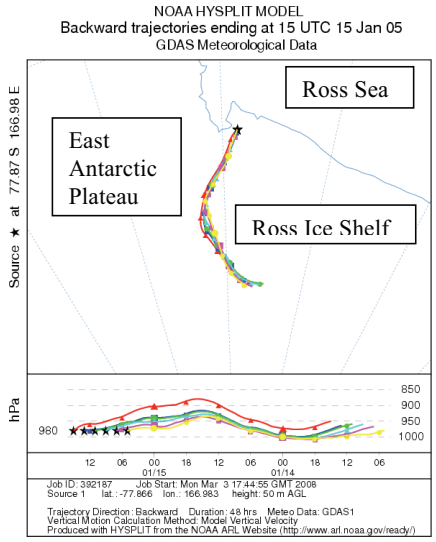

Figure 4: Back trajectory analysis ending at 20 UTC 24 January 2007 exemplifies how a majority of air originates from the south of the Ross Island region.

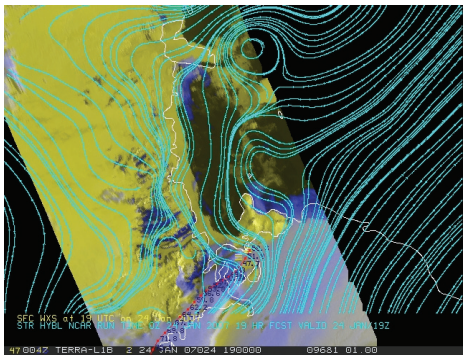

Figure 5: RGB PCI fog satellite imagery with AMPS streamlines at the second sigma layer above the surface and HYSPLIT back trajectory valid at 19 UTC 24 January 2007.

5. Summary and Conclusions

The examination of fog occurrence in the Ross Island region of the Antarctic has found most austral summer fog events to be "advective." Satellite observations along with corroborating model and back trajectory analyses reveal austral summer fog events often form outside the current Mac Weather AWS fog network. The analysis identifies two key source areas. The primary region is from the south and east of Ross Island over the Ross Ice Shelf. A secondary region, of very few events not shown here, is from the north and east along the northern Scott Coast of McMurdo Sound.

Acknowledgements

The author wishes to thank Professor Charles R. Stearns (1925-2010) for his commitment to Antarctic observations. Thanks to Professor Steve Ackerman for his support and advice. The author gratefully acknowledges the NOAA Air Resources Laboratory for the provision of the HYSPLIT model on the READY website used in this effort. This effort was partially supported by the National Science Foundation Office of Polar Programs Grant No. ANT-0636873.

References

[1] Hillger, D. W.: Meteorological features from principal component image transformations of GOES imagery. *Proceedings of the International Symposium on Optical Science, Engineering, and Instrumentation*, Denver, CO, 4-9 August, SPIE, vol. 2812, 111-121. 1996.

[2] Stull, R.B.: *An Introduction to Boundary Layer Meteorology*. Kluwer, 666 pp., 1988.

[3] Croft, P.J., R.L. Pfost, J.M. Medlin, and G.A. Johnson: Fog Forecasting for the Southern Region: A Conceptual Model Approach. *Wea. Forecasting*, **12**, 545-556, 1997.

[4] Rolph, G. D.: Real-time Environmental Applications and Display sYstem (READY) NOAA Air Resources Laboratory, Silver Spring, MD. [Available online at http://arl.noaa.gov/ready/hysplit4.html.], 2003.

[5] Draxle, R .R. and G. D. Rolph: HYSPLIT (Hybrid Single-Particle Lagrangian Integrated Trajectory). NOAA Air Resources Laboratory, Silver Spring, MD. [Model access via NOAA ARL Ready Website http://www.arl.noaa.gov/ready/hysplit4.html], 2003.

[6] Powers, J. G., A. J. Monaghan, A. M. Cayette, D. H. Bromwich, Y-H. Kuo, and K. W. Manning: Real-time mesoscale modeling over Antarctica: The Antarctic Mesoscale Prediction System (AMPS). *Bull. Amer. Met. Soc.*, **84**, 1533-1545, 2003.

5th International Conference on Fog, Fog Collection and Dew
Münster, Germany, 25–30 July 2010
FOGDEW2010-151

How does canopy wetness shape evapotranspiration in a mountain cloud forest

H.-S. Chu, S.-C. Chang, Y.-Z. Lin, and Y.-J. Hsia
Department of Natural Resources and Environmental Studies, National Dong Hwa University, Hualien, Taiwan

Interception plays an important role in the hydrological characteristics of cloud forest ecosystems due to frequent wetness of the canopy. The dynamics of this canopy interception processes are ecologically important for partitioning between interception evaporation and transpiration. Long term meteorological observations at the Chi-Lan Mountain site (24°35'N, 121°25'E) indicated that fog weather accounts for one third of the time on a year around and mainly prevails in the late afternoon and evening. However, it is still not clear how long the interception water could last on canopy surface under such diurnal foggy patterns and how this wetness further shapes the partition between interception evaporation and transpiration.

In order to explore the evapotranspiration patterns under wet canopy conditions, three-month intensive experiment was conducted at the CLM site from 2009/4/28 to 7/21. Eddy covariance method was applied to measure the net water vapor exchange between ecosystem and atmosphere. An open/closed-path eddy covariance system, including a sonic anemometer (Campbell CSAT3), an open path infrared gas analyzer (Licor LI7500) and a closed path infrared gas analyzer (Licor LI7000), was mounted at 1.8-fold of canopy height. The S-type sap flow sensors (Ecomatik SF-L) were mounted at 1.3 m height of trunk on five representative Chamaecyparis obtusa var. formosana trees as an index of transpiration rate. Three leaf wetness sensors (Campbell LW237) and two infrared surface thermometers (Apogee IRTS-P) were added to monitor the wetness and surface temperature of canopy.

The result showed that canopy wetness played a crucial role in partitioning the interception evaporation and transpiration at this forest stand. Evapotranspiration either under wet or dry canopy conditions was mainly driven by the evapotranspiration demand, as indicated by the potential evapotranspiration. However, evapotranspiration was lower for dry canopy condition. While total evapotranspiration rate increased with evapotranspiration demand, transpiration did not follow the increasing trend. Transpiration under dry canopy condition increased linearly with evapotranspiration demand and leveled off as evapotranspiration demand exceeded around 3 mmole m-2 s-1. This flatten trend reflected that water stress could develop at this forest under higher evapotranspiration demand even the soil was moist. On the other hand, transpiration under wet canopy condition was reduced while evapotranspiration increased, which reflected that canopy wetness possibly reduced the capability of transpiration. Complex of canopy wetness probably played an important role in partitioning the interception evaporation and transpiration under this wet canopy condition.

The diurnal courses of weather and water status during the experimental period showed fog typically formed in the afternoon and dissipated before midnight. Canopy surface was gradually wetted a few hours after the initiation of fog events. In the beginning hours of fog events during the late afternoon, canopy surface was only slightly wetted. Fog reduced solar irradiance but transpiration still was driven by the reduced evapotranspiration demand. As fog persisted in the following nighttime, canopy surface wetness increased and only trivial water vapor fluxes were observed due to lack of energy for evaporation and the cease of transpiration. As incident radiation rose after dawn, leaf temperature increased, intercepted water on the canopy surface was evaporated and canopy surface dry quickly in the morning. Both interception evaporation and transpiration contributed significantly to ecosystem water vapor fluxes during these drying periods till canopy surface was completely dry and transpiration dominated thereafter.

5th International Conference on Fog, Fog Collection and Dew
Münster, Germany, 25–30 July 2010
FOGDEW2010-152

Effects of foggy conditions on the measurement of stem respiration in a cloud forest in Taiwan

S. C. Chang, H. K. Wang, Y. C. Lin and Y. J. Hsia
Department of Natural Resources and Environmental Studies, National Dong Hwa University, Hualien, Taiwan
(scchang@mail.ndhu.edu.tw / Fax: +886-3-8633260)

Abstract

Stem CO_2 efflux of a *Chamaecyparis obtusa* var. *formosana* forest ecosystem was measured at the Chi-Lan Mountain site in northern Taiwan. The site is located at an altitude of 1650 m and is subjected to frequent fog coverage around the year. Stem CO_2 efflux was measured continuously at 1 m height by horizontally mounting an automatic soil respiration chamber system (LI-8100 Survey Chamber, LI-COR) on the stem surface. Under clear weather, e. g. on May 16, 2009, the diurnal stem CO_2 efflux rate vs. stem temperature showed a clear hysteresis loop. The daytime stem CO_2 efflux rates were lower than the potential values, which were predicted by the nighttime stem temperature-stem CO_2 efflux relation. The magnitude of the daytime depression of the stem CO_2 efflux was positively correlated with the sapflow velocity. On the contrary, when the site was submerged in fog during the daytime, the hysteresis did not take place and the very low sapflow velocities caused only minor decrease in the daytime stem CO_2 efflux compared to those in nighttime. In May 2009, the daily accumulated daytime depression of stem CO_2 efflux ranged from 0.54 to 7.70 mmol m^{-2}. The daily daytime foggy time had a negative linear correlation with the amount of daily depression. The stem CO_2 efflux measured by the chamber method might significantly underestimate the stem respiration rate. In a clear day the daytime total stem CO_2 efflux may represent only 85% of the stem respiratory CO_2. However, in a foggy day, 99% of the respired CO_2 might diffuse out of the bark and be detected by the chamber system.

1. Introduction

Aboveground woody tissue respiration is a significant component of carbon flux in forested ecosystems because it may return 5-15% of gross primary production to the atmosphere. Worldwide great uncertainties have been shown in quantifying stand-scale stem respiration from the chamber measurements due to the large spatial and temporal variations within an ecosystem. More detailed studies are thus needed also for the modeling purpose.

As part of the carbon project at the Chi-Lan Mountain (CLM) long-term ecosystem research site, we conducted the stem respiration measurements in 2008-2009. Both the spatial and temporal variability of stem CO_2 efflux were evaluated for the upscaling to the stand scale. In this paper we present the part of the continuous measurement in 10-min frequency. The results might offer an opportunity for elucidating the controlling mechanism of stem respiration in the humid subtropical region.

2. Material and methods

2.1 The study site

The study was conducted at the Chi-Lan Mountain site (24˚35'N, 121˚25'E) located in northern Taiwan. Long-term ecosystem research program including the study of carbon budget has been carried out since 2002. This mountainous forest ecosystem is subjected to frequent foggy condition and the *Chamaecyparis obtusa* var. *formosana* stand adds more than 300 mm yr^{-1} of fog deposition to its 4350 mm yr^{-1} precipitation [2]. Due to the high soil water content and the relatively low annual air temperature (13.8 ˚C), the soil respiration rate was estimated to be an extremely low value of 1.6 ton C ha^{-1} yr^{-1} [1].

2.2 Setup of the measurements

The stem CO_2 efflux was measured using the LI-8100 Automated Soil CO_2 Flux System (LI-COR Biosciences, USA). PVC collars of 10 cm in diameter were mounted on the stem surface and the LI-8100-102 Survey Chamber was attached horizontally to the collar by measurement. Measurements of spatial variation at 1 m height were

done on 25 *C. obtusa* var. *formosana* trees. Three of which were selected for the investigation of vertical gradient by measuring at 1, 2, 4, and 6 m height. The measurements were performed every 4 weeks. For the rest of time, the chamber was mounted on one of the trees for continuous measurement in a frequency of once per 10 min. Stem temperature beside 7 of the collars was monitored using thermisters installed 0-3 cm into the stem.

The meteorological and ecophysiological parameters used in this study, including the horizontal visibility and the sapflow rate, were part of the monitoring program at the CLM site.

3. Results and discussion

The temporal variation of stem CO_2 efflux followed an obvious diurnal pattern as well as a seasonal pattern. The similar trend of stem temperature and stem CO_2 efflux, as shown in May 2009 (Figure 1), depicts a significant correlation between them. The stem CO_2 efflux (F, in [μmol C m^{-2} s^{-1}]) grows exponentially with the stem temperature (T, in [°C]):

$$F = -0.523 + e^{-0.506+0.069*T} \qquad (1)$$

with R^2=0.90.

While the dependence of stem CO_2 efflux on stem temperature seems apparent at the monthly time scale, the diurnal course of the efflux rate showed a clear hysteresis with stem temperature. Figure 2 gives a typical example of the hysteresis for clear days at the CLM site. The nighttime stem CO_2 efflux rates were higher than the daytime ones giving the same stem temperature. This phenomenon is well recognized in the literature [3] and the deviation of daytime efflux rates from the nighttime values results mainly from the upward transport of dissolved CO_2 in the xylem sap when transpiration takes place. The bubble size in Figure 2, an indication of the strength of sapflow rate, clearly suggests its relation with the amount of deviation of daytime to nighttime stem CO_2 efflux rate.

To quantify the effect of transpiration on the measurement of stem CO_2 efflux, the "daytime depression (DD)" of the stem CO_2 efflux was calculated as follows: (1) a daily potential CO_2 efflux function was derived by fitting the nighttime efflux rate and the respective stem temperature to a linear equation; (2) for each daytime measurement, the potential daytime CO_2 efflux was calculated using the respective stem temperature and the function derived above; (3) the DD was calculated by subtracting the potential efflux rate with the actual efflux rate.

Taking the data in May 16, 2009 as an example again, the DDs calculated for the daytime measurement points (from 06:00 to 18:00) showed a significant

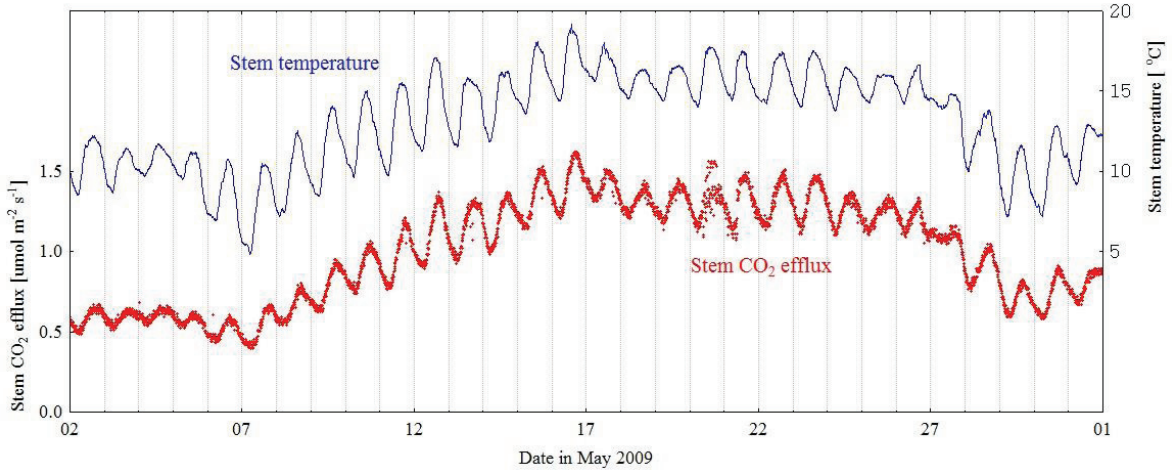

Figure 1: Stem CO_2 efflux and stem temperature of a *Chamaecyparis obtusa* var. *formosana* tree in May 2009 at the CLM site.

positive linear correlation with the sapflow rates (R^2=0.92) (Figure 3).

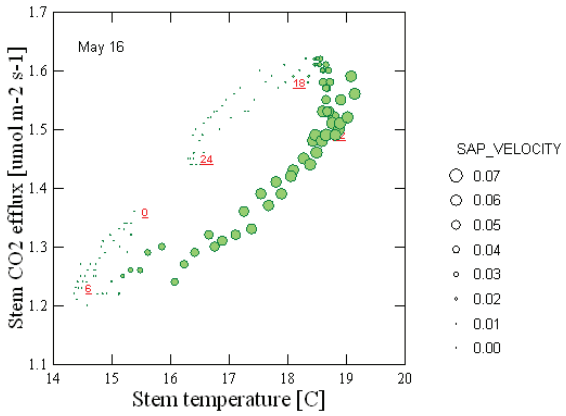

Figure 2: Dependence of stem CO_2 efflux on stem temperature in a clear day (May 19, 2009). The underlined numbers indicate the time of the day. The size of the circles represents the rate of sapflow [cm min^{-1}].

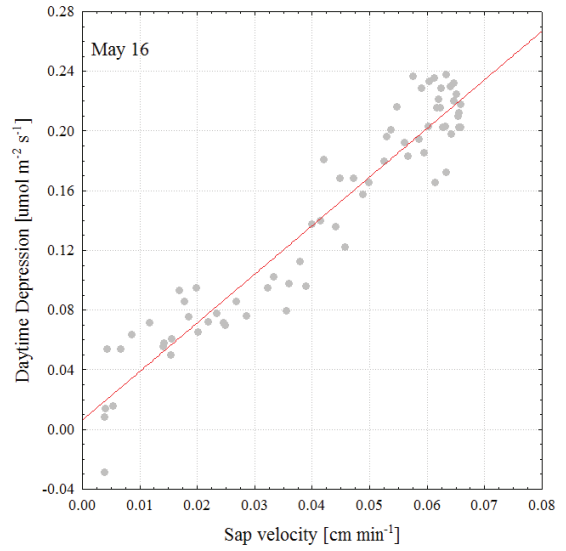

Figure 3: The dependence of the daytime depression on the sapflow rate for a clear day of May 16, 2009 at the CLM site. The points represents the daytime (06:00 to 18:00) 10-min measurements. The solid line is the linear regression curve.

In contrast with the clear days, the diurnal course of stem CO_2 efflux for the foggy days did not present any clear hysteresis pattern. Figure 4 shows an example of foggy day on May 24, 2009, with total fog duration amounted to 310 min. On this day, the daytime efflux-temperature relation did not depart much from that in the nighttime. It seems that only minor part of the respired CO_2 was transported upwards under the very low daytime average sapflow velocity of 0.026 cm min^{-1}. On the contrary, the average sapflow velocity on May 16, 2009 was 0.046 cm min^{-1}. The 77% higher sapflow velocity on that clear day has caused the daytime depression of the stem CO_2 efflux.

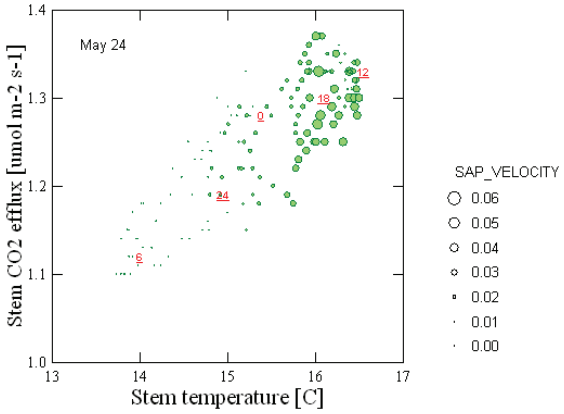

Figure 4: Dependence of stem CO_2 efflux on stem temperature in a foggy day (May 24, 2009). The underlined numbers indicate the time of the day. The size of the circles represents the rate of sapflow [cm min^{-1}].

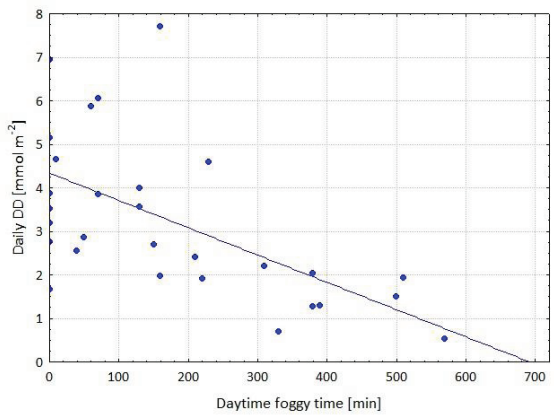

Figure 5: Relation between daily daytime depression (DD) and daily daytime foggy time in May 2009 at the CLM site. The solid line represents the linear regression curve.

To get more insight into the effect of foggy condition on the stem CO_2 efflux, the daily accumulated daytime depression was calculated for each day of May 2009. The daily DD ranged from 0.54 to 7.70 mmol C m^{-2} d^{-1}, with the low values being from the heavy foggy days (Figure 5). When the daily foggy time was longer than 300 min, the depression was up to 2 mmol C m^{-2} d^{-1}. However, in clearer days, the depression as well as the variation of depression got higher, indicating a more complicated control over the distribution of respired CO_2 in the stem.

The effects of foggy conditions on the stem CO_2 efflux measurement might have some ecological implications. The frequent occurrence of fog in the cloud forests, where the transpiration rates are low, might guarantee a less biased estimation of stem respiration by the chamber method. The measured stem CO_2 efflux might significantly underestimate the stem respiration rate of the living cells in the stem. As the case at the CLM site showed, in a clear condition the daytime total stem CO_2 efflux may represent only 85% of the stem respiratory CO_2. However, in a foggy day 99% of the CO_2 evolved from the respiration might diffuse out of the bark and be detected by the chamber system.

4. Conclusions

At the CLM site, the climatic condition might strongly influence the stem CO_2 efflux rate measured by chamber method. Under clear weather, the transpiratory water movement in the xylem reduced the amount of CO_2 efflux rate. Daily export of dissolved CO_2 might amount to 7.7 mmol C m^{-2} d^{-1}., or 15% of the total respired CO_2. On the contrary, in the foggy days the CO_2 efflux rate represented a significant part of the respired CO_2 in the stem.

Acknowledgements

We thank the Forest Conservation and Management Administration, Veterans Affairs Commission for permission of using the study site and for the help in the construction of the tower. We also thank C. W. Lai and H. S. Chu for their help in data analysis. The project was funded by Environmental Protection Administration, Taiwan and National Science Council, Taiwan.

References

[1] Chang, S. C., Tseng, K. H., Hsia, Y. J., Wang, C. P. and Wu, J. T.: Soil respiration in a subtropical montane cloud forest in Taiwan, Agricultural and Forest Meteorology, Vol. 148, pp. 788-798, 2008.

[2] Chang, S. C., Yeh, C. F., Wu, M. J., Hsia, Y. J. and Wu, J. T.: Quantifying fog water deposition by in situ exposure experiments in a mountainous coniferous forest in Taiwan, Forest Ecology and Management, Vol. 224, pp. 11-18, 2006.

[3] Teskey, R. O., Saveyn, A., Steppe, K. and McGuire, M. A.: Origin, fate and significance of CO_2 in tree stems, New Phytologist, Vol. 177, pp. 17-32, 2008.

5th International Conference on Fog, Fog Collection and Dew
Münster, Germany, 25–30 July 2010
FOGDEW2010-153

A 15-year dataset of mountain cloud chemistry observed in northern Taiwan

N-H. Lin (1), J.-C. Jao (1), and C.-M. Peng (2)

(1) Department of Atmospheric Sciences, National Central University, Chung-Li, Taiwan, (2) WeatherRisk Explore Inc., Taipei, Taiwan

The purpose of this study is to characterize the chemistry of the wintertime clouds observed in northern Taiwan. The experiment of cloud water collection on an hourly basis for each event was conducted at Bamboo Mt. ($\sim$1100 m MSL) during the winters of 1996-2010. In total, 130 events with 4589 samples were obtained. In general, there cloud events can be categorized into two cloud types associated with northeast monsoon flow and frontal passage. The average pH for all events ranged in 3.21-5.85, with a mean of 4.26 for all samples. On average, the dominant ions in collected cloud water were Na^+, Cl^-, SO_4^{2-}, NO_3^-, and NH_4^+. The first two seasalt ions generally can account for more than 50% of total ion concentration. In addition to the statistic analysis, the parameters of Acidifying Potential (AP), Neutralizing Potential (NP and Seasalt Potential (SP) were also introduced to characterize the cloud water chemistry. Associated backward trajectories of airflows for corresponding events were calculated in order to investigate the long-range transport of regional air pollutants. As a consequence, most of the backward trajectories were primarily originated from eastern coastal areas of China for cloud events associated with prevailing northeast monsoon flows. In contrast, the source regions of air mass can extend to central China for the cloud events associated with frontal passages. The source/receptor relationship between source regions and cloud chemistry was further studied. The results indicated that regional air pollutant can be possibly carried through clouds to Taiwan via the long-range transport.

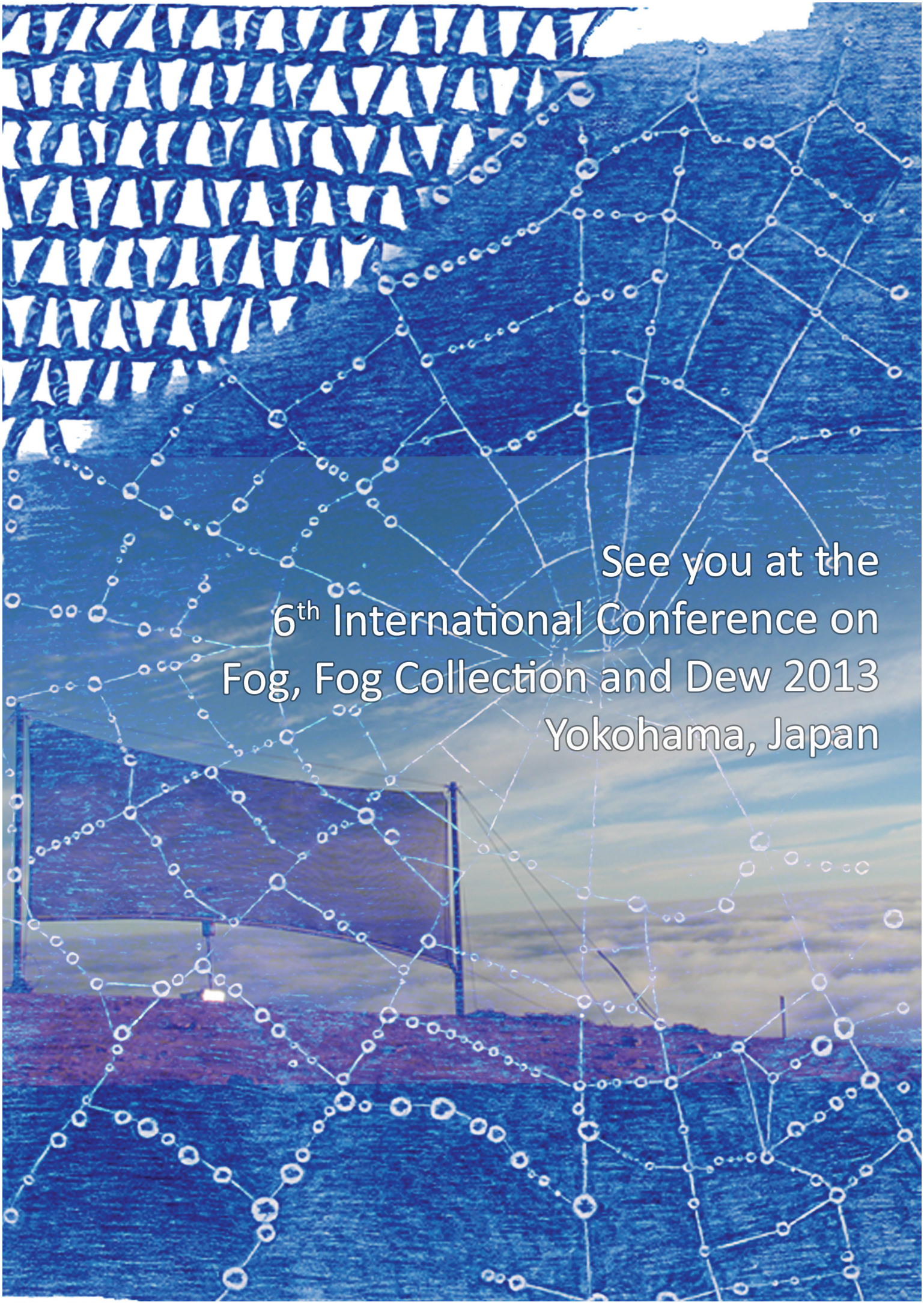
See you at the
6th International Conference on
Fog, Fog Collection and Dew 2013
Yokohama, Japan